The Icacinaceae from the Paleogene of the Paris Basin

Cédric del Rio

Cédric del Rio. The Icacinaceae from the Paleogene of the Paris Basin. Paleontology. Muséum national d'histoire naturelle - MNHN PARIS, 2018. English. NNT : 2018MNHN0011 . tel-02366974

HAL Id: tel-02366974
https://theses.hal.science/tel-02366974
Submitted on 17 Nov 2019

MUSEUM NATIONAL D'HISTOIRE NATURELLE
Ecole Doctorale Sciences de la Nature et de l'Homme – ED 227

Année 2018 **N° attribué par la bibliothèque**
|_|_|_|_|_|_|_|_|_|_|_|_|

THESE

Pour obtenir le grade de

DOCTEUR DU MUSEUM NATIONAL D'HISTOIRE NATURELLE

Spécialité : Paléontologie

Présentée et soutenue publiquement par

Cédric DEL RIO

Le 16 novembre 2018

Les Icacinaceae du Paléogène du Bassin de Paris

Sous la direction de **: Monsieur Dario De Franceschi, Maître de Conférences**
et Monsieur Thomas Haevermans, Maître de Conférences

JURY :

M. Manchester, Steven R.	**Professor, Florida Museum of Natural History, Gainsville (32611-7800)**	**Rapporteur**
M^{me} Nadot, Sophie	**Professeur, Université Paris-Sud, Orsay (091)**	**Rapporteur**
M^{me} Crasquin, Sylvie	**Directeur de recherche CNRS, Sorbonne Université, Paris (075)**	**Examinateur**
M^{me} Decombeix, Anne-Laure	**Chargée de recherche CNRS, Université de Montpellier, Montpellier (034)**	**Examinateur**
M^{me} Meyer-Berthaud, Brigitte	**Directeur de recherche CNRS, Université de Montpellier, Montpellier (034)**	**Examinateur**
M. De Franceschi, Dario	**Maitre de Conférences, Muséum national d'Histoire naturelle, Paris (075)**	**Directeur de Thèse**

Remerciements

Je tiens tout d'abord à remercier mes directeurs de thèse, Dario De Franceschi et Thomas Haevermans, pour m'avoir donné l'opportunité d'effectuer cette thèse dans de bonnes conditions. Etant basé dans le bâtiment de Paléobotanique, j'ai plus étroitement travaillé avec Dario De Franceschi au quotidien, je tiens à le remercier plus spécialement pour le temps qu'il m'a accordé, l'aide qu'il m'a apportée et la bonne humeur qu'il a su m'insuffler.

Cette thèse a été effectuée au sein de deux laboratoires, le Centre de recherche sur la paléobiodiversité et les paléoenvironnements (UMR7207) ainsi que dans l'Institut de Systématique, Evolution et Biodiversité (UMR7205). Je tiens à remercier Sylvie Crasquin et Philippe Grandcolas de m'avoir accueilli dans ces deux laboratoires. Je remercie également le Labex BCDiv (CNRS-MNHN) qui a financé cette thèse et plus particulièrement Myriam Méziou et Anne-Cécile Haussonne pour s'être occupées avec une efficacité sans pareille de mes ordres de missions, de mes billets d'avions et de mes retours de missions.

Je remercie les responsables des herbiers qui m'ont accueilli avec gentillesse et qui m'ont permis de visiter de belles collections ; Sovanmolly Hul pour l'Herbier de Paris, ainsi que Myriam Gaudeul pour les demandes de prélèvements, Petra De Block pour l'Herbier de Meise et Roxali Bjmoer pour l'Herbier de Leiden.

Mes remerciements vont également à tous les gens qui m'ont aidé durant ma thèse. Je pense particulièrement à Michel Lemoine qui m'a permis d'accéder au macroscope et au MEB d'Archéobotanique, Lilian Cazes et Philippe Loubry pour l'accès au MEB de Paléontologie et qui m'ont été d'une grande aide, Amandine Blin pour m'avoir permis d'utiliser le macroscope de la plateforme de morphométrie, Marie-Béatrice Forel pour m'avoir permis d'utiliser dans de bonnes conditions le MEB de Jussieu (décidément !), Angélina Bastos pour son aide administrative à de multiples moments, Thierry Deroin pour l'aide qu'il m'a apportée lors de mes tentatives de faire des lames d'endocarpes, enfin à Yohan Despres pour le moulage de la surface du seul et unique spécimen de *Paleophytocrene* que j'ai étudié durant cette thèse.

Je voudrais remercier mes collaborateurs, en particulier Gregory W. Stull et Bernard Bodo qui m'ont aidé à divers moments de la thèse.

Le bon déroulement de cette thèse est en grande partie attribuable à mon comité de thèse qui m'a suivi avec efficacité tout le long de ces trois années. Je voudrais pour cela remercier ses membres, Hervé Sauquet, Antoine Zazzo, Timothée Le Péchon, Brigitte Meyer-Berthaud et Sylvie Crasquin.

Le bâtiment de paléobotanique est comme une petite famille et on y travaille plutôt bien. C'est dans cette ambiance sympathique que j'ai pu effectuer ma thèse sans flancher. Je remercie pour cela Marc Godinot (et ses Carambars!) Jean Dejax, Eloïse Zoukouba (merci pour l'Awallé !), Olivier Bethoux, Peggy Vincent et Nathalie Bardet. Je voudrais en particulier remercier Anaïs Boura pour son énergie et pour son aide sans faille en début de thèse. Mes remerciements vont également à Guillaume Cousin, ses petites blagues et pour cette guerre incessante entre la partie gauche et la partie droite du bâtiment, guerre qui, me dit-on, n'a pas trouvée d'issue favorable ni à l'un ni à l'autre des camps ; malgré l'intervention de l'aviation. Je remercie également Rémi Allemand, mon colocataire de bureau, avec qui nous avons fondé la Team Endo- et affronté bien des périls, la canicule, le froid mordant, les vaisseaux ennemis, le lundi matin ! Je remercie Mélanie Tanrattana pour les longues pauses que nous avons prises et l'accueil de son bureau. Enfin, je remercie Pauline Robat pour sa gentillesse et sa présence durant toute ma thèse.

Mes amis de promotion, je vous dois des remerciements particulièrement chaleureux. Cinq ans ! Je remercie particulièrement Valentin Seizilles de Mazancourt (qui m'a plus d'une fois dépanné en latin), Romain Sabroux et Martial Plasse, pour tous ces moments passés à trainer à la ménagerie, auprès de notre (nos) Kookaburra préférés. Je remercie également Jean-Christophe Theil et Damien Olivier pour leur bonne humeur tout au long de ces trois années. Enfin, je remercie Cindy Lim, soutien infaillible en toute chose, tu m'as apporté tout ce qu'il me fallait pour réussir ces trois dernières années. Tu es également une correctrice attentionnée de cette thèse, tâche ingrate s'il en est.

Je remercie mes parents pour m'avoir permis de faire mes études à Toulouse, puis à Paris, ce n'était pas gagné ! Je remercie également mon frère pour son intérêt pour ma thèse. J'ai une pensée particulière pour Jeanne Perramond qui, je pense, aurait été fière de me voir terminer cette thèse. *Si tout va bien, tous les buts sont atteints.*

Je tiens enfin à remercier le jury de cette thèse pour sa lecture attentive de mon travail.

Table of content

Introduction

1. The Icacinaceae family

1.1. Brief taxonomic history

In 1823, Adrien de Jussieu (1797 – 1853) described a new genus called "*Icacina*" in reference to "*la ressemblance que les branches de cet arbre offrent dans leur port avec celle de l'Icaco, espèce de Chrysobolon*." (The similarity of the shape of the tree branches with the *Icaco*, species of *Chrysoblon*) and not attributed to a special family (Jussieu, 1823). Jussieu's drawing *Icacina senegalensis* (Fig. 1) illustrated all the vegetative and reproductive characters of this new genus. He shows that there is no character in particular but a combination of characters for the recognition of *Icacina*.

In 1841, George Bentham (1800 – 1884) proposed a tribe named Icacineae, putting together *Gomphandra*, *Icacina*, *Apodytes*, *Leretia* and *Pogopetalum* in the Olacineae order (Bentham, 1841). The diagnosis of this new tribe used ovary and seed characters such as the pendulous ovule.

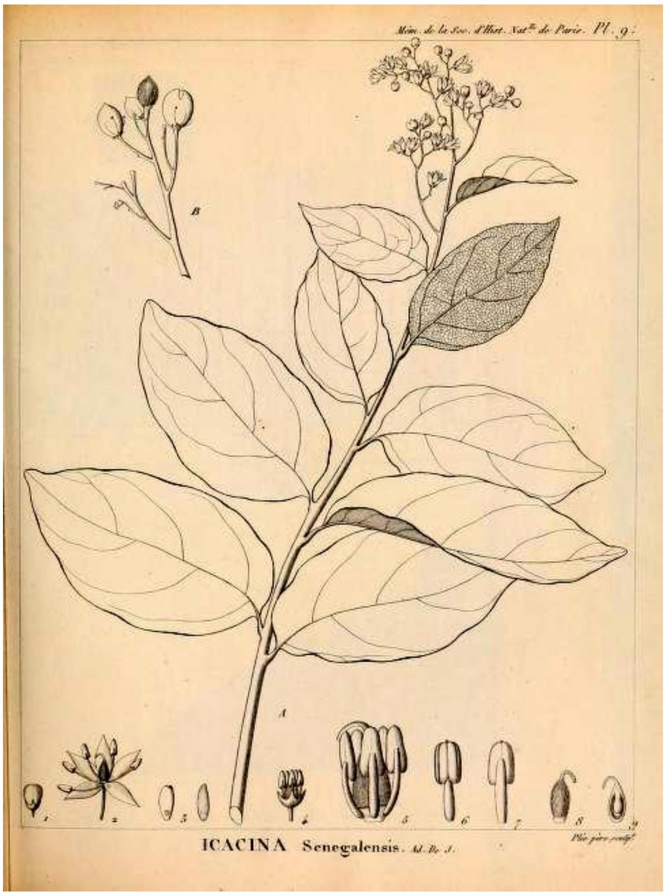

Figure 1. First representation of *Icacina senegalensis* by Adrien de Jussieu.

In 1852, John Miers (1789 – 1879) considered the Icacineae tribe as not closely related to the Olacaceae family (asterids) and changed the taxonomic rank of this group: he described the Icacinaceae family and added the following genera to this new group: *Mappia*, *Rhaphiostylis*, *Stemonurus*, *Phlebocalymna*, *Sarcostigma*, *Poraqueiba*, *Pennantia*, *Ptycopetalum* and *Desmostachys* (Miers, 1851). He considered this family as close to the Celastraceae and Aquifoliaceae (rosids).

In 1897, Adolf Engler (1844 – 1930) reviewed the Icacinaceae family and described three sub-familia: Icacinoideae, Lophopyxidoideae, and Cardiopterygoideae (Engler, 1897). The Icacinoideae sub-familia is divided into four tribes: Icacineae, Iodeae, Sarcostigmateae, and Phytocreneae. The Icacinaceae family contains 38 genera.

In 1942, Hermann Sleumer (1906 – 1993) only considered the Icacinoideae sub-familia as part of he Icacinaceae family and confirmed the four tribes described by A. Engler. The Icacinaceae family contains 58 genera; this is the widest definition of this family and we are referring to this definition when we use the term Icacinaceae s.l. in posterior articles and in this thesis. He considered this family as a member of Sapindales (rosids).

This last article was published in a context of intensive work about the wood anatomy and global morphology of Icacinaceae (Howard, 1940, 1942a, 1942b, 1942c, 1942d, 1943, Bailey and Howard, 1941a, 1941b, 1941c,) and was followed by other precise taxonomic studies of pubescence, crystals (Heintzelman and Howard, 1948) and pollen (Dahl, 1952, Lobreau Callen, 1972, 1973). However, those articles failed to find diagnostic characters for the family.

In 1997, Armen Takhtajan (1910 – 2009) proposed the Icacinales order, which includes Icacinaceae and Aquifoliaceae (rosids) together (Takhtajan, 1997).

In 1998, The Angiosperm phylogeny group (APG, 1998) considered Icacinaceae as unassigned to a particular order but was listed in the Euasterids clade based on molecular phylogeny. On this article, Icacinaceae is considered as a member of Euasterids rather than rosids.

In 2001, Jesper Kårehed showed that the Icacinaceae family is a polyphyletic group (Kårehed, 2001) with molecular and morphological data. He defined the Icacinaceae s.s. in the Garryales order and placed some genera in Aquifoliales and Apiales orders. In particular, Kårehed formed a new family, Stemonuraceae, and used the Cardiopteridaceae family for the genera included in the Aquifoliales. This new circumscription of Icacinaceae s.s. includes 36 genera in four groups: *Icacina*, *Cassinopsis*, *Emmotum*, and *Apodytes*.

In 2008, Frederic Lens and collaborators show that the Icacinaceae s.s. is a basal lamiid group (Lens et al., 2008). According to this study, the Icacinaceae s.s. have simple perforation plates in vessels (except for *Cassinopsis*), which is not the case for other excluded former Icacinaceae.

In 2014, with the study of James W. Byng and collaborators, Icacinaceae s.s. sensu Kårehed is considered as a probable non-monophyletic group.

Finally, in 2015, Gregory W. Stull and collaborators delimited a new Icacinaceae s.s. family with only the Icacina group sensu Kårehed (2001) accepted, using new molecular data set (Stull et al., 2015). Icacinaceae s.s. contains only 23 genera with about 160 species and is a basal lamiid group close to the Oncothecaceae family. Both families are in the newly defined Icacinales order. Those taxonomic assignments are accepted and used in the APG IV (APG, 2016). Stull and collaborators proposed four clades in the Icacinaceae family (Fig. 2).

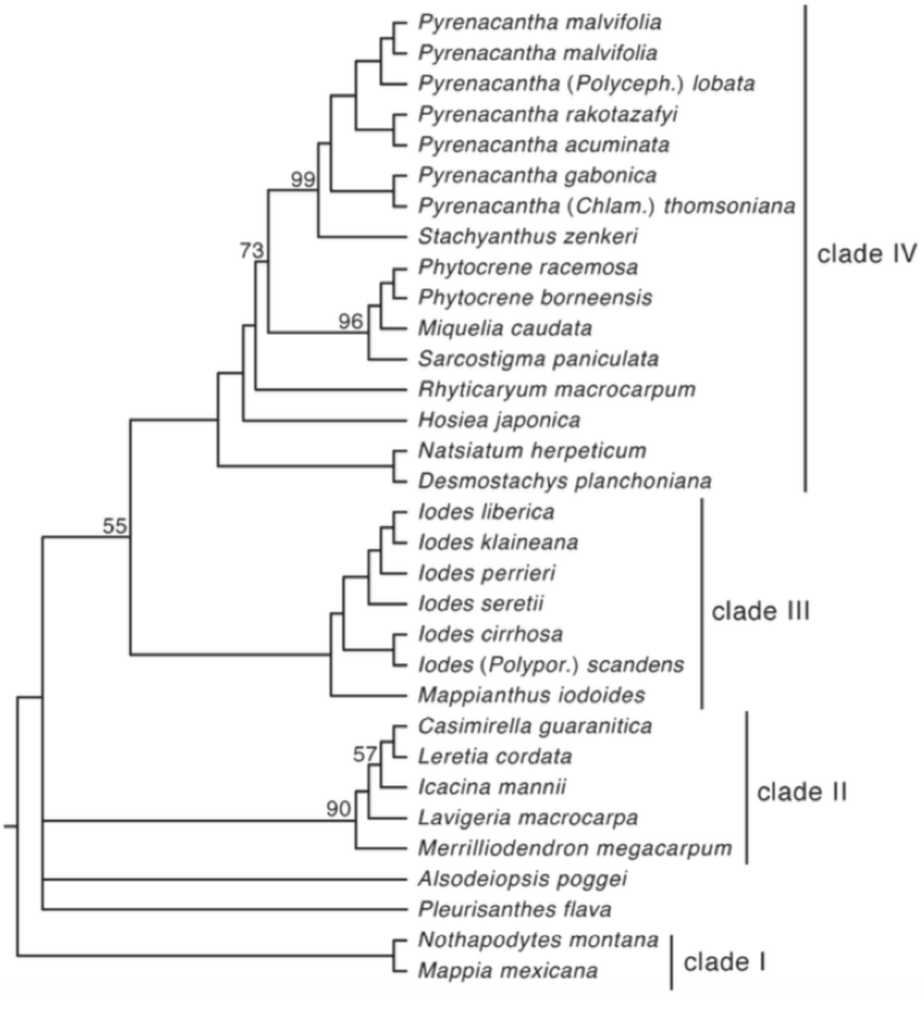

Figure 2. Icacinaceae phylogeny from Stull et al. 2015. Note: this phylogeny shows the Icacinoideae group and excludes *Cassinopsis*.

The clade II includes genera traditionally considered in Icacineae tribe. Other groups include genera from more than two traditional tribes. In the following parts, we only described the Icacinaceae s.s. sensu Stull et al., 2015.

1.2. Habitus and biogeography

Most of the species in the Icacinaceae family are lianas but some of them are trees or shrubs. In particular, clade III and IV are characterized by lianas or climbing shrubs. Species forming a tree are scarce and are only present in *Cassinopsis* and in some species of the clade I and II. Most of the species from both clades are shrubs. The family is mainly tropical to sub-tropical with some exceptions such as the genus *Hosiea*, which is more temperate. We found the Icacinaceae family in four main areas: Asia, Africa, Madagascar and South America (Fig. 3, Table 1.).

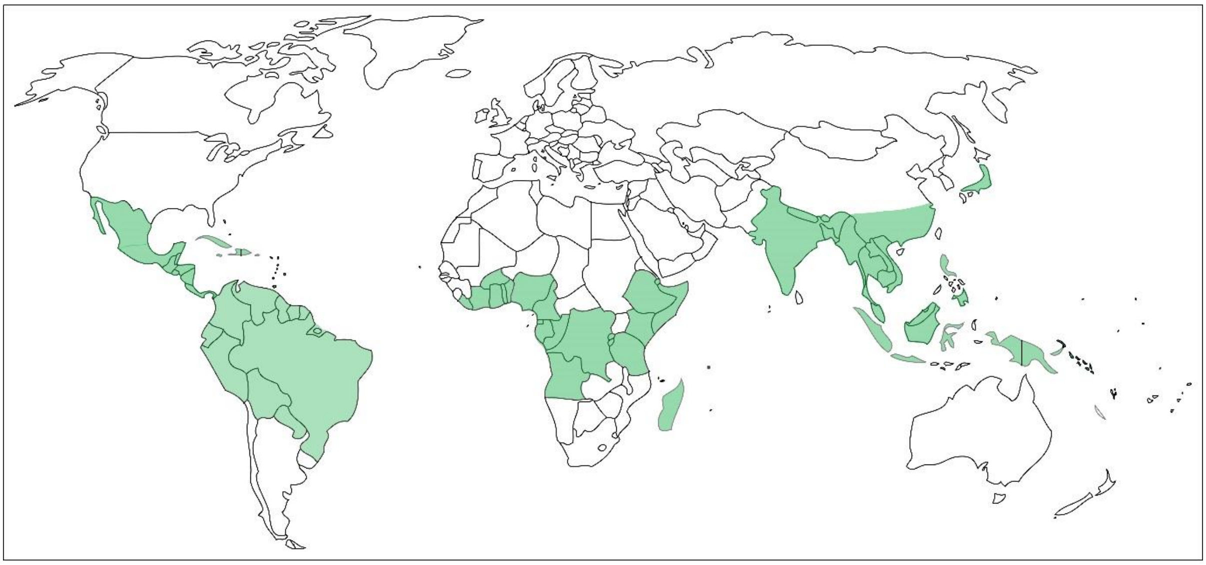

Figure 3. Modern distribution of the Icacinaceae family.

The Icacinaceae s.l. were also present in the Oceanian area, they will not be considered as following the monophyletic definition of the Icacinaceae species. This lack of species in this area remains surprising in the current phylogenetically context because the Oncothecaceae family, which includes only one genus and species, is restricted to Oceania (Morat and Veillon, 1988). The Asian area and in particular the Malaysian area are the most diversified for this family with about 60 species and 13 genera.

TABLE 1. Distribution of species and genera of Icacinaceae

Area	**Number of species**	**Number of genera**
Asia	60	13
Africa	54	8
South America	20	4
Madagascar	18	4
Total	152	23

The African area also contains a comparable number of species but low genera diversity, found mainly in the equatorial forest (Congo, Cameroon, and Gabon). The South American area contains few species and genera in the North-eastern area up to Mexico, whereas Madagascar seems to be particularly rich in Icacinaceae. Only four genera are shared between these areas: *Cassinopsis* and *Desmostachys* (Africa-Madagascar), *Iodes* and *Pyrenacantha* (Africa-Madagascar-Asia). This shows a strong endemism in general for the Icacinaceae genera and species. The number of species by genus is very variable (Table 2.). *Pyrenacantha* is the most diversified genus in terms of species richness followed by the *Iodes* genus. It is noteworthy that those two genera are both distributed in three different areas and are climbers too. Most genera of Icacinaceae comprise less than ten species and five genera are represented by only one species, mostly from the Asian area.

TABLE 2. Number of species by genus of Icacinaceae.

Genus	*Pyrenacantha*	*Iodes*	*Rhyticaryum*	*Phytocrene*	*Miquelia*	*Alsodeiopsis*	*Casimirella*	*Nothapodytes*
Total species	35	23	12	11	9	8	7	7
Genus	*Pleurisanthes*	*Cassinopsis*	*Mappia*	*Desmotachys*	*Icacina*	*Stachyanthus*	*Hosiea*	*Lavigeria*
Total species	7	6	6	5	5	4	2	2
Genus	*Mappianthus*	*Sarcostigma*	*Leretia*	*Merrilliodendron*	*Natsiatopsis*	*Natsiatum*	*Sleumeria*	
Total species	2	2	1	1	1	1	1	

1.3. Morphological characteristics

The family has no single morphological diagnostic character but can only be defined by their combinations. The exceptions are common in all traits and thus we can understand the difficulties of some authors from the past two hundred years to define a monophyletic group from the Icacinaceae family. However, global tendencies are shown and we will highlight these characters without hiding the true diversity.

The leaves are commonly alternate, simple, entire with a pinnate veination, brochidodromous secondary veins and percurrent tertiary veins (Fig. 4, A). This kind of leaves is very common and typical of tropical floras. The petiole size is variable as well as the apex and the base shapes, the pilosity and the size of the leaves (Fig. 4). We found in *Iodes* and *Cassinopsis* some examples of opposite leaves. In *Hosiea*, which is a temperate genus from China, we can observe teeth on the margin of the leaves and craspedodromous secondary veins (Fig. 4, B). *Phytocrene palmata* has mesophyll palmate leaves (Fig. 4, C), a very uncommon character in the Icacinaceae family. Domatia were occasionally present, as in the *Mappia* genus leaves (Potgieter & Duno, 2016). Stomatal type of Icacinaceae s.s. is mostly cyclocytic but also anomocytic; the stomatal index is very variable (Van Staveren & Baas, 1973, Baas, 1974).

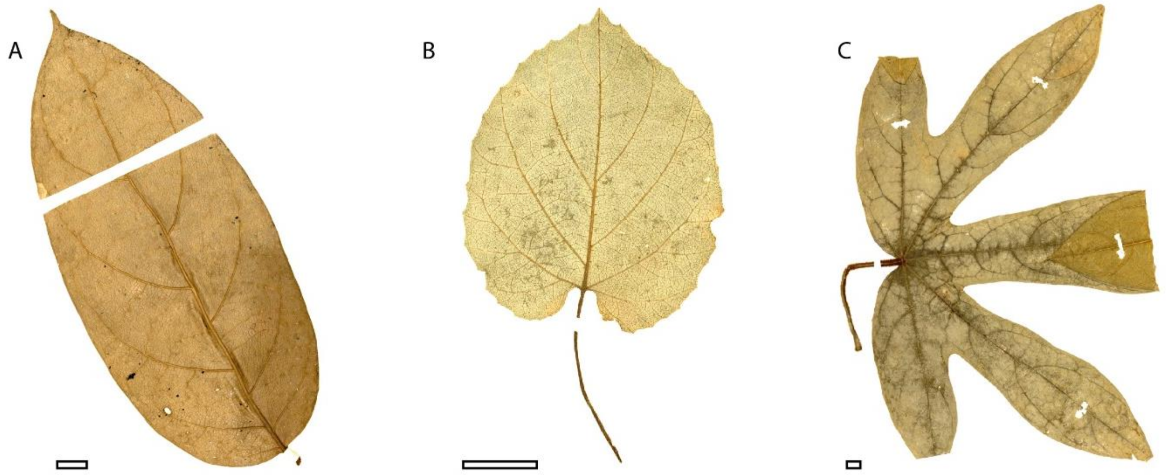

Figure 4. Different types of leaves of Icacinaceae. (A) *Icacina claessensii* De Wild (P04495399, P); (B) *Hosiea sinensis* (Oliv.) Hemql. & E.H. Wilson (P04513501, P); (C) *Phytocrene palmata* Wall. (P04513410, P). Scale bar: 1 cm.

Druses and rhombies crystals are found in leaves of Icacinaceae but also in flowers and woods (Heintzelman & Howard, 1948).

Tendrils were found in the *Iodes* and *Mappianthus* genera (clade III) and also in *Natsiatopsis*. They could be associated with a liana habitus even if all lianas do not have tendrils (as *Pyrenacantha*).

The anatomy of the wood in the Icacinaceae is mainly characterised by simple perforation plates of vessels (except for *Cassinopsis* which has scalariform perforation plates) but also by alternate vessels, short vessel elements, banded and vasicentric axial parenchyma, multiseriate rays and the occurrence of cambial variants (Bailey and Howard, 1941b, Lens et al., 2008).

The shape of the inflorescence is much diversified in Icacinaceae family, cauliflorous, axillary or terminal (Fig. 5). The inflorescence could be panicles, cymes, spikes, racemes or in heads (Fig. 5). There is no particular tendency for these characters in the Icacinaceae family. The inflorescence was used only in the definition of some genera. Indeed, *Alsodeiopsis* and *Leretia* only have axillary panicles, *Desmostachys* and *Rhytycaryum* axillary spikes, *Mappia*, *Hosiea* and *Mappianthus* axillary cymes, *Lavigeria* cauliferous panicles, *Phytocrene* is mostly in heads (Fig. 5, B) and all *Stachyanthus* species have cauliferous and racemose inflorescences (Fig. 5, A).

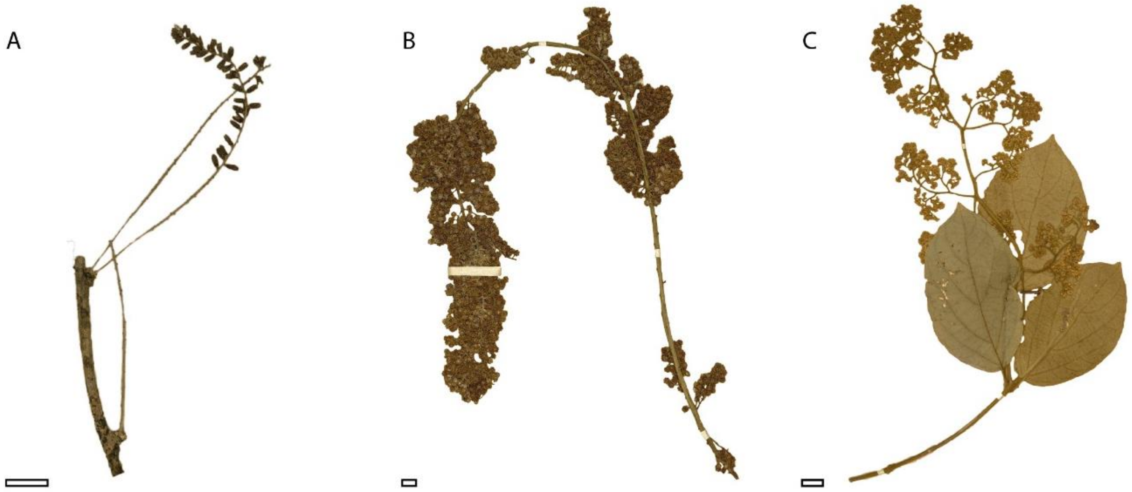

Figure 5. Different types of inflorescence in Icacinaceae. (A) *Stachyanthus zenkeri* Engl. (P05030980, P); (B) *Phytocrene bracteata* Wall. (P05221882, P); (C) *Iodes cirrhosa* Turcz (P06672323, P). Scale bar: 1 cm.

However, we found almost all combination available in *Iodes* and *Pyrenacantha* groups. For example, *Iodes cirrhosa* has axillary cymes (Fig. 5, C) whereas *Iodes klaineana* tends to have axillary panicles. The most diverse group for inflorescence types is *Pyrenacantha*, which has species with head, spike, and raceme types, axillary or cauliferous.

Flowers are always with a radial symmetry and are very small (< 10 mm) with marked differences between genera. For example, flowers from *Desmostachys* (8-10 mm) are significantly larger than those from *Iodes* (2-3 mm - Villiers, 1973)

Flowers are bisexual (Fig. 6, A) or unisexual (Fig. 6, B, D). Following the last phylogeny (Fig. 2), the clade III only has unisexual flowers (Fig. 6, B) and the clade IV has a marked tendency for unisexual flower too (Fig. 6, D). On the opposite, the clades I and II have bisexual flowers (Fig. 6, A, C). The calyx is clearly divided (Fig. 6, A-B) or cupular (Fig. 6, C) and occasionally absent in the *Pyrenacantha* genus (Fig. 5, D). Petals are valvate, four or five (sometimes, the number of petals varies in function of the flower sex) mainly gamopetal at the base but free in the clade II (Fig. 6, A). We also found free petals in *Mappia* (clade I, Fig. 6, C), *Iodes* (clade III) and *Pyrenacantha* (clade IV). The petal apices are generally inflexed (Fig. 6, A, C), except in *Hosiea*, *Natsiatum* and some *Iodes*, *Desmostachys* and *Pyrenacnatha* species (Fig. 6, B, D).

The petals could be curved abaxially (Fig. 6, B). There are simple hairs outside the petals in almost all species of Icacinaceae with few exceptions.

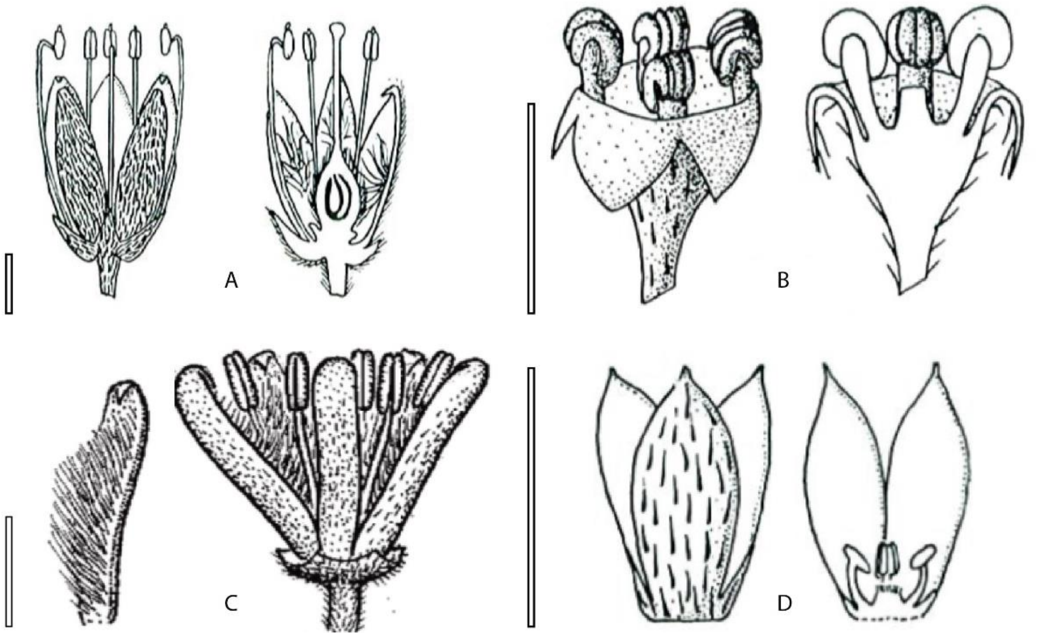

Figure 6. Examples of flower from the four clades defined by Stull et al. 2015. (A) *Icacina manii* Oliv. ; (B) *Iodes africana* Welw. Ex Oliv. Male flower; (C) *Mappia multiflora* Lundell; (D) *Pyrenacantha vogeliana* Baill. male flower. Drawings from Villiers, 1973 (A, B and D) and from Angulo et al., 2013 (C). Scale bar: 2 mm.

The stamen insertion is generally free. We observe a variation in the length of the filament (Fig. 6) and the shape of the anther is not constant (in particular in the shape of the anther from *Iodes africana*, Fig. 6, B).

The pollen of Icacinaceae is small in general (< 20 μm), with various shapes and ornamentations (Lobreau-Callen, 1972, 1973). Indeed, the clade III and clade IV have porate pollen (except in *Desmostachys* and *Hosiea*), the clade II has colporate pollen and the clade I colpate pollen. Therefore, this character seems to be a good key for Icacinaceae's phylogeny. However, this character is not significant for Icacinaceae's placement in the Lamiid clade. The ornamentation of the Icacinaceae pollen is generally echinate but the clade II is composed of species with reticulate pollen. Little is known about the pollination of Icacinaceae but insects seem to be important pollinators for this family. For example, *Icacina oliviformis* is pollinated by Hymenoptera (Fay, 1993), *Nothapodytes amamianus* by Diptera and Lepidoptera (Nagamasu & Kato, 2004) and *Nothapodytes nimmoniana* by Hymenoptera (incl. five species of ants), Diptera and Lepidoptera (Sharma et al., 2011).

Among all characters, the fruit of the Icacinaceae seems to be the most significant character-bearing organ for the recognition of the family. In all the species of Icacinaceae, the fruit is a drupe containing two anatropous and pendulous ovules, among which, only one becomes mature. The fruit is mostly bisymmetrical and asymmetrical at the apex. Despite this unity of characters, the fruit of the Icacinaceae family is highly variable in shape, size, and endocarp ornamentation. We found smooth, reticulate and/or rugose ornamentation on the surface of the endocarp, with or without pits (Fig. 7). The occurrence of pits, in particular, could be a diagnostic trait for the clade IV (Stull et al., 2015, Fig. 7, C, D).

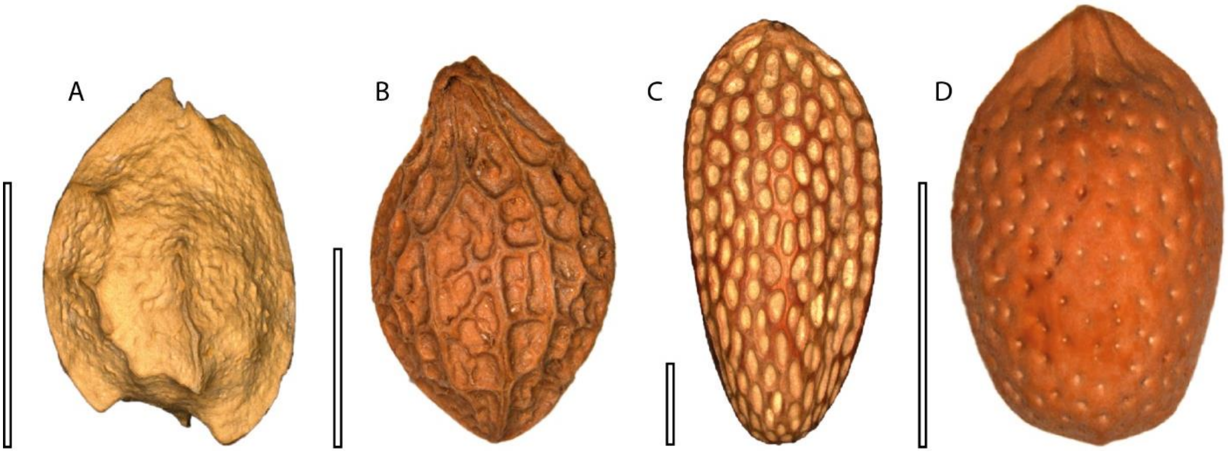

Figure 7. Examples of the diversity within the endocarp ornamentation of the Icacinaceae family. (A) *Iodes cirrhosa* Turcz (P06672331, P); (B) *Rhyticaryum fasciculatum* Becc. (K000271837, K); (C) *Phytocrene oblonga* Wall. (S.N., P); (D) *Pyrenacantha capitata* H. Perrier (P00440639, P). Scale bar: 10 mm.

The pits are generally followed by tubercles inside the locule and penetrate in the seed's tissue (Potgieter & Wyk, 1994). Reticulation pattern formed by ridges (Fig. 7, B) is found in all clade and seems to be an ancestral character for this family. Rugosities are scattered on the endocarp surface of some species such as *Iodes cirrhosa* and some *Icacina* species (Fig. 7, A).

The endocarp wall is composed of sclerotic and digitate cells more or less oriented. We also found a small layer, lining the endocarp locule, occasionally with rounded protuberance from each cell, the papillae (Potgieter & Wyk, 1994).

The fruits are generally red, occasionally green and seem to be dispersed by animals. Indeed, fruits of Icacinaceae are consumed by bats (Kuhlmann & Ribeiro, 2016), birds (Ganesh & Davidar, 2001, Potgieter & Duno, 2016); and mammals: one occurrence of tapirs eating Icacinaceae fruits has been recorded (Bodmer, 1991), some baboons eating fruit from *Icacina oliviformis* (Fay, 1993) and some occurrences from a widespread primate (*Homo sapiens*) that eat and use Icacinaceae fruits and other parts (see ethnobotany part) has been also signalled. One species, *Merriliodendron megacarpum* shows a spongious endocarp, longitudinally grooved and lacunose (Sleumer, 1971). This species seems to be adapted to seawater dispersion as suggested by Sleumer (1971).

Finally, the seed has a minute embryo and a copious endosperm, generally non-ruminate (Corner, 1976).

1.6. Ethnobotany and medicinal use

The Icacinaceae family was traditionally used in different manners and countries. In Africa, the Icacinaceae were intensively used. Roots, leaves, and fruit of *Icacina oliviformis* or false yam, are eaten in numerous countries (Fay, 1987, 1993, Dei et al., 2015, Catarino et al., 2016) and used for cattle feeding in agriculture (Roessler et al., 2017). This species is also used in medicine in order to cure black stains (Cisse et al., 2016) in Senegal. Leaves of *Icacina mannii* and *I. senegalensis* were used to cure malaria respectively in Ivory Coast and Senegal (Sarr et al., 2011, Kipre et al., 2017). Oil extracted from *Icacina trichanta* was used to treat pelvic pain in Nigeria (Okieimen et al., 2018). The leaves of *Alsodeiopsis mannii* were used as herbal tea in order to cure headaches and fever in Cameroon (Jiofack et al., 2010). The roots of *Pyrenacantha staudtii* were put in water and then administrated orally in order to cure ulcers for cattle in Niger (Soladoye et al., 2010, Saganuwan, 2017). In addition, *Lavigeria macrocarpa* has an edible refreshing fruit (MNHN-P-P04494836) and *Iodes africana* was used to cure the gall (MNHN-P-P03951983,). In Asia, the Icacinaceae family was also used as medical plants: in India, the whole plant of *Natsiatum herpeticum* was used to cure headache and influenza (Jain & Dam, 1979, Sarkar et al., 2017) and the whole plant of *Nothapodytes nimmoniana* was used as anti-viral (Prashanth Kumar & Shiddamallayya, 2016); in China, *Iodes vitigenia* was used against injuries (Zheng & Xing, 2009). Finally, we only found one occurrence of plant used in South America: roots of *Leretia cordata* were used as fattening, tonic and against malaria in the Paranapura basin, Peruvian Amazon (Odonne et al., 2013).

The chemical medicine also used Icacinaceae's properties to produce some primordial drugs in current pharmacopoeia. Terpenoid indole alkaloids from *Mappianthus* genus are tested for its anti-canceral potential activity (Jiang et al., 2017, Wei et al., 2018, Zhang et al., 2018). The production of camptothecin, a quinolone indole alkaloid, was used in cancer treatment and can be found in several species on Icacinaceae from *Nothapodytes*, *Icacina* and *Merrilliodendron* genus (Arisawa et al., 1981, Roja and Heble, 1994, Zhou et al., 2000, Lorence and Nessler, 2004, Wu et al., 2008, Ramesha et al., 2013, Soujanya et al., 2017). The antimalarial effect of *Icacina senegalensis* has been tested as well as the therapeutic potential against painful, inflammatory and feverish condition of ethanoic root bark extract (David-Oku et al., 2014, 2015, 2016) with conclusive results. The anti-microbial effect of the extract from *Icacina trichanta* has also been shown (Otun et al., 2015).

1.7. The fossil record

As shown above, the Icacinaceae family interested the botanists, local population and chemical medicine. Additionally, this family is also an interesting work field for the paleobotanists. Indeed, this family possesses an extensive fossil record with a great range of areas and epochs (Fig. 8). This family is commonly found in the major fruit and seed outcrops, mainly during the Eocene epoch (an example of endocarp Fig. 8, A). In North America, the Middle Eocene Nut Bed Flora from Oregon contains about 20 000 specimens and 173 species with eight species (in five genera) belongs to the Icacinaceae family (Manchester, 1994). Extensive works show a wide diversity from the Paleogene fruits of Icacinaceae in North America (Crane et al., 1990, Pigg et al., 2008, Rankin et al., 2008, Stull et al., 2011, 2012, Allen et al., 2015).

The most iconic formation for fruits and seeds remains was the London Clay (Reid & Chandler, 1933). Many sites, from early to middle Eocene age, compose the London Clay. In the introduction of the widest study of the London Clay (Reid & Chandler, 1933), authors precise, that about 120 000 fruits and seeds were collected in the sites. Due to the lignite preservation, almost all specimens were decayed by pyritisation. Among these numerous specimens, 685 fossils were identified as Icacinaceae in six genera with only one modern genus (*Iodes*).

In Germany, the Messel biota from the middle Eocene is rich in fruits and seeds remains. In particular in Icacinaceae endocarps with 156 species which ten belong to the Icacinaceae family. Other studies from the Palaeogene of Europe show a widespread view of the diversity of Icacinaceae during this period (Chandler, 1925, 1961a, 1961b, 1962, Knobloch & Mai, 1986, Fairon-Demaret & Smith, 2002). Other major and minor sites for the Paleogene Icacinaceae family records are known in the Paris basin (see the following section) and are studied in this thesis.

Among all occurrences of Icacinaceae fruit and seed fossils, we also have species from South America (Stull et al., 2012) and North Africa (Chandler, 1954). Finally, a species has also been found in the Middle East, but its belonging to the Icacinaceae is doubtful (Soudry & Gregor, 1997). Leaves (Fig. 8, B), wood and pollen (Fig. 8, C) were also attributed to Icacinaceae

(Shilkina, 1956, Wolfe, 1977, Tanai, 1990, Cavagnetto, 2000, Allen et al., 2015, Del Rio et al., 2017) but in terms of family assignation, these species can be more or less questionable.

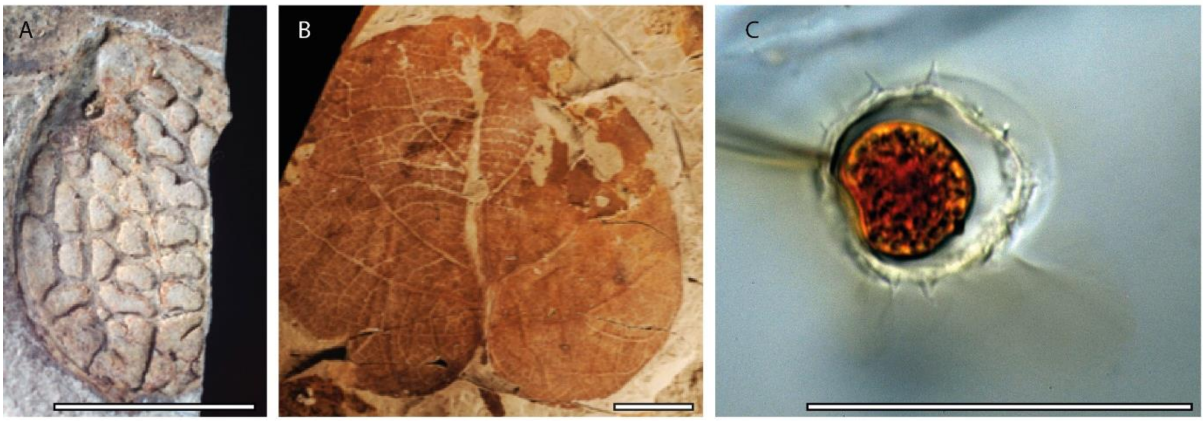

Figure 8. Examples of fossil remains attributed to the Icacinaceae family. (A) *Iodes brownii* (Berry) Stull, Adams, Manchester et Collinson; (B) *Goweria bluerimensis* S.E. Allen, Stull, & Manchester; (C) Pollen of *Icacinanthium tainiaphorum* Del Rio & De Franceschi. A & B modified from Allen et al. 2015, C modified from Del Rio et al. 2017. Scales: A = 5 mm, B = 10 mm, C = 50 µm.

In addition, the Icacinaceae fossil remains were used as a paleoclimatic clue and contribute to the characterization of the Boreotropical forest definition. A forest that occurs during the Eocene (Wolfe, 1975). The Icacinaceae fossils also played an important role in the understanding of the dispersion between Europe and North America during the early-middle Eocene (Manchester, 1994, Stull et al., 2011, Allen et al., 2015).

2. The Paris Basin

2.1. Brief definition and history

The "Bassin de Paris" or "Bassin parisien" (Paris Basin, or Parisian Basin) is one of the greatest French sedimentary basin covering about 110 000 km^2 and with 3000 m of depth (Perrodon & Zabek, 1991). The basin is now delimited by the Ardennes block, the Armorican massif, the Central massif and is on a hercynian base (Perrodon & Zabek, 1991). The Paris Basin is composed of sediments strata in a cup, from the Triassic up to the Pliocene age (about 250 Ma of sediments, Fig. 9). The geology of the Paris Basin was composed of many marines' transgressions and regressions that ended only during the beginning of the Miocene. This is the subsidence mainly during the Mesozoic period, which allows the sediment to be conserved with at least 2900 m of deposited sediments (Gély et al., 2014) in cup. The subsidence decreases during the Cainozoic period with only a deposit of sediment of about 250 m high (Mégnien, 1980a). These sediments were marine, lacustrine or fluviatile. The oldest sediments outcrop on the periphery of the basin, whereas the newest sediments are mostly remaining in the center (Fig. 9). The Paris Basin was not horizontal, since it is folded by a series of synclines and anticlines caused by the Pyrenean-Alpine movement during the Cenozoic period.

The first geological map of the Paris basin was from George Cuvier (1769 – 1832) and Alexandre Brongniart (1770 – 1847), but these authors did not define the Paris Basin (Cuvier and Brongniart, 1811). Jean-Baptiste d'Omalius d'Halloy (1783 – 1875) was the first to describe the "Bassin de Paris" in his work of the section between Guéret and Hirson (Omalius d'Halloy, 1816). Others geological sections were made thereafter and in particular from d'Alcide D'Orbigny (1802 – 1857) who defined stages and nine stratotypes in the Paris Basin. Thus, this basin is considered as the cradle of stratigraphy (De Wever et al., 2002). This is especially Gustave Dolfus who defined the Sparnacian and the Cuisian stratotypes (early and middle Ypresian) always used regionally (Dollfus, 1880). Paul Lemoine was the first in the beginning of the XX^th^ century to propose a view of the Paris Basin in concentric zones, a representation that is still used today (Lemoine, 1911), based on wells. Other studies, based on the Lemoine's work, define more precisely the Paris Basin geological structure and led to the production of a geological synthesis (Mégnien, 1980a). In particular, the AGBP association (Association des Géologues du Bassin de Paris) regularly published new data and studies since 1964 (Gély et al., 2014).

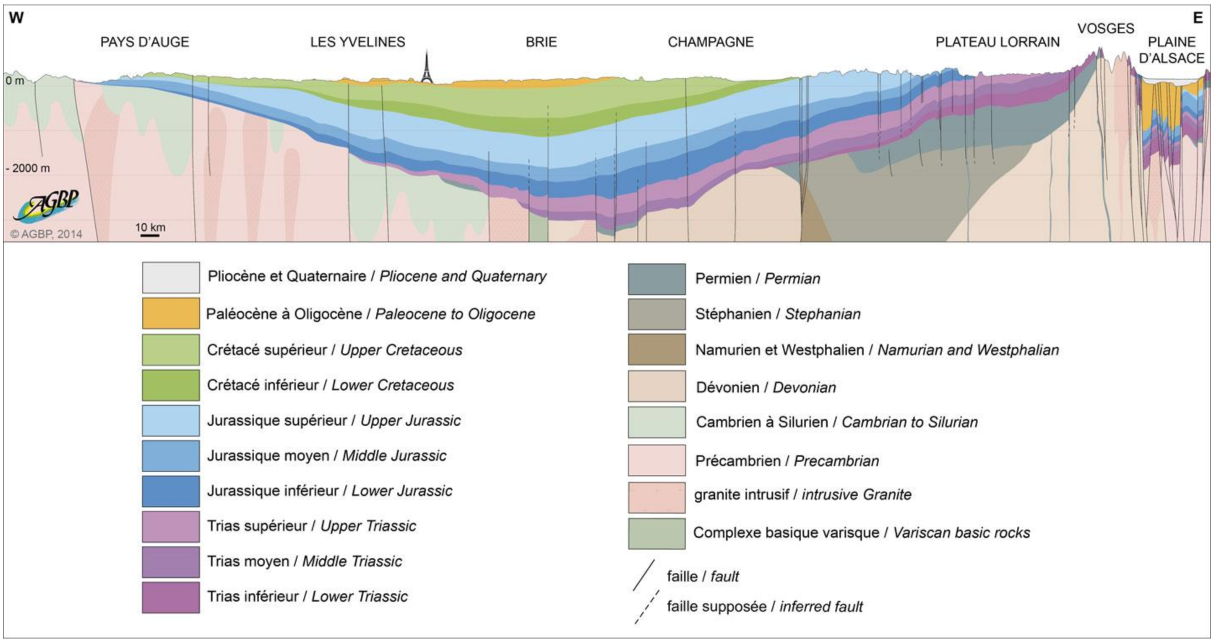

Figure 9. Simplified geological section of the Paris Basin. From AGBP (2014).

2.2. The Paris Basin and the Icacinaceae

Intensive work was made in Palaeogene palaeontology in the Paris Basin (Mégnien, 1980a). Terrestrial faunal remains were studied from several lacustrine or lagoon sites mainly for Eocene age (Louis, 1996; Nel et al., 1999, Smith et al., 2014). Numerous studies have been made in the palynoflora remains of the Paris Basin mainly by two authors, Gruas-Cavagnetto (Cavagnetto, 1967, 2000, Gruas-Cavagnetto, 1967a, 1967b, 1968, 1974, 1976, 1978, 1987, Gruas-Cavagnetto & Bui, 1976, Gruas-Cavagnetto & Cerceau-Larrival, 1982) and Kedves (Kedves, 1967a, 1967b, 1968a, 1968b, 1969, 1970, 1992, 1997, 1998, 1999, Kedves & Pradutz, 1970). Flora macro-rests were also found as in the "Traversins de Sézanne" of Thanetian age, with almost only leaves remains (Saporta, 1868, Mouton, 1970). A preliminary study shows that Icacinaceae macro-rests were found in the Paris Basin in five sites, which are "Grès de Belleu", Prémontré, Passy, Le Quesnoy and Rivecourt (Table 3., Fig. 10). The stratigraphy and biochronology of those sites are well known (Schmidt-Kittler et al., 1987; Aubry et al., 2005) as shown in the Table 3.

In particular, two main sites were recently published with endocarp Icacinaceae illustrations or Icacinaceae identifications, the Rivecourt site (Oise) from the Late Thanetian (Smith et al., 2014) and the Le Quesnoy site (Oise) from the early Ypresian (Nel et al., 1999).

The Rivecourt site (or “Petit Pâtis”) is part of sandy and lignite layers within the upper part of the Bracheux Formation. The sediment indicates that this site corresponds to an ancient fluvial or fluvio-estuarine depositional environment; the sedimentology and lithostratigraphy of this site were previously published in detail (Smith et al., 2014). The site has a rich vertebrate assemblage assimilated to the Clarkforkian North American Age. For the flora diversity, we found abundant wood, other vegetative structures, fruits, and seeds, preserved as lignite or charcoal. The reproductive structure is generally less than 20 mm and with morphological and anatomical details preserved. The preliminary study shows a great diversity of Angiosperm families as Anacardiaceae, Arecaceae, Betulaceae, Icacinaceae, Menispermaceae, Piperaceae and Vitaceae. In particular, we found numerous endocarps attributed to the Icacinaceae family (see Fig. 4, R-S, Smith et al., 2014). Another unpublished study shows three potential Icacinaceae wood species.

TABLE 3. Stratigraphy of the Paris basin, with carpoflora sites with Icacinaceae family in bold and mammal (MP) and pollen (NP) biochronology. Source: Schmidt-Kittler et al. 1987, Aubry et al. 2005

Stage	sub-stage	Paris Basin	MP	NP
Ypresian	**Cuisian**	**Grès de Belleu**, sable de Cuise, argiles de Troenes, **Prémontré**, Saint Agnan	MP10	
		Sables d'Aizy		
		Tuffeau de Mont Notre Dame, sables de Laon, Formation de Varengeville	MP9	NP12
	Sparnacian facies	Grès d'Urcel, de Bruyère-la-comptesse, de Challvoie. Faluns à cyrènes et à huitres		
		Sables de Sincerny, Argilmes de Sarron, Sables de Pourcy		NP11
		Sables d'Auteuil: **Passy**	MP8	
		Argiles à lignites du Soissonais et plastiques de Vaugirard		NP10
		Calcaires de Clairoix, Mortemer, Cap d'Ally, Marnes de Sincerny, Dormans, Chenais (p.p.), Cendrier de Paris, Lamorlaye, Montgiroux, Conglomerat de Meudon, **Le Quesnoy**	MP7	
Thanetian		Sables de Bracheux, **Rivecourt**		NP9
		Traversins de Sézanne	MP6	

The Le Quesnoy site (or Houdancourt, also called "Creil" in some publications) is part of the "*argiles à lignite du Soisonnais*" composed of alternating clayey and sandy layers with amber and lignite. The sediment indicates that this site corresponds to an ancient fluvial depositional environment. The amber is probably originated from a Caesalpiniaceae resin (De Franceschi & De Ploëg, 2003). In this amber, a rich insect fauna was founded (Lacau et al., 2000, Nel et al., 2003, 2004a, 2004b, Menier et al., 2004, Nel & Prokop, 2006, Michez et al., 2007, Brasero et al., 2009, Aria et al., 2011, Nel et al., 2011, Robin et al., 2016) with pollen (De Franceschi et al., 2000, Dejax et al., 2001). In addition, some flowers were also recorded (Nel et al., 1999, Del Rio et al., 2017) and one fruit in amber (Nel et al., 1999). Like for the Rivecourt sites, Le Quesnoy has a rich vertebrate assemblage (Nel et al., 1999, Hervet, 2006, Marandat et al., 2012, Bronnert et al., 2017) and plants with a great diversity of palynoflora (Cavagnetto, 2000), abundant wood, fruits and seeds remains (Nel et al., 1999, Jacques & De Franceschi, 2005). In particular, Icacinaceae, Menispermaceae, and Vitaceae are the most abundant families. Numerous endocarps, pollen and a flower in amber (Cavagnetto, 1967, Del Rio et al., 2017) represent the Icacinaceae family.

Figure 10. Geological map showing the emplacement of the five sites with Icacinaceae remains. Colours: Light grey= Upper Cretaceous, dark grey= Cenozoic. Modified from the synthèse géologique du Bassin de Paris (Mégnien, 1980b).

These two sites have a high diversity and both sites share some taxa as, for example, the Icacinaceae family. In addition, the two sites are geographically separated from less than ten kilometers and are very close in age (Fig. 10). The main difference is that Rivecourt site is before the Paleocene-Eocene thermal maximum (or PETM, see below), whereas the Le Quenoy site is after the PETM. Thus, **these macrorest floras constitute a great opportunity to study the PETM variation in floral elements**.

3. Background for the Paleocene Eocene thermal maximum

3.1. Age and temperature

A global warming at the end of the Paleocene has been highlighted since 1991 (Kennett & Stott, 1991) in view of an abrupt shift in carbon and oxygen isotope ratio (carbon isotope excursion or CIE) and confirmed later, as shown in Fig. 11 (Zachos et al., 2001, 2008). The Paleocene–Eocene boundary, linked with the base of the CIE was defined by the placement of a Global Boundary Stratotype section (GSSP) in the Dababiya section in Egypt (Luterbacher et al., 2000) and was dated of about 56 Ma. The Paleocene-Eocene thermal maximum was an abrupt event in the geological scale. Indeed, the total duration of this event was estimated to about 115–220 ka (Röhl et al., 2007, Aziz et al., 2008, Murphy et al., 2010) but with an onset shorter, corresponding to 8–23 ka (Zachos, 2005, Aziz et al., 2008). Study highlights that the PETM was composed of the release of two pulses of carbon, the first less than 2 000 years (Bowen et al., 2014). During this short event, the marine temperature increases of about 5°C (Kennett & Stott, 1991, Zachos et al., 2001). However, other studies estimate that the temperatures reached up to 8°C in some area and in particular in the USA and the Arctic continent (Sluijs et al., 2006, Zachos et al., 2006, Weijers et al., 2007). In terrestrial remains (mammal’s tooth enamel, leaves, soil), studies estimated that the temperature rose about 5–7°C (Fricke et al., 1998, Koch et al., 2003, Wing et al., 2005, Bowen et al., 2014).

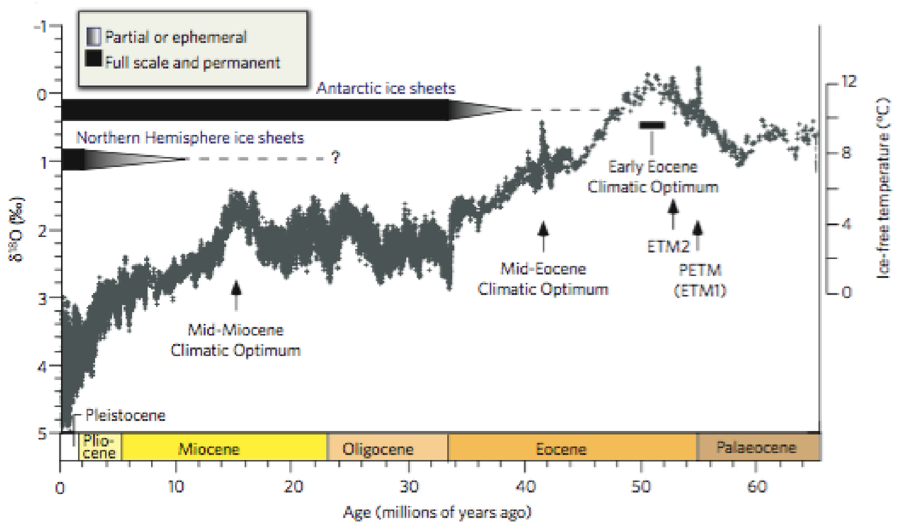

Figure 11. Evolution of atmospheric CO_2 levels and global climate over the past 65 Ma. Modified from Zachos et al., 2008.

3.2. Causes of the PETM

A massive and rapid release of carbon was recorded during the Paleocene-Eocene boundary (McInerney & Wing, 2011, Wright & Schaller, 2013, Bowen et al., 2014) which disturbed the carbon cycle. The initial carbon pulse was estimated with a magnitude of 3 000 Pg (10^5g) C (Zeebe et al., 2009) to about 7 000 Pg C (Panchuk et al., 2008). Sources of the carbon are intensively discussed in the literature. An extra-terrestrial primary cause of perturbation was proposed with arguments in favour of the impact of a comet with about a 10 km circumference (Kent et al., 2003). The recent discovery of silicate glass spherules on the Atlantic margin actualized this theory (Schaller et al., 2016). The volcanism in the North Atlantic Volcanic Province (Svensen et al., 2004, Storey et al., 2007, Rampino, 2013, Gutjahr et al., 2017) could be at the origin of the massive release of carbon in the atmosphere. In particular, a recent study considers that the volcanism could reject in the atmosphere more than 10 000 Pg C, the main release of carbon (Gutjahr et al., 2017), with only one event. The circum-Caribbean explosive volcanism has a sedimentary record close to the PETM and could be at the origin of the reordering of the ocean circulation, which induces the global warming (Bralower et al., 1997). A hypothesis involving the burning of coal and peats was proposed (Kurtz et al., 2003). However, this hypothesis was refuted because there was no increase in combustion shown during the PETM (Moore & Kurtz, 2008).

During the Palaeogene, permafrost could store a vast quantity of carbon in Antarctica, and may be released, increasing the initial warming due to other sources (DeConto et al., 2010). A desiccation of a major epicontinental seaway could be a major source of carbon during the PETM (Higgins & Schrag, 2006). The orbital forcing has also been considered as a potential cause or help for the increase of the temperature (Lourens et al., 2005). In all cases, these hypotheses are not sufficient to explain the increase in temperature. Thus, the initial perturbation (regardless of the source) could be the cause of the destabilization of the methane clathrates, methane contained in solid water (Dickens et al., 1995, 1997, Bowen et al., 2014). This destabilization of methane clathrates may amplify the initial perturbation. There is a debate about the place of the methane clathrates in the PETM, but some authors consider it as the main driver of the global warming (Zeebe et al., 2009, Gehler et al., 2016). Finally, the causes of the PETM are probably complex, multiples and far from being resolved.

3.3. Biological consequences of the PETM

In the marine ecosystems, we record a mass extinction of benthic foraminifera with a loss of 30–50% of the diversity (Thomas, 2007), a rapid turnover of larger foraminifera (Pujalte et al., 2009) and diversification of planktonic foraminifera (Kelly et al., 1998). Ostracods seem to be equally or less touched by environmental changes (Steineck & Thomas, 1996, Webb et al., 2009). Studies show a rapid turnover in Ostracods' diversity associated with the PETM (Speijer & Morsi, 2002, Morsi et al., 2011). Calcerous nanofossils show slight increases or decreases of diversity and nanofossil favoring oligotrophic conditions became most abundant during the PETM (Gibbs et al., 2006, Agnini et al., 2007b, Bown & Pearson, 2009).

In terrestrial ecosystems, the first appraisal of some modern mammal groups as Perissodactyla and Primates at the base of the Eocene was shown, probably due to migrations in Europe and North America of faunas from Asia (Gingerich, 2000, 2003, 2006, Godinot & de Broin, 2003, Smith et al., 2006, 2014, Hooker, 2015). Squamates also show dispersions during the PETM (Godinot & de Broin, 2003, Smith, 2009).

This event caused changes in floral composition (Wing et al., 2005). In particular, palynological studies show changes in the palynoflora with, in general, a more diverse flora (especially Angiosperm) in the Basal Eocene and from little to major changes in composition (Cavagnetto, 2000, Collinson et al., 2009, Jaramillo et al., 2010, Garel et al., 2013, 2014). The cessation of fire and the marked seasonality could explain the change in vegetal composition during the PETM (Collinson et al., 2009, Garel et al., 2013). Little is known about the impact of the PETM on the vegetation from the flora fossil macrorests, or the rate of interaction between leaves and herbivorous insects increased during the PETM (Currano, 2008). A study estimates that during the PETM, the flora changed from a thermophilic evergreen laurophyllous forest to a strongly evergreen thermophilic forest rich in climbers (Collinson & Hooker, 2003). The frequency of untoothed leaf margin increases during the Eocene reveals a warmer flora (Traiser et al., 2018). Therefore, precise studies of macrorest across the PETM are needed to confront the results with palynoflora and to increase the understanding of the floral changes.

4. Problematics of the thesis

This thesis aims to answer the following questions:

(1) What is the impact of the PETM on the Icacinaceae Miers family in the Paris Basin?
(2) What inferences can be made for the changes in the Icacinaceae family during the Palaeogene?

In order to answer these two questions, we undertook the following studies:

In the first part (Chapt. I & II), we establish a referential of modern fruits and endocarp species. We propose a morpho-anatomical approach of modern species in order to compare them with fossils remains. Indeed, this type of studies has never been made at the scale of the Icacinaceae family. We will discuss the diversity of endocarp, especially for the *Iodes* genus, and the value of endocarps in species recognition.

In the second part (Chapt. III-VII), we study the Icacinaceae fossils from the Paris Basin. We first study Icacinaceae from the Paleocene (Rivecourt site). These fossils were primary endocarps with a good morpho-anatomical preservation. An abnormal endocarp specimen in particular attracted our attention. The implication of the anatomy of this specimen was discussed. Three potential Icacinaceae wood from Rivecourt were studied. Finally, a chemical-study was tried on the seed remains due to their peculiar texture and colour. Thereafter, we worked on the Icacinaceae from the Eocene. Le Quesnoy site shows endocarps morpho-anatomically preserved. A flower in amber was found, associated with pollen and attributed to the Icacinaceae family. Next, we studied the other sites of the Paris Basin, which only have endocarps remains. Finally, we discuss the diversity of the Icacinaceae, their affinities (in particular in the light of phylogeny) and the changes through the PETM in the Paris Basin (1).

In the third part (Chapt. VIII, IX), we try to place the Icacinaceae from the Paris Basin in a global perspective. We will discuss the fossil diversity for the Icacinaceae s.s., the paleobiogeography of the family, especially for the *Iodes* genus and we propose an ecological and biogeographical interpretation (2). We highlight the contribution of the Paris Basin fossils in the understanding of the global paleobiogeography of the Icacinaceae. Finally, we use our morpho-anatomical data from modern and fossil species with molecular data together to infer the divergence dating and the biogeographic history of the family. We will discuss on the implication of these analyses in the understanding of changes in the Icacinaceae family during the Palaeogene (2) and the implication of global patterns for understanding the changes occurring in the Paris Basin during the PETM (1).

Chapter I

Fruits and endocarps of extant Icacinaceae

Icacinaceae Miers is a well-described family in numerous floras used as guide in Herbaria or for expedition sampling (Kerr, 1911, De La Bâthie, 1952, Boutique, 1960, Sleumer, 1971, Villiers, 1973, Jansen-Jacobs, 1979, De Roon, 1994, 2003, Peng & Howard, 2008, Duno de Stephano, 2013). The flowers, inflorescences, vegetative parts and the wood anatomy vary and were used for taxonomic classification. Nevertheless, the fruit description is often succinct and the endocarp especially scarcely studied. In botanical literature, precise studies of fruits of Icacinaceae s.s. have been done for *Pyrenacantha* (*P. grandifolia*, *P. scandens* and *P. kaurabassana,* Potgieter & van Wyk, 1994) and *Cassinopsis* (*C. ilicifolia* and *C. tinifolia*, Potgieter & van Wyk, 1993). However, despite the fact that only drupaceous fruits are found in this family, the diversity of shape, anatomy and ornamentation is very important and could be used in the sub-family level classification. Moreover, the fossil record of Icacinaceae is mainly based on endocarp specimens (Reid & Chandler, 1933, Manchester, 1994, Collinson et al., 2012). In Paleobotany, the study of endocarps remains crucial in order to understand past floras and their affinities with extant vegetation. A few paleobotanical studies show extant specimens (Manchester, 1994, Stull et al., 2012), but not in detail.

In this chapter, we described 88 fruits and endocarps of Icacinaceae species (about 56% of the total diversity). The objectives are (1) to provide a survey and produce a reference for this family, (2) to produce a natural key of genera and species for each genus with two and more species and (3) to discuss the diversity and the value of endocarps in species assignment.

I.1. Material and method

I.1.1. Samples and preparation

Endocarps were obtained from fruits that were removed from herbarium sheets. Preliminary tests showed that removing the mesocarp might damage the cellular structure of the outer part of the endocarp. When one specimen represents a species, we conduced the following protocol: fruits were first hydrated in boiling water during 10 minutes. Then, cross sections were made in the fruits using a classical scalpel, before being dried via silica-gel. Samples were then coated with gold-palladium for examination with a Scanning Electron Microscope (SEM, model Jeol JCM6000 instrument), facilitating the observation of anatomical features, especially the endocarp wall layers (called here units) and the locule surface (sometimes with papillae). Then, we re-hydrated the specimens in boiling water during 10 minutes and remove the exocarp and mesocarp using a classical scalpel. Finally, we studied under a binocular microscope (Wild M3Z) and imaged with a Leica DFC 420 camera the endocarp surface. When at least two specimens represent a species, we conduce the anatomical and morphological studies separately using two fruits. The adhesion and hardness of the mesocarp vary considerably among species and genera. For extreme case of hardness (ex. *Rhyticaryum macrocarpum*) the mesocarp was slashed and put back again into boiling water for a few minutes. Measures were taken using the ImagJ Software (Rasband, 2016).

The sampling contains 88 species among the 158 accepted extent species (Appendix 1) of Icacinaceae s.s. We added five Icacinaceae s.l. (now Metteniusaceae) and one Oncothecaceae in order to provide out-groups in our analysis. This sampling comes from many Herbaria, mainly the Muséum national d'Histoire naturelle in Paris (P, acronym following Holmgren et al., 1990) but also from the Royal Botanic Garden Kew (K), the Naturalis Biodiversity Center (L, U, WAG), the Botanic Garden Meise (BR), Kunming Institute of Botany (KUN) and the Missouri Botanical Garden (MO). The voucher information (country, date and identity of the herbarium) can be found at the end of each species' descriptions. The specimen(s) used for the endocarp and fruit descriptions are in italic, whereas the specimens used only for the fruit description are in normal font. Only one or two specimens represent each of these species. However, we consider these specimens as a good source of information concerning the diversity in anatomy and morphology. Furthermore, some species were described in flora only from a few herbarium sheets and thus the descriptions presented here are in a certain point similar to other floral studies.

The sampling covers almost all the geographic areas, Africa (39/54 species), Asia (32/60), Madagascar (12/18), but is weaker in South American (5/20) species. In term of genera representation, the sample lacks of three monospecific genera (*Merrilliodendron*, *Natsiatopsis* and *Sleumeria*) and *Casimirella,* which contains seven species. This last genus is from South America and explains mostly the lack of sample for this area.

I.1.2. Elements of description

We adopted classical elements of description following previous literature, especially for the orientation of the fruit as well as in other groups (Jacques, 2009b). The endocarps are oriented along two axes, Apical-Basal and Dorsal-Ventral (Fig. I.1). The primary vascular bundle runs on/in or above the dorsal part of the endocarp. Overall, we observe two basic types of endocarps in Icacinaceae family: the ridged (Fig. I.1, A) and pitted (Fig. I.1, B) form. In the ridged form, vertical ridges form a diffuse pattern, but often additional horizontal ridges span vertical ridges creating a reticulate pattern of areoles. On these areoles, free-ending ridges and simple or in arbuscular shape (in reference of arbuscle of mychorization) are occasionally found. In the pitted form, circular to elongate pits are more or less randomly or longitudinally arranged. Small ridges are also found at the apical part but also diffuse ridges in some species. The diameter and number of pits varies between species, as they are associated with tubercles, protruding more or less into the locule cavity.

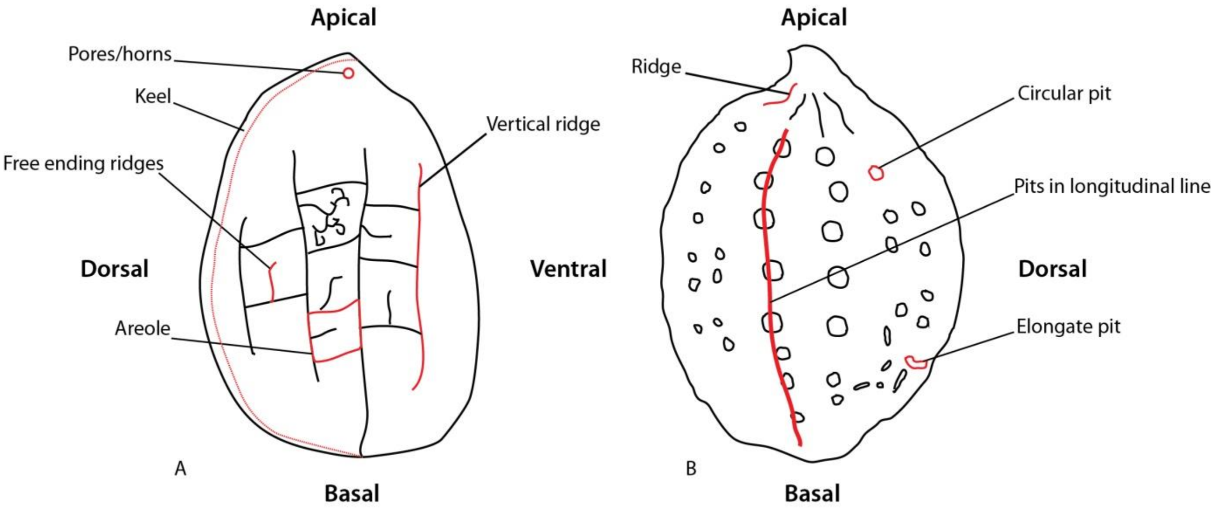

Figure I.1. General ornamentation of Icacinaceae endocarps. Endocarp ridged (A); endocarp pitted (B).

For the tubercle shape, we partially followed the nomenclature developed by G.W. Stull (Stull et al., 2012), but we adapted the descriptions for this new survey (Fig. I.2, A–G). We defined two main categories—first tubercles protruding into the endocarp locule (Fig. I.2, A–E) and second tubercles, which are not protruding into the endocarp locule (Fig. I.2, F–G). For the first category, we defined five forms. All considerations are made in transverse section of the fruit. The conical shape (Fig. I.2, A) is defined as a tubercle wider than long, composed of short sclerotic cells. The elongate-flattened shape (Fig. I.2, B) corresponds to a tubercle longer than wide and vertically flattened like a blade with more or less short sclerotic cells. The peg-shaped tubercles (Fig. I.2, C) have parallel sides with a truncated apex, more or less flattened, with elongated cells. The cylindrical tubercles (Fig. I.2, D) are the largest form, often longer than 2 mm and wider than other forms, composed of numerous elongate cells forming a cylindrical structure, with a capitate apex (or at least inflated apex). The spiny tubercles (Fig. I.2, E) are the most commonly found tubercle type and corresponds to spiny like shape with elongate cells and an acute apex. The not-protruding category divided in two clear types one, the areole-shaped pit (Fig. I.2, F), a polygonal cavity delimited by the wall and the spiny-like pit (Fig. I.2, G), a thin cavity with an acute apex.

The shape of Icacinaceae hairs was previously discussed for the pistil, corolla, filaments and endocarp locule (Heintzelman & Howard, 1948), but not for the epicarp. We follow partially the former nomenclature, but we added some other shapes, which are described for the first time for the Icacinaceae fruits. The papillae-like shape (Fig. I.2, H) corresponds to small structures on the epicarp comparable to the papillae on the locule of some endocarp as in the *Iodes* species. The small ovoid hairs with an acuminate apex (Fig. I.2, I) are the thickest hair type. The apex of the uncinate hairs (Fig. I.2, J) forms a hook. The simple hairs with granular ornamentation (Fig. I.2, K) is the most common shape on the epicarp of Icacinaceae. Finally, the long and thin hairs (Fig. I.2, L) are visible with the naked eye and form a pilose indumentum. Occasionally, the long and thin hairs are associated with small and thin hairs at the base, forming what we call a cluster of hairs (not drawn here, in the Fig. I.2).

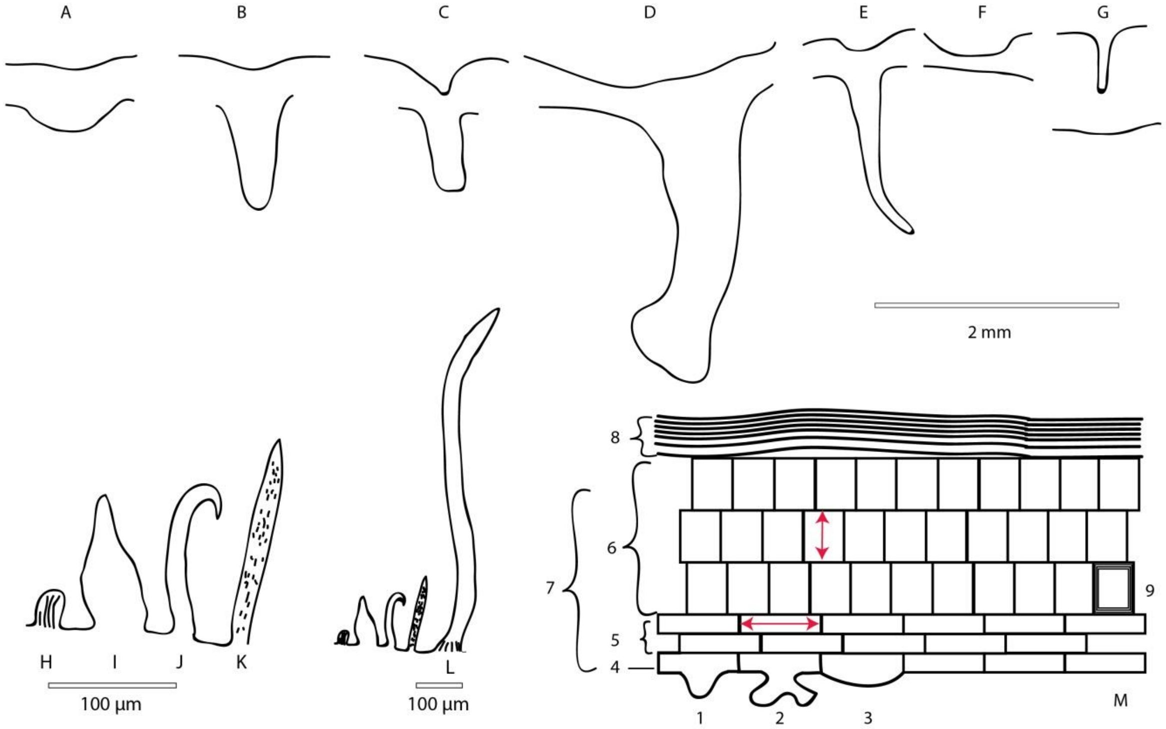

Figure I.2. Tubercle shapes in transverse section (A–G), conical (A), elongate-flattened shape (B), peg-shaped (C), cylindrical (D), spiny (E), areole-like pit (F) and spiny pit (G); hairs shape (H–L), papillae like (H), small ovoid hairs with an acuminate apex (I), uncinate hairs (J), simple hairs with granular ornamentation (K), long and thin hairs (L); endocarp wall anatomy (M), rounded papillae (1), large papillae (2), inflated cell (3), periclinally oriented cells lining the locule (4), periclinally oriented cells (5), anticlinally oriented cells (6), endocarp wall (7), mesocarp wall (8), multi-layered wall (9).

The endocarp wall's structure is relatively constant across all Icacinaceae fruits (Fig. I.2, M). The cell walls are sclerotic and digitate in shape. The basal rows of the wall seem to be globally comprised periclinally oriented cells (Fig. I.2, M 5), with the innermost, lining the locule surface, composed of cells with thinner walls. This inner row could either exhibits rounded to large papillae (Fig. I.2, M 1, 2), or just inflated cells (Fig. I.2, M 3). Differences between papillae and inflated cells are occasionally difficult to distinguish. To describe these rows, we occasionally added anticlinally oriented and/or isodiametrical cell rows (Fig. I.2, M 6) which were relatively easy to distinguish. We often observed a row between the mesocarp and the endocarp with small anticlinally oriented or isodiametrical cells, which is difficult to attribute to the inner part of the mesocarp or the outer part of the endocarp. We guess that this layer is likely part of the endocarp because cells seem to be sclerotic, in contrast with the cells of the mesocarp (Fig. I.2, M 8). The cell wall could be simple or composed of secondary wall; we named this structure multi-layered secondary wall (Fig. I.2, M 9).

An Xper^3 key, developed in the Chapter II, could help the understanding of this survey and bring some further informations about this work.

I.2. Fruit description of Icacinaceae s.s.

Icacinaceae Miers

Plates I–XXIX

<u>Fruit</u> drupe elliptical to globular, asymmetrical at the apex, occasionally accrescent, laterally compressed, mainly red-black when mature, glabrous, strigose, pubescent or pilose with a wide diversity of hairs, mainly simple hairs with granular ornamentation but also papillae like expansion, small ovoid hairs with an acuminate apex, long and thin hairs and uncinate hairs. Calyx mainly persistent occasionally separated from the fruit by a gynophore.

<u>Endocarp</u> cream to brown in color, bilaterally symmetrical, unilocular, single-seeded, elliptical to globular, lenticular to globular in transverse section. A keel often surrounds the endocarp in the plane of symmetry, occasionally faintly apparent or with a channel. Apex, acute to flattened, asymmetrical or slightly asymmetrical, base symmetrical or cleft in one side, rounded to acute. Outer part of the endocarp smooth, rugose, ridged and/or pitted, scarcely hairy. Endocarp primary vascular strand outside the endocarp wall or in a channel on the keel or inside the wall. Endocarp wall composed of packed interlocking digitate and sclerotic cells with different units, occasionally homogeneous. Locule with tubercles or without protuberances, mainly lacunose. Locule surface smooth, papillate or with inflated cells, occasionally hairy.

Key of genera

1	Wall with homogeneous isodiametric cells	*Cassinopsis*
+	Wall divided into distinct layers/units or not only isodiametric	2
2	Presence of hairs on the locule surface	3
+	Absence of hairs on the locule surface	4
3	Endocarp width about 40 mm, endocarp wall more than 700 µm	*Lavigeria*
+	Endocarp width about 13 mm, endocarp wall less than 400 µm	*Leretia*
4	Locule surface with papillae expansions	5
+	Locule surface without papillae expansions	6
5	Surface of endocarp pitted	7
+	Surface of endocarp non-pitted	8
6	Presence of hairs on the endocarp surface	*Pleurisanthes*
+	Absence of hairs on the endocarp surface	9
7	Tubercles conical	*Miquelia*
+	Tubercles spiny, cylindrical, peg-shaped or elongate	*Pyrenacantha*
8	Endocarp primary vascular strand inside endocarp wall	*Iodes*
+	Endocarp primary vascular strand outside endocarp wall or in a channel	10
9	Surface of endocarp pitted	11
+	Surface of endocarp non-pitted	12
10	Endocarp completely smooths	*Iodes*
+	Endocarp ridged or rugose, irregular	13
11	Pits forming shallow mounds not protruding inside the locule	*Phytocrene*
+	Pits forming tubercles protruding inside the locule	14
12	Endocarp thickness > 12 mm	*Icacina*
+	Endocarp thickness < 10.2 mm	15
13	Endocarp length about 12 mm	*Hosiea*
+	Endocarp length > 15 mm	16
14	Tubercles conical	*Stachyanthus*
+	Tubercles spiny, cylindrical, peg-shaped or elongate	*Pyrenacantha*
15	Endocarp ridged and reticulates	17
+	Endocarp rugose, irregular	18
16	Endocarp almost smooth, irregularly rugose but without clear protuberant structures	*Sarcostigm*a
+	Endocarp rugose with clear protuberant structures or ridged	19

17	Endocarp oblong	*Alsodeiopsis*
+	Endocarp elliptical	20
18	Presence of ornamentation bulge or horns on the apex	21
+	No ornamentation on the apex	*Mappia*
19	Endocarp rugose, irregular	*Mappianthus*
+	Endocarp ridged with a reticular or diffuse ornamentation	*Rhyticaryum*
20	Endocarp length 9 mm, 4–5 areoles formed by ridges on each face	*Natsiatum*
+	Endocarp length > 11 mm, 20–30 areoles formed by ridges on each face	*Desmostachys*
21	Presence of horn-like protrusions sub-apically	*Desmostachys*
22	Presence of bulge at the apex	23
23	Ornamentation with mounds, occur in Madagascar	*Desmostachys*
+	Ornamentation more granular, occur in Asia	*Nothapodytes*

***Alsodeiopsis* Oliv. in Benth.**

Plate I, Plate II. 1–9

Fruit drupe oblong to slightly elliptical, asymmetrical, laterally compressed, red when mature, epicarp strigose, with simple type of yellow hairs with granular ornamentation, more or less reticulate when dry. Calyx persistent.

Endocarp cream to brown in color, bilaterally symmetrical, unilocular, single-seeded, oblong in lateral view, lenticular in transverse section. A keel surrounds the endocarp in the plane of symmetry. Apex with a central pit, asymmetrical in lateral view, base rounded and symmetrical. Outer part of the endocarp ridged, delimiting a reticulate pattern of thin rounded to angular ridges. The ridges delimit irregular small to much extended areoles with simple freely ending ridgelets or in arbuscles. Vasculature on endocarp surface follows the reticulum. Endocarp primary vascular strand outside the endocarp wall or in a channel on the keel. Endocarp wall composed of packed interlocking digitate and sclerotic cells with globally two or three stratified units at least a row with a periclinally orientation cells; Locule surface smooth, often clearly lacunate.

Key of species

1	Endocarp brown with large ridges	*Alsodeiopsis manii*
+	Endocarp cream with thin ridges	2

2 Endocarp primary vascular strand outside the endocarp wall, base rounded *Alsodeiopsis staudtii*
\+ Endocarp primary vascular strand in a channel on the keel, base more flattened 3
3 Endocarp 13 mm length, endocarp wall 180–232 µm thick *Alsodeiopsis poggei*
\+ Endocarp 16 mm length, endocarp wall 256–302 µm thick *Alsodeiopsis zenkeri*

Alsodeiopsis mannii **Oliv.**

Plate I. 1–9

<u>Fruit</u> drupe oblong, asymmetrical at the apex, laterally compressed, red when mature, epicarp strigose, with simple yellow hairs with granular ornamentation, reticulate when dry, mesocarp about 200–250 µm thick when dry. Length 10–40 mm, width 8–15 mm, thickness 5–8 mm.

<u>Endocarp</u> brown in color, bilaterally symmetrical, unilocular, single-seeded, oblong in lateral view, lenticular in transverse section, length 19.2 mm, width 7.7 mm, thickness 6 mm. A keel surrounds the endocarp in the plane of symmetry. Apex slightly asymmetrical in lateral view, with a central pit in apical view, base rounded and symmetrical. Outer part of the endocarp ridged with 4–6 main ridges longitudinally with two of them reaching the point of the base on each face. Ridges rounded and large, delimiting a reticulate pattern, faintly apparent, enclosing about 40 small areoles, with simple free-ending ridges. Endocarp wall 120–136 µm thick excluding ridges (163–185 µm thick including ridges). Vasculature on endocarp surface resting on ridges and endocarp primary vascular strand outside the endocarp wall. Endocarp wall composed of packed interlocking digitate and sclerotic cells with globally three stratified cell units: the outermost is composed of 2–3 rows of isodiametrical to periclinally oriented cells, cells 12.7–21.7 µm in width, with a simple cell wall, followed by a unit of 6–7 rows of periclinally oriented cells, cells 8–19 µm in width, with a 5–6-layered secondary wall. The innermost row contains small, periclinally oriented cells, about 6.7 µm in width, with a uni-layered cell wall. Locule surface smooth.

<u>Studied specimen</u> *N. Hallé & J. F. Villiers 4579, Gabon, 1968, MNHN-P-P04504542; N. Hallé 1269, Gabon, 1961, MNHN-P-P04504541;* A. Gentry 33411, Gabon, 1981, MNHN-P-P04495966; F.J. Breteler 15615, Gabon, 2000, MNHN-P-P01068095; N. Hallé 2442, Gabon, 1963, MNHN-P-P04504543.

Alsodeiopsis poggei **Engl.**

Plate I. 10–18

<u>Fruit</u> drupe oblong, asymmetrical at the apex, laterally compressed, red when mature, epicarp strigose with simple yellow to white hairs with granular ornamentation, smooth when dry.

Mesocarp about 75 µm thick when dry. Calyx persistent. Length 10–19 mm, width 5–10 mm, thickness 4.0–5.1 mm.

Endocarp cream in color, bilaterally symmetrical, unilocular, single-seeded, oblong in lateral view, lenticular in transverse section, length 13.1 mm, width 6.9 mm, thickness 4.5 mm. A keel surrounds the endocarp in the plane of symmetry. Apex asymmetrical in lateral view, with a central pit in apical view, base rounded, almost flattened and symmetrical. Outer part of the endocarp ridged with about three main longitudinal ridges (with other small longitudinal ridges), the median ridge reaching the point of the base. Ridges rounded-angular and thin, delimiting a reticulate pattern, enclosing about 20–60 small areoles with free-ending ridges in an arbuscle shape inside. Endocarp wall 135–156 µm thick excluding ridges (180–232 µm thick including ridges). Vasculature on endocarp surface resting on ridges and endocarp primary vascular strand in a channel on the keel. Endocarp wall composed of packed interlocking digitate and sclerotic cells with globally three unicellular and a multicellular units: the outermost unit is composed of 1–2 rows of isodiametrical to periclinally oriented cells, cells 12.3–24.1 µm in width and with a simple cell wall, followed by a unit with 8–12 rows of periclinally oriented cells, cells 9–23 µm in width and with a multi-layered secondary wall. The innermost row contains small periclinally oriented cells, about 9 µm in width and with a simple cell wall, inflated into the locule surface.

Studied specimen *P. Sita 1872, Congo, 1969, MNHN-P-P04495916* ; A. Hladik 1859, s.p., 1971 MNHN-P-P04495893; M. Ekitiké 48, Cameroon, 1986, MNHN-P-P04495907; R. Letouzey 4485, Cameroon, 1962, MNHN-P-P04495897; C. Farron 4577, Congo, 1965, MNHN-P-P04495914.

***Alsodeiopsis staudtii* Engl.**

Plate I. 19–27

Fruit drupe oblong, asymmetrical at the apex, laterally compressed, red when mature, epicarp strigose with simple yellow hairs with granular ornamentation, reticulate when dry, mesocarp about 300–400 µm thick when dry. Calyx persistent. Length 10–22 mm, width 5–15 mm, thickness 5.6–7.0 mm.

Endocarp cream in color, bilaterally symmetrical, unilocular, single-seeded, oblong in lateral view, lenticular in transverse section, length 18.9 mm, width 7.1 mm, thickness 3.5 mm. A keel surrounds the endocarp in the plane of symmetry. Apex asymmetrical in lateral view, with a central pit in the apical view, base rounded and symmetrical. Outer part of the endocarp ridged with about 2–3 main longitudinal ridges, very branched, which the median ridge reaching the point of the base. Ridges slightly angular and thin, delimiting a reticulate pattern with a random global aspect, enclosing about 40–45 irregular areoles with free-ending ridges in an arbuscle shape inside. Endocarp wall 151–295 µm thick excluding ridges (256–302 µm thick including ridges). Vasculature on endocarp surface resting on ridges and endocarp primary vascular strand outside endocarp wall. Endocarp wall composed of packed interlocking digitate and sclerotic cells with globally periclinally orientation, about 14 cell rows, 13–20 µm in width. Locule surface smooth.

Studied specimen *J.J.F.E. de Wilde 8304, Cameroon, s.d., BR000002146852 (Br)*; *H. Jacques-Felix 9190, Cameroon, 1967, MNHN-P-P04495847;* J.J. Bos 4276, Cameroon, 1969, MNHN-P-P05036812 ; D. Kenfack 1073, Cameroon, 1998, MNHN-P-P05036862 ; M.A. Mwangoka & C. Kayombo 101, Tanzania, 1998, MNHN-P-P05036843; J. J. F. E. de Wilde 8304, Cameroon, 1975, MNHN-P-P04534452.

***Alsodeiopsis zenkeri* Engl.**

Plate II. 1–9

Fruit drupe oblong, asymmetrical at the apex, laterally compressed, red when mature, epicarp strigose with simple yellow hairs with granular ornamentation, reticulate when dry. Mesocarp about 70–80 µm thick when dry. Calyx persistent. Length 12.0–17.3 mm, width 5–8 mm, thickness 2.0–5.9 mm.

Endocarp cream in color, bilaterally symmetrical, unilocular, single-seeded, oblong in lateral view, lenticular in transverse section, length 16 mm, width 7.2 mm, thickness 4.4 mm. A keel surrounds the endocarp in the plane of symmetry. Apex asymmetrical in lateral view, with a central pit in the apical view, base flattened and slightly asymmetrical. Outer part of the endocarp ridged with about three main longitudinal ridges which the median ridge and the lateral ridge, in the opposite side of the apical asymmetry, reaching the point of the base. Ridges slightly angular and thin, delimiting a reticulate pattern, enclosing about 50–60 polygonal areoles with free-ending ridges inside, more or less in an arbuscle shape. Endocarp wall 102–157 µm thick excluding ridges (about 186 µm thick including ridges.) Vasculature on endocarp surface resting on ridges and endocarp primary vascular strand in a channel on the keel. Endocarp wall composed of packed interlocking digitate and sclerotic cells with globally two unicellular and a multicellular unit; the outermost rows are composed of 10–11 periclinally oriented cells, cells 9–15 µm in width and with multilayered secondary wall. The innermost cell row contains small periclinally oriented cells, cells about 8–9 µm in width, inflated in the locule surface.

Studied specimen *W.J.J. O. de Wilde 1549, Cameroon, 1963, MNHN-P-P04495824*; W. J. J. O. de Wilde 1549, Cameroon, 1963, MNHN-P-P04495824; W. J. J. O. de Wilde 2662b, Cameroon, 1964, MNHN-P-P04495825.

***Cassinopsis* Sond.**

Plate II. 10–26, Plate III. 1–9

Fruit drupe globular to elliptical, asymmetrical, occasionally laterally compressed, brown-black when mature, epicarp glabrous. Calyx persistent.

Endocarp cream to brown in color, bilaterally symmetrical, unilocular, single-seeded, elliptical to globular in lateral view, lenticular to globular in transverse section. A keel surrounds the endocarp in the plane of symmetry. Apex asymmetrical in lateral view, base symmetrical. Outer part of the endocarp ridged with thin to large rounded and diffuse ridges (i.e., not reticulate) sometimes erased. Vasculature on endocarp surface follows the reticulum of ridges or in a channel. Endocarp primary vascular strand outside or inside the endocarp wall. Endocarp wall thick. Endocarp wall composed of packed interlocking digitate and sclerotic cells, homogeneous, without preferential orientations of cells. Locule surface smooth, occasionally lacunate or with a cluster of hairs.

Key of species

1 Endocarp 6 mm length with the endocarp primary vascular strand inside the endocarp wall *Cassinopsis madagascariensis*

\+ Endocarp > 6 mm length with the endocarp primary vascular strand outside the endocarp wall 2

2 Endocarp globular, surface smooth *Cassinopsis ilicifolia*

\+ Endocarp elliptical, surface clearly ridged *Cassinopsis ciliata*

***Cassinopsis ciliata* Baker**

Plate II. 10–18

Fruit drupe elliptical, apex acute, brown when mature, epicarp glabrous, smooth when dry. Mesocarp 200–400 μm thick when dry. Calyx persistent. Length 13–23 mm, width 5–7 mm, thickness 8.0–9.4 mm.

Endocarp brown in color, compressed in the dorso-ventral axis, bilaterally symmetrical, unilocular, single-seeded, elliptical in lateral view, lenticular in transverse section, length 12.9 mm, width 6.5 mm, thickness 8.8 mm. A keel surrounds the endocarp in the plane of symmetry. Apex acute, asymmetrical in lateral view, base rounded and symmetrical. Outer part of the endocarp ridged with about three main longitudinal ridges which the median ridge, thicker than other ridges, reaching the point of the base up to the apex. Ridges thin and rounded, forming a diffuse pattern of small and interconnected ridges from the main ridge, which are more or less alternate in the length. Endocarp wall 544–761 μm excluding ridges (744–940 μm thick including ridges). Vasculature on the endocarp surface resting on ridges and endocarp primary vascular strand outside the endocarp wall. Endocarp wall composed of packed interlocking digitate and sclerotic cells with about 20 isodiametrical cells quite homogeneous with only differences in size between the 13–17 outermost cell rows with 45–60 μm in diameter and the 5–7 innermost cell rows, cells 20–35 μm in diameter, all with 6–7 layered secondary cell wall. Locule surface smooth and lacunose.

Studied specimen *H. Perrier De La Bathie 4671, Madagascar, 1932, MNHN-P-P00441031.*

Cassinopsis ilicifolia **(Hochst.) Sleumer**

Plate II. 19–25

Fruit drupe globular, asymmetrical at the apex, laterally compressed, brown when mature, epicarp glabrous with traces left by the vasculature. Mesocarp 210–272 μm thick when dry. Calyx persistent. Length 9.5 mm, width 8.6 mm, thickness 5.2 mm.

Endocarp cream in color, bilaterally symmetrical, unilocular, single-seeded, globular in lateral view, lenticular in transverse section, length 7.6–8.7 mm, width 7.8 mm, thickness 4.4 mm. A keel surrounds the endocarp in the plane of symmetry. Apex asymmetrical in lateral view, base rounded and asymmetrical. Outer part of the endocarp globally smooth with only minute channels. Endocarp wall 600–640 μm thick. Vasculature on endocarp surface resting on the channels and endocarp primary vascular strand outside the endocarp wall. Endocarp wall composed of packed interlocking digitate and sclerotic cells with about 24 rows of isodiametrical oriented cells quite homogeneous, 25–55 μm in diameter, cells with 7–8 layered secondary wall. Locule surface smooth, not lacunose.

Studied specimen *C.D. Louwsburg 2730, Natal, 1969, WAG1462859 (WAG)*; R. J. Rodin 3952, South Africa, 1948, MNHN-P-P05193345.

Cassinopsis madagascariensis **Baill.**

Plate III. 1–9

Fruit drupe elliptical, asymmetrical at the apex, brown when mature, epicarp glabrous, ridged when dry. Mesocarp about 100 μm thick when dry. Calyx persitent. Length 5–8 mm, width 3.5–5.0 mm, thickness 3.0–4.8 mm.

Endocarp cream in color, bilaterally symmetrical, unilocular, single-seeded, elliptical to globular in lateral view, globular in transverse section, length 6 mm, width 5 mm, thickness 4 mm. A keel surrounds the endocarp in the plane of symmetry. Apex slightly flattened, asymmetrical in lateral view, base rounded and symmetrical. Outer part of the endocarp ridged with about 5–6 main longitudinal ridges which the median and two lateral ridges reaching the point of the base. Ridges thin and rounded, forming a diffuse pattern, interconnected from the main ridges alternate in the length. Endocarp wall 520–750 µm thick excluding ridges (660–980 µm thick including ridges). Vasculature on endocarp surface resting on ridges and endocarp primary vascular strand inside the endocarp wall in a thicker part of the keel. Endocarp wall composed of packed interlocking digitate and sclerotic cells with about 20 rows of isodiametrical to anticlinally oriented cells quite homogeneous, cells 30–55 µm in width and with a multi-layered cell wall. A row line the locule surface with inflated cells, 15–18 µm in width, with a simple cell wall. Locule surface with a cluster of 3–6 simple and wide hairs, not lacunose.

Studied specimen *P. P. Lowry et al. 5162, Madagascar, 1999, MNHN-P-P00724815.*

Desmostachys **Planch. ex Miers**

Plate III. 10–25, Plate IV. 1–18

Fruit drupe elliptical, laterally compressed, red when mature, epicarp strigose to pubescent composed of simple yellow hairs with granular ornamentation, smooth to reticulate when dry. Calyx persistent.

Endocarp cream to brown in color, bilaterally symmetrical, unilocular, single-seeded, elliptical in lateral view, lenticular to globular in transverse section. A keel often surrounds the endocarp in the plane of symmetry, occasionally not visible. Apex more or less asymmetrical in lateral view, base symmetrical. Outer part of the endocarp rugose or ridged with diffuse or reticulate pattern of sharp to angular ridges. When reticulate, the ridges delimit polygonal areoles with or without free-ending ridges. Endocarp often possessing a symmetrical pair of horn-like protrusions compressed on the keel, positioned eccentrically and subapically on the apical endocarp faces each with a central pit, occasionally lost or replaced by an apical bulge. Vasculature on the endocarp surface follows the reticulum of ridges or is found between ridges/mounds. Endocarp primary vascular strand outside the endocarp wall or in a channel on the keel. Endocarp wall composed of packed interlocking digitate and sclerotic cells with at least one row of periclinally oriented cells. Locule surface smooth more or less lacunate.

Key of species

1 Endocarp surface exclusively rugose *Desmostachys planchoniana*

\+ Endocarp surface ridged, occasionally with rugosities 2
2 Endocarp ridged and rugose with a diffuse pattern of ridges *Desmostachys vogelii*
\+ Endocarp exclusively ridged with a reticulate pattern of ridges 3
3 Fruit length about 11 mm, ridges sharp and areoles with free-ending ridges *Desmostachys oblongifolius*
\+ Fruit length about 20–25 mm, ridges angular and areoles without free-ending ridges *Desmostachys tenuifolius*

***Desmostachys oblongifolius* (Engl.) Villiers**

Plate III. 10–16

Fruit drupe elliptical, asymmetrical at the apex, laterally compressed, red when mature, epicarp strigose with yellow simple hairs with granulates ornamentation, reticulate when dry. Mesocarp 50–70 µm thick when dry. Calyx persistent. Length 9–15 mm, width 6.3–10.0 mm, thickness 5.0–6.6 mm.

Endocarp cream in color, bilaterally symmetrical, unilocular, single-seeded, elliptical in lateral view, lenticular to globular in transverse section, length 11.3 mm, width 6.8 mm, thickness 4.5 mm. A keel surrounds the endocarp in the plane of symmetry. Apex slightly asymmetrical, base rounded and slightly asymmetrical. Outer part of the endocarp ridged with about 4-5 main longitudinal ridges which the median and occasionally a lateral ridge reaching the point of the base. Ridges sharp and thin, delimiting a reticulate pattern enclosing 20–25 polygonal areoles with inside free-ending ridges. Endocarp wall 112–154 µm thick excluding ridges (260–330 µm thick including ridges). Vasculature of endocarp resting on ridges and endocarp primary vascular strand outside the endocarp wall. Endocarp wall composed of packed interlocking digitate and sclerotic cells with 9–11 rows of periclinally oriented cells, cells 8–15 µm in width and with a 5–6 layered secondary wall. Locule surface smooth, lacunose.

Studied specimen *R. Letouzey 8309, Cameroon, 1966, MNHN-P-P04495051.*

***Desmostachys planchonianus* Miers**

Plate III. 17–25

Fruit drupe elliptical, asymmetrical at the apex, laterally compressed, red when mature, epicarp strigose with simple yellow hairs with granular ornamentation, rugose when dry. Mesocarp 250–300 µm thick when dry. Calyx persistent. Length 10–16 mm, width 7–12 mm, thickness 5.0–5.8 mm.

Endocarp cream in color, bilaterally symmetrical, unilocular, single-seeded, elliptical in lateral view, lenticular in transverse section, length 11.1 mm, width 7.8 mm, thickness 3.5 mm. Apex asymmetrical with a bulge shape, base rounded, slightly asymmetrical. Outer part of the endocarp rugose, irregular, with 20–25 mounds longitudinally arranged and spaced by 4–5 channels. Small rugosities parse the surface of endocarp. A channel surrounds the endocarp in the plane of symmetry. Vasculature of endocarp on the channel between mounds and endocarp primary vascular strand outside the endocarp wall. Endocarp wall 245–290 µm thick excluding mounds (338–474 µm thick including mounds). Endocarp wall composed of packed interlocking digitate and sclerotic cells with globally two multicellular units: the outermost unit with 7–10 rows of anticlinally oriented cells, cells16–21 µm in width and with a multi-layered secondary wall; the innermost unit with 7–10 rows of periclinally oriented cells, cells 20–27 µm in width and with a multi-layered secondary wall (about 5 layers). Locule surface smooth.

Studied specimen *B. Lewis & S. Razafimandimbison 735, Madagascar, 1993, MNHN-P-P04561640* ; R. Rabevohitra et al. 4810, Madagascar, 2003, MNHN-P-P04561628 ; R. Rabevohitra et al. 4658, Madagascar, 2003, MNHN-P-P04561629; J. Rabenantoandro et al. 1155, Madagascar, 2002, MNHN-P-P04561630.

Desmostachys tenuifolius **Oliv.**

Plate IV. 1–9

Fruit drupe elliptical, asymmetrical at the apex, laterally compressed, red when mature, epicarp strigose with simple yellow hairs with granular ornamentation, smooth when dry. Mesocarp 750–820 µm thick when dry. Calyx persistent. Length 21–25 mm, width 9–15 mm, 5.0–10.2 mm.

Endocarp cream in color, bilaterally symmetrical, unilocular, single-seeded, elliptical in lateral view, lenticular in transverse section, length 18.4 mm, width 9.2 mm, thickness 8.5 mm. A keel surrounds the endocarp in the plane of symmetry. Apex slightly asymmetrical in bulge, base sub-acute, symmetrical. Outer part of the endocarp ridged with 4–6 main longitudinally ridges, the median and a lateral one reaching the point of the base on each face. Ridges, angular and broad almost rectangular, with a median channel clearly visible, delimiting a reticulate pattern enclosing 20–24 polygonal areoles longitudinally elongate. The ridges merge with the bulge at the apex. Vasculature of endocarp in the channel on the ridges and endocarp primary vascular strand in a gutter on the keel. Endocarp wall 180–200 µm thick excluding ridges (320–385 µm thick including ridges). Endocarp wall composed of packed interlocking digitate and sclerotic cells with globally 17 rows of periclinally oriented cells, cells 7–16 µm in width and with a multi-layered secondary wall. Locule surface smooth and lacunose.

Studied specimen *J. J. Bos 4277, Cameroon, 1969, MNHN-P-P04495129.*

Desmostachys vogelii **(Miers) Stapf**

Plate IV. 10 –18

Fruit drupe elliptical, asymmetrical at the apex, red when mature, epicarp pubescent with yellow simple hairs with granular ornamentation, reticulate-rugose when dry. Mesocarp thin. Calyx persistent. Length 14–21.4 mm, width 10.0–11.1 mm, thickness 7.0–11.2 mm.

Endocarp brown in color, bilaterally symmetrical, unilocular, single-seeded, elliptical in lateral view, globular in transverse section, length 19.4 mm, width 10.7 mm, thickness 10 mm. A sharp keel, sinuous and serrated, surrounds the endocarp in the plane of symmetry. Apex acute and asymmetrical, base rounded, slightly asymmetrical. Outer part of the endocarp rugose and ridged. Ridges sharp and diffuse with only a median ridge serrated and reaching the point of the base, then bifurcating at the third of the endocarp length and going upward to the apex. Surface covered by about 70 rugged protuberances evenly distributed and "ridges" which form small vertically and longitudinally elongate mounds. Endocarp possessing a symmetrical pair of horn-like protrusions situated at the merging between the apex and the median ridge each with a central pit. Vasculature free, endocarp primary vascular stand outside the endocarp wall. Endocarp wall 370–477 μm thick excluding ridges (1200–1380 μm including ridges). Endocarp wall composed of packed interlocking digitate and sclerotic cells with globally three stratified cell units: the outermost with 1–2 rows of isodiametric oriented cells, cells about 27–40 μm in diameter and with simple wall; followed by a unit of 15–21 rows of anticlinally oriented cells, cells about 19–24 μm in width and with 4–5 layered secondary wall; the innermost unit with 5–6 rows of periclinally oriented cells, cells about 9–14 μm in width and with a multi-layered secondary wall. Locule surface smooth and lacunose.

Studied specimen *Service forestier 364, Côte d'Ivoire, 1931, MNHN-P-P04495087*; Service forestier 446, Côte d'Ivoire, 1931, MNHN-P-P04495088; W. J. J. O. de Wilde 514, Ivory Coast, 1963, MNHN-P-P04495094; C. C. H. Jongkind 4975, Ivory Coast, 2000, WAG.1463136 (WAG).

Hosiea **Hemsl. & E.H. Wilson**

Plate IV. 19–25, Plate V. 1–9

Fruit drupe elliptical, slightly asymmetrical at the apex; laterally highly compressed, red-brown when mature, epicarp glabrous. Calyx persistent.

Endocarp cream in color, bilaterally symmetrical, unilocular, single-seeded, elliptical in lateral view, lenticular in transverse section. A small keel surrounds the endocarp in the plane of symmetry. Apex slightly asymmetrical in lateral view, base rounded and symmetrical. Outer part of the endocarp with thin rounded to sharp ridges delimiting a reticulate pattern. Ridges delimit areoles with most having freely ending ridgelets inside. Vasculature of the endocarp free or on ridges and endocarp primary vascular strand outside the endocarp wall. Endocarp wall thin with small expansion corresponding to the ridges, divided into distinctive units, at least one unit with anticlinally oriented cells (outer part) and another with periclinally oriented cells (inner part). Locule surface with regularly spaced and large papillae, irregular in shape. Locule surface lacunate.

Key of species

1	Endocarp ridges sharp	*Hosiea japonica*
+	Endocarp ridges rounded	*Hosiea sinensis*

Hosiea japonica **Makino**

Plate IV 19 –25

Fruit drupe elliptical, laterally highly compressed, red when mature, epicarp glabrous, mesocarp about 200 µm thick when dry.

Endocarp cream in color, bilaterally symmetrical, unilocular, single-seeded, elliptical in lateral view, lenticular in transverse section, length 12.5 mm, width 8.1 mm, thickness 1.5 mm. A small keel surrounds the endocarp in the plane of symmetry. Apex asymmetrical, base rounded symmetrical. Outer part of the endocarp ridged with 2–3 main longitudinal ridges which the median reaching the point of de base. Ridges thin and sharp, delimiting a reticulate pattern enclosing 15–18 irregular areoles, generally with a free-ending ridge inside areoles. Vasculature of the endocarp in the ridges and endocarp primary vascular strand outside the endocarp wall. Endocarp wall 180–235 µm thick excluding ridges (262–302 µm including ridges). Endocarp wall composed of packed interlocking digitate and sclerotic cells with globally three stratified units: the outermost unit with 11–12 rows of anticlinally oriented cells, cells 14–26 µm in width, then a 3–4 rows of periclinally oriented and thick walled cells, cells 11–22 µm in width and with a multi-layered secondary wall; the innermost row is composed of periclinally oriented cells, cells thick, 6 µm in width and with a simple wall, which line the locule with regularly spaced and large to rounded papillae, 12.2–21.0 (avg. 14.6 µm) in diameter. Locule lacunate.

Studied specimen *Okudai 60474*.

Hosiea sinensis **(Oliv.) Hemsl. & E.H. Wilson**

Plate V. 1–9

Fruit drupe elliptical, slightly asymmetrical at the apex, laterally highly compressed, red-brown when mature, epicarp glabrous, reticulate when dry. Mesocarp about 70 µm thick when dry. Calyx persistent. Length 13–18 mm, width 8.1 mm, thickness 3.9 mm.

Endocarp cream in color, bilaterally symmetrical, unilocular, single-seeded, elliptical in lateral view, lenticular in transverse section, length 12.6 mm, width 7.8 mm, thickness 1.1 mm. A small keel surrounds the endocarp in the plane of symmetry. Apex asymmetrical, base rounded and symmetrical. Outer part of the endocarp ridged with 3–4 main longitudinal ridges, the median reaching the point of de base. Ridges thin and rounded delimiting a reticulate pattern enclosing 14–20 areoles, generaly with a free-ending ridge inside areoles. Vasculature of the endocarp free and endocarp primary vascular strand outside the endocarp wall. Endocarp wall 161–202 µm thick excluding ridges (about 250 µm thick including ridges). Endocarp wall composed of packed interlocking digitate and sclerotic cells, with globally three stratified cell units: the outermost ones with 5–10 rows of anticlinally oriented cells, cells 10–13 µm in width, followed by a unit of 5–7 rows of periclinally oriented cells, cells 15–19 µm in width and with a 4–8 layered secondary wall, the innermost unit with a single row of periclinally oriented cells, cells about 6 µm in width and with a simple cell wall, which line the locule with regularly spaced and large papillae, 11–21 µm in diameter, about 1000 papillae by 0.25 mm^2. Locule lacunate.

Studied specimen *M. l'abbé Farges s.n., China, s.d., MNHN-P-P04513501.*

Icacina **A. Juss.**

Plate V. 10–26, Plate VI

Fruit drupe elliptical, occasionally slightly globular, asymmetrical at the apex, red brown to dark when mature, epicarp glabrous or yellowish pubescent with short globular to papillae like hairs, which line the surface and simple hairs with granular ornamentation or only simple hairs but without ornamentation; fruit ridged when dry. Calyx persistent.

Endocarp cream in color, bilaterally symmetrical, unilocular, single-seeded, elliptical in lateral view, globular to lenticular in transverse section. A keel surrounds the endocarp in the plane of symmetry or faintly visible. Apex flat or acute always asymmetrical in the lateral view, base symmetrical. Outer part of the endocarp irregularly rugose or ridged with diffuse or reticular pattern of rounded to sharp ridges. Vasculature follows the ridges or resting between rugosities. Endocarp primary vascular strand outside or inside the endocarp wall. Endocarp wall composed of packed interlocking digitate and sclerotic cells with at least one row with periclinally oriented cells. Locule surface smooth and faintly lacunate.

Key of species

1	Keel surrounding the endocarp clearly visible, rugose ornamentation with numerous mounds	2
+	Keel faintly apparent, ridged ornamentation	3
2	Apex flat, length about 18 mm	*Icacina oliviformis*
+	Apex acute, length about 25 mm	*Icacina mannii*
3	Ridges sharp, delimiting a more or less sparse reticulation	4
+	Ridges rounded, diffuse, some very short	*Icacina guessfeldtii*
4	Ridges up to 430 μm thick, keel faintly apparent without vascular bundle inside	*Icacina claessensii*
+	Ridges up to 730 μm thick, keel thick with a vascular bundle inside	*Icacina trichanta*

***Icacina claessensii* De Wild**

Plate V. 10–17

Fruit drupe elliptical, asymmetrical at the apex, red when mature, epicarp glabrous, ridged with diffuse long arbuscle when dry. Mesocarp 200–250 μm thick. Calyx persistent. Length 24–26 mm, width 18.3 mm, thickness 14.0–17.5 mm.

Endocarp cream in color, bilaterally symmetrical, unilocular, single-seeded, elliptical in lateral view, globular in transverse section, length 23 mm, width 17.6 mm, thickness 17 mm. A keel faintly apparent with a median channel surrounds the endocarp in the plane of symmetry. Apex flattened, asymmetrical, base rounded and slightly asymmetrical at the opposite of the apex asymmetry. Outer part of the endocarp ridged with 3–4 main ridges longitudinally, the median and a lateral ridge reaching the point of the base. Ridges sharp and thin with a median channel, delimiting a partial and sparse reticulation, about 16–17 areoles with some areoles transversally extended to the two third of the endocarp length and others small and randomly positioned, with free-ending ridges, occasionally arbuscle-like. Endocarp possessing a symmetrical pair of pores, positioned eccentrically and subapically at the apical end of the median ridge, each with a central pit. Vasculature of the endocarp on the channel of the ridges and endocarp primary vascular strand outside the endocarp wall. Endocarp wall 240–362 μm thick excluding ridges (400–430 μm including ridges). Endocarp wall composed of packed interlocking digitate and sclerotic cells, with globally two stratified units: the outer ones composed of 3–4 rows of isodiametrical oriented cells, cells 18–28 µm in diameter, and the inner ones with 10–13 rows of periclinally oriented cells, cells 13–21 µm in width and with a multi-layered secondary wall. Locule surface smooth and lacunate.

Studied specimen *C. Evard 5094, Congo, s.d., BR0000015572356 (BR)*; R.P. Klaine 959, Gabon, 1897, MNHN-P-P04495392.

***Icacina guessfeldtii* Asch.**

Plate V. 18–26

Fruit drupe elliptical to obovate, asymmetrical at the apex, red when mature, epicarp glabrous, ridged when dry. Mesocarp 400–600 µm thick when dry. Calyx persistent. Length 21–30 mm, width 15–20 mm, thickness 12.0–19.4 mm.

Endocarp cream in color, bilaterally symmetrical, unilocular, single-seeded, obovate in lateral view, globular in transverse section, length 26.3 mm, width 17 mm, thickness 16.5 mm. A keel surrounds the endocarp wall in the plane of symmetry, with one part flattened containing a vascular bundle embedded in the endocarp wall. Apex flattened, asymmetrical, base acute slightly asymmetrical. Outer part of the endocarp ridged and rugose, with a median ridge reaching the point of the base and running nearly the apex but without reaching it. Two-three laterals irregular and disconnected ridges run in more or less the endocarp length. Ridges rounded with a slight median channel, forming a diffuse pattern, occasionally forming an arbuscle-like branched. A few isolated mounds cover the surface randomly. Endocarp possessing a symmetrical pair of horn-like protrusions compressed on the keel, positioned eccentrically and subapically on the apical endocarp face, each with a central pit. Endocarp wall 263–306 µm thick excluding ridges (470–560 µm including ridges). Vasculature of the endocarp on the channel of the ridges but also free. Endocarp wall composed of packed interlocking digitate and sclerotic cells with about 15 rows of periclinally oriented cells, cells 20–27 µm in width and apparently with simple wall. Locule surface smooth slightly lacunate.

Studied specimen *J. Gillet 2674, Congo, s.d., BR0000015572677 (BR)*; A. Bouquet 28, Congo, 1964, MNHN-P-P04495336.

***Icacina mannii* Oliv.**

Plate VI. 1–9

Fruit drupe elliptical, apex acute and asymmetrical, laterally compressed, brown when mature, epicarp pubescent with two types of hairs, simple hairs with granular ornamentation and small papillae-like hair expansions which line the fruit; faintly rugose when dry. Mesocarp 200–400 µm thick when dry. Calyx persistent. Length 25–35 mm, width 16.5–26.0 mm, thickness 10–17 mm.

Endocarp cream in color, bilaterally symmetrical, unilocular, single-seeded, elliptical in lateral view, lenticular in transverse section, length 25.6 mm, width 16.3 mm, thickness 12 mm. A keel surrounds the endocarp in the plane of symmetry with one part flattened in dorsal view containing a vascular bundle embedded on the endocarp wall, keel bordered by two longitudinal channel. A channel surrounds the ventral part. Apex acute forming a rectangular protuberance, asymmetrical, base rounded-acute and slightly asymmetrical. Outer part of the endocarp rugged with about 90 mounds more or less square polygonal with a free-ending channel inside more or less branched. Mounds organized in 9–12 longitudinal lines separated by 5–6 main longitudinal channels. The main channel on each face reaching pores positioned sub-apically in the apical protuberance. Vasculature of the endocarp in the channels between mounds and branched in the channel's mounds. Endocarp wall 289–372 µm thick excluding mounds (460–544 µm including mounds). Endocarp wall composed of packed interlocking digitate and sclerotic cells, with globally two stratified units: the outermost ones with 8–9 rows of anticlinally oriented to isodiametric cells, cells 22–31 µm in width, the inner unit composed of 5–6 rows of periclinally oriented cells, cells 14–21 µm in width and with a four layered secondary wall. Locule surface smooth, lacunate.

Studied specimen *J. Koechlin 2334, Brazzaville, 1953, MNHN-P-P04495011*; J. Koechlin 633, Brazzavile, 1950, MNHN-P-P04495012; R.P. Klaine 489, Gabon, 1897, MNHN-P-P04495007.

***Icacina oliviformis* (Poir.) J.Raynal**

Plate VI. 10 –18

Fruit drupe elliptical, apex asymmetrical, red-brown when mature, epicarp pubescent with small ovoid hairs with an acuminate apex. Mesocarp 420–620 µm thick when dry. Calyx persistent. Length 17–23 mm, width 13–16 mm, thickness 9–14 mm.

Endocarp cream in color, bilaterally symmetrical, unilocular, single-seeded, elliptical in lateral view, globular in transverse section, length 18 mm, width 13.1 mm, thickness 14 mm. A keel surrounds the endocarp in the plane of symmetry, with one part flattened in dorsal view containing a vascular bundle embedded on the endocarp wall. Keel bordered by two longitudinal channels and an other part with only a channel instead of the keel in ventral view. Apex flat, asymmetrical, base rounded-acute and slightly asymmetrical. Outer part of the endocarp rugose with about 70–80 mounds more or less square polygonal with a free-ending channel inside, more or less branched. Mounds organized in 7–8 longitudinal lines separated by three main longitudinal channels. The main channel on each face reaching a horn-like protrusion positioned sub-apically, with a central pit. Vasculature of the endocarp in the channels between mounds and in the channel's mounds. Endocarp wall 288–307 µm thick excluding mounds (588–661 µm including mounds). Endocarp wall composed of packed interlocking digitate and sclerotic cells with globally two stratified units: the outermost unit with 7–8 rows of anticlinally oriented to isodiametrical cells, cells 24–34 µm in width, the inner unit with 8–9 rows of periclinally oriented cells, cells 16–21 µm in width and with a four-layered secondary wall. Locule surface smooth, lacunate.

Studied specimen *M. Dybowski 698, Congo, 1892, MNHN-P-P04495750*; Peyre de Fabrègues 3610, Central African Republic, 1978, MNHN-P-P04495743; J. Trochain 3367, Senegal, s.d., MNHN-P-P04495790.

Icacina trichantha **Oliv.**

Plate VI. 19–27

Fruit drupe elliptical, asymmetrical at the apex, brown-black when mature, epicarp pubescent, with simple yellow hairs, reticulate when dry. Mesocarp about 300 µm thick when dry. Calyx persistent. Length 30.8–34.0 mm, width 17–24 mm, thickness 12.0–18.7 mm.

Endocarp cream in color, bilaterally symmetrical, unilocular, single-seeded, elliptical in lateral view, globular in transverse section, length 27.4 mm, width 17 mm, thickness 14 mm. A keel surrounds the endocarp in the plane of symmetry, with the thicker margin containing a vascular bundle embedded in the endocarp wall. Apex greatly asymmetrical in lateral view, base rounded, slightly asymmetrical. Outer part of the endocarp ridged with about four main ridges, two lateral ridges reaching the point of the base. Ridge sharp and rectangular with a median channel, delimiting a reticulate pattern mostly developed in the upper half part of the endocarp length and most diffuse in the lower half part. The reticulum enclosed 10–20 irregular, more or less polygonal areoles with free-ending ridges inside. Endocarp possessing a symmetrical pair of horn-like protrusions compressed on the keel, positioned eccentrically and subapically on the apical endocarp faces each with a central pit. Endocarp wall 270–315 µm thick excluding ridges (362–735 µm including ridges). Vasculature of the endocarp resting on the channel of the ridges. Endocarp wall composed of packed interlocking digitate and sclerotic cells with globally three stratified units: the outermost ones with 4–6 rows of anticlinally oriented to isodiametrical cells, cells 19–30 µm in width and with a 5 layered secondary wall , the median unit is composed of 4–8 rows of periclinally oriented cells, cells 20–27 µm in width and more or less with simple secondary wall, the innermost unit contains one row of periclinally oriented cells, which line the locule surface with inflated cells, 8–13 μm in width, with a simple secondary wall. Locule surface smooth, lacunose.

Studied specimen *J. C. Okafor fhi 34969, Nigeria, 1955, MNHN-P-P04495708.*

Iodes **Blume**

Plate VII-X, Plate XI. 1–18

Fruit drupe elliptical, asymmetrical at the apex, occasionally globular, laterally compressed, red to brown when mature, epicarp strigose or pubescent scarcely pilose with simple hairs with granular ornamentation and/or uncinate hairs or long and thin hairs, ridged or rudged-rugose to smooth when dry. Calyx persistent.

Endocarp cream to brown in color, bilaterally symmetrical, unilocular, single-seeded, elliptical, occasionally globular in lateral view, lenticular, occasionally globular in transverse section. A keel often surrounds the endocarp in the plane of symmetry with the thicker margin containing a vascular bundle embedded in the endocarp wall, a gutter containing the vascular bundle occasionally replace the keel. Apex asymmetrical in lateral view, base cleft at the base or symmetrical. Outer part of the endocarp smooth, rugged/rugose and/or ridged with diffuse to reticulate rounded to sharp ridges with or without free-ending ridges. Secondary ridges (i.e. small ridges delimiting a reticulation inside or between primary reticulation/ridges) occasionally present. Endocarp possessing a symmetrical pair of horn-like protrusions compressed on the keel, sometimes much reduced and forming pores, positioned eccentrically and subapically on the apical endocarp faces, each with a central pit, or with a unique central pit at the apex. Vasculature resting on ridges when present, occasionally between ridges or rugosities. Endocarp wall composed of packed interlocking digitate and sclerotic cells with at least one unit with rows of periclinally oriented cells. Locule surface with regularly spaced and rounded papillae. Locule surfaces more or less lacunate.

Key of species

1	Endocarp with pores or horns at the apex	2
+	Endocarp with apical pits or without any aperture	3
2	Endocarp with pores	4
+	Endocarp with horn-like protrusions	5
3	Outer part of the endocarp smooth	*I. seguinii*
+	Outer part of the endocarp ridged	6

4	Endocarp globular in lateral view, less than 12 mm length	*I. perrieri*
+	Endocarp elliptical in lateral view, more than 30 mm length	*I. yatesii*
5	Endocarp base cleft on one side	7
+	Endocarp base symmetrical	8
6	Pattern of ridges diffuse	*I. liberica*
+	Pattern of ridges reticulate	9
7	Pattern of ridges delimiting a few areoles, length of endocarp more than 12.6 mm	*I. ovalis*
+	Pattern of ridges diffuse, length of endocarp less than 12.6 mm	10
8	Endocarp about 32 mm length,	*I. balansae*
+	Endocarp about 15 mm length	*I. scandens*
9	Fruit pilose, endocarp wall 222–245 µm excluding ridges	*I. seretii*
+	Fruit glabrous, strigose or pubescent, endocarp wall less than 200 µm thick excluding ridges	11
10	Rugose ornamentation present in the surface of endocarp, secondary ridges absent	*I. cirrhosa*
+	Rugose ornamentation not present, secondary ridges present	*I. philippiensis*
11	Number of areoles low, about 1 to 3	*I. kamerounensis*
+	Number of areoles high	12
12	Fruit glabrous, endocarp with numerous areoles, ridges faintly distinct and endocarp less than 8 mm length	*I. madagascariensis*
+	Fruit pubescent to strigose, endocarp with max 25 areoles with free-ending ridges, ridges very distinct, and endocarp more than 10 mm length	13
13	Areoles about 13–15 in each face, surface rugose	*I. klaineana*
+	Areoles about 21–25 in each face, surface not rugose	*I. africana*

Iodes africana **Welw. ex Oliv.**

Plate VII. 1–9

<u>Fruit</u> drupe, elliptical, slightly asymmetrical at the apex, laterally compressed, brown when mature, epicarp strigose with simple yellow hairs with granular ornamentation, reticulate when dry. Mesocarp about 300 µm thick when dry. Calyx persistent. Length 11.2–15.0 mm, width 8.4–11.1 mm, thickness about 6 mm.

<u>Endocarp</u> cream in color, bilaterally symmetrical, unilocular, single-seeded, elliptical, lenticular in transverse section, length 10.8–11.7 mm, width 8.5–9.1 mm, thickness about 4.5

mm. A keel surrounds the endocarp in the plane of symmetry with the thicker margin containing a vascular bundle embedded in the endocarp wall. Apex asymmetrical in lateral view, base rounded, slightly flattened, symmetrical. Outer part of the endocarp ridged with three main longitudinal ridges (up to eight counting small longitudinal ridges) more or less branched with all reaching the point of the base. Ridges rounded and thin, enclosing 21–25 longitudinal and polygonal areoles with small free-ending ridges, occasionally absent. Vasculature of the endocarp resting on ridges and free in the mesocarp thickness. Endocarp wall 154–171 µm thick excluding ridges (268–277 µm including ridges). Endocarp wall composed of packed interlocking digitate and sclerotic cells with globally three stratified units: the outermost layer with about 0–6 isodiametrical oriented cells, 24–32 µm in width and with a multi-layered cell wall, followed by 5–10 rows of periclinally oriented cells, cells 9–13 µm in width and with a 5–6 layer cell's wall, the innermost with one row of periclinally oriented cells, cells about 8.5 µm in width and with an uni-layered cell wall, covering the inner endocarp surface with regularly spaced and rounded papillae, 14.3–17.4 (avg. 16.1 µm) in diameter with about 810–840 papillae per 0.25 mm^2. Locule surface lacunate.

Studied specimen *R.P. Tisserant s.n., Oubangui, 1948, MNHN-P-P03951984*; *R.P. Klaine 3505, Gabon, 1904, MNHN-P-P03951995*; J.J. Bos 5089, Cameroon, 1969, MNHN-P-P03951958; A. Bouquet 833, Congo, 1964, MNHN-P-P03951922.

Iodes balansae Gagnep.

Plate VII. 10–13

Fruit drupe elliptical, asymmetrical at the apex, laterally compressed, red when mature, epicarp strigose-pubescent with simple yellow hairs with granular ornamentation, reticular when dry. Mesocarp about 200 µm thick when dry. Calyx persistent. Length 25–38 mm, width 14–20 mm.

Endocarp brown in color, bilaterally symmetrical, unilocular, single-seeded, elliptical, lenticular in transverse section, length 32.7 mm, width 15.2 mm. A keel surrounds the endocarp in the plane of symmetry with the thicker margin containing a vascular bundle embedded in the endocarp wall. Apex greatly asymmetrical, base acute, symmetrical. Outer part of the endocarp ridged with two types of ridges, the primary ridges composed of one main median ridge, which reaches the point of the base and two lateral ridges in general which runs to or close to the apex up to the 2/3 of the endocarp length. Primary ridges rectangular and thin with a median channel, forming a diffuse pattern with short lateral free-ending ridges. Secondary ridges thin and rounded delimiting a dense reticulum at the surface of the endocarp enclosing numerous areoles. Endocarp possessing a symmetrical pair of horn-like protrusions compressed on the keel, positioned eccentrically and subapically on the apical endocarp faces each with a central pit. Vasculature of the endocarp resting on the channel of the ridges and free in the mesocarp thickness. Endocarp wall 434–450 μm thick excluding ridges (550–600 μm thick including secondary ridges and 1300 μm thick including primary ridges). Endocarp wall composed of packed interlocking digitate and sclerotic cells with globally three stratified cell units: the outermost layer with about 12 isodiametrical to anticlinally oriented cells, followed by 7 periclinally oriented cells, the innermost periclinally oriented one, the cells line the locule surface with rounded papillae, about 20 μm in diameter. Locule lacunate.

<u>Studied specimen</u> *KUN 0647593 (KUN)*; B. Balansa 3981, Vietnam, 1888, MNHN-P-P00698073.

Remarks: Cells detail not really visible, this is why I decided to do not mention the size of the cells. The detail of the inner surface of the endocarp is decayed, but we distinguish few papillae.

***Iodes cirrhosa* Turcz.**

Plate VII. 14 –23

<u>Fruit</u> drupe elliptical, asymmetrical at the apex, cleft at the base, laterally compressed, red when mature, epicarp pubescent composed of simple type of yellow hairs with granular ornamentation, ridged when dry. Mesocarp 270–320 μm thick when dry. Length 12–20 mm, width 10–15 mm, thickness 7–10 mm.

<u>Endocarp</u> cream in color, bilaterally symmetrical, unilocular, single-seeded, elliptical, lenticular in transverse section, length 12.6 mm, width 9.5 mm, thickness 4.5 mm. A keel surrounds the endocarp in the plane of symmetry with the thicker margin containing a vascular bundle embedded in the endocarp wall. Apex asymmetrical with an acute protuberance in both side in lateral view, base flat and cleft on the opposite side, with two acute protuberance in the continuity of the keel in both sides. Outer part of the endocarp ridged and faintly rugose with two thin rectangular to sharp ridges on each face, the median ridge runs to the base up to the two-thirds of the length and the second ridge runs up to the sub-apical part, on the opposite side to the apex asymmetry. Endocarp possessing a symmetrical pair of horn-like protrusions compressed on the keel, positioned eccentrically and subapically on the apical endocarp faces each with a central pit. Endocarp wall 380–405 μm thick excluding ridges (813–1064 μm thick including ridges. Endocarp wall composed of packed interlocking digitate and sclerotic cells with globally three stratified units, sometimes quite homogeneous; the outermost unit with 15–17 rows of isodiametrical, occasionally anticlinally oriented cells, cells 22–49 μm in diameter and

with a uni-layered cell wall, followed by 3–4 rows of small periclinally oriented cells, cells 7–10 μm in width and with an uni-layered cell wall, the locule epiderma composed of one row of periclinally oriented cells, cells about 6.5 μm in width and with an uni-layered thin cell wall, covering the inner endocarp surface with regularly spaced and sessile rounded papillae, 8.6–15.5 (avg. 10.2 μm) in diameter, with about 460 papillae per 0.25 mm^2. Locule surface lacunate.

<u>Studied specimen</u> *B. Hayata 672, "Indo-chine", 1921, MNHN-P-P06672331*; E. Poilane 6622, "Indo-chine", s.d., MNHN-P-P06672332.

Remarks: the endocarp was considered as "smooth inside" (Sleumer, 1971). Here we demonstrate that the locule is densely covered by papillae. These papillae are filmy and thus difficult to observe without SEM view.

Iodes kamerunensis **Engl.**

Plate VIII. 1–9

<u>Fruit</u> drupe elliptical, asymmetrical at the apex, epicarp pubescent with yellow simple hairs with granular ornamentation, reticulate when dry. Mesocarp 135–150 μm thick when dry. Calyx persistent. Length 10.0–12.4 mm, width 7.0–9.6 mm, thickness 6.0–8.9 mm.

<u>Endocarp</u> cream in color, bilaterally symmetrical, unilocular, single-seeded, elliptical, globular in transverse section, length 10.9 mm, width 9.9 mm, thickness 7.5 mm. A keel surrounds the endocarp in the plane of symmetry, with the thicker margin containing a vascular bundle embedded in the endocarp wall, occasionally divided in two part sub-apically. Apex asymmetrical in lateral view, base rounded-flat and symmetrical. Outer part of the endocarp ridged with three main ridges longitudinally, the median ridge reaches the point of the base then dichotomises at the 2/3 of the endocarp. The remaining 1/3 of the endocarp length is ridgeless. Ridges rounded and thin, each with a median channel, enclosing 1–3 polygonal areoles, extended transversally and longitudinally. Vasculature of the endocarp resting on the channel of the ridge. Endocarp wall 154–181 μm thick excluding ridges (460–470 μm thick including ridges). Endocarp wall composed of packed interlocking digitate and sclerotic cells quite homogenous, with 9–12 isodiametric oriented cells, 14–26 μm in width. Locule surface unknown, lacunate.

<u>Studied specimen</u> *G.A. Zenker 2032, Cameroon, 1899, MNHN-P-P03951972.*

Remarks: A tissue (placenta? Degradation?) masks the surface of the locule.

Iodes klaineana **Pierre**

Plate VIII. 10–18

<u>Fruit</u> drupe elliptical, asymmetrical at the apex, laterally compressed, red when mature, epicarp densely pubescent with simple yellow short hairs with a granular ornamentation and simple longer hairs without ornamentation, ridged when dry. Mesocarp 240–300 μm thick when dry. Calyx persistent. Length 11.0–13.6 mm, width 7.0–11.0 mm, thickness 4–7.1 mm.

<u>Endocarp</u> cream in color, bilaterally symmetrical, unilocular, single-seeded, elliptical in lateral view, lenticular in transverse section, length 12.1 mm, width 7.6 mm, thickness 6.3 mm. A keel surrounds the endocarp in the plane of symmetry with the thicker margin containing a vascular bundle embedded in the endocarp wall. Apex slightly asymmetrical in lateral view, without aperture, base rounded and symmetrical. Outer part of the endocarp ridged with 4–5 main ridges longitudinally, the median ones runs from the point of the base up to the point of the apex. Ridges rounded, thin, with a median channel, delimiting a reticulate pattern sparse sub-apically and sub-basally, denser in other part, enclosing 13–15 polygonal areoles with a free-ending ridge more or less marked inside. Vasculature of the endocarp resting on the channel of the ridges. Endocarp wall 128–173 μm thick excluding ridges (300–360 μm thick including ridges). Endocarp wall composed of packed interlocking digitate and sclerotic cells with at least two stratified cell units: the outermost ones with 5–9 rows of isodiametrical to anticlinally oriented cells, cells 22.7–29.0 μm in width and with a multi-layered secondary wall (about 3–4), the innermost unit with 1–5 rows of periclinally oriented cells, cells 13–14 μm in width and with a multi-layered secondary wall. Locule surface unknown, lacunate.

<u>Studied specimen</u> *R.P. Klaine 3064, Gabon, 1902, MNHN-P-P04472306;* J.J.F.E. de Wilde 606, Gabon, 1983, MNHN-P-P04472313;

Iodes liberica **Stapf**

Plate VIII. 19–27

<u>Fruit</u> drupe elliptical to obovoid, asymmetrical at the apex, laterally compressed, red when mature, epicarp sparsely strigose with simple yellow hairs with granular ornamentation, ridged when dry. Mesocarp about 200 μm when dry. Calyx not persistent. Length 8.0–11.9 mm, width 5.0–7.8 mm, thickness 5.5–7.4 mm.

<u>Endocarp</u> brown in color, bilaterally symmetrical, unilocular, single-seeded, elliptical to obovoid in lateral view, globular in transverse section, length 10.4 mm, width 7.1 mm, thickness about 7 mm. A keel surrounds the endocarp in the plane of symmetry with the thicker margin containing a vascular bundle embedded in the endocarp wall. Apex slightly asymmetrical in lateral

view without aperture, base rounded-acute, symmetrical. Outer part of the endocarp sparsely ridged, with one median ridge running longitudinally, beginning to the point of the base and reaching the 2/3 of the endocarp length. Ridges angular-sharp, thin, with a median channel, forming a sparse diffuse pattern from the median ridge, absent at the 1/3 apical length. Vasculature of the endocarp resting on the channel of the ridge. Endocarp wall 138–172 μm thick excluding ridges (257–266 μm thick including ridges). Endocarp wall composed of packed interlocking digitate and sclerotic cells with at least two unicellular and multicellular units: the outermost unit with 1 anticlinally-isodiametrical oriented cells, 16.1–22.7 μm in width, the innermost unit with 8–9 periclinally oriented cells, 8.8–22 μm in width and with a multi-layered cell wall, about 6–11. Locule surface unknown, not lacunate.

Studied specimen *J.G. Adam 3833, Guinea, 1949, MNHN-P-P04472332*; J. G. Adam 5788, Guinea, 1949, MNHN-P-P04472335; J. G. Adam 5252, Guinea, 1949, MNHN-P-P04472330; A. Jolly s.n., Ivory Coast, 1906, MNHN-P-P04472370; A. J. M. Leewenberg 2527, Ivory Coast, 1959, MNHN-P-P04472371.

Iodes madagascariensis **Baill.**

Plate IX. 1–9

Fruit drupe, elliptical, slightly asymmetrical at the apex, laterally compressed, brown when mature, epicarp glabrous, granular, faintly ridged when dry. Mesocarp 135–214 μm thick when dry. Calyx not persistent. Length 7–9 mm, width 4–5 mm, thickness 4.4–5.0 mm.

Endocarp cream in color, bilaterally symmetrical, unilocular, single-seeded, elliptical in lateral view, lenticular in transverse section, length 7.6–8.0 mm, width about 4.6 mm, thickness about 4.3 mm. A keel surrounds the endocarp in the plane of symmetry with the thicker margin containing a vascular bundle embedded in the endocarp wall. Apex slightly asymmetrical in lateral view without aperture, base rounded, symmetrical. Outer part of the endocarp ridged delimiting a reticulate pattern of ridges rounded, thin and faintly apparent and with a median channel, ridges enclosing more than 80 small polygonal areoles distributed over the entire surface of the endocarp. Vasculature of the endocarp resting on the channel of the ridge. Endocarp wall 165–201 μm thick excluding ridges (227–265 μm thick including ridges). Endocarp wall composed of packed interlocking digitate and sclerotic cells with at least two unicellular and multicellular units: the outermost unit with about 11 rows of more or less periclinally to isodiametrical oriented cells, cells 18.9–27.0 μm in width and with 7–8 secondary layer cell's wall, the innermost unit with one row of small periclinally oriented cells, cells 7.9–9.6 μm in width and with an uni-layered cell wall, cover the inner endocarp surface with regularly spaced and rounded papillae, about 13.3 µm in diameter. Locule not lacunate.

Studied specimen *Chapelier s.n., Madagascar, s.d., MNHN-P-P04472113*; *McPherson 18809 (MO)*; Chapelier s.n., Madagascar, s.d., MNHN-P-P04472112.

Iodes ovalis **Blume**

Plate IX. 10 –18

Fruit drupe elliptical, asymmetrical at the apex, cleft at the base, laterally compressed, epicarp strigose with simple yellow hairs with granular ornamentation and small papillae-like hairs expansion which lines the fruit; reticular when dry. Mesocarp 142–242 µm thick when dry. Calyx persistent. Length 15–25 mm, width 10.0–11.4 mm, thickness 8–9 mm.

Endocarp cream in color, bilaterally symmetrical, unilocular, single-seeded, elliptical in lateral view, lenticular in transverse section, length 17.8 mm, width 11 mm, thickness 8.6 mm. A keel surrounds the endocarp in the plane of symmetry with the thicker margin containing a vascular bundle embedded in the endocarp wall. Apex asymmetrical and acute in lateral view, base flattened and cleft on the opposite side with two acute protuberances in the continuity of the keel in both sides. Outer part of the endocarp ridged and faintly rugose with 3–4 main longitudinal ridges, delimiting a reticulate pattern enclosing 3–4 large polygonal areoles. Ridges thin, rectangular, with a median channel, interconnected with some very short free-ending ridges. Rugosities distributed over the entire surface. Endocarp possessing a symmetrical pair of horn-like protrusions, positioned eccentrically and subapically on the apical endocarp faces, each with a central pit. Endocarp wall 314–375 µm thick excluding ridges (about 490 µm thick including ridges). Endocarp wall composed of packed interlocking digitate and sclerotic cells with globally three stratified units: the outermost unit with 16–19 rows of isodiametric, occasionally anticlinally oriented cells, cells with an uni-layered thick cell wall, followed by a unit with 6–11 rows of periclinally oriented cells; the innermost unit of one row of periclinally oriented cells, cells with an uni-layered thin cell wall, lining the surface of the locule with regularly spaced and rounded papillae, 9.2–11.8 (avg. 10.1 µm) in diameter, at least 220 per 0.25 mm^2. Locule lacunate.

Studied specimen *Hiep HLF 203 (MO)*; Kunz?, Celebes, 1863, MNHN-P-P04504863.

Iodes perrieri **Sleumer**

Plate IX. 19–27

Fruit drupe globular, symmetrical at the apex, brown when mature, epicarp strigose with simple yellow hairs with granular ornamentation, finely ridged when dry. Mesocarp 88–111 μm thick when dry. Calyx persistent. Length 11–17 mm, width 11.3–15.0 mm, thickness 10–12 mm.

Endocarp cream in color, bilaterally symmetrical, unilocular, single-seeded, globular in lateral view and transverse section, length 11.5 mm, width 10.9 mm, thickness 9.2 mm. A thin and delicate keel surrounds the endocarp in the plane of symmetry with the thicker margin containing a vascular bundle embedded in the endocarp wall. Apex slightly asymmetrical, base rounded, symmetrical. Outer part of the endocarp ridged with two types of ridges. The primary ridges composed of three main longitudinally ridges, the median ridge and a ridge on the side of the apical asymmetry reaching the point of the base. Primary ridges thin, rounded and forming a sparse diffuse pattern. Secondary ridges thin and sharp, delimiting a dense reticulum enclosing numerous areoles. Endocarp possessing a symmetrical pair of pores, positioned eccentrically and subapically on the apical endocarp faces. Vasculature of the endocarp resting on ridges. Endocarp wall 317–338 μm thick excluding ridges (340–426 μm thick including ridges). Endocarp wall composed of packed interlocking digitate and sclerotic cells with globally three stratified units: all with cells with an uni-layered cell wall; the outermost unit with 3–11 rows of isodiametrical to anticlinally oriented cells, cells 23.7–44.0 μm in width, followed by 3–9 rows of periclinally oriented cells, cells 20–27 μm in width, the innermost unit with one row of periclinally oriented cells, cells 12–18 μm in width, covers the inner endocarp surface with regularly spaced and rounded papillae, 12.3–18.0 (avg. 14.9 μm) in diameter, with about 448 papillae per 0.25 mm^2. Locule lacunate.

Studied specimen *Perrier De La Bâthie 17843, Madagascar, 1926, MNHN-P-P04472108*; J. Leandri 468, Madagascar, 1932, MNHN-P-P04472110; C .C.H Jongkind 3385, Madagascar, 1996, MNHN-P-P05279694; C.C.H. Jongkind 3696, Madagascar, 1997, MNHN-P-P05274867.

Iodes philippinensis **Merr.**

Plate X. 1–9

Fruit drupe oblong, asymmetrical at the apex, laterally compressed, red when mature, epicarp pubescent-strigose with simple yellow hairs with granular ornamentation and uncinate hairs, ridged when dry. Mesocarp about 50 μm thick when dry. Calyx persistent. Length 11–15 mm, width 7.5–12.0 mm, thickness 5–10 mm.

Endocarp brown in color, bilaterally symmetrical, unilocular, single-seeded, oblong in lateral view, hexagonal in transverse section, length 12.4 mm, width 7.6 mm, thickness 6.5 mm. A keel surrounds the endocarp in the plane of symmetry, with the thicker margin containing a vascular bundle embedded in the endocarp wall. Apex asymmetrical and almost flat with two uncinate protuberances in lateral view; base flattened and cleft on the opposite side, with two acute protuberance in the continuity of the keel in both sides. Outer part of the endocarp ridged with two types of ridges, the primary ridges composed of two main longitudinal ridges, which run from the sub-basal part up to the sub-apical part of the endocarp length. Primary ridges quite large and rectangular, forming a diffuse pattern with only 2–3 lateral free-ending ridges. Secondary ridges thin and rounded, delimiting a dense reticulum at the surface of the endocarp enclosing numerous areoles. Endocarp possessing a symmetrical pair of horn-like protrusions, positioned on the bigger uncinate protuberance at the apex. Vasculature of the endocarp resting on ridges. Endocarp wall 229–282 µm thick excluding ridges (285–296 µm including secondary ridges and 360–396 µm including primary ridges). Endocarp wall composed of packed interlocking digitate and sclerotic cells, with globally four unicellular and multicellular units: the outermost unit with about 5 rows of isodiametrical oriented cells, cells 12.5–16.5 µm in width and with an uni-layered cell wall, followed by a unit with about 6 rows of isodiametric-anticlinally oriented cells, cells 21.4–28.3 in width, then a unit with about 5 rows of periclinally oriented cells, cells 8.1–11.9 µm in width and with a multi-layered cell wall; the innermost unit of one row of periclinally oriented cells, cells 6.7–6.9 µm in width, covers the surface of the locule (detail of the surface unknown). Locule lacunate.

Studied specimen *A.D.E. Elmer 16418, Phillipines, 1916, MNHN-P-P04504850.*

***Iodes scandens* (Becc.) Utteridge & Byng**

Plate X. 10–17

Fruit drupe, elliptical, asymmetrical at the apex, laterally compressed, epicarp pubescent. Length 20 mm, width 15 mm, thickness 15 mm.

Endocarp brown in color, bilaterally symmetrical, unilocular, single-seeded, elliptical in lateral view, lenticular in transverse section, length 14.7 mm, width 12.9 mm, thickness 11.2 mm. A keel surrounds the endocarp in the plane of symmetry with the thicker margin containing a vascular bundle embedded in the endocarp wall. Apex rounded and asymmetrical, base rounded, slightly asymmetrical. Outer part of the endocarp ridged with two main longitudinal ridges, the median runs from the point of the base up the ½ of the endocarp length, and then divided in some smaller ridges and a lateral ridge, which runs from the sub-base up to the sub-apex. Ridges rectangular, thin, with a median channel, delimiting a reticulate pattern enclosing 13–18 irregular ridges, with free-ending ridges in arbuscle-shape. Vasculature of the endocarp surface in the channel of the ridge. Endocarp possessing a symmetrical pair of horn-like protrusions compressed on the keel, positioned eccentrically and subapically on the apical endocarp faces, each with a central pit. Endocarp wall 502–564 µm thick excluding ridges (652–672 µm including ridges). Endocarp wall composed of packed interlocking digitate and sclerotic cells with globally three stratified units: the outermost unit with 11–13 rows of anticlinally oriented cells, cells 14.0–43.1 µm in length, followed by a unit with 6–8 rows of periclinally oriented cells, cells 21.1–25.6 µm in width and with a multi-layered cell wall. The innermost unit of one row of periclinally oriented cells, cells 9.3–9.8 µm in width, and with a uni-layered cell wall, covers the surface of the locule, apparently with rounded papillae (detail of the surface poorly preserved). Locule lacunate.

Studied specimen *No voucher (MO).*

***Iodes seguinii* (H.Lév.) Rehder**

Plate X. 18–26

Fruit drupe elliptical to oblong, laterally compressed, red when mature, epicarp pubescent with uncinate yellow hairs, smooth when dry. Mesocarp thin when dry. Length 15–23 mm, width 10–16 mm, thickness 5.0–7.9 mm.

Endocarp brown in color, bilaterally symmetrical, unilocular, single-seeded, oblong in lateral view, lenticular in transverse section, length 16.5 mm, width 11 mm, thickness 8.1 mm. A channel surrounds the endocarp in only one side in the plane of symmetry. Apex asymmetrical, flattened in the lateral view, base flattened and symmetrical. Outer part of the endocarp smooth with thin faintly apparent channels, 3–4 main longitudinally. Vasculature of the endocarp on the channels and endocarp primary vascular strand inside the channel surrounding the endocarp. Endocarp wall 173–226 µm thick. Endocarp wall composed of packed interlocking digitate and sclerotic cells, with 12 rows of periclinally oriented cells, cells 9.9–15.4 µm in width and with a uni-layered cell wall. Locule surface apparently smooth, not lacunate.

Studied specimen *Abbé Cavalerie 3932, Chine, 1913, MNHN-P-P05279333.*

***Iodes seretii* (De Wild.) Boutique**

Plate XI. 1–9

Fruit drupe elliptical, asymmetrical at the apex, laterally compressed, red when mature, epicarp pilose with long and thin yellow hairs and simple yellow hairs with granular ornamentation.

Mesocarp 132–162 µm thick when dry. Calyx persistent. Length 11.6–15.5 mm, width 8.5–10.0 mm, thickness 5.6 mm.

Endocarp brown in color, bilaterally symmetrical, unilocular, single-seeded, elliptical in lateral view, lenticular in transverse section, length 11.6 mm, width 8.7 mm, thickness 5.9 mm. A keel surrounds the endocarp in the plane of symmetry with the thicker margin containing a vascular bundle embedded in the endocarp wall. Apex slightly asymmetrical in lateral view, with a central pit in apical view, base rounded, symmetrical. Outer part of the endocarp ridged with 3–4 main longitudinally ridges (6-7 with small longitudinal ridges), the median and two lateral ridges reaching the point of the base and run up to the sub-apical part of the endocarp length. Ridges thin, rounded to rectangular with a median channel, delimiting a reticulate pattern enclosing 23–25 polygonal and longitudinal extended areoles. Surface of endocarp finely covered by ridgelets-rugosities. Vasculature of the endocarp resting on the channel of the ridges. Endocarp wall 227–245 µm thick excluding ridges (320-386 µm including ridges). Endocarp wall composed of packed interlocking digitate and sclerotic cells with globally three stratified units: the outermost unit with 1–3 rows of isodiametrical oriented cells (Mesocarp?), cells 12.2–17.2 µm in width, and with an uni-layered cell wall, followed by a unit with 15 rows of periclinally oriented cells, cells 9.4–13.2 µm in width and with 5–6 layered cell wall, the innermost unit with one row of periclinally oriented cells, cells 5.4–8.7 µm in width and with an uni-layered cell wall, covers the inner endocarp surface with regularly spaced and rounded papillae, 11.8–13.7 (avg. 12.7 µm) in diameter. Locule lacunate.

Studied specimen *D. Thomas & M. Etuge 63, Cameroon, s.d., BR0000015596772 (BR)*; Ekwuno PFO 370 (MO).

Iodes yatesii **Merr.**

Plate XI. 10–18

Fruit drupe elliptical, laterally compressed, brown when mature, length 25–34 mm, width 15–17 mm, thickness 11–13 mm.

Endocarp cream in color, with a cork-like texture, bilaterally symmetrical, unilocular, single-seeded, elliptical in lateral view, lenticular in transverse section, length 33.8 mm, width 17 mm, thickness 10.7 mm. A keel surrounds the endocarp in the plane of symmetry with the thicker margin containing a vascular bundle embedded in the endocarp wall. Apex asymmetrical in lateral view, base rounded, symmetrical. Outer part of the endocarp ridged with two types of ridges. The primary ridges composed of three main ridges longitudinally, the median ridge reaching the point of the base. Primary ridges large, rectangular, with a median channel and with wavelets ornamentation from both sides of the channel; delimiting a reticulate pattern enclosing 7–8 square-polygonal areoles expended transversally. Secondary ridges thin and sharp, delimiting a dense reticulum at the surface of the endocarp enclosing numerous areoles. Vasculature of the endocarp resting on the channel of the ridges. Endocarp possessing a symmetrical pair of pores, positioned eccentrically and subapically on the apical endocarp faces. Endocarp wall 258–322 µm thick excluding ridges (433–597 µm thick including the secondary ridges and about 959 µm thick including primary ridges). Endocarp wall composed of packed interlocking digitate and faintly sclerotic cells, with globally three stratified units, all cells with an uni-layered cell wall: the outermost unit with about 2–4 rows of isodiametrical to anticlinally oriented cells, cells 30.7–32.6 µm in width, followed by a unit with 11 rows of periclinally oriented cells, cells 11.9–21.0 µm in width, the innermost unit with one row of periclinally oriented cells, cells 6.3–8.4 µm in width, covers the inner endocarp surface with papillae. Locule lacunate.

<u>Studied specimen</u> *Burley 1577 (K)*; H. S. Yates 1342, Sumatra, s.d. MNHN-P-P04504846.

***Lavigeria* Pierre**

Plate XI. 19–21

<u>Fruit</u> drupe elliptical, red when mature, epicarp pilose and pubescent composed of simple hairs with granular ornamentation and of long and thin hairs, rugose when dry. Calyx apparently not persistent.

<u>Endocarp</u> cream in color, bilaterally symmetrical, unilocular, single-seeded, elliptical in lateral view, globular in transverse section. A keel surrounds the endocarp in the plane of symmetry, with the thicker margin containing a vascular bundle embedded in the endocarp wall. Apex slightly asymmetrical in lateral view, base symmetrical. Outer part of the endocarp rugose. Vasculature of the endocarp on longitudinal furrows into the endocarp wall. Endocarp wall composed of packed interlocking digitate and sclerotic cells with at least one unit with row of periclinally oriented cells. Locule surface smooth and hairy, not lacunose.

***Lavigeria macrocarpa* (Oliv.) Pierre**

Plate XI. 19–21

<u>Fruit</u> drupe, elliptical, red when mature, epicarp pilose and pubescent with long and thin red hairs and simple hairs with granular ornamentation, rugose when dry. Mesocarp about 14 mm thick. Calyx apparently not persistent. Length 53–95 mm, width 40–58 mm.

<u>Endocarp</u> cream in color, bilaterally symmetrical, unilocular, single-seeded, elliptical in lateral view, globular in transverse section, Length 58 mm, width 37 mm. A keel surrounds the

endocarp in the plane of symmetry, with the thicker margin containing a vascular bundle embedded in the endocarp wall. Apex slightly asymmetrical in the lateral view, base rounded, symmetrical. Outer part of the endocarp rugose, with about 3–4 main longitudinally large mounds in longitudinal rows. A fold of the wall forms the mounds. Vasculature of the endocarp on some longitudinal furrows into the endocarp wall. Endocarp wall 694–850 µm thick without and with ridges. Endocarp wall composed of packed interlocking digitate and sclerotic cells with globally two multicellular units: the outermost unit with 15 rows of isodiametric cells, cells 20.5–58.5 µm in width, the innermost unit with 15 rows of periclinally oriented cells, cells 10.3–32.0 µm in width and with 5–7 layered cell wall. Inner endocarp smooth with long and thin hairs. Locule surface fold, not lacunate.

Studied specimen *Bos 4098 (MO); R. Letowsey 8970, Cameroon, 1968; N. Hallé 3734, Gabon, 1966, MNHN-P-P04494807; J.J. Wieringa 5840, Cameroon, 2007, WAG. 1398985 (WAG).*

Leretia **Vell.**

Plate XII. 1–9

Fruit drupe elliptical, apex asymmetrical, red-black when mature, epicarp glabrous, channels with vasculature visible when dry. Calyx persistent.

Endocarp cream in color, bilaterally symmetrical, unilocular, single-seeded, elliptical and elongate in lateral view, globular in transverse section. Apex slightly asymmetrical in lateral view, base symmetrical. Outer part of the endocarp smooth with some longitudinal shallows channels containing the vasculature of the endocarp. Endocarp primary vascular strand inside the endocarp wall. Endocarp wall composed of packed interlocking digitate and sclerotic cells with at least one unit with rows of periclinally oriented cells. Locule surface smooth and hairy, slightly lacunose.

Leretia cordata **Vell.**

Plate XII. 1–9

Fruit drupe elliptical, apex asymmetrical, red-black when mature, epicarp glabrous, channels with vasculature marked when dry. Mesocarp 200–240 µm hick when dry. Calyx persistent. Length 20–50 mm, width 13–30 mm, thickness 12.7–16.0 mm.

Endocarp cream in color, bilaterally symmetrical, unilocular, single-seeded, elliptical to oblong in lateral view, globular in transverse section, length 22.5 mm, width 13 mm, thickness 12.3 mm. A channel surrounds the endocarp in only one side in the plane of symmetry. Apex slightly asymmetrical in lateral view, base rounded, slightly asymmetrical. Outer part of the endocarp smooth with about 3 main shallow channels containing the vasculature of the endocarp. Endocarp primary vascular strand inside the endocarp wall. Endocarp wall 353–386 µm thick. Endocarp wall composed of packed interlocking digitate and sclerotic cells with globally 12–14 rows of periclinally oriented cells, cells 16.3–33.0 µm in width and with 6–10 layered cell wall. Inner endocarp smooth with long and thin hairs. Locule surface slightly lacunose.

Studied specimen *J.C. Solomon 17073, Bolivia, 1987, U. 1343377 (U)*; Centre Orstom 4687, Guyane, 1981, MNHN-P-P05221896.

Mappia **Jacq.**

Plate XII. 10–26, Plate XIII. 1–8

Fruit drupe elliptical to globular, laterally compressed, red when mature, epicarp glabrous.

Endocarp cream in color, bilaterally symmetrical, unilocular, single-seeded, elliptical to globular in lateral view, lenticular in transverse section. A keel surrounds the endocarp in the plane of symmetry. Apex asymmetrical in lateral view, base symmetrical. Outer part of the endocarp rugose, almost smooth. Vasculature of the endocarp generally resting between rugosities. Endocarp primary vascular strand outside the endocarp wall. Endocarp wall composed of packed interlocking digitate and sclerotic cells with at least one unit with rows of periclinally oriented cells and another with rows of anticlinally oriented cells. Locule surface smooth, sometimes slightly lacunose.

Key of species

1	Endocarp surface quite smooth	*2*
+	Endocarp surface rugose with channels and mounds	*Mappia multiflora*
2	Endocarp elliptical, without clear ridges	*Mappia racemosa*
+	Endocarp globular, short ridge at the apex	*Mappia longipes*

Mappia longipes **Lundell**

Plate XII. 10 –18

Fruit drupe globular, symmetrical at the apex, laterally compressed, red when mature, epicarp glabrous, smooth or slightly rugose when dry. Mesocarp about 350 µm thick when dry. Calyx persistent. Length 18.8 mm, width 14.7 mm, thickness 10.4 mm.

Endocarp cream in color, bilaterally symmetrical, unilocular, single-seeded, globular in lateral view, lenticular in transverse section, length 15.8 mm, width 13.6 mm, thickness 10.2 mm. A keel surrounds the endocarp in the plane of symmetry with a central channel. Apex slightly asymmetrical in lateral view, base rounded, symmetrical with a small rounded protuberance at the point of the base. Outer part of the endocarp smooth with sparse rugosities randomly distributed. A short ridge reaches the apex and runs transversally and sub-apically over 0.5 mm at the most. Vasculature of the endocarp free and endocarp primary vascular strand outside the endocarp wall. Endocarp wall 714–809 µm thick. Endocarp wall composed of packed interlocking digitate and sclerotic cells with globally two multicellular units: the outermost unit with about 17 rows of anticlinally oriented cells, cells 21.7–32.8 µm in width and with uni- and multi-layered cell walls, the innermost unit with 14 rows of periclinally oriented cells, cells 16.9–26.7 µm in width. Inner endocarp smooth, not lacunate.

<u>Studied specimen</u> *M. Guillermo Ibarra 72, Mexico, 1982, U. 1343380 (U).*

Mappia multiflora **Lundell**

Plate XII. 19–26

<u>Fruit</u> drupe elliptical, apex slightly acuminate and asymmetrical, laterally compressed, length 14–26 mm, width 10–20 mm, thickness 10–13 mm.

<u>Endocarp</u> cream in color, bilaterally symmetrical, unilocular, single-seeded, elliptical-globular in lateral view, lenticular in transverse section, length 16.4 mm, width 11.3 mm, thickness 9.3 mm. A channel surrounds the endocarp in the plane of symmetry. Apex slightly asymmetrical and acute, base rounded and symmetrical. Outer part of the endocarp rugose with about 2–3 main longitudinal channels that separate irregular mounds. Vasculature of the endocarp resting on the channel, between rugosities and endocarp vascular primary strand in the channel surrounding the endocarp. Endocarp wall 692–795 µm thick with and without rugosities. Endocarp wall composed of packed interlocking digitate and sclerotic cells, with globally two multicellular units: the outermost unit with 13 rows of anticlinally oriented cells, cells 16.8–30.2 µm in width, the innermost unit with 20 rows of periclinally oriented cells, cells 13.5–28.2 µm in width. Inner endocarp smooth, lacunate.

<u>Studied specimen</u> *Contreras 6781.*

Mappia racemosa **Jacq.**

Plate XIII. 1–8

<u>Fruit</u> drupe elliptical or globular, asymmetrical at the apex, laterally compressed, epicarp glabrous, length 10–23 mm, width 8–11 mm, thickness 6–13 mm.

Endocarp cream in color, bilaterally symmetrical, unilocular, single-seeded, elliptical in lateral view, lenticular in transverse section, length 12 mm, width 8.8 mm, thickness 6.9 mm. A keel surrounds the endocarp in the plane of symmetry. Apex slightly asymmetrical and acute, base rounded, symmetrical with a small rounded protuberance at the point of the base. Outer part of the endocarp rugose, irregular, distributed randomly at the surface. Vasculature of the endocarp free, endocarp vascular primary strand in the channel surrounding the endocarp. Endocarp wall 373–468 µm thick excluding rugosities (535–545 µm thick including rugosities). Endocarp wall composed of packed interlocking digitate and sclerotic cells, with globally two multicellular units: the outermost unit with 10–12 rows of anticlinally oriented cells, cells 15.7–34.0 µm in width and with a uni-layered cell wall; the innermost unit with 10 rows of periclinally oriented cells, cells 13.8–19.8 µm in width and with a multi-layered cell wall. Locule surface smooth, not lacunate.

Studied specimen *H. A. Van Hermann 250, West Indies, 1904, MNHN-P-P04513543*; C. Wright 1389, Cuba, s.d., MNHN-P-P04513544.

***Mappianthus* Hand.-Mazz.**

Plate XIII. 9–17

Fruit drupe elliptical, asymmetrical at the apex, laterally compressed, red when mature, epicarp strigose with simple yellow hairs with granular ornamentation, faintly rugose when dry. Calyx persistent.

Endocarp cream in color, bilaterally symmetrical, unilocular, single-seeded, elliptical, lenticular in transverse section. Keel absent. Apex asymmetrical in lateral view with a sub apical pore on each face, base symmetrical. Outer part of the endocarp rugose, irregular. Vasculature of the endocarp resting between rugosities. Endocarp primary vascular strand in a gutter in the symmetrical axis. Endocarp wall composed of packed interlocking digitate and sclerotic cells with at least one unit with rows of periclinally oriented cells and another with rows of anticlinally cells. Locule surface with regularly spaced and rounded papillae, relatively sparse, lacunose.

***Mappianthus iodoides* Hand.-Mazz.**

Plate XIII. 9–17

Fruit drupe elliptical, asymmetrical at the apex, laterally compressed, red-green when mature, epicarp strigose with simple yellow hairs with granular ornamentation, faintly rugose when dry. Mesocarp 100–200 µm thick when dry. Calyx persistent. Length 20–37 mm, width 10.0–17.7, thickness 4–8 mm.

Endocarp cream in color, bilaterally symmetrical, unilocular, single-seeded, elliptical in lateral view, lenticular in transverse section, length 25.5 mm, width 12.8 mm, thickness 6.9 mm. A channel surrounds the endocarp in the plane of symmetry. Apex asymmetrical, acute in lateral view; base rounded, symmetrical. Outer part of the endocarp rugose with about 73–91 mounds more or less square polygonal with inside a free-ending channel more or less branched. Mounds organized in 5–6 longitudinal lines separated by four main longitudinal channels. The main channel on each face reaching a pore positioned sub-apically. Vasculature of the endocarp in the channels between mounds and branching out in the channel's mounds, endocarp primary strand in the channel surrounding the endocarp and half-embedded. Endocarp wall 293–329 μm thick excluding mounds (484–496 μm thick including mounds). Endocarp wall composed of packed interlocking digitate and sclerotic cells, with globally three stratified units: the outermost unit with 1–4 rows of isodiametrical, occasionally anticlinally oriented cells, cells 26–35 μm in width, followed by a unit with 7–10 rows of periclinally oriented cells, cells 24.6–29.0 μm in width and with a 5–9 layered cell wall, the innermost unit with one row of periclinally oriented cells, cells 10.1–13.8 μm in width and with an uni-layered cell wall, cover the inner endocarp surface with regularly spaced and rounded papillae, 21.9–30.6 (avg. 25.6 μm) in diameter with about 138 papillae per 0.25 mm^2. Locule lacunate.

Studied specimen *A. N. Steward & H.C. Cheo 1093, China, 1933, MNHN-P-P045135385*; Cavalerie 1518, China, s.d., MNHN-P-P05274868.

***Miquelia* Meisn.**

Plate XIII. 18–23; Plate XIV. 1–17

Fruit drupe ovoid to elliptical with the apex occasionally acuminate or accrescent, laterally compressed, red when mature, epicarp strigose to pubescent composed of yellow simple hairs with granular ornamentation and uncinate hairs, more or less ridged when dry. Calyx persistent separated from the fruit by a gynophore.

Endocarp brown in color, bilaterally symmetrical, unilocular, single-seeded, elliptical to ovoid or partially globular in lateral view, lenticular in transverse section. A keel surrounds the endocarp in the plane of symmetry. Apex slightly asymmetrical in lateral view with a sub apical pore on each face, occasionally absent, base symmetrical. Outer part of the endocarp pitted and ridged or rugose. Pits large, exclusively circular and organized in longitudinal lines. Pits being associated with small, conical, tuberculate extensions into the locule. Ridges thin to large in reticulate pattern, delimiting a few polygonal areoles. Vasculature of the endocarp resting on the ridges. Endocarp primary vascular strand outside the endocarp wall. Endocarp wall composed of packed interlocking digitate and sclerotic cells, with at least one unit with rows of periclinally oriented cells. Locule surface with regularly spaced and rounded papillae, occasionally lacunate, often hardly discernible.

Key of species

1	Endocarp ovoid, about 8 mm length	*Miquelia celebica*
+	Endocarp elliptic, > 13.5 mm length	2
2	Endocarp wall thick (> 1mm), 8–9 pits longitudinally	*Miquelia caudata*
+	Endocarp wall thin (< 0.2 mm), 3–4 pits longitudinally	*Miquelia assamica*

Miquelia assamica **(Griff.) Mast. ex B.D.Jacks.**

Plate XIII. 18–23

<u>Fruit</u> drupe elliptical, asymmetrical and with an acumen at the apex, laterally compressed, epicarp glabrous, reticulate when dry. Calyx persistent separated from the fruit by a gynophore. Length 9.0–13.5 mm, width 8.0–9.3 mm, thickness about 5 mm.

<u>Endocarp</u> brown in color, bilaterally symmetrical, unilocular, single-seeded, elliptical in lateral view, lenticular in transverse section, length 13.5 mm, width 8.9 mm. A keel surrounds the endocarp in the plane of symmetry. Apex slightly asymmetrical with an acute apex in lateral view and an apical hole in the apical view, base rounded and symmetrical. Outer part of the endocarp pitted, ridged and "rugose". Ridges large and rounded, faintly apparent, with three main longitudinal ridges delimiting a reticulate pattern enclosing a few polygonal areoles. Rugosities on top of ridges, mostly present on the margin of the endocarp and mainly positioned on the transversally ridges. Pits large, 1–2 mm, exclusively circular and organized in longitudinal lines, 3–4 pits longitudinally and transversally (about 12 pits per face). Pits being associated with conical, tuberculate extensions into the locule, about 240 μm in length inside the endocarp. Endocarp primary vascular strand outside the endocarp wall. Endocarp wall about 182–210 μm thick (with and without ridges, the ridges are mainly formed by a fold of the wall not by thickening). Endocarp wall composed of packed interlocking digitate and sclerotic cells, with globally two stratified units: the outermost unit with about 12 rows of periclinally oriented cells, cells 13.4–28.0 μm in width and with a multi-layered cell wall, the innermost unit with one row of periclinally oriented cells, cells 8.2–11.0 μm in width and with an uni-layered cell wall, cover the inner endocarp surface with regularly spaced and rounded papillae, 13–18 (avg. 16 μm) in diameter. Locule lacunate.

Studied specimen *No voucher "15023"*;?, Celebes, MNHN-P-P04513530.

Miquelia caudata **King**

Plate XIV. 1–8

Fruit drupe elliptical, apex accrescent, elongate in acumen, laterally compressed, red when mature, epicarp strigose with simple yellow hairs with granular ornamentation, faintly ridged when dry. Calyx persistent separated from the fruit by a gynophore. Length 23–30 mm, width 13–18 mm, thickness 7–10 mm.

Endocarp brown in color, bilaterally symmetrical, unilocular, single-seeded, elliptical in lateral view, lenticular in transverse section, length 17 mm, width 12.2 mm, thickness 8.2 mm. A keel surrounds the endocarp in the plane of symmetry. Apex slightly asymmetrical with an acute apex in lateral view and an apical hole, base rounded and symmetrical. Outer part of the endocarp pitted and ridged. Ridges sharp and thin, with three main longitudinal ridges, the median ridge reaching the point of the base and runs up to the 2/3 of the endocarp length and the two lateral ridges reaching the point of the apex and run up to almost the base. The two lateral ridges are each connected with four transversal ridges enclosing three areoles (ended by the keel). Pits large (0.4–1.2 mm in diameter) exclusively circular and organized in longitudinal lines, 8–9 pits longitudinally and about 6 pits transversally of which one pits occur between each main longitudinally ridges and two pits occur between laterals ridges and the keel (about 44–48 pits per face). Pits being associated with conical, tuberculate extensions into the locule, about 302 μm in length inside the endocarp. Endocarp primary vascular strand outside the endocarp wall. Cell details of endocarp wall unknown. Inner surface with regularly spaced and rounded papillae, 13.2–18.0 (avg. 15.9 μm) in diameter with about 600–800 papillae per 0.25 mm^2. Locule lacunate.

Studied specimen *Mohd, Shah & Sidek 1168, Malay, 1965, L2289517 (L); Othman S.56069 (MO).*

Miquelia celebica **Blume**

Plate XIV. 9–17

Fruit drupe ovoid, laterally compressed, red when mature, epicarp pubescent with yellow uncinate hairs, ridged when dry. Mesocarp 143–240 μm thick when dry. Calyx persistent separated from the fruit by a gynophore. Length 8–17 mm, width 7–12 mm, thickness 6 mm.

Endocarp brown in color, bilaterally symmetrical, unilocular, single-seeded, ovoid in lateral view, lenticular in transverse section, length 8 mm, width 7.8 mm, thickness 3 mm. A keel surrounds the endocarp in the plane of symmetry. Apex slightly asymmetrical with an acute apex in lateral view and a sub-apical pore, base slightly rounded, symmetrical. Outer part of the endocarp pited and ridged. Ridges rounded and thin to large, with three main longitudinal ridges, the median ridge runs from the base up to the 2/3 of the endocarp length and the two lateral ridges reaching the point of the apex and run up to almost the base. The two lateral ridges are each connected with some transversal ridges free or connected with the keel. Pits large (0.4–0.9 mm in diameter) exclusively circular and organized in longitudinal lines, 3–5 pits longitudinally and 4 pits transversally of which one pits occur between each main longitudinally ridges and one pits between lateral ridges and the keel (about 17–19 pits per face). Pits being associated with conical, tuberculate extensions into the locule, about 400 μm in length inside the endocarp. Vasculature resting on ridges, endocarp primary vascular strand outside the endocarp wall. Endocarp wall about 170–270 μm thick (with and without ridges, the ridges are mainly formed by a fold of the wall not by thickening). Endocarp wall composed of packed interlocking digitate and sclerotic cells, with globally three stratified units: the outermost unit with 2–4 rows of isodiametrical oriented cells, cells 13.0–22.7 μm in width, followed by about 5 rows of periclinally oriented cells, cells 8.5–17.7 μm in width and with a multi-layered cell wall, the innermost unit with one row of periclinally oriented cells, cells 8.6–15.4 μm in width and with a uni-layered cell wall, covers the inner endocarp surface with regularly spaced and rounded papillae, 12.6–16.0 (avg. 14 μm) in diameter. Locule lacunate.

<u>Studied specimen</u> *V. Gal (?) 23, Celebes, 1923, L.2289530 (L)*;?, Celebes, 1840, L.0014929 (L); Ramos 80631 (K).

***Natsiatum* Buch.-Ham. ex Arn.**

Plate XIV. 18–26

<u>Fruit</u> drupe elliptical to ovoid, apex slightly asymmetrical, black when mature, epicarp strigose with simple yellow hairs with granular ornamentation. Calyx persistent.

<u>Endocarp</u> cream in color, bilaterally symmetrical, unilocular, single-seeded, elliptical to ovoid in lateral view, lenticular in transverse section. A keel surrounds the endocarp in the plane of symmetry. Apex slightly asymmetrical in lateral view, base symmetrical. Outer part of the endocarp ridged with a reticulate pattern of thin and rounded ridges delimiting polygonal areoles. Vasculature in the channels of the ridges. Endocarp primary vascular strand in a gutter on the keel. Endocarp wall composed of packed interlocking digitate and sclerotic cells, with at least one unit with a row of periclinally oriented cells. Locule surface smooth and lacunose.

Natsiatum herpeticum **Buch.-Ham. ex Arn.**

Plate XIV. 18–26

Fruit drupe elliptical to ovoid, apex slightly asymmetrical, black when mature, epicarp strigose with simple yellow hairs with granular ornamentation. Mesocarp 98–126 µm thick when dry. Calyx persistent. Length 10.2–15.0 mm, width 7.6–10.0 mm, thickness 5.6 mm.

Endocarp cream in color, bilaterally symmetrical, unilocular, single-seeded, elliptical to ovoid in lateral view, lenticular in transverse section, length 9 mm, width 7 mm, thickness 5.1 mm. A keel surrounds the endocarp in the plane of symmetry with a central channel. Apex asymmetrical and acute in lateral view, base rounded, symmetrical. Outer part of the endocarp ridged, faintly apparent, but with at least two main longitudinal ridges, the median ridge reaching the point of the base. Ridges thin and rounded, with a median channel, delimiting a sparse reticulum with only 3–4 polygonal areoles visible. Vasculature in the channels of the ridges, endocarp primary vascular strand semi-embedded into the endocarp wall in the channel of the keel. Endocarp wall 280–370 µm thick excluding ridges (432–531 µm thick including ridges). Endocarp wall composed of packed interlocking digitate and sclerotic cells with globally two stratified units: the outermost unit with 0–3 row(s) of isodiametrical oriented cells (mesocarp-endocarp cell transition), cells 15.1–19.7 µm in width and with an uni-layered cell wall, the innermost unit with 12–16 rows of periclinally oriented cells, cells 12.7–21.5 µm in width and with a multi-layered cell wall. Locule surface unknown, lacunate.

Studied specimen *H. B. Cale s.n., China, 1903, MNHN-P-P04513511.*

Remarks: In literature (Stull et al., 2011) a figure shows the endocarp of *Natsiatum herpeticum* in a better preservation. They have more areoles and free-ending ridges not seen here. We consider that the development of the endocarp in our sample is stopped or decayed by fungal attacks (see global discussion).

Nothapodytes **Blume**

Plate XV. 1–15

Fruit drupe elliptical to almost oblong, asymmetrical at the apex, laterally compressed, red-black when mature, epicarp strigose composed of simple yellow hairs with granular ornamentation, rugose when dry. Calyx persistent.

Endocarp cream to brown, bilaterally symmetrical, unilocular, single-seeded, elliptical to oblong in lateral view, lenticular to globular in transverse section. A keel surrounds the endocarp in the plane of symmetry. Apex asymmetrical in lateral view with a sub-apical bulge, base symmetrical. Outer part of the endocarp rugose, irregular. Vasculature of the endocarp resting between the rugosities. Endocarp primary vascular strand in the gutter in the plane of symmetry or outside the endocarp wall. Endocarp wall composed of packed interlocking digitate and sclerotic cells with globally rows of periclinally oriented cells. Locule surface smooth, not lacunate.

Key of species

1 Endocarp oblong, globular in transverse section, endocarp wall > 200 μm

Nothapodytes nimmoniana

2 Endocarp elliptical, lenticular in transverse section, endocarp wall < 200 μm

Nothapodytes pittosporoides

Nothapodytes nimmoniana **(J.Graham) Mabb.**

Plate XV. 1–9

<u>Fruit</u> drupe oblong, asymmetrical at the apex, laterally compressed, red-black when mature, epicarp strigose with simple yellow-white hairs with granular ornamentation, rugose when dry. Mesocarp 108–189 μm thick when dry. Calyx persistent. Length 10–20 mm, width 6–10 mm, thickness 3.0–7.3 mm.

<u>Endocarp</u> brown, bilaterally symmetrical, unilocular, single-seeded, oblong in lateral view, globular in transverse section, length 14 mm, width 7.2 mm, thickness 6.6 mm. A channel surrounds the endocarp in the plane of symmetry on one side. Apex asymmetrical in lateral view with a sub-apical bulge with an aperture in the plane of symmetry, base rounded symmetrical. Outer part of the endocarp rugose, irregular. Rugosities extended longitudinally and organized in 3–4 longitudinal lines, separated by 3–4 main longitudinal channels. Vasculature of the endocarp inside the channels and endocarp primary vascular strand inside the channel surrounding the endocarp. Endocarp wall 208–295 μm thick excluding (336 μm thick including rugosities). Endocarp wall composed of packed interlocking digitate and sclerotic cells, with globally 16 rows of periclinally oriented cells, cells 11.6–23.7 μm in width and with a multi-layered cell wall. Endocarp apparently smooth, lacunate.

<u>Studied specimen</u> *A. H. H. Jayasuriya 1922, Ceylon, 1975, L2289443 (L);* Thomson 359 ?, s.p., s.n., MNHN-P-P04513576 ; Thwaites 492, Ceylan, s.d., MNHN-P-P04513579 .

Nothapodytes pittosporoides **(Oliv.) Sleumer**

Plate XV. 10–18

Fruit drupe elliptical, asymmetrical at the apex, laterally compressed, red when mature, epicarp strigose with simple yellow hairs with granular ornamentation, rugose when dry. Mesocarp 72–129 µm thick when dry. Calyx persistent. Length 10–20 mm, width 6–9 mm, thickness 4.0–6.7 mm.

Endocarp cream in color bilaterally symmetrical, unilocular, single-seeded, elliptical, lenticular in transverse section, length 10.7 mm, width 7.3 mm, thickness 6.7 mm. A channel surrounds the endocarp in the plane of symmetry. Apex asymmetrical in lateral view, with a sub-apical bulge with an aperture in the plane of symmetry, base rounded symmetrical. Outer part of the endocarp rugose, irregular. Rugosities extended longitudinally and organized in 3–4 longitudinal lines separated by 3–4 main longitudinal channels. Vasculature of the endocarp inside the channels and endocarp primary vascular strand inside the channel surrounding the endocarp, half-embedded. Endocarp wall 164–197 µm thick excluding rugosities. Endocarp wall composed of packed interlocking digitate and sclerotic cells, with globally 7–8 rows of periclinally oriented cells, cells 14.2–26.8 µm in width and with a multi-layered (about 6) cell wall. Locule surface smooth, lacunate.

Studied specimen *? 4118, China, s.d., MNHN-P-P04513559*; J. Cavalerie 3164, China, 1907, MNHN-P-P04449925.

Phytocrene **Wall.**

Plate XV. 19–26, Plate XVI, Plate XVII

Fruit drupe elliptical to oblong, asymmetrical and accrescent at the apex, laterally compressed, yellow red when mature, and epicarp pubescent to pilose composed of cluster of yellow to red hairs or long and thin hairs. Calyx persistent or absent.

Endocarp brown, bilaterally symmetrical, unilocular, single-seeded, elliptical to ovoid in lateral view, occasionally obovoid, lenticular to elliptical in transverse section. A keel surrounds rarely the endocarp in the plane of symmetry. Apex asymmetrical in lateral view, with a sub-apical pairs of horn-like protrusions occasionally much reduced and forming pores each with a central pits, base symmetrical. Outer part of the endocarp pitted, occasionally ridged or rugose, irregular. Pits being associated with shallow mound, spiny or polygonal in shape, not protrude beyond the wall. Endocarp primary vascular strand outside the endocarp wall. Endocarp wall composed of packed interlocking digitate and sclerotic cells with at least one unit with rows of periclinally oriented cells and another with rows of anticlinally oriented cells. Locule surface smooth, generally not lacunose.

Key of species

1	Pits looking like areoles	2
+	Pits looking like spines	3
2	Endocarp about 14 mm length, endocarp wall thin (114–154 μm thick), pits with a median free-ending ridge	*Phytocrene anomala*
+	Endocarp about 26 mm, length, endocarp wall thick (542–591 μm thick), pits without a free-ending-ridge	*Phytocrene oblonga*
3	Endocarp clearly ridged	*Phytocrene hirsuta*
+	Endocarp not clearly ridged	4
4	Pits 60–65 on each face, finely reticulate	*Phytocrene bracteata*
+	Pits > 90 on each face, not finely reticulate	5
5	Endocarp 40–60 mm length, oblong	*Phytocrene macrophylla*
+	Endocarp < 40 mm length, not oblong	6
6	Endocarp ob-ovoid, 125–130 pits per face	*Phytocrene borneensis*
+	Endocarp ovoid, 168–178 pits per face	*Phytocrene palmata*

***Phytocrene anomala* Merr.**

Plate XV. 19–26

Fruit drupe elliptical, slightly asymmetrical and accrescent at the apex, laterally compressed, yellow-orange when mature, epicarp pilose with a cluster of yellow hairs. Calyx persistent. Length 20–25 mm, width 11–15 mm, thickness 8.0–10.1 mm.

Endocarp cream in color, bilaterally symmetrical, unilocular, single-seeded, elliptical in lateral view, lenticular in transverse section, length 14.4 mm, width 10 mm, thickness 6 mm. No clear keel surrounds the endocarp in the plane of symmetry, but thin trace of keel present in the upper part. Apex slightly asymmetrical and acute in lateral view, base rounded, symmetrical. Outer part of the endocarp pitted. Pits circular to elongate (areole-like shape), about 0.8–1.7 mm in diameter, representing most of the surface of the endocarp, more or less organized longitudinally with about 8–10 pits longitudinally and 6–7 pits transversally (about 35–45 pits per face). Each pits with a central mound or one free-ending ridge inside. Pits not protrude beyond the wall. Vasculature free, endocarp primary vascular strand outside the endocarp wall. Endocarp possessing a symmetrical pair of horn-like protrusions compressed on the keel, positioned eccentrically and subapically on the apical endocarp faces each with a central pit. Endocarp wall about 330 µm thick excluding pits (114–154 µm thick including pits). Endocarp wall (excluding pits) composed of packed interlocking digitate and sclerotic cells with globally three stratified units: the outermost with 3–5 rows of anticlinally oriented cells, cells 12.3–24.5 µm in width, followed by 9–10 rows of periclinally oriented cells and with a multi-layered cell wall, about 10.2–14.2 µm. The innermost row of periclinally oriented cells, cells 13.0–20.7 µm in width and with a uni-layered cell wall, lining the locule surface with inflated cells. Locule with rounded protuberance due to the thickening of the wall under the pits.

Studied specimen *M. Ramos 1840, Borneo, 1920, L.2289425 (L); Patrick et al. SAN 118639, Malaysia, 1986, K000183648 (K).*

Phytocrene borneensis **Becc.**

Plate XVI. 1–8

Fruit drupe obovoid, slightly asymmetrical and widely accrescent at the apex, laterally compressed, yellow-brown when mature, epicarp pilose with a cluster of yellow hairs. Mesocarp thin but thick at the accrescent part when dry. Calyx not persistent. Length 56 mm, width 14 mm.

Endocarp brown, bilaterally symmetrical, unilocular, single-seeded, obovoid in lateral view, lenticular in transverse section, length 39.1 mm, width 17.3 mm, thickness 9 mm. No clear keel surrounds the endocarp in the plane of symmetry, but thin trace of keel present in the upper part. Apex asymmetrical and emarginate in lateral view, base acute, symmetrical. Outer part of the endocarp pitted. Pits circular in the ½ upper part and more elongate in the ½ lower part of the endocarp, relatively thin, 0.2–0.4 mm in diameter, randomly arranged with about 12–13 pits longitudinally and 10–11 pits transversally (about 125–130 pits per face). Pits spiny not protrude beyond the wall. Vasculature free, endocarp primary vascular strand outside the endocarp wall. Endocarp possessing a symmetrical pair of pores, positioned eccentrically and subapically on the apical endocarp faces. Endocarp wall 681–766 µm thick excluding pits (307–351 µm thick including pits). Endocarp wall (excluding pits) composed of packed interlocking digitate and sclerotic cells, with globally three stratified units: the outermost with about 16 rows of anticlinally oriented cells, cells 32.8–45.7 µm in width, followed by a unit with about 9 rows of periclinally oriented cells, cells 14.5–24.0 µm in width. The innermost row of periclinally cells, cells 9.7–11.4 µm in width and with a uni-layered cell wall, lining the locule surface with inflated cells. Locule covered with rounded protuberances due to the thickening of the wall under the pits.

Studied specimen *No voucher, Borneo, 1979, L.2289394 (L).*

***Phytocrene bracteata* Wall.**

Plate XVI. 9–16

Fruit drupe, ovoid with a symmetrical and accrescent apex elongate, laterally compressed, yellow-brown when mature, epicarp pilose with a cluster of yellow hairs. Mesocarp thin but thick at the accrescent part when dry. Calyx not persistent. Length 45–80 mm, width 15–23 mm, thickness 10.0–11.6 mm.

Endocarp brown in color, bilaterally symmetrical, unilocular, single-seeded, ovoid in lateral view, lenticular in transverse section, length 30.5–40.0 mm, width 16.4–20.0 mm, thickness 11–15 mm. No clear keel surrounds the endocarp in the plane of symmetry, but thin trace of keel present in the upper part. Apex slightly asymmetrical and emarginated in lateral view, base rounded, symmetrical. Outer part of the endocarp pitted and faintly ridged. Pits circular, occasionally elongate, relatively thin, 0.3–0.6 mm in diameter, randomly arranged with about 11–12 pits longitudinally and 5–7 pits transversally (about 60–65 pits per face). Pits spiny not protrude beyond the wall. Ridges faintly apparent, rounded, delimiting a pseudo-reticulum at the surface enclosing numerous areoles. Vasculature free, endocarp primary vascular strand outside the endocarp wall. Endocarp possessing a symmetrical pair of pores, positioned eccentrically and subapically on the apical endocarp faces. Endocarp wall 615–684 µm thick (ridges height insignificant, about 250 µm including pits). Endocarp wall (excluding pits) composed of packed interlocking digitate and sclerotic cells with globally three stratified units: the outermost unit with 10–11 rows of anticlinally oriented cells, 22.0–38.0 µm in width, followed by a unit with 17–18 rows of periclinally oriented cell, cells 11.7–21.9 µm in width and with a multi-layered cell wall occasionally with an uni-layered cell wall. The innermost unit of one row of periclinally oriented cells, cells 4.3–7.3 µm in width and with a uni-layered cell wall, lining the locule surface with inflated cells. Locule with rounded protuberances due to the thickening of the wall under the pits.

Studied specimen *W.S. Kurz s.n., Malaysia, s.d., MNHN-P-P00868411*; A. D. E. Elmer 21444, Borneo, s.d., MNHN-P-P04513389.

***Phytocrene hirsuta* Blume**

Plate XVI. 17–24

Fruit drupe elliptical, with a symmetrical and accrescent apex elongate, laterally compressed, red when mature, epicarp pilose with a cluster of yellow-red hairs. Mesocarp thin but thick at the accrescent part when dry. Calyx not persistent. Length 30–45 mm, width 15–20 mm, thickness 15–16 mm.

Endocarp brown in color, bilaterally symmetrical, unilocular, single-seeded, elliptical in lateral view, lenticular in transverse section, length 20–35 mm, width 16 mm, thickness 11 mm. No clear keel surrounds the endocarp in the plane of symmetry, but trace of keel present in the upper part. Apex asymmetrical slightly emarginate in lateral view, base rounded, symmetrical. Outer part of the endocarp pitted and ridged. Pits circular, thin, 0.4–0.8 mm in diameter, randomly arranged with about 13–14 pits longitudinally and 8–11 pits transversally (about 145–150 pits per face). Pits mainly spiny and occasionally capitate not protrude beyond the wall. Ridges large and flattened, diffuse, with three main ridges longitudinally (8-10 counting all longitudinal ridges), the median ridge reaches a sub-basal area and runs up to the 2/3 of the endocarp length; the two lateral ridges run from the apex and are interconnected together in the sub-apical point which have a pore, become diffuse and faintly apparent in the ½ of the endocarp length with some transversal and longitudinal free-ending ridges interconnected. Vasculature free, endocarp primary vascular strand outside the endocarp wall. Endocarp wall 1035–1055 µm thick excluding pits. Detail of wall unknown. Locule surface with inflated cells. Locule with rounded protuberances due to the thickening of the wall under the pits.

Studied specimen *O. Beccari HB.2497/98, Celebes, 1874, L.2289338 (L).*

Phytocrene macrophylla (Blume) Blume

Plate XVII. 1–9

Fruit drupe, elliptical, with a symmetrical and accrescent apex elongate, laterally compressed, red when mature, epicarp pilose with a cluster of yellow-red hairs. Mesocarp 330–400 µm thick but thicker at the accrescent part when dry. Calyx not persistent. Length 55–130 mm, width 19–30 mm.

Endocarp cream in color, bilaterally symmetrical, unilocular, single-seeded, oblong in lateral view, lenticular in transverse section, length 40–60 mm, width 13.3–25.0 mm, thickness 8–20 mm. No clear keel surrounds the endocarp in the plane of symmetry, but trace of keel present in the upper part. Apex asymmetrical, emarginate in lateral view, base acute, slightly asymmetrical. Outer part of the endocarp pitted and ridged. Pits primary longitudinally elongate, occasionally two pits are merged, 0.4–1.0 mm in diameter, more or less longitudinally arranged, with about 11–12 pits longitudinally and 7–9 pits transversally (about 90–105 pits per face). Pits shortly rounded, not protrude beyond the wall. Ridges rounded limited to two laterals ridges not branched, solely present at the 1/3 apical part of the endocarp length. The two lateral ridges reach the apex and are interconnected in a sub-apical point, which shows a pore. Endocarp primary vascular strand outside the endocarp wall. Endocarp wall 550–660 µm thick excluding pits (285 μm thick including pits). Endocarp wall (excluding pits) composed of packed interlocking digitate and sclerotic cells with globally three stratified units: the outermost unit with about 10–16 rows of anticlinally oriented cells, cells 15.5–23.3 μm in width, followed by a unit with about 13–19 rows of periclinally oriented cells, cells 10.5–12.6 μm in width. The innermost unit of one row of periclinally oriented cells, cells 8.2–9.02 μm in width, lining the locule surface with inflated cells. Locule with rounded protuberances due to the thickening of the wall under the pits.

<u>Studied specimen</u> *J. & M.S. Clemens 26544 Bis, Borneo, 1931, L.2289632 (L)*; A. D. E. Elmer 15960, Philippine, 1916, MNHN-P-P04513397.

Phytocrene oblonga **Wall.**

Plate XVII. 10–18

<u>Fruit</u> drupe, obovoid, symmetrical and accrescent at the apex, laterally compressed, red when mature, epicarp pilose with long and thin yellow hairs. Mesocarp thin but thicker in the accrescent part when dry. Calyx not persistent. Length 30–44 mm, width 15.0–25.0 mm, thickness 9–10 mm.

<u>Endocarp</u> brown in color, bilaterally symmetrical, unilocular, single-seeded, elliptical to oblong in lateral view, lenticular in transverse section, length 26.5 mm, width 12.3 mm, thickness 7 mm. No clear keel surrounds the endocarp in the plane of symmetry. Apex asymmetrical in lateral view, base rounded, slightly symmetrical. Outer part of the endocarp pitted. Pits elongate longitudinally (areole-like shape), about 1.4–2.8 mm length, representing most of the surface of the endocarp, more or less organized longitudinally with about 12 pits longitudinally and 7–12 pits transversally (about 81–105 pits per face). Pits not protrude beyond the wall. Endocarp primary vascular strand outside the endocarp wall. Endocarp possessing a symmetrical pair of horn-like protrusions compressed on the keel, positioned eccentrically and subapically on the apical endocarp faces each with a central pit. Endocarp wall about 542–591 μm thick excluding pits (about 200 μm thick including pits). Endocarp wall (excluding pits) composed of packed interlocking digitate and sclerotic cells with globally three stratified units: the outermost unit with about 17 rows of anticlinally oriented cells, cells 10.3–19.3 μm in width and apparently with an uni-layered cell wall (at least in the first cell row), followed by about 4 rows of periclinally oriented cells, cells 13.9–18.6 μm in width and with a multi-layered cell wall. The innermost unit of one row of periclinally oriented cells, cells 17.0–29.8 μm in width and with a uni-layered cell wall, lining the locule surface with the inflated cells. Locule with rounded protuberances due to the thickening of the wall under the pits.

Studied specimen *No voucher*; A. Chevalier 1499, Indochine, 1920, MNHN-P-P04513413.

Phytocrene palmata **Wall.**

Plate XVII. 19–26

Fruit drupe ovoid, slightly asymmetrical and accrescent at the apex, laterally compressed, yellow when mature, epicarp pilose with a cluster of hairs. Mesocarp thin but thicker in the accrescent part when dry. Calyx not persistent. Length 35–55 mm, width 16–25 mm, thickness about 13 mm.

Endocarp brown in color, bilaterally symmetrical, unilocular, single-seeded, ovoid in lateral view, lenticular in transverse section, length 29.3 mm, width 18 mm, thickness 13 mm. A keel surrounds the endocarp in the plane of symmetry. Apex slightly asymmetrical in lateral view, base rounded, symmetrical. Outer part of the endocarp pitted and faintly ridged. Pits circular, occasionally elongate, thin, 0.3–0.8 mm in diameter, randomly arranged with about 11–13 pits longitudinally and 8–11 pits transversally (about 168–178 pits per face). Pits spiny to shortly rounded, not protrude beyond the wall. Ridges rounded limited to two laterals ridges not branched, solely present at the 1/3–1/2 apical part of the endocarp length. The two lateral ridges reach the apex and are interconnected in the sub-apical point, which have on a horn-like protrusion with a central pit. Endocarp primary vascular strand outside the endocarp wall. Endocarp wall 594–627 µm thick excluding pits (300–400 µm thick including pits). Endocarp wall (excluding pits) composed of packed interlocking digitate and sclerotic cells, with globally three stratified units: the outermost unit with about 14 rows of anticlinally oriented cells, cells 22.3–34.6 µm in length, followed by a unit with about 5 rows of periclinally oriented cells, cells 15.8–22.9 µm in width. The innermost unit of one row of periclinally oriented cells, cells about 11 µm in width and with an uni-layered cell wall, lining the locule surface with inflated cells. Locule with rounded protuberances due to the thickening of the wall under the pits.

Studied specimen *Jacobs 8155 (MO).*

Pleurisanthes **Baill.**

Plate XVIII. 1–9

Fruit drupe elliptical, acuminate and slightly accrescent at the apex, red when mature, epicarp pubescent with small ovoid hairs with an acuminate apex, rugose-ridged when dry. Calyx not persistent.

Endocarp cream in color, tomentose, bilaterally symmetrical, unilocular, single-seeded, elliptical in lateral view, lenticular to globular in transverse section. A channel surrounds the endocarp in the plane of symmetry. Apex slightly asymmetrical in lateral view, base symmetrical.

Outer part of the endocarp with irregular and longitudinal rugosities spaced by longitudinal folds. Dense long and yellow-white hairs cover the surface. Vasculature of the endocarp resting between the rugosities. Endocarp primary vascular strand outside the endocarp wall. Endocarp wall composed of packed interlocking digitate and sclerotic cells at least one unit with rows of periclinally oriented cells and another with row of anticlinally oriented cells. Locule surface smooth, widely lacunate.

Pleurisanthes flava **Sandwith**

Plate XVIII. 1–9

Fruit drupe elliptical, acuminate and slightly accrescent at the apex, red when mature, epicarp pubescent with small ovoid hairs with an acuminate apex, rugose-ridged when dry. Mesocarp 131–163 µm thick when dry. Calyx not persistent. Length 11.0–12.7 mm, width 9.0–10.2 mm, thickness 8.0–8.5 mm.

Endocarp cream in color, tomentose with long and simple hairs forming a “layer” in transversal view of about 200 µm thick, bilaterally symmetrical, unilocular, single-seeded, elliptical in lateral view, lenticular to globular and folded in transverse section, length 11.6 mm, width 10.2 mm, thickness 8.6 mm. A channel surrounds the endocarp in the plane of symmetry. Apex asymmetrical in lateral view with a central pit in apical view, base rounded, symmetrical. Outer part of the endocarp rugose with some elongate and large mounds organized in 4–5 longitudinal lines separated by four channels. Vasculature resting into the channels. Endocarp primary vascular strand in the channel surrounding the endocarp. Endocarp wall 260–353 µm thick with and without mounds, (a fold of the wall mainly forms the rugosities not by thickening). Endocarp wall composed of packed interlocking digitate and sclerotic cells with globally two multicellular units: the outermost unit with 6–7 rows of anticlinally oriented cells, cells 24.7–57.2 µm in length, and the innermost unit with 2–3 rows periclinally oriented cells, cells 9.5–17.3 µm in width. Locule smooth, highly lacunate.

Studied specimen *J. J. Pipoly 10168, Guyana, 1987, MNHN-P-P05279044.*

Pyrenacantha **Hook.**

Plate XVIII. 10–27, Plate XIX–XXV, Plate XXVI. 1–9

Fruit drupe elliptical to globular, apex accrescent elongate, sometimes widely inflated, laterally compressed or not, yellow to black when mature, epicarp pubescent to pilose composed of simple, small ovoid with an acuminate apex, long and thin or uncinate hairs, yellow, occasionally red or white; occasionally ridged when dry. Calyx absent or persistent often separated from the fruit by a gynophore more or less extended.

Endocarp brown to cream in color, bilaterally symmetrical, unilocular, single-seeded, elliptical-ovoid to globular, rarely triangular in lateral view, lenticular to globular in transverse section. A keel, more or less visible, surrounds the endocarp in the plane of symmetry. Apex asymmetrical in lateral view, base symmetrical. Outer part of the endocarp pitted and ridged delimiting a reticulate pattern, which in general surround the pits, more or less marked. Sometimes the ridges are no longer visible except at the apex. Pits more or less circular, in longitudinal lines or random, being associated with a tubercle, which protrude beyond the wall with various shapes, spiny, peg-shaped, cylindrical or longitudinally elongate. Vasculature of the endocarp free. Endocarp primary vascular strand outside the endocarp wall. Endocarp wall composed of packed interlocking digitate and sclerotic cells with at least one layer with rows of periclinally oriented cells. Locule surface often with regularly spaced and rounded to large papillae, occasionally only present at the apex of the tubercle, smooth in some cases, not clearly lacunose.

Key of species

1	Endocarp elliptical-ovoid, obovoid or globular in lateral view	2
+	Endocarp triangular in lateral view	*Pyrenacantha macrocarpa*
2	Tubercle < or = 1 mm elongate-flattened or peg-shaped	3
+	Tubercle > 1 mm spiny or cylindrical	4
3	Tubercle peg-shaped	5
+	Tubercle elongate-flattened shape	6
4	Tubercle spiny	7
+	Tubercle cylindrical	8
5	Locule surface smooth, tubercle capitate at the apex, often bifid	*Pyrenacantha klaineana*
+	Locule surface papillae, tubercle with apex not elaborated	9
6	Endocarp ovoid to globular in lateral view, less than 50 pits per face	10
+	Endocarp elliptical to ob-ovoid, more than 50 pits per face	11
7	Pits on the surface small, max. 400 µm, tubercle apex not elaborated	12
+	Pits on the surface wider, max. 1450 µm, tubercle apex capitate or not	13
8	Endocarp 9 mm length with diffuse ridges	*Pyrenacantha sylvestris*
+	Endocarp more than 10 mm length with reticulate ridges	14

9 Endocarp with more than 200 pits per face *Pyrenacantha vogeliana*

\+ Endocarp with less than 190 pits per face 15

10 Thickness of the wall 275–325 µm, at least 40 pits per face *Pyrenacantha anhydathoda*

\+ Thickness of the wall 420–500 µm, at last 36 pits per face *Pyrenacantha gossweileri*

11 Endocarp ob-ovoid, 18.5 mm length, with a reticulum of ridges enclosing 37–55 areoles *Pyrenacantha soyauxii*

\+ Endocarp elliptical, 14.8 mm length, with a reticulum of ridges enclosing 5–7 areoles *Pyrenacantha thomsoniana*

12 Endocarp width 15 mm *Pyrenacantha longirostrata*

\+ Endocarp width 7.2 mm 16

13 Thickness of endocarp wall less than 400 µm 17

\+ Thickness of endocarp wall more than 400 µm 18

14 Endocarp length about 19 mm, number of pits more than 100 pits per face *Pyrenacantha laetivirens*

\+ Endocarp length less than 12 mm, number of pits less than 45 pits per face 19

15 Endocarp length about 15.4 mm, thickness of the wall 290–300 µm, about 100 pits per face *Pyrenacantha rakotozafyi*

\+ Endocarp length less than 14.4 mm, thickness of the wall more than 400 µm, more than 120 pits 20

16 Endocarp 11 mm length 21

\+ Endocarp 14 mm length *Pyrenacantha lebrunii*

17 Number of pits per face about 80–93 *Pyrenacantha tropophila*

\+ Number of pits per face about 107–114 *Pyrenacantha capitata*

18 Endocarp lenticular in transverse section, surface ridged and pitted or only pitted 22

\+ Endocarp globular in transverse section, surface only pitted 23

19 Tubercle length more than 2 mm, endocarp length 12 mm, endocarp wall more than 300 µm *Pyrenacantha cordicula*

\+ Tubercle length less than 2 mm, endocarp length 10.8 mm, endocarp wall less than 300 µm *Pyrenacantha staudtii*

20 Ridges sharp, diameter of the surface pits less than 300 µm, pits 170–184 on each face *Pyrenacantha kaurabassana*

\+ Ridges rounded, diameter of the surface pits more than 300 µm, pits 120–140 on each face *Pyrenacantha malvifolia*

21	Endocarp with a prominent median ridge, which cross the endocarp	*Pyrenacantha acuminata*
+	Endocarp without a prominent median ridge, which cross the endocarp	*Pyrenacantha puberula*
22	Endocarp pitted and ridged, with elongate pits	*Pyrenacantha hunblotii*
+	Endocarp pitted only with circular pits	*Pyrenacantha glabrescens*
23	Endocarp pits surfaces 145–150 on each face	*Pyrenacantha ambrensis*
+	Endocarp pits surfaces 159–173 on each face	*Pyrenacantha andapensis*

***Pyrenacantha acuminata* Engl.**

Plate XVIII. 10–18

<u>Fruit</u> drupe elliptical, acuminate and accrescent at the apex, laterally compressed, epicarp pubescent with simple yellow hairs with granular ornamentation, ridged when dry. Mesocarp 192–612 μm thick when dry. Calyx persistent. Length 12–17 mm, width 8–12 mm, thickness 4–8 mm.

<u>Endocarp</u> brown in color, bilaterally symmetrical, unilocular, single-seeded, elliptical in lateral view, lenticular in transverse section, length 11 mm, width 8.4 mm, thickness 5.5 mm. A keel surrounds the endocarp in the plane of symmetry. Apex slightly asymmetrical and acute in lateral view, base rounded, symmetrical. Outer part of the endocarp pitted and ridged. Pits circular and thin, about 0.2–0.3 mm in diameter, randomly arranged with 8–11 pits longitudinally and 8–9 pits transversally (about 93–106 pits per face). Pits being associated with spiny tubercles, protruding into the locule cavity, about 983–1718 μm in length and 352–456 μm in diameter at the base of the tubercle. Number of cells of tubercles 17–18 in width, sclerotic, digitate and elongate. Ridges rounded and thin, more or less diffuse, faintly apparent, with a median prominent ridge running longitudinally from the base up to the apex. Vasculature of the surface free, endocarp primary vascular strand outside the endocarp wall. Endocarp wall 243–302 μm (thick excluding pits). Endocarp wall (excluding pits) composed of packed interlocking digitate and sclerotic cells, with globally three stratified units: the outermost unit is composed of 1–2 rows of isodiametric to periclinally oriented cells, cells 11.8–20.1 μm in width and with a uni-layered cell wall, followed by a unit with 9–11 rows of periclinally oriented cells, cells 7.0–35.6 μm in width and with about 6 layered cell walls. The innermost unit of one row of periclinally oriented cells, cells 9.16–17.0 μm in width and with a uni-layered cell wall, lining the locule surface with inflated to papillate cells. Locule not lacunate.

Studied specimen *R.P. Tisserant s.n., Congo, 1951, MNHN-P-P04495460*; (?) 1863, s.p., 1900, MNHN-P-P04495455; R. Letouzey 9166, Cameroon, 1968, MNHN-P-P04495454.

Pyrenacantha ambrensis **Labat, El-Achkar & R.Rabev**.

Plate XVIII. 19 –27

Fruit drupe, elliptical to globular, accrescent at the apex, brown-orange when mature, epicarp pubescent with small ovoid yellow hairs with an acuminate apex and simple hairs with granular ornamentation, ridged when dry. Mesocarp 480–500 μm thick when dry. Calyx persistent separated from the fruit by an extended gynophore. Length 25–30 mm, width 19–22 mm, thickness 15.0–16.6 mm.

Endocarp brown in color, bilaterally symmetrical, unilocular, single-seeded, elliptical to globular in lateral view, globular in transverse section, length 22.5 mm, width 17 mm, thickness 15 mm. No clear keel surrounds the endocarp in the plane of symmetry, but trace of keel present in the upper part. Apex with an acute protuberance, asymmetrical in lateral view, base rounded, symmetrical. Outer part of the endocarp pitted. Pits circular, occasionally elongate, 0.4–1.4 mm length longitudinally, randomly arranged with 11–12 pits longitudinally and 12–15 pits transversally (about 145–150 pits per face). Pits being associated with spiny tubercles protruding into the locule cavity, about 3–4 mm in length and 647–931 μm in diameter at the base of the tubercle, faintly capitate at the apex. Number of cells of tubercles 26–27 in width, sclerotic, digitate and elongate. Vasculature of the surface free, endocarp primary vascular strand outside the endocarp wall. Endocarp wall 569–601 μm thick (excluding pits). Endocarp wall (excluding pits) composed of packed interlocking digitate and sclerotic cells, with globally three stratified units: the outermost unit with 8–14 rows of anticlinally oriented cells, cells 17.8–50.5 μm in length, followed by 3–9 rows of periclinally oriented cells, cells 17.7–23.7 μm in width. The innermost unit of one row of periclinally oriented cells, cells 0.5–1.4 μm in width and with a uni-layered cell wall, lining the locule surface with regularly spaced and sessile rounded papillae, papillae 7.6–13.1 (avg. 10.6 μm) in diameter, with about 1000 papillae per 0.25 mm^2 . Locule surface not lacunate.

Studied specimen *O. Andrianantoanina & A. Solotiana 62, Madagascar, 1993, MNHN-P-P00440603*.

Remarks: The innermost one row of periclinally cells, which has low width, could be collapsed because of the dry inside the locule.

Pyrenacantha andapensis **Labat, El-Achkar & R.Rabev.**

Plate XIX. 1–9

Fruit drupe, elliptical to globular, accrescent at the apex, laterally compressed, brown-orange when mature, epicarp pubescent with small ovoid yellow hairs with an acuminate apex and simple hairs with granular ornamentation, ridged when dry. Mesocarp 620–1541 µm thick when dry. Calyx persistent separated from the fruit by an extended gynophore. Length 20–26 mm, width 20–26 mm, thickness 17.4–26.0 mm.

Endocarp brown in color, bilaterally symmetrical, unilocular, single-seeded, globular in lateral view, globular in transverse section, length 19.9 mm, width 18.2 mm, thickness 14 mm. No clear keel surrounds the endocarp in the plane of symmetry, but trace of keel present in the upper part. Apex with an acute protuberance, asymmetrical in lateral view, base rounded, symmetrical. Outer part of the endocarp pitted. Pits circular, occasionally elongate, 0.2–1.1 mm length longitudinally, randomly arranged with 10–11 pits longitudinally and 13–15 pits transversally (about 159–173 pits per face). Pits being associated with spiny tubercles protruding into the locule cavity, about 3–4 mm in length and 600–655 µm in diameter at the base of the tubercle, capitate at the apex. Number of cells of tubercles 20–21 in width, sclerotic, digitate and elongate. Vasculature of the surface free, endocarp primary vascular strand outside the endocarp wall. Endocarp wall 512–569 µm thick (excluding pits). Endocarp wall (excluding pits) composed of packed interlocking digitate and sclerotic cells, with globally three stratified units: the outermost unit with about 7–8 rows of anticlinally oriented cells, cells 19.0–29.9 µm in length, followed by 9–10 rows of more isodiametrical or occasionally periclinally oriented cells, cells 21.0–33.5 µm in diameter and with a multi-layered cell wall. The innermost unit of one row of isodiametrical oriented cells, cells 14–18 µm in diameter and with a uni-layered cell wall. Regularly spaced and rounded papillae line the locule surface, 9.7–17 (avg. 13.9 µm) in diameter. Locule surface not lacunate.

Studied specimen *D. Ravelonarivo et al. 72, Madagascar, 1994, MNHN-P-P00440605.*

Pyrenacantha anhydathoda **(Villiers) Byng & Utteridge**

Plate XIX. 10–17

Fruit drupe, ovoid to globular, accrescent at the apex, laterally compressed, red when mature, epicarp pubescent with simple red to yellow hairs with granular ornamentation, ridged when dry. Mesocarp about 100 µm thick when dry. Calyx persistent. Length 34–35 mm, width 12–20 mm, thickness 7–8 mm.

Endocarp brown in color, bilaterally symmetrical, unilocular, single-seeded, ovoid to globular in lateral view, lenticular in transverse section, length 10.6 mm, width 11.4, thickness 5.5 mm. A sharp keel surrounds the endocarp in the plane of the symmetry. Apex acute, asymmetrical in lateral view, base rounded, symmetrical. Outer part of the endocarp pitted and ridged. Pits primary elongate, 0.3–0.9 mm in length longitudinally, randomly arranged with about 5 pits longitudinally and 8 pits transversally (about 40–42 pits per face). Pits being associated with an elongate-flattened tubercles protruding into the locule cavity, about 412–874 μm in length and 400–450 μm in diameter at the base of the tubercle. Ridges rounded and thin, with a median ridge running longitudinally from the point of the apex to the ½ of the endocarp length and then splitted in two parts, merging with two lateral ridges. Ridges delimiting a reticulate pattern with 12–14 areoles. Secondary ridges delimiting small areoles more or less enclosing each pit. Vasculature of the surface free, endocarp primary vascular strand outside the endocarp wall. Endocarp wall 276–326 μm thick excluding ridges (about 460 μm thick including ridges). Endocarp wall (excluding pits) composed of packed interlocking digitate and sclerotic cells, with globally three stratified units: the outermost unit composed of 2–4 rows of anticlinally oriented cells, cells 15.4–27.4 μm in length and with an uni-layered cell wall, followed by a unit with 14–16 rows of periclinally oriented cells, cells 8.0–14.2 μm in width and with a multi-layered cell wall. The innermost unit of one row of periclinally oriented cells, cells 7.7–15.6 μm in width and with a uni-layered cell wall. Regularly spaced and rounded to large papillae line the locule surface, 10.9–18.3 (avg. 14.8 μm) in diameter. Locule surface not lacunate.

Studied specimen *A. P. Teilles (?) 100, Gabonica, s.d., MNHN-P-P04494750*; R.P. Klaine 1571, s.d., 1889, MNHN-P-P00418164.

Pyrenacantha capitata **H.Perrier**

Plate XIX. 18–26

Fruit drupe, elliptical, slightly accrescent at the apex, laterally compressed, epicarp pilose with long and thin yellow hairs, ridged when dry. Mesocarp 360–400 μm thick when dry. Calyx persistent. Length 17–21 mm, width 8–12 mm, thickness 4–6 mm.

Endocarp cream in color, bilaterally symmetrical, unilocular, single-seeded, elliptical in lateral view, lenticular in transverse section, length 17.1 mm, width 10.4 mm, thickness 4.5 mm. No clear keel surrounds the endocarp in the plane of symmetry, but trace of keel present in the upper part. Apex with an acute "protuberance" but flattened laterally, asymmetrical in lateral view, base rounded, symmetrical. Outer part of the endocarp pitted and ridged with only 1–2 longitudinal ridges present in the apical flattened part. Pits circular, occasionally elongate, 0.2–0.6 mm in diameter, more or less randomly arranged with 10–13 pits longitudinally and 8–10 pits transversally (about 107–114 pits per face). Pits being associated with spiny tubercles protruding into the locule cavity, about 1500 μm in length and 420–620 μm in diameter at the base of the tubercle. Number of cells of tubercles 20–23 in width, sclerotic, digitate and elongate. Vasculature of the surface free, endocarp primary vascular strand outside the endocarp wall. Endocarp wall 246–289 μm thick (excluding pits). Endocarp wall (excluding pits) composed of packed interlocking digitate and sclerotic cells, with globally three stratified units: the outermost unit composed of 4–7 rows of anticlinally to isodiametrical oriented cells, cells 15.4–28.9 μm in length and with an uni-layered cell wall, followed by a unit with 9–12 rows of periclinally oriented cells, cells 10.0–11.2 μm in width and with a multi-layered cell wall. The innermost unit of one row of periclinally oriented cells, cells 5.0–9.9 μm in width and with a uni-layered cell wall, lining the locule surface with more or less flattened cells. Locule surface not lacunate.

<u>Studied specimen</u> *F. Ratovoson et al. 678, Madagascar, 2002, MNHN-P-P00440639*; T. Andriamihajarivo et al. 638, Madagascar, 2005, MNHN-P-P06807829.

Pyrenacantha cordicula **Villiers**

Plate XX. 1–9

<u>Fruit</u> drupe, elliptical, slightly accrescent at the apex, laterally compressed, epicarp pubescent with simple yellow hairs with granular ornamentation, ridged when dry. Mesocarp 225–425 μm thick when dry. Calyx persistent separated from the fruit by a small gynophore. Length 17 mm, width 11.6 mm, thickness 9.3 mm.

<u>Endocarp</u> brown in color, bilaterally symmetrical, unilocular, single-seeded, elliptical to ob-ovoid in lateral view, lenticular in transverse section, length 12 mm, width 8 mm, thickness 5 mm. No clear keel surrounds the endocarp in the plane of symmetry, but trace of keel present in the upper part. Apex with an acute “protuberance” laterally flattened, asymmetrical in lateral view, base rounded, symmetrical. Outer part of the endocarp pitted and ridged. Pits primarily elongate, occasionally circular, 0.6–1.3 mm in length, arranged in longitudinal lines with 6–7 pits longitudinally and transversally (about 40–45 pits per face). Pits being associated with cylindrical tubercles protruding into the locule cavity, about 2.5 mm in length and 1 mm in diameter at the base of the tubercle, capitate at the apex. Number of cells of tubercles about 45 in width, sclerotic, digitate and elongate. Ridges rounded and large delimiting a dense reticulum enclosing all pits in an areole. Vasculature of the surface free, endocarp primary vascular strand outside the endocarp wall. Endocarp wall 332–438 μm thick (excluding pits). Endocarp wall (excluding pits) composed of packed interlocking digitate and sclerotic cells, with globally three stratified units:

the outermost is composed of 1–2 rows of isodiametric to periclinally oriented cells, cells 8.6–10.7 µm in width and with a uni-layered cell wall, followed by a unit with about 17 rows of periclinally oriented cells, cells 9.5–25.3 µm in width and with a multi-layered cell wall. The innermost unit of one row of periclinally oriented cells, cells 5.5–5.8 µm in width and with and uni-layered cell wall, lining the locule surface with more or less flattened cells. Locule surface not lacunate.

Studied specimen *M. Etuge & D. Thomas 28, Cameroon, 1986, MNHN-P-P00557873.*

***Pyrenacantha glabrescens* (Engl.) Engl.**

Plate XX. 10–18

Fruit drupe, elliptical, slightly accrescent at the apex, laterally compressed, red when mature, epicarp pubescent with uncinate yellow hairs, slightly ridged when dry. Mesocarp 250–300 µm thick when dry. Calyx persistent separated from the fruit by a small gynophore. Length 24.3–35.0 mm, width 15–18 mm, thickness 10.0–11.4 mm.

Endocarp brown in color, with a cardboard-like texture, bilaterally symmetrical, unilocular, single-seeded, elliptical, lenticular in transverse section, length 21.7 mm, width 13.7 mm, thickness 10 mm. No clear keel surrounds the endocarp in the plane of symmetry, but trace of keel present in the upper part. Apex, asymmetrical in lateral view, base rounded, symmetrical. Outer part of the endocarp pitted. Pits circular, 0.6–1.3 mm in diameter, randomly arranged with 10–12 pits longitudinally and 8–9 transversally (about 60–80 pits per face). Pits being associated with spiny tubercles protruding into the locule cavity. Vasculature of the surface free, endocarp primary vascular strand outside the endocarp wall. Endocarp wall 550–638 µm thick (excluding pits). Endocarp wall (excluding pits) composed of packed interlocking digitate and sclerotic cells, with globally three stratified units: the outermost with 7–8 rows of anticlinally oriented cells, cells 31.3–56 µm in length, followed by a unit with 6–7 rows of periclinally oriented cells, cells 26.2–31.0 µm in width. The innermost unit of one row of periclinally oriented cell, cells 13.8–14.4 µm in width, lines the endocarp. Locule surface not lacunate.

Studied specimen *A. Chevalier 17326, Ivory coast, 1906, MNHN-P-P04495475*; J. de Koning 6802, Ivory Coast, 1976, MNHN-P-P06807655.

Remark: The specimens studied were attacked inside by a saprophytic fungus. This could explain the peculiar texture of the endocarp. Thus, the tubercles are atrophied (see below for preservation issues discussion).

***Pyrenacantha gossweileri* (Exell) Byng & Utteridge**

Plate XX. 19–27

Fruit drupe, ovoid, accrescent at the apex with an inflated cap, which represents the ½ of the length of the fruit, laterally compressed, epicarp strigose with simple yellow hairs with granular ornamentation. Mesocarp 130–140 µm thick when dry. Calyx not persistent. Length 16.0–16.8 mm, width 11.3–16.0 mm, thickness 7.5–12.0 mm.

Endocarp brown in color, bilaterally symmetrical, unilocular, single-seeded, ovoid to globular in lateral view, lenticular in transverse section, length 10.7 mm, width 10.5 mm, thickness 7.1 mm. A sharp keel surrounds the endocarp in the plane of symmetry. Apex acute, asymmetrical in lateral view, base rounded, symmetrical. Outer part of the endocarp pitted and ridged. Pits primary elongate, 0.5–1.7 mm length longitudinally, randomly arranged with about 6 pits longitudinally and transversally (about 33–36 pits per face). Pits being associated with elongate-flattened tubercles protruding into the locule cavity, about 724 µm in length and 716 µm in diameter at the base of the tubercle. Number of cells of tubercles about 15 in width, sclerotic, digitate and not elongate. Ridges rounded and thin, with a median ridge running longitudinally from the point of the apex down to sub-basal area of the endocarp length and two lateral ridges (with two other lateral ridgelets). Ridges delimiting a reticulate pattern with 14–15 areoles. Secondary ridges delimiting small areoles more or less enclosing each pit. Vasculature of the surface free, endocarp primary vascular strand outside the endocarp wall. Endocarp wall 423–498 µm thick excluding ridges (about 700 µm thick including ridges). Endocarp wall (excluding pits) composed of packed interlocking digitate and sclerotic cells, with globally three stratified units: the outermost unit with 3–4 rows of isodiametric to anticlinally oriented cells, cells 10.4–43.2 µm in length and with a uni-layered cell wall, followed by 8–12 rows of periclinally oriented cells, cells 13.0–15.9 µm in width and with a multi-layered cell wall. The innermost unit of one row of periclinally oriented cells, cells 6.3–10.3 µm in width and with an uni-layered cell wall, lining the locule surface with regularly spaced and rounded to large papillae, 14.9–18.8 (avg. 16.1 µm) in diameter. Locule surface not lacunate.

Studied specimen *Y. Attims 42, Congo, 1969, MNHN-P-P04494730.*

***Pyrenacantha humblotii* (Baill. ex Grandid.) Sleumer**

Plate XXI. 1–9

Fruit drupe, elliptical, slightly accrescent at the apex, laterally compressed, red when mature, epicarp pilose-pubescent with simple yellow hairs with granular ornamentation, ridged when dry. Mesocarp 440–560 µm thick when dry. Calyx persistent separated from the fruit by an elongate gynophore. Length 17–22 mm, width 11–20 mm, width 5–13 mm.

Endocarp cream in color, bilaterally symmetrical, unilocular, single-seeded, elliptical in lateral view, lenticular in transverse section, length 17 mm, width 11.7 mm, thickness 7.4 mm. No clear keel surrounds the endocarp in the plane of symmetry, but trace of keel present in the upper part. Apex with an acute "protuberance" laterally flattened, asymmetrical in lateral view, base rounded, symmetrical. Outer part of the endocarp pitted and ridged. Pits primarily elongate, 0.4–1.3 mm in diameter, more or less randomly arranged with 9–13 pits longitudinally and 10–12 pits transversally (about 115–130 pits per face). Pits being associated with spiny tubercles protruding into the locule cavity, about 2021–2883 μm in length and 548–628 μm in diameter at the base of the tubercle, more or less capitate at the apex. Number cells of tubercles 16–20 in width, sclerotic, digitate and elongate. Ridges rounded and large delimiting a dense reticulum enclosing all pits in an areole. Vasculature of the surface free, endocarp primary vascular strand outside the endocarp wall. Endocarp wall 480–566 μm thick (excluding pits). Endocarp wall (excluding pits) composed of packed interlocking digitate and sclerotic cells, with globally three stratified cell units: the outermost with 3–4 rows of isodiametric to anticlinally oriented cells, cells 8.3–12.8 μm in length and with an uni-layered cell wall, followed by a unit with about 13–14 rows of periclinally oriented cells, cells 16.9–56.3 μm in width and with a multi-layered cell wall. The innermost unit of one row of periclinally oriented cells, cells 9.2–11.9 μm in width and with a uni-layered cell wall, lining the locule surface with regularly spaced and rounded papillae, 10.5–20.0 (avg. 15.3 μm) in diameter. Locule surface not lacunate.

Studied specimen *M. Nicoll, P. Lowry & A. Rakotozafy 570, Madagascar, 1987, MNHN-P-P00440635*. REH 334, Madagascar, s.d., MNHN-P-P06637527; Humblot s.n., Madagascar, s.d., MNHN-P-P00440634.

Pyrenacantha kaurabassana **Baill.**

Plate XXI. 10–18

Fruit drupe, elliptical, accrescent at the apex, laterally compressed, epicarp strigose with simple yellow hairs with granular ornamentation. Mesocarp 200–260 μm thick when dry. Calyx persistent separated from the fruit by an elongate gynophore. Length 13–20 mm, width 8.0–9.2 mm, thickness 5–7 mm.

Endocarp cream in color, bilaterally symmetrical, unilocular, single-seeded, elliptical in lateral view, lenticular in transverse section, length 14.4 mm, width 8.2 mm, thickness 6 mm. A keel surrounds the endocarp in the plane of symmetry. Apex with an acute "protuberance" flattened, asymmetrical in lateral view, base rounded, symmetrical. Outer part of the endocarp pitted and ridged. Pits exclusively circular, 0.2–0.3 mm in diameter, more or less longitudinally arranged with

14–18 pits longitudinally and about 10 pits transversally (about 170–184 pits per face). Pits being associated with peg-shaped tubercles protruding into the locule cavity, about 658–700 μm in length and 267–326 μm in diameter at the base of the tubercle. Ridges sharp and thin delimiting a dense reticulum enclosing all pits in an areole. Vasculature of the surface free, endocarp primary vascular strand outside the endocarp wall. Endocarp wall 427–469 μm thick (excluding pits). Endocarp wall (excluding pits) composed of packed interlocking digitate and sclerotic cells, with globally three stratified units: the outermost with 1–2 rows of isodiametric oriented cells, cells 8.0–12.6 μm in length and with an uni-layered cell wall, followed by a unit with 11–12 rows of periclinally oriented cells, cells 15.0–44.3 μm in width and with a multi-layered cell wall. The innermost unit of one row of periclinally oriented cells, cells 8.9–12.2 μm in width and with a uni-layered cell wall, lining the locule surface with regularly spaced and rounded papillae, 12.3–27.8 (avg. 21 μm) in diameter. Locule surface not lacunate.

Studied specimen *A. Gomes e Sousa 1584, Moçambique, 1933, MNHN-P-P04495513.* R.P. Sacleux 787, Côte orientale d'Afrique, 1888, MNHN-P-P04495512; Orège ? , Cap, s.d., MNHN-P-P04495509.

Pyrenacantha klaineana **Pierre ex Exell & Mendonça**

Plate XXI. 19–27

Fruit drupe, elliptical, accrescent at the apex, laterally compressed, black when mature, epicarp pubescent with simple yellow hairs with granular ornamentation, ridged when dry. Calyx persistent separated from the fruit by an elongate gynophore. Length 20–25 mm, width 11–16 mm, thickness 7–9 mm.

Endocarp cream in color, bilaterally symmetrical, unilocular, single-seeded, elliptical in lateral view, lenticular in transverse section, length 17.9 mm, width 9.5 mm, thickness 7 mm. No keel surrounds the endocarp in the plane of symmetry. Apex and base rounded, symmetrical or slightly asymmetrical in lateral view. Outer part of the endocarp pitted. Pits circular, occasionally elongate, 0.1–0.3 mm in diameter, randomly arranged with 18–19 pits longitudinally and 12–17 pits transversally (about 242 pits per face). Pits being associated with peg-shaped tubercles protruding into the locule cavity, about 698–982 μm in length and 388–576 μm in diameter at the base of the tubercle, bifid and/or capitate at the apex. Number of cells of tubercles 16–17 in width, sclerotic, digitate and elongate. Vasculature of the surface free, endocarp primary vascular strand outside the endocarp wall. Endocarp wall 130–185 μm thick (excluding pits). Endocarp wall (excluding pits) composed of packed interlocking digitate and sclerotic cells, with globally two stratified units: the outermost unit with 8–10 rows of periclinally oriented cells, cells 9.2–17.2

µm in width and with a multi-layered cell wall. The innermost unit of one row of periclinally oriented cells, cells 3.6–7.6 µm in width and with a uni-layered cell wall, lining the locule surface. Locule surface not lacunate.

Studied specimen *A. J. M. Leewenber 4523, West Africa, 1962, MNHN-P-P04495495*; R.P. Klaine 1299, Gabon, s.d., MNHN-P-P04495499; R.P. Klaine 1383, Gabon, 1899, MNHN-P-P04495503.

Pyrenacantha laetevirens **Sleumer**

Plate XXII. 1–9

Fruit drupe, elliptical, accrescent at the apex, laterally compressed, epicarp pubescent with simple yellow hairs with granular ornamentation, slightly ridged when dry. Mesocarp 313–566 µm thick when dry. Calyx persistent occasionally separated from the fruit by an elongate gynophore. Length 19–40 mm, width 13–26 mm, thickness 7–20 mm.

Endocarp cream in color, bilaterally symmetrical, unilocular, single-seeded, elliptical in lateral view, lenticular in transverse section, length 18.9 mm, width 12.3 mm, thickness 8 mm. No clear keel surrounds the endocarp in the plane of symmetry, but trace of keel present in the upper part. Apex with an acute "protuberance" laterally flattened, asymmetrical in lateral view, base rounded, symmetrical. Outer part of the endocarp pitted and ridged. Pits primarily elongate, 0.3–1.3 mm length, randomly arranged with about 10 pits longitudinally and 9–10 pits transversally (about 108–115 pits per face). Pits being associated with cylindrical tubercles protruding into the locule cavity, about 1979–2340 µm in length and 675–1085 µm in diameter at the base of the tubercle, more or less capitate at the apex. Number of cells of tubercles 26 in width, sclerotic, digitate and elongate. Ridges faintly rounded to rectangular and large delimiting a dense reticulum enclosing all pits in an areole. Vasculature of the surface free, endocarp primary vascular strand outside the endocarp wall. Endocarp wall 370–400 µm thick excluding pits. Endocarp wall (without pits) composed of packed interlocking digitate and sclerotic cells with globally three stratified units: the outermost unit with about 7 rows of isodiametric to occasionally anticlinally oriented cells, cells 16.1–33.4 µm in length and with an uni-layered cell wall, followed by a unit with about 8 rows of periclinally oriented cells, cells 22.4–34.3 µm and with an uni-layered cell wall. The innermost unit of one row of periclinally oriented cells, cells 5.0–8.3 µm in width, lining the locule surface. Locule surface not lacunate.

Studied specimen *H. Grevé 234, Madagascar, s.d., MNHN-P-P00440649*; H. Perrier De La Bathie 1985, Madagascar, 1923, MNHN-P-P00440648.

***Pyrenacantha lebrunii* Boutique**

Plate XXII. 10–18

Fruit drupe elliptical, acuminate and accrescent at the apex, laterally compressed, epicarp pubescent with simple yellow hairs with granular ornamentation, ridged when dry. Mesocarp 130–300 µm thick when dry. Calyx persistent separated from the fruit by a short gynophore. Length 16.0–18.4 mm, width 9.6–11.0 mm, thickness 3–5 mm.

Endocarp brown in color, bilaterally symmetrical, unilocular, single-seeded, elliptical in lateral view, lenticular in transverse section, length 13.9 mm, width 8.8 mm, thickness 4.1 mm. A keel surrounds the endocarp in the plane of symmetry. Apex slightly asymmetrical and acute in lateral view, base rounded, symmetrical. Outer part of the endocarp pitted and ridged. Pits circular, occasionally elongate, 0.2–03 mm in diameter, randomly arranged with 9–11 pits longitudinally and about 8 pits transversally (about 105–107 pits per face). Pits being associated with spiny tubercles, protruding into the locule cavity, about 836–1500 µm in length and about 500 µm in diameter at the base of the tubercle. Number of cells of tubercles about 22 in width, sclerotic, digitate and elongate. Ridges rounded and thin, more or less diffuse, enclosing 4–5 areoles, faintly apparent, with a ridge running longitudinally from the base up to the apex. Vasculature of the surface free, endocarp primary vascular strand outside the endocarp wall. Endocarp wall 221–280 µm thick excluding ridges (370–455 µm including ridges). Endocarp wall (excluding pits) composed of packed interlocking digitate and sclerotic cells, with globally three stratified units: the outermost unit with about 2 rows of isodiametrical oriented cells, cells 11.3–22.2 µm in length and with an uni-layered cell wall, followed by a unit with about 11 rows of periclinally oriented cells, cells 16.3–33.2 µm in width and with a multi-layered cell wall. The innermost unit of one row of periclinally oriented cells, cells 7.5–15.5 µm in width and with a uni-layered cell wall, lining the locule surface with more or less inflated-papillate cells. Locule surface not lacunate.

Studied specimen F.J. Breteler 2933, Cameroon, 1962, MNHN-P-P04472184.

***Pyrenacantha longirostrata* Villiers**

Plate XXII. 19–25

Fruit drupe, elliptical, accrescent at the apex, laterally compressed, red when mature, epicarp pubescent with uncinate yellow hairs. Length 28–35 mm, width 16–20 mm, thickness 6–8 mm.

Endocarp brown in color, bilaterally symmetrical, unilocular, single-seeded, elliptical in lateral view, lenticular in transverse section, width 15 mm, thickness 6 mm. A keel surrounds the endocarp in the plane of symmetry. Apex slightly asymmetrical and acute in lateral view. Outer part of the endocarp pitted and ridged. Pits circular, occasionally elongate, 0.1–0.3 mm in diameter, randomly arranged with 11–12 pits transversally. Pits being associated with spiny tubercles, protruding into the locule cavity, about 1200 μm in length and about 386–472 μm in diameter at the base of the tubercle, apex occasionally bifid. Number of cells of tubercles about 14 in width, sclerotic, digitate and elongate. Ridges rounded and thin apparently diffuse, faintly apparent. Vasculature of the surface free, endocarp primary vascular strand outside the endocarp wall. Endocarp wall 350–400 μm thick excluding ridges (484–534 μm thick including ridges). Endocarp wall (excluding pits and ridges) composed of packed interlocking digitate and sclerotic cells, with globally two stratified units: the outermost unit with about 11 rows of periclinally oriented cells, cells 11.2–32.8 μm in width and with a multi-layered cell wall. The innermost unit of one row of periclinally oriented cells, cells 9.8–16.2 μm in width and with a uni-layered cell wall, lining the locule surface with regularly spaced and rounded papillae, 8.7–15.7 (avg. 13.7 μm) in diameter with about 190 papillae per 0.25 mm^2. Locule surface not lacunate.

Studied specimen *R. Letouzey 14156, Cameroun, s.d., (K).*

Remarks: Endocarp specimen with only the upper part preserved, rare in herbarium sheets.

Pyrenacantha macrocarpa **(A. Chev. ex Hutch. & Dalziel) Byng & Utteridge**

Plate XXIII. 1–8

Fruit drupe, elliptical accrescent at the apex (represented about half of the length), laterally compressed, epicarp pilose with long and thin hairs and simple yellow white hairs with granular ornamentation. Mesocarp thin when dry. Calyx persistent separated from the fruit by a more or less elongated gynophore. Length 42.4–70.0 mm, width 20–25 mm, thickness 9–10 mm.

Endocarp cream in color, bilaterally symmetrical, unilocular, single-seeded, triangular in lateral view, lenticular in transverse section, length 20.6 mm, width 16.4 mm, thickness 9.5 mm. A keel surrounds the endocarp in the plane of symmetry. Apex flattened and slightly asymmetrical with a “protuberance” flattened in lateral view, base rounded almost acute, symmetrical. Outer part of the endocarp pitted and ridged. Pits circular, occasionally elongate, 0.5–1.6 mm in diameter, arranged in longitudinal lines with 9–10 pits longitudinally and 8–9 pits transversally (about 83–84 pits per face). Pits being associated with elongate-flattened tubercles, protruding into the locule cavity, about 710–1084 μm in length and 227–279 μm in diameter at the base of the tubercle. Ridges rounded-rectangular, thin delimiting a dense reticulum enclosing all pits in an areole, especially differentiable to the wall at the apex. Vasculature of the surface free, endocarp primary vascular strand outside the endocarp wall. Endocarp wall 534 μm thick excluding pits.

Endocarp wall (excluding pits) composed of packed interlocking digitate and sclerotic cells, with globally three stratified units poorly preserved. The innermost of one row of periclinally oriented cells, cells 3.3–10.5 µm in width and with a uni-layered cell wall, lining the locule surface with inflated cells. Locule surface not lacunate.

Studied specimen *J. De Koning 4918, Ivory Coast, s.d., BR0000015570635 (Br)*; *N. Lovi 3952, Ivory Coast, 1954, MNHN-P-P04494747;* A. Chevalier 17216, Ivory Coast, 1907, MNHN-P-P00418166; J. Stone, J. Amponsah & M. Chintoh 3421, Ghana, 1999, MNHN-P-P06807826.

Remarks: wall poorly preserved in the studied specimen due to the preparation (see discussion about preservation issues below)

Pyrenacantha malvifolia **Engl.**

Plate XXIII. 9–17

Fruit drupe, elliptical, shortly accrescent at the apex, laterally compressed, epicarp strigose with simple yellow hairs with granular ornamentation, ridged when dry. Mesocarp 450–560 µm thick when dry. Calyx persistent. Length 16 mm, width 10.2 mm, thickness 6.5 mm.

Endocarp cream in color, bilaterally symmetrical, unilocular, single-seeded, elliptical in lateral view, lenticular in transverse section, length 12.6 mm, width 8.7 mm, thickness 6 mm. A keel surrounds the endocarp in the plane of symmetry. Apex acute and asymmetrical in lateral view, base rounded, symmetrical. Outer part of the endocarp pitted and ridged. Pits circular, occasionally elongate, about 0.3 mm in diameter, randomly arranged with 9–14 pits longitudinally and 10–12 pits transversally (about 120–140 pits per face). Pits being associated with peg-shaped tubercles, protruding into the locule cavity, about 625–693 in length, 227–279 µm in diameter at the base of the tubercle. Number of cells of tubercles about 15–16 in width, sclerotic, digitate and shortly elongate. Ridges faintly apparent rounded and diffuse which a median ridge, which runs to the base up to the apex. Vasculature of the surface free, endocarp primary vascular strand outside the endocarp wall. Endocarp wall 440–516 µm (excluding pits). Endocarp wall (excluding pits) composed of packed interlocking digitate and sclerotic cells, with globally three stratified units: the outermost is composed of 2–3 rows of isodiametric to periclinally oriented cells, cells 11.5–17.0 µm in width and with a uni-layered cell wall, followed by a unit with about 15 rows of periclinally oriented cells, cells 10.6–43.6 µm in width and with 6–9 layered cell wall. The innermost unit of one row of periclinally oriented cells, cells 5.7–12.3 µm in width and with a uni-layered cell wall, lining the locule surface with regularly spaced and rounded-large papillae. Locule surface not lacunate.

Studied specimen *P. Polill 475, s.p., 1961,?.*

Pyrenacantha puberula **Boutique**

Plate XXIII. 18–26

Fruit drupe elliptical, acuminate and accrescent at the apex, laterally compressed, epicarp pubescent with uncinate yellow hairs, slightly ridged when dry. Mesocarp 230–312 μm thick when dry. Calyx persistent separated from the fruit by a short gynophore. Length 19.7 mm, width 11.4 mm, thickness 4.6 mm.

Endocarp brown in color, bilaterally symmetrical, unilocular, single-seeded, elliptical in lateral view, lenticular in transverse section, length 11 mm, width 7.2 mm, thickness 4.5 mm. A keel surrounds the endocarp in the plane of symmetry. Apex slightly asymmetrical and acute in lateral view, base rounded, symmetrical. Outer part of the endocarp pitted and ridged. Pits circular, occasionally elongate, about 0.2–0.4 mm in diameter, randomly arranged with 9–11 pits longitudinally and 8–10 pits transversally (about 85–100 pits per face). Pits being associated with spiny tubercles, protruding into the locule cavity, about 977–1100 μm in length and 285–361 μm in diameter at the base of the tubercle. Number of cells of tubercles about 17 in width, sclerotic, digitate and elongate. Ridges rounded and thin, more or less diffuse, faintly apparent, with a median ridge running longitudinally from the base up to the apex. Vasculature of the surface free, endocarp primary vascular strand outside the endocarp wall. Endocarp wall 177–184 μm thick (excluding pits). Endocarp wall (excluding pits) composed of packed interlocking digitate and sclerotic cells, with globally three stratified units: the outermost is composed of 1–3 rows of isodiametric to periclinally oriented cells, cells 7.5–14.6 μm in width and with a uni-layered cell wall, followed by a unit with about 10 rows of periclinally oriented cells, cells 10.2–32.5 μm in width and with a multi-layered cell wall. The innermost unit of one row of periclinally oriented cells, cells 4.1–10.0 μm and with a uni-layered cell wall, lining the locule surface with inflated to papillate cells, 11.2–21.8 (avg. 17.3 μm) in diameter. Locule not lacunate.

Studied specimen *C. Evrard 601, Congo, 1955, BR0000013148430 (BR).*

Pyrenacantha rakotozafyi **Labat, El-Achkar & R.Rabev.**

Plate XXIV. 1–9

Fruit drupe elliptical, slightly accrescent at the apex, laterally compressed, epicarp pubescent with uncinate yellow hairs, ridged when dry. Mesocarp 70–200 μm when dry. Calyx persistent. Length 16.0–18.2 mm, width 9.0–10.8 mm, thickness 5–7 mm.

Endocarp cream in color, bilaterally symmetrical, unilocular, single-seeded, elliptical in lateral view, lenticular in transverse section, length 15.4 mm, width 10 mm, thickness 6.6 mm. A keel surrounds the endocarp in the plane of symmetry. Apex rounded-flattened, asymmetrical in lateral view, base rounded, symmetrical. Outer part of the endocarp pitted and ridged. Pits primarily elongate, 0.2–0.4 in length, arranged in longitudinal lines with 12–14 pits longitudinally and 8–9 pits transversally (about 100–110 pits per face). Pits being associated with peg-shaped tubercles, protruding into the locule cavity, 828–905 µm in length and 311–327 µm in diameter at the base of the tubercle. Number of cells of tubercles about 16 in width, sclerotic, digitate and elongate. Ridges rounded and thin, more or less diffuse, faintly apparent. Vasculature of the surface free, endocarp primary vascular strand outside the endocarp wall. Endocarp wall 288–304 µm thick (excluding pits). Endocarp wall (excluding pits) composed of packed interlocking digitate and sclerotic cells, with globally two stratified units: the outermost unit with about 12 rows of periclinally oriented cells, cells 14.7–32.3 µm in width and with a multi-layered cell wall. The innermost unit of one rows of periclinally oriented cells, cells 4.1–10.0 µm in width and with an uni-layered cell wall, lining the locule surface with inflated cells or regularly spaced and large papillae cells (generally at the apex of the tubercle), 12.5–20.0 µm in diameter. Locule not lacunate.

Studied specimen *F. Barthelat 1764, Mayotte, 2007, MNHN-P-P00631418.*

Pyrenacantha soyauxii **(Engl.) Byng & Utteridge**

Plate XXIV. 10–18

Fruit drupe, elliptical accrescent at the apex and forming an inflated cap (represented about half of the length), laterally compressed, epicarp pilose with long and thin yellow hair. Mesocarp about 100 µm thick when dry. Calyx persistent separated from the fruit by a short gynophore. Length 33–50 mm, width 11.2–26.0 mm, thickness 8.6–12.0 mm.

Endocarp cream in color, bilaterally symmetrical, unilocular, single-seeded, ob-ovoid in lateral view, lenticular in transverse section, length 18.5 mm, width 10.5 mm, thickness 7 mm. A keel surrounds the endocarp in the plane of symmetry. Apex flattened and slightly asymmetrical with a “protuberance” flattened in lateral view, base rounded almost acute, symmetrical. Outer part of the endocarp pitted and ridged. Pits primarily elongate, arranged in longitudinal lines with 10–11 pits longitudinally and 8–9 pits transversally (about 60–70 pits per face). Pits being associated with elongate-flattened tubercles, protruding into the locule cavity, 523–813 µm in length and 554–651 µm in diameter at the base of the tubercle. Number of cells of tubercles 25–26 in width, sclerotic, digitate and not elongate, more or less anticlinal-isodiametric. Ridges rounded, thin delimiting a dense reticulum enclosing all pits in an areole. Vasculature of the surface free, endocarp primary vascular strand outside the endocarp wall. Endocarp wall about 400 µm thick (excluding pits). Endocarp wall (excluding pits) composed of packed interlocking digitate and sclerotic cells, with globally three stratified units: the outermost unit with 4–6 rows of anticlinally oriented to isodiametrical cells, cells 20.5–37.0 μm in length, followed by a unit with 11–13 rows of periclinally oriented cells, cells 7.1–16.2 μm in width. The innermost unit of one row of periclinally oriented cells, cells 5.1–9.0 μm in width and with an uni-layered cell wall, lining the locule surface with regularly spaced and rounded papillae or inflated cells, 9.1–23.7 (avg. 13.9 μm) in diameter with about 1300 papillae/inflated cells per 0.25 mm^2. Locule not lacunate.

Studied specimen *R.P. Klaine 1469, Gabon, 1899, MNHN-P-P04494736*;

***Pyrenacantha staudtii* (Engl.) Engl.**

Plate XXIV. 19–27

Fruit Drupe, ob-avoid, slightly accrescent at the apex, laterally compressed, epicarp pubescent with simple yellow hairs with granular ornamentation, ridged when dry. Mesocarp 350–410 μm thick when dry. Calyx persistent. Length 12–20 mm, width 10–12 mm, thickness 7–9 mm.

Endocarp brown in color, bilaterally symmetrical, unilocular, single-seeded, elliptical to ob-ovoid in lateral view, lenticular in transverse section, length 10.8 mm, width 9 mm, thickness 6.7 mm. No clear keel surrounds the endocarp in the plane of symmetry, but trace of keel present in the upper part. Apex with an acute "protuberance" flattened, asymmetrical in lateral view, base rounded, symmetrical. Outer part of the endocarp pitted and ridged. Pits primarily elongate and arranged in longitudinal lines with 5–7 pits longitudinally and 7–8 pits transversally (about 38–43 pits per face). Pits being associated with cylindrical tubercles, protruding into the locule cavity, about 1.8 mm in length and 0.6 mm in diameter at the base of the tubercle, capitate at the apex. Number of cells of tubercles about 30 in width, sclerotic, digitate and elongate. Ridges rounded and large delimiting a dense reticulum enclosing all pits in an areole. Vasculature of the surface free, endocarp primary vascular strand outside the endocarp wall. Endocarp wall 244–295 μm thick (excluding pits). Endocarp wall (excluding pits) composed of packed interlocking digitate and sclerotic cells with globally two stratified units: the outermost unit with 12 rows of periclinally oriented cells, cells 14.7–21.8 μm thick. The innermost unit of one row of periclinally oriented cells, cells 7.3–9.0 μm in width and with a uni-layered cell wall, lining the locule surface. Locule not lacunate.

Studied specimen *R.P. Tisserant 1737, Congo, 1950, MNHN-P-P04472207*; J. N. Asonganyi 448, Cameroon, 1982, MNHN-P-P05279462; F.J. Breteler 2968, Cameroon, 1962.

Pyrenacantha sylvestris **S.Moore**

Plate XXV. 1–9

Fruit drupe elliptical, acuminate and accrescent at the apex, laterally compressed, brown when mature, epicarp pubescent with simple yellow hairs with granular ornamentation and uncinate yellow-red hairs, ridged when dry. Mesocarp 170–300 µm thick when dry. Calyx persistent. Length 10.2–12.0 mm, width 8.5–12.0 mm, thickness 3.5–5.6 mm.

Endocarp brown in color, bilaterally symmetrical, unilocular, single-seeded, elliptical in lateral view, lenticular in transverse section, length 9 mm, width 7.4 mm, thickness 5 mm. A sharp keel surrounds the endocarp in the plane of symmetry. Apex slightly asymmetrical and acute in lateral view, base rounded, symmetrical. Outer part of the endocarp pitted and ridged. Pits elongate and thin, about 0.1–0.5 mm in length, randomly arranged with 6–7 pits longitudinally and 5–8 pits transversally (about 44–54 pits per face). Pits being associated with cylindrical tubercles, protruding into the locule cavity, about 1307–1549 µm in length and 488–604 µm in diameter at the base of the tubercle, capitate or bifid at the apex. Number of cells of tubercles about 28 in width, sclerotic, digitate and elongate. Ridges rounded and thin, more or less diffuse, faintly apparent, with a median ridge running longitudinally from the base up to the apex. Vasculature of the surface free, endocarp primary vascular strand outside the endocarp wall. Endocarp wall 189–228 µm thick (excluding pits). Endocarp wall (excluding pits) composed of packed interlocking digitate and sclerotic cells, with globally three stratified units: the outermost unit with 2–3 rows of anticlinally to isodiametrical oriented cells, cells 11.8–18.5 µm in length and with a uni-layered cell wall, followed by 9–10 rows of periclinally oriented thick cells, cells 13.1–17.9 µm in width and with a multi-layered cell wall. The innermost unit of one row of periclinally oriented cells, cells 8.4–14.7 µm in width and with a uni-layered cell wall, lining the locule surface with inflated to papillate cells. Locule not lacunate.

Studied specimen *N. Hallé 3598, Gabon, 1964, MNHN-P-P04472269*; J. Florence 2002, Gabon, 1979, MNHN-P-P04472191.

Pyrenacantha thomsoniana **(Bail.) Byng & Utteridge**

Plate XXV. 10–18

Fruit drupe, elliptical, accrescent elongate at the apex (representing 4/5 of the fruit length), laterally compressed, epicarp pilose with long and thin yellow hairs. Mesocarp thin when dry. Calyx persistent separated from the fruit by an elongate gynophore. Length 45–80 mm, width 14–18 mm, thickness 7–12 mm.

Endocarp brown in color, bilaterally symmetrical, unilocular, single-seeded, elliptical in lateral view, lenticular in transverse section, length 14.8 mm, width 11.5 mm, thickness 6.8 mm. A keel surrounds the endocarp in the plane of symmetry. Apex slightly asymmetrical in lateral view, base rounded, symmetrical. Outer part of the endocarp pitted and ridged. Pits circular, occasionally elongate, 0.3–0.6 mm in diameter, randomly arranged with 7–12 pits longitudinally and 9–11 pits transversally (about 74–83 pits per face). Pits being associated with elongate-flattened tubercles, protruding into the locule cavity, 634–761 μm in length and about 670 μm in diameter at the base of the tubercle. Number of cells of tubercles 20 in width, sclerotic, digitate and not elongate, more or less anticlinal-isodiametric. Ridges rounded and thin, with 5–6 ridges longitudinally, the median ridge runs to the base up to the apex. Ridges delimiting a reticulate pattern enclosing 5–7 areoles. Secondary ridges delimiting small areoles more or less enclosing each pits. Vasculature of the surface free, endocarp primary vascular strand outside the endocarp wall. Endocarp wall 376–433 μm thick excluding ridges (520–590 μm thick including ridges). Endocarp wall (excluding pits) composed of packed interlocking digitate and sclerotic cells with globally three stratified units: the outermost unit with 3–6 rows of anticlinally oriented cells, cells 11.9–35.3 μm in length and with an uni-layered cell wall, followed by a unit with 5–9 rows of periclinally oriented cells, cells 9.7–18.6 μm in width and with a multi-layered cell wall. The innermost unit of one row of periclinally oriented cells, cells 6.9–9.9 μm in width and with a uni-layered cell wall, lining the locule surface with regularly spaced and rounded papillae, 7.1–11.2 (avg. 9.1 μm) in diameter, with 650–920 papillae per 0.25 mm^2. Locule not lacunate.

<u>Studied specimen</u> *M. Le Testu 1038, Gabon, 1907, MNHN-P-P04494723*; Equipe ?, Central African Republic, 1947, MNHN-P-P04494725 ; Equipe ? , Central African Republic, 1949, MNHN-P-P04494720.

Pyrenacantha tropophila **Labat, El-Achkar & R. Rabev.**

Plate XXV. 19–26

<u>Fruit</u> drupe, elliptical to globular, accrescent at the apex, brown-orange when mature, epicarp pubescent with long and thin yellow hairs and simple yellow hairs with granular ornamentation, ridged when dry. Length 25–32 mm, width 17–25 mm, thickness 16–18 mm.

<u>Endocarp</u> brown in color, bilaterally symmetrical, unilocular, single-seeded, elliptical to ovoid in lateral view, globular in transverse section, length 20 mm, width 14.1 mm, thickness 12 mm. No clear keel surrounds the endocarp in the plane of symmetry, but trace of keel present in the upper part. Apex with an acute protuberance flattened, asymmetrical in lateral view, base rounded, symmetrical. Outer part of the endocarp pitted. Pits circular, occasionally elongate, 0.7–1.3 mm length longitudinally, randomly arranged with 9–12 pits longitudinally and 8–10 pits transversally (about 80–93 on each face). Pits being associated with spiny-cylindrical tubercles,

protruding into the locule cavity, 2290–2702 µm in length and 992–1264 µm in diameter at the base of the tubercle, capitate at the apex. Number of cells of tubercles 33 in width, sclerotic, digitate and elongate. Vasculature of the surface free, endocarp primary vascular strand outside the endocarp wall. Endocarp wall 374–394 µm thick (excluding pits). Endocarp wall (excluding pits) composed of packed interlocking digitate and sclerotic cells, with globally three stratified units: the outermost unit is composed of 2–5 rows of isodiametric to periclinally oriented cells, cells 7.5–13.0 µm in width and with a uni-layered cell wall, followed by a unit with about 18 rows of periclinally oriented cells, cells 10.8–21.0 µm in diameter and with a multi-layered cell wall. The innermost unit of one row of periclinally oriented cells, cells 10.7–16.5 µm in width and with an uni-layered cell wall, lining the locule surface with regularly spaced and rounded (scarcely large) papillae, 11.8–27.0 (avg. 16.9 µm) in diameter. Locule surface not lacunate.

<u>Studied specimen</u> *H. Perrier de la Bâthie 1746, Madagascar, 1904, MNHN-P-P00441092*; H. Perrier de la Bâthie 1621, Madagascar, s.d., MNHN-P-P00440610.

Pyrenacantha vogeliana **Baill.**

Plate XXVI. 1–9

<u>Fruit</u> drupe, elliptical, accrescent at the apex, red when mature, laterally compressed, epicarp strigose with simple yellow hairs with granular ornamentation. Mesocarp 141–170 µm thick when dry. Calyx persistent. Length 17.4 mm, width 9.2 mm, thickness 7.2 mm.

Endocarp cream in color, bilaterally symmetrical, unilocular, single-seeded, elliptical in lateral view, lenticular in transverse section, length 14.6 mm, width 8.3 mm, thickness 6.6 mm. A keel surrounds the endocarp in the plane of symmetry. Apex with an acute "protuberance" flattened, asymmetrical in lateral view, base rounded, symmetrical. Outer part of the endocarp pitted and ridged. Pits exclusively circular, 0.1–0.2 mm in diameter, more or less longitudinally arranged with 12–18 pits longitudinally and 13–14 pits transversally (about 200–210 pits per face). Pits being associated with peg-shaped tubercles, protruding into the locule cavity, about 852–1057 µm in length and 273–286 µm in diameter at the base of the tubercle. Vasculature of the surface free, endocarp primary vascular strand outside the endocarp wall. Endocarp wall 300–477 µm thick (excluding pits). Endocarp wall (excluding pits) composed of packed interlocking digitate and sclerotic cells with globally two stratified units: the outermost with about 19 rows of periclinally oriented cells, cells 9.0–59.7 µm in width and with a uni-layered cell wall. The innermost unit of one row of periclinally oriented cells, cells 5.7–8.5 µm in width and with a uni-layered cell wall, lining the locule surface with regularly spaced and rounded papillae, 10.0–19.4 (avg. 15 µm) in diameter. Locule surface not lacunate.

<u>Studied specimen</u> *R.P. Sacleux 1873," Côte orientale d'Afrique", s.d., MNHN-P-P04472242;* R.P. Klaine 1803, Gabon, 1900, MNHN-P-P04472246.

Remarks: perhaps an error of identification in herbarium sheet, the global shape of the endocarp could not correspond to other sheets herbarium.

Rhyticaryum **Becc.**

Plate XXVI. 10–25, Plate XXVII, Plate XXVIII. 1–18

<u>Fruit</u> drupe, elliptical, asymmetrical at the apex, laterally compressed, red when mature, epicarp strigose with simple hairs with granular ornamentation or glabrous, ridged when dry. Calyx persistent.

<u>Endocarp</u> brown–cream in color, bilaterally symmetrical, unilocular, single-seeded, elliptical in lateral views, lenticular in transverse section. A keel surrounds the endocarp in the plane of symmetry. Apex asymmetrical in lateral view with a sub-apical pair of pores, occasionally absent, base symmetrical. Outer part of the endocarp ridged, rarely rugose, ridges diffuse, or delimiting a reticulate pattern, enclosing polygonal areoles with freely ending ridgelet. Ridges rounded, occasionally sharp. Vasculatures of the endocarp resting on the ridges. Endocarp primary vascular strand outside the endocarp wall or in a channel on the keel. Endocarp wall composed of packed interlocking digitate and sclerotic cells at least with one unit with rows of periclinally oriented cells and another with rows of anticlinally oriented cells. Locule surface covered by large to rounded and regularly spaced papillae. Locule lacunate.

Key of species

1	Endocarp 28.8–36.3 mm length, thickness of endocarp wall 800–950 µm	*Rhyticaryum macrocarpum*
+	Endocarp less than 23.6 mm length, thickness of endocarp wall less than 600 µm	2
2	Primary endocarp vasculature in a gutter	*Rhyticaryum novoguineensis*
+	Primary endocarp vasculature outside the endocarp wall	3
3	Endocarp ridged reticulate	4
+	Endocarp ridged diffuse	*Rhyticaryum oleraceum*
4	Pores sub-apical present, thickness of endocarp wall less than 250 µm	*Rhyticaryum elegans*
+	Pores sub-apical absent, thickness of endocarp wall more than 300 µm	5

5 Areole 15–21 on each face, thickness of endocarp wall 514–575 μm *Rhyticaryum fasciculatum*
\+ Areoles less than 15 on each face, thickness of endocarp less than 500 μm 6
6 Fruit strigose, endocarp width about 10 mm *Rhyticaryum longifolium*
\+ Fruit glabrous, endocarp width about 13 mm *Rhyticaryum racemosum*

***Rhyticaryum elegans* G.Schellenb.**

Plate XXVI. 10–17

<u>Fruit</u> drupe elliptical, laterally compressed, red when mature, epicarp strigose with simple yellow hairs with granular ornamentation, ridged when dry. Mesocarp 50–72 μm thick when dry. Calyx persistent. Length 16.3–18.0 mm, width 8.2–9.0 mm, thickness 5–7 mm.

<u>Endocarp</u> brown in color, bilaterally symmetrical, unilocular, single-seeded, elliptical in lateral view, lenticular in transverse section, length 15.2 mm, width 7.2 mm, thickness 5.8 mm. A keel surrounds the endocarp in the plane of symmetry. Apex acute, asymmetrical in lateral view, base rounded, symmetrical. Outer part of the endocarp ridged with 2–4 main longitudinal ridges, the median ridge reaching the point of the base. Ridges rounded and thin with a median channel, almost diffuse but enclosing about 6 longitudinal and polygonal areoles with free-ending ridges. Endocarp possessing a symmetrical pair of pores, positioned eccentrically and subapically at the apical end of the median ridge. Vasculature on endocarp surface resting in the channels of ridges, endocarp primary vascular strand outside the endocarp wall. Endocarp wall 174–246 μm thick excluding ridges (280–370 μm thick including ridges). Endocarp wall composed of packed interlocking digitate and sclerotic cells, with globally three stratified units all with a uni-layered cell wall: the outermost unit with 0–2 row(s) of isodiametric-anticlinally oriented cells, cells 15.9–23.5 μm in length, followed by a unit with 8–10 rows of anticlinally oriented cells, cells 18.0–20.9 μm in width. The innermost unit of one row of periclinally oriented cells, cells 6.7–11.0 μm in width, lining the locule surface with regularly spaced and large papillae, 9.1–20.7 (avg. 15.1 μm) in diameter with 500–900 (avg. 637 papillae) per 0.25 mm^2. Locule surface lacunate.

<u>Studied specimen</u> *R. Schlechter 18681, Papouasie, 1908, MNHN-P-P04513302.*

***Rhyticaryum fasciculatum* Becc.**

Plate XXVI. 18–25

<u>Fruit</u> drupe, elliptical, laterally compressed, red when mature, epicarp sparsely strigose with simple yellow hairs with granular ornamentation. Mesocarp thin. Length 13.0–20.5 mm, width 10–15 mm, thickness 7–9 mm.

Endocarp brown in color, bilaterally symmetrical, unilocular, single-seeded, elliptical in lateral view, lenticular in transverse section, length 20.5 mm, width 12.3 mm, thickness 9 mm. A keel surrounds the endocarp in the plane of symmetry. Apex truncate, slightly inflated and asymmetrical in lateral view, base rounded, symmetrical. Outer part of the endocarp ridged with about four ridges longitudinally, the median ridge reaching the point of the base. Ridges rounded and thin with a median channel, enclosing 15–21 polygonal areoles elongate longitudinally with free-ending ridges, some in arbuscle-shape. Vasculature on endocarp surface resting in the channels of ridges, endocarp primary vascular strand outside the endocarp wall. Endocarp wall 514–575 μm thick excluding ridges (751–989 μm thick including ridges). Endocarp wall composed of packed interlocking digitate and sclerotic cells, with globally three stratified units: the outermost unit with about 14 rows of anticlinally oriented cells, cells 24.6–54.4 μm in length and with an uni-layered cell wall, followed by a unit with about 8 rows of periclinally oriented cells, cells 18.1–25.1 μm in width and with 6–7 layered cell wall. The innermost unit of one row of periclinally oriented cells, cells 8.7–11.9 μm in width and with a uni-layered cell wall, lining the locule surface with regularly spaced and large papillae, 7.2–21.0 (avg. 13.9 μm) in diameter with 710 papillae per 0.25 mm^2. Locule surface lacunate.

Studied specimen *Heu Her 4, Indonesia, s.d., K000271837 (K).*

Rhyticaryum longifolium **K.Schum. & Lauterb.**

Plate XXVII. 1–9

Fruit drupe elliptical, asymmetrical at the apex, laterally compressed, red when mature, epicarp strigose with simple red hairs with granular ornamentation, ridged when dry. Mesocarp 110–130 μm thick when dry. Calyx persistent. Length 18.2–25.0 mm, width 11.4–17.0 mm, thickness 7.6–10.0 mm.

Endocarp cream in color, bilaterally symmetrical, unilocular, single-seeded, elliptical in lateral view, lenticular in transverse section, length 16.8–17.0 mm, width 10.7–11.9 mm, thickness 7.6–8.1 mm. A keel surrounds the endocarp in the plane of symmetry. Apex truncate, slightly inflated and asymmetrical in lateral view, base rounded, symmetrical. Outer part of the endocarp ridged with about five longitudinal ridges, the median ridge reaching the point of the base. Ridges sharp to slightly rounded and thin with a median channel, enclosing 7–11 polygonal areoles with small free-ending ridges. Vasculature on endocarp surface resting in the channels of ridges, endocarp primary vascular strand outside the endocarp wall. Endocarp wall 312–445 μm thick excluding ridges (740–840 μm thick including ridges). Endocarp wall composed of packed interlocking digitate and sclerotic cells, with globally three stratified units all with an uni-layered cell wall: the outermost unit with 2–3 rows of anticlinally oriented cells, cells 14.1–20.5 μm in length, followed by a unit with about 13 rows of periclinally oriented cells, cells 15.6–40.3 µm in width. The innermost unit of one row of periclinally oriented cells, cells 10.1–17.4 µm in width, lining the locule surface with regularly spaced and rounded papillae, 9.5–18.8 (avg. 12.7 µm) in diameter with 550 papillae per 0.25 mm^2. Locule surface lacunate.

Studied specimen *Jacobs 9671 (L)* ; *Bowers 84, Papua New Guinea, 1962, L2292735 (L)*; W. Takeuchi & J. Kulang 11657, Papua New Guinea, 1996, MNHN-P-P05279704.

Rhyticaryum macrocarpum **Becc.**

Plate XXVII. 10–18

Fruit drupe, elliptical, laterally compressed, red when mature, epicarp glabrous, ridged when dry. Mesocarp thick, leather-like texture. Calyx apparently not persistent. Length 35–43 mm, width 25–30 mm, thickness 15 mm.

Endocarp brown in color, bilaterally symmetrical, unilocular, single-seeded, elliptical in lateral view, lenticular in transverse section, length 28.8–36.3 mm, width 21.5–28.0 mm, thickness 13.7–14.6 mm. A keel surrounds the endocarp in the plane of symmetry. Apex slightly flattened, asymmetrical in lateral view, base rounded-truncate or cleft at the base, symmetrical. Outer part of the endocarp sparsely rugose and ridged with about 2–5 longitudinal ridges, the median ridge reaching the point of the base and run up to the apex. Ridges rounded and more or less large, enclosing about 0–5 polygonal areoles, occasionally without transversal ridges. Endocarp possessing a symmetrical pair of pores, positioned eccentrically and subapically at the apical end of the median ridge. Endocarp primary vascular strand outside the endocarp wall. Endocarp wall 800–950 µm thick excluding ridges (about 1300 µm thick including ridges). Endocarp wall composed of packed interlocking digitate and sclerotic cells, with globally three stratified units: the outermost unit with about 17 rows of anticlinally oriented cells, cells 16.4–47.7 µm in length and with a more or less multi-layered cell wall, followed by a unit with about 14 rows of periclinally oriented cells, cells 16.4–27.1 µm in width and with a multi-layered cell wall. The innermost unit of one row of periclinally oriented cells, lining the locule surface with regularly spaced and large papillae, 19.4–32.7 (avg. 25.0 µm) in diameter with 400 papillae per 0.25 mm^2. Locule surface lacunate.

Studied specimen *W. Vink 11381, New Guinea, 1961, L2293146 (L); Katik 46856 (MO).*

***Rhyticaryum novoguineense* (Warb.) Sleumer**

Plate XXVII. 19–26

Fruit drupe elliptical, asymmetrical at the apex, laterally compressed, red when mature, epicarp strigose with simple yellow hairs with granular ornamentation, ridged when dry. Mesocarp 120–340 μm thick when dry. Calyx persistent. Length 17.0–21.1 mm, width 13.2–15.0 mm, thickness 5.0–9.2 mm.

Endocarp cream in color, bilaterally symmetrical, unilocular, single-seeded, elliptical in lateral view, lenticular in transverse section, length 19.8 mm, width 12.4–12.5 mm, thickness 8.7 mm. A keel surrounds the endocarp in the plane of symmetry with a central gutter. Apex slightly inflated and asymmetrical in lateral view, base rounded, symmetrical. Outer part of the endocarp ridged with 5–6 ridges longitudinally, the median runs from the point of the base up to the apex. Ridges rounded and thin with a median channel, enclosing about 22 polygonal areoles with small free-ending ridges. Endocarp possessing a symmetrical pair of pores, positioned eccentrically and subapically at the apical end of the median ridge. Vasculature on endocarp surface resting in the channels of ridges, endocarp primary vascular strand inside the gutter in the keel. Endocarp wall 391–405 μm thick excluding ridges (624–654 μm thick including ridges). Endocarp wall structure unknown. Locule surface with rounded papillae, lacunate.

Studied specimen *A. Millar, NGF 40764, Papua New Guinea, 1968, L.2293149 (L).*

Remarks: the structure of the wall has been crushed in the process of material preparation (see below preservation issues).

***Rhyticaryum oleraceum* Becc.**

Plate XXVIII. 1–9

Fruit drupe elliptical, slightly asymmetrical, laterally compressed, red when mature, epicarp glabrous, ridged when dry. Mesocarp 260–270 μm thick when dry. Calyx apparently not persistent. Length 17–26 mm, width 10.0–15.7 mm, thickness 7.4–10.0 mm.

Endocarp cream in color, bilaterally symmetrical, unilocular, single-seeded, elliptical in lateral view, lenticular in transverse section, length 23.6 mm, width 15.7 mm, thickness 8.7 mm. A keel surrounds the endocarp in the plane of symmetry. Apex slightly inflated and asymmetrical in lateral view, base rounded, symmetrical. Outer part of the endocarp ridged with three main ridges longitudinally. Ridges rounded and thin, forming a relaxed diffuse pattern with two ridges reaching the point of the apex and running more or less up to the 2/3 of the length and a median ridge reaching the point of the base up to the 1/3 of the endocarp length. Vasculature on endocarp surface resting in ridges, endocarp primary vascular strand outside the endocarp wall. Endocarp wall 157–188 µm thick excluding ridges (about 420 µm including ridges). Endocarp wall composed of packed interlocking digitate and sclerotic cells, with globally three stratified units: the outermost unit with 5–7 rows of anticlinally oriented cells, cells 17.2–29.4 µm in length and with a uni-layered cell wall, followed by a unit with 2–3 rows of periclinally oriented cells, cells 15.4–24.0 µm in width and with a multi-layered cell wall. The innermost unit of one row of periclinally oriented cells, cells 4.3–6.0 µm in width and with a uni-layered cell wall, lining the locule surface with regularly spaced and large papillae, 8.9–28.3 (avg. 15.0 µm) in diameter. Locule surface lacunate.

Studied specimen *P. Buwalda 4471, Moluccas isld., 1938, L2293162 (L).*

Rhyticaryum racemosum **Becc.**

Plate XXVIII. 10–18

Fruit drupe elliptical, asymmetrical at the apex, laterally compressed, red when mature, epicarp glabrous, ridged when dry. Mesocarp 70–200 µm thick when dry. Calyx persistent. Length 15–18 mm, width 10.0–13.8 mm, thickness 8–10 mm.

Endocarp cream in color, bilaterally symmetrical, unilocular, single-seeded, elliptical in lateral view, lenticular in transverse section, length 17.1 mm, width 13.3 mm, thickness 10 mm. A keel surrounds the endocarp in the plane of symmetry. Apex asymmetrical in lateral view, base rounded, symmetrical. Outer part of the endocarp ridged with three longitudinal ridges, the median ridge reaches the point of the base and runs up to the apex. Ridges sharp and thin with a median channel, delimiting a reticulate pattern enclosing about 10 irregular areoles, each with a free-ending ridge more or less branched. Vasculature on endocarp surface resting in the channels of ridges, endocarp primary vascular strand outside the endocarp wall. Endocarp wall 363–391 µm thick excluding ridges (520–686 µm thick including ridges). Endocarp wall composed of packed interlocking digitate and sclerotic cells, with globally three stratified units: the outermost unit with about 8 rows of anticlinally to isodiametric oriented cells, cells 15.7–28.7 µm in length and with an uni-layered cell wall, followed by a unit with about 11 rows of periclinally oriented cells, cells 8.1–20.0 µm in width and with a multi-layered cell wall. The innermost unit of one row of periclinally oriented cells, cells 5.9–7.4 µm in width and with a uni-layered cell wall, lining the locule surface with regularly spaced and large papillae, 8.0–27.0 (avg. 16.4 µm) in diameter with about 790 papillae per 0.25 mm^2. Locule surface lacunate.

Studied specimen *Royen 3448, New Guinea, 1954, L.2293115 (L).*

Sarcostigma **Wight & Arn.**

Plate XXVIII. 19–32

Fruit drupe elliptical, slightly asymmetrical or symmetrical, laterally compressed, red-black when mature, epicarp pubescent with simple hairs with granular ornamentation or uncinate hairs, occasionally ridged when dry. Calyx persistent or not.

Endocarp cream in color, bilaterally symmetrical, unilocular, single-seeded, elliptical in lateral view, lenticular in transversal view. A keel or a gutter surrounds the endocarp in the plane of symmetry. Apex asymmetrical in lateral view, with a sub-apical pair of horn-like protrusions, which have a central pit, base symmetrical. Outer part of the endocarp rugose, irregular, almost smooth. Vasculatures of the endocarp free. Endocarp primary vascular strand outside the endocarp wall or in a gutter on the keel. Endocarp wall composed of packed interlocking digitate and sclerotic cells with at least one unit with row(s) of periclinally oriented cells and another with rows of anticlinally oriented cells. Locule surface covered by rounded and regularly spaced papillae. Locule lacunate.

Key of species

1 Endocarp globular in transverse section, 13 mm width, endocarp primary vascular strand outside endocarp wall *Sarcostigma paniculata*

\+ Endocarp lenticular in transverse section, 16 mm width, endocarp primary vascular strand in a gutter *Sarcostigma klenii*

Sarcostigma kleinii **Wight & Arn.**

Plate XXVIII. 19–24

Fruit drupe elliptical, laterally compressed, red when mature, epicarp pubescent with simple yellow hairs with granular ornamentation. Mesocarp 313–343 μm thick when dry. Calyx persistent. Length 22–35 mm, width 16–23 mm, thickness 10–15 mm.

Endocarp cream in color, bilaterally symmetrical, unilocular, single-seeded, elliptical in lateral view, lenticular in transverse section, length 21 mm, width 16 mm, thickness 9.9 mm. A gutter surrounds the endocarp in the plane of the symmetry with a median thin ridge. Apex rounded and asymmetrical in lateral view, base rounded and symmetrical. Outer part of the endocarp more or less smooth, slightly rugose with irregular mounds, randomly arranged and faintly apparent. Endocarp possessing a symmetrical pair of horn-like protrusions compressed on the keel, positioned eccentrically and subapically on the apical endocarp faces each with a median pit. A ridgelet reach the horns and runs to the wall transversally and sub-apically. Vasculature on endocarp surface free, endocarp primary vascular strand in the gutter surrounding the endocarp. Endocarp wall 496–513 μm thick excluding rugosities (614 μm thick including rugosities). Endocarp wall composed of packed interlocking digitate and sclerotic cells, with globally three stratified units: the outermost unit with about 13 rows of anticlinally oriented cells, cells 17.6–35.8 μm in length, followed by a unit with 10 rows of periclinally oriented cells, cells 13.0–17.2 μm in width and globally with a multi-layered cell wall, but not the 2–3 last rows. The innermost unit of one row of periclinally oriented cells, cells 5.8–6.1 μm in width and with a uni-layered cell wall, lining the locule surface. Detail of the locule surface unknown.

Studied specimen *King's Collector s.n., 1890, (K)*; DDS_14043, Vietnam, 2008, MNHN-P-P06807860.

Remarks: A fongic attack mask the surface of the locule (see preservation issues bellow).

Sarcostigma paniculata **Pierre**

Plate XXVIII. 25–32

Fruit drupe elliptical, slightly asymmetrical at the apex, laterally compressed, brown-black when mature, epicarp pubescent with uncinate yellow hairs, ridged when dry. Mesocarp 200–250 μm thick when dry. Calyx persistent. Length 30–38 mm, width 15–23 mm, thickness 9.0–13.4 mm.

Endocarp cream in color, bilaterally symmetrical, unilocular, single-seeded, elliptical in lateral view, lenticular to globular in transverse section, length 26.1–27.6 mm, width 12.9–14.0 mm, thickness 10.5–10.8 mm. A keel surrounds the endocarp in the plane of the symmetry. Apex acute, asymmetrical in lateral view, base rounded and symmetrical. Outer part of the endocarp smooth, more or less rugose but faintly apparent. Endocarp possessing a symmetrical pair of horn-like protrusions compressed on the keel, positioned eccentrically and subapically on the apical endocarp face each with a central pit. Vasculature on endocarp surface free, endocarp primary vascular strand outside the endocarp wall. Endocarp wall 474–490 μm thick. Endocarp wall composed of packed interlocking digitate and sclerotic cells, with globally three stratified units: the outermost unit with about 14 rows of anticlinally oriented cells, cells 20.3–40.5 μm in length and with a uni-layered cell wall, followed by a unit with about 7 rows of periclinally oriented cells, cells 16.1–22.4 μm in width and with a multi-layered cell wall. The innermost unit of one row of periclinally oriented cells, cells 6.7–8.7 μm in width and with an uni-layered cell wall, lining the locule surface with regularly spaced and rounded papillae, 12.8–20.6 (avg. 15.7 μm) in diameter with about 1020–1070 papillae per 0.25 mm^2. Locule surface not lacunate.

<u>Studied specimen</u> *E. Poilane 6677, Vietnam, 1923, MNHN-P-P05279454*; DDS_14047, Vietnam, 2008, MNHN-P-P06807857.

***Stachyanthus* Engl.**

Plate XXIX

<u>Fruit</u> drupe, elliptical, acute-acuminate at the apex, laterally compressed, yellow or blue when mature, epicarp strigose to pubescent with simple hairs with granular ornamentation and/or uncinate hairs, rugulate-ridged or smooth when dry. Calyx persistent.

<u>Endocarp</u> cream to brown in color, bilaterally symmetrical, unilocular, single-seeded, elliptical in lateral view, lenticular in transverse section. A keel surrounds the endocarp in the plane of symmetry. Apex asymmetrical, base symmetrical. Outer part of the endocarp pitted and ridged. Pits more or less circular, being associated with conical tubercles. Ridges forming a diffuse pattern, faintly apparent. Vasculatures of the endocarp free. Endocarp primary vascular strand outside the endocarp. Endocarp wall composed of packed interlocking digitate and sclerotic cells, with at least one unit with rows of periclinally oriented cells. Locule surface smooth and lacunate.

Key of species

1	Endocarp 22 mm length, ridges sharp	*Stachyanthus zenkeri*
+	Endocarp < 17 mm length, ridges rounded	2
2	Endocarp length 17 mm, pits per face 150–160	*Stachyanthus donisii*
+	Endocarp length 11 mm, pits more than 180	*Stachyanthus occidentalis*

***Stachyanthus donisii* (Boutique) Boutique**

Plate XXIX. 1–9

<u>Fruit</u> drupe, elliptical, slightly asymmetrical at the apex, laterally compressed, yellow-blue when mature, epicarp strigose with simple yellow hairs with granular ornamentation and uncinate yellow hairs, rugulate when dry. Mesocarp about 200 µm thick when dry. Calyx persistent. Length 17.0–18.6 mm, width 10.0–10.4 mm, thickness about 7 mm.

<u>Endocarp</u> cream in color, bilaterally symmetrical, unilocular, single-seeded, elliptical in lateral view, lenticular in transverse section, length 16.9 mm, width 9.8 mm, thickness 6.3 mm. A keel surrounds the endocarp in the plane of symmetry. Apex acute and asymmetrical in lateral view, base rounded, symmetrical. Outer part of the endocarp pitted and ridged. Pits circular in the

center, most elongate laterally, 0.2–0.6 (avg. 0.3 mm) in diameter, randomly arranged with 12–16 pits longitudinally and 9–11 pits transversally (about 153–155 pits per face). Pits being associated with conical tubercles, protruding into the locule cavity, about 364–418 µm in length and 768–819 µm in diameter at the base of the tubercle. Cells of tubercles sclerotic, digitate and periclinal. Ridges rounded and thin, faintly apparent, with one median ridge reaching the point of the apex and running up to the 1/3 of the endocarp length. Ridges forming a diffuse pattern of ridges interconnected from the median ridge up to the keel, branched in arbuscle-like shape. Vasculature on endocarp surface free, endocarp primary vascular strand outside the endocarp wall. Endocarp wall 110–216 µm thick excluding ridges (about 220 µm thick including ridges). Endocarp wall composed of packed interlocking digitate and sclerotic cells, with globally two stratified units: the outermost composed of about 10–11 rows of periclinally oriented cells, cells 8.3–26.4 µm in width and with a multi-layered cell wall. The innermost unit of one row of periclinally oriented cells, cells 7.7–9.7 µm in width and with a uni-layered cell wall, lining the locule surface. Locule smooth.

Studied specimen *J.H. Laurent 423, Congo, 1948, BR0000005850273 (BR).*

***Stachyanthus occidentalis* (Keay & É. Miège) Boutique**

Plate XXIX. 10–18

Fruit drupe, elliptical, acuminate and asymmetrical at the apex, laterally compressed, epicarp pubescent with simple yellow hairs with granular ornamentation. Mesocarp 201–216 µm thick when dry. Calyx persistent. Length 9.0–12.4 mm, width 6.0–8.5 mm, thickness 3.0–5.4 mm.

Endocarp cream in color, bilaterally symmetrical, unilocular, single-seeded, elliptical in lateral view, lenticular in transverse section, length 11.3 mm, width 8.1 mm, thickness 5.1 mm. A keel surrounds the endocarp in the plane of symmetry. Apex acute and asymmetrical in lateral view, base rounded, symmetrical. Outer part of the endocarp pitted and ridged. Pits circular in the center, most elongate laterally, 0.1–0.3 (avg. 0.2 mm) in diameter, randomly arranged with 12–14 pits longitudinally and 11 pits transversally (about 184 pits per face). Pits being associated with conical tubercles, protruding into the locule cavity, about 244–248 µm in length and 377–382 µm in diameter at the base of the tubercle. Cells of tubercles sclerotic, digitate and periclinal. Ridges rounded and thin, faintly apparent, with one median ridge reaching the point of the apex and running up to the point of the base. Ridges forming a diffuse pattern of ridges interconnected from the median ridge up to the keel. Vasculature on endocarp surface free, endocarp primary vascular strand outside the endocarp wall. Endocarp wall 145–165 µm thick (excluding ridges). Endocarp wall composed of packed interlocking digitate and sclerotic cells, with globally two stratified units: the outermost unit with 9–10 rows of periclinally (occasionally isodiametric-like shape) oriented cells, cells 6.3–24.7 µm in width. The innermost unit of one row of periclinally oriented cells, cells 6.0–11.5 µm in width and with a uni-layered cell wall, lining the locule surface. Locule smooth.

Studied specimen *A. Chervalier 23794, Somalie (?), 1910, MNHN-P-P04495077* ; ? 3104, Ivory Coast, 1955, MNHN-P-P04495080 .

Stachyanthus zenkeri **Engl.**

Plate XXIX. 19–27

Fruit drupe, elliptical, acute at the apex, laterally compressed, epicarp pubescent with uncinate yellow hairs, ridged when dry. Mesocarp 204–264 µm thick when dry. Calyx persistent. Length 24–30 mm, width 14–18 mm, thickness 9–12 mm.

Endocarp brown in color, bilaterally symmetrical, unilocular, single-seeded, elliptical in lateral view, lenticular in transverse section, length 22.3 mm, width 13.8 mm, thickness 8.8 mm. A keel surrounds the endocarp in the plane of symmetry. Apex acute and asymmetrical in lateral view, base rounded, symmetrical. Outer part of the endocarp pitted and ridged. Pits exclusively circular, 0.2–0.3 mm in diameter, more or less organized in longitudinal lines with 14–18 pits longitudinally and 9–10 pits transversally (about 162–164 pits per face). Pits being associated with conical tubercles, protruding into the locule cavity, about 320 µm in length and about 701 µm in diameter at the base of the tubercle. Cells of tubercles sclerotic, digitate and periclinal. Ridges sharp and thin, with three longitudinal ridges, the median ones runs from the point of the base up to the the apex and the two lateral ridges run sub-basally up to the 2/3 of the endocarp length and then are interconnected with the median ridge. Vasculature on endocarp surface free, endocarp primary vascular strand outside the endocarp wall. Endocarp wall 277–477 µm thick excluding ridges (800–960 µm thick including ridges). Endocarp wall composed of packed interlocking digitate and sclerotic cells, with globally three stratified units: the outermost unit with 3–4 rows of isodiametric-anticlinally (mesocarp?) oriented cells, cells 13.5–19.2 µm in width and with an uni-layered cell wall, followed by a unit with 11–12 rows of periclinally oriented cells, cells 18.0–21.4 µm in width and with a multi-layered cell wall. The innermost unit of one row of periclinally oriented cells, cells 6.3–10.0 µm in width and with a uni-layered cell wall, lining the locule surface. Locule smooth.

Studied specimen *Carvalho 3626, Guiana, 1988, MNHN-P-P05030978.*

I.3. Fruit description of Icacinaceae s.l.

Metteniusaceae H. Karst. Ex Schnizl.

Plate XXX, Plate XXXI. 1–15

***Apodytes dimidiata* E.Mey. ex Arn.**

Plate XXX. 1–9

Fruit drupe, black when dry, laterally compressed and elongate in width. Fruit laterally truncate with a fleshy appendage (red but black in dry condition) attached at the truncate part. Epicarp glabrous, ridged when dry. Mesocarp about 80–100 µm thick when dry. Calyx persistent. Length about 6 mm, width about 10 mm, thickness about 3 mm.

Endocarp brown in color, bilaterally symmetrical, unilocular, single seeded, globular-truncate in lateral view, length 5.5 mm, width 7.6 mm. Outer part of the endocarp ridged with rounded diffuse and thin ridges with about 10 ridges laterally expanded. Vasculature on endocarp surface free, endocarp primary vascular strand outside the endocarp wall. Endocarp wall 177–266 µm thick (excluding ridges). A sclerotic mass, about 1.3 mm thick, are developed from the wall in the truncate part of the endocarp. Endocarp wall composed of packed of sclerotic cells with globally two units: The outermost unit with 4–7 rows of more or less anticlinally oriented cells, cells 29–86 µm in width and with a multi-layered cell wall. The innermost unit of one row of periclinally oriented cells, cells 13.0–16.5 µm in width and with a uni-layered cell wall, lining the locule surface, forming ripples (the cells have a triangular shape).

Studied specimen *R. Ranaivojaona et al. 114, Madagascar, 1997, MNHN-P-P05279728*; S.T. Malcomber et al. 1212, Madagascar, 1992, MNHN-P-P00379386; H. Perrier De La Bathie 19254, Madagascar, 1933, MNHN-P-P0044068; M.Y. Ammann, M.C Madiomanana & A.J. Tahinarivo MYA495, Madagascar, 2009, MNHN-P-P05279690; G. Simon, L. Festo & G. Massawe 527, Kenya, 2000, MNHN-P-P04499342.

Remarks: the sclerotic mass in the truncate part could be a mechanical reinforcement due to the connection in this part with the fleshy appendage.

***Dendrobangia boliviana* Rusby**

Plate XXX. 10–17

Fruit drupe, laterally compressed, black when dry, elliptical, epicarp glabrous. Mesocarp about 190 µm thick when dry. Calyx persistent. Length 15–20 mm, width 6.0–10.4 mm, thickness about 6.1 mm.

Endocarp cream in color, bilaterally symmetrical, unilocular, single seeded, elliptical in lateral view, triangular or pyriforme in transverse section, length 14.5 mm, width 8.1 mm, thickness 5.9 mm. A large channel is visible in dorsal view, followed by a keel in ventral view. Apex and base slightly asymmetrical in lateral view. Outer part of the endocarp rugose-granulate, homogeneous. Vasculature on endocarp surface free, endocarp primary vascular strand outside the endocarp wall. Endocarp wall 300–320 µm thick. Endocarp wall composed of packed of sclerotic cells, with globally two units: the outermost unit with 6–8 rows of anticlinally-isodiametrical oriented cells, cells 27.4–38.4 µm in width and with apparently only a uni-layered cell wall, followed by 1-5 rows of periclinally oriented cells, cells 23.8–35.2 µm width and with a multi-layered cell wall, cells in tunnel shape (very elongate cells).

Studied specimen *O. Poncy 2800, Guyane, 2015, MNHN-P-P00784576.*

***Emmotum nitens* (Benth.) Miers**

Plate XXX. 18–27

Fruit drupe, black when dry, globular, epicarp glabrous. Calyx persistent. Length 10–15 mm, width 10–15 mm, thickness 15–18 mm.

Endocarp cream in color, bilaterally symmetrical, trilocular, three seeded, globular in lateral view and transverse section, flattened in the apex-base axis, length 10.4 mm, width 14.9 mm, thickness 15 mm. A keel surrounds the endocarp in dorsal view only. Apex and base flattened in lateral view. Outer part of the endocarp rugose with long and brittle rugosities. Endocarp wall in two part, the outer part, about 400 µm thick (930–1230 µm with rugosities) surrounds the three inner locule wall (350–390 µm thick) surrounding the seeds. The outer part of the endocarp has circular holes piercing the wall, about 110 µm in diameter. Endocarp wall composed of packed, sclerotic, isodiametric and homogeneous cells (inner and outer walls), 59.4–111.9 µm in diameter and with a uni-layered cell wall. Cells punctuate and with spikes inside.

Studied specimen *R. M. Harley & R. Souza 10028, Brazil, 1968, MNHN-P-P05279304*; M. Claussen 1838, Brazil, 1969, MNHN-P-P04513313; R. Quevedo 927, Bolivia, 1993, MNHN-P-P04513320; R. M. Harley et al. 15081, Brazil, 1974, MNHN-P-P04513269; A. Glaziou 22041, Brazil, 1894, MNHN-P-P04513276.

Remarks: the holes piercing the outer part of the wall could be gaz exchange ways between the outer and inner part of the locules. We do not have idea about the significance of the spikes inside the endocarp cells.

Pittosporopsis kerii **Craib**

Plate XXXI. 1–7

Fruit drupe, brown when dry, oblong but slightly oblique, epicarp glabrous. Mesocarp do not covers the apex, forming a circle around the style, 55–80 µm thick when dry, finely reticulate. Calyx persistent. Length 12.8 mm, width 8 mm, thickness 7.9 mm.

Endocarp cream in color, slightly bilateral, unilocular, single seeded, oblong in lateral view, globular in transverse section, length 12 mm, width 7.5 mm, thickness 7.5 mm. Apex acute and asymmetrical, base rounded and symmetrical. Outer part of the endocarp ridged with more than 10 ridges longitudinally. Ridges round and thin, a few or not interconnected. Vasculature free or inside the endocarp wall, occasionally at the base of the wall. Endocarp wall 145–192 µm thick. Endocarp wall composed of 7–9 rows of sclerotic, periclinally oriented, oblong and homogeneous cells, cells 15.5–24.7 µm in width. Inner locule smooth, not lacunate.

Studied specimen *M.F. Newman et al. LAO 831, Laos, 2005, MNHN-P-P05279702.*

Platea parvifolia **Merr. & Chun**

Plate XXXI. 8–15

Fruit drupe, laterally compressed, black when dry, ovoid-elongate, acute at the apex, epicarp glabrous. Mesocarp thin when dry. Length 30–34 mm, width 13.5–15.0 mm, thickness 13.7 mm.

Endocarp brown in color, slightly bilaterally symmetrical, unilocular, single-seeded, elliptical in lateral view, globular in transverse section, length 33.2 mm, width 12.2 mm, thickness 12.5 mm. Apex acute and asymmetrical, base rounded and symmetrical. Outer part of the endocarp rugose with about 62–65 mounds more or less square polygonal with inside a free-ending channel more or less branched. Mounds organized in 3–4 longitudinal lines separated by 2–3 main longitudinal channels. The main channel on each face reaching a pore positioned sub-apically. Vasculature of the endocarp in the channels between mounds and in the channel's mounds. Endocarp wall 500–550 µm thick. Endocarp wall composed of 11–21 rows of sclerotic, periclinally oriented, elongated and homogeneous cells, cells 18.0–44.8 µm in width. Inner endocarp surface smooth not lacunate.

Studied specimen *W. T. Tsang 27299, China, 1936, MNHN-P-P04518074.*

Oncothecaceae Kobuski ex Airy Shaw

Plate XXXI. 16–21

Oncotheca balansae **Baill.**

Plate XXXI. 16–21

Fruit drupe, brown–black when dry, more or less globular, but flattened in the axis apex-base. Epicarp glabrous. Calyx persistent. Length 10.4 mm, width 16.7 mm, thickness 16.7 mm.

Endocarp Brown in color, with five locules and five seeds, globular in transverse section. Outer part of the endocarp smooth. Endocarp wall with two parts, the outer part surrounding the inner locule walls, but outer and inner walls fused and difficult to dissociate. All walls about 2 mm thick, inner endocarp wall (locule) about 200 µm thick composed of crystalliferous cells. Endocarp wall composed of sclerotic cells, with globally two stratified units: the outermost unit with numerous rows of isodiametric cells, cells 28.3–44.0 µm in width, the smallest on the inner part of the endocarp wall. The innermost unit of one row of periclinally oriented cells, cells 2.4–3.3 µm in width, lining the locule surface with inflated and elongate cells.

Studied specimen *H.S. Mackee 37671, New-Caledonia, 1979, MNHN-P-P00180992.*

Remarks: The mesocarp is strongly attached to the endocarp wall. The structure of the endocarp is difficult to break due to the thickness of the endocarp wall.

I.4. Discussion

I.4.1. Diversity of Icacinaceae endocarp

Among all genera of the Icacinaceae, a great diversity is shown here in the epicarp hairs, the mesocarp thickness, the ornamentation of the endocarp, the shape of the tubercle (if present), the structure and the thickness of the endocarp and the nature of the layer lining the locule.

These characters and also others allowed the separation in most cases genera and species (see below and keys for more informations).

Despite these differences, the endocarp traits permit the differentiation of the Icacinaceae s.s. with Icacinaceae s.l. (here now species from *Metteniusaceae*). In particular, the structure of the endocarp wall but also the wall of the endocarp cells gives a good anatomical differentiation. Therefore, we can define some fruit anatomy criteria for the Icacinaceae s.s. affinities. This shows the value of precise descriptions and illustrations of the endocarp anatomy in taxonomy studies and especially in fossil taxonomy applications.

The endocarp length varies from six to 58 mm. This great disparity could be due to a great diversity of habitat niches, a difference of vegetative structuration (tree, shrub or liana) and frugivorous syndrome (Tiffney, 1984), because almost all species of Icacinaceae s.s. are eaten by animals and partially by human beings. In fossil records, we have some endocarps smaller than all modern species, including in this survey as *Iodes sinuosa*, *Iodes parva* (Del Rio et al. 2018), *Iodes germanica* (Knobloch & Mai, 1986*)*, and *Palaeophytocrene hammenii* (Stull et al., 2012). For this last species, it is assumed that this genus is extinct, so the comparison is impossible with extant species. For the three other *Iodes* species, taphonomic processes, especially during the lignitization, could alter the length of the endocarp. However, this low length could also correspond to an adaptation of an extinct habitat or these fossils could reveal an early diversification without frugivorous constraints for *Iodes* genus.

Some surprising shapes or structures in the Icacinaceae fruits and endocarps suppose to consider this family as very diversified in endocarp's shapes. In the most diversified genus, *Pyrenacantha*, we found cap at the apex of the fruits in some species formerly assigned to *Chlamydocarya* Baill., in particular *P. gossweileri*, *P. soyauxii*, *P. macrocarpa* and *P. thomsoniana*. In the flora of Cameroon (Villiers, 1973) from a previous developmental study (Villiers, 1971), this structure was interpreted as from the development of the ovary in a cap, inflated or in tube, whereas this structure was considered in the 19th century as part of the perianth (Baillon, 1874). This may need a complementary developmental study. The cap is often longer than the fruit s.s. especially for *P. thomsoniana*. The potential function of the cap has never been discussed yet. During the process of preparation of the endocarp study, we noticed that *P. soyauxii* remains at the surface of the water, the cap acting as a floating function. This species as many species of *Pyrencantha* is a quite common liana along streams. We can form the hypothesis that this structure, at least when inflated can favor the dispersion of the species by waters.

The hairs on some *Phytocrene* species, particularly *P. borneensis*, *P. bracteata, P. hirsuta* and *P. oblonga* are long, thin and in clusters. These hairs are irritating or very sharp easily penetrating into the skin (Sleumer, 1971 and personal observation). This structure could act as a repulsive apparatus for frugivorous species.

Endocarp of *Pleurisanthes flava* possesses hairs directly attached to it and forming a layer in the upper part in cross section. This trait is apparently not observed in literature. Baillon seems to ignore the shape of the fruit (Baillon, 1874), as well as later Howard in his work about new world genera of Icacinaceae (Howard, 1942). Among the diverse extant flora, the fruits are quickly described, but not this trait (De Roon, 1994, 2003, Duno de Stephano, 2013). Thus, this is the first time that these special hairs in this genus have been highlighted. These hairs could be a diagnostic character for the species or for the genus; however, we have too few specimens for a conclusion.

Cassinopsis ciliata endocarp is thicker than large. In dorsal view (Plate II. 12), we show distinctly the difference of size compared to the lateral view (Plate II. 13). This fruit was earlier represented (Perrier De La Bâthie, 1952), but it seems that there is a confusion between the dorsal view with the lateral view.

We found hairs on the locule surface in *Leretia*, *Lavigeria* and *Cassinopsis madagascariensis.* For this last species, the hairs are different from the two other genera in forming a cluster of large hairs, whereas the hairs in *Leretia* and *Lavigeria* are quite long and thin. In the description of this species and in the flora of Madagascar, there are no mentions of these hairs (Baillon, 1874, Perrier De La Bâthie, 1952). This character is unique in the genus *Cassinopsis* and can be used as a diagnostic character for this species. For *Leretia* the hairs inside the locule were mentioned in literature (Jansen-Jacobs, 1979, Duno de Stephano, 2013) as for the *Lavigeria* genus (Villiers, 1973). *Casimirella,* not studied here, also have hairs on the locule surface (De Roon, 1994). The three genera are phylogenetically close, forming with *Icacina* a clade in molecular phylogeny (Byng et al., 2014, Stull et al., 2015). These characters could be synapomorphic for this group, implying a lost of hairs for *Icacina* in the current phylogenetic framework.

A gynophore, more or less elongate, was shown for *Miquelia* and *Pyrenacantha* genera, often cut by the bagging of the fruits in the herbarium. These two genera are close in the recent phylogeny, but no phylogenetical reconstruction show both genera as sister groups. Thus, it could be one more exemple of convergence rather than a phylogenetical signal. However, the phylogeny of Icacinaceae is, until now, not enough resolved to conclude.

Finally, among all genera of Icacinaceae s.s., *Desmostachys* remains the most variable, as shown in the global key. With the endocarp characters only, it remains difficult to assume that this genus is natural, except considering its trend to have a bulge or a complex apex. In fact, the great diversity of ornamentation and size is very surprising. The original description of *Desmostachys* highlights floral traits to argue the genus' value (Miers, 1852), from specimens native from Madagascar only (*D. planchonianus*). The position of the flowers in the inflorescences is diagnostic for the genus (Villiers, 1973). However, no phylogeny studies including the type species and other species from Africa have been made (Byng et al., 2014, Stull et al., 2015). Indeed, *Desmostachys* is placed in a clade with *Pleurisanthes*, *Alsodeiopsis*, and *Mappianthus* in the Byng and collaborators' study, including *Desmostachys brevipes* (Engl.) Sleumer and *Desmostachys vogelii* (Byng et al., 2014). Contrarywise, *Desmostachys planchionianus* seems to be close to *Natsiatum* (Stull et al., 2015). However, both studies do not use the same data and thus are weakly comparable for the placement of the *Desmostachys* genus. The type species is very different from the other species of the genus and explains in a greater part the variation observed in this genus. Therefore, a global phylogenenetic analysis could be necessary to choose the following two alternatives: (1) the genus is monophyletic and a disjunction of area divided the genus in two kind of shapes; (2) the genus is not monophyletic and we have two different genera: one with the type species and another one with the African species.

I.4.2. Diversity of *Iodes* endocarp

The *Iodes* genus is the only one to have the following three characters: papillae on the inner locule surface, ridged ornamentation on the endocarp and vascular bundle embedded in the endocarp wall. However, *Iodes seguinii* misses these characters. The placement of this species in molecular and/or morphological phylogeny is essential for all conclusions about this genus but morphological evidences seem to argue about the placement of this species in the *Iodes* genus. The flora of China (Peng & Howard, 2008) precises that the endocarp of this species is « smooth, slightly grooved or reticulate ». We do not see any reticulate endocarp for this species; the sample of this shape could be a good key in order to understand morphological changes in this species. This form could be simply due to a lack of sclerotization of the ovary in comparison with other *Iodes* species during the fruit development, which could explain the lack of suture for the vascular bundle and the lack of ridges. Though, without developmental studies this remains a hypothesis. The vascular bundle inside the endocarp wall is rare in Icacinaceae family and frequently used for fossil *Iodes* endocarp identification in fossil records. We also found this character in *Icacina*, *Cassinopsis*, *Lavigeria* and *Leretia*. *Icacina* species have a ridged pattern on the endocarp surface as *Iodes* genus too but *Icacina* species do not have papillae. Thus, we need all three characters to argue about an assignation to the *Iodes* genus. We note that *Icacina* species endocarps were generally longer and wider than those of *Iodes* species and globular in transverse section. This could indicate, in some cases, when the papillae lack in fossil specimens, that the specimen still belongs to the *Iodes* genus. *Iodes* species from Asia differ from African ones by some characters. Asian species posses a pair of horn-like protrusions or pores, are longer in size (Asian species 12.4–33.8 mm vs African species 10.4–12.1 mm) and generally are less reticulate than African species. Reticulation of fossil *Iodes* species is with or without few free-ending ridges inside areoles. In modern *Iodes* species, a reticulate pattern without free ending-ridges is rare. Therefore, we can consider fossil species as belonging to this genus as a unique and extinct form that increases the diversity observed in this group.

I.4.3. Value of the endocarp in species recognition

Some fossil sites provided almost only fruits, endocarp and seeds remains. These remains bring informations about species diversity, flora composition and paleoenvironment parameters. For the Icacinaceae family, most of the fossil records are endocarps. In this work, we compared the diversity between sites of the Paris Basin and we mainly determined some endocarp species. Thus, the value of the endocarp in species recognition is crucial for this survey, which could give us some information about the delimitation of species.

The different keys proposed in this survey show that in almost all cases, the endocarps from different living species are differentiable. However, *Pyrenacantha ambrensis*, *Pyrenacantha andapensis* and *Pyrenacantha tropophila* are identical in almost all characters. They are provided by the same study (Labat et al. 2006) and are very similar in shape. The main characters on the Labat key to differentiate *Pyrenacantha ambrensis* to *Pyrenacantha andapensis* are the texture of the leaves (papyrus-like or coriaceous) or the shape of fruit between *Pyrenacantha andapensis* and *Pyrenacantha tropophila*. Phylogenetic studies are needed to clarify the status of these three species from Madagascar. *Pyrenacantha lebrunii* and *Pyrenacantha puberula* are very similar in endocarp shape and differ mostly by their size. The endocarp sample is reduced and thus it is possible that these endocarps were not discriminable in reality. In the *Pyrenacantha* genus, some different species have the same endocarp shape. However, the shape of the tubercles allows the differenciation of most species. Therefore, with only endocarp material, we can succeed to differentiate a good proportion of species but not all of them; the study of fossil endocarp can therefore underestimate the number of species. However, this is not completely generalizable for other genera. For exemple, the *Phytocrene* and *Iodes* species are all highly differentiable whereas *Rhyticaryum* and *Stachyanthus* are like the *Pyrenacantha* genus with very homogeneous endocarps.

The *Alsodeiopsis* genus shows that the shape of ridges can be a key to differentiate some species. The structuration of the ridges could differentiate species in the *Iodes* genus. The size of the endocarps was an indication for the differentiation of species as for exemple in the *Miquelia* genus; however, this character seems valuable when there is an important gap in the size (see also in *Nothapodytes* genus).

Finally, we also encountered the case where one species has two types of endocarps. For exemple, *Rhyticaryum macrocarpum* shows endocarp with diffuse pattern of ridges and a base cleft on one side (Plate XXVII. 10–13) and another endocarp shows reticulate pattern and rounded base (Plate XXVII. 16). In fossil remains, these two shapes could be interpreted as two close species. We do not encounter this case in other species with two or more endocarps.

To conclude, the endocarp is a good organ to differentiate Icacinaceae species, sometimes with clear characters or with slight variations of a structure. The size is significant when a gap is visible. Nevertheless, we risk more to underestimate than overestimate the number of species in using endocarp remains only.

I.4.4. Stomata and papillae on the locule

We found some stomata on the endocarp locule, especially for the following species: *Pyrenacantha malvifolia* (Fig. I.3, 1), *Rhyticaryum macrocarpum* (Fig. I.3, 2), *Stachyanthus donisii* (Fig. I.3, 3) and *Stachyanthus occidentalis* Fig. I.3, 3). These occurrences have previously been noticed (Potgieter & van Wyk, 1994) for *Pyrenacantha kaurabassana* and *Pyrenacantha grandiflora*.

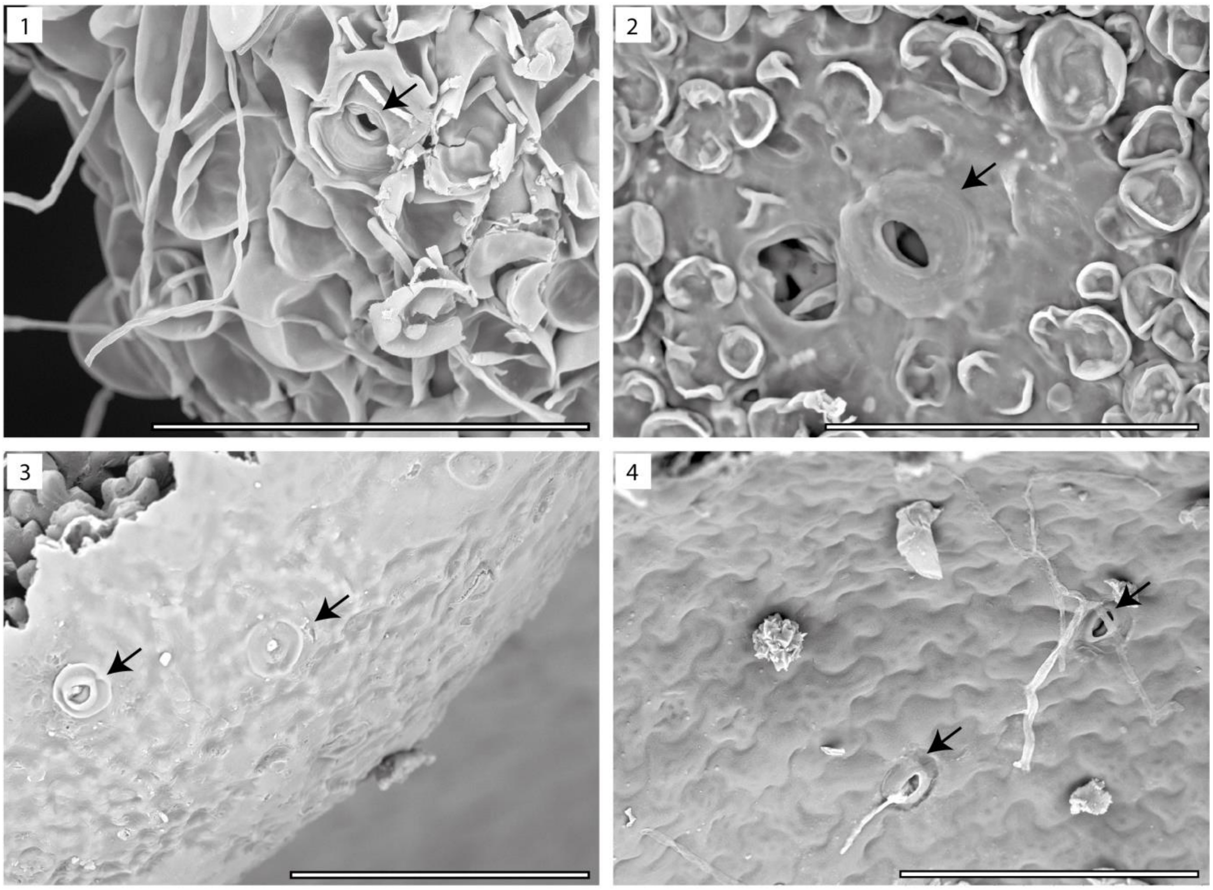

Figure I.3. SEM view of stomata on the locule surface (arrow), *Pyrenacantha malvifolia* (1), *Rhyticaryum macrocarpum* (2), *Stachyanthus donisii* (3), and *Stachyanthus occidentalis* (4). Scale: 100 µm.

We expand here the observation for at least two other genera in the Icacinaceae familly. Potgieter and van Wyk (1994) consider these stomata as gaz exchange apparatus between the outside and inner part of the seed. In particular, the stomata seem to be denser at the apex of the tubercles, which enter into the seed up to the embryo. The observations confirm this hypothesis.

Papillae are often present on the locule of *Pyrenacantha*, especially at the apex of the tubercle but also in others genera, as *Iodes* and *Rhyticaryum*. These papillae are directly linked with the testa or the seed. They consist in a rounded or large swelling of the last cell layer, more or less punctuate. Thus, papillae increase the contact surface between the seed and the endocarp and could have similar gaz transfert function than stomata or nutriment transfert function (pitted wall).

I.4.5. Preservation issue

Among the 88 Icacinaceae s.s. endocarps sectioned for anatomical studies, 15 showed fungi wall and inner locule attacks (17 %). Among all 19 genera studied here, 10 possesses species with fungal attacks: *Desmostachys*, *Hosiea*, *Icacina*, *Iodes*, *Miquelia*, *Natsiatum*, *Phytocrene*, *Pyrenacantha*, *Rhyticaryum* and *Sarcostigma*. This relativly large proportion of attacks remains a problem for anatomical studies due to the limited endocarp resources. In fact, the anatomy of the endocarp was deeply damaged as for exemple for *Pyrenacantha glabrescens* (Plate XX. 16) where the tubercles were atrophied and the endocarp wall was deeply eaten by fungi and having a cardboard texture. Another exemple of catastrophic preservation can be seen in *Natsiatum herpeticum* where the endocarp wall structure is preserved, but not the outer and inner ornamentations (Plate XIV. 19–26, Fig. I.3, 3). This lack of ornamentation could be due to the saprophytic attack that stops the development of the fruit. In our knowledge, these specimens were not related to a special period of collect, the range of collect ranging from 1874 to 1966. In the same way, no precise geographical origin or Herbarium could explain the fungal attacks. We identified two types of fungi: the first, forming oblong and echinulate spores (14/15 cases, Fig I.3. 1), the second, forming rounded and not echinulate spores (only one case, *Pyrenacantha glabrescens*, Fig I.4. 2). Unfortunately, we are unable to identify the responsible fungus. We suppose that the echinate and round form belong to Ascomycota group. Despite the esthetic value of these organisms, the inner surface of the locule that carries some anatomical information was not observable in most cases (Fig. I.4, 3).

A reflexion should begin in the future to decide how to collect and maintain fresh fruits in a good preservation as well as for DNA preservation in the past decade (Chase & Hills, 1991, Gaudeul & Rouhan, 2013, Rouhan & Gaudeul, 2014). Simple ethanol fixing solution could be enough for this purpose, but not always easy to be done on the field. In the fossil record, we also found saprophytic attacks inside the endocarp wall (See chapter III), but we do not found spores associated to the hyphae.

Another problem, but less frequently encountered in this study, is the sample of immature fruit. We collected one immature specimen for *Iodes vitiginea* (Hance) Hance (voucher: J. F. Maxwell 92-328) without clues that indicates it (Fig. I.4, 4). The anatomical study revealed poorly differentiated layers in the pericarp (Fig. I.4, 5) and papillae not well developed (Fig. I.3, 6). Thus, we decided to not include this species in our survey. This kind of errors could be resolved in two different ways: (1) the author of the sample specifies the nature of its material in the herbarium label sheet and/or (2) the author of the sample cut a single fruit and add it in the herbarium material. Several scientists (personal observation in herbarium) have adopted this last solution.

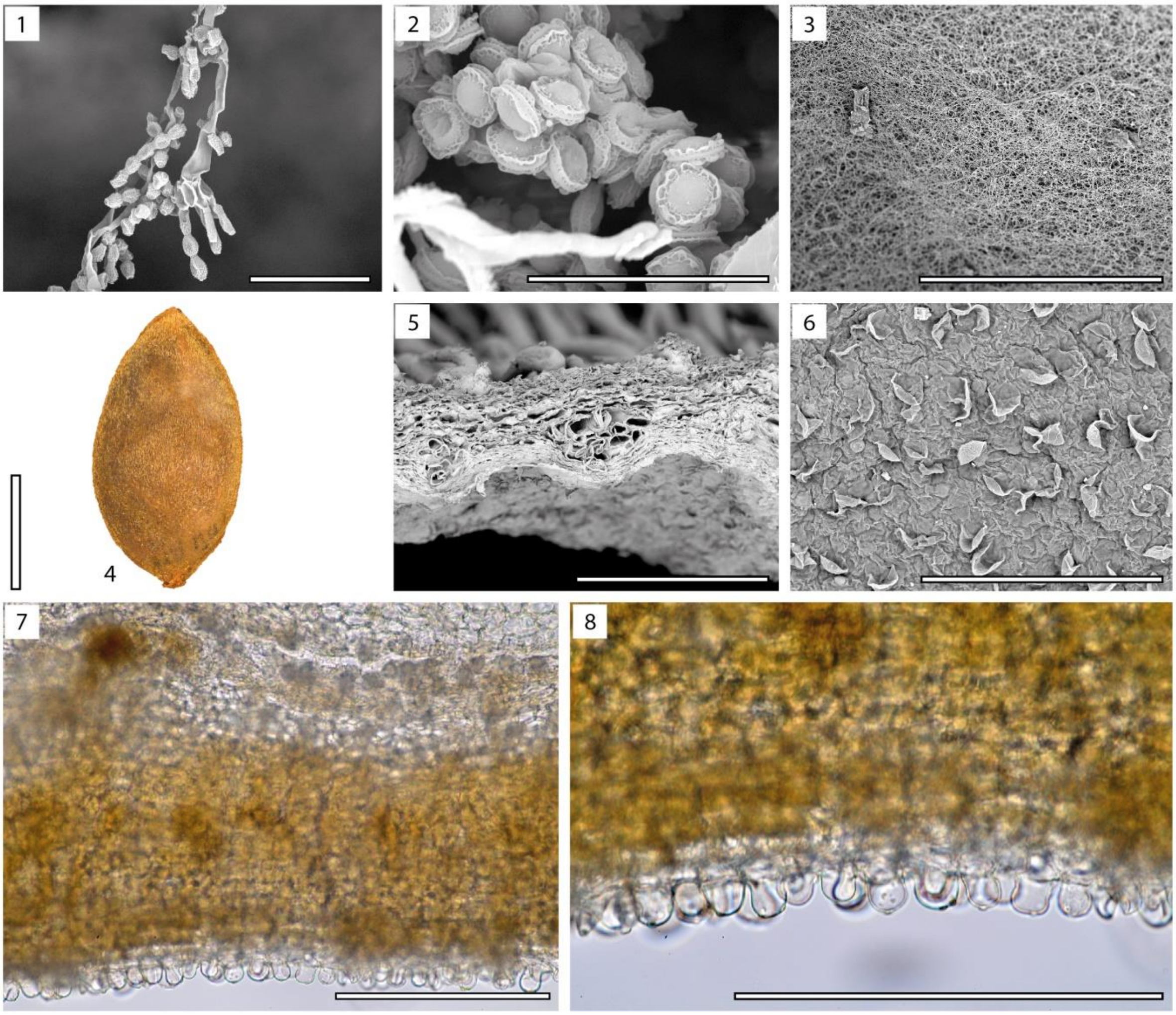

Figure I.4. Preservation issue. Fungal mycellium and echinate spore from *Desmostachys vogelii* (1), fungi rounded spore from *Pyrenacantha glabrescens* (2), dense mycellian filament on the locule from *Natsiatum herpeticum* (3), lateral view of *Iodes vitiginea* (4), SEM view of the pericarp not differentiated from *Iodes vitiginea* in transverse section (5), same showing the papillae on the locule (6), Cross section of *Iodes africana* endocarp view from the microscope (7), same with magnification (8). Scale: 4 = 10 mm ; 3 = 500 µm ; 5–8 = 200 µm ; 1, 2 = 20 µm.

The process in order to study anatomical endocarps could be partially destructive. The best exemple is the scratch of cell wall of the endocarp due to the scalpel use (for exemple for *Phytocrene hirsuta*, Plate XVI. 23, 24). No rule exists about the success of the cut but we think that it depends on the texture of the endocarp and the organisation of the cell wall. Some genera as *Iodes* or *Alsodeiopsis* are easy to cut correctly whereas *Phytocrene* or *Miquelia* are very difficult. In order to guarantee or systematize non-destructive cuts, we tested a technique using microtome instrument after the inclusion of specimens in epoxy resin. This technique, usually used in wood anatomy, allows the preparation of samples for microscopy. The result for *Iodes africana* fruit shows the cells layers (units) and the papillae in transverse section (Fig. I.3, 7, 8). However, the endocarp wall is a hard structure, and we could make only sample of about 50 µm thick for *Iodes africana*. Moreover, the wall of *Iodes africana* is part of the smaller walls in the Icacinaceae family, so potentially easiest than some species to cut. Several cell layers overlap for *Iodes africana* and the result is not very convincing. Another issue is that we destroyed at least half of the specimen in the process.

When we have only one specimen representing one species, this technique does not allow the preparation of transversal view of the pericarp and morphological view of the endocarp together. Further, the technique for preparing specimens is slow and requires several weeks of process. SEM view for living species have the additional advantage to produce the same images as fossil analysis and the materials are directly comparable. We envisioned the use of liquid nitrogen in order to improve the cut of the endocarp, but we could not test this solution.

I.4.6. Limit and prospect

This study aims to give a survey of the Icacinaceae fruits and endocarps. This survey could be useful for paleocarpological studies but also for botanical taxonomy. The fruit has often been neglected in order to establish diagnostic characters. However, we show here that the fruit could be important for discriminate species, genera and families. Despite the intake of information from this survey, the lack of intra-specific variation, especially for the endocarp, is the clear limitation.

We can try to remediate this in encouraging the sampling of fruits and in establishing a protocol of conservation for them as for the DNA in current expeditions. The survey covers only half of Icacinaceae species, an extended effort could be realized in the future studies in order to complete observations and to propose an atlas of all valid species of Icacinaceae. This study shows the value of anatomy in carpological studies. This survey construction could be recycled for other studies focusing on other families.

The keys presented here are "natural" and thus follows a predefined path. In addition, some primary characters for these keys are hard to observe and need intensive anatomical work. To remediate to this, we should use the software Xper^2 (Ung et al. 2010). Indeed, this software allows identifying specimens starting to any characters and could be a good opportunity to propose keys that are more accurate (see Chapter II).

Conclusion of the chapter

This study shows the great diversity of fruit and endocarp in the Icacinaceae family, in particular in term of hairs' shape, the ornamentation of the endocarp, the shape of tubercles, when they are present; the apex structure and the vascularisation. These characters and others allow discriminating almost all species. The digitate cells on the endocarp wall seem to be a good character to differentiate Icacinaceae s.s. from Icacinaceae s.l. now mainly Metteniusaceae. Some particularities are noted, as the presence of hairs in the locule for the *Leretia*, *Lavigeria* and *Cassinopsis* genera, a cap at the apex of some *Pyrenacantha* species, hairs at the surface of the endocarp for *Pleurisanthes* and the presence of gynophores for *Miquelia* and *Pyrenacantha* genera.

The *Iodes* species are easily recognizable by three characters: ridges at the endocarp surface, vascular bundle inside the endocarp wall and papillae on the locule surface. Some genera share one or two of these characters, only the presence of the three characters seem to be diagnostic. However, the global shape of the endocarp could orientate the identification in case of decay.

Stomata, papillae and tubercles were found in the locule surface. These three structures seem to have the same functional aim: allowing gaz exchange between the seed and the exterior.

Some specimens studied in this study were decayed by fungi attack. It is probably possible to pay attention of the sampling of the fruits during expeditions, using a protocol limiting the contamination in the same way as ADN sampling.

Plates

Plate I

Alsodeiopsis mannii Oliv.
(N. Hallé & J. F. Villiers 4579)
1. – Lateral view of the dried fruit.
2. – Lateral view of the endocarp showing a reticulate pattern of ridges.
3. – Dorsal view showing a keel surrounding the endocarp.
4. – Second lateral view.
5. – Apical view.
6. – Basal view.
7. – SEM view of seed and pericarp in transverse section.
8. – Detail showing the mesocarp on the top and the endocarp wall at the bottom.
9. – SEM view of the vascular bundle in a channel (arrow).

Alsodeiopsis poggei Engl.
(P. Sita 1872)
10. – Lateral view of the dried fruit.
11. – Lateral view of the endocarp showing a reticulate pattern of ridges.
12. – Dorsal view showing the keel surrounding the endocarp.
13. – Second lateral view.
14. – Apical view.
15. – Basal view.
16. – SEM view of the simple hairs on the epicarp surface.
17. – SEM view of the endocarp wall in transverse section.
18. – SEM view of the vascular bundle in a channel (arrow).

Alsodeiopsis staudtii Engl.
(J.J.F.E. de Wilde 8304)
19. – Lateral view of the dried fruit.
20. – Lateral view of the endocarp showing a reticulate pattern of ridges.
21. – Dorsal view showing a keel surrounding the endocarp.
22. – Second lateral view.
23. – Apical view.
24. – Basal view.
25. – Lateral view showing the vascularisation on the ridges.
26. – SEM view of the pericarp in transverse section with a vascular bundle (arrow).
27. – SEM view of the simple hairs on the epicarp surface.

Scale: 1–6, 10–15, 19–24 = 10 mm; 7, 25 = 1 mm; 9, 18, 26 = 500 µm; 8, 16, 17, 27 = 200 µm.


1


2


3


4


5


6

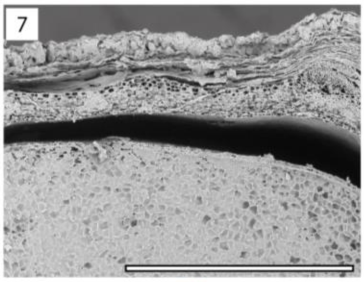
7

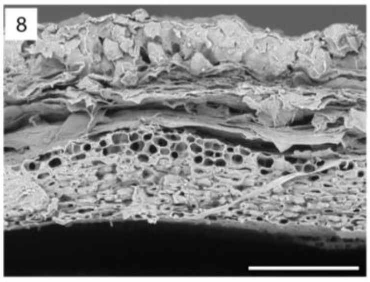
8

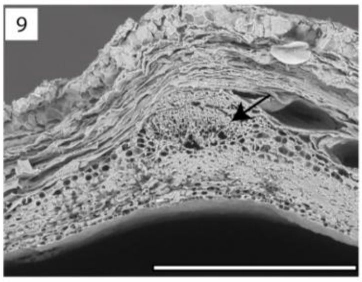
9


10


11


12


13


14


15

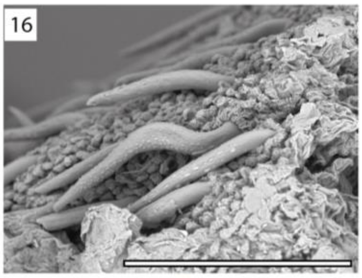
16

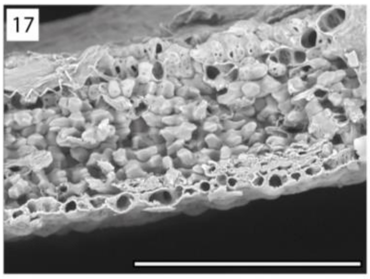
17

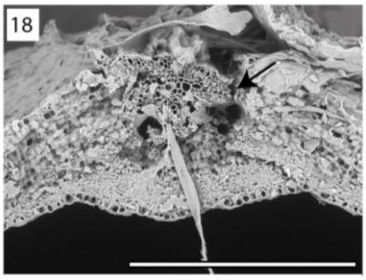
18


19


20


21


22


23


24

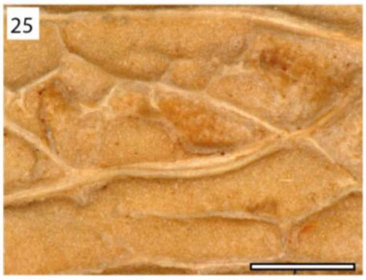
25

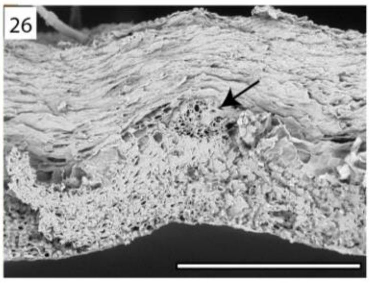
26

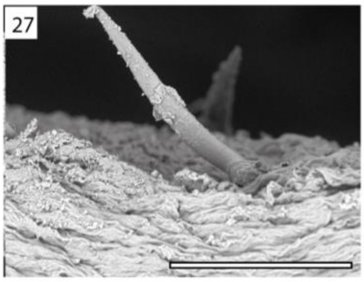
27

Plate II

Alsodeiopsis zenkeri Engl.
(*W.J.J. O. de Wilde 1549)*
1. – Lateral view of the dried fruit.
2. – Lateral view of the endocarp showing a reticulate pattern of ridges.
3. – Dorsal view showing a keel surrounding the endocarp.
4. – Second lateral view.
5. – Apical view.
6. – Basal view.
7. – SEM view of the pericarp in transverse section.
8. – SEM view of simple hairs on the epicarp surface.
9. – SEM view of the vascular bundle in a channel (arrow).

Cassinopsis ciliata Baker
(*H. Perrier De La Bathie 4671)*
10. – Lateral view of the dried fruit.
11. – Lateral view of a broken endocarp showing a reticulate pattern of ridges.
12. – Dorsal view showing the keel surrounding the endocarp.
13. – Second lateral view.
14. – Apical view.
15. – Basal view.
16. – Transverse section of the fruit.
17. – SEM view of the endocarp wall in transverse section.
18. – Detail of the same section showing endocarp cells wall at the center of the wall.

Cassinopsis ilicifolia (Hochst.) Sleumer
(*C.D. Louwsburg 2730*)
19. – Lateral view of the dried fruit.
20. – Lateral view of a part of the endocarp (apex missing).
21. – Dorsal view showing a keel surrounding the endocarp.
22. – Second lateral view.
23. – Basal view.
24. – SEM view of the pericarp in transverse section.
25. – Detail of the same showing the cells wall.

Scale: 1–6, 10–15 = 10 mm; 16, 19–23 = 2.5 mm; 9, 24 = 500 µm; 7, 8, 25 = 100 µm; 18 = 50 µm.

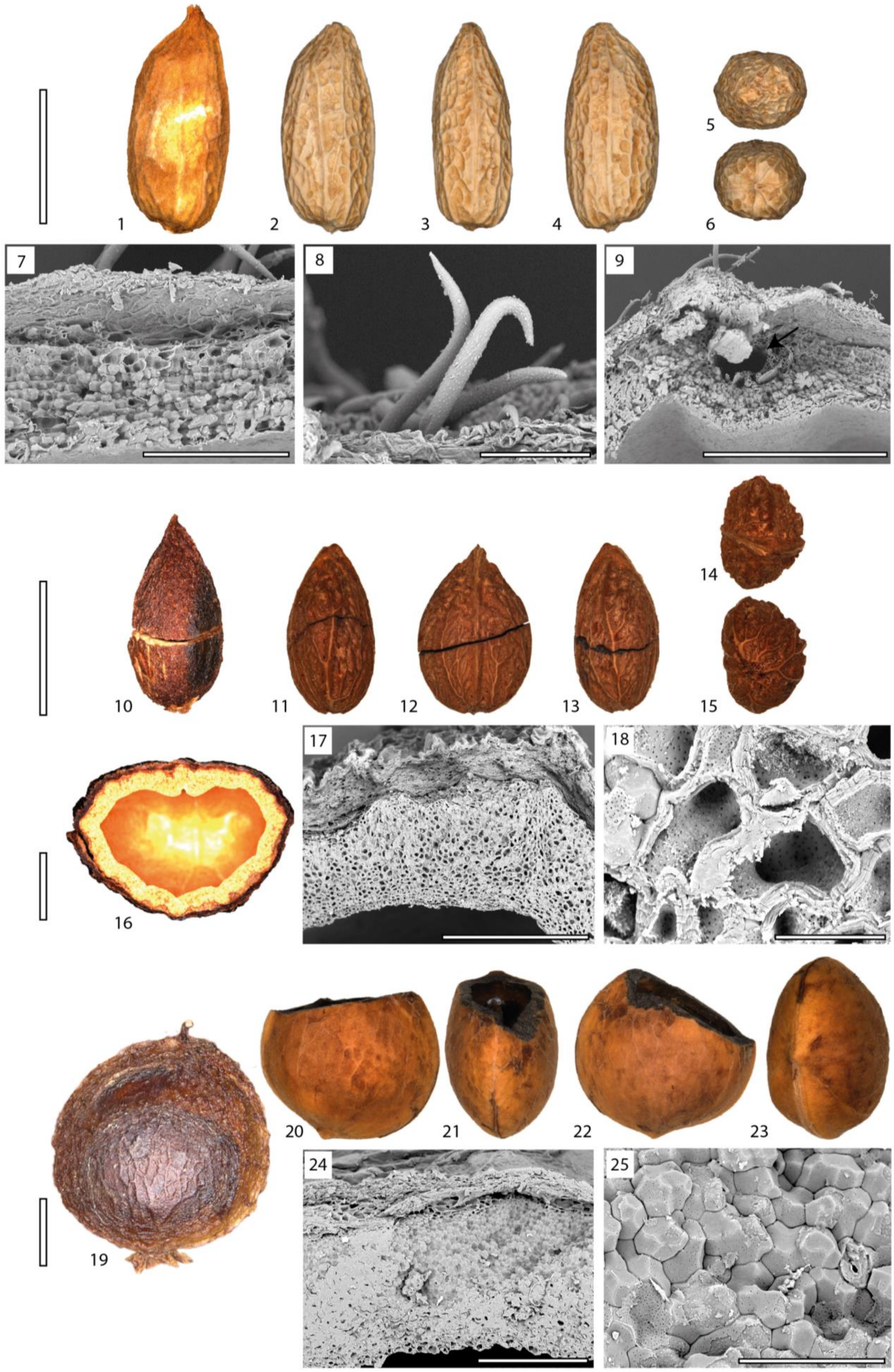
1
2
3
4
5
6
7
8
9
10
11
12
13
14
15
16
17
18
19
20
21
22
23
24
25

Plate III

Cassinopsis madagascariensis Baill.
(*P. P. Lowry et al. 5162*)
1. – Lateral view of a broken fruit.
2. – Lateral view of a broken endocarp showing a reticulate pattern of ridges.
3. – Dorsal view showing a keel surrounding the endocarp.
4. – Second lateral view.
5. – Apical view.
6. – Basal view.
7. – SEM view of the pericarp in transverse section.
8. – Same with magnification showing the cells wall.
9. – SEM view of the inner endocarp surface showing cluster of hairs inside.

Desmostachys oblongifolius (Engl.) Villiers
(*R. Letouzey 8309*)
10. – Lateral view of the dried fruit.
11. – Lateral view of a broken endocarp showing a reticulate pattern of ridges.
12. – Dorsal view showing the keel surrounding the endocarp.
13. – Second lateral view.
14. – Apical view.
15. – Basal view.
16. – SEM view of the pericarp in transverse section.

Desmostachys planchonianus Miers
(*B. Lewis & S. Razafimandimbison 735*)
17. – Lateral view of the dried fruit.
18. – Lateral view of the endocarp showing the roughness.
19. – Dorsal view showing a keel surrounding the endocarp.
20. – Second lateral view.
21. – Apical view.
22. – Basal view.
23. – SEM view of the endocarp in transverse section.
24. – Detail of the basal part showing periclinally oriented cells.
25. – Detail of the upper part showing anticlinally oriented cells.

Scale: 1–6, 10–15, 17–22 = 5 mm; 7 = 1 mm; 16 = 500 μm; 23 = 300 μm; 9 = 200 μm; 25 = 100 μm; 8, 24 = 50 μm.

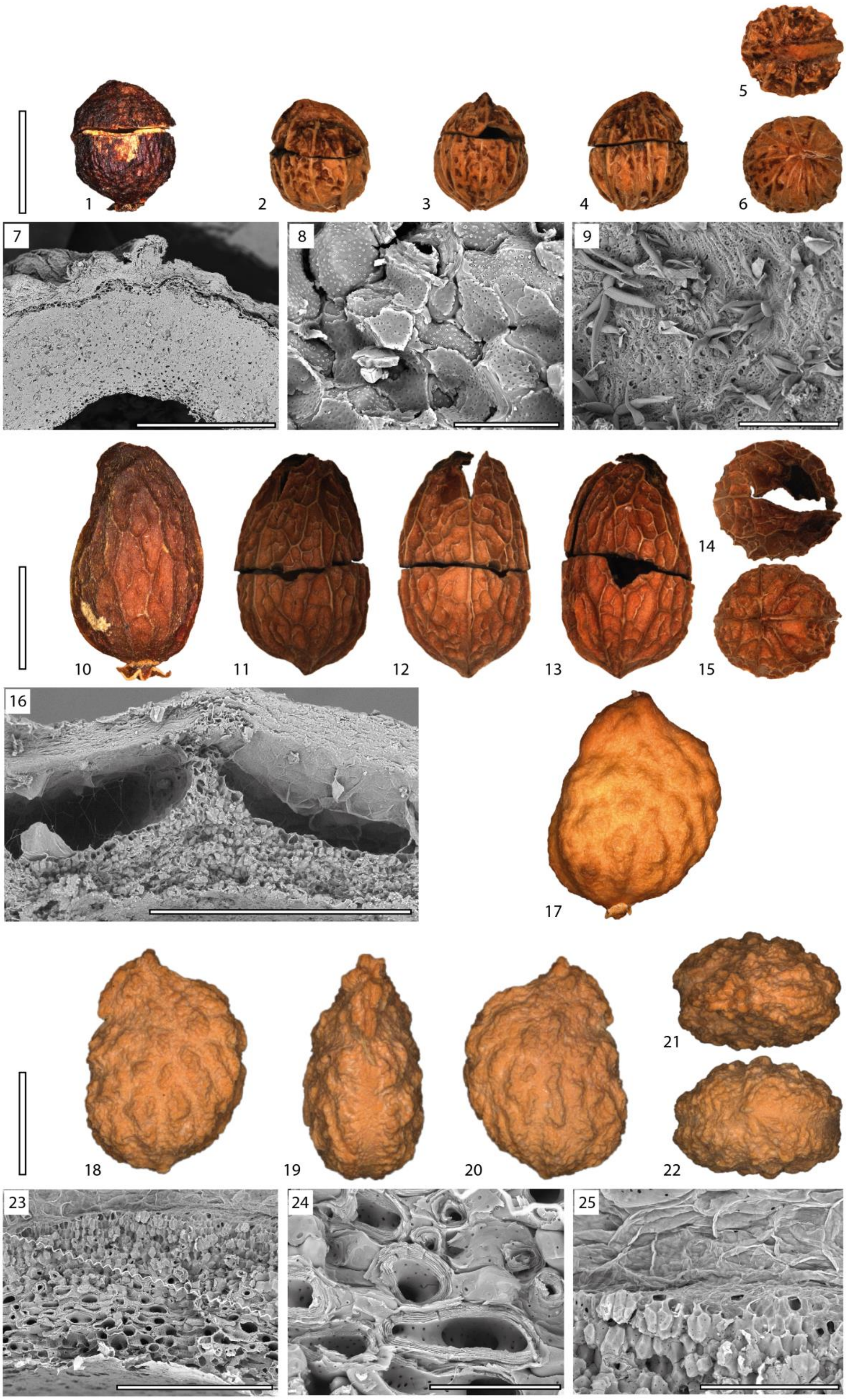
1
2
3
4
5
6
7
8
9
10
11
12
13
14
15
16
17
18
19
20
21
22
23
24
25

Plate IV

Desmostachys tenuifolius Oliv.
(J.J. Bos 4277)
1. – Lateral view of the dried fruit.
2. – Lateral view of the endocarp showing a reticulate pattern of ridges.
3. – Dorsal view showing a keel surrounding the endocarp.
4. – Second lateral view.
5. – Apical view.
6. – Basal view.
7. – SEM view of pericarp in transverse section.
8. – SEM view of the endocarp in transverse section.
9. – SEM view of the vascular bundle in a channel.

Desmostachys vogelii (Miers) Stapf.
(*Service forestier 364*)
10. – Lateral view of the dried fruit.
11. – Lateral view of the endocarp showing the ridges and roughness.
12. – Dorsal view showing the keel surrounding the endocarp.
13. – Second lateral view.
14. – Apical view.
15. – Basal view.
16. – SEM view of a ridge in transverse section.
17. – SEM view of the endocarp wall in transverse section.
18. – SEM view of simple hairs in epicarp surface.

Hosiea japonica Makino
(*Okudai 60474*)
19. – Lateral view of the endocarp showing a reticulate pattern of ridges.
20. – Dorsal view showing a keel surrounding the endocarp.
21. – Second lateral view.
22. – SEM view of the endocarp wall in transverse section.
23. – Same with magnification showing the cells wall.
24. – SEM view of the inner layer of the endocarp wall, showing papillae.
25. – The same enlarged.

Scale: 1–6, 10–15, 19–21 = 10 mm; 7, 16, 22 = 1 mm; 9, 17 = 500 µm; 8, 25 = 100 µm; 23 = 300 µm; 8, 18 = 200 µm; 24, 25 = 20 µm.

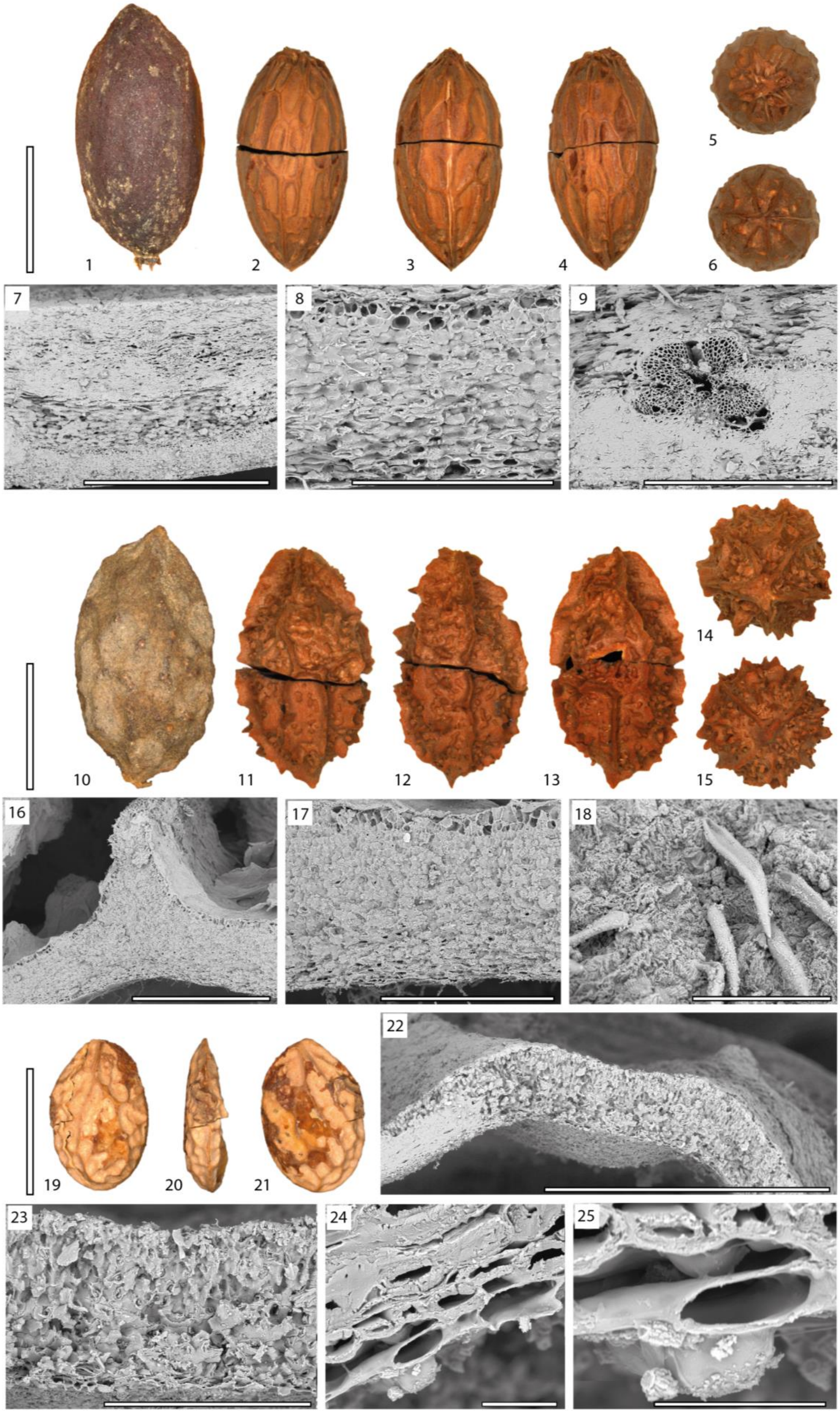
1
2
3
4
5
6
7
8
9
10
11
12
13
14
15
16
17
18
19
20
21
22
23
24
25

Plate V

Hosiea sinensis (Oliv.) Hemsl. & E.H. Wilson
(*M. l'abbé Farges s.n.*)
1. – Lateral view of the dried fruit.
2. – Lateral view of the endocarp showing a reticulate pattern of ridges.
3. – Dorsal view showing a keel surrounding the endocarp.
4. – Second lateral view.
5. – Apical view.
6. – Basal view.
7. – SEM view of pericarp in transverse section.
8. – SEM view of the endocarp cells wall in transverse section.
9. – SEM view of papillae lining the locule.

Icacina claessensii De Wild
(*C. Evard 5094*)
10. – Lateral view of the dried fruit.
11. – Lateral view of a broken endocarp showing the ridges.
12. – Dorsal view showing the keel surrounding the endocarp.
13. – Second lateral view.
14. – Apical view.
15. – Basal view.
16. – SEM view of the endocarp with ridges and separated mesocarp in transverse section.
17. – SEM view of the endocarp wall in transverse section.

Icacina guessfeldtii Asch.
(*J. Gillet 2674*)
18. – Lateral view of the dried fruit.
19. – Lateral view of a broken endocarp showing a reticulate pattern of ridges.
20. – Dorsal view of the endocarp.
21. – Second lateral view.
22. – Apical view.
23. – Basal view.
24. – Detail of the apical view showing the pair of horn-like protrusions.
25. – SEM view of the pericarp in transverse section showing the vascular bundle in the endocarp wall (arrow).
26. – SEM view of the endocarp periclinally oriented cells.

Scale: 1–6, 10–15, 18–23 = 10 mm ; 24 = 2 mm ; 16, 25 = 1 mm ; 7, 17, 26 = 200 µm ; 8, 9 = 50 µm.

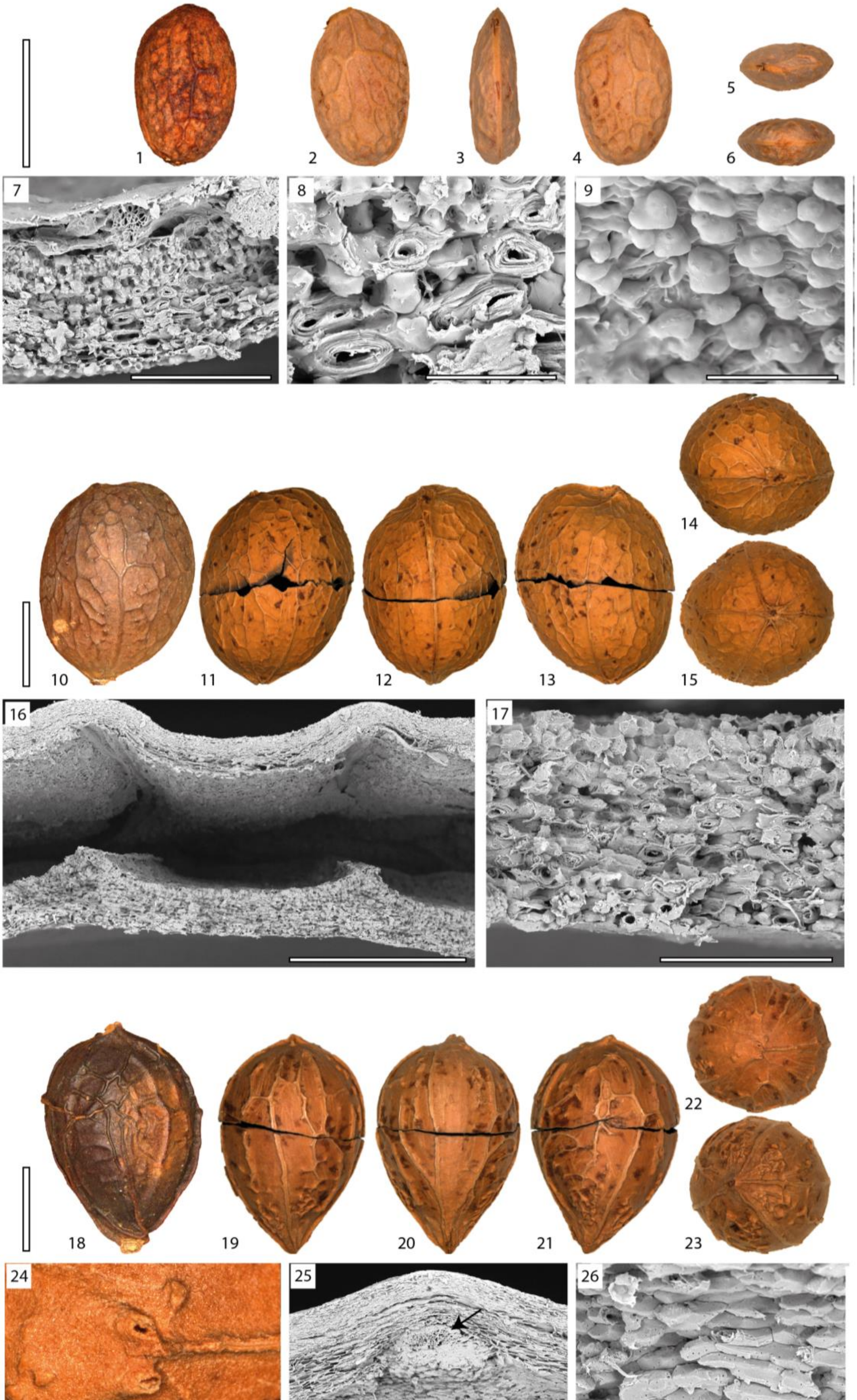
1
2
3
4
5
6
7
8
9
10
11
12
13
14
15
16
17
18
19
20
21
22
23
24
25
26

Plate VI

Icacina mannii Oliv.
(*J. Koechlin 2334*)
1. – Lateral view of the dried fruit.
2. – Lateral view of the endocarp showing the mounds.
3. – Dorsal view of the endocarp.
4. – Second lateral view.
5. – Apical view.
6. – Basal view.
7. – SEM view of the vascular bundle embedded in endocarp wall in transverse section (arrow).
8. – SEM view of the endocarp wall in transverse section.
9. – SEM view of the papillae-like hairs on epicarp.

Icacina oliviformis (Poir.) J.Raynal
(*M. Dybowski 698*)
10. – Lateral view of a broken fruit.
11. – Lateral view of a broken endocarp showing the mounds.
12. – Dorsal view of the endocarp.
13. – Apical view.
14. – Basal view.
15. – Detail of apical view showing horn-like protrusions (arrows).
16. – SEM view of the vascular bundle embedded in endocarp wall in transverse section (arrow).
17. – SEM view of the endocarp wall in transverse section.
18. – SEM view of the ovoid hairs with an acuminate apex on the epicarp.

Icacina trichanta Oliv.
(*J.C. Okafor fhi 34969*)
19. – Lateral view of the dried fruit.
20. – Lateral view of a broken endocarp showing the ridges.
21. – Dorsal view showing a keel surrounding the endocarp.
22. – Second lateral view.
23. – Apical view.
24. – Basal view.
25. – SEM view of the vascular bundle embedded in endocarp wall in transverse section (arrow).
26. – SEM view of a ridge in transverse section.
27. – SEM view of the endocarp wall in transverse section.

Scale: 1–6, 10–14, 19–24 = 10 mm ; 7, 15, 25 = 1 mm ; 16, 26 = 500 µm; 8, 27 = 300 µm, 17 = 200 µm; 9, 18 = 100 µm.


1
2
3
4
5
6
7
8
9
10
11
12
13
14
15
16
17
18
19
20
21
22
23
24
25
26
27

Plate VII

Iodes africana Welw. Ex Oliv.
(*R.P. Tisserant s.n.*)
1. – Lateral view of the dried fruit.
2. – Lateral view of the endocarp showing a reticulate pattern of ridges.
3. – Dorsal view of the endocarp.
4. – Second lateral view.
5. – Apical view.
6. – Basal view.
7. – SEM view of the pericarp in transverse section.
8. – SEM view of the endocarp wall in transverse section and papillae on the inner surface.
9. – SEM surface view of the papillae lining the locule.

Iodes balansae Gagnep.
(KUN 0647593)
10. – Lateral view of the dried fruit.
11. – Lateral view of a part of the endocarp showing the double reticulation.
12. – SEM view of primary ridges in transverse section.
13. – SEM view of secondary ridges in transverse section.

Iodes cirrhosa Turcz
(*B. Hayata 672*)
14. – Lateral view of the dried fruit.
15. – Lateral view of the endocarp showing the ridges and roughness.
16. – Dorsal view showing a keel surrounding the endocarp.
17. – Second lateral view.
18. – Apical view.
19. – Basal view.
20. – SEM view of the vascular bundle embedded in endocarp wall in transverse section of the pericarp (arrow).
21. – SEM view of an endocarp ridge in a transverse section of the pericarp.
22. – SEM view of the lower part of the endocarp wall in transverse section and papillae on the inner surface.
23. – SEM surface view of the papillae lining the locule.

Scale: 1–6, 10, 11, 14–19 = 10 mm; 12 = 1 mm; 13, 20, 21 = 500 µm; 7, 9 = 300 µm; 8, 23 = 50 µm; 22 = 20 µm.

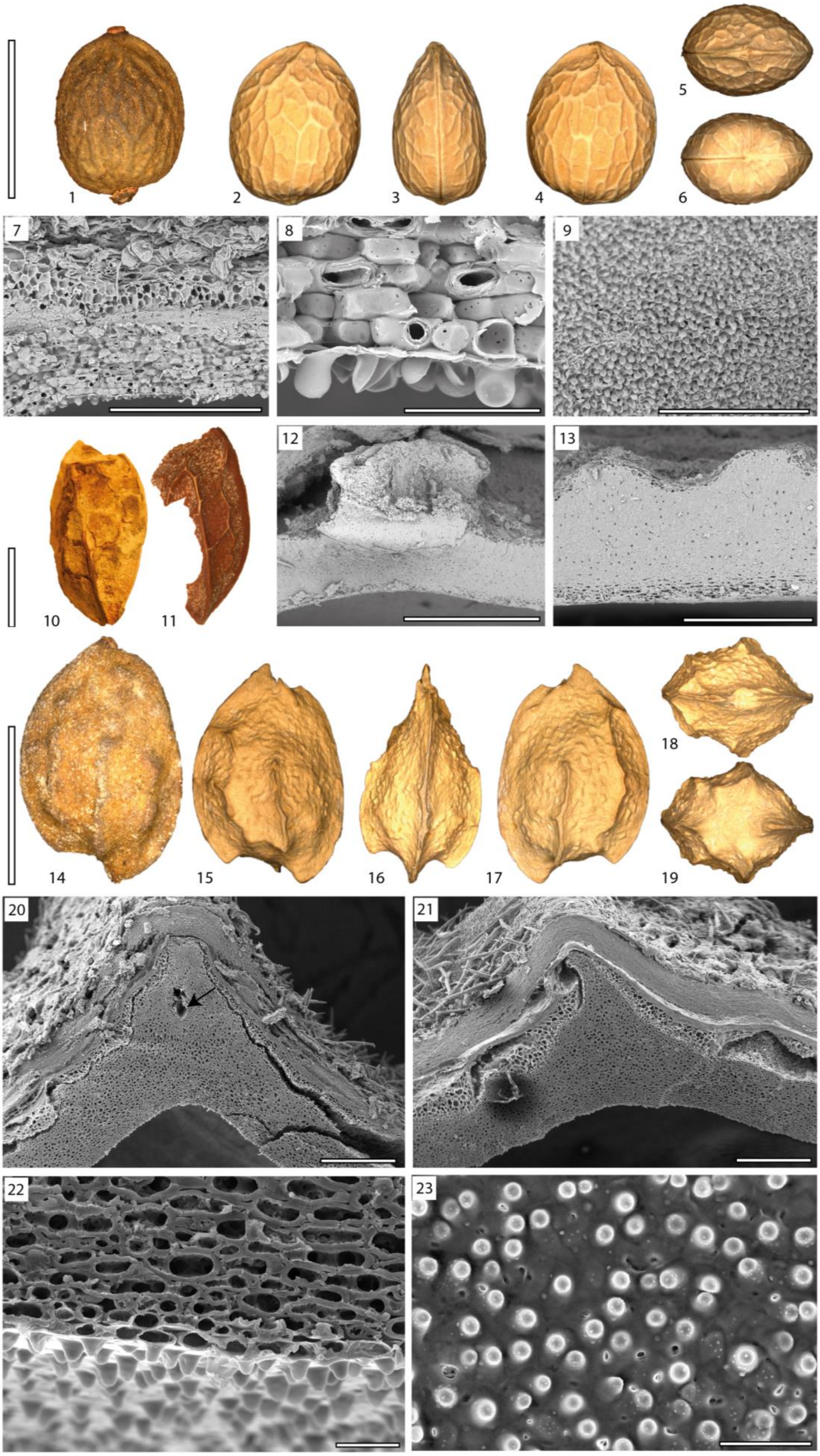
1
2
3
4
5
6
7
8
9
10
11
12
13
14
15
16
17
18
19
20
21
22
23

Plate VIII

Iodes kamerunensis Engl.
(*G.A. Zenker 2032*)
1. – Lateral view of the dried fruit.
2. – Lateral view of a broken endocarp showing a reticulate pattern of ridges.
3. – Dorsal view showing a keel surrounding the endocarp.
4. – Second lateral view.
5. – Apical view.
6. – Basal view.
7. – SEM view of the vascular bundle embedded in the endocarp wall (arrow) in a transverse section of the pericarp.
8. – SEM view of a ridge in transverse section of the pericarp.
9. – SEM view of the endocarp wall in transverse section.

Iodes klaineana Pierre
(*R.P. Klaine 3064*)
10. – Lateral view of the dried fruit.
11. – Lateral view of the endocarp showing a reticulate pattern of ridges.
12. – Dorsal view showing the keel surrounding the endocarp.
13. – Second lateral view.
14. – Apical view.
15. – Basal view.
16. – SEM view of the vascular bundle embedded in the endocarp wall (arrow) in a transverse section of the pericarp.
17. – SEM view of a ridge in transverse section of the pericarp.
18. – SEM view of the cells wall of the endocarp.

Iodes liberica Stapf
(*J.G. Adam 3833*)
19. – Lateral view of a broken dried fruit.
20. – Lateral view of a broken endocarp showing a reticulate pattern of ridges.
21. – Dorsal view showing a keel surrounding the endocarp.
22. – Second lateral view.
23. – Apical view.
24. – Basal view.
25. – SEM view of the vascular bundle embedded in the endocarp wall (arrow).
26. – SEM view of a ridge and endocarp wall in transverse section.
27. – Portion of the endocarp wall.

Scale: 1–6, 10–15, 19–24 = 10 mm; 7, 16, 25 = 1 mm; 8, 17 = 500 µm; 26 = 300 µm; 9 = 200 µm; 27 = 100 µm; 18 = 50 µm.

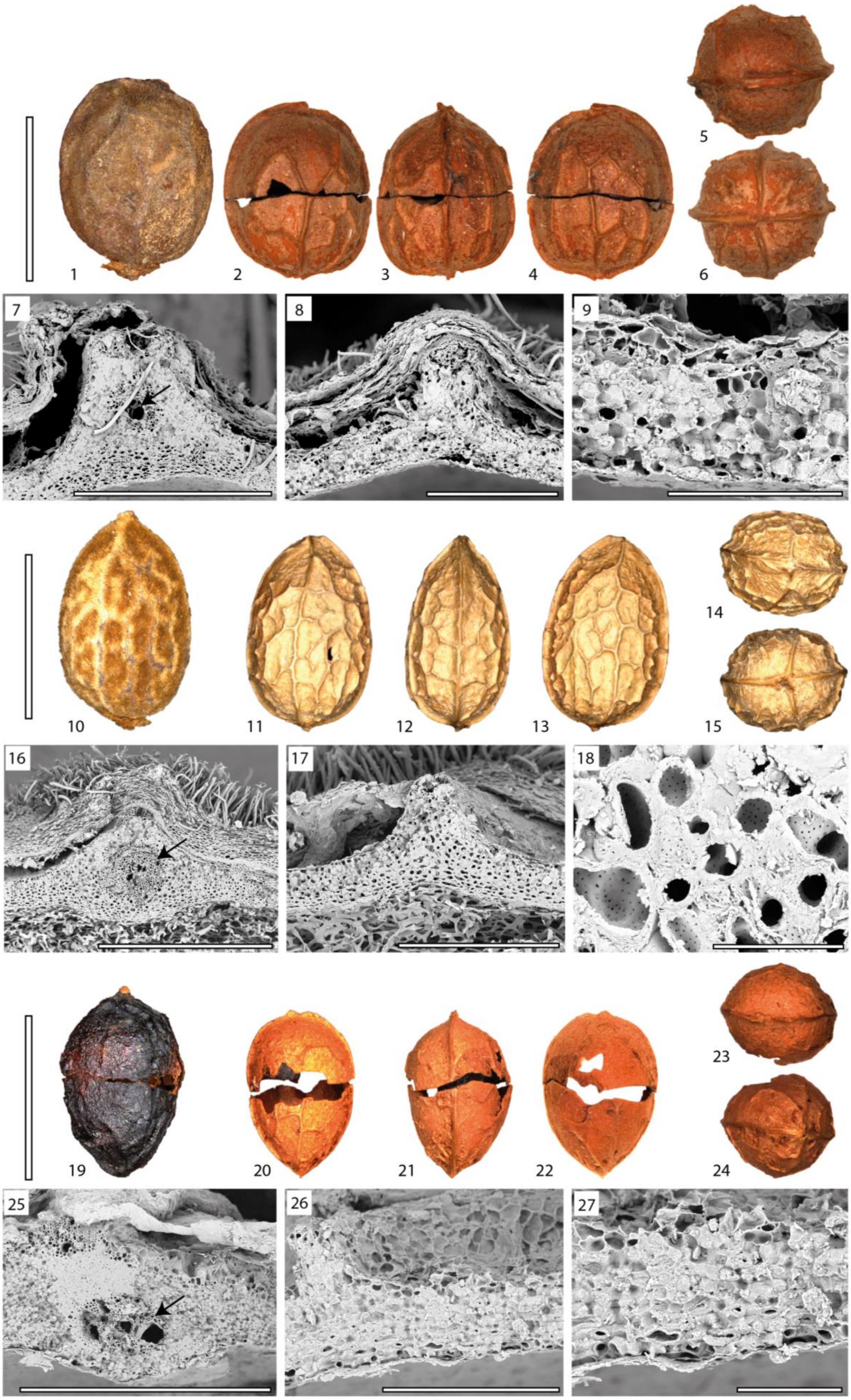
1
2
3
4
5
6
7
8
9
10
11
12
13
14
15
16
17
18
19
20
21
22
23
24
25
26
27

Plate IX

Iodes madagascariensis Baill.
(*Chapelier s.n.*)
1. – Lateral view of the dried fruit.
2. – Lateral view of a broken endocarp showing a reticulate pattern of ridges.
3. – Dorsal view showing a keel surrounding the endocarp.
4. – Second lateral view.
5. – Apical view.
6. – Basal view.
7. – SEM view of the pericarp in a transverse section showing the vascular bundle embedded in the endocarp wall (arrow).
8. – Other view of the pericarp in a transverse section showing the endocarp wall .
9. – Detail showing the papillae on the locule surface.

Iodes ovalis Blume
(*Hiep HLF 203*)
10. – Lateral view of a broken dried fruit.
11. – Lateral view of a broken endocarp showing the reticulation and roughness.
12. – Dorsal view showing the keel surrounding the endocarp.
13. – Second lateral view.
14. – Apical view.
15. – Basal view.
16. – SEM view of the vascular bundle embedded in the endocarp wall (arrow).
17. – SEM view of a ridge in transverse section.
18. – SEM view of the papillae on the locule surface.

Iodes perrieri Sleumer
(*Perrier De La Bâthie 17843)*
19. – Lateral view of the dried fruit.
20. – Lateral view of the endocarp showing a reticulate pattern of faintly marked ridges.
21. – Dorsal view of endocarp.
22. – Second lateral view.
23. – Apical view.
24. – Basal view.
25. – SEM view of a ridge and endocarp wall in transverse section.
26. – Detail showing the endocarp cells wall in the upper part.
27. – SEM view of the papillae on the locule surface.

Scale: 1–6, 10–15, 19–24 = 10 mm; 16 = 1 mm; 7, 8, 17, 25 = 500 µm; 26 = 200 µm; 9, 18, 27 = 50 µm.

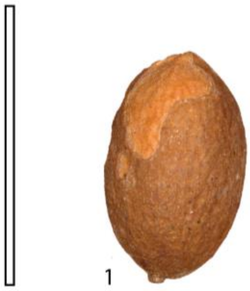
1


2


3


4


5


6

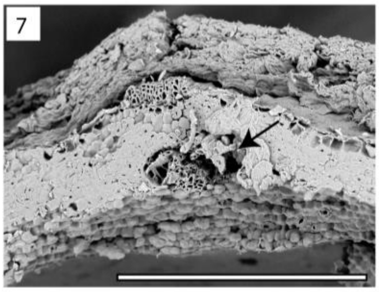
7

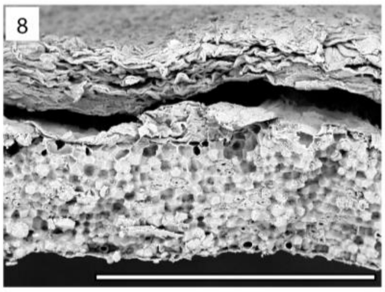
8

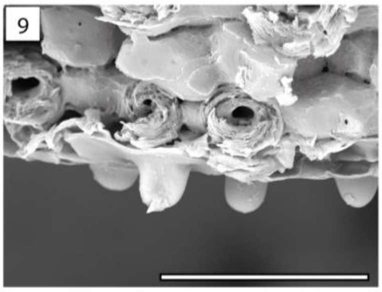
9


10


11


12


13

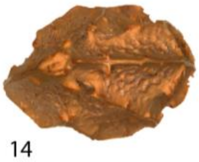
14

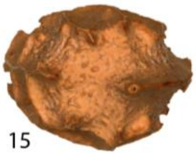
15

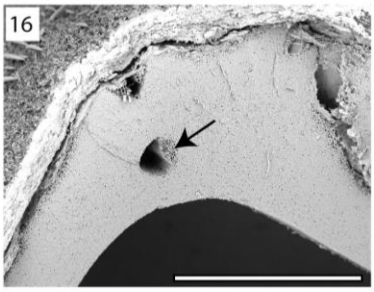
16

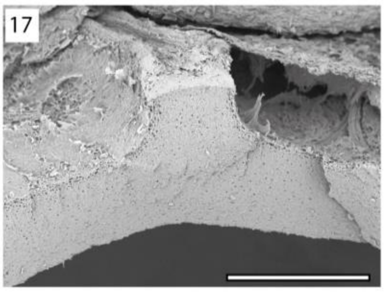
17

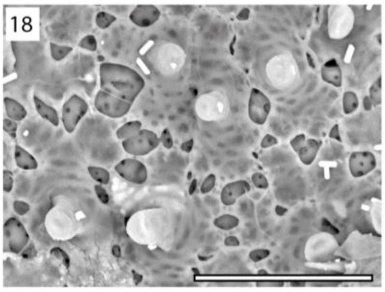
18


19


20


21


22


23


24

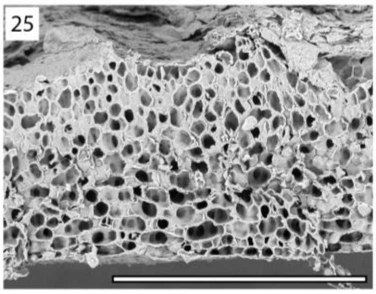
25

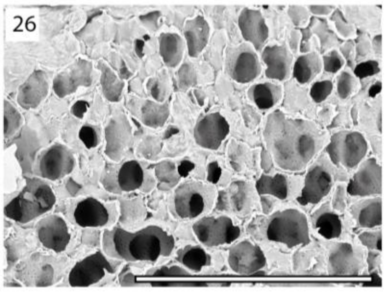
26

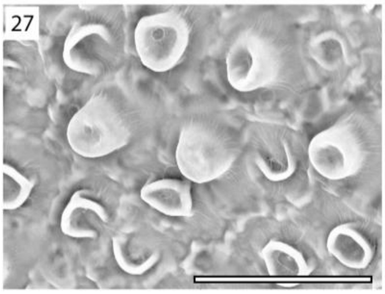
27

Plate X

Iodes philippiensis Merr.
(*A.D.E. Elmer 16418)*
1. – Lateral view of the dried fruit.
2. – Lateral view of a broken endocarp showing the primary ridges and secondary reticulation.
3. – Dorsal view showing a keel surrounding the endocarp.
4. – Second lateral view.
5. – Apical view.
6. – Basal view.
7. – SEM view of the uncinate hairs on the epicarp surface.
8. – SEM view of the vascular bundle embedded in the endocarp wall (arrow) seen in a transverse section of the pericarp.
9. – SEM view of the endocarp wall in transverse section.

Iodes scandens (Becc.) Utteridge & Byng
(*No voucher, MO*)
10. – Lateral view of the endocarp showing a reticulate pattern of ridges.
11. – Dorsal view showing the keel surrounding the endocarp partially splitted on the same plan.
12. – Second lateral view.
13. – Apical view.
14. – Basal view.
15. – SEM view of a ridge in transverse section.
16. – SEM view of the endocarp wall in transverse section.
17. – SEM view of the endocarp cells and potential papillae on the locule surface (arrow).

Iodes seguinii (H. Lév.) Rehder
(*Abbé Cavalerie 3932*)
18. – Lateral view of the dried fruit.
19. – Lateral view of the endocarp showing the smooth surface with the vasculature on a faintly marked channel.
20. – Dorsal view of endocarp showing the channel.
21. – Second lateral view.
22. – Apical view with the channel seen on the left side.
23. – Basal view.
24. – SEM view of the channel containing the vascular bundle.
25. – SEM view of endocarp wall in transverse section.
26. – Detail showing the endocarp basal cells wall.

Scale: 1–6, 10–14, 18–23 = 10 mm; 7, 15 = 1 mm; 8, 16, 24 = 500 µm; 9, 25 = 200 µm; 26 = 50 µm; 17 = 30 µm.

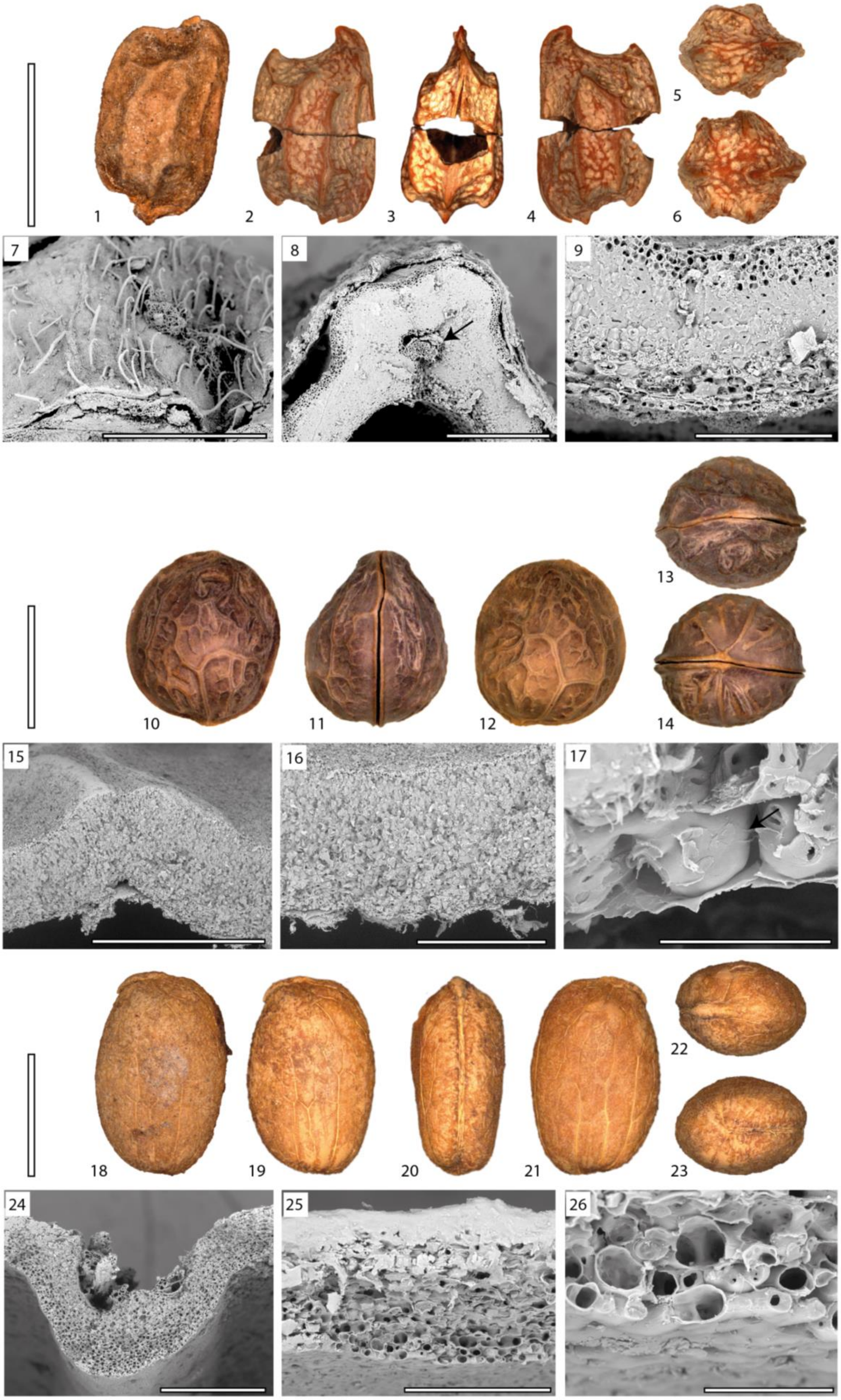
1
2
3
4
5
6
7
8
9
10
11
12
13
14
15
16
17
18
19
20
21
22
23
24
25
26

Plate XI

Iodes seretii (De Wild.) Boutique
(*D. Thomas & M. Etuge 63*)
1. – Lateral view of a broken dried fruit.
2. – Lateral view of the endocarp showing a reticulate pattern of ridges.
3. – Dorsal view showing a keel surrounding the endocarp.
4. – Second lateral view.
5. – Apical view.
6. – Basal view.
7. – SEM view of the pilose indumentum on the epicarp surface and of a transverse section of the pericarp.
8. – SEM view of the vascular bundle embedded in the endocarp wall (arrow) in a transverse section of the pericarp.
9. – SEM view of basal endocarp cells in a transverse section and papillae on the locule surface.

Iodes yatesii Merr.
(*Burley 1577*)
10. – Lateral view of the endocarp showing the double reticulation.
11. – Dorsal view showing the keel surrounding the endocarp.
12. – Second lateral view.
13. – Apical view.
14. – Basal view.
15. – Magnification of areoles showing the secondary reticulation.
16. – SEM view of the vascular bundle embedded in the endocarp wall (arrow).
17. – SEM view of primary and secondary ridges in transverse view.
18. – Detail of the right part of the same section showing the cells organization in endocarp wall and secondary ridges.

Lavigeria macrocarpa (Oliv.) Pierre
19. – Lateral view of the endocarp showing ridges/roughness. (*R. Letowsey 8970*)
20. – Transverse section of the endocarp showing the vascular bundle (arrow) embedded in the endocarp wall. (*N. Hallé 3734*)
21. – SEM view of the same showing the endocarp wall and the locule with simple hairs (arrow). (*Bos 4098*)

Scale: 1–6, 10–14, 19, 20 = 10 mm; 7, 21 = 2 mm; 15, 17 = 1 mm; 8, 16, 18 = 500 µm ; 9 = 50 µm.

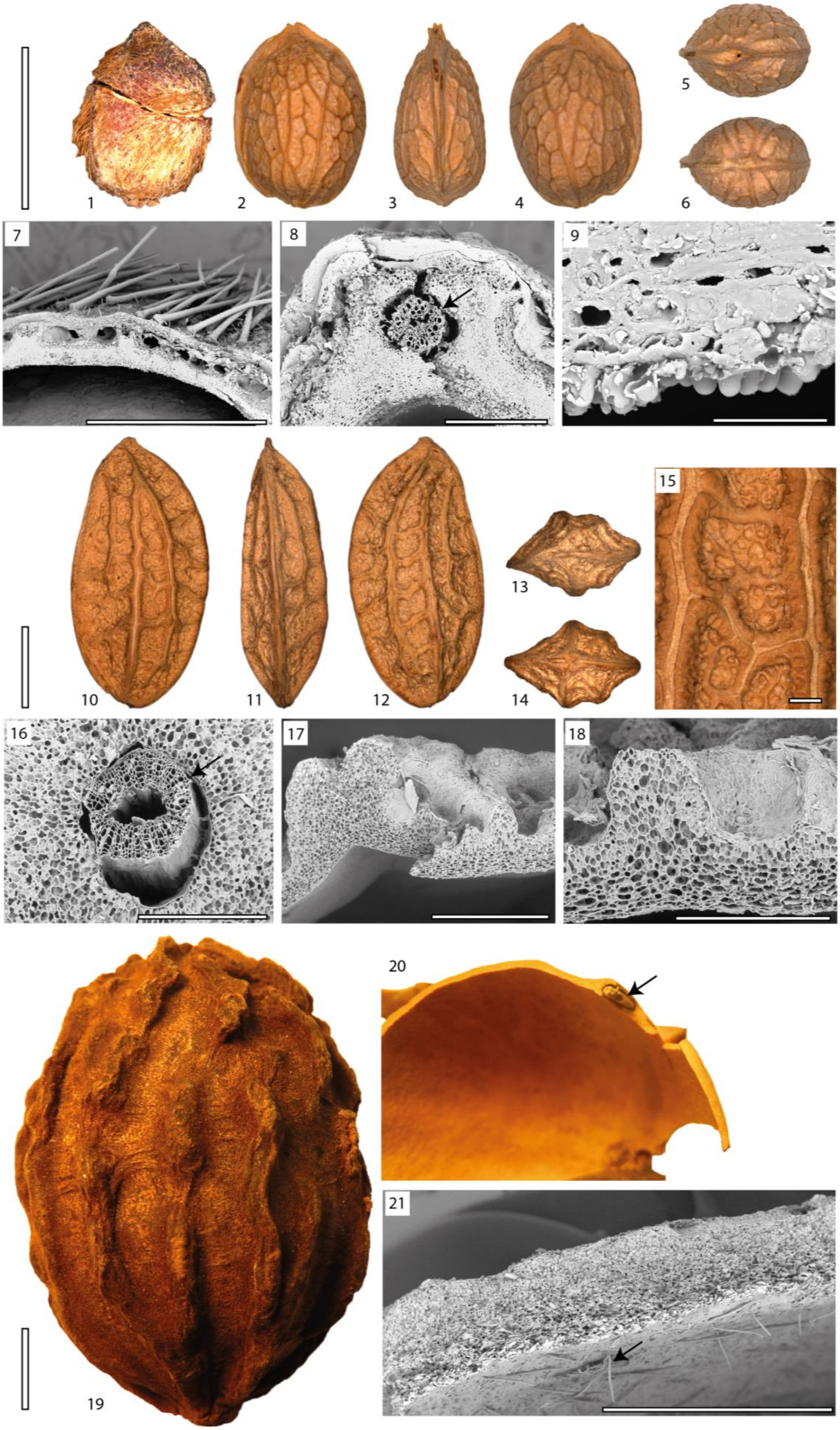
1
2
3
4
5
6
7
8
9
10
11
12
13
14
15
16
17
18
19
20
21

Plate XII

Leretia cordata Vell.
(*J.C. Solomon 17073*)
1. – Lateral view of the dried fruit.
2. – Lateral view of a broken endocarp showing channels and vascularization.
3. – Dorsal view showing a keel surrounding the endocarp.
4. – Second lateral view.
5. – Apical view.
6. – Basal view.
7. – SEM view of the vascular bundle embedded in the endocarp wall (arrow).
8. – SEM view of the endocarp wall in transverse section.
9. – Detail showing cells wall of the endocarp.

Mappia longipes Lundell
(*M. Guillermo Ibarra 72*)
10. – Lateral view of the dried fruit.
11. – Lateral view of a broken endocarp showing faint roughness.
12. – Dorsal view showing the keel surrounding the endocarp.
13. – Second lateral view.
14. – Apical view.
15. – Basal view.
16. – SEM view of the pericarp in transverse section.
17. – SEM view of the endocarp in transverse section.
18. – Detail showing anticlinally oriented cells.

Mappia multiflora Lundell
(*Contreras 6781*)
19. – Lateral view of the endocarp showing the channels and the vasculature.
20. – Dorsal view of endocarp (with a broken part at left apex).
21. – Second lateral view.
22. – Apical view.
23. – Basal view.
24. – SEM view of a transverse section showing a channel with the vascular bundle (arrow).
25. – SEM view of the endocarp wall in transverse section.
26. – Enlargement showing anticlinal oriented cells wall detail and vasculature on the endocarp.

Scale: 1–6, 10–15, 19–23 = 10 mm; 7, 16, 24 = 1 mm; 17, 25 = 500 µm; 8 = 300 µm; 26 = 200 µm; 9 = 100 µm; 18 = 50 µm.

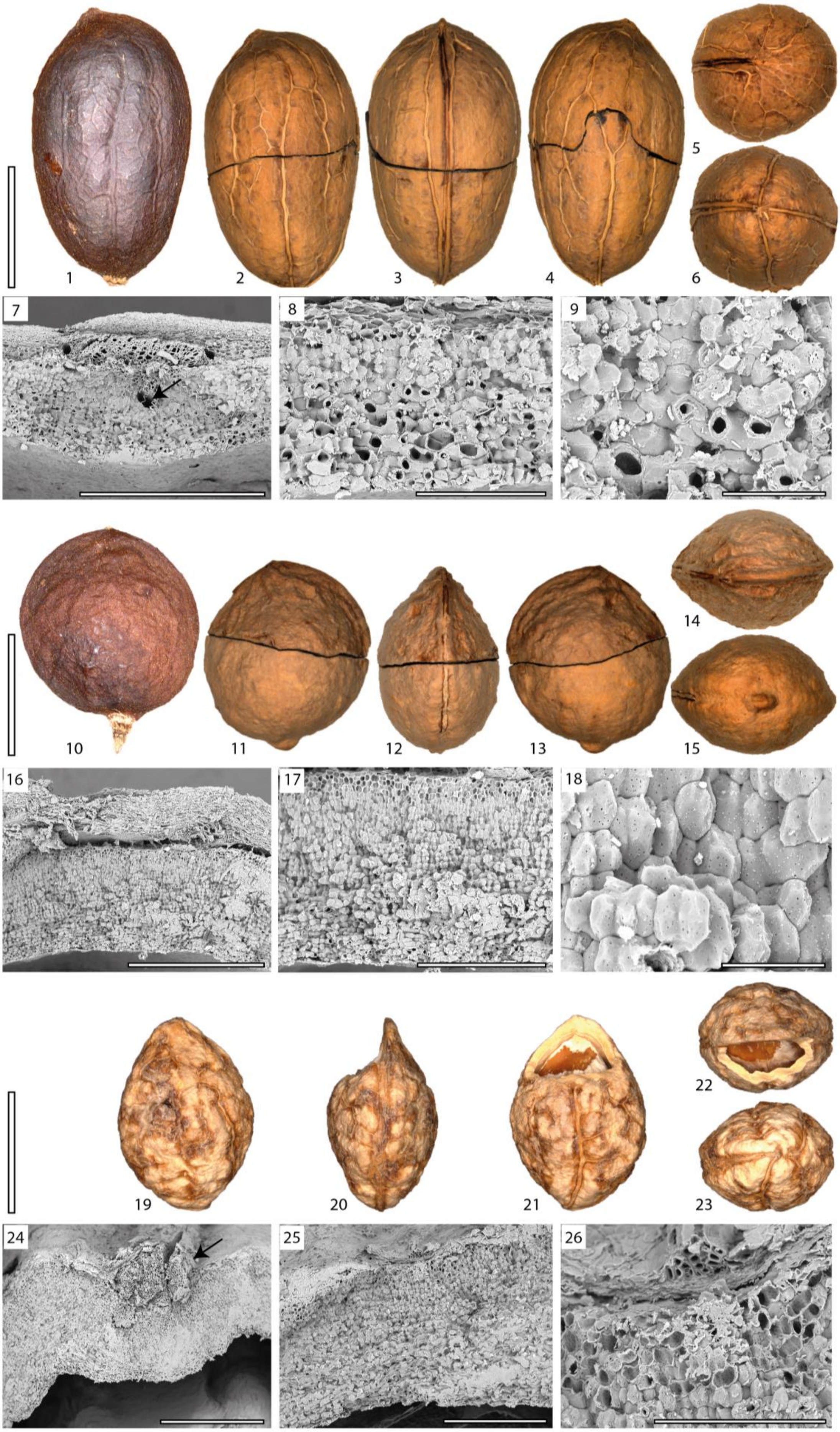
1
2
3
4
5
6
7
8
9
10
11
12
13
14
15
16
17
18
19
20
21
22
23
24
25
26

Plate XIII

Mappia racemosa Jacq.
(*H.A. Van Hermann 250*)
1. – Lateral view of the endocarp showing its rough surface.
2. – Dorsal view showing a keel surrounding the endocarp.
3. – Second lateral view.
4. – Apical view.
5. – Basal view.
6. – SEM view of the endocarp wall in transverse section.
7. – Detail showing anticlinally oriented outer layer cells.
8. – Detail showing periclinally oriented inner layer cells.

Mappianthus iodoides Hand.-Mazz.
(*A.N. Steward & H.C. Cheo 1093*)
9. – Lateral view of a broken dried fruit.
10. – Lateral view of the endocarp showing the mounds.
11. – Dorsal view.
12. – Second lateral view.
13. – Apical view.
14. – Basal view.
15. – SEM view of a pericarp transverse section showing the channel with the vascular bundle.
16. – SEM view of the pericarp transverse section.
17. – SEM surface view of the papillae in the locule.

Miquelia assamica (Griff.) Mast. ex B.D. Jacks.
(*No voucher "15023")*
18. – Lateral view of the endocarp showing the pits and ridges.
19. – Second lateral view.
20. – SEM view of the endocarp wall in transverse section.
21. – Detail showing the cells layers of endocarp wall.
22. – Other detail showing the conical tubercle.
23. – SEM view of the inner part of the endocarp and the papillae in transverse section.

Scale: 1–5, 9–14, 18, 19 = 10 mm; 20 = 1 mm; 6, 15, 16, 22 = 500 µm ; 17, 21 = 300 µm; 7, 8 = 100 µm; 23 = 50 µm.

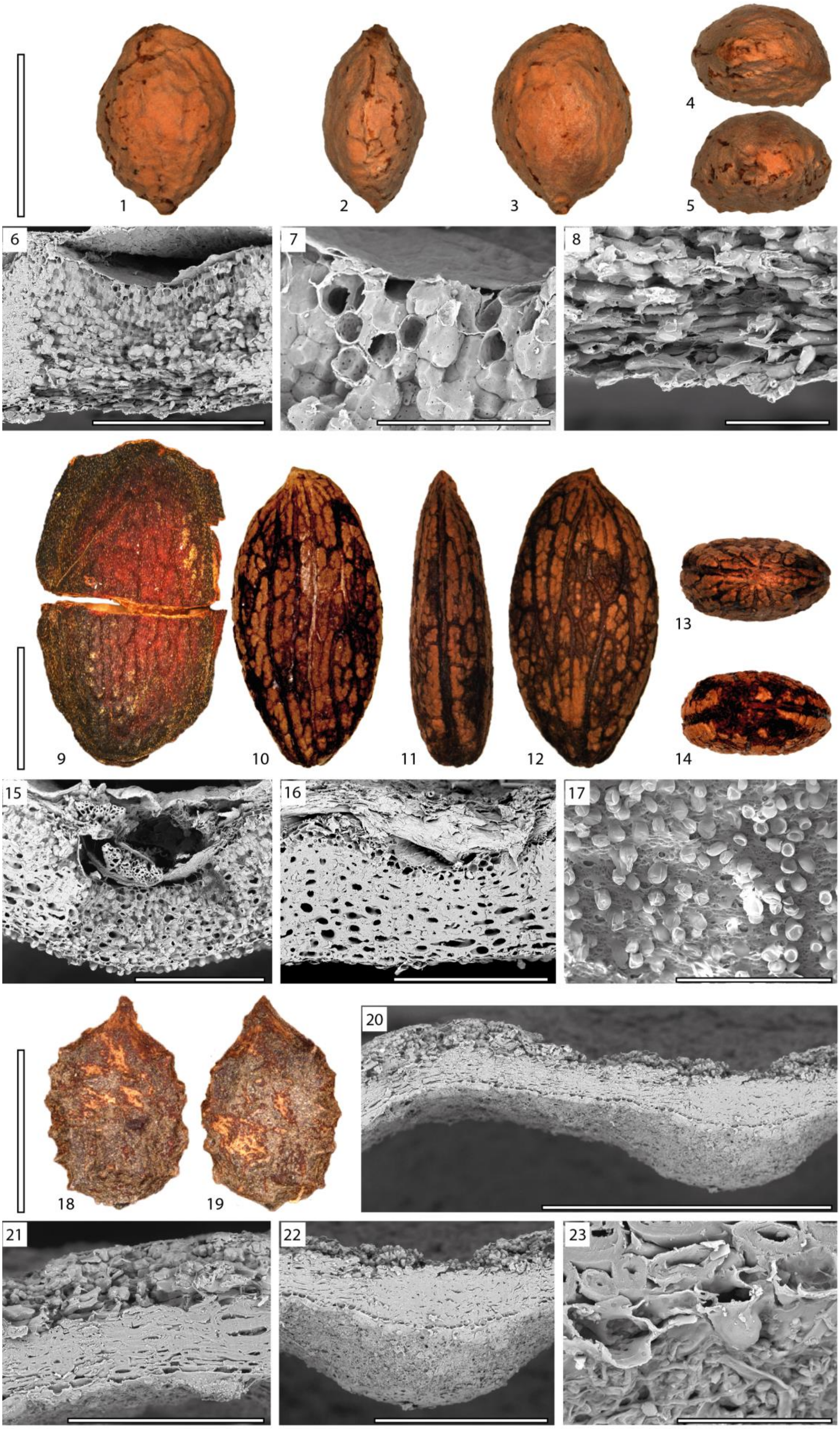
1
2
3
4
5
6
7
8
9
10
11
12
13
14
15
16
17
18
19
20
21
22
23

Plate XIV

Miquelia caudata King
(*Mohd, Shah & Sidek 1168)*
1. – Lateral view of the dried fruit with acuminate apex and an elongate gynophore (here broken).
2. – Lateral view of the endocarp showing ridges and pits.
3. – Dorsal view showing a keel surrounding the endocarp.
4. – Second lateral view.
5. – Apical view.
6. – Basal view.
7. – SEM view of the conical tubercle in the locule.
8. – SEM view of the papillae on the tubercle surface.

Miquelia celebica Blume
(*V. Gal (?) 23*)
9. – Lateral view of the dried fruit with an elongate gynophore.
10. – Lateral view of the endocarp showing ridges and pits.
11. – Dorsal view showing the keel surrounding the endocarp.
12. – Second lateral view.
13. – Apical view.
14. – Basal view.
15. – SEM view of the pericarp in transverse section showing a ridge.
16. – SEM view of the pericarp in transverse section showing the conical tubercle.
17. – SEM view of the inner part of the endocarp in transverse section showing papillae.

Natsiatum herpeticum Buch.-Ham. ex Arn.
(*H.B. Cale s.n*)
18. – Lateral view of a broken dried fruit.
19. – Lateral view of a broken endocarp showing the ridges.
20. – Dorsal view of endocarp showing the keel surrounding the endocarp.
21. – Second lateral view.
22. – Apical view.
23. – Basal view.
24. – SEM view of the pericarp in transverse section showing the channel with the vascular bundle (arrow).
25. – SEM view of the pericarp in transverse section showing the ridge.
26. – Detail showing cells wall of the endocarp.

Scale: 1–6, 9–14, 18–23 = 10 mm; 15, 24 = 1 mm 7, 16, 25 = 500 µm; 26 = 200 µm; 8, 17 = 50 µm.

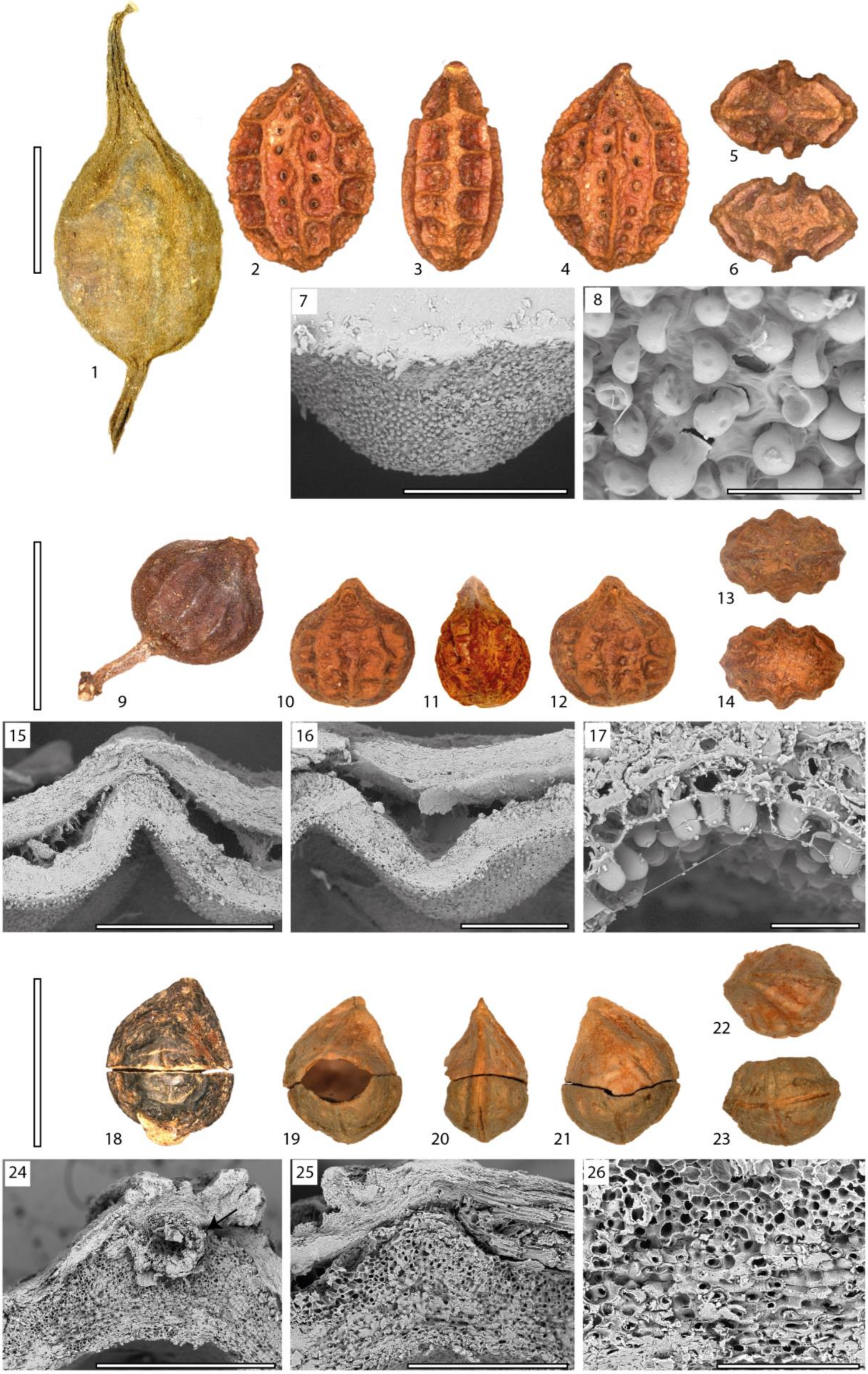
1
2
3
4
5
6
7
8
9
10
11
12
13
14
15
16
17
18
19
20
21
22
23
24
25
26

Plate XV

Nothapodytes nimmoniana (J. Graham) Mabb.
(*A.H.H. Jayasuriya 1922)*
1. – Lateral view of the dried fruit.
2. – Lateral view of a broken endocarp showing the roughness.
3. – Dorsal view of the endocarp with a channel.
4. – Second lateral view.
5. – Apical view.
6. – Basal view.
7. – SEM view of the pericarp in transverse section.
8. – Detail showing the inner part of the endocarp cells.
9. – Other detail showing the outer part of the endocarp cells.

Nothapodytes pittosporoides (Oliv.) Sleumer
(? 4118, P)
10. – Lateral view of the dried fruit.
11. – Lateral view of the endocarp showing the roughness.
12. – Dorsal view of the endocarp with a channel.
13. – Second lateral view.
14. – Apical view.
15. – Basal view.
16. – SEM view of a pericarp transverse section showing the vascular bundle in a channel.
17. – SEM view of a pericarp transverse section with a vasculature between mesocarp and endocarp.
18. – SEM view of the endocarp cells wall in transverse section.

Phytocrene anomala Merr.
(*M. Ramos 1840)*
19. – Lateral view of the dried fruit with an accrescent apex.
20. – Lateral view of the endocarp showing the pits in areole-like pit.
21. – Dorsal view of the endocarp.
22. – Second lateral view.
23. – Apical view.
24. – Basal view.
25. – SEM view of the endocarp showing a pit in transverse section.
26. – SEM view of the endocarp wall in transverse section.

Scale: 1–6, 10–15, 19–24 = 10 mm; 7, 16, 17, 25 = 500 µm; 18 = 300 µm; 8, 9 = 200 µm; 26 = 100 µm.


1
2
3
4
5
6
7
8
9
10
11
12
13
14
15
16
17
18
19
20
21
22
23
24
25
26

Pate XVI

Phytocrene borneensis Becc.
(*No voucher, L*)
1. – Lateral view of the dried fruit with a widely accrescent apex.
2. – Lateral view of a broken endocarp showing the pits.
3. – Dorsal view of the endocarp.
4. – Second lateral view.
5. – Apical view.
6. – Basal view.
7. – SEM view of endocarp wall in transverse section.
8. – SEM view of the spiny like shaped pits in transverse section.

Phytocrene bracteata Wall.
(*W.S. Kurz s.n*)
9. – Lateral view of the dried fruit with a widely accrescent apex.
10. – Lateral view of the endocarp showing the reticulation and pits.
11. – Dorsal view of the endocarp.
12. – Second lateral view.
13. – Apical view.
14. – Basal view.
15. – SEM view of the endocarp wall in transverse section.
16. – SEM view of the spiny shaped pits in transverse section.

Phytocrene hirsuta Blume
(*O. Beccari HB.2497/98*)
17. – Lateral view of the dried fruit with a widely accrescent apex.
18. – Lateral view of the endocarp showing the pits and ridges.
19. – Dorsal view of the endocarp.
20. – Second lateral view.
21. – Apical view.
22. – Basal view.
23. – SEM view of the endocarp wall in transverse section.
24. – SEM view of the spiny shaped pits in transverse section here enlarged towards the locule.

Scale: 1–6, 9–14, 17–22 = 10 mm; 7, 8, 15, 16, 23, 24 = 500 µm.

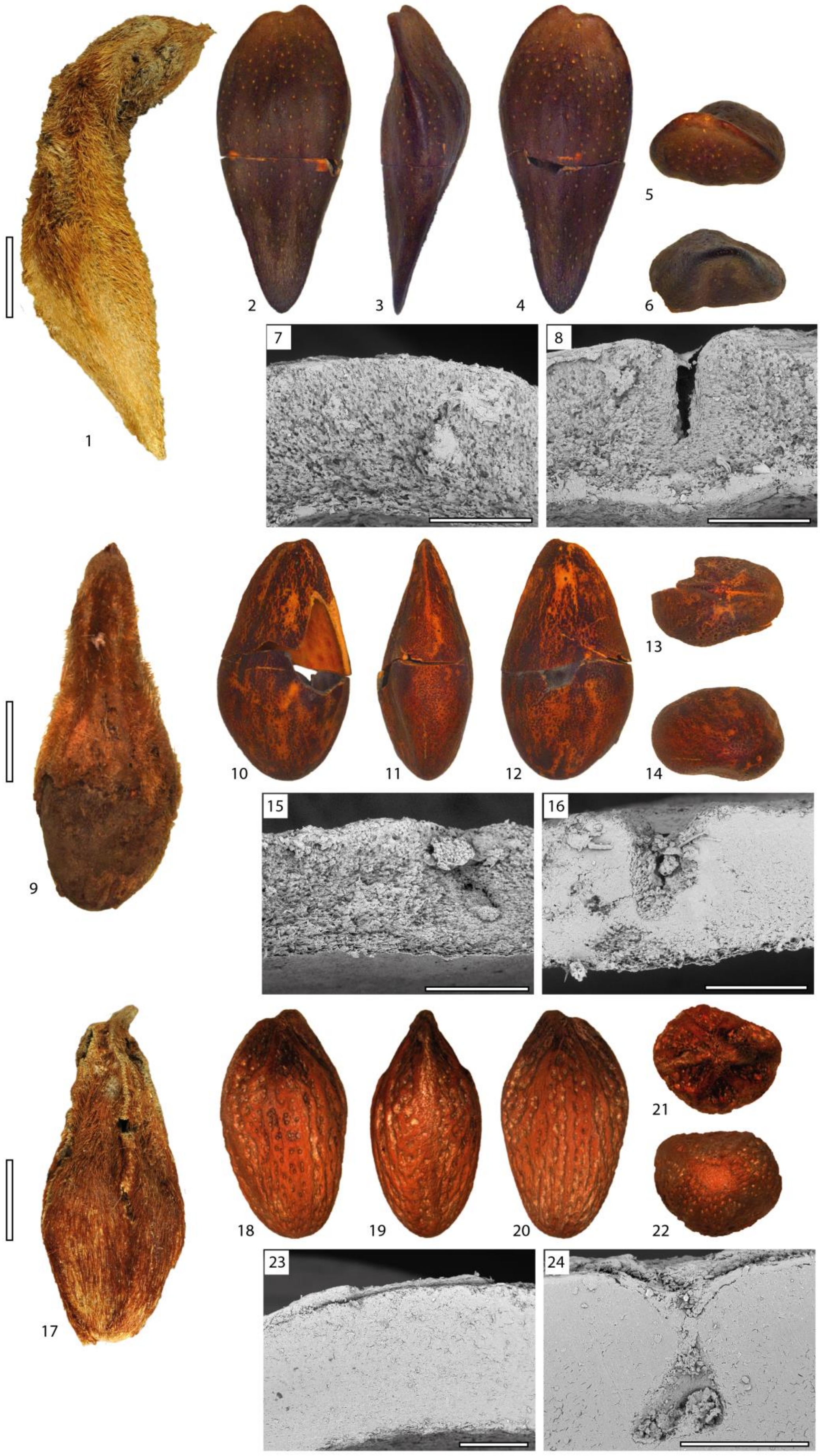
1
2
3
4
5
6
7
8
9
10
11
12
13
14
15
16
17
18
19
20
21
22
23
24

Plate XVII

Phytocrene macrophylla (Blume) Blume
(J. & M.S. Clemens 26544 Bis)
1. – Lateral view of the dried fruit with an accrescent apex.
2. – Lateral view of a broken endocarp showing the pits.
3. – Dorsal view of the endocarp.
4. – Second lateral view.
5. – Apical view.
6. – Basal view.
7. – SEM view of pericarp in transverse section.
8. – SEM view of the endocarp showing a spiny shaped pit in transverse section.
9. – SEM view of the cluster of hairs on the epicarp surface.

Phytocrene oblonga Wall.
(No voucher, P)
10. – Lateral view of the dried fruit with an accrescent apex..
11. – Lateral view of the endocarp showing the areole-like pits.
12. – Dorsal view of the endocarp.
13. – Second lateral view.
14. – Apical view.
15. – Basal view.
16. – SEM view of the endocarp showing a pit in transverse section.
17. – SEM view of the endocarp wall in transverse section.
18. – SEM view of inflated cells on the locule surface.

Phytocrene palmata Wall.
(*Jacobs 8155*)
19. – Lateral view of a broken endocarp showing the pits.
20. – Dorsal view of the endocarp showing the keel.
21. – Second lateral view.
22. – Apical view.
23. – Basal view.
24. – SEM view of the endocarp in transverse section
25. – SEM view of the endocarp in transverse section showing a spiny shaped pit.
26. – Detail showing cells on and around the pit.

Scale: 1–6, 10–15, 19–23 = 10 mm; 7–9, 16, 24, 25 = 500 μm; 26 = 200 μm; 17, 18 = 100 μm.


1


2


3


4


5


6

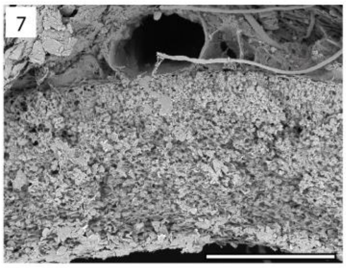
7

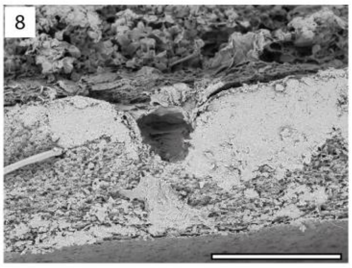
8

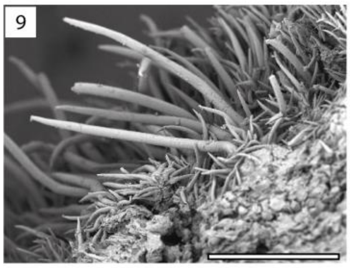
9


10

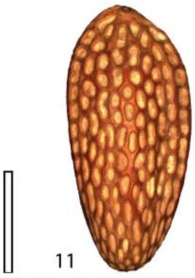
11


12


13

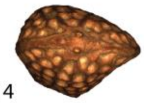
14

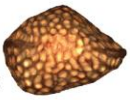
15

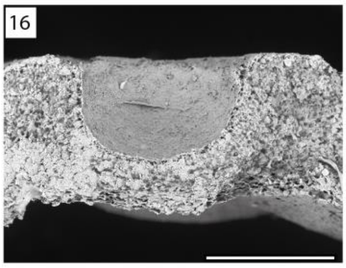
16

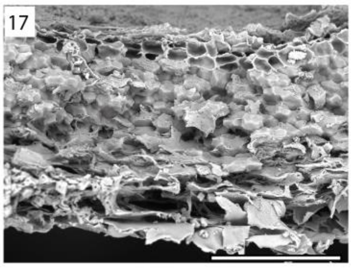
17

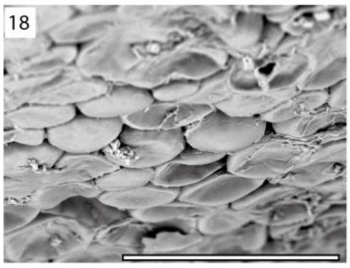
18

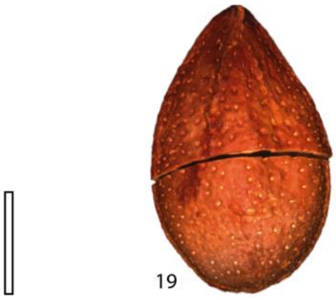
19


20


21


22


23

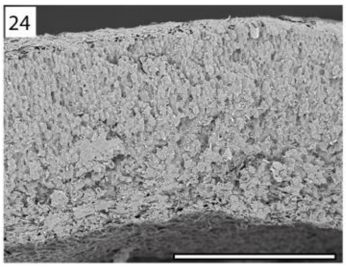
24

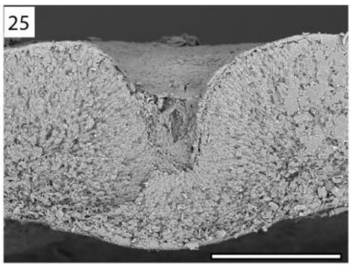
25

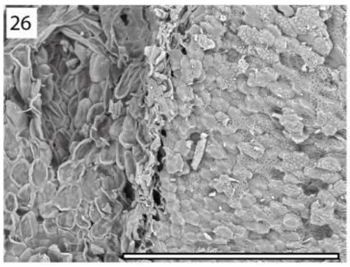
26

Plate XVIII

Pleurisanthes flava Sandwith
(*J.J. Pipoly 10168*)
1. – Lateral view of the dried fruit.
2. – Lateral view of a broken endocarp showing mounds and hairs-like fibres.
3. – Dorsal view of the endocarp.
4. – Second lateral view.
5. – Apical view.
6. – Basal view.
7. – SEM view of the pericarp with a vasculature in an endocarp channel (arrow).
8. – SEM view of the endocarp wall in transverse section.
9. – SEM view of the small ovoid hairs with an acuminate apex in the epicarp surface.

Pyrenacantha acuminata Engl.
(*R.P. Tisserant s.n.*)
10. – Lateral view of the dried fruit.
11. – Lateral view of the endocarp showing the pits and the main ridge.
12. – Dorsal view of the endocarp.
13. – Second lateral view.
14. – Apical view.
15. – Basal view.
16. – SEM view of the endocarp in transverse section showing spiny tubercles.
17. – SEM view of tubercle cells in longitudinal section of the tubercule.
18. – SEM view of the endocarp wall in transverse section.

Pyrenacantha ambrensis Labat, El-Achkar & R. Rabev.
(*O. Andrianantoanina & A. Solotiana 62*)
19. – Lateral view of the dried fruit with an elongate gynophore here broken.
20. – Lateral view of a broken endocarp showing circular pits.
21. – Dorsal view of the endocarp showing the keel.
22. – Second lateral view.
23. – Apical view.
24. – Basal view.
25. – SEM view of the pericarp in transverse section.
26. – SEM view of the endocarp wall in transverse section.
27. – SEM view of cells of the tubercle in its longitudinal section.

Scale: 1–6, 10–15, 19–24 = 10 mm; 16, 25 = 2 mm; 7 = 1 mm; 18, 26 = 500 µm; 8, 27 = 300 µm; 9, 17 = 100 µm.

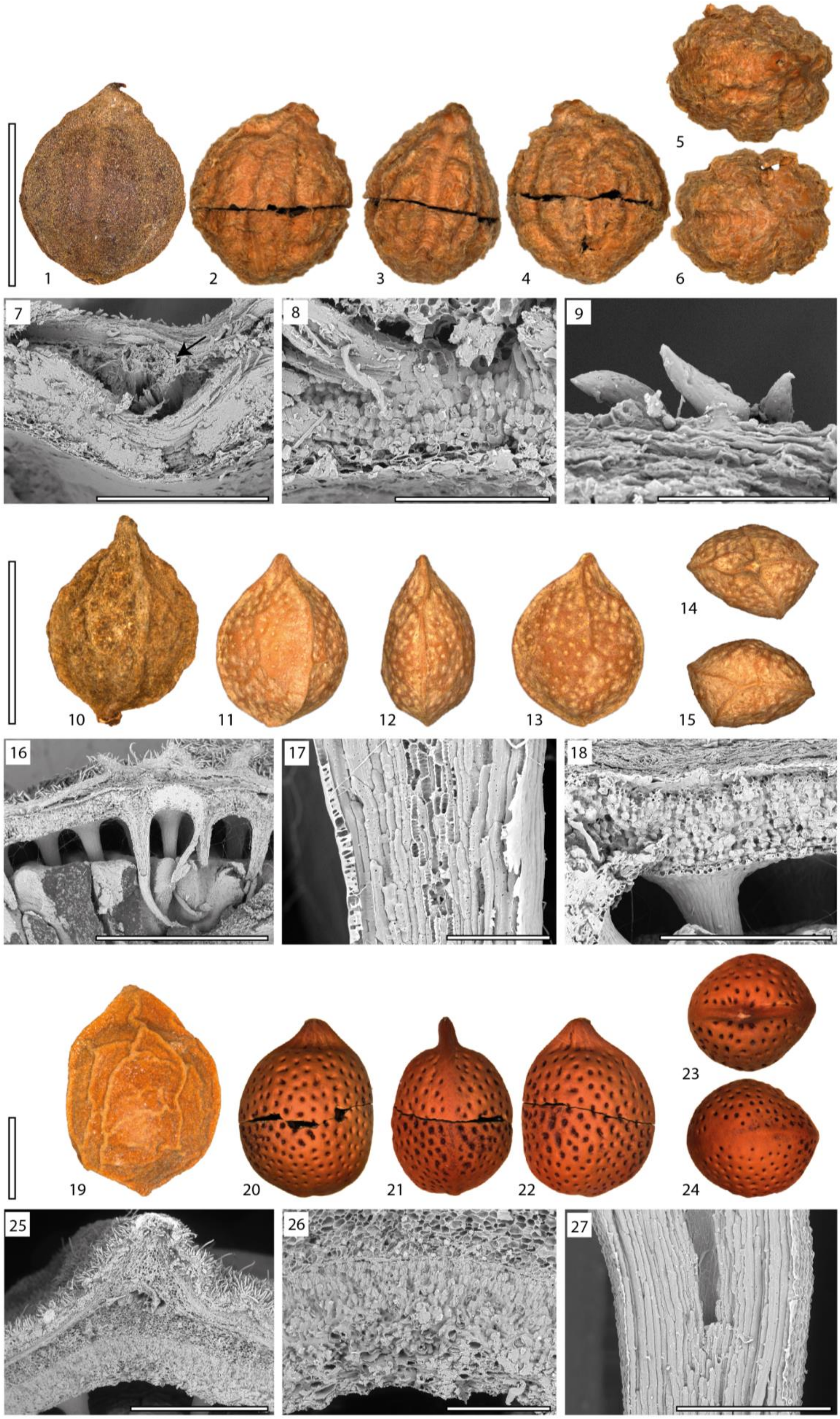
1
2
3
4
5
6
7
8
9
10
11
12
13
14
15
16
17
18
19
20
21
22
23
24
25
26
27

Plate XIX

Pyrenacantha andapensis Labat, El-Achkar & R.Rabev.
(*D. Ravelonarivo et al. 72*)
1. – Lateral view of the dried fruit with an elongate gynophore here boken.
2. – Lateral view of a broken endocarp showing the pits.
3. – Dorsal view of the endocarp.
4. – Second lateral view.
5. – Apical view.
6. – Basal view.
7. – SEM view of the endocarp wall in transverse section and spiny tubercles.
8. – SEM view of the inner part cells of the endocarp wall in transverse section, and the innermost layer that line the locule with papillae.
9. – SEM view of the small ovoid hairs with an acuminate apex on the epicarp surface.

Pyrenacantha anhydathoda (Villiers) Byng & Utteridge
(*A.P. Teilles (?) 100*)
10. – Lateral view of the endocarp showing the pits and the main ridges.
11. – Dorsal view of the endocarp.
12. – Second lateral view.
13. – Apical view.
14. – Basal view.
15. – SEM view of the endocarp showing elongate flattened tubercles.
16. – SEM view of the endocarp wall in transverse section.
17. – SEM view of spherical papillae lining the locule surface.

Pyrenacantha capitata H.Perrier
(*F. Ratovoson et al. 678*)
18. – Lateral view of the dried fruit with a short gynophore.
19. – Lateral view of the endocarp showing the pits.
20. – Dorsal view of the endocarp.
21. – Second lateral view.
22. – Apical view.
23. – Basal view.
24. – SEM partial view of the fruit in transverse section showing spiny tubercles and long and thin hairs on the epicarp.
25. – SEM view of the pericarp in transverse section.
26. – SEM view of the cells of the tubercle in its longitudinal section.

Scale: 1–6, 10–14, 18–23 = 10 mm; 7, 24 = 2 mm; 15, 25 = 1 mm; 9 = 500 µm; 16, 26 = 300 µm; 8 = 200 µm; 17 = 30 µm.


1


2


3


4


5


6

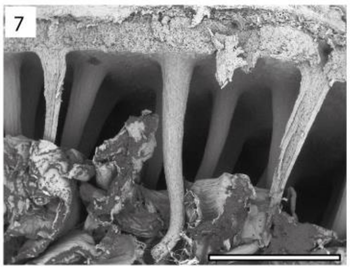
7

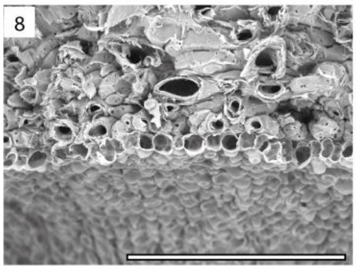
8

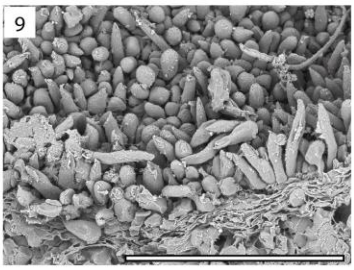
9


10


11


12


13


14

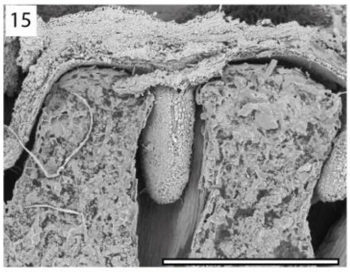
15

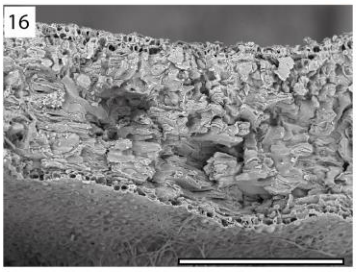
16

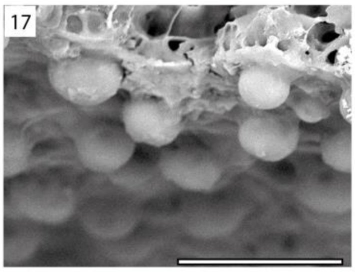
17


18


19


20


21


22


23

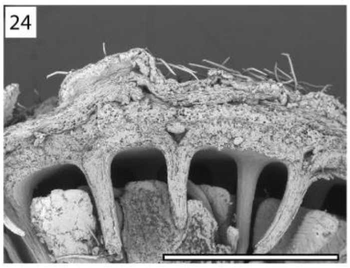
24

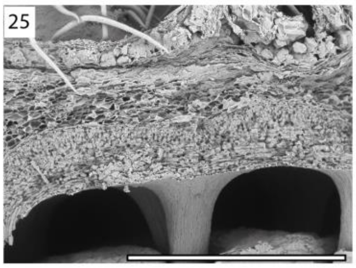
25

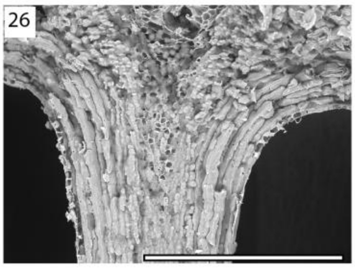
26

Plate XX

Pyrenacantha cordicula Villiers
(*M. Etuge & D. Thomas 28*)
1. – Lateral view of the dried fruit with a short gynophore.
2. – Lateral view of the endocarp showing the pits and ridges.
3. – Dorsal view of the endocarp.
4. – Second lateral view.
5. – Apical view.
6. – Basal view.
7. – SEM view of the endocarp showing cylindrical tubercles.
8. – SEM view of cells of the tubercle in its transverse section.
9. – SEM view of the endocarp wall in transverse section.

Pyrenacantha glabrescens (Engl.) Engl.
(*A. Chevalier 17326*)
10. – Lateral view of the dried fruit with a short gynophore.
11. – Lateral view of the endocarp showing the pits (decayed).
12. – Dorsal view of the endocarp.
13. – Second lateral view.
14. – Apical view.
15. – Basal view.
16. – SEM view of the atrophied spiny tubercles.
17. – SEM view of the pericarp in transverse section.
18. – SEM view of the uncinate hairs on the epicarp.

Pyrenacantha gossweileri (Exell) Byng & Utteridge
(*Y. Attims 42*)
19. – Lateral view of the dried fruit with a inflated cap and ending by a short tube.
20. – Lateral view of the endocarp showing the pits and ridges.
21. – Dorsal view of the endocarp showing the keel.
22. – Second lateral view.
23. – Apical view.
24. – Basal view.
25. – SEM view of the fruit and seed in transverse section.
26. – SEM detail of transverse section of the endocarp showing an elongate flattened tubercle diving in a seed pit.
27. – SEM view of the inner layers of the endocarp showing papillae lining the locule surface.

Scale: 1–6, 10–15, 19–24 = 10 mm; 7, 25 = 2 mm; 16, 17 = 1 mm; 8, 26 = 500 µm; 9, 18 = 300 µm; 27 = 50 µm.

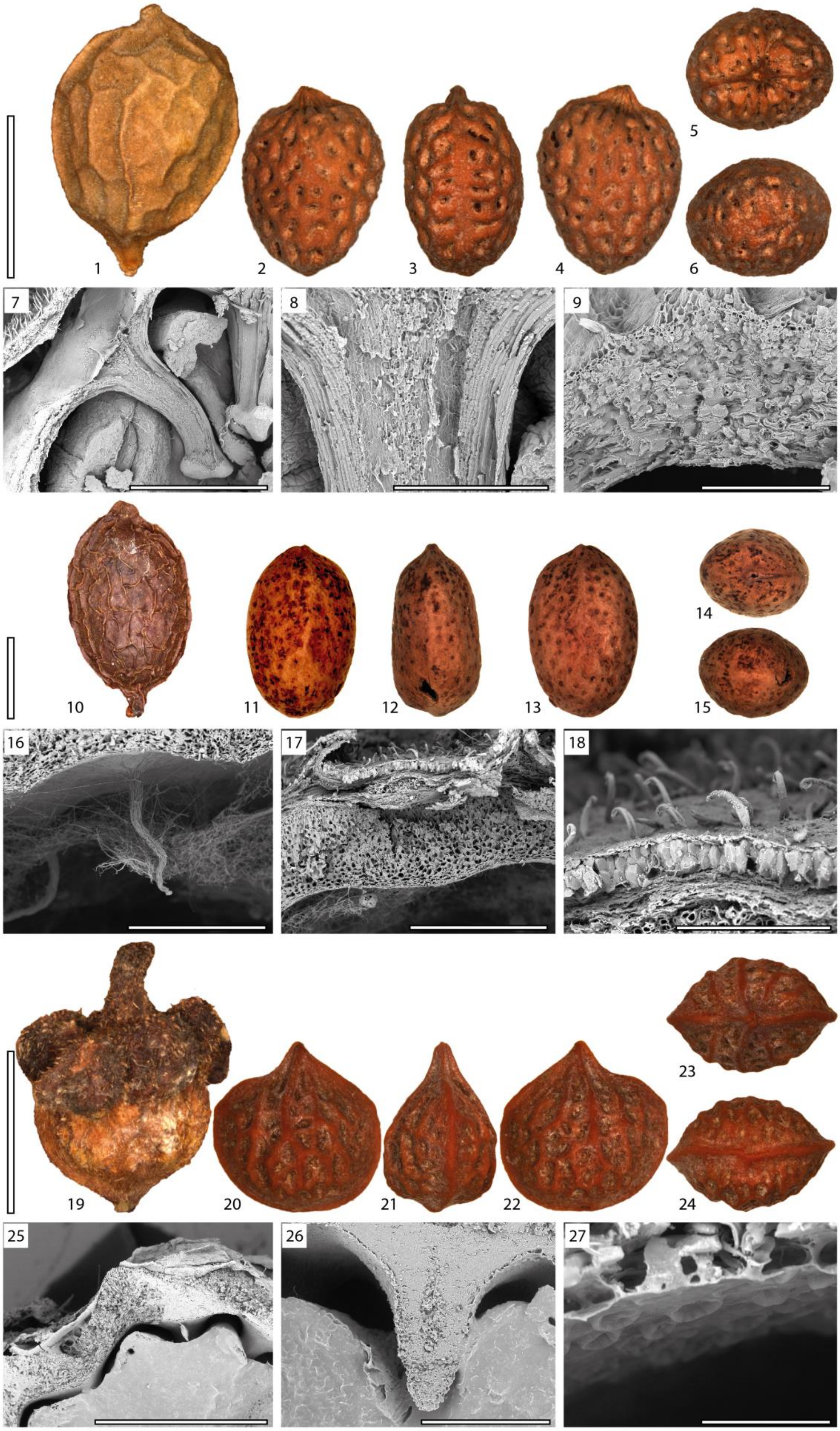
1
2
3
4
5
6
7
8
9
10
11
12
13
14
15
16
17
18
19
20
21
22
23
24
25
26
27

Plate XXI

Pyrenacantha humblotii (Baill. ex Grandid.) Sleumer
(*M. Nicoll, P. Lowry & A. Rakotozafy 570*)
1. – Lateral view of the dried fruit with a broken gynophore.
2. – Lateral view of the endocarp showing the pits and ridges.
3. – Dorsal view of the endocarp.
4. – Second lateral view.
5. – Apical view.
6. – Basal view.
7. – SEM view of the fruit in transverse section showing endocarp with spiny tubercles expanding between the seed cells.
8. – SEM view of tubercle cells in its logitudinal section.
9. – SEM view of the papillae on the tubercle surface.

Pyrenacantha kaurabassana Baill.
(*A. Gomes e Sousa 1584*)
10. – Lateral view of the dried fruit with a portion of the gynophore.
11. – Lateral view of a broken endocarp showing the pits and sharp ridges.
12. – Dorsal view of the endocarp showing the keel.
13. – Second lateral view.
14. – Apical view.
15. – Basal view.
16. – SEM view of the peg-shaped tubercles in a transverse section of the pericarp (Note the presence of fungal hyphae).
17. – SEM view of the endocarp wall in transverse section.
18. – SEM view of the papillae on the tubercle surface.

Pyrenacantha klaineana Pierre ex Exell & Mendonça
(*A.J.M. Leewenber 4523*)
19. – Lateral view of the dried fruit with a gynophore here broken.
20. – Lateral view of the endocarp showing the pits.
21. – Dorsal view of the endocarp showing the keel.
22. – Second lateral view.
23. – Apical view.
24. – Basal view.
25. – SEM view of the capitate peg-shaped tubercles.
26. – SEM view showing cells of the tubercle in its longitudinal section.
27. – SEM view of the endocarp wall in transverse section.

Scale: 1–6, 10–15, 19–24 = 10 mm; 7 = 2 mm; 16, 25 = 1 mm; 17 = 500 µm; 8 = 300 µm; 18 = 200 µm; 26, 27 = 100 µm; 9 = 50 µm.


1
2
3
4
5
6
7
8
9
10
11
12
13
14
15
16
17
18
19
20
21
22
23
24
25
26
27

Plate XXII

Pyrenacantha laetevirens Sleumer
(*H. Grevé 234*)
1. – Lateral view of the dried fruit with a short gynophore here partially broken.
2. – Lateral view of a broken endocarp showing the pits and flattened reticulation.
3. – Dorsal view of the endocarp.
4. – Second lateral view.
5. – Apical view.
6. – Basal view.
7. – SEM view of the cylindrical tubercle between seed cells.
8. – SEM view of the pericarp in transverse section showing the regular tomentum on the epicarp.
9. – SEM view of the endocarp in transverse section.

Pyrenacantha lebrunii Boutique
(F.J. Breteler 2933)
10. – Lateral view of the dried fruit with a short gynophore and elongate apex.
11. – Lateral view of a broken endocarp showing the pits and ridges.
12. – Dorsal view of the endocarp showing the keel.
13. – Second lateral view.
14. – Apical view.
15. – Basal view.
16. – SEM view of pericarp with the spiny tubercles and corresponding seed cavities separated each other after retraction of the seed tissue of due to drying.
17. – Detail of the endocarp in transverse section showing the wall and tubercle cells.
18. – Other detail showing simple hairs on the epicarp.

Pyrenacantha longirostrata Villiers
(*R. Letouzey 14156*)
19. – Lateral view of the apical part of the endocarp showing the pits and ridges.
20. – Second lateral view.
21. – Internal view showing spiny tubercles.
22. – Apical view.
23. – SEM view of the endocarp in transverse section showing wall and tubercle cells.
24. – SEM view of uncinate hairs on the epicarp.
25. – SEM view of papillae on the locule.

Scale: 1–6, 10–15, 19, 20, 22 = 10 mm; 7, 16 = 2 mm; 8, 21 = 1 mm; 23 = 500 µm; 9, 17, 18 = 300 µm; 24 = 100 µm; 25 = 30 µm.

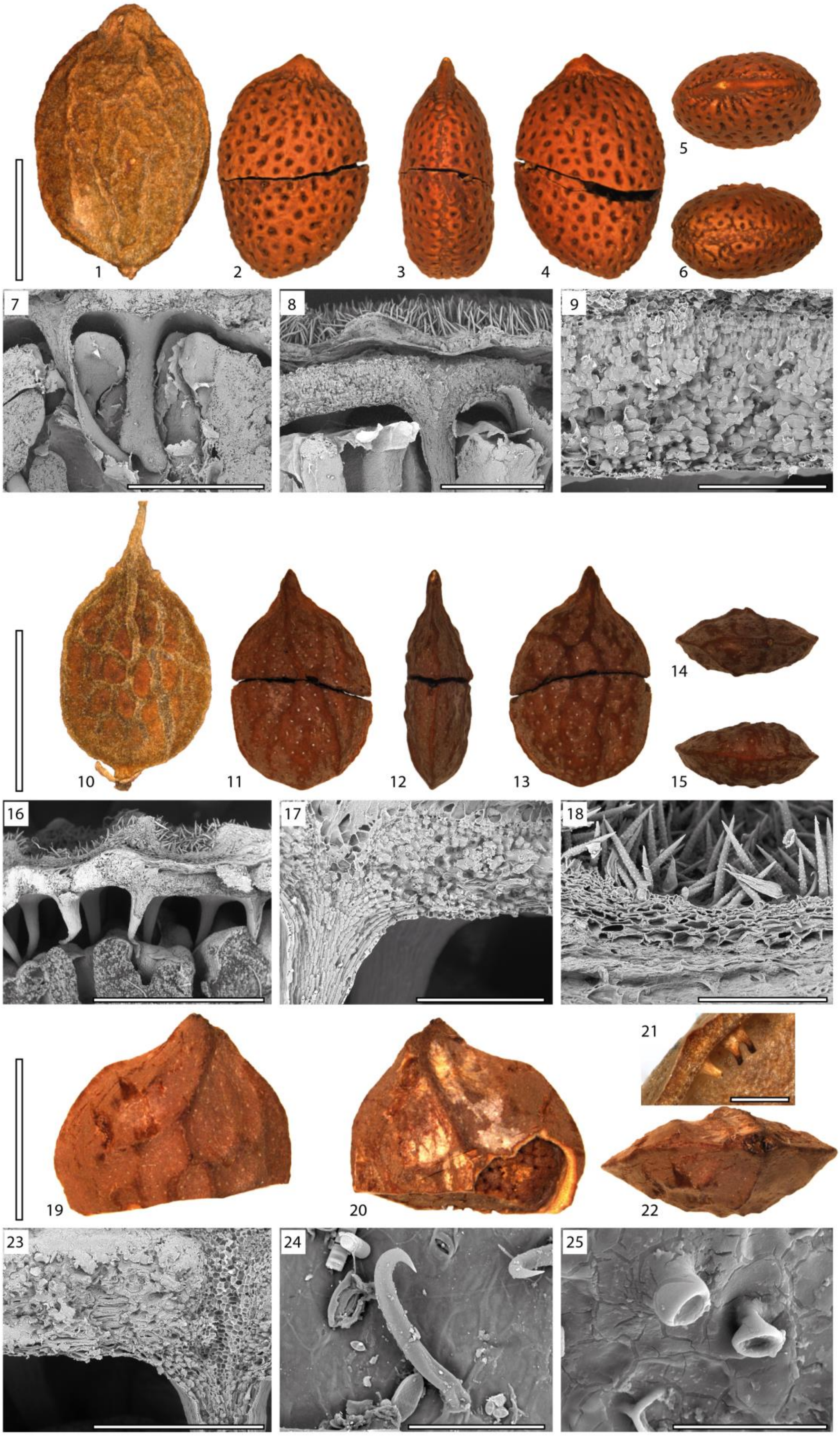
1
2
3
4
5
6
7
8
9
10
11
12
13
14
15
16
17
18
19
20
21
22
23
24
25

Plate XXIII

Pyrenacantha macrocarpa (A. Chev. ex Hutch. & Dalziel) Byng & Utteridge
(*J. De Koning 4918*)
1. – Lateral view of the dried fruit with a short gynophore and an inflated cap ending by an elongate tube.
2. – Lateral view of the endocarp showing the pits.
3. – Dorsal view of the endocarp showing a keel.
4. – Second lateral view.
5. – Apical view.
6. – Basal view.
7. – SEM view of the outer surface with pits and transverse section of the endocarp showing wall and elongate-flattened tubercles between seed tissues.
8. – SEM view of the inner layers of the endocarp wall.

Pyrenacantha malvifolia Engl.
(*P. Polill 475*)
9. – Lateral view of the dried fruit with a short gynophore.
10. – Lateral view of a broken endocarp showing the pits and ridges.
11. – Dorsal view of the endocarp showing the keel.
12. – Second lateral view.
13. – Apical view.
14. – Basal view.
15. – SEM view of the pericarp in transverse section showing peg-shaped tubercles on the inner part of the endocarp.
16. – Detail of longidudinal section of the tubercle showing the cell layers.
17. – Other detail showing the papillae and one stomata (arrow) on the apex of a tubercle.

Pyrenacantha puberula Boutique
(*C. Evrard 601*)
18. – Lateral view of the dried fruit with a short gynophore and a short acuminate apex.
19. – Lateral view of the endocarp showing the pits.
20. – Dorsal view of the endocarp showing the keel.
21. – Second lateral view showing the pitted seed in the left bottom part (pericarp missing area).
22. – Apical view.
23. – Basal view.
24. – SEM view of the fruit in transverse section showing spiny tubercles entering in the pitted seed.
25. – SEM view of the endocarp in transverse section showing the wall and the base of tubercle wall.
26. – SEM view of the papillae on the apex of the tubercle.

Scale: 1–6, 9–14, 18–23 = 10 mm; 7, 15, 24 = 2 mm; 25 = 300 µm; 16, 26 = 200 µm; 8, 17 = 50 µm.

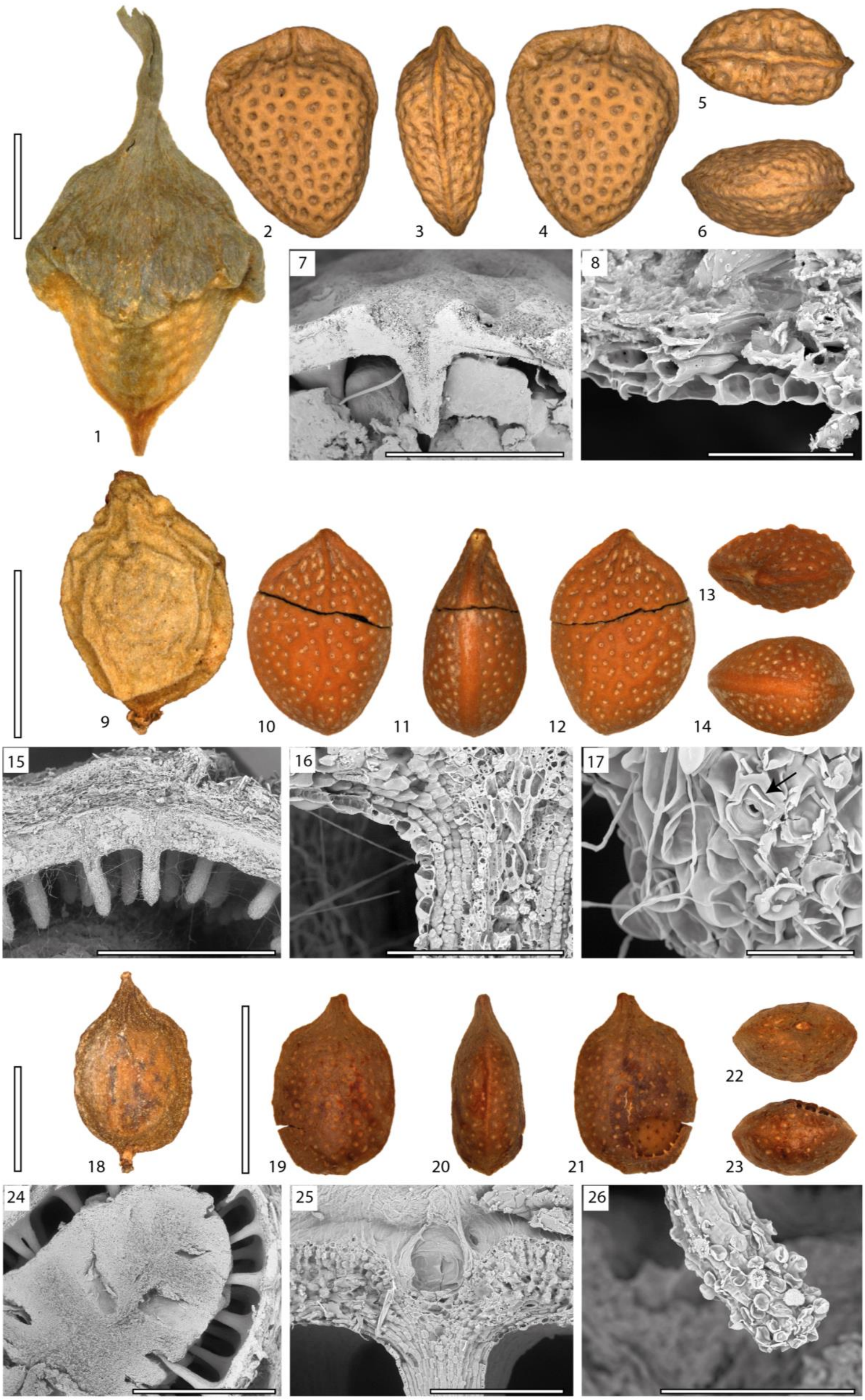
1
2
3
4
5
6
7
8
9
10
11
12
13
14
15
16
17
18
19
20
21
22
23
24
25
26

Plate XXIV

Pyrenacantha rakotozafyi Labat, El-Achkar & R.Rabev.
(*F. Barthelat 1764*)
1. – Lateral view of the dried fruit.
2. – Lateral view of a broken endocarp showing the pits.
3. – Dorsal view of the endocarp showing the keel.
4. – Second lateral view.
5. – Apical view.
6. – Basal view.
7. – SEM view of the endocarp in transverse section showing peg-shaped tubercles.
8. – Detail showing the tubercle base and endocarp cells in transverse section.
9. – SEM view of the uncinate hairs on the epicarp.

Pyrenacantha soyauxii (Engl.) Byng & Utteridge
(*R.P. Klaine 1469*)
10. – Lateral view of the dried fruit with a short gynophore (broken here) and an inflated cap at the apex.
11. – Lateral view of a broken endocarp showing the pits and ridges.
12. – Dorsal view of the endocarp showing the keel.
13. – Second lateral view.
14. – Apical view.
15. – Basal view.
16. – SEM view of an elongate flattened tubercle.
17. – SEM view of an elongate flattened tubercle in its longitudinal section.
18. – Detail showing the endocarp wall in transverse section.

Pyrenacantha staudtii (Engl.) Engl.
(*R.P. Tisserant 1737*)
19. – Lateral view of the dried fruit.
20. – Lateral view of the endocarp showing the pits and ridges.
21. – Dorsal view of the endocarp showing the keel.
22. – Second lateral view.
23. – Apical view.
24. – Basal view.
25. – SEM view of fruit in transverse section showing the cylindrical tubercles between seed tissues.
26. – Detail of a tubercle base and endocarp cells in transverse section.
27. – SEM view of the capitate tubercle apices.

Scale: 1–6, 10–15, 19–24 = 10 mm; 25 = 2 mm; 7 = 1 mm; 16–18, 26, 27 = 500 µm; 8 = 300 µm; 9 = 100 µm.

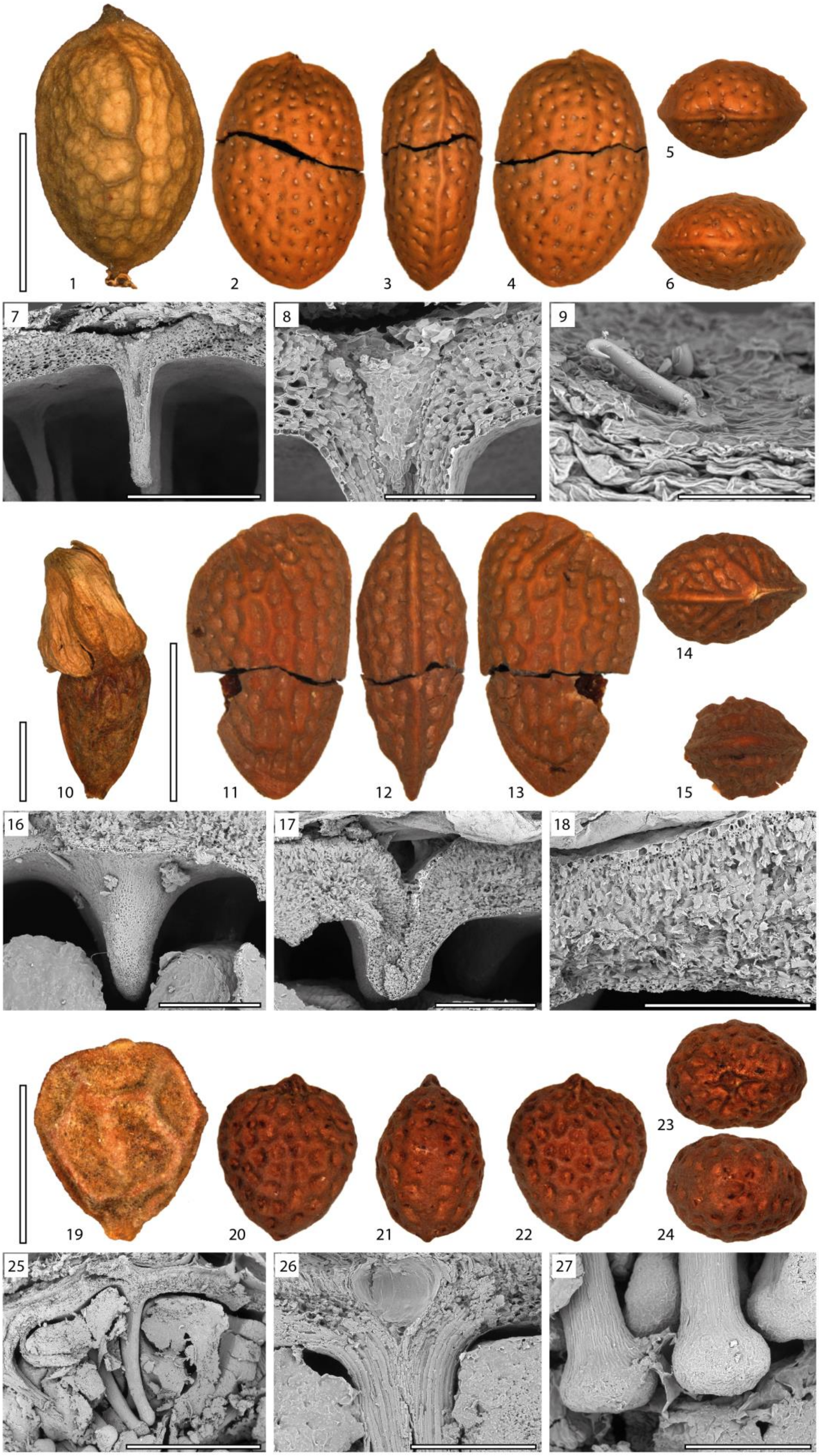
1
2
3
4
5
6
7
8
9
10
11
12
13
14
15
16
17
18
19
20
21
22
23
24
25
26
27

Plate XXV

Pyrenacantha sylvestris S.Moore
(*N. Hallé 3598*)
1. – Lateral view of the dried fruit.
2. – Lateral view of the endocarp showing the pits and ridges.
3. – Dorsal view of the endocarp showing the keel.
4. – Second lateral view.
5. – Apical view.
6. – Basal view.
7. – SEM view of the fruit in transverse section showing cylindrical tubercles inserted between seed tissues.
8. – Detail of a tubercle base and endocarp cells in transverse section.
9. – Detail of the pericarp showing endocarp bellow the mesocarp and epicarp covered by dense simple hairs.

Pyrenacantha thomsoniana (Bail.) Byng & Utteridge
(*M. Le Testu 1038*)
10. – Lateral view of the dried fruit with short gynophore and a cap ending in a very long tip.
11. – Lateral view of the endocarp showing the pits and ridges.
12. – Dorsal view of the endocarp showing the keel.
13. – Second lateral view.
14. – Apical view.
15. – Basal view.
16. – SEM view of the pericarp in transverse section showing the elongate flattened tubercles.
17. – SEM view of pericarp showing the long and thin hairs on the epicarp.
18. – SEM view of the endocarp wall in transverse section bearing the tubercules.

Pyrenacantha tropophila Labat, El-Achkar & R. Rabev.
(*H. Perrier de la Bâthie 1746*)
19. – Lateral view of the endocarp showing the pits.
20. – Dorsal view of the endocarp.
21. – Second lateral view.
22. – Apical view.
23. – Basal view.
24. – SEM view of the endocarp and seed in transverse section showing the spiny tubercles .
25. – Detail of longitudinal section of a tubercle base.
26. – Detail showing inner layers of the endocarp and the papillae emerging from the locule surface.

Scale: 1–6, 10–15, 19–23 = 10 mm; 7, 17, 24 = 2 mm; 16, 18 = 1 mm; 9 = 500 µm; 8, 25 = 300 µm; 26 = 50 µm.

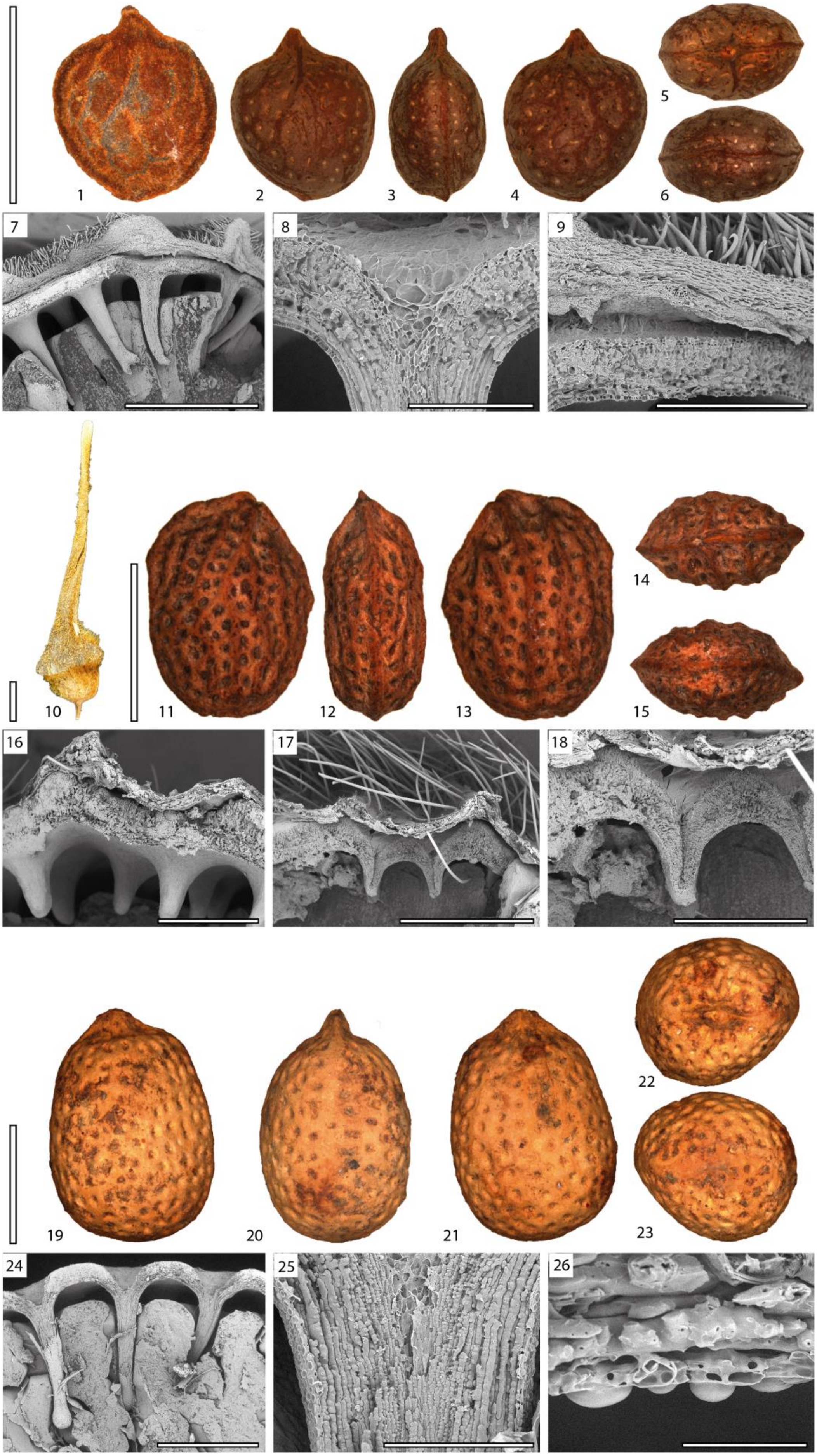
1
2
3
4
5
6
7
8
9
10
11
12
13
14
15
16
17
18
19
20
21
22
23
24
25
26

Plate XXVI

Pyrenacantha vogeliana Baill.
(*R.P. Sacleux 1873*)
1. – Lateral view of the dried fruit.
2. – Lateral view of the endocarp showing the pits and faintly marked ridges.
3. – Dorsal view of the endocarp showing the keel.
4. – Second lateral view.
5. – Apical view.
6. – Basal view.
7. – SEM view of the endocarp in a transverse section showing peg-shaped tubercles.
8. – SEM view of a longitudinal section of the "pipe-like" tubercle showing cells and central lacuna.
9. – SEM view of the endocarp in transverse section.

Rhyticaryum elegans G.Schellenb.
(*R. Schlechter 18681*)
10. – Lateral view of the dried fruit.
11. – Lateral view of a broken endocarp showing a reticulate pattern of ridges.
12. – Second lateral view.
13. – Basal view.
14. – Magnification of the lateral view showing the pore at the apex (arrow).
15. – SEM view of the pericarp in transverse section showing a ridge.
16. – Other view the endocarp and mesocarp in transverse section.
17. – Detail of the inner layers of the endocarp with papillae lining the locule surface.

Rhyticaryum fasciculatum Becc.
(*Heu Her 4*)
18. – Lateral view of the endocarp showing a reticulate pattern of ridges.
19. – Dorsal view of the endocarp showing the keel.
20. – Second lateral view.
21. – Apical view.
22. – Basal view.
23. – SEM view of the endocarp wall in transverse section.
24. – Detail showing the cell arrangement.
25. – Other detail of inner part of the endocarp showing the papillae lining the locule surface.

Scale: 1–6, 10–13, 18–22 = 10 mm; 7, 14, 23 = 1 mm; 15, 16, 24 = 500 µm; 9 = 300 µm; 8 = 200 µm; 25 = 100 µm; 17 = 50 µm.

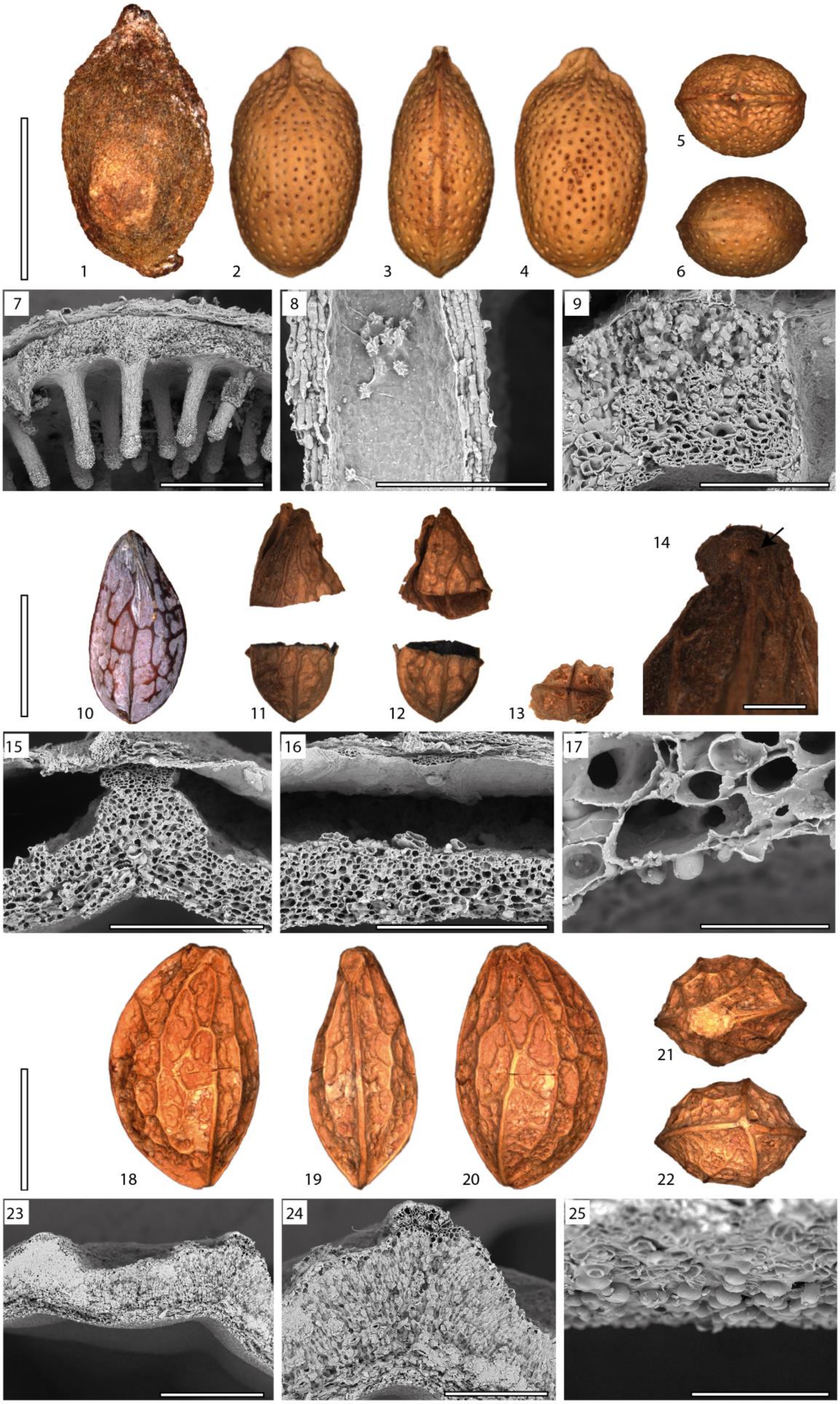
1
2
3
4
5
6
7
8
9
10
11
12
13
14
15
16
17
18
19
20
21
22
23
24
25

Plate XXVII

Rhyticaryum longifolium K.Schum. & Lauterb.
(*Jacobs 9671*)
1. – Lateral view of the dried fruit.
2. – Lateral view of the endocarp showing a reticulate pattern of ridges.
3. – Dorsal view of the endocarp showing the keel.
4. – Second lateral view.
5. – Apical view.
6. – Basal view.
7. – SEM view of the keel in transverse section.
8. – SEM view of the pericarp in transverse section showing the ridges and endocarp wall.
9. – SEM view of papillae lining the locule surface.

Rhyticaryum macrocarpum Becc.
(*W. Vink 11381*)
10. – Lateral view of the dried fruit.
11. – Lateral view of the endocarp showing the ridges.
12. – Dorsal view of the endocarp showing the keel.
13. – Second lateral view.
14. – Apical view.
15. – Basal view.
16. – Lateral view of other specimen showing the reticulum of ridges. (*Katik 46856*)
17. – SEM view of the endocarp wall in transverse section.
18. – SEM view of papillae lining the locule surface.

Rhyticaryum novoguineense (Warb.) Sleumer.
(*A. Millar, NGF 40764*)
19. – Lateral view of the dried fruit.
20. – Lateral view of the endocarp showing a reticulate pattern of ridges.
21. – Dorsal view of the endocarp showing the keel.
22. – Second lateral view.
23. – Apical view.
24. – Basal view.
25. – SEM view of the pericarp in transverse section.
26. – SEM view of the papillae lining the locule surface.

Scale: 1–6, 10–16, 19–24 = 10 mm; 7, 8, 17, 25 = 1 mm; 18, 26 = 100 µm; 9 = 50 µm.

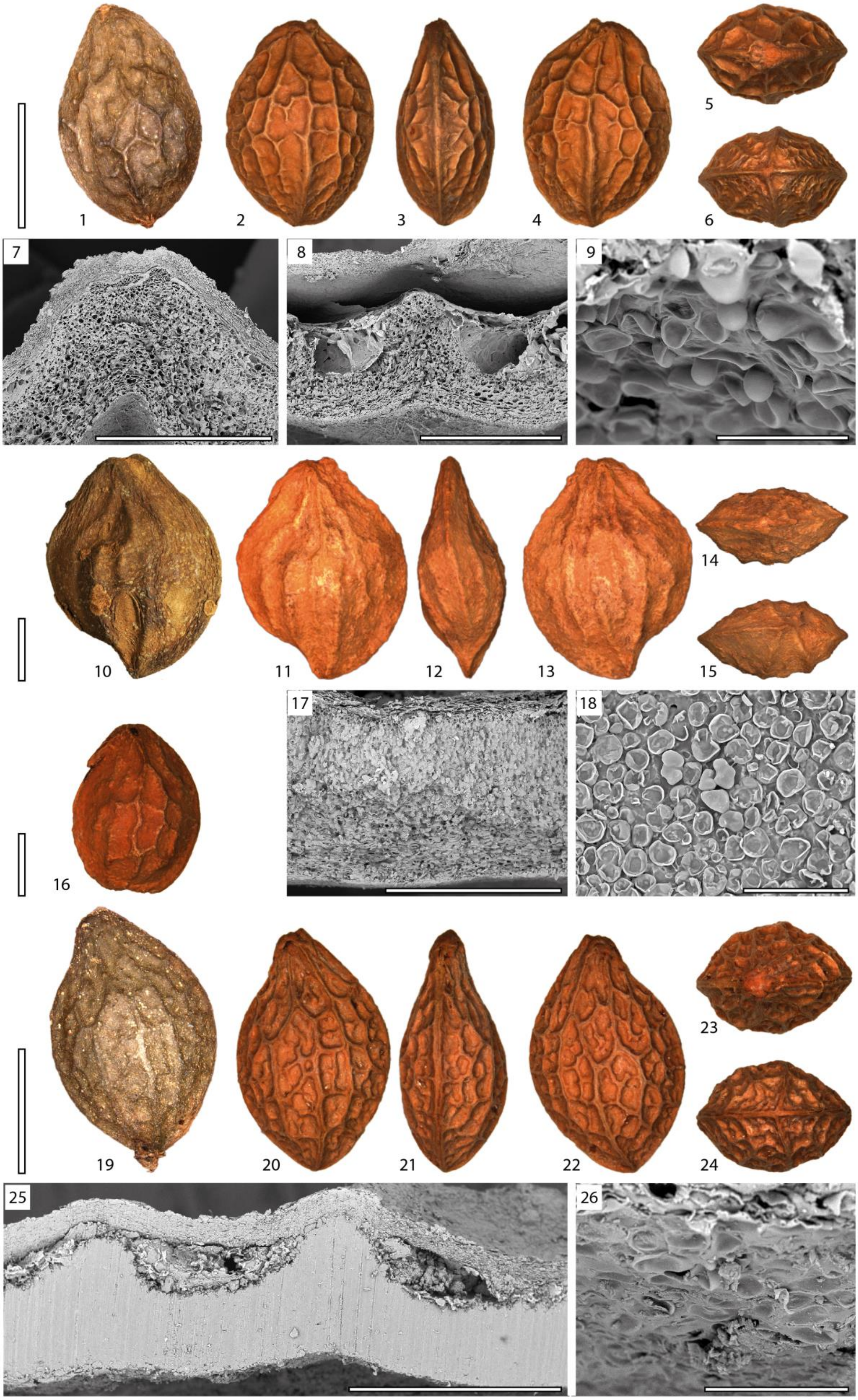
1
2
3
4
5
6
7
8
9
10
11
12
13
14
15
16
17
18
19
20
21
22
23
24
25
26

Plate XXVIII

Rhyticaryum oleraceum Becc.
(*P. Buwalda 4471*)
1. – Lateral view of the dried fruit.
2. – Lateral view of a broken endocarp showing the ridges.
3. – Dorsal view of the endocarp showing the keel.
4. – Second lateral view.
5. – Apical view.
6. – Basal view.
7. – SEM view of the keel in transverse section.
8. – SEM view of the endocarp wall in transverse section.
9. – SEM view of papillae lining the locule surface.

Rhyticaryum racemosum Becc.
(*Royen 3448*)
10. – Lateral view of the dried fruit.
11. – Lateral view of a broken endocarp showing a reticulate pattern of ridges.
12. – Dorsal view of the endocarp showing the keel.
13. – Second lateral view.
14. – Apical view.
15. – Basal view.
16. – SEM view of a ridge in transverse section.
17. – SEM view of the endocarp wall in transverse section.
18. – SEM view of papillae lining the locule surface.

Sarcostigma kleinii Wight & Arn.
(*King's Collector s.n.*)
19. – Lateral view of a broken endocarp showing the faint ornamentation.
20. – Dorsal view of the endocarp.
21. – Second lateral view.
22. – Apical view.
23. – Basal view.
24. – SEM view of the endocarp wall in transverse section.

Sarcostigma paniculata Pierre
(*E. Poilane 6677*)
25. – Lateral view of the dried fruit.
26. – Lateral view of a broken endocarp showing the low ornamentation.
27. – Dorsal view of the endocarp showing the keel.
28. – Second lateral view.
29. – Apical view.
30. – Basal view.
31. – SEM view of the endocarp wall in transverse section.
32. – SEM view of the papillae lining the locule surface.

Scale: 1–6, 10–15, 19–23, 25–30 = 10 mm; 16 = 1 mm; 7, 17, 24, 31 = 500 µm; 8 = 200 µm; 18, 32 = 100 µm; 9 = 50 µm.

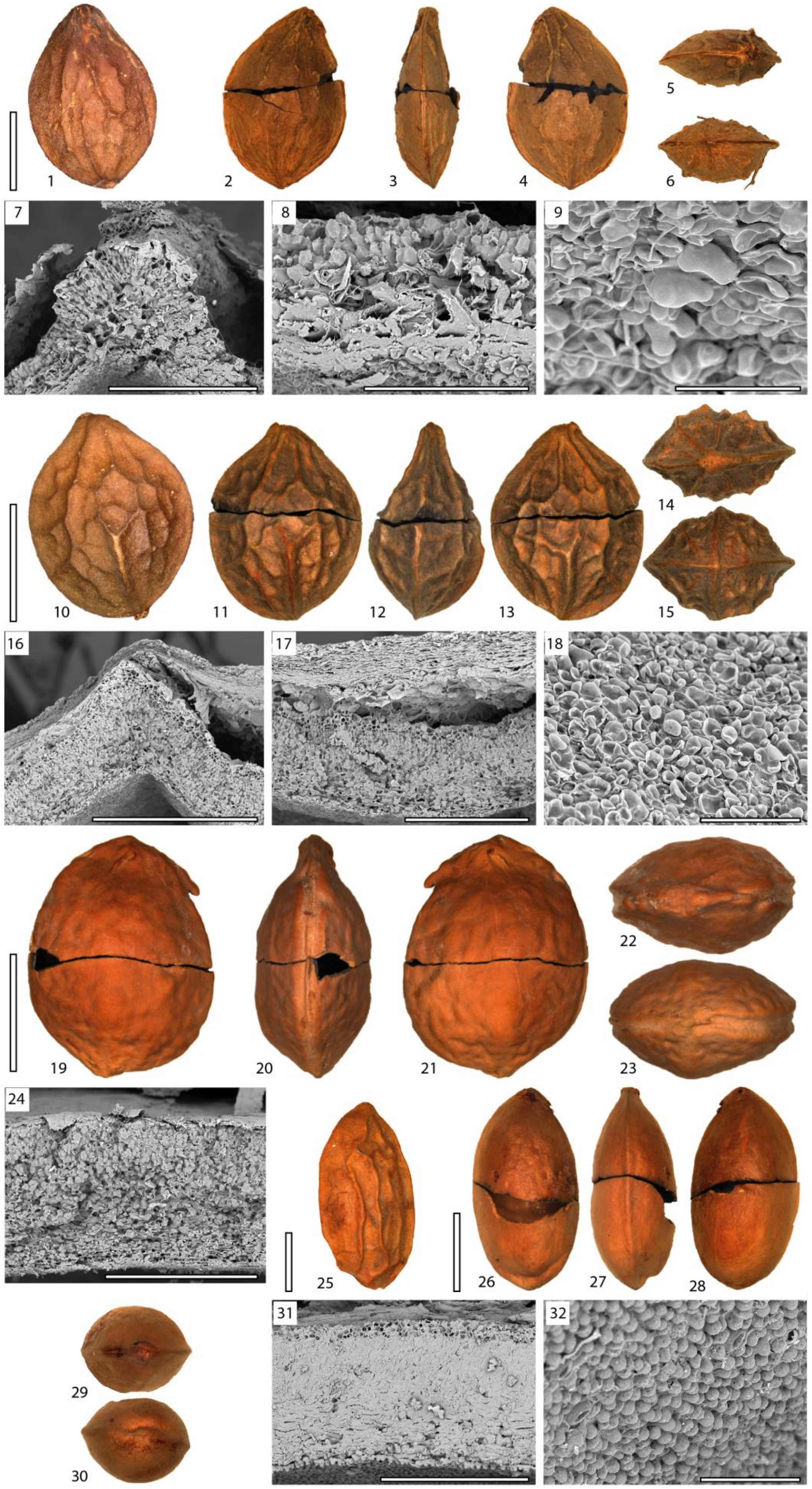
1
2
3
4
5
6
7
8
9
10
11
12
13
14
15
16
17
18
19
20
21
22
23
24
25
26
27
28
29
30
31
32

Plate XXIX

Stachyanthus donisii (Boutique) Boutique
(*J.H. Laurent 423*)
1. – Lateral view of the dried fruit.
2. – Lateral view of the endocarp showing the pits and ridges.
3. – Dorsal view of the endocarp showing the keel.
4. – Second lateral view.
5. – Apical view.
6. – Basal view.
7. – SEM view from the locule side of the conical tubercles.
8. – SEM view of the endocarp in transverse section, showing the conical tubercle cell arrangement.
9. – Detail showing the central tubercle cells.

Stachyanthus occidentalis (Keay & É. Miège) Boutique
(*A. Chervalier 23794*)
10. – Lateral view of the dried fruit.
11. – Lateral view of the endocarp showing the pits and ridges.
12. – Dorsal view of the endocarp showing the keel.
13. – Second lateral view.
14. – Apical view.
15. – Basal view.
16. – SEM view from the locule side of the conical tubercles.
17. – SEM view of the pericarp in transverse section showing conical tubercles .
18. – Detail of the endocarp wall.

Stachyanthus zenkeri Engl.
(*Carvalho 3626*)
19. – Lateral view of the dried fruit.
20. – Lateral view of a broken endocarp showing the pits and ridges.
21. – Dorsal view of the endocarp showing the keel.
22. – Second lateral view.
23. – Apical view.
24. – Basal view.
25. – SEM view in transverse section of the pericarp of the ridges and conical tubercles.
26. – Detail on the pericarp in transverse section.
27. – Other detail showing the endocarp wall.

Scale: 1–6, 10–15, 19–24 = 10 mm; 25 = 2 mm; 26 = 1 mm; 8, 17, 27 = 500 µm; 7 = 300 µm; 16, 18 = 200 µm; 9 = 50 µm.

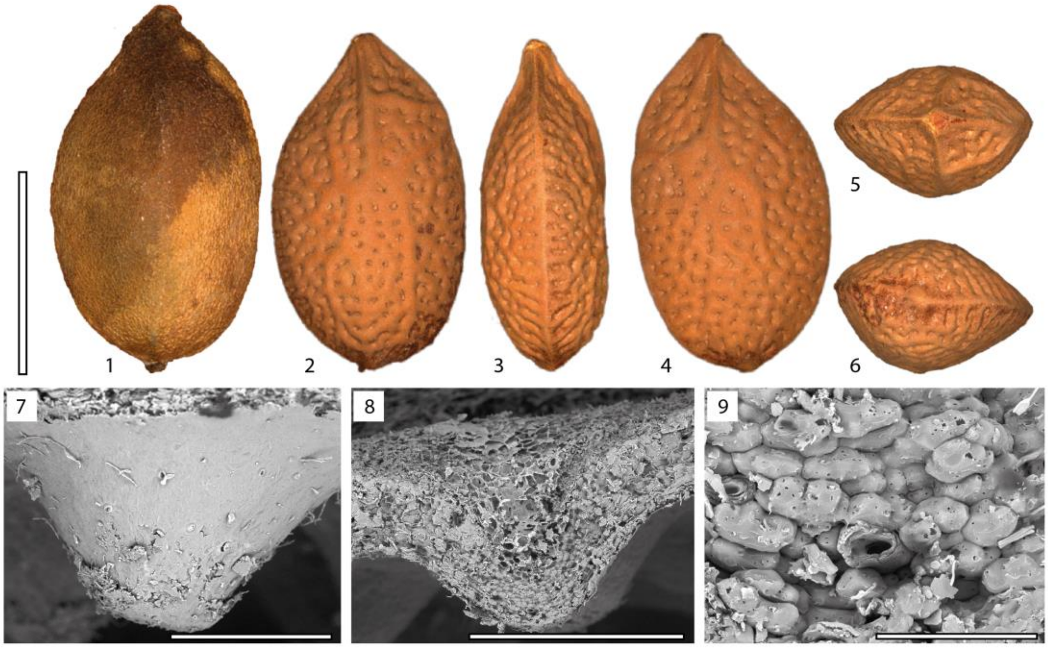
1
2
3
4
5
6
7
8
9

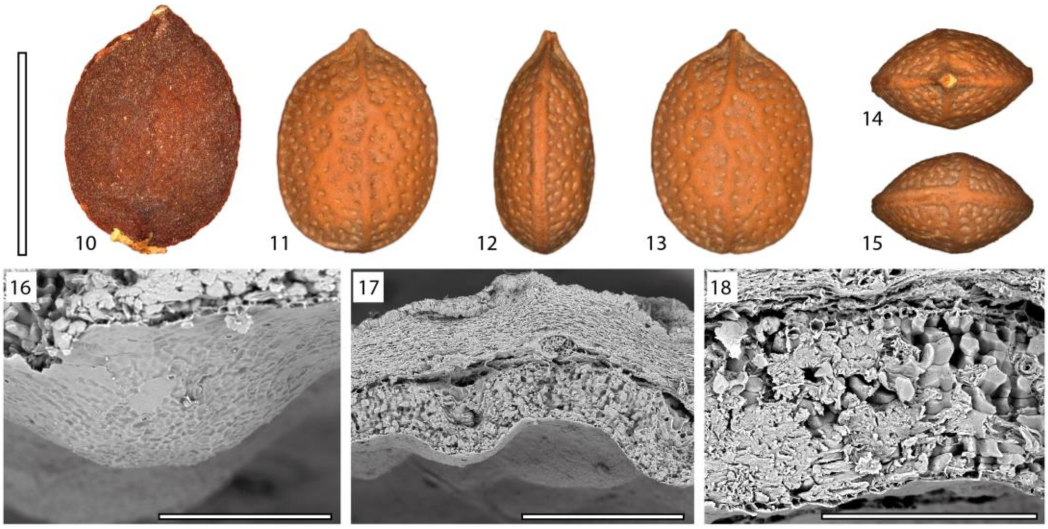
10
11
12
13
14
15
16
17
18

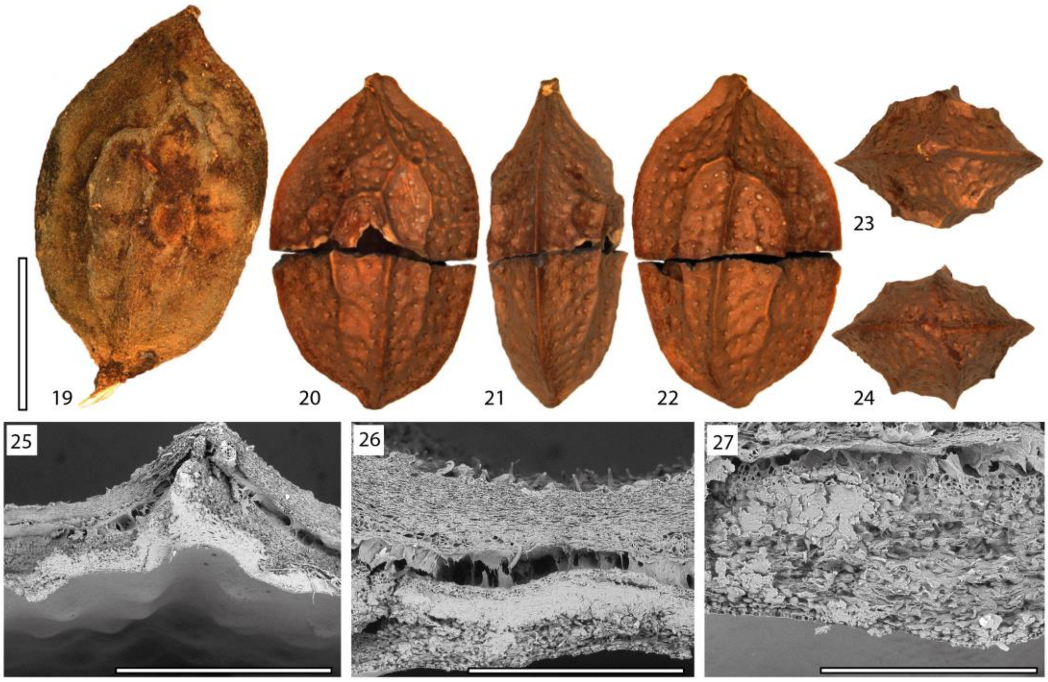
19
20
21
22
23
24
25
26
27

Plate XXX

Apodytes dimidiata E.Mey. ex Arn.
(*R. Ranaivojaona et al. 114*)
1. – Lateral view of the asymmetrical fruit with calice and style.
2. – Dorsal view of the fruit.
3. – Second Lateral view of the dried fruit.
4. – Apical view.
5. – Basal view.
6. – Lateral view of the endocarp showing lateral ridges.
7. – SEM view of the sclerotic mass in the ventral part of the fruit.
8. – SEM view of the endocarp wall in transverse section.
9. – Detail showing the layer of elongate cells lining the locule.

Dendrobangia boliviana Rusby
(*O. Poncy 2800*)
10. – Lateral view of the dried fruit.
11. – Lateral view of the endocarp showing the inconspicuous roughness.
12. – Dorsal view of the endocarp showing the enlarged channel.
13. – Second lateral view.
14. – Apical view showing the marked enlarged channel on the left side.
15. – Basal view.
16. – SEM view of the endocarp wall in transverse section.
17. – Detail of another part of the endocarp in transverse section.

Emmotum nitens (Benth.) Miers
(*R. M. Harley & R. Souza 10028*)
18. – Lateral view of the dried fruit.
19. – Lateral view of the endocarp showing the coarse expansions.
20. – Dorsal view of the endocarp showing the keel.
21. – Second lateral view.
22. – Transverse section of the endocarp in apical view.
23. – Apical view.
24. – Basal view.
25. – SEM view of a detail of the outer endocarp wall showing porate cell wall with thorn expansions.
26. – SEM view of pores on the outer endocarp wall.
27. – SEM view of the inner endocarp wall in transverse section showing the same cells than the inner endocarp wall.

Scale: 1–6, 10–15, 18–24 = 10 mm; 7 = 2 mm; 26, 27 = 500 µm; 8 = 300 µm; 25 = 200 µm; 9 = 50 µm.

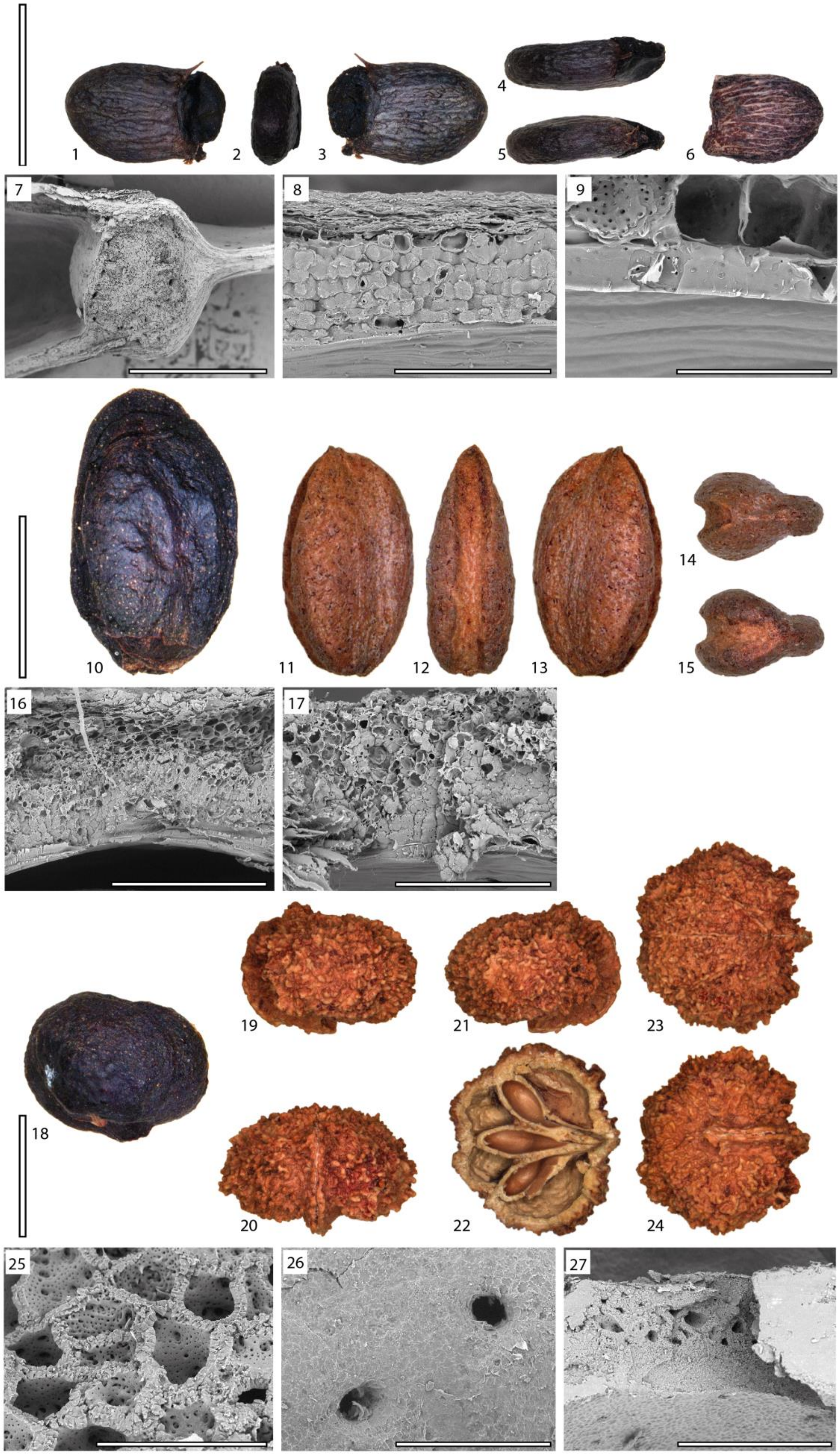
1
2
3
4
5
6
7
8
9
10
11
12
13
14
15
16
17
18
19
20
21
22
23
24
25
26
27

Plate XXXI

Pittosporopsis kerii Craib
(*M.F. Newman et al. LAO 831*)
1. – Lateral view of the dried fruit.
2. – Lateral view of the endocarp showing ridges.
3. – Apical view.
4. – Basal view.
5. – SEM view of the endocarp wall in transverse section showing vascular tissues in both sides.
6. – Other SEM view of the endocarp wall in transverse section showing the tree main layers.
7. – Detail showing the cell of the medium layer walls.

Platea parvifolia Merr.& Chun
(*W.T. Tsang 27299*)
8. – Lateral view of the dried fruit.
9. – Lateral view of the endocarp showing the mounds.
10. – Dorsal view of the endocarp.
11. – Second lateral view.
12. – Apical view.
13. – Basal view.
14. – SEM view of the endocarp wall in transverse section.
15. – Detail showing the endocarp cell walls and their organization.

Oncotheca balansae Baill.
(*H.S. Mackee 37671*)
16. – Lateral view of the dried fruit.
17. – Apical view.
18. – Basal view.
19. – SEM view of the outer and inner endocarp wall.
20. – SEM view of the inner endocarp wall showing prismatic crystal.
21. – SEM view of the locule surface lined by elongate cells.

Scale: 1–4, 8–13, 16–18 = 10 mm; 19 = 1 mm; 14 = 500 µm; 20 = 300 µm; 5, 6, 21 = 200 µm; 15 = 100 µm; 7 = 50 µm.


1
2
3
4
5
6
7
8
9
10
11
12
13
14
15
16
17
18
19
20
21

Chapter II

E-identification of fruits and endocarps of extant Icacinaceae

Among all challenges of the taxonomic studies, may be the most important are: the availability of the so-called raw data, the standardization of the descriptions, and the understanding by all of the descriptors used. This last point could be underestimated in the "background noise" in taxonomic studies. The length of the endocarps, tubercles, lamina or flower could underlie a plurality of methods, the material used, and of course the differences in accuracy. Thus, we should propose for each character, and states of characters used a definition and/or an explanatory diagram. In this way, a manual of leaf architecture was made (Leaf architecture working group, 1999) in order to remediate to the last two points. For the Angiosperm wood, a database was settled (Inside wood) in order to standardize, and host the row data (Wheeler, 2011). In addition, this database was based on IAWA list of characters greatly illustrated, and explained (Wheeler et al., 1989). Recently, new databases have been made using the Xper^2 software (Ung et al., 2010), with the most important achievement published for botanical studies were Palm-ID (Thomas, 2011, Thomas & De Franceschi, 2013), Pl@ntWood (Sarmiento et al., 2011), and a key of Amazonian ferns (Zuquim et al., 2017). These databases allow us to define items (species), and descriptive model (characters). Diverse functionalities can be used, especially interactive identification that permit the identification of a specimen starting from any descriptor.

The taxonomy of the Icacinaceae family was intensively studied (Perrier De La Bathie, 1944, Sleumer, 1969, 1971, Villiers, 1973, Jansen-Jacob, 1979, De Roon, 1994, Labat et al. 2006, Peng & Howard 2008, Duno De Stephano, 2013). However, the descriptions of some organs as fruits and endocarps are often succinct. For example, in the Flora of China, the information relative of *Iodes cirrhosa* fruit is:" *Drupe red when mature, ovoid-globose, 2-2.6 × 1.2-2 cm, pulp thick, laterally compressed, pubescent, polygonous reticulate-lacunose when dry."* (Peng & Howard, 2008). In fact, the fruits and endocarps are less used in taxonomic considerations and identifications. However, paleobotanical remains clearly attributed to Icacinaceae are mainly endocarp (Reid & Chandler, 1933, Manchester, 1994, Collinson et al., 2012). Therefore, this "taxonomic detail" remains crucial in the paleobotanical context.

In this chapter, we proposed the first database using Xper^3 (the online version of the Xper^2) dedicated to the Icacinaceae fruits and endocarps from modern species. Our aims are (1) to put row data of morphological and anatomical studies available online, (2) to propose a standardisation of characters, (3) to explain the descriptors used and (4) to propose an interactive and natural key assisted by computer.

II.1. Material and methods

The sampling contains 88 species among the 158 accepted extent species (Appendix 1) of Icacinaceae s.s. We added five Icacinaceae s.l. (now Metteniusaceae), and one Oncothecaceae in order to provide out-group in our analysis. This sampling is from diverse Herbarium, mainly the Muséum national d'Histoire naturelle in Paris (P, acronym following Holmgren et al., 1990) but also from the Royal Botanic Garden Kew (K), the Naturalis Biodiversity Center (L, U, WAG), the Botanic Garden Meise (BR), Kunming Institute of Botany (KUN), and the Missouri Botanical Garden (MO). The sampling covers all Icacinaceae area but lack of South American species. In term of genera representation, the sample lacks of three monospecific genera (*Merrilliodendron*, *Natsiatopsis* and *Sleumeria*), and *Casimirella,* which contain seven species. This last genus is from South-America, which explains in part the lack of sample for this area. The endocarps/fruits were studied morphologically and anatomically by SEM using Jeol JCM6000 instrument and measures were made by ImagJ software.

The Xper^3 online database was used (Ung et al., 2010) in order to implement descriptions and observations made. The interface proposes tabs (Fig. II.1, A) as following: items (specimens), descriptive model (characters and state of characters), description (link between the two previous tabs) and identification, which generate an interface for assisted identification. The database also was implemented in the local software Xper^2 in order to have access to the statistic part of the database (power of discrimination of characters, number of pictures, complements of descriptions etc.).

II.2. Results

The Xper^3 key for the Icacinaceae is available at this following link: http://www.xper3.fr/xper3GeneratedFiles/publish/identification/-8704055676548069962/mkey.html
The database contains 94 Items (Fig. II.1, B) with for each the associated studied specimens (Fig. II.1, C) and finally morphological and anatomical pictures (Fig. II.1, D). The database contains 652 illustrations associated with these items and descriptors.

Fifty-six (56) descriptors were defined, 52 of them with associated images and 121 states were used (average number of states by descriptors = 2.16); among them, 103 are illustrated. Six descriptors are precise by 23 sub-descriptors. The character ranking causes inapplicable characters. For example, the length of the tubercle depends on the presence of tubercle. If the user chooses the tubercle as absent, all characters related to the tubercle disappear from the identification interface. In the descriptive model we have chosen the view of characters in the form of a list (one to fifty-six, following the order of entry into the base) or in dependency hierarchy. We recommend to use this last option.

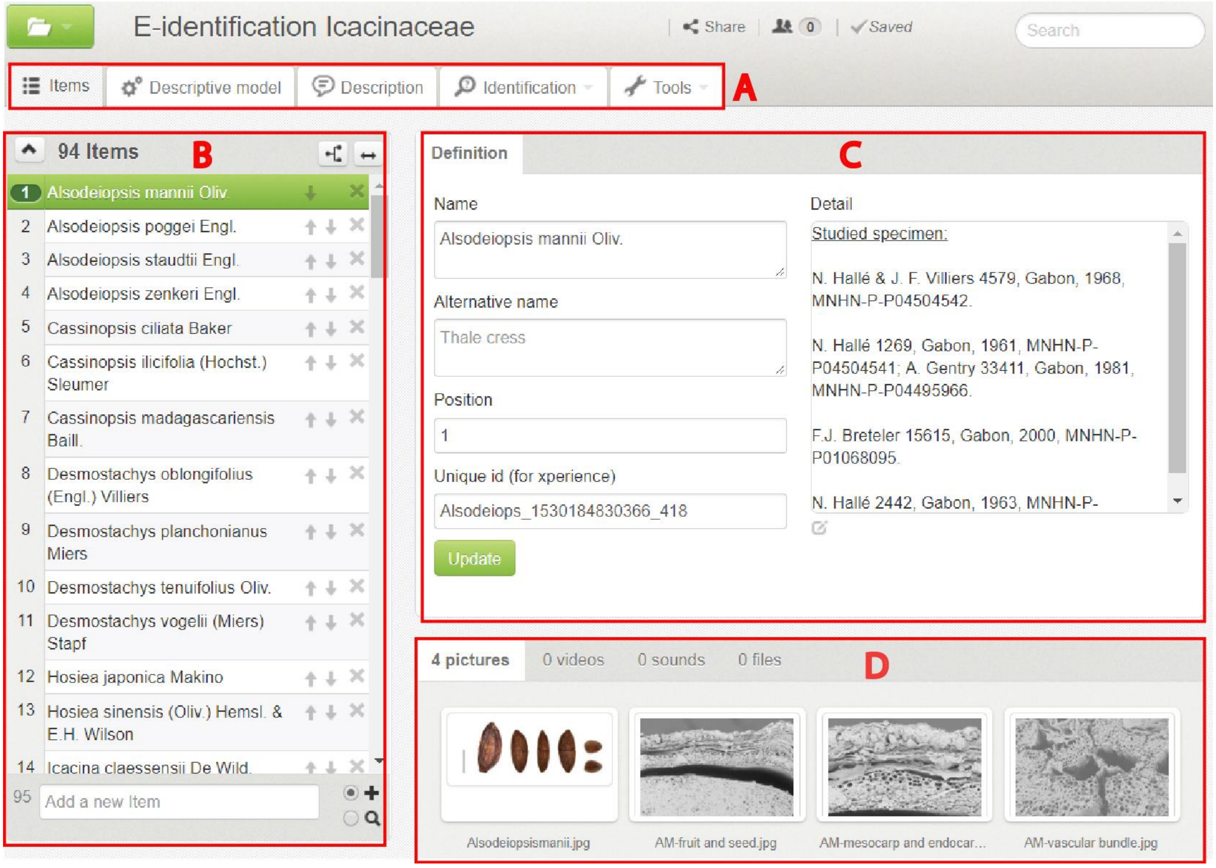

94 Items

1 Alsodeiopsis mannii Oliv.
2 Alsodeiopsis poggei Engl.
3 Alsodeiopsis staudtii Engl.
4 Alsodeiopsis zenkeri Engl.
5 Cassinopsis ciliata Baker
6 Cassinopsis ilicifolia (Hochst.) Sleumer
7 Cassinopsis madagascariensis Baill.
8 Desmostachys oblongifolius (Engl.) Villiers
9 Desmostachys planchonianus Miers
10 Desmostachys tenuifolius Oliv.
11 Desmostachys vogelii (Miers) Stapf
12 Hosiea japonica Makino
13 Hosiea sinensis (Oliv.) Hemsl. & E.H. Wilson
14 Icacina claessensii De Wild.
95 Add a new Item

Name: Alsodeiopsis mannii Oliv.

Alternative name: Thale cress

Position: 1

Unique id (for xperience): Alsodeiops_1530184830366_418

Detail

Studied specimen:

N. Hallé & J. F. Villiers 4579, Gabon, 1968, MNHN-P-P04504542.

N. Hallé 1269, Gabon, 1961, MNHN-P-P04504541; A. Gentry 33411, Gabon, 1981, MNHN-P-P04495966.

F.J. Breteler 15615, Gabon, 2000, MNHN-P-P01068095.

N. Hallé 2442, Gabon, 1963, MNHN-P-

Figure II.1. Item view in the Xper^3 database. (A) tabs, (B) list of items, (C) sheet of *Alsodeiopsis mannii* with studied specimens, (D) pictures attached to the sheet.

Another available option allows us to form a group of characters. Here, we do not use this option, despite it could be useful for the future development of the base, (see discussion part). We have 18 numerical and 38 categorical descriptors. The descriptors in dependent hierarchy are as following:

1. Fruit type: 1 = Drupe; 2 = Berry; 3 = Samara

All Icacinaceae species (and outgroup used here) have drupe fruit.

2. Fruit color: 1 = Green; 2 = Red; 3 = Brown; 4 = Black; 5 = Yellow; 6 = Blue
3. Fruit: length
4. Fruit: width
5. Fruit: thickness

6. Epicarp indumentum type: 1 = Glabrous; 2 = Pilose; 3 = Pubescent; 4 = Strigose

+ 7. Epicarp hair type: 1 = Papillae like expansion; 2 = "globular"; 3 = Uncinate; 4 = Simple; 5 = Long and thin; 6 = Cluster of hairs **Inapplicability condition (Glabrous)**

+ 8. Epicarp hair color: 1 = Red; 2 = White; 3 = Yellow **Inapplicability condition (Glabrous)**

9. Epicarp additional structure: 1 = None; 2 = Apex elongate; 3 = Cap at the apex elongate; 4 = Cap at the apex inflated

10. Endocarp presence of a keel: 1 = Yes; 2 = No

11. Endocarp shape in lateral view: 1 = Elliptical; 2 = Globulose; 3 = Obovoid; 4 = Triangular; 5 = Oblong

12. Endocarp shape in transverse section: 1 = Lenticular; 2 = Globulose; 3 = Triangular

13. Endocarp apex structure: 1 = Absent; 2 = Horns; 3 = Pores; 4 = Bulge

14. Endocarp base morphology: 1 = Symmetrical (no basal cleft); 2 = Cleft on one side

15. Endocarp: length

16. Endocarp: width

17. Endocarp: thickness

18. Endocarp wall: thickness

19. Endocarp surface structures: 1 = Ridged; 2 = Pitted; 3 = Rugose, irregular; 4 = Smooth

+ 20. Endocarp ridging pattern: 1 = Reticulate; 2 = Diffuse **Inapplicability condition (Pitted, Rugose, irregular, Smooth)**

+ 27. Areoles freely ending ridgelets: 1 = Yes; 2 = Rare or No **Inapplicability condition (Diffuse)**

+ 36. Areole number closed by ridges **Inapplicability condition (Diffuse)**

+ 40. Endocarp wall: Thickness with ridges/rugosity **Inapplicability condition (Pitted, Smooth)**

+ 22. Pits arrangement: 1 = In longitudinal lines; 2 = Random **Inapplicability condition (Ridged, Rugose, irregular, Smooth)**

+ 25. Pits: diameter **Inapplicability condition (Ridged, Rugose, irregular, Smooth)**

+ 41. Pits: number by faces **Inapplicability condition (Ridged, Rugose, irregular, Smooth)**

+ 23. Pits: number longitudinally **Inapplicability condition (Ridged, Rugose, irregular, Smooth)**

+ 24. Pits: number transversally **Inapplicability condition (Ridged, Rugose, irregular, Smooth)**

+ 21. Pits shape: 1 = Mainly circular; 2 = Primarily elongate **Inapplicability condition (Ridged, Rugose, irregular, Smooth)**

- + 50. Ridges secondary: 1 = Yes; 2 = No **Inapplicability condition (Pitted, Smooth, Rugose, irregular)**
- + 37. Ridges shape: 1 = Rounded; 2 = Sharp; 3 = Angular **Inapplicability condition (Pitted, Smooth, Rugose, irregular)**
- + 29. Tubercles presence: 1 = Yes; 2 = No **Inapplicability condition (Ridged, Rugose, Irregular, Smooth)**
  - + 32. Tubercles morphology: 1 = Conical; 2 = Elongate-flattened; 3 = Peg shaped; 4 = Cylindrical; 5 = Spiny; 6 = "Shallow mound" not protrude beyond wall **Inapplicability condition (No)**
    - + 33. Tubercle apex morphology: 1 = Not elaborated (more or less rounded or pointed); 2 = Capitate (Swollen head); 3 = Biphid **Inapplicability condition («Shallow mound" not protrude beyond wall)**
    - + 34. Tubercle: length **Inapplicability condition («Shallow mound" not protrude beyond wall)**
    - + 51. Shallow mound invagination shape: 1 = Spiny; 2 = Areoles **Inapplicability condition (Elongate-flattened, Cylindrical, Spiny, Peg shaped, Conical)**
    - + 56. Tubercle: number of cells CT **Inapplicability condition («Shallow mound"not protrude beyond wall)**

+ 35. Tubercle diameter **Inapplicability condition (No)**

26. Endocarp surface vasculature: 1 = Resting on ridges; 2 = Resting between ridges/mounds; 3 = On the channel of endocarp; 4 = Free

28. Endocarp primary vascular strand position: 1 = Outside endocarp wall; 2 = in a gutter or channel; 3 = Inside endocarp wall

30. Locule: microtomography : 1 = Smooth; 2 = Papillate; 3 = Inflated

- + 44. Papillae: density **Inapplicability condition (Smooth, Inflated)**
- + 43. Papillae: diameter **Inapplicability condition (Smooth, Inflated)**
- + 42. Papillae shape: 1 = Rounded; 2 = Large **Inapplicability condition (Smooth, Inflated)**

31. Locule hairs: 1 = Yes; 2 = No

38. Ridges number reaching the base: 1 = zero; 2. = one; 3 = two; 4 = four; 5 = six

39. Vertical ridges number: 1 = zero; 2 = one; 3 = two; 4 = three; 5 = four; 6 = five; 7 = >5

45. Endocarp wall layers: 1 = Divided into distinctive units; 2 = Homogeneous

46. Endocarp wall cells orientation: 1 = Periclinal; 2 = Anticlinal; 3 = Isodiametric

47. Locule number: 1 = One; 2. = Three; 3 = Five

48. Locule lacunate: 1 = Yes; 2. = No

49. Geographical sampling: 1 = Africa; 2 = Asia; 3 = South America; 4 = Oceania; 5 = Madagascar

52. Endocarp: thicker than wide: 1 = Yes; 2 = No
53. Fruit: fleshy appendage: 1 = Yes; 2 = No
54. Fruit: gynophore: 1 = Yes; 2 = No
55. Endocarp hairs: 1 = Yes; 2 = No

The discriminative power of all descriptors is available in the Appendix 2 with three indices, Xper, Sokal & Michener and Jaccard. In addition, we can propose different descriptor weight (one to three) in order to put forward the most pertinent characters. In our cases, we promoted the characters which were directly visible.

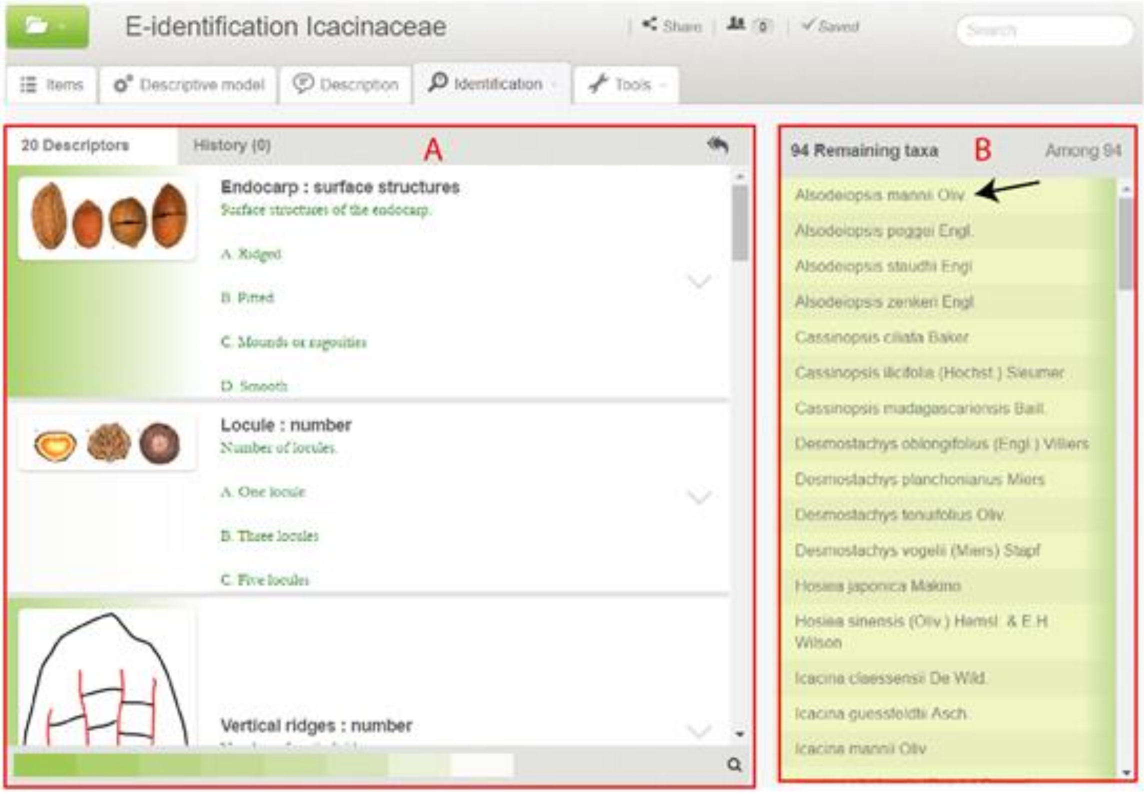

Figure II.2. Interactive identification view in Xper3 database. (A) descriptors, (B) remaining items.

The database contains 5264 potential combinations. Among them, 4101 combinations are applicable and 1163 combinations are inapplicable. The database was completed at 95.5% with 194 unknown data. These unknown data are mainly due to decayed from fungi attacks or the low preservation of endocarps /fruits sampling. However, the less described species is *Miquelia assamica* (Griff.) Mast. ex B.D.Jacks. with 17.9 % of lacunae, showing the relatively good filling rate.

The identification table proposes an interactive identification with a table showing the descriptors (Fig. II.2, A) illustrated and a remaining taxa table (Fig. II.2, B). The user can begin the identification of the specimen by any descriptors. When the user clicks on a descriptor, the different character state appear. The user can choose several states of characters.

The choice of the character states induces a loss of taxa in the B part (Fig. II.2). After identification or when it remains some possibilities after using all available characters in the studied specimens, the user can click on the name of the remaining taxa (Fig. II.2, B, Arrow) and obtain in one sheet all the available information for the species (Fig. II.3): the species name (Fig. II.3, A), all pictures associated to the species in the database (Fig. II.3, B), the studied specimens (Fig. II.3, C) and all character states associated to this species. Thus, the user can check the value of the identification made following the interactive identification. A history of characters used is available (Fig. II.2, A) in case of the user need to come back to the characters if an error occurs during the identification.

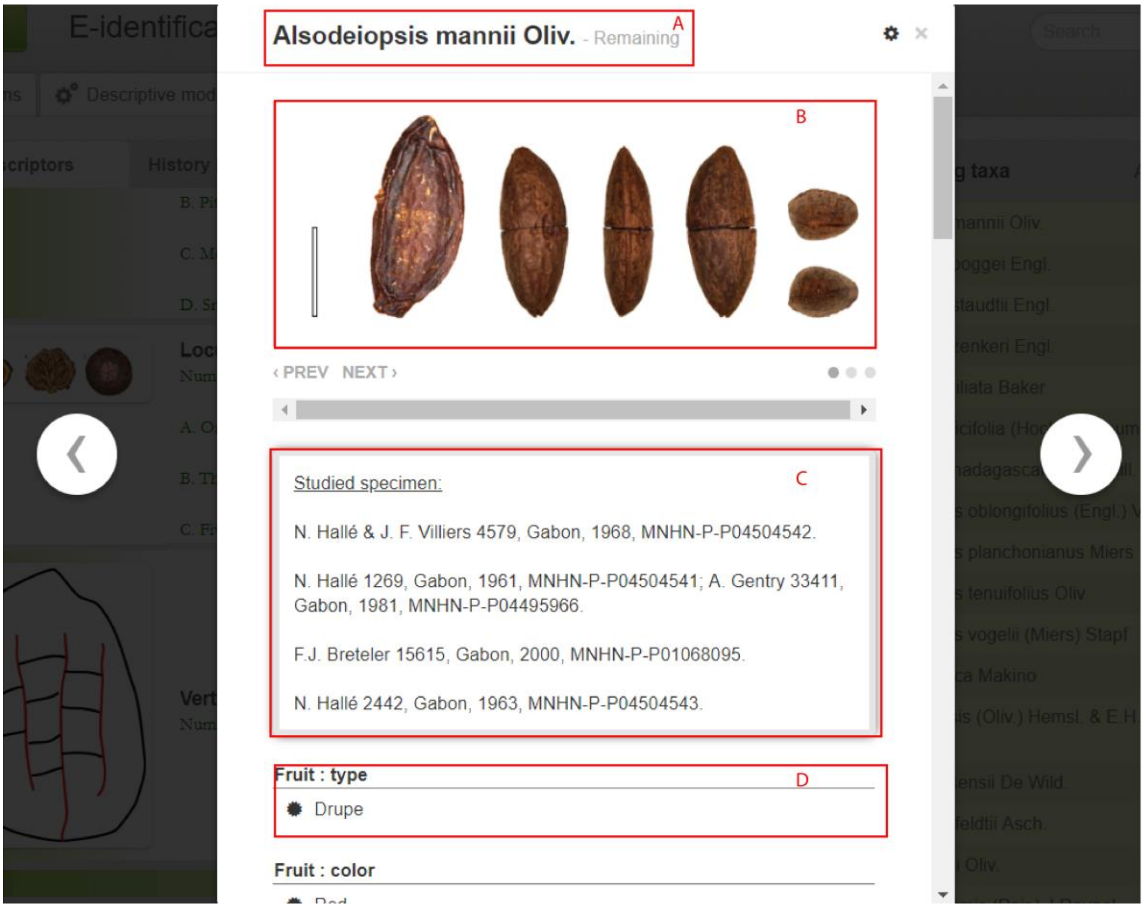

Alsodeiopsis mannii Oliv. - Remaining

Studied specimen:

N. Hallé & J. F. Villiers 4579, Gabon, 1968, MNHN-P-P04504542.

N. Hallé 1269, Gabon, 1961, MNHN-P-P04504541; A. Gentry 33411, Gabon, 1981, MNHN-P-P04495966.

F.J. Breteler 15615, Gabon, 2000, MNHN-P-P01068095.

N. Hallé 2442, Gabon, 1963, MNHN-P-P04504543.

Fruit : type

● Drupe

Fruit : color

Figure II.3. View of remaining taxa in Interactive identification tab. (A) scientific name of the species, (B) pictures associated to the species, (C) studied specimens, (D) characters and character states of the species.

This interactive identification is available online. We can transfer the database in the Xper^2 software but in all cases, we need a computer. The identification table proposes to generate an identification key from IKEY+ (Burguiere et al., 2012) based on the database, power of discrimination of characters and weight made by the author of the database. The key has between 113 (Xper method) and 126 entries (Jaccard method). In average, we need 5.8 paths to obtain the identification of the specimen. The result of the Key with 113 entries (Xper method) is available in Appendix 3.

II.3. Discussion & perspectives

No items possess recovering identification in the database with others. This confirms that the fruits and endocarps characters are good organs for specific identifications: for the Icacinaceae family, the endocarps and fruits characters seem to be enough to identify species. The key with only 113 entries (5.8 average paths by species) shows that these characters are promising in taxonomic assignment. However, the quantitative characters, which have the best power of discrimination are difficult to use in identification because of the lack of intra-specific diversity. One of the future perspectives is to increase this diversity in order to increase the reliability of these characters.

The database could be completed to include fossils and other modern species. We also consider this base as adaptable to other groups with drupaceous fruits. For the other fruit types, we can add character boxes linked to the fruit types, and make a general database of fruits, not only drupe remains. Another perspective is to create groups of descriptors of other organs as leaves, wood, and flower characters in order to have the most complete, and standardised descriptions on Icacinaceae family.

A sub-base could be created in a phylogenetic perspective. Actually, not all characters are adapted to a phylogenetic analysis but this database could be the first step, and we can select /modify characters in order to build a phylogenetic matrix. In fact, the formation of a nexus file is easily accessible by an option of the software. This could be a great opportunity to use this morphological, and anatomical database in order to include fossil endocarp remains in recent molecular phylogeny. In this thesis we used a sub-base of this database in the Chapter VII in order to include fossil endocarp from the Paris Basin in a molecular phylogeny, and in the Chapter IX in a perspective work including other morphological characters and fossils in a molecular phylogeny. In a widest perspective, this database was used as practical basis in this thesis in order to compare, and confirm diagnosis characters of fossils from Paris Basin.

Finally, this database can be shared, and this can lead to a collaborative work around the taxonomy of Icacinaceae, with applications of these data's in identification, and phylogeny.

Conclusion of the chapter

The Xper^3 database proposed here responds to the need of the availability of the raw data, the standardization of the descriptions, and the understanding by all of the used descriptors. This base measure the discriminative power of each characters, and verifies the discrimination of all taxa. An assisted key is available, and a natural key can be done. As a dynamic structure, the base can evolve in function of the needs of the users.

Chapter III

Fruit studies of the Icacinaceae family from the Paris Basin Paleocene

The Rivecourt site is the most ancient site containing Icacinaceae remains in the Paris Basin (Smith et al., 2014). Among the numerous endocarp and seed remains, about 70 very well preserved endocarps belongs to the Icacinaceae family and especially to the *Iodes* genus. This chapter is divided in three parts:

The first part describe five new species from the endocarp remains. This part correspond to an accepted article published in earth and environmental science transactions of the royal society of Edinburgh: **Del Rio, C., Thomas, R., De Franceschi, D., 2018. Fruits of Icacinaceae Miers from the Paleocene of the Paris Basin (Oise, France). Earth Environ. Sci. Trans. R. Soc. Edinb. DOI: 10.1017/S1755691018000221**

The second part is a comment about a double endocarp (teratology) which give information about the ovules. This part was submitted to Adansonia: **Del Rio, C., De Franceschi, D. He has two, and they dangle nicely: an abnormal fossil fruit from Rivecourt (Oise, France). Adansonia, Submitted.**

The third part is a chemical study of the seeds. These seeds were soft and have a cream colour contrasting with the lignitic sediment. The chemical studies were conducted in collaboration with Bernard Bodo (Professor, UMR7245 CNRS/MNHN). This part is only formatted for this thesis.

III.1. Fruits of Icacinaceae Miers from the Paleocene of the Paris Basin (Oise, France)

III.1.1. Introduction

Icacinaceae Miers are a family of trees, shrubs, and lianas with a pantropical distribution. This family has been traditionally characterized by having two pendulous ovules (with only one reaching maturity), drupaceous fruits, hermaphroditic flowers, and simple leaves (Kårehed, 2001). However, the lack of clear synapomorphic characters has led to confusion regarding the taxonomy and phylogeny of the family. Indeed, Icacinaceae s.l. included about 54 genera and 400 species classified mostly by wood characters (Engler, 1897, Sleumer, 1942). Since the beginning of the twenty-first century, multiple phylogenetic studies focused on morphology and molecular data (Soltis, 2000, Kårehed, 2001, Lens et al., 2008, Byng et al., 2014, Stull et al., 2015) have greatly clarified Icacinaceae phylogeny, leading to the recognition of a reduced circumscription of the family, including 23 genera and about 160 species. This clade, along with Oncothecaceae Kobuski ex Airy Shaw, is included in the newly recognized order Icacinales (APG, 2016), which is sister to all other lamiids (Stull et al., 2015).

Icacinaceae s.s. is well known in the fossil record, especially from the Paleogene of Europe (Reid & Chandler, 1933; Chandler, 1961a, Chandler 1961b, Chandler, 1962, Collinson, 1983, Knobloch & Mai, 1986, Cleal et al., 2001, Fairon-Demaret & Smith, 2002) and North America (Crane et al., 1990, Manchester, 1994, Manchester, 1999, Pigg & Wher, 2002, Pigg et al., 2008, Rankin et al., 2008, Stull et al., 2011, Stull et al., 2012, Allen et al., 2015). However, a few records of Icacinaceae have also been reported from South America (Stull et al., 2012), the Middle East (Soudry & Gregor, 1997), Africa (Chandler, 1954, Chester, 1955), and Japan (Tanai, 1990). Although the fossil record of Icacinaceae includes a notable diversity of genera, the modern genus *Iodes* is perhaps the most diverse and abundantly represented (excluding the unnatural form genus *Icacinicarya*). Fruits of modern and fossil *Iodes* are characterized by an elliptical to globulose shape, an external reticulate pattern, a papillate layer on the inner endocarp surface (locule wall), and the presence of a vascular bundle running from the base to the apex, embedded in the endocarp wall.

Here we describe five species of Icacinaceae fossil endocarps from late Paleocene of Rivecourt deposit (Oise, France). An initial report on the flora and fauna from the Rivecourt outcrop was presented by Smith et al. (2014). The present work provides a detailed treatment of Icacinaceae fossils from this outcrop. This represents the first detailed study of Icacinaceae from the Paris Basin, and will be followed by other studies focused on other sites from the important basin, which, with the exception of a work on Menispermaceae (Jacques & De Franceschi, 2005), remains understudied in terms of its palaeocarpology.

All the species present in Rivecourt possess the diagnostic characters of the genus *Iodes,* as described below. Therefore, we generated a key including the fossils from Rivecourt and all other described fossil species of *Iodes* to aid in the differentiation and identification of fossil *Iodes*. Moreover, we propose a new combination for *Iodes israelii* Soudry & Gregor, *Icacinicarytes israelii* (Soudry & Gregor) Del Rio, Thomas & De Franceschi, because this fossil species lacks the diagnostic morphological and anatomical characters of *Iodes*. The significance of papillae (i.e., small bumps lining the locule wall) has already been discussed for *Iodes* fossil from several sites. We propose here standardization in terminology of this character in accordance with new data observed on the Rivecourt fossils. A potential link between late Paleocene flora of Europe and the modern Asian flora is suggested, based on morphological similarities shared between the fossils presented here and modern species from Asia.

III.1.2. Material and methods

III.1.2.1. Material

The lignitic fossil specimens were collected from the Rivecourt site (Oise, France) in 2009 and 2012, from lignitic sandy layers of fluvial to fluvio-estuarine deposits. These deposits date from late Paleocene (MP6b about 57-56 Ma; Smith et al., 2014). Among numerous other plant macrofossils mainly preserved as lignitic, carbonized, or piritized material, about 70 nearly complete endocarps as well as some lignitic fragments assigned to Icacinaceae were collected. Herbarium samples examined for comparison are listed in Appendix 4.

III.1.2.2. Method of collection

Almost all specimens were collected by screen washing of fossiliferous sediments on meshes of 5, 2, and 1 mm and density separated from the denser mineralized material in water. The obtained lignite was then washed with tap water and dried in a ventilated oven at 45°C. Sorting was done using binocular microscopes (Mantis Elite). The specimens are kept in plastic boxes with renewed silica gel. All samples are stored at the Muséum national d'Histoire naturelle of Paris for study and will be held at the Musée Vivenel in Compiègne (Oise, France) for permanent storage.

III.1.2.3. Method of observation

All specimens were studied with a binocular microscope (Wild M3Z) and imaged with a Leica DFC 420 camera. Measures were taken using the ImagJ Software (Rasband, 2016). Cell diameters and papillae were measured 10 times for each species, using random selections of the specimens. Samples were coated with gold-palladium for examination by Scanning Electron Microscopy (SEM), using a Jeol JCM6000 instrument, facilitating observation of anatomical features, especially the endocarp wall layers and papillae.

III.1.3. Results

III.1.3.1. Systematics

All fossils presented here share the common features of Icacinaceae: globular to elliptical shape, bilateral endocarp with asymmetrical apex, presence of a keel surrounding the endocarp and single-seeded fruit. Moreover, they are consistent with the genus *Iodes* in possessing a reticulate pattern formed by longitudinal and vertical ridges (which delimit polygonal areoles), a vascular bundle embedded in the wall of endocarp, papillae on the inner endocarp surface, and a pair of subapical horn-like protrusions (which are present in some, but not all, modern species of *Iodes*). However, additional anatomical and morphological characters permit the differentiation and description of five new species.

The most differentiated endocarp walls are composed of four cells layers of one or several successive cell rows. The outermost cells layer is identified as the "apical sclerotic layer," the second as the "isodiametric cell layer," the third as the "basal sclerotic layer," and the last as the "locule epiderma layer." We follow the same nomenclature for all wall preservations regardless of their layer development and position (in cases of absence or reduction). We sometimes found seeds in broken endocarps with remnant testa, suggesting that some unbroken specimens might also contain seeds. With a beige colour and a soft texture, these seeds demonstrate the high quality of the lignitic preservation at the Rivecourt and a chemical study focused on seeds is in progress.

Icacinaceae Miers

Genus *IODES* Blume

Species - Iodes sinuosa Del Rio, Thomas & De Franceschi, sp. nov.

Fig. III.1 A-L

Diagnosis. Endocarp elliptical with reticulate pattern of sharp, thin and sinuous ridges, which delimit about 16–17 polygonal areoles on each lateral face with few or no freely ending ridgelets. Endocarp possessing a symmetrical pair of horn-like protrusions compressed on the keel, positioned eccentrically and subapically. Endocarp wall 0.22–0.24 mm thick and 0.35–0.39 mm thick with ridges. Inner endocarp surface densely covered with regularly spaced and sessile rounded papillae. Length of endocarp: 4.65–5.3 mm; width about 3.66 mm.

Etymology. *”sinuosa”* refers to the sinuous pattern of the ridges on the endocarp surface.

Holotype. Riv. PPB 157.

Stratigraphy. Late Paleocene.

Type locality. Rivecourt (Oise, France).

Paratypes. Riv. PPB 146, Riv. PPB 147, Riv. PPB 190.

Description. Endocarp bilaterally symmetrical, unilocular, single-seeded, elliptical, lenticular in transverse section; length 4.65–5.3, avg. 4.97 mm (SD= 0.61, n=2), width 3.66 mm, thickness 2.49 mm; outer part of endocarp covered with a reticulate pattern of sharp, thin and sinuous ridges with 3–4 irregular longitudinal ridges, which delimit 16–17 polygonal areoles on each lateral face with few or no freely ending ridgelets; a keel surrounds the fruit in the plane of symmetry with the thicker margin containing a vascular bundle embedded in the endocarp wall. Endocarp possessing a symmetrical pair of horn-like protrusions compressed on the keel, positioned eccentrically and subapically on the endocarp faces, with each protrusion containing a central pit or channel. Endocarp wall 0.22–0.24, avg. 0.23 mm (SD=0.03, n=2) thick without ridges and 0.35–0.39, avg. 0.37 mm (SD=0.02, n=2) with ridges. Wall composed of four unicellular and multicellular cells layers, the outermost corresponding to an apical sclerotic layer of two or three cells thick, difficult to distinguish, sometimes absent due to erosion on the areoles showing the layer in one row of isodiametric cells; cells 0.022–0.036 mm of diameter (Riv. PPB 146), the basal sclerotic layer forms much of the thickness of the endocarp wall and is composed of numerous cells. Inner endocarp surface densely covered with regularly spaced and sessile rounded papillae, which correspond to the cell expansions of the locule epiderma layer with interdigitated cells; papillae diameter 0.011–0.015 mm (Riv. PPB 146 and Riv. PPB 147); the number of papillae per 0.25 mm^2 is 600 (Riv. PPB 146).

Remarks. This species is represented by four lignitic endocarps and a few fragments. It is very distinctive from the other species in having sharp, sinuous and small ridges (Fig. III.1 G-H), a short overall endocarp length (Fig. III.1 A-F) and a high density of sessile rounded papillae (Fig. III.1 J-L). *Iodes sinuosa* differs from *I. eocenica*, *I. brownii* and *I. corniculata* by its relatively short length and width. It is close to *I. acutiformis* in terms of overall length, ridge sharpness, and papillae morphology. However *I. sinuosa* has a more obtuse and asymmetrical apex and a more elliptical endocarp. In addition, the horn-like protrusions do not exceed the endocarp in the lateral view in this new species, in contrast to specimens of *I. acutiformis* (see in particular Plate 13, fig. 1. H; Chandler, 1962). Thus, we consider these two species to be closely related but with consistent differences allowing for their separation. The cell wall layer is well preserved (Fig. III.1 H) with four distinctive unicellular and multicellular layers. This corresponds to the most differentiated wall of the *Iodes* from Rivecourt's site. Considering that the wall is complete and undamaged, the sharpness of the ridges is considered a bonafide taxonomic feature rather than a consequence of taphonomic degradation. Indeed, we do not recognize any abrasion on the external or internal endocarp wall. The inner surface shows papillae in anatomical position (Fig. III.1 J-K).

Species - *Iodes parva* Del Rio, Thomas & De Franceschi, sp. nov.
Fig. III.1 M-X

Diagnosis. Endocarp elliptical to globulose with a reticulate pattern of rounded and thin to large ridges, which delimit 11–20 polygonal areoles on each lateral face, with a few or no freely ending ridgelets. Endocarp possesses a symmetrical pair of horn-like protrusions compressed on the keel, positioned eccentrically and subapically. Endocarp wall 0.16–0.26 mm thick and 0.4–0.56 mm thick with ridges. Inner endocarp surface densely covered with regularly spaced and sessile rounded papillae. Length of endocarp: 4.38–6.05 mm; width of endocarp: 3.49–5.19 mm.

Etymology. *"parva"* refers to the small size of the endocarp.

Holotype. Riv. PPB 188.

Stratigraphy. Late Paleocene.

Type locality. Rivecourt (Oise, France).

Paratypes. Riv. PPB 18, Riv. PPB 131, Riv. PPB 139, Riv. PPB 148, Riv. PPB 153, Riv. PPB 158, Riv. PPB 162, Riv. PPB 165, Riv. PPB 189.

Additional specimens. Riv. PPB 129, Riv. PPB 130, Riv. PPB 132, Riv. PPB 133, Riv. PPB 134, Riv. PPB 135, Riv. PPB 136, Riv. PPB 142, Riv. PPB 143, Riv. PPB 168, Riv. PPB 184, Riv. PPB 192.

Description. Endocarp bilaterally symmetrical, unilocular, single-seeded, elliptical to globulose, lenticular in transverse section; length 4.38–6.05, avg. 5 mm (SD=0.49, n=7), width 3.49–5.19 avg. 4.34 mm (SD=0.63, n=7), thickness 2.6–3.53, avg. 3.06 mm (SD=0.65, n=2); outer part of endocarp with reticulate pattern of rounded and thin to large ridges with 4–6 longitudinal ridges, which delimit 11–20 polygonal areoles on each lateral face with a few or no freely ending ridgelets; a keel surrounds the fruit in the plane of symmetry with the thicker margin containing a vascular bundle embedded in the endocarp wall. Endocarp possessing a symmetrical pair of horn-like protrusions compressed on the keel, positioned eccentrically and subapically on the apical endocarp faces each with a central pit; Endocarp wall 0.16–0.26, avg. 0.21 mm (SD=0.04, n=3) thick without ridges and 0.4–0.56, avg. 0.51 mm (SD=0.07, n=3) with ridges. Wall composed of three unicellular and multicellular cell layers, the outermost correspond to a layer in one row of isodiametric cells, cells 0.039–0.047 mm diameter (Riv. PPB 158). The basal sclerotic layer forming the main part the endocarp wall thickness and is composed of 12–14 periclinal cells 0.023–0.031 mm high, 0.041–0.054 mm wide (Riv. PPB 18). Inner endocarp surface is densely covered by regularly spaced, minute and sessile rounded papillae, which correspond to cell expansions of the locule epiderma (uni-stratified layer) with interdigitated cells; papillae diameter 0.010–0.014 mm (Riv. PPB 158 and Riv. PPB 18), the number of papillae per 0.25 mm^2 is 510–1060 (Riv. PPB 158 and Riv. PPB 18).

Remarks. Nine uncompressed specimens, preserved as lignite, represent this species. Additional compressed specimens are assigned to *Iodes parva* because of the similarity of the anatomical characters, even if they are compressed in the plane of symmetry, thus wider, and generally fragmented. These differences appear to be due to taphonomic processes. Note that almost all fragmented specimens come from the same trench in Rivecourt site, perhaps indicating a local accumulation or preservation bias. *I. parva* differs from the other species in having a small endocarp size (Fig. III.1 M-R & U), rounded thin to large ridges (Fig. III.1 S-T), and a high density of sessile, rounded papillae (Fig. III.1 V-W). In particular, *I. parva* differs from other previously described fossil species by the combination of small endocarp size (compared to *I. corniculata*, *I. eocenia* and *I. brownii*) and rounded ridges (compared to *I. acutiformis* and *I. sinuosa*). This species, however, is perhaps closely related to *I. corniculata* from the London Clay given their similar pattern of ridges and number of areoles. The first layer of the endocarp wall corresponds to the isodiametric cell layer. These specimens have lost their apical sclerified layer and a part of the isodiametric cell layer. Inside the areoles we can find some remains of this lost apical sclerotic layer but the majority of the exterior endocarp is composed of isodiametric and digitate cells (Fig. III.1 S-T). The measure of the wall is therefore biased and underestimated, which can explain the differences between thin and large ridges between individuals. The basal sclerotic layer of the wall is very well preserved. We show cells with a very thick wall organized in layers (Fig. III.1 T), from which an upper part is composed of anticlinal cells in order to form the ridges while the lower part remains periclinal. The locule epidermal layer is preserved with papillae in its anatomical place, very similar to *Iodes sinuosa* (Fig. III.1 V-W).

Species - Iodes reidii Del Rio, Thomas & De Franceschi, sp. nov.
Fig. III.2 A-I

Diagnosis. Endocarp elliptical with a reticulate pattern of angular to rounded and thin ridges, which delimit 9–19 polygonal areoles on each lateral face with few or no freely ending ridgelets. Endocarp possesses a symmetrical pair of horn-like protrusions compressed on the keel, positioned eccentrically and subapically. Endocarp wall 0.25–0.27 mm thick and about 0.8 mm thick with ridges. Length of endocarp: 9.2–10.8 mm; width of endocarp: 6.68–7.55 mm.

Etymology. This species is named in memory of Eleanor M. Reid, for her important contributions to Paleobotany, particularly Paleocarpology.

Figure III.1. (A-L) *Iodes sinuosa* sp. nov. (A-E) Holotype specimen (Riv. PPB 157). (A) Lateral view of endocarp showing the reticulum pattern of sharp and sinuous ridges. (B) Dorsal view showing the keel, open in the middle, surrounding the fruit. (C) Lateral view of second face of endocarp. (D) Apical view showing the small pair of horns. (E) Basal view. (F) Lateral view of specimen deformed Riv. PPB 190. (G) SEM view of reticulum of sinuous ridges of Riv. PPB 146. (H) Same with magnification showing wall layers and ridges in transversal section. (I) Detail showing the apical sclerotic layer in outermost, the isodiametric cell layer and the beginning of the basal sclerotic layer. (J-L) SEM view of sessile rounded papillae of Riv. PPB 146 in different magnification. (M-X) *Iodes parva* sp. nov. (M-Q) Holotype specimen (Riv. PPB 188). (M) Lateral view of endocarp showing the reticulum of rounded ridges with sub-apical horns. (N) Dorsal view showing the keel surrounding the fruit. (O) Lateral view of second face of endocarp. (P) Apical view showing the pair of horns. (Q) Basal view. (R) Lateral view of Riv. PPB 139. (S) SEM view of endocarp Riv. PPB 18 wall and ridges forming areoles. (T) Same with magnification under wall in transverse section. (U) Lateral view of Riv. PPB 165. (V-X) SEM view of sessile rounded papillae of Riv. PPB 18 in different magnification. Scale bars: (A-F) 5 mm, (G-H) 200 μm, (I) 50 μm, (J) 50 μm, (K) 20 μm, (L) 5 μm, (M-R & U) 5 mm, (S-T) 200 μm, (V) 50 μm, (W) 20 μm, (X) 5 μm.

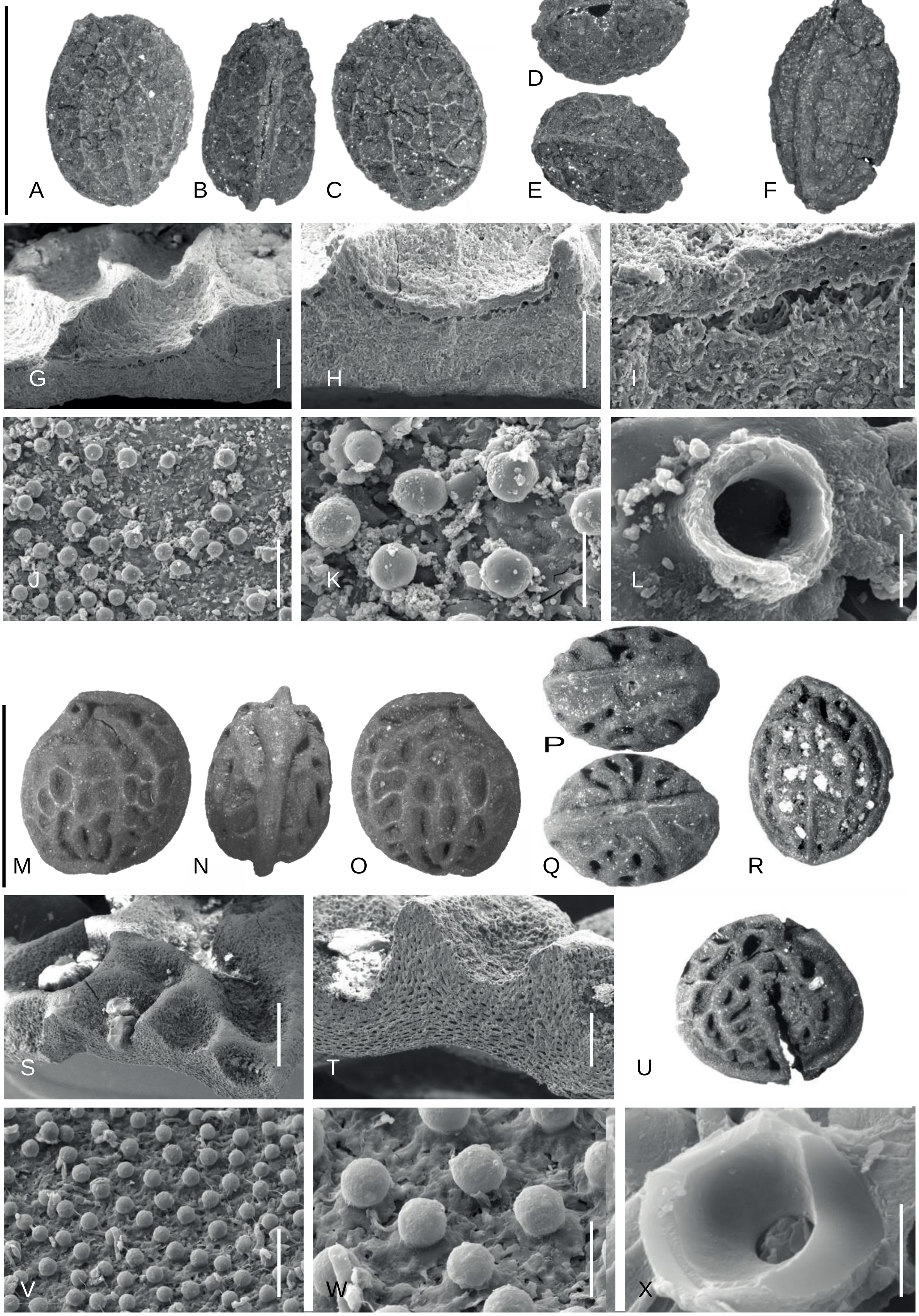
A
B
C
D
E
F
G
H
I
J
K
L
M
N
O
P
Q
R
S
T
U
V
W
X

Holotype. Riv. PPB 138.

Stratigraphy. Late Paleocene.

Type locality. Rivecourt (Oise, France).

Paratypes. Riv. PPB 154, Riv. PPB 160, Riv. PPB 191.

Description. Endocarp bilaterally symmetrical, unilocular, single-seeded, elliptical, laterally compressed in the plane of symmetry, lenticular in transverse section; length 9.2–10.8, avg. 9.85 mm (SD=0.84, n=3), width 6.68–7.55 avg. 7.21 mm (SD=0.4, n=4), thickness 2.9–4.6, avg. 3.75 mm (SD=0.8, n=4); outer part of endocarp with reticulate pattern of angular to rounded and thin ridges with 4–5 longitudinal ridges, which delimit 9–19 polygonal areoles on each lateral face, with few or no freely ending ridgelets; a keel surrounds the fruit in the plane of symmetry with the thicker margin containing a vascular bundle embedded in the endocarp wall. Presence of a symmetrical pair of horn-like protrusions compressed on the keel, positioned eccentrically and subapically on the apical endocarp faces, each with a central pit; Endocarp wall 0.25–0.27 mm thick without ridges and 0.8 mm with ridges. Wall contains two unicellular and multicellular cells layers. The outermost corresponds to a layer in one row of isodiametric cells, cells 0.025–0.036 mm diameter (Riv. PPB 160 and Riv. PPB 138). The basal sclerotic layer forms the essential of the thickness of the endocarp wall and is composed of 12–13 periclinal rows of isodiametric thin walled cells, 0.012–0.022 mm high, 0.022–0.040 mm wide (Riv. PPB 160). Inner endocarp surface degraded.

Remarks. Four lignitic specimens represent this species. Only one of them is transversally broken on the basal part (Riv. PPB 160). This species differs from the other species by the smaller size of the endocarp wall and cell walls and the larger size of the thin ridges, which form deep areoles (Fig. III.2 G-I), as well as the overall large size of the endocarp (Fig. III.2 A-F). Endocarps of *I. reidii* differs from those of *I. corniculata* in being slightly longer, with a more elliptical shape, a more acute base, and horn-like protrusions that seem to be more compressed on the keel (see plate 14, 35-36; Reid & Chandler, 1933). It also differs from *I. brownii* in having a thinner wall, an apex that is less acute, and horn-like protrusions that seems to be more compressed on the keel. Nevertheless, *I. brownii* was described from specimens on shale-sand siltstones, making difficult direct comparison with specimens on lignitic sediments. *I. reidii* differs from *I. eocenica* by its smaller length and width. For all these reasons, we decided to describe a new species, acknowledging its close affinities with *I. brownii* and *I. corniculata*. The endocarp wall is abraded on the outermost and on the innermost parts. The apical sclerotic layer and locule epidermal layer are lost in the broken specimen (Fig. III.2 H). We did not find papillae on the inner surface of the wall (missing layer), but we consider this a result of taphonomic degradation or tearing (see general discussion). The cell walls of the basal sclerotic layer are very thin compared to the cells of *Iodes parva* and *Iodes tubulifera*.

Species - Iodes tubulifera Del Rio, Thomas & De Franceschi, sp. nov.
Fig. III.2 J-U

Diagnosis. Endocarp elliptical with a reticulate pattern of sharp and thin ridges, which delimit at least 21 polygonal areoles on each lateral face, with few or no freely ending ridgelets. Endocarp possessing a symmetrical pair of horn-like protrusions prominent (i.e., not compressed) on the keel, positioned eccentrically and subapically. Endocarp wall 0.26 mm thick and 0.38 mm thick with ridges. Inner endocarp surface densely covered with regularly spaced and tubular papillae. Length of endocarp about 10 mm.

Etymology. *"tubulifera"* refers to tubular morphology of the papillae on the inner surface of endocarp.

Holotype. Riv. PPB 141.

Stratigraphy. Late Paleocene.

Type locality. Rivecourt (Oise, France).

Description. Endocarp bilaterally symmetrical, unilocular, single-seeded, elliptical, laterally compressed in the plane of symmetry; length 10 mm, width unknown (estimated about 6 mm), thickness 2.08 mm; outer part of endocarp with reticulate pattern of sharp and thin ridges with at least 5 irregular longitudinal ridges, which delimit at least 21 polygonal areoles on each lateral face with few or no freely ending ridgelets; a keel surrounds the fruit in the plane of symmetry with the thicker margin containing a vascular bundle embedded in the endocarp wall and the other part thin. Endocarp possessing a symmetrical pair of horn-like protrusions prominent from the keel, positioned eccentrically and subapically on the apical endocarp faces, each with a central pit; Endocarp wall 0.26 mm thick without ridges and 0.38 mm with ridges. Wall composed of four layers of one or several successive cell rows, the outermost correspond to an apical sclerotic layer, cells difficult to distinguish, sometimes absent by erosion on the areoles, which show the isodiametric unistratified cell layer, cells 0.040–0.069 mm diameter. The basal sclerotic layer forming the major part of the endocarp wall thickness is composed of 6–8 sclerotized and periclinal cell rows 0.013–0.031 mm high, 0.034–0.081 mm wide. Inner endocarp surface densely covered with regularly spaced, minute and tubular papillae which correspond to a cell expansion of the locule epiderma layer in one row of interdigitated cells; papillae diameter 0.016–0.019 mm, about 270 papillae per 0.25 mm^2.

Remarks. This species is represented by a single specimen (Fig. III.2 J-N). The specimen is longitudinally broken, thus the width is not known. It differs from the others in having sharp ridges, a thin endocarp wall (Fig. III.2 P-R), and low, dense tubular papillae (Fig. III.2 S-U). The horns are prominent compared to the keel (Fig. III.2- J), to a greater extent than other species from this deposit but similar to *I. brownii* and *I. corniculata* (Reid & Chandler, 1933, Allen et al., 2015). However, *I. tubulifera* differs from both species by its sharp ridges and tubular papillae. The wall is irregularly preserved; one part is differentiated into four layers like *Iodes sinuosa* (Fig. III.2 P), but without a good preservation of the cells, while another part lacks complete layers, but with good cellular preservation (Fig. III.2 Q).

Figure III.2. (A-I) *Iodes reidii* sp. nov. (A-E) Holotype specimen (Riv. PPB 138). (A) Lateral view of endocarp showing the reticulum of rounded ridges, which delimit deep areoles, with sub-apical horns. (B) Dorsal view showing the keel surrounding the fruit. (C) Lateral view of second face of endocarp. (D) Apical view showing the pair of horns. (E) Basal view. (F) Lateral view of Riv. PPB 191 specimen. (G) SEM view of reticulum of Riv. PPB 160. (H) Same with focus on wall in transverse section. (I) Detail showing small wall. (J-U) *Iodes tubulifera* sp. nov. (J-N) Holotype specimen (Riv. PPB 141). (J) Lateral view of endocarp showing the sub-apical horns and the reticulum of sharp ridges. (K) Dorsal view showing the keel surrounding the fruit. (L) Lateral view of second face of endocarp. (M) Apical view showing the pair of horns. (N) Basal view. (O) SEM view of reticulum ridges. (P) Transverse section of wall showing layers. (Q) Detail of cell preservation. (R) Same with magnification showing basal sclerotic layer and locule epiderma layer with papillae. (S-U) SEM view of tubular papillae in different magnification. Scale bars: (A-F) 5 mm, (G) 1 mm, (H) 200 μm, (I) 100 μm, (J-N) 5 mm, (O) 500 μm, (P-Q) 200 μm, (R) 20 μm, (S) 50 μm, (T) 20 μm (U) 5 μm.

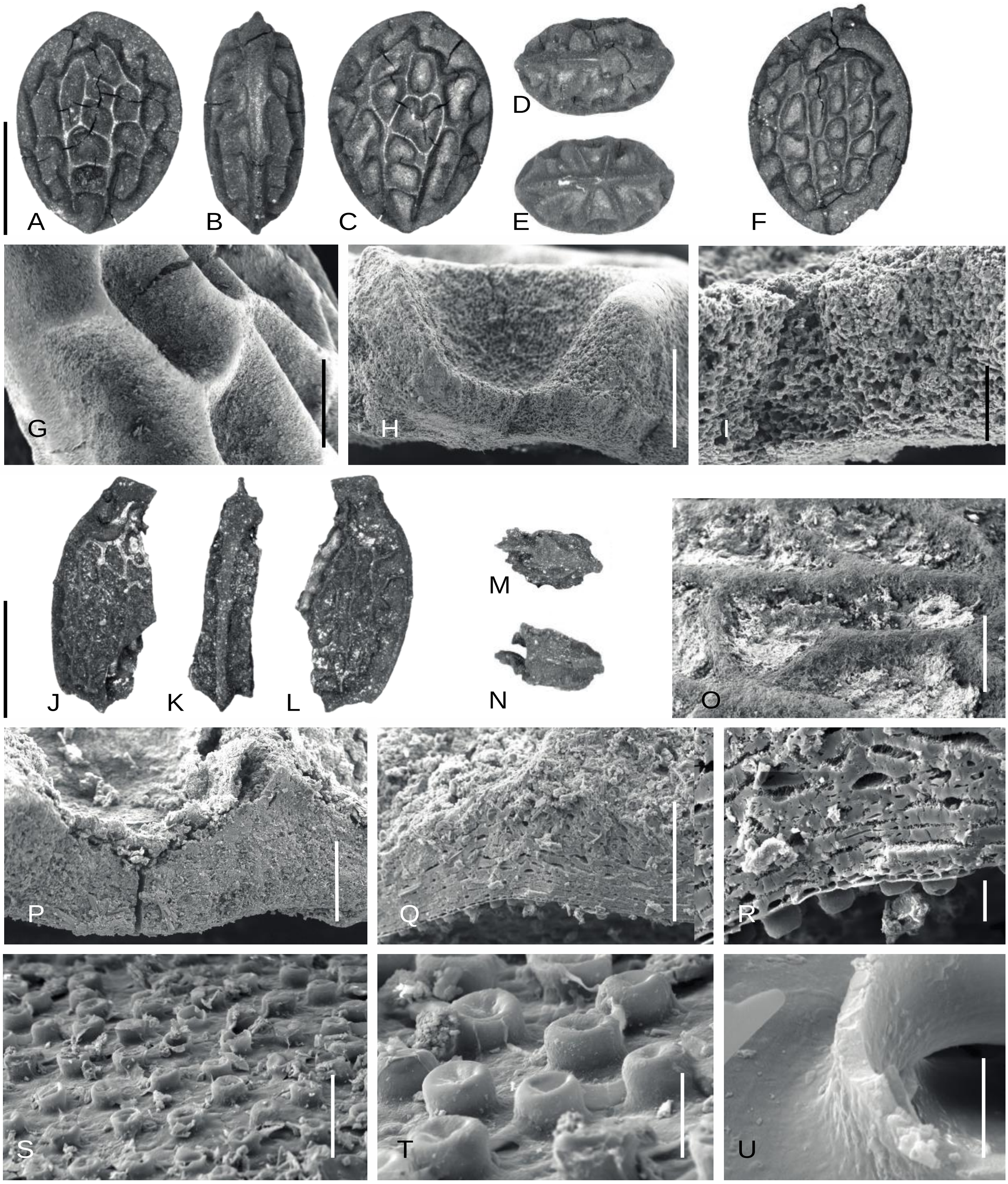
A
B
C
D
E
F
G
H
I
J
K
L
M
N
O
P
Q
R
S
T
U

Species - *Iodes rivecourtensis* Del Rio, Thomas & De Franceschi, sp. nov.
Fig. III.3 A-K

Diagnosis. Endocarp elliptical to globulose with a reticulate pattern of rounded and large ridges, which delimit 8–22 polygonal areoles on each lateral face with few or no freely ending ridgelets. Endocarp possessing a symmetrical pair of horn-like protrusions compressed on the keel, positioned eccentrically and subapically. Endocarp wall 0.32–0.7 mm thick (without ridges) and 0.38–1.59 mm thick with ridges. Inner endocarp surface densely covered with regularly spaced and tubular papillae. Length of endocarp: 8.2–12.04 mm, width of endocarp: 6.2–9.9 mm.

Etymology. *"rivecourtensis"* refers to the Rivecourt locality, where these numerous fossils were found.

Holotype. Riv. PPB 156.

Stratigraphy. Late Paleocene.

Type locality. Rivecourt (Oise, France).

Paratypes. Riv. PPB 19, Riv. PPB 128, Riv. PPB 137, Riv. PPB 140, Riv. PPB 145, Riv. PPB 149, Riv. PPB 150, Riv. PPB 151, Riv. PPB 152, Riv. PPB 155, Riv. PPB 161, Riv. PPB 163, Riv. PPB 164, Riv. PPB 166, Riv. PPB 167, Riv. PPB 169, Riv. PPB 170, Riv. PPB 171, Riv. PPB 172, Riv. PPB 173, Riv. PPB 174, Riv. PPB 175, Riv. PPB 176, Riv. PPB 178, Riv. PPB 179, Riv. PPB 182, Riv. PPB 183, Riv. PPB 185, Riv. PPB 186, Riv. PPB 187, Riv. PPB 193, Riv. PPB 194, Riv. PPB 195, Riv. PPB 196, Riv. PPB 197.

Description. Endocarp bilaterally symmetrical, unilocular, single-seeded often well preserved with testa remains, elliptical to globulose, laterally compressed in the plane of symmetry; length 8.2–12.04, avg. 9.2 mm (SD=0.83, n=21), width 6.3–9.9, avg. 9.1 mm (SD=0.99, n=13), thickness 2.76–5.9, avg. 4.05 mm (SD=0.82, n=16); outer part of endocarp with reticulate pattern of rounded and large ridges with 4–6 longitudinal ridges, which delimit 8–22 polygonal areoles on each lateral face with few or no freely ending ridgelets; a keel surrounds the fruit in the plane of symmetry with the thicker margin containing a vascular bundle embedded in the endocarp wall. Presence of a symmetrical pair of horn-like protrusions compressed on the keel, positioned eccentrically and subapically on each endocarp faces, each with a central pit; Endocarp wall 0.32–0.7, avg. 0.5 mm (SD=0.1, n=24) thick without ridges and 0.38–1.59, avg. 1.19 mm (SD=0,23, n=23) with ridges. Wall composed of three layers of one or several successive cell rows, the outermost corresponds to the layer in one row of isodiametric cells, cells 0.015–0.046 mm diameter (13 specimens). The basal sclerotic layer forms the bulk of the thickness of the endocarp wall and is composed of numerous sclerotized cells. Inner endocarp surface is densely covered with regularly spaced, minute and tubular papillae, which correspond to cell expansions of the locule epidermal layer, with papillae often apparent on the testa; papillae diameter 0.013–0.017 mm (Riv. PPB 140), 126–260 papillae per 0.25 mm². Testa with rectangular to polygonal cells, 0.016–0.024 mm diameter.

Remarks. This species is the most abundantly represented in the Rivecourt site with 36 specimens. It differs from the other species in having large ridges: they represent almost an area wider than the areoles' (Fig. III.3 A-F). This species also has a very thick wall and thick ridges (Fig. III.3 G-H). Endocarps of this species differ from *I. corniculata* by their greater length and width, their larger ridges, their more compressed horn-like protrusions, and their denser papillae. These features also distinguish *I. rivecourtensis* from *I. brownii*, but *I. trivecourtensis* also has a notably thicker endocarp wall with papillae showing a smaller diameter. Finally, endocarps of *I. rivecourtensis* differ from those of *I. eocenica* by their smaller length and width and their denser reticulum pattern on the endocarp surface. Seeds are well preserved with remains of testa. The first wall layer corresponds to the second one in *Iodes sinuosa*. The basal sclerotic layer is composed of numerous sclerotized intermixed cells (Fig. III.3 H). The inner surface of endocarp is generally incomplete due to abrasion, with a few tubular papillae in anatomical place (Fig. III.3 I). Indentations from the papillae are generally present on the testa (Fig. III.3 J-K), providing a good indication of the original position of the papillae. However, the shape, diameter, and density are difficult to appreciate on testa (see general discussion).

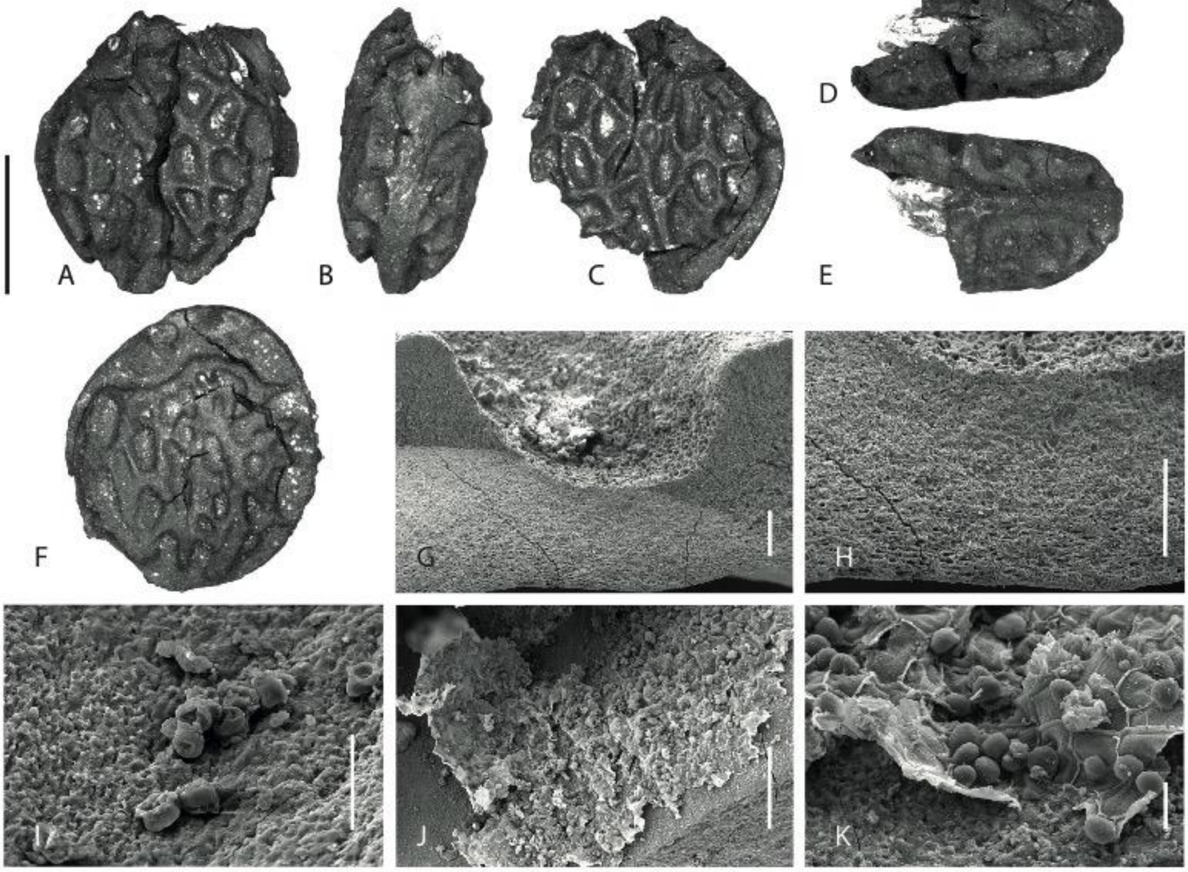

Figure III.3. *Iodes rivecourtensis* sp. nov. (A-E) Holotype specimen (Riv. PPB 156). (A) Lateral view of endocarp showing the sub-apical horn and a reticulum of large ridges. (B) Dorsal view showing the keel surrounding the fruit. (C) Lateral view of second face of endocarp. (D) Apical view showing the pair of horns. (E) Basal view. (F) Lateral view of Riv. PPB 170 showing the sub-apical horn and a reticulum of particular large ridges. (G) SEM view of endocarp wall and ridges of Riv. PPB 145 in transverse section. (H) Detail showing cell preservation. (I) SEM view of tubular papillae of Riv. PPB 194. (J) SEM view of testa remaining for Riv. PPB 187. (K) Same with magnification showing papillae includes on the testa. Scale bars: (A-F) 5 mm, (G-H) 200 μm, (I) 20 μm, (J) 200 μm, (K) 20 μm.

III.1.3.2. Key of fossil species attributed to the genus *Iodes*

The following key highlights the differences between *Iodes* fossil species found in literature and those described in this study. Rivecourt species are shown in bold.

1 Endocarp with external reticulation, sub-apical horn-like protrusions or at least pores/ channels are present on each face ____________ 2
1 Endocarp with external reticulation, but lacking horn-like protrusions or pores/ channels on each face ____________ 3

2 Endocarp reticulations with frequent free-ending ridges ____________ *I. bilinica*
2 Endocarp reticulations without free-ending ridges, or few ____________ 4

3 Endocarp reticulation with free-ending ridges ____________ *I. occidentalis*
3 Endocarp reticulation without free-ending ridges, or few ____________ 5

4 Fossil elliptical to globulose, length: 13.5–15 mm, width: 12 mm ____________ *I. eocenica*
4 Fossil elliptical to globulose, length: 8–12 mm, width 5.5–9.9 mm ____________ 6
4 Fossil elliptical to globulose, length: < 6.05 mm, width: <5.2 mm ____________ 7

5 Endocarp length: 20 mm, width: 18 mm, with a few areoles ____________ *Croomiocarpon mississippiensis*
5 Endocarp length: 8–12.5 mm, width: 4–7.5 mm, with 30–50 areoles ____________ *I. multireticulata*
5 Endocarp length: 4–5 mm, width: 2.6–3.2 mm, with > 20 areoles ____________ *I. germanica*

6 Horn-like protrusion prominent compared with the keel ____________ 8
6 Horn-like protrusion compressed on the keel ____________ 9

7 Apex obtuse and asymmetrical ____________ 10
7 Apex acute almost symmetrical without deformation ____________ *I. acutiformis*

8 Ridges sharp and thin, length: 10 mm, tubular papillae (270 per 0.25 mm^2), wall 0.26 mm and 0.38 mm with ridges ____________ ***I. tubulifera* sp. nov.**
8 Ridges angular to rounded ____________ 11

9 Large longitudinal ridges (at least the central ridge), wall 0.32–0.7 mm and 0.38–1.59 mm with ridges, length: 8.2–12.04 mm, width: 6.3–9.5 mm ____________ ***I. rivecourtensis* sp. nov.**

9 Thin longitudinal ridges (at least the central ridge), wall 0.25–0.27 mm and 0.8 mm with ridges, length: 9.2–10.8 mm, width: 6.68–7.55 mm ***I. reidii*** **sp. nov.**

10 Ridges sharp and thin, sinuous, wall 0.22–0.24 mm and 0.35–0.39 mm with ridges, short rounded papillae (600 per 0.25 mm^2), length: 4.6–5.3 mm, width: 2.5–3.7 mm ***I. sinuosa*** **sp. nov.**
10 Ridges round and large to thin, wall 0.16 to 0.26 mm and 0.4–0.56 mm with ridges, short rounded papillae (510–1060 per 0.25 mm^2), length: 4.38–6.05 mm, width 3.5–5.2 mm ***I. parva*** **sp. nov.**

11 Endocarp ornamented by 20–25 areoles, wall 0.3–0.4 mm, length: 7.5–9.5 mm, width: 5–7.5 mm *I. brownii*
11 Endocarp ornamented by 15–20 areoles, thickness of wall unknown, length: 8–9 mm, width: 5.5– 7 mm *I. corniculata*

III.1.4. General Discussion

III.1.4.1. Species included in the key

The key is restricted to fossils traditionally assigned to the modern genus *Iodes* in the literature and especially in a recent revision (Stull et al., 2016): we agree that the doubtful specimen *Iodes israelii* (Soudry & Gregor, 1997) should be excluded from the genus *Iodes*. The specimen does not possess the features diagnostic of *Iodes*: presence of vascular bundle embedded in the wall of endocarp and papillae on the inner surface (locule) of the endocarp. The specimen has no anatomically preserved structures. For all these reasons, we transfer the species to the genus *Icacinicaryites* Pigg Manchester & DeVore, which encompasses endocarps "resembling *Icacinocarya* but lacking anatomical detail needed for more precise assignment" (Pigg et al., 2008).

Icacinicaryites israelii (Soudry & Gregor) Del Rio, Thomas & De Franceschi **comb. nov.**; basyonym: *Iodes israelii* Soudry & Gregor, Cret. Research 18: 161-178. 1997.

We included *Croomiocarpon mississippiensis* in this key because it shares numerous features with *Iodes* including the presence and position of a vascular bundle. The specimen has no papillae, but it is likely a result of abrasion (see below discussion of anatomical significance of papillae). *Croomiocarpon* perhaps should be considered as a synonym of *Iodes*. However, the huge size of the specimen and the substantial thickness of the endocarp wall may justify a different genus name.

I. eocenica is included in the key as a species with horn-like protrusions because we can observe these structures in the illustration of this species in Fig. 13, Pl 15 (Reid & Chandler, 1933).and this feature is additionally noted in the legend.

III.1.4.2. Anatomical significance of papillae

The density and the size of the papillae are commonly included in descriptions of Icacinaceae endocarp fossils (Table 1). However, due to a lack of preservation, these characters are often difficult to observe. In the literature, densities were measured in several ways: following a line, within a defined area, or by simple descriptions such as "regularly spaced" or "closely spaced." The first mention of this feature is found in Reid & Chandler (1933) for *Iodes corniculata*, presented as the number of papillae per 0.25 mm^2. More recently, this character formulation was used by Allen et al. (2015) for *Iodes occidentalis*. Likewise, we also recommend using this original metric (number of papillae per 0.25 mm^2) when the fossil is fairly well preserved for a measure of the density.

For the new species from Rivecourt, we found a higher density than in all other publications. For example, both *I. corniculata* and *I. multireticulata* (*sensu* Manchester, 1994) have 3–4 papillae per 0.25 mm^2. We suppose that the small number of papillae could be explained by taphonomic bias or miscalculation. Additionally, the testa in some cases might tear the inner surface of endocarp, which supports the papillae (Fig. III.3 J-K). This tearing might explain the lack of papillae for some specimens in the literature, e.g., *Croomiocarpon mississippiensis* (Stull et al., 2011). The species *Iodes rivecourtensis* seems to be a good illustration of this phenomenon. We found the highest densities of papillae in cavities that appeared protected from tearing (Fig. III.3 I). The analysis of the intact testa on the preserved seed shows papillae, but unfortunately not the entire density, which leads to underestimation of the original density. It is possible to calculate an approximation of the original density by measuring the distance from the closest neighbouring papilla for each papilla. In fact, it seems that all preserved locular epidermal cells potentially wear a papilla and the distance could be estimated as the distance between the center of two neighboring cells

The size of papillae always seems to be between 10 and 20 µm. Indeed, we found for the most well-preserved anatomical specimens (*Paleophytocrene vancouverensis, P. pseudopersica, Iodicarpa lenticularis,* and species from this study) a very similar result. Reid & Chandler (1933) measure 50 µm for papillae of *I. multireticulata,* but according to Manchester's comment (Manchester, 1994), these measures might correspond to the hole left by tearing of the papillae. Likewise, the measure of the papillae in *I. brownii* (30 µm) is based on the same type of measurement. Furthermore, the size of papillae is difficult to measure on the testa of the seeds because the traces left by the papillae are generally bigger than the original structures.

Table 1 Comparative table of papillae feature of fossil Icacinaceae endocarp.

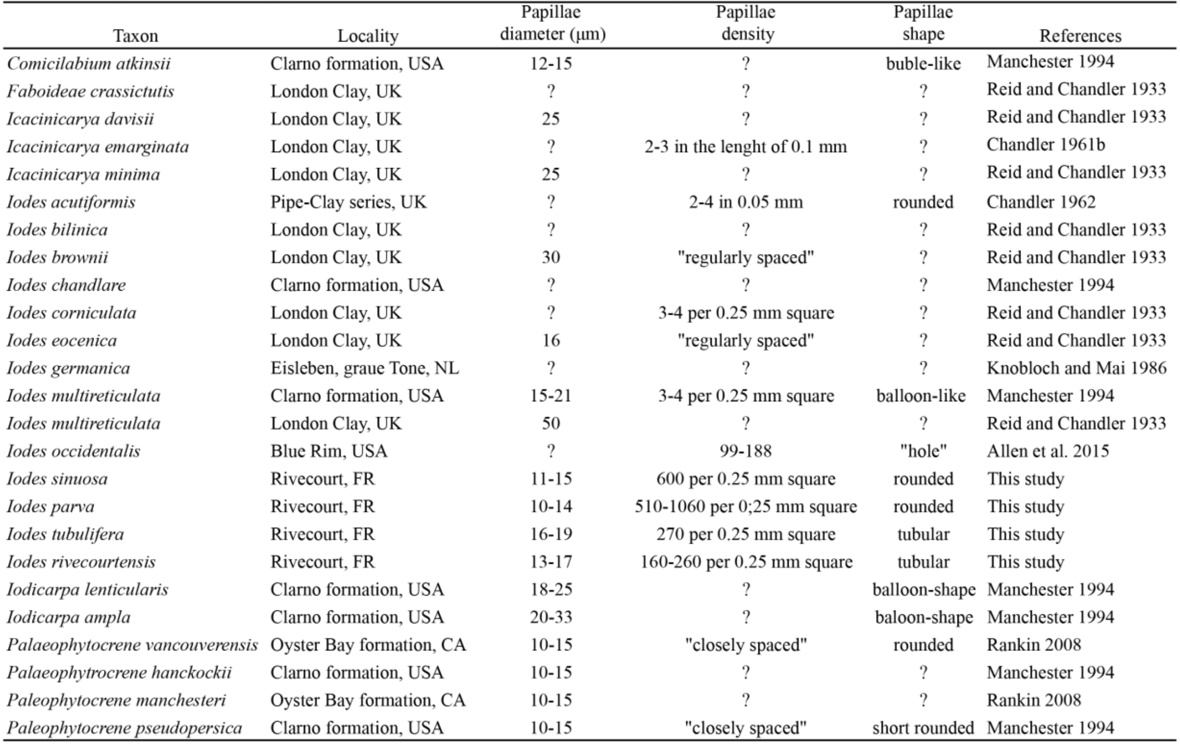

Taxon	Locality	Papillae diameter (µm)	Papillae density	Papillae shape	References
Comicilabium atkinsii	Clarno formation, USA	12-15	?	buble-like	Manchester 1994
Faboideae crassictutis	London Clay, UK	?	?	?	Reid and Chandler 1933
Icacinicarya davisii	London Clay, UK	25	?	?	Reid and Chandler 1933
Icacinicarya emarginata	London Clay, UK	?	2-3 in the lenght of 0.1 mm	?	Chandler 1961b
Icacinicarya minima	London Clay, UK	25	?	?	Reid and Chandler 1933
Iodes acutiformis	Pipe-Clay series, UK	?	2-4 in 0.05 mm	rounded	Chandler 1962
Iodes bilinica	London Clay, UK	?	?	?	Reid and Chandler 1933
Iodes brownii	London Clay, UK	30	"regularly spaced"	?	Reid and Chandler 1933
Iodes chandlare	Clarno formation, USA	?	?	?	Manchester 1994
Iodes corniculata	London Clay, UK	?	3-4 per 0.25 mm square	?	Reid and Chandler 1933
Iodes eocenica	London Clay, UK	16	"regularly spaced"	?	Reid and Chandler 1933
Iodes germanica	Eisleben, graue Tone, NL	?	?	?	Knobloch and Mai 1986
Iodes multireticulata	Clarno formation, USA	15-21	3-4 per 0.25 mm square	balloon-like	Manchester 1994
Iodes multireticulata	London Clay, UK	50	?	?	Reid and Chandler 1933
Iodes occidentalis	Blue Rim, USA	?	99-188	"hole"	Allen et al. 2015
Iodes sinuosa	Rivecourt, FR	11-15	600 per 0.25 mm square	rounded	This study
Iodes parva	Rivecourt, FR	10-14	510-1060 per 0;25 mm square	rounded	This study
Iodes tubulifera	Rivecourt, FR	16-19	270 per 0.25 mm square	tubular	This study
Iodes rivecourtensis	Rivecourt, FR	13-17	160-260 per 0.25 mm square	tubular	This study
Iodicarpa lenticularis	Clarno formation, USA	18-25	?	balloon-shape	Manchester 1994
Iodicarpa ampla	Clarno formation, USA	20-33	?	baloon-shape	Manchester 1994
Palaeophytocrene vancouverensis	Oyster Bay formation, CA	10-15	"closely spaced"	rounded	Rankin 2008
Palaeophytrocrene hanckockii	Clarno formation, USA	10-15	?	?	Manchester 1994
Paleophytocrene manchesteri	Oyster Bay formation, CA	10-15	?	?	Rankin 2008
Paleophytocrene pseudopersica	Clarno formation, USA	10-15	"closely spaced"	short rounded	Manchester 1994

For a few specimens, the shape of the papillae is defined in literature. In all articles describing this feature, we found the same general shape with differences in the papillae elevation. Chandler was the first to use the term of “rounded” for the shape of the papillae for *I. acutiformis,* while Manchester used terms as “bubble-like,” "balloon-like,” “balloon-shaped,” or “short rounded” for species from the Clarno formation. We suggest using the term “sessile rounded” for the papillae without elevation (Fig. III.1 J-K, V-W). We designated the new term “tubular” for papillae that are parallel side and flattened apex. This type of papilla is evident in well-preserved specimens of *Iodes tubulifera* (Fig. III.2 S-U) and in less well-preserved specimens of *Iodes rivecourtensis* (Fig. III.3 I-K). Mainly, this shape is wider than the short-rounded shape and sparser (Fig. III.1 J-L; Fig. III.2 S-U). Furthermore, the wall of the papillae, visible in broken examples, is less thick in tubular form than short rounded form (Fig. III.2 U).

III.1.4.3. Biogeographical significance of horns

The fossil species described here are considered a part of the modern genus *Iodes*. Reid & Chandler (1933) highlighted the affinities of *I. corniculata* with the modern species *I. africana*.

The modern genus *Iodes* is present in Africa (Boutique, 1960, Villiers, 1973), Indo-Malaysia (Sleumer, 1971, Peng & Howard, 2008) and Madagascar (De La Bâthie, 1952). Like Stull et al.

(2016), we did not found horns on the living African species (Fig. III.4 A-B), but did find them on several Indo-Malaysian species, such as *Iodes cirrhosa* (Fig. III.4 C-D). These horns are very close to those of *Iodes tubulifera*, *I. brownii* and *I. corniculata*; additionally, all species from the Rivecourt Paleocene site had this feature. According to this shared feature, we suggest a close affinity between the Paleocene fossil species and modern Asian *Iodes*. Affinities between Palaeogene European and present Asian floras and faunas are indicated in several studies (Wolfe, 1975, Smith et al., 2006, Smith et al. 2014), suggesting the modern Indo-Malaysian flora and fauna could be a relict area. A migration of this *Iodes* group to North America during the PETM (Wolfe, 1975, Manchester, 1999), corresponding to tropical habitat expansion (Wing et al., 2005), seems likely and would explain the link between *I. corniculata* and *I. brownii* (Allen et al., 2015).

Complete morphological and phylogenetic studies are needed on this clade and other related genera to elucidate the biogeographic history of this group. New fossils from other sites of the Paris Basin, still under study, could also show new character combinations and lead to more accurate biogeographical interpretations.

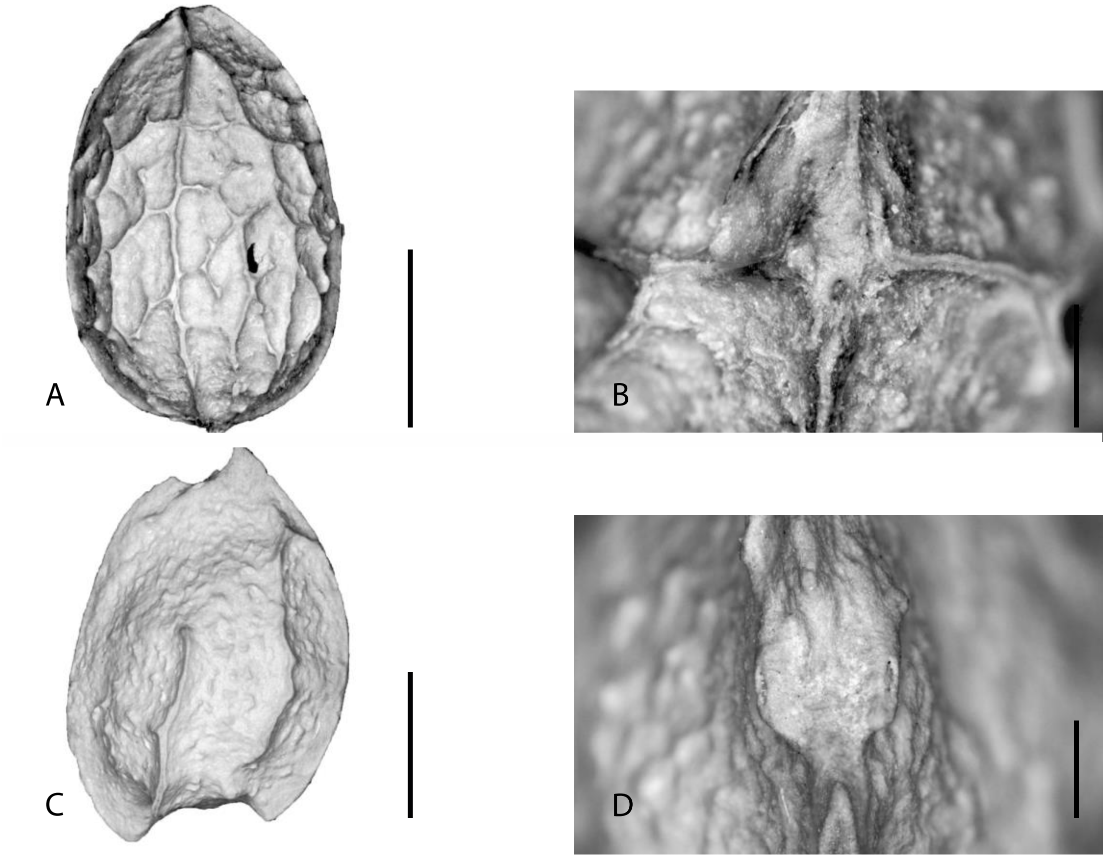

Figure III.4. (A) Lateral view of *Iodes klaineana* showing reticulum pattern of ridges. (B) Same in apical view showing the apical hole. (C) Lateral view of *Iodes cirrhosa* showing sub-apical horn and two major ridges. (D) Same in apical view showing pair of horns. Scale bars: (A, C) 5 mm, (B, D) 1 mm.

Acknowledgments

We thank Lafarge Granulats for logistic help to carry out the excavation on the Rivecourt site, the Musée Vivenel for allowing study of the fossil specimens, and the staff of the Paris Herbarium (MNHN P) for the modern endocarp sample loan and access to herbarium sheets. We thank Gregory Stull for improving the English.This work was supported by a grant from Agence Nationale de la Recherche under the LabEx ANR-10-LABX-0003-BCDiv, in the program “Investissements d’avenir” n_ ANR-11-IDEX-0004-02 and by the CR2P.

III.2. He has two, and they dangle nicely: an abnormal fossil fruit from Rivecourt (Oise, France).

III.2.1. Introduction

The Rivecourt site (Thanetian from Oise, France (Smith et al., 2014) shows numerous fruits, endocarps and seeds whose about 70 endocarp specimens are distributed in five *lodes* species (Del Rio et al. 2018). Among the 36 specimens of *Iodes rivecourtensis*, one of them caught our attention. Numbered as Riv. PPB19 and figured upside down in the presentation of the Rivecourt'site (Smith et al., 2014, Fig. III.4T), this specimen shows quite exceptional and "abnormal" characters, which led us to research the origin and the significance of these particularities.

III.2.2. Material and Method

The lignitic fossil endocarp Riv. PPB19 was studied in detail as well as the herbarium (P) fruits, which have been surveyed for comparison. Among them, three sheets have been sampled for special fruits with rare morphology described here, *Iodes africana* Welw. Ex Oliv. (P03951984 and P03951995) and *Pyrenacantha vogelianna* Baill. (P04472242).

The fossil and extant specimens were studied with a binocular microscope (Wild M3Z) and imaged with a Leica DFC 420 camera.

III.2.3. Results

The endocarp (Fig. III.5 A–D) shows two horn-like protrusions per face. A total of four, as shown on the endocarp apex, (Fig. III.5 D) versus only two horn-like protrusions on usual specimens (Fig. III.5 E). Moreover, the endocarp is divided laterally into two twin parts (Fig. III.5 C) and thus presents two locules: one of them has a seed inside, which is still preserved. The locule of the other part remains unknown. This configuration in two parts explains the wideness of this specimen (ratio length/wide = 0.82) compared to the usual type (ratio l/w =1.14).

This fossil fruit is affected by teratology, but this is not an isolated case. Our attention was also intrigued by other species, in extant Icacinaceae family. We found, among the more than 4 000 fruit specimens present in the Paris Herbarium (P), two comparable examples, which indicates a low rate of appraisal of the "abnormal case" (roughly 0.5 ‰). In the species *Iodes africana* (Fig. III.5 F–H), only one specimen, among the 404 specimens (max 2.5‰) has two locules clearly divided into two lateral parts (Fig. III.5 F); all locules contain a developed seed (Fig. III.5 G). This abnormal endocarp is wider than the standard single-seeded type (Fig. III.5 H) characteristic of the family. In the species *Pyrenacantha vogeliana* (Fig. III.5 I–K), we also find an abnormal specimen, among 147 present in the herbarium (max 6.8‰). In this specimen, the endocarp is clearly divided into two parts (Fig. III.5 I, J). In cross section, we observe a wall making the link between the two parts. Each locule possesses tubercles positioned as in the usual type (Fig. III.5 J).

III.2.4. Discussion

Since extant Icacinaceae Miers are a family with two pendulous ovules where only one reaches the maturity (Kårehed, 2001), here we have cases where both ovules are fertilized and become seeds. The development of the two ovules into seeds induces the development of two symmetrical units of endocarp linked by a wall. This observation in extant species allows us to conclude that the same process explains the observation made on the specimen Riv. PPB19. Furthermore, this abnormal specimen suggests that *Iodes rivecourtensis* had two pendulous ovules, where generally only one matures. This observation corroborates the fact that this fossil species possesses all characters of the members of Icacinaceae family.

Moreover, the development of both ovules induced the formation of four horn-like protrusions, instead of two. This structure is considered as "the point of entry of two vascular bundles into the locule (supplying the two apical ovules characteristic of icacinaceous fruits)" (Allen et al., 2015). This explanation is partially not congruent with our observation, each ovule needing two horns. The horns may be a starting point of the vascularization towards the internal part of the endocarp which permit its setting up. The role of these apical structures remains unresolved and development studies in extant *Iodes* with horns is necessary. In all cases, these four horn-like protrusions show that the development of both seeds should duplicate the vasculature of the fruit.

A similar case has been mentioned in the fossil record in the London Clay outcrops (Reid & Chandler, 1933) for *Iodes multireticulata* Reid & Chandler (see in particular plate 15, fig. 8) within one hundred specimens. Reid and Chandler proposed the same explanation about the development of the two ovules, but without certitudes. In other sites with numerous Icacinaceae fossils, we did not found other cases (Knobloch & Mai, 1986, Manchester, 1994, Collinson et al., 2012); this should be a rare case of special development of these fruits in the past.

Figure III.5. (A–D) abnormal *Iodes rivecourtensis* specimen (Riv. PPB19.), (A–B) lateral view showing the two horn-like protrusions (arrows), (C) broken parts showing one of the two locules, in cream colour, the remains of a seed still embedded in the endocarp, (D) same in apical view showing the four horn-like protrusions (arrows) ; (E) *I. rivecourtensis* usual type (Riv. PPB 156.)

showing one horn-like protrusion (arrow); (F–G) Abnormal *Iodes africana*, (F) lateral view showing the clear two twin parts, (G) two mature seeds from the abnormal fruit; (H) standard single-seeded fruit of *Iodes africana*; (I–J) abnormal *Pyrenacantha vogeliana,* (I) lateral view showing the clear two parts, (J) cross section of the abnormal fruit; (K) usual fruit of *Pyrenacantha vogeliana*.

The fossil sample also reveals that even this particular morphology is rare; its occurrence is present since more than 56 My (Paleocene) in this family and has been maintained as a possible development in several taxa until now.

Acknowledgments

We thank Lafarge Granulats for the logistic help to carry out the excavation on the Rivecourt site, the Musée Vivenel for allowing us to study of the fossil specimens, and the staff of the Paris Herbarium (MNHN P) for the modern endocarp sample loan and access to herbarium sheets. We thank Valentin Seizilles De Mazancourt for the good idea of the title. This work was supported by a grant from Agence Nationale de la Recherche under the LabEx ANR-10-LABX-0003-BCDiv, in the program "Investissements d'avenir" n_ ANR-11-IDEX-0004-02 and by the CR2P.

III.3. Chemical studies of Icacinaceae fossil seeds from the Rivecourt site (Thanetian, Oise, France)

III.3.1. Introduction

Numerous chemical studies exist on the extant Icacinaceae family especially with the Camptothecin research, but not only, using fruits, tubers or leaves (Rasoanaivo et al., 1990, Lorence & Nessler, 2004, Wu et al., 2008, Ramesha et al., 2013, Chen et al., 2015, Otun et al., 2015, David-Oku et al., 2016, Zhang et al., 2016, Datkhile et al., 2017, Feiz Haddad et al., 2017, Jiang et al., 2017, Soujanya et al., 2017, Suma et al., 2017, Wei et al., 2018). Otherwise, in another study some authors tried to make a link between taxonomy and evolution of terpenoids in the Icacinaceae group s.l. (Kaplan et al., 1991), showing a potential source of chemical taxonomic identification.

Among the Icacinaceae specimens from Rivecourt site (Thanetian, Oise, France); some have seeds remains (Del Rio et al., 2018). These seeds show a cream colour (Fig. III.6 A–C) contrasting with other lignitic fossils. We found seeds alone (Fig. III.6 A–B) or inside endocarps, mainly for *Iodes rivecourtensis* Del Rio & De Franceschi (Fig. III.6 C). The MEB view of the seed structure shows an agglomerate material very different in shape and even in organisation compared to the endocarp structure (Fig. III.6 D). All these observations led us to raise the question about the nature of these remains: is-it organic or mineral? Do we have recognisable molecules or chemical structure?

III.3.2. Material and method

The specimens were imaged with a Leica DFC 420 camera. The specimen Riv. PPB 186 was coated with gold-palladium for examination by Scanning Electron Microscopy (SEM), using a Jeol JCM6000 instrument. Two seeds have been weighed, Riv. PPB 180 and Riv. PPB 126. These seeds were powdered and introduced into two tubes and measured above and 3.1 ml of CH_2CL_2 (dichloromethane) was added thereto as an effective solvent on many organic products (fat, oils, resin, etc.). The tubes were mixed several times over a period of 24 hours.

The dichloromethane was then transferred into balloons. The rotary evaporator was used to remove the dichloromethane from the samples by evaporation at low pressure. Then the balloons were weighed again. The difference corresponds to the weight of the extract. The extracts were dissolved with a substance similar to chloroform but enriched in deuterium ($CDCl_3$)

and sent for NMR (nuclear magnetic resonance) analysis. It is a spectroscopy technique that exploits the magnetic properties of certain atomic nuclei. The supernatant was dissolved in methanol (CH_3OH) for 24 hours, used as an interesting solvent for peptides, protein etc. Finally, the The methanol solution was transferred into balloons and then evaporated before being sent for NMR analysis.

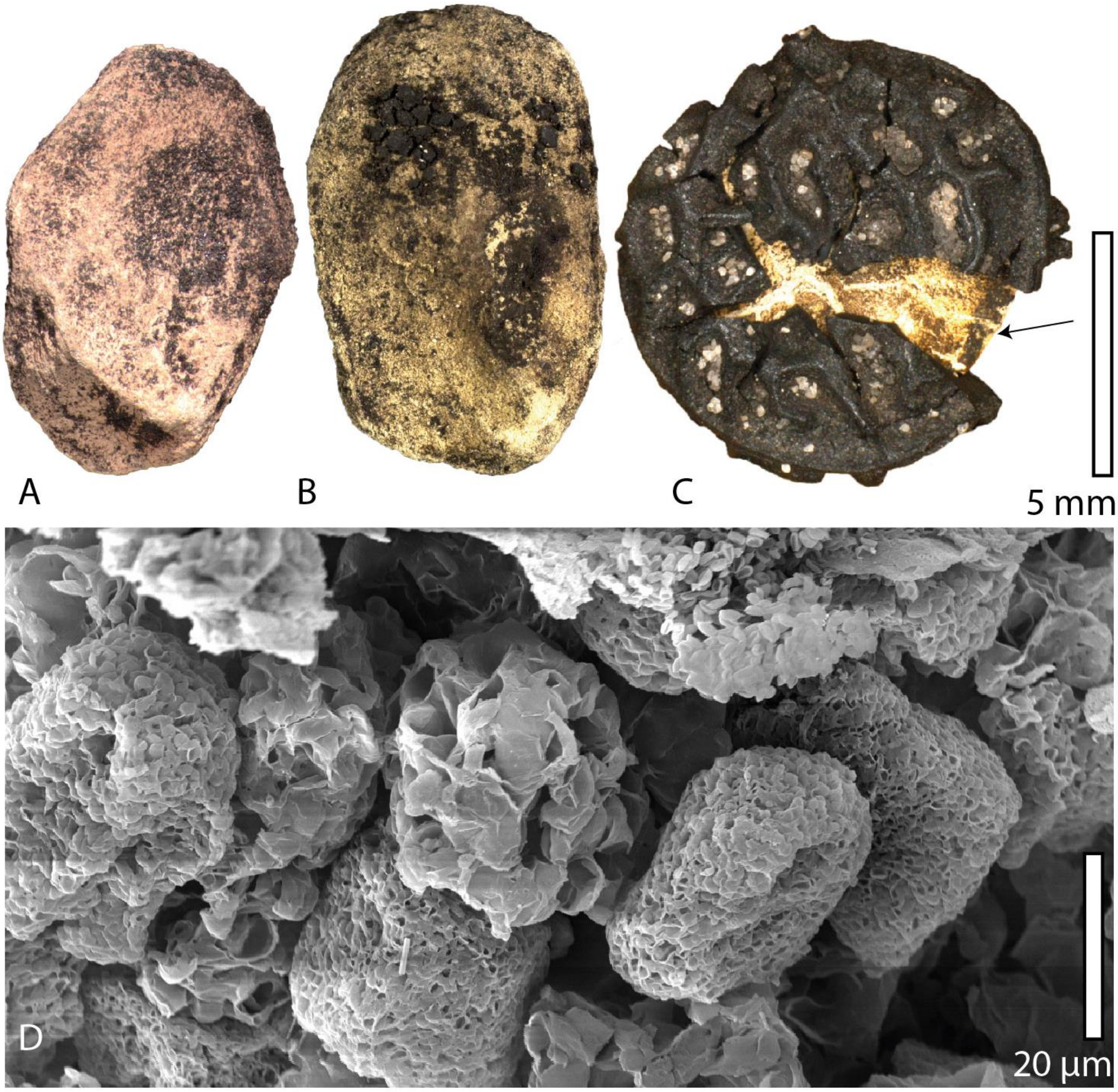

Figure III.6. (A) Lateral view of free seed (Riv. PPB 180); (B) other lateral view of free seed (Riv. PPB 126); (C) endocarp of a specimen of *Iodes rivecourtensis* (Riv. PPB 169) showing the seed (arrow); (D) SEM view of seed cell contains (Riv. PPB 186).

III.3.3. Results

Our experiment was guided by a preliminary combustion test that has been made on a small piece of fossil seed. This test was conclusive after the emission of the flame, which demonstrates that the seed is mainly composed of organic matter as the resulting ash is in very small quantity, like for living plant seeds. The seeds weight for Riv. PPB 180 is 17 mg and for Riv. PPB 126, 23 mg. The extract obtained with the use of dichloromethane corresponds to 0.7 mg for Riv. PPB 180 and 2 mg for Riv. PPB 126. The NMR analysis shows the same pattern for the two seeds, we present here (Fig. III.7) only the result for Riv. PPB 126. The NMR shows two peaks, a peak at about 0.8 ppm corresponding to CH_3 and another one at about 1.2 ppm corresponding to CH_2 (Fig. III.7). Those peaks may indicate the presence of lipid molecules. However, the molecular structure of the lipids is impossible to reconstruct due to the low quantity of extract. Unfortunately, the methanol dissolvent did not show any result.

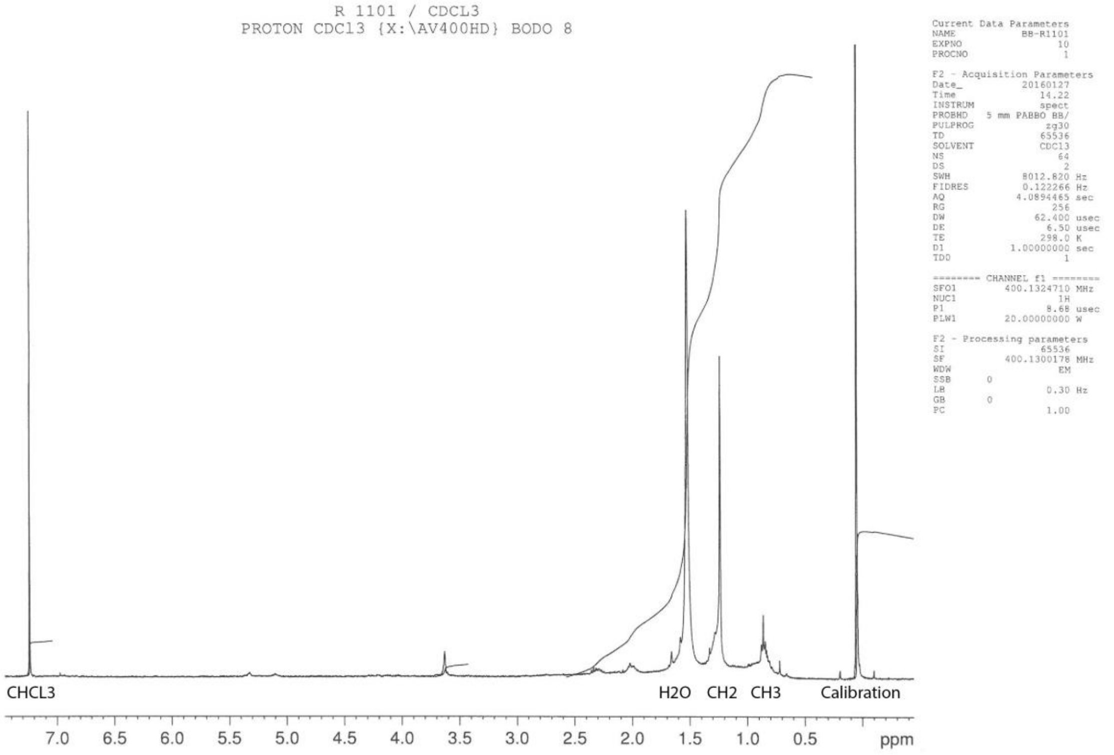

```
Current Data Parameters
NAME              BB-R1101
EXPNO                   10
PROCNO                   1

F2 - Acquisition Parameters
Date_             20160127
Time                 14.22
INSTRUM              spect
PROBHD   5 mm PABBO BB/
PULPROG               zg30
TD                   65536
SOLVENT              CDCl3
NS                      64
DS                       2
SWH               8012.820 Hz
FIDRES            0.122266 Hz
AQ               4.0894465 sec
RG                     256
DW                  62.400 usec
DE                    6.50 usec
TE                   298.0 K
D1              1.00000000 sec
TD0                      1

======== CHANNEL f1 ========
SFO1           400.1324710 MHz
NUC1                    1H
P1                    8.68 usec
PLW1           20.00000000 W

F2 - Processing parameters
SI                   65536
SF             400.1300178 MHz
WDW                     EM
SSB       0
LB                    0.30 Hz
GB        0
PC                    1.00
```

Figure III.7. Result of the NMR analysis showing the presence of CH_3 and CH_2 for Riv. PPB 126.

III.3.4. Discussion

The presence of organic matter in fossil record is rare but not isolated. Scientists found chemical compound in a wide diversity of species and epochs (Briggs & Summons, 2014). In plants, a Mesozoic conifer fossil possesses some lipids (Marynowski et al., 2007). In Cenozoic era, an unsaturated fatty acid was determinated on Palaeogene fruits and seeds (Niklas, 1982). This finding in Rivecourt site, unresolved on the seed chemical nature, shows anyway the exceptional preservation of fossils and the presence of high rate preserved organic matter.

Conclusion of the chapter

The Rivecourt site reveal five species of *Iodes* from 70 anatomically well preserved lignitic specimens. These species have in common a vascular bundle on the endocarp wall, papillae at the locule surface; ridges at the surface of the endocarp and sub-apical horn-like protrusions in each face. This last character is common in the modern Asian *Iodes* species and could be a clue for affinities between European Paleocene and modern Asian floras. Among the 70 specimens, the Riv. PPB19 specimen is divided in two parts with two horns by faces and suggest the abnormal development of the two pendulous ovules (instead of only one). This specimen confirms that these species belongs to the Icacinaceae family. The study of the seed, with an unusual colour and texture, which contrasts with the rest of the outcrop, shows that there are organic matters but the chemical characterisation, was not possible regarding its available amount. All these studies demonstrate the good preservation of the fossils from the Rivecourt site and the need to study them.

Chapter IV

Expected Icacinaceae wood in Rivecourt site (Thanetian, Oise, France) and the affinity of *Icacinoxylon* Shilk.

Among all fossil species attributed to the Icacinaceae family, some of them are fossil wood (Greguss, 1969, Petrescu & Dragastan, 1972, Wheeler et al., 1987). The affinity of these fossils with this extant family was augmented by comparative studies (Bailey & Howard, 1941a, 1941b, 1941c). Fossils were attributed to the fossil genus *Icacinoxylon* (affinity with *Citronella*, Shilkina, 1956) and *Gomphandroxylon* (affinity with *Gomphandra*, Bande & Khatri, 1980). Since, a wide phylogenetic study including wood characters have been made (Lens et al., 2008), corroborating the exclusion of *Citronella* and *Gomphandra* from Icacinaceae s.s (Kårehed, 2001, Stull et al., 2015).

In Rivecourt site (Thanetian, Oise, France), Icacinaceae are well represented among macrofossils fruits and seeds, especially with numerous endocarps (Smith et al., 2014). In this site, many lignitic or coalified fossil woods have been found. A preliminary study (Gabaix-Hiale, 2014) revealed three potential *Icacinoxylon* woods among hundreds of samples. These woods have indistinct growth rings boundaries, a diffuse-porous wood and scalariform perforation plates. All these observations led us to raise the following questions: Do these woods belong to the genus *Icacinoxylon* and/or to the Icacinaceae family? What information can they bring about their past ecology? This chapter concerns the study of these three wood samples, their identification and potential affinities.

IV.1. Material and method

We studied three wood samples from Rivecourt site. The lignitic or coalified fossil woods were found in a same layer as fruits, endocarps and seeds in this site. The specimens have been included in epoxy resin then transverse, radial and tangential sections were prepared following the standard techniques (Hass & Rowe, 1999). After that, the specimens were observed with an optic microscope Nikon Eclipse80i and photographed with a Nikon D300 camera. We used the database "Inside Wood" (Wheeler, 2011) in order to compare with extant and extinct species on the base of the characters proposed by the IAWA Committee (Wheeler et al., 1989).

IV.2. Results

Specimen number PPB 26

Description. Wood diffuse-porous (Fig. IV.1 A). Growth rings absent. Vessel predominantly solitary (+ 90%), oval to round, average 32 per mm^2; tangential diameter 52–102 μm (average 69.5 μm); vessel elements 540 μm long. Scalariform perforation plate; bar number 20–40 (Fig.

IV.1 G). Vessel-ray pit apparently simple. Fiber libriform with simple pits. Ray commonly 4 to 10 seriate; 4–12 rays per tangential mm (average 6 per tangential mm), > 1mm high (Fig. IV.1 D); ray heterocellular with more than 4 rows of square cells and body raw cells procumbent. Axial parenchyma diffuse-in-aggregate and scanty paratracheal.

Inside wood code tested 2p 5p 9p 14p 17p 300p 41p 48p 53p 61p 77p 78p 98p 102p 103p 302p 108p 115p

Identification. This fossil is characterized in having (1) diffuse-porous wood consisting of predominantly of solitary vessels, (2) Scalariform perforation plate with 20–40 bars, (3) Ray heterocellular and commonly 4–10 seriate, and (4) Axial parenchyma diffuse-in-aggregate and scanty paratracheal. The specimen fossil closely resembles to *Spiroplatanoxylon shilkinae* (Greguss) Süss (invalid species, see below) and *Spiroplatanoxylon hortobágyii* (Greguss) Süss, but it mainly differs by the absence of helical thickenings in vessel elements. The specimen is also close to *Protoatherospermoxylon kraeuselii* Mädel (Monimiaceae), but differs by the absence of oil or mucilage cells. *Plataninium obbruxellense* Stockmans matches with this specimen, but since this species has a majority of unknown characters, the direct comparison is impossible. *Mastixioxylon microporosum* Gottwald (Cornaceae) differs from PPB26 by having fiber with distinctly bordered pits and axial parenchyma diffuse. *Cyrilloxylon europaeum* Burgh (Cyrillaceae) have fibers with distinctly bordered pits that allow the separation with specimen from Rivecourt. The specimen PPB26 could be particularly close, or associated to *Icacinoxylon* genus, sharing with it some relevant characters as diffuse-porous wood consisting of predominantly solitary vessels, scalariform perforation plates and heterocellular rays. Among the genus, *Icacinoxylon crassiradiatum* Gottwald seems to be close, but have more than 100 vessels per mm^2 and less solitary vessels than the specimen PPB26. Thus, this specimen seems to be unique.

Affinities. Among extant species, PPB26 resembles Symplocaceae (ex. *Symplocos cochinchinensis* (Lour.) S. Moore) or Cunoniaceae (Pullea), but mainly differs by the presence of fibers with simple to minutely bordered pits. *Turpinia ovalifolia* Elmer, whatever that is close in ray and vessel characters lacks of parenchyma diffuse in aggregate. These groups are quite far apart in the classification (APG IV) and allow us to consider them as unresolved regarding the affinities considerations.

Specimen number PPB 34

Description. Wood diffuse-porous (Fig. IV.1 B), trace of cicatrization visible, Growth rings absent. Vessel predominantly solitary (+ 90%), oval to round, average 26 per mm^2; tangential diameter 63–148 µm (average 100 µm). Scalariform perforation plate; bar number 20–40. Intervessel pits alternate and opposite, 2.3 to 3.8 µm in diameter. Vessel-ray pit apparently simple (Fig. IV.1 H). Fiber libriform with simple pits (Fig. IV.1 E). Ray commonly 4 to 10 seriate; 4–12 rays per tangential mm (average 6 per tangential mm), > 1 mm high; ray heterocellular with more than four rows of square cells and body raw cells procumbent. Axial parenchyma diffuse and scanty paratracheal.

Inside wood code tested 2p 5p 9p 14p 21p 22p 24p 300p 41p 42p 48p 61p 76p 78p 98p 102p 302p 108p 115p

Identification. This fossil is characterized in having (1) diffuse-porous wood consisting of predominantly solitary vessels, (2) Scalariform perforation plate with 20–40 bars, (3) Intervessel pits alternate and opposite (4) Ray heterocellular and commonly 4–10 seriate, and (5) Axial parenchyma diffuse and scanty paratracheal. The fossil specimen closely resembles to *Plataninium obbruxellense* Stockmans, but differs by the mean tangential diameter of vessel lumina. Moreover, this species has a majority of unknown characters making the direct comparison impossible. *Cyrilloxylon europaeum* Burgh (Cyrillaceae) is close to this specimen but lacks simple fiber as well as *Ericaceoxylon parenchymatosum* Burgh (Ericaceae). *Spiroplatanoxylon shilkinae* (Greguss) Süss differs by the presence of helical thickenings in vessel elements. The specimen PPB34 could be particularly close or associated to *Icacinoxylon* genus, with whom it shares some relevant characters as diffuse-porous wood consisting of predominantly solitary vessels, scalariform perforation plate and heterocellular rays. However, no fossil species seems to be very close to this specimen. The closest could be *Icacinoxylon* sp. 2 (Herendeen, 1991), but they have intervessel pits scalariform and not alternate, and the description of this species has a majority of unknown characters.

Affinities. Among extant species, PPB34 resembles the genus *Cassinopsis* and the species *Symplocos pilosiuscula* Brand, but differs by the presence of fibers with simple to minutely bordered pits and axial parenchyma scantly paratracheal. The specimen could be close to *Ctenolophon englerianus* Mildbr in almost all characters but differs radically by the absence of prismatic crystals in ray cells and gums and other deposits in heartwood vessels. Thus, affinities with extant species allow this wood to be considered as a likely member of asterid clade.

Specimen number PPB 40

Description. Wood diffuse-porous (Fig. IV.1 C), Growth rings absent. Vessel predominantly solitary (+ 90%), oval to round, average 61 per mm^2; tangential diameter 44–72 µm (average 64 µm). Scalariform perforation plate; bar number 20–40. Intervessel pits alternate and opposite, 4.4 to 7.2 µm in diameter. Vessel-ray pit apparently simple. Fiber libriform with simple pits (Fig. IV.1 E). Ray commonly 4 to 10 seriate; 4–12 rays per tangential mm (average 5.6 per tangential mm), > 1 mm high; ray heterocellular with more than 4 rows of square cells and body raw cells procumbent. Axial parenchyma diffuse. Prismatic crystals present.

Inside wood code tested 2p 5p 14p 17p 21p 22p 24? 41p 49p 61p 76p 98p 102p 107p 302p 115p 136p

Identification. This fossil is characterized in having (1) diffuse-porous wood consisting of predominantly solitary vessels, (2) Scalariform perforation plate with 20–40 bars, (3) Intervessel pits alternate and opposite (4) Ray heterocellular and commonly 4–10 seriate, and (5) Axial parenchyma diffuse. The fossil specimen closely resembles to some fossil woods, this specimen seems to be close to *Spiroplatanoxylon romanicum* Petrescu (Süss), and *Spiroplatanoxylon shilkinae* (Greguss) Süss, ancient member of *Icacinoxylon* (see below for nomenclature issues), but it differs by the absence of helical thickenings in vessel elements.

This specimen could be close to *Mastixioxylon microporosum* Gottwald (Cornaceae) but differs by having fiber with distinctly bordered pits and no intervessel pits opposite. *Cyrilloxylon europaeum* Burgh (Cyrillaceae) have fibers with distinctly bordered pits and no prismatic crystal that allow the separation with the specimen from Rivecourt. The specimen PPB40 could be particularly close or associated with *Icacinoxylon* genus, with who it shares some relevant characters as diffuse-porous wood consisting of predominantly of solitary vessels, scalariform perforation plate and ray heterocellular. Among the genus, *Icacinoxylon densiporosum* Petrescu has close description but shows ring boundaries. *Icacinoxylon crassiradiatum* Gottwald seems to be close but has more than 100 vessels per mm^2 and less solitary vessels than the specimen PPB40. Thus, this specimen seems to be unique.

Affinities. Among extant species, PPB40 matches with *Octoknema borealis* (Octoknemaceae,). However, this extant species has scalariform perforation plates mainly with less than 20 bars and the axial parenchyma is absent, only occasionally diffuse. *Ilex mitis* (L.) Radlk. (Aquifoliaceae) also matches with the description from PPB40. However, this extant species possesses scalariform intervessel pits. *Symplocacos* is close to this specimen but has fibers with distinctly bordered pits. *Erythrospermum candidum* (Achariaceae) corresponds to PPB40 but differs in having no axial parenchyma. Some *Araliaceae* species (e.g. *Apiopetalum glabratum)* shows comparable description but differs in at least one character; *Apiopetalum glabratum* has smaller perforation plates and *Schefflera elegantissima* axial parenchyma scanty paratracheal instead of axial parenchyma diffuse. Thus, it is difficult to propose a clear affinity for this specimen event if some affinities may indicate an asterids affinity of this fossil wood.

IV.3. Discussion

IV.3.1. Consideration about identifications

The three woods described here seem to be very comparable in having diffuse-porous wood consisting of predominantly solitary vessels, Scalariform perforation plate with 20–40 bars and ray heterocellular and commonly 4–10 seriate. The tangential vessel diameter and the number of the vessel per mm^2 are comparable. For PPB34 and PPB40, we also found intervessel pits alternate and opposite. The axial parenchyma is always present, diffuse, diffuse-in-aggregate and/or scantly paratracheal. Therefore, we may consider these three specimens as part of the same species with few differences. This point is corroborating with the identification of the three specimens, which are very similar. Differences could be due to taphonomic process (bad preservation of some structures as intervessel pits in PPB26) or intra-specific variability or the provenance of the wood i.e. not the same part of the plant.

Affinity with the *Icacinoxylon* genus is considered because all specimens share the main characters of this genus: Wood diffuse-porous consisting of predominantly of solitary vessels scalariform perforation plates and heterogeneous rays. Moreover, the genus *Icacinoxylon* is probably defined on the base of ancestral (or plesiomorph) characters. Indeed, the affinity with Icacinaceae was argued in the basis of ancient taxonomic works. Phylogenetic studies allow the recognition of Icacinaceae as a non-monophyletic group (Kårehed, 2001, Byng et al., 2014, Stull et al., 2015).

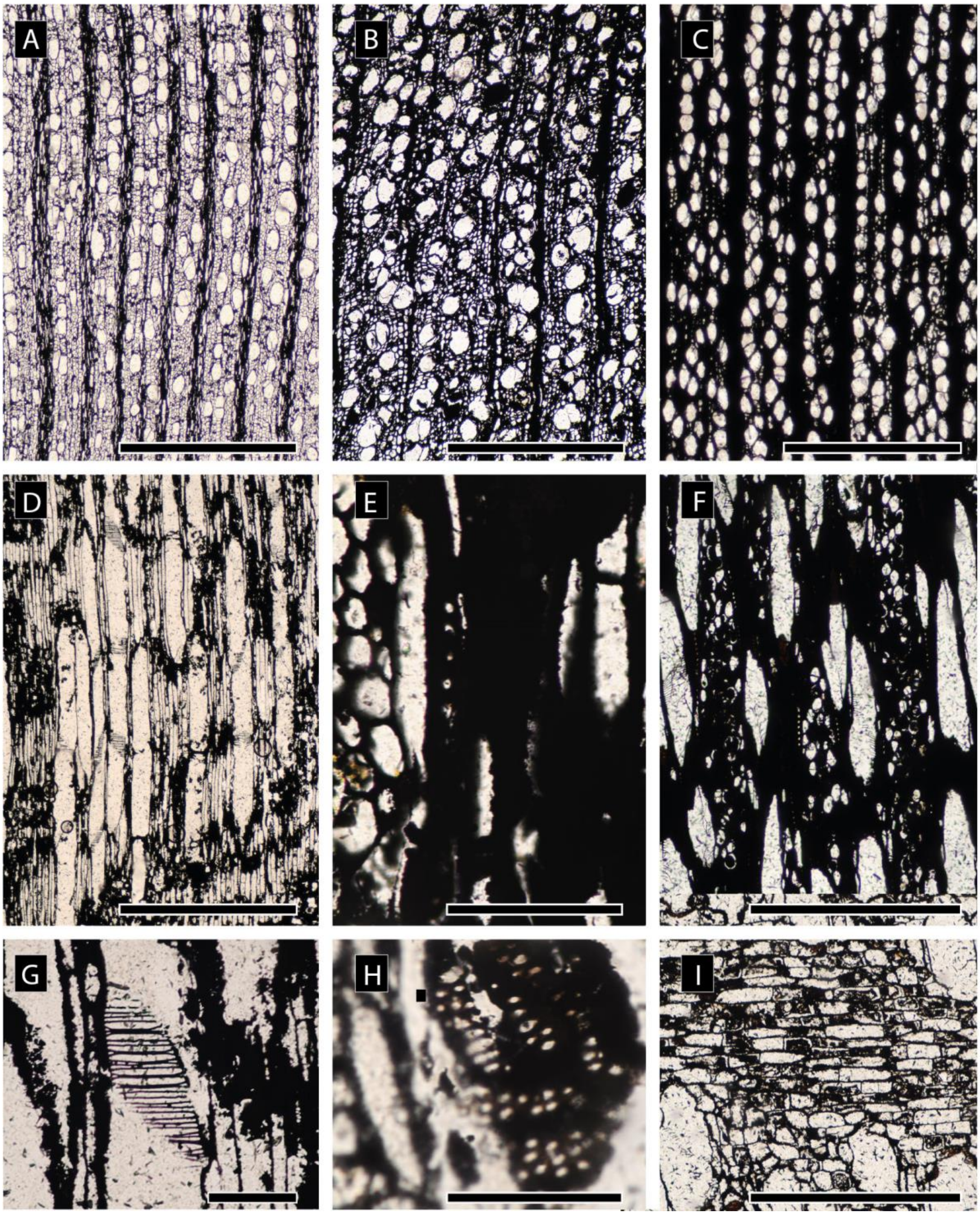

Figure IV.1. (A–C) transverse section of (A) PPB26, (B) PPPB34, (C) PPB40. Note the diffuse-porous wood, with more or less solitary vessels and without ring boundaries; (D–H) tangential section, (D) large rays, 4–10 seriate (PPB26), (E) fibers with simple pits (PPB34), (F) large rays, 4–10 seriate, about 4–12 rays per millimeter (PPB40), (G) scalariform perforation plate with 20–40 bars (PPB26), (H) vessel ray pits apparently simple (PPB 34); (I) radial section, rays heterocellular, body ray cells procumbent with mostly 2–4 rows of upright margin cells. Scale bars: A–D = 1 mm; E, G, H= 0.1 mm; F, I = 0.5 mm.

Icacinaceae s.s. (excluding *Cassinopsis* genus) have simple perforation plates that excludes the affinity with our specimens and with *Icacinoxylon* in general. All genera (excluding *Cassinopsis*) with scalariform perforation plates are now considered as belonging to Cardiopteridaceae, Metteniusaceae and Aquifoliaceae families. Thus, the comparative group for the *Icacinoxylon* affinities belongs to multiple origins in the asterid clade. *Cassinopsis* is the earliest diverging genus in the Icacinaceae clade. The scalariform perforation plate, very common in the asterid clade (e.g. Ericales and Cornales) could be a retention or plesiomorphic characters in this genus.

IV.3.2. Relations between *Spiroplatanoxylon* and *Icacinoxylon*

Süss (2007) described a new extinct genus, *Spiroplatanoxylon* and transferred all *Icacinoxylon* with helical thickening in vessel elements in this new group. Among these species, he replaced *Icacinoxylon citronelloides*, type species of *Icacinoxylon,* in his new genus; so *Icacinoxylon* should be in synonymy of *Spiroplatanoxylon.* However, Süss gave in author name of *Icacinoxylon citronelloides,* Greguss 1969 instead of Shilkina. In fact, Greguss (1969) describes a fossil wood as belonging to the type species described by Shilkina, despite some differences. Süss estimated that the Greguss'specimen belongs to his new genus and transferred it with the specific epithet *citronelloides* Greguss 1969. However, the species *Icacinoxylon citronelloides* Greguss 1969 does not exist, because Greguss never described a new species from this specimen. Süss had to define a new species from the Greguss description before making a new combination. Consequently, *Spiroplatanoxylon citronelloides* (Greguss) Süss is not valid. It's important for the nomenclature to differentiate *Icacinoxylon citronelloides* Shilkina (valid) and *Spiroplatanoxylon citronelloides* sensus Greguss. In the database "Inside wood", only the second one is present.

Conclusion of the chapter

The three wood specimens from the Rivecourt site may belong to the same species. These specimens could correspond to the *Icacinoxylon* fossil genus in having the key characters of this group. However, the recognition of this genus was made in the basis of the polyphyletic definition of the Icacinaceae group. Icacinaceae s.s. have simple perforation plates (excluding *Cassinopsis*); *Icacinoxylon* Shilkina is no longer considered as an extinct group of Icacinaceae. The comparative group for the *Icacinoxylon* affinities belongs to multiple origins in the asterid clade, which indicates that these woods belong to this clade, but that precise affinities in order or family rank remain unclear. Thereby, no Icacinaceae s.s. wood have been identified until now in the fossil records. Without giving information in the evolution of Icacinaceae clade, these three specimens show no ring boundaries, which allow us to consider the seasonality in Rivecourt site during the end of the Paleocene as few marked which agrees with previous ecological considerations (Smith et al., 2014, Del Rio et al., 2018).

Chapter V

Two new species of *Iodes* (Icacinaceae) from the Le Quesnoy locality (Ypresian, Oise, France)

Icacinaceae are a family of trees, shrubs, and climbers with a pantropical distribution. Traditionally, the family contained about 54 genera and 400 species (Sleumer, 1942). However, the lack of clear synapomorphies led to confusions around the taxonomy and phylogeny of this group. Recent phylogenetic studies using morphological and molecular data have greatly clarified Icacinaceae phylogeny, allowing the recognition of a monophyletic—and much reduced—circumscription of 23 genera and about 150 species (Kårehed, 2001, Lens et al., 2008, Byng et al., 2014, Stull et al., 2015). This clade, along with the family Oncothecaceae, is now placed in the order Icacinales (APG, 2016), which is sister to all other lamiids (Stull et al., 2015). The Icacinaceae s.s. are well known in the fossil record in Paleogene localities from Europe, such as the London Clay flora (Reid and Chandler, 1933, Chandler, 1961a, 1961b, 1962, Collinson, 1983, Cleal et al., 2001, Stull et al., 2016), the Messel biota (Collinson et al., 2012), and the Dormaal Formation (Fairon-Demaret and Smith, 2002). Remains from the Paleogene of North America are also well documented (Crane et al., 1990, Manchester, 1994, Manchester, 1999, Pigg and Wher, 2002, Pigg et al., 2008, Rankin et al., 2008, Stull et al., 2011, Stull et al., 2012, Allen et al., 2015). In addition, several fossils of the family are known from South America (Stull et al., 2012) and Egypt (Manchester and Tiffney, 1993); additional material has been reported from Africa (Chandler, 1954, Chester, 1955) and Japan (Tanai, 1990), but the affinities of these fossils are more dubious.

Multiple clades of Icacinaceae are diagnosable by fruit characters—for example, the genus *Iodes* Blume is characterized by elliptical to globular endocarps, lenticular in transverse section, with an external reticular pattern, a papillae layer on the inner surface (locule), and a vascular bundle running from the base to the apex embedded in the endocarp wall. *Iodes*, which contains ~23 extant species, is the most abundantly represented genus of Icacinaceae in the fossil record.

These endocarp features are present in numerous fossils from the Le Quesnoy site, suggesting the presence of *Iodes* at this Paleogene locality. The faunal and floral diversity of the Le Quesnoy amber locality (Ypresian, Oise, France) was first studied by Nel et al. (1999). Particular elements of the flora have been examined; for example, there are studies focused on flowers and pollen grains preserved in amber (De Franceschi et al., 2000, De Franceschi and De Ploëg, 2003; Del Rio et al., 2017), lignitic fossil fruits and seeds (Nel et al., 1999), and Menispermaceae endocarps (Jacques and De Franceschi, 2005). However, the diversity of the flora remains understudied.

In this chapter, we describe two species of *Iodes* based on fossil endocarps and document a species already described recently from the Rivecourt site (Del Rio et al., 2018); we also document multiple seeds specimens attributed to Icacinaceae, without specific affinity. We discuss the morphological variation of modern and fossil *Iodes* endocarps, establishing a context for assessing the systematic affinities of the new species.

This chapter was submitted in **Review of Paleobotany & Palynology** in collaboration with Dario De Franceschi and Gregory W. Stull.

V.1. Material and methods

V.1.1. Material

The lignitic fossil specimens were collected from Le Quesnoy locality (Houdancourt, Oise, France) from 1996 to 2000, from the lignitic clay sediments of Le Quesnoy outcrop, representing the lower Eocene (for location and geological setting, see De Franceschi and De Ploëg, 2003, Smith et al., 2014). Based upon the mammalian fauna, these sediments are dated at MP7 (Lower Ypresian, ~56 Ma), with corroboration from palynological studies (Nel et al., 1999, Cavagnetto, 2000). This corresponds to the Sparnacian facies of the Lower Ypresian (Lower Eocene).

Approximately 185 nearly complete endocarps of Icacinaceae were collected, primarily representing lignified samples, but some pyritized specimens were also obtained. In addition, some lignitic fragments assigned to Icacinaceae were also collected. The fossils are kept in the palaeobotanical collections of the Muséum national d'Histoire naturelle (MNHN) at Paris, collection De Franceschi - De Ploëg. Endocarps of living species of *Iodes* were sampled from herbarium specimens (Tab.1), obtained from the Muséum national d'Histoire naturelle de Paris (P), the Royal Botanic Garden Kew (K), the Botanic Garden Meise (BR) and the Missouri Botanical Garden (MO). We sampled 14 of the 23 extant species of *Iodes*, spanning the biogeographic breadth of the genus, providing us a relatively comprehensive picture of its morphological diversity. Voucher information is available in appendix.

V.1.2. Method of collection

The fruits were extracted and sieved from the lignitic clay sediments. The fossils were slowly dried after being washed in water and diluted in hydrogen peroxide and then they were kept in dry conditions. Once dried, the different sediment fractions were sorted using a binocular microscope (Mantis Elite). The pyritized samples are stored with a dehydration agent (silica-gel).

Table 1. Comparative table of features of fossil and modern endocarps of *Iodes*

Species	Endocarp length	Endocarp width	Endocarp thickness	Endocarp ornamentation	Endocarp ridging pattern	Apex vascular structure	Freely ending ridgelets	Number of areoles	Shape of ridges	Ridges at the point of the base	Ridges vertically	Thickness of endocarp wall
Croomiocarpon missippiensis Stull, Manchester & Moore	20	18	?	Ridged	Reticulate	Absent (Bulge)	Rare or absent	9–11	Angular	1	3	1140–1160
Hosiea pterojugata Mai	4–6	4–5	?	Ridged	Reticulate	?	Rare or absent	?	?	?	?	?
Iodes acuta **Del Rio & De Franceschi**	**5.8–8.0**	**3.6–5.4**	**?**	**Ridged**	**Reticulate**	**Absent (Bulge)**	**Rare or absent**	**10–25**	**Sharp**	**2**	**3 & 6**	**80–130**
Iodes acutiform (is?) Chandler	6	3.5–4	?	Ridged	Reticulate	Horns	Rare or absent	15–15	Sharp	?	4 & 3	200
Iodes africana Welw. ex Oliv.	10.8–11.7	8.5–9.1	4.5	Ridged	Reticulate	Absent	Present	21–25	Rounded	6	3	154–171
Iodes balansae Gagnep.	32.7	15.2	?	Ridged	Diffuse & Reticulate	Horns	Present	?	Angular	2	3	434–450
*Iodes bilinica (*Ettingshausen) Stull, Adams, Manchester et Collinson	9–16	7–11	5–6	Ridged	Reticulate	Pores	Present	?	Sharp	2	3 & 5	650–650
Iodes brownii (Berry) Stull, Adams, Manchester et Collinson	7.5–9.5	5–7.5	?	Ridged	Reticulate	Horns	Rare or absent	20–25	Rounded (?)	2	5 & 6 & 7	300–400
Iodes cirrhosa Turcz.	12.6	9.5	4.5	Ridged & Rugose	Diffuse		Not applicable	Not applicable	Rounded	0 & 2	2	381–405
Iodes corniculata Reid & Chandler	8–9	5.5–7.0	4	Ridged	Reticulate	Horns	Not applicable	15–20	Rounded	2	3 & 4	?
Iodes eocenica Reid et Chandler	13.5–15	12.0	5–6	Ridged	Reticulate	Horns	Rare or absent	?	Rounded	2	2	?
Iodes germanica Knobloch & Mai	4–5	2.6–3.2	?	Ridged	Reticulate	Absent (?)	Rare or absent	20	?	?	2 & 3	?
Iodes kamerunensis Engl.	10.9	9	7.5	Ridged	Reticulate	Absent	Present	1–3	Rounded	2	1	154–181
Iodes klaineana Pierre	12.1	7.6	6.3	Ridged	Reticulate	Absent	Present	13–15	Rounded	2	3	128–173
Iodes liberica Stapf	10.4	7.1	7	Ridged	Diffuse	Absent	Not applicable	Not applicable	Sharp	2	1	138–172
Iodes madagascariensis Baill.	7.6–8	4.6	4.3	Ridged	Reticulate	Absent	Rare or absent	About 80	Rounded	4	2 & 3	165–201
Iodes multireticulata Reid et Chandler	8–12.5	4–7.5	3.4	Ridged	Reticulate	Absent	Rare or absent	30–50	Rounded	2	4 & 5	?
Iodes occidentalis S.E. Allen, Stull & Manchester	7.1	6.2	?	Ridged	Reticulate	Absent	Present	26	Rounded	2	4 & 3	640
Iodes ovalis Blume	17.8	11	8.6	Ridged & Rugose	Reticulate	Horns	Present	3–4	Angular	2	3	314–375
Iodes parva Del Rio, Thomas & De Franceschi	4.4–6	3.5–5.2	2.6–3.5	Ridged	Reticulate	Horns	Rare or absent	11–20	Rounded	2	4 & 5 & 6	160–260
Iodes perrieri Sleumer	11.5	10.9	9.2	Ridged	Diffuse	Pores	Not applicable	Not applicable	Sharp	4	2	317–338
Iodes philippinensis Merr.	12.4	6–7.6	5–6.5	Ridged	Diffuse	Horns	Not applicable	Not applicable	Rounded	0 & 2	2	229–282
Iodes redii Del Rio, Thomas & De Franceschi F	9.2–10.8	6.7–7.5	2.9–4.6	Ridged	Reticulate	Horns	Rare or absent	9–19	Rounded	4	4 & 5	250–270
Iodes rigida **Del Rio & De Franceschi**	**3.7–9.3**	**3.0–6.5**	**?**	**Ridged**	**Reticulate**	**Absent**	**Rare or absent**	**0–20**	**Angular**	**2**	**5**	**260–500**
Iodes rivecourtensis Del Rio, Thomas & De Franceschi	8.2–12.0	6.3–9.9	2.8–5.9	Ridged	Reticulate	Horns/Pores	Rare or absent	8–22	Rounded	2	4 & 5 & 6	320–700
Iodes scandens (Becc.) Utteridge & Byng	14.7	12.9	11.2	Ridged	Reticulate	Horns	Present	13–18	Angular	2	2 & 3	502–564
Iodes seguinii (H, Lév.) Rehder	16.5	11.0	8.1	Smooth	Not applicable	Absent	Not applicable	Not applicable	Not applicable	0	0	173–226
Iodes seretii (De Wild.) Boutique	11.6	8.7	5.9	Ridged	Reticulate	Absent	Rare or absent	23–25	Rounded & Angular	6	3 & 4	227–245
Iodes sinuosa Del Rio, Thomas & De Franceschi	4.6–5.3	3.7	2.5	Ridged	Reticulate	Horns	Rare or absent	16–17	Sharp	2	3 & 4	220–240
Iodes tubulifera Del Rio, Thomas & De Franceschi	10	6	2	Ridged	Reticulate	Horns	Rare or absent	21	Sharp	2	5	260
Iodes yatesii Merr.	33.8	17	10.7	Ridged	Reticulate	Pores	Present	7–8	Angular	2	3	258–322
*Palaeohosiea marchiaca (*Mai*)* Kvaček & Bůžek	6–10	4–7	?	Ridged	Reticulate	Horns (?)	Rare or absent	?	?	?	?	?
Palaeohosiea suleticensis Kvaček & Bůžek	15–20	13–16	?	Ridged	Reticulate	Absent (?)	Rare or absent	?	?	1(?)	2 & 3	?

Table 1. Continued.

Species	Thickness of endocarp wall with ridges	Diameter of papillae	Density of papillae	Cell composition of endocarp wall	Orientation of endocarp wall cells	Geological period	Geographical sampling	References
Croomiocarpon missippiensis Stull, Manchester & Moore	2200-2500	?–?	?–?	?	?	Eocene	North America	Stull et al., 2011
Hosiea pterojugata Mai	?	?	?	?	?	Paleocene	Europe	Mai, 1987
Iodes acuta **Del Rio & De Franceschi**	**180–390**	**10–18**	**230–410**	**Divided into distinctive layers**	**Isodiametric & Periclinal**	**Eocene**	**Europe**	**This study**
Iodes acutiform (is?) Chandler	?	?	900–1600	?	?	Eocene	Europe	Chandler, 1962
Iodes africana Welw. ex Oliv.	268–277	14.3–17.4	810–840	Divided into distinctive layers	Periclinal & Isodiametric	Extant	Africa	This study
Iodes balansae Gagnep.	543–1311	20	?	Divided into distinctive layers	Periclinal & Isodiametric	Extant	Asia	This study
*Iodes bilinica (*Ettingshausen) Stull, Adams, Manchester et Collinson	1000	?	?	?	?	Eocene	Europe	Chandler, 1925, Kvaček and Bůžek, 1995, Collinson, 2012
Iodes brownii (Berry) Stull, Adams, Manchester et Collinson	?	30	?	?	?	Eocene	North America	Allen et al., 2015, Stull et al., 2016
Iodes cirrhosa Turcz.	813–1064	8.6–15.3	462	Divided into distinctive layers	Isodiametric & Periclinal	Extant	Asia	This study
Iodes corniculata Reid & Chandler	?	?	?	?	?	Eocene	Europe	Reid and Chandler, 1933
Iodes eocenica Reid et Chandler	?	16	?	?	?	Eocene	Europe	Reid and Chandler, 1933
Iodes germanica Knobloch & Mai	?	?	?	?	?	Cretaceous	Europe	Knobloch and Mai, 1986, Mai, 1987
Iodes kamerunensis Engl.	460–470	?	?	Homogeneous	Isodiametric	Extant	Africa	This study
Iodes klaineana Pierre	300–360	?	?	Divided into distinctive layers	Isodiametric & Periclinal	Extant	Africa	This study
Iodes liberica Stapf	257–266	?	?	Divided into distinctive layers	Isodiametric & Periclinal	Extant	Africa	This study
Iodes madagascariensis Baill.	227–265	13.3	?	Divided into distinctive layers	Periclinal & Isodiametric	Extant	Madagascar	This study
Iodes multireticulata Reid et Chandler	?	50	?	?	?	Eocene	Europe	Reid and Chandler, 1933
Iodes occidentalis S.E. Allen, Stull & Manchester	?	30–50	99–180	?	?	Eocene	North America	Allen et al., 2015
Iodes ovalis Blume	490	9.2–11.8	?	Divided into distinctive layers	Isodiametric & Periclinal	Extant	Asia	This study
Iodes parva Del Rio, Thomas & De Franceschi	400–560	10–14	510–1060	Divided into distinctive layers	Isodiametric & Periclinal	Paleocene & Eocene	Europe	Del Rio et al., accepted
Iodes perrieri Sleumer	340–426	12.3–18	448	Divided into distinctive layers	Isodiametric & Periclinal	Extant	Madagascar	This study
Iodes philippinensis Merr.	360–387	?	?	Divided into distinctive layers	Isodiametric & Periclinal	Extant	Asia	This study
Iodes redii Del Rio, Thomas & De Franceschi F	800	?	?	Divided into distinctive layers	Isodiametric & Periclinal	Paleocene	Europe	Del Rio et al., accepted
Iodes rigida **Del Rio & De Franceschi**	**430–580**	**10–26**	**290–570**	**Divided into distinctive layers**	**Isodiametric & Periclinal**	**Eocene**	**Europe**	**This study**
Iodes rivecourtensis Del Rio, Thomas & De Franceschi	380–1590	13–17	126–260	Divided into distinctive layers	Isodiametric & Periclinal	Paleocene	Europe	Del Rio et al., accepted
Iodes scandens (Becc.) Utteridge & Byng	652–672	?	?	Divided into distinctive layers	Periclinal &Anticlinal	Extant	Asia	No voucher (MO).
Iodes seguinii (H, Lév.) Rehder	?	?	?	Homogeneous	Periclinal	Extant	Asia	This study
Iodes seretii (De Wild.) Boutique	320–386	11.8–13.7	?	Divided into distinctive layers	Isodiametric & Periclinal	Extant	Africa	BR0000015596772
Iodes sinuosa Del Rio, Thomas & De Franceschi	350–390	11–15	600	Divided into distinctive layers	Isodiametric & Periclinal	Paleocene	Europe	Del Rio et al., accepted
Iodes tubulifera Del Rio, Thomas & De Franceschi	380	16–19	270	Divided into distinctive layers	Isodiametric & Periclinal	Paleocene	Europe	Del Rio et al., accepted
Iodes yatesii Merr.	430–959	?	?	Divided into distinctive layers	Isodiametric & Periclinal	Extant	Asia	This study
*Palaeohosiea marchiaca (*Mai*)* Kvaček & Bůžek	?	16–25	?	?	?	Paleocene	Europe	Kvaček and Bůžek, 1995
Palaeohosiea suleticensis Kvaček & Bůžek	?	15–20	?	?	?	Oligocene	Europe	Kvaček and Bůžek, 1995

V.1.3. Method of observation

All specimens were studied with a binocular microscope (Wild M3Z) and imaged with a Leica DFC 420 camera. Measures were taken using the ImageJ Software (Rasband 2016). Cell diameters and papillae were measured 10 times for each species, using random selections of the specimens. Multiple samples were coated with gold-palladium for examination by Scanning Electron Microscopy (SEM), using a Jeol JCM6000 instrument, facilitating observation of anatomical features, especially the endocarp wall layers and papillae.

V.2. Systematics

The general fruit features of Icacinaceae are present in the species described here: bilateral endocarps, usually elliptical, with an asymmetrical apex and containing a single-seeded. The fossils show additional features generally associated with the *Iodeae* tribe (which is now understood to by polyphyletic; see Stull et al., 2015): the presence of a keel surrounding the endocarp, the pattern of ridges at the surface (which delimitate areoles), and papillae on the inner endocarp surface. However, these features combined with a vascular bundle inside the endocarp wall and notably round papillae suggest affinities with *Iodes*, which can be distinguished from other genera of Icacinaceae based on this unique combination of characters. Additionally, more subtle characters permit the recognition of three species, two of which are newly described here.

Order- Icacinales Tiegh.
Family- Icacinaceae Miers
Genus- *Iodes* Blume
Species- *Iodes rigida* Del Rio and De Franceschi sp. nov.
Plate I, 1-12

Diagnosis. Endocarp bilaterally symmetrical, elliptical to ovate, occasionally globular, with a reticulate pattern of rectangular ridges that delimit about 11 polygonal areoles on each face, with few or no freely ending ridgelets. A keel surrounds the endocarp in the plane of symmetry, with the thicker margin containing a vascular bundle embedded in the endocarp wall. Endocarp possessing an apical hole. Endocarp wall about 0.26–0.50 mm thick (excluding ridges; 0.43–0.58

mm including ridges). Inner endocarp surface densely covered with regularly spaced, sessile papillae, rounded in shape with small punctuations/depressions on the surface. Length of endocarp 3.72–9.29 mm, width 3.01–6.54mm.

Etymology. From rigidus (L = rigid), in reference to the strong ridges of the endocarp structure.

Holotype. MNHN.F. 44593.

Stratigraphy. Early Eocene.

Type locality. Le Quesnoy (Oise, France).

Paratypes. MNHN.F.44547., MNHN.F.44548., MNHN.F.44555., MNHN.F.44557., MNHN.F.44558., MNHN.F.44560., MNHN.F.44561., MNHN.F.44563., MNHN.F.44564., MNHN.F.44565., MNHN.F.44566., MNHN.F.44567., MNHN.F.44568., MNHN.F.44570., MNHN.F.44572., MNHN.F.44573., MNHN.F.44575., MNHN.F.44577., MNHN.F.44578., MNHN.F.44579., MNHN.F.44580., MNHN.F.44581., MNHN.F.44582., MNHN.F.44583., MNHN.F.44584., MNHN.F.44585., MNHN.F.44586., MNHN.F.44587., MNHN.F.44588., MNHN.F.44589., MNHN.F.44590., MNHN.F.44591., MNHN.F.44592., MNHN.F.44594., MNHN.F.44595., MNHN.F.44596., MNHN.F.44597., MNHN.F.44598., MNHN.F.44599., MNHN.F.44600., MNHN.F.44601., MNHN.F.44602., MNHN.F.44603., MNHN.F.44604., MNHN.F.44606., MNHN.F.44607., MNHN.F.44608., MNHN.F.44609., MNHN.F.44610., MNHN.F.44611., MNHN.F.44612., MNHN.F.44613., MNHN.F.44615., MNHN.F.44616., MNHN.F.44617., MNHN.F.44618., MNHN.F.44619., MNHN.F.44620., MNHN.F.44621., MNHN.F.44622., MNHN.F.44623., MNHN.F.44624., MNHN.F.44625., MNHN.F.44626., MNHN.F.44627., MNHN.F.44629., MNHN.F.44630., MNHN.F.44631., MNHN.F.44632., MNHN.F.44633., MNHN.F.44635., MNHN.F.44637., MNHN.F.44640., MNHN.F.44641., MNHN.F.44642., MNHN.F.44645., MNHN.F.44646., MNHN.F.44647., MNHN.F.44649., MNHN.F.44650., MNHN.F.44651., MNHN.F.44653., MNHN.F.44654., MNHN.F.44655., MNHN.F.44656., MNHN.F.44657., MNHN.F.44658., MNHN.F.44659., MNHN.F.44661., MNHN.F.44662., MNHN.F.44663., MNHN.F.44665., MNHN.F.44666., MNHN.F.44667., MNHN.F.44670., MNHN.F.44672., MNHN.F.44673., MNHN.F.44674., MNHN.F.44675., MNHN.F.44678., MNHN.F.44679., MNHN.F.44680., MNHN.F.44681., MNHN.F.44683., MNHN.F.44684., MNHN.F.44685., MNHN.F.44686., MNHN.F.44688., MNHN.F.44689., MNHN.F.44690., MNHN.F.44691., MNHN.F.44692., MNHN.F.44693., MNHN.F.44695.,

MNHN.F.44697., MNHN.F.44698., MNHN.F.44699., MNHN.F.44703., MNHN.F.44711., MNHN.F.44712., MNHN.F.44713., MNHN.F.44714., MNHN.F.44716., MNHN.F.44717.

Description. Endocarp bilaterally symmetrical, unilocular, single-seeded, elliptical to ovate (Plate I, 1–6), occasionally globular, lenticular in transverse section; length, 3.72–9.29 (avg. 6.25 mm; SD= 0.89, n=115), width 3.01–6.54 (avg. 4.79 mm; SD=0.73, n=110). Outer part of endocarp with reticulate pattern of "I-Beam" ridges, a particular shape of rectangular ridges with a channel on the median apical part of the surface corresponding to the trace left by the outer vasculature at the boundary between endocarp and mesocarp (Plate I, 7), occasionally preserved. Each endocarp face generally includes five longitudinal ridges (Plate I, 1–6); Ridges without connexions or delimiting up to 20 polygonal areoles on each lateral face, avg. 11, with few or no freely ending ridgelets. A keel surrounds the endocarp in the plane of symmetry (Plate I, 2) with the thicker margin containing a vascular bundle embedded in the endocarp wall (Plate I, 10). Endocarp possessing an apical hole (Plate I, 4). Endocarp wall 0.26–0.50 thick excluding ridges (avg. 0.38 mm; SD=0.1, n=4), 0.43–0.58 thick including ridges (avg. 0.51 mm; SD=0.06, n=9); see Plate I, 8). Wall composed of packed, interlocking digitate and sclerotic cells in a layer with about four units of cell rows; the outermost unit consists of numerous apical cell rows, difficult to distinguish; the second unit corresponds to a single row of isodiametrical cells, 0.039–0.104 mm in diameter; the basal sclerotic unit is composed of numerous rows of periclinal cells, 0.019-0.050 mm in length. Inner endocarp surface is densely covered with regularly spaced, sessile papillae, rounded in shape with small punctuations on the surface (Plate I, 11–12); the papillae correspond to the cell expansions of the locule epidermal layer; papillae diameter 0.010–0.026 mm (MNHN.F.44601., MNHN.F.44607., MNHN.F.44666., MNHN.F.44667., MNHN.F.44698., MNHN.F.44703.); the number of papillae per 0.25 mm^2 is between 290 and 570 (MNHN.F.44601., MNHN.F.44666., MNHN.F.44667., MNHN.F.44698., MNHN.F.44703.).

Remarks. This is the most abundant species at the Le Quesnoy site, with 125 endocarps and a few fragments. The single row of isodiametric cells is a fragile zone (Plate I, 8). Almost all broken specimen show a ridge section with this layer; papillae are very heterogeneous in form ranging from small to elongate to relatively large (Plate I, 10 & 11). The pattern of ridges is generally consistent across all specimens (Fig. V.1), but we show the extreme forms of this species in Fig. V.1. The ridge pattern is composed first of one ridge, on the medial part of each face, which begins at the base (or almost the base) and runs up two thirds of the length of the endocarp (Fig. V.1). Two series of ridges (noted 2 & 2' and 3 & 3' on Fig. V.1) running along each side complete the longitudinal ridges, with the secondary ones (2 & 2') well developed and the third ones (3 & 3') more or less developed. The occurrence of all ridges depends on the global shape of the endocarp. Punctuations in the papillae could correspond to an exchange zone between endocarp and seed.

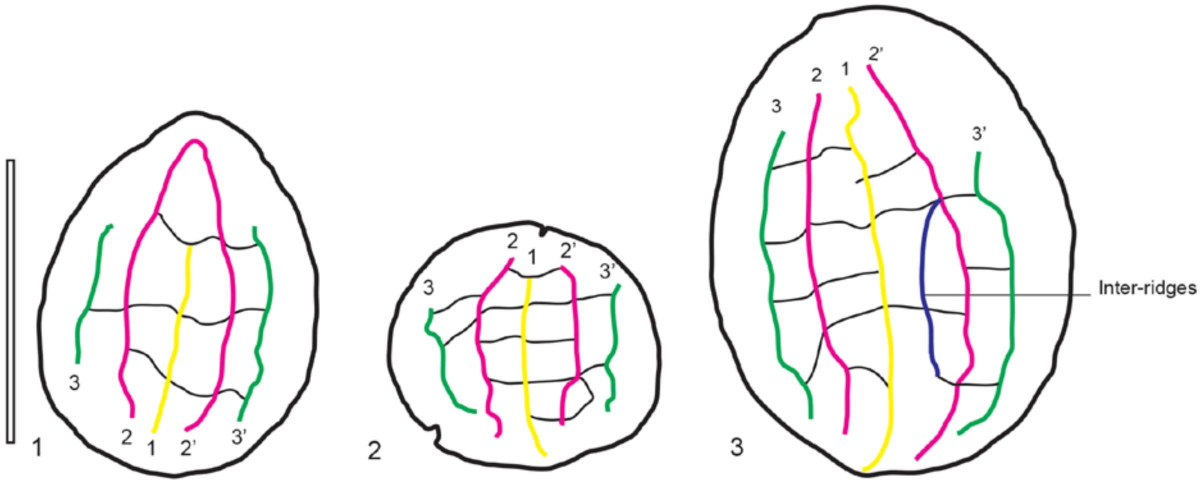

Figure V.1. Reticulation pattern of *Iodes rigida*. (1) MNHN.F.44593, (2) MNHN.F.44557. and (3) MNHN.F.44621. Scale bar: 5 mm.

Systematic affinity. This species differs from others in having a hole at the apex (Plate I, 4), a pattern of reticulation that delimits some areoles (Plate I, 1, 3 & 6), the "I-beam" ridge structure (Plate I, 8), and the punctuated and heterogeneous sessile, rounded papillae (Plate I, 12). Despite overlap in size, this species differs from *I. acuta* in having rectangular ridges and endocarp walls twice as thick. It differs from *I. parva* in lacking horn-like protrusions and possessing distinctive rectangular ridges. *Iodes rigida* differs from *I. bilinica*, *I. eocenica*, *I. acutiformis*, *I. brownii,* I. *corniculata* and all the other species from Rivecourt site (Del Rio et al., 2018) in having no horn-like protrusions but rather an apical hole. In addition, this species differs from *I. bilinica* in size and in having no free-ending ridges; from *I. eocenica* in having a clearly smaller size (3.7–9.3 mm vs 13.5–15 mm, Tab.1); from *I. acutiformis* in lacking an acute apex and having rectangular, rather than sharp, ridges; from *I. brownii* by its different pattern of ridges and distinct endocarp wall shape (?) and from *I. corniculata* in having rectangular ridges. It differs from *I. occidentalis* (Allen et al., 2015) in having no free-ending ridges, fewer areoles, and rectangular ridges. This species seems to be close to *I. multireticulata* Reid and Chandler from the London Clay (Reid and Chandler, 1933) sharing the apical hole and a pattern of reticulation without free-ending ridges (Stull et al., 2016). However, specimens from Le Quesnoy are generally smaller in size, with a length of 3.7–9.3 mm compared to 8.0–12.5 mm for *I. multireticulata*. In addition, *I. rigida* has a maximum of 20 areoles per endocarp face, which is less than *I. multireticulata* (30–50 areoles per face). The most important distinction is the shape of the ridges: the rectangular ridges of *I. ridiga* do not correspond to those described and illustrated for *I. multireticulata* (Reid and Chandler, 1933). Finally, the papillae diameter of *I. multireticulata* is more greater than that of *I. rigida* (50 vs max 26 µm), but this last difference could be due to taphonomic bias. *I. germanica* seems to be close to these new species but is typically smaller and shows more areoles and less vertical ridges (Knobloch and Mai, 1986). However, the lack of detail provided for the papillae and ridge characters in the original description of *I. germanica* makes difficult a thorough comparison. The length of *Paleohosiea suleticensis* species (here considered as potential *Iodes* species, see general discussion) is considerably greater than *I. rigida* (15–20 mm vs 3.7–9.3 mm). Finally, *Paleohosiea marchiaca* seems to be very close in shape and size but has low, rounded ridges, which are distinct from the ridges of *I. rigida*.

Species - *Iodes acuta* Del Rio and De Franceschi sp. nov.
Plate I, 13-24

Diagnosis. Endocarp bilaterally symmetrical, unilocular, single-seeded, elliptical to ovate, with a reticulate pattern of sharp and sinuous ridges, which delimit about 17 polygonal areoles on each face with few or no freely ending ridgelets. A keel surrounds the endocarp in the plane of symmetry with the thicker margin containing a vascular bundle embedded in the endocarp wall. Endocarp possessing an apical outgrowth composed of the main ridge that runs from the base up to the apex and a protuberance from the keel merged. Endocarp wall about 0.08–0.19 mm thick excluding ridges (0.18–0.39 mm including ridges). Inner endocarp surface densely covered with regularly spaced more or less punctuated and sessile rounded papillae. Length of endocarp about 5.8–8.0 mm, width about 3.61–5.42 mm.

Etymology. From acutus (L=sharpened, made sharp) in reference of the shape of ridges.

Holotype. MNHN.F.44571.

Stratigraphy. Early Eocene.

Type locality. Le Quesnoy (Oise, France).

Paratypes. MNHN.F.44551., MNHN.F.44553., MNHN.F.44554., MNHN.F.44576., MNHN.F.44605., MNHN.F.44614., MNHN.F.44634., MNHN.F.44668., MNHN.F.44682., MNHN.F.44687., MNHN.F.44696., MNHN.F.44700., MNHN.F.44701., MNHN.F.44704., MNHN.F.44705., MNHN.F.44718., MNHN.F.44719.

Description. Endocarp bilaterally symmetrical, unilocular, single-seeded, elliptical to ovate (Plate I, 14–18), lenticular in transverse section; length 5.8–8.0 (avg. 6.91 mm; SD= 0.79, n=12), width 3.61–5.42 (avg. 4.76 mm; SD=0.63, n=13). Outer part of endocarp with a reticulate pattern of sharp and sinuous ridges (Plate I, 19). Each face of the endocarp with 3–6 longitudinal ridges, which delimit 10–25 polygonal areoles on each lateral face, avg. 17, with few or no freely ending ridgelets. A keel surrounds the endocarp in the plane of symmetry (Plate I, 14), with the thicker margin containing a vascular bundle embedded in the endocarp wall (Plate I, 22). Endocarp possessing an apical outgrowth (Plate I, 16) composed of the main ridge that runs from the base up to the apex and a protuberance from the keel merged; Endocarp wall 0.08–0.19 thick excluding ridges (avg. 0.13 mm; SD=0.04, n=3); 0.18–0.39 thick including ridges (avg. 0.29 mm; SD=0.08, n=4). Wall composed of packed interlocking digitate and sclerotic cells with four units of unicellular and multicellular cell rows (Plate I, 20–21); the outermost unit corresponds to an apical sclerotic layer of numerous cell rows, difficult to distinguish; the second unit corresponds to one row of isodiametric-oriented cells, 0.035–0.041 mm in diameter; the basal sclerotic unit is composed of numerous rows of periclinal cells. Inner endocarp surface densely covered with regularly spaced, more or less punctuated, sessile papillae, rounded in shape (Plate I, 23–24), which correspond to the cell expansions of the locule epiderma layer; papillae diameter 0.010–0.018 mm (MNHN.F.44554., MNHN.F.44668., MNHN.F.44705., MNHN.F.44718.); the number of papillae per 0.25 mm2 is between 230 and 410 (MNHN.F. 44554., MNHN.F.44668.).

Remarks. This species is represented by 18 lignitic fossils from Le Quesnoy. Two morphotypes are remarquable, one elongate (Plate I, 18) and one more elliptical with a thicker and more delicate keel (Plate I, 13-17). Despite these conspicuous features, the anatomical data allow consideration of these two shapes as an intraspecific variation, showing the great plasticity of this species. The wall is exceptionally thin for an icacinaceous endocarp. We show numerous mycelium filaments between papillae (Plate I, 23-24). These filaments have the same lignitic nature of endocarp, indicating that the mycelium represents a probable saprophytic consumption before fossilisation.

Systematic affinity. This new species is distinct from the others due to its unique apical outgrowth, composed of the main ridge that runs from the base up to the apex and a protuberance from the keel merged (Plate I, 16), a very thin wall (Plate I, 20-21), and sharp ridges (Plate I, 19). It differs from *I. rigida* and *I. parva* in having sharp ridges. *Iodes acuta* shares this shape of ridges with *I. acutiformis*, *I.bilinica*, *I.sinuosa* and *I. tubulifera*, all species from European Eocene sites; other species have clearly rounded or rectangular ridges (Tab. 1). *I. acutiformis* has a thicker endocarp wall (200 µm vs max. 130 µm) and an acute apex, which is not found in *I. acuta*. In addition, the papillae seem to be denser in *I. acutiformis*, but we do not have information about the shape and diameter of the papillae for comparison. *I. acuta* differs from *I. bilinica* (Collinson et al., 2012) in overall size (5.8–8.0 mm vs 9.0–16.0 mm length), the absence of free-ending ridges, and endocarp thickness (for *I. bilinica*, 650 µm, Tab.1). *I. germanica* is smaller than *I. acuta* and is not well described, making it difficult to more thoroughly assess the affinities between these two species.

The shape of the ridges in transverse section of the new species (Plate I, 20) resembles that of *I. sinuosa* from the Rivecourt site (Del Rio et al., 2018), suggesting potential affinities, despite the differences in apex morphology, overall size, endocarp wall thickness, and papillae density. Finally, *I. tubulifera* has a greater size and shows tubular papillae not found in *I. acuta*.

Species - *Iodes parva* Del Rio, Thomas and De Franceschi
Plate II, 1-12

Stratigraphy. Late Paleocene
Additional stratigraphy. Early Eocene

Type locality. Rivecourt (Oise, France).
Additional locality. Le Quesnoy (Oise, France)

Specimens: MNHN.F.44549., MNHN.F.44550., MNHN.F.44552., MNHN.F.44556., MNHN.F.44562., MNHN.F.44569., MNHN.F.44628., MNHN.F.44638., MNHN.F.44639., MNHN.F.44648., MNHN.F.44660., MNHN.F.44706., MNHN.F.44707., MNHN.F.44709., MNHN.F.44710., MNHN.F.44730.

Description (Le Quesnoy specimens). Endocarp bilaterally symmetrical, unilocular, single-seeded Endocarp shape elliptical to ovate (Plate II, 1–6), lenticular in transverse section; length 4.27–7.10, avg. 5.47 mm (SD= 0.95, n=15), width 3.20–5.48, avg. 4.34 mm (SD=0.77, n=14). Outer part of the endocarp with a reticulate pattern of rounded and thin ridges (Plate II, 7), each face of the endocarp with 3–6 longitudinal ridges, which delimit 9–23 polygonal areoles on each lateral face, avg. 17, with few or no freely ending ridgelets.

Plate I

1-12. *Iodes rigida* Del Rio and De Franceschi sp. nov.

1. Lateral view of endocarp showing the reticulate pattern of ridges, Holotype specimen (MNHN.F.44593.).
2. Same in dorsal view showing the keel surrounding the fruit.
3. Same in lateral view showing the second face of endocarp.
4. Same in apical view showing the hole.
5. Same in basal view showing the trace left by the peduncle.
6. Lateral view of another specimen (MNHN.F.44564.) showing a comparable reticulum.
7. SEM view of ridges showing trace left by vascular bundles (MNHN.F.44655.).
8. SEM transverse view of wall and ridge (MNHN.F.44697.).
9. SEM transverse view showing the basal sclerotic layer and locule epidermal layer with papillae in contact with seed cells. (MNHN.F.44607.).
10. SEM view of the vascular bundle (arrow) inside the endocarp wall (MNHN.F.44601.).
11. SEM view of the papillae on the locule lining.
12. Same with magnification showing punctuation under papillae.

13-24. *Iodes acuta* Del Rio and De Franceschi sp. nov.

13. Lateral view of endocarp showing the reticulum of ridges, Holotype specimen (MNHN.F.44571.).
14. Same in dorsal view showing the keel surrounding the fruit.
15. Same in lateral view showing the second face of the endocarp.
16. Same in apical view showing the hole.
17. Same in basal view showing the trace left by the peduncle.
18. SEM lateral view of another specimen (MNHN.F.44696.) showing reticulum of sharp ridges.
19. SEM view of reticulum of sharp ridges (MNHN.F.44705.).
20. Same in transverse view of wall and ridges.
21. Same with magnification focused on cell layers.
22. View of the vascular bundle (arrow) inside the endocarp wall (MNHN.F.44701.).
23. Same with magnification showing mycological filaments.
24. Same with magnification focused on non-punctuated papillae.

Scale bar: 5 mm = 1-6, 13-18; 1 mm = 22; 500 µm = 7, 19; 200 µm = 8, 10, 20; 50 µm = 9, 11, 21, 23; 20 µm = 24; 5 µm = 12.

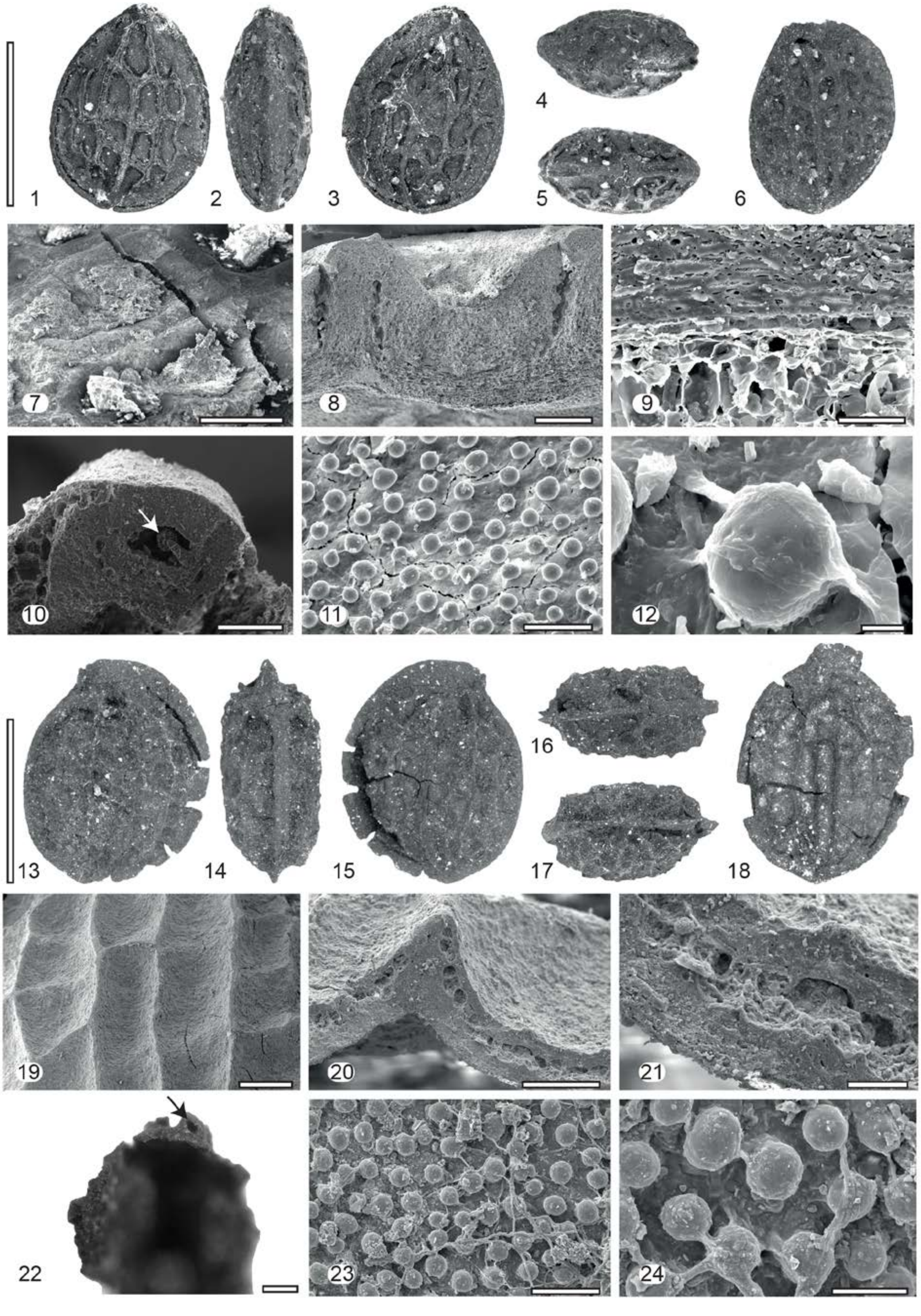
1
2
3
4
5
6
7
8
9
10
11
12
13
14
15
16
17
18
19
20
21
22
23
24

A keel surrounds the endocarp in the plane of symmetry (Plate II, 2), with the thicker margin containing a vascular bundle embedded in the endocarp wall. Endocarp possessing a symmetrical pair of horn-like protrusions compressed on the keel (Plate II, 1–6, arrows), positioned eccentrically and subapically on the apical endocarp faces, each with a central pit. Endocarp wall 0.10–0.17, avg. 0.13 mm (SD=0.05, n=2) thick (excluding ridges, 0.21–0.32, avg. 0.26 mm (SD=0.08, n=2) including ridges). Wall composed of packed interlocking digitate and sclerotic cells with four units of unicellular and multicellular layers (Plate II, 8); the outermost unit corresponds to an apical sclerotic layer of numerous cell rows, difficult to distinguish and often absent by abrasion; the second unit corresponds to one row of isodiametric cells; the basal sclerotic unit is composed of numerous cell rows. Inner endocarp surface densely covered with regularly spaced, sessile, rounded papillae (Plate II, 10–12), which correspond to the cell expansions of the locule epidermal layer; papillae diameter 0.014–0.020 mm (MNHN.F.44706., MNHN.F.44709.); the number of papillae per 0.25 mm2 is between 300 and 500 (MNHN.F.44706., MNHN.F.44709.). Testa with rectangular to polygonal cells, 0.020–0.027 X 0.008–0.014 mm.

Remarks. This species is represented by 16 fossils from Le Quesnoy. They are very different from the others specimens from Le Quesnoy in having horn-like protrusions (Plate II, 4). The wall and ridges are not well preserved on the endocarps (Plate II, 7-8), whereas the papillae are well preserved and clearly lack punctuations on the surface (Plate II, 11-12). These fossils are the most decayed among *Iodes* remains examined here; however, the seeds are well preserved and include testa remains.

Sytematic affinity. Specimens with horn-like protrusions are included within our concept of *I. parva* (Plate II, 1-12). Minor quantitative differences are noted: the wall and ridges are smaller, papillae are wider and the density is lower on Le Quesnoy specimens compared to the Rivecourt ones. However, the wall of the Le Quesnoy specimens is poorly preserved compared to those of Rivecourt (Plate II, 8). The different size could be a consequence of crushing of the cells during the taphonomic process for the Le Quesnoy specimens. In contrast, papillae cells of *I. parva* from Rivecourt are retracted and non-touching, whereas the same layer of specimens from Le Quesnoy is uniform and cells are contiguous. This cell retraction could explain the smaller size of papillae in the Rivecourt endocarps (Del Rio et al., 2018). Differences in papillae density remain problematic, although the lower values in *I. parva* from Rivecourt correspond to the higher values in the Le Quesnoy specimens. Overall, the specimens from these two sites show high levels of affinity, supporting their recognition as a single species.

Icacinaceae Incertae Sedis sp.
Plate II, 13–18

Description. Seeds elliptical in shape (Plate 2, 13–15), lenticular in transverse section, slightly asymmetrical to completely asymmetrical at the apex; length 6.31–8.56, avg. 7.52 mm (SD= 0.7, n=10), width 4.67–6.00, avg. 5.49 mm (SD=0.37, n=10). Outer surface smooth (Plate II, 16–17); anatomical structure unknown (Plate II, 18).

Specimens. MNHN.F.44720., MNHN.F.44721., MNHN.F.44722., MNHN.F.44723., MNHN.F.44724., MNHN.F.44725., MNHN.F.44726., MNHN.F.44729., MNHN.F.44731., MNHN.F.44732., MNHN.F.44733.

Remarks. Ten mineralized seeds represent this type. Due to mineral preservation (Plate II, 18), it is difficult to distinguish the hilum and the micropyle, but the asymmetrical shape of the apex is a clue for the position of both structures (Plate II, 13-15). A trace surrounds the seed (Plate II, 17); probably due to the shape of the bilateral endocarp, that embeds it. The trace left by the raphe is absent for all the specimens, probably a result of the taphonomic processes. The wall is mineralized and thin (Plate II, 16).

Systematic affinity Mineralized seeds found in Le Quesnoy are very similar in shape with seeds of Icacinaceae documented from the Dormaal formation (Fairon-Demaret and Smith, 2002). However, the specimens from Le Quesnoy are bigger than the Dormaal's specimens. We suspect a close affinity between these taxa, but without anatomical information, it is impossible to determine. The size of these seeds may indicate a species of Icacinaceae with much bigger endocarps than the other species from the Le Quesnoy site, but we could not find remains of the corresponding endocarp.

Plate II

1-12. *Iodes parva* Del Rio, Thomas and De Franceschi

1. Lateral view of endocarp showing the reticulum of ridges and sub-apical horn-like protrusions, (MNHN.F.44562.).
2. Same in dorsal view showing the keel surrounding the fruit.
3. Same in lateral view showing the second face of endocarp.
4. Same in apical view showing the ridges and sub-apical horn-like protrusions.
5. Same in basal view showing the trace left by the peduncle.
6. Lateral view of another specimen (MNHN.F.44556.).
7. SEM view of reticulum of ridges showing tearing of primary layer (MNHN.F.44628.).
8. Same in transverse view of wall and ridge.
9. Same with a view of the locule epidermal layering showing remnant testa in contact with the endocarp.
10. SEM view of locule epiderma layer showing numerous sessile, rounded papillae (MNHN.F.44709.)
11. Same with magnification.
12. Same with magnification showing unpunctuated cells under papillae.

13-18. Icacinaceae *insertae sedis*

13. Lateral view of seed showing smooth surface and asymmetrical apex (MNHN.F.44725.).
14. Other example in the same configuration (MNHN.F.44724.).
15. Other example in the same configuration (MNHN.F.44723.).
16. SEM view of broken apex of seeds (MNHN.F.44731.).
17. Same in apical view showing trace surrounding the seed.
18. Same in lateral view showing the mineralized surface.

Scale bar: 5 mm = 1-6, 13-15; 1 mm = 16; 500 μm = 7, 17; 200 μm = 8, 10; 100 μm = 9; 50 μm = 11; 20 μm = 12, 18.

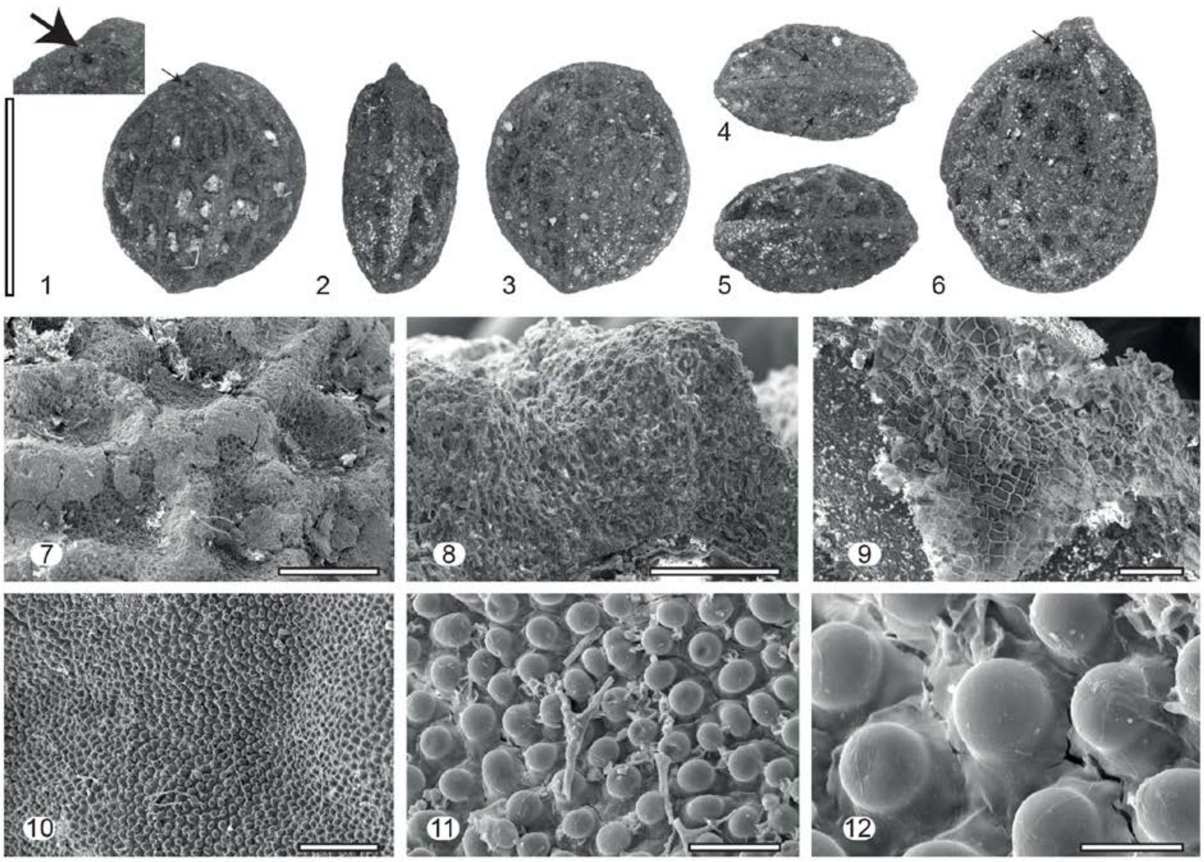
1
2
3
4
5
6
7
8
9
10
11
12

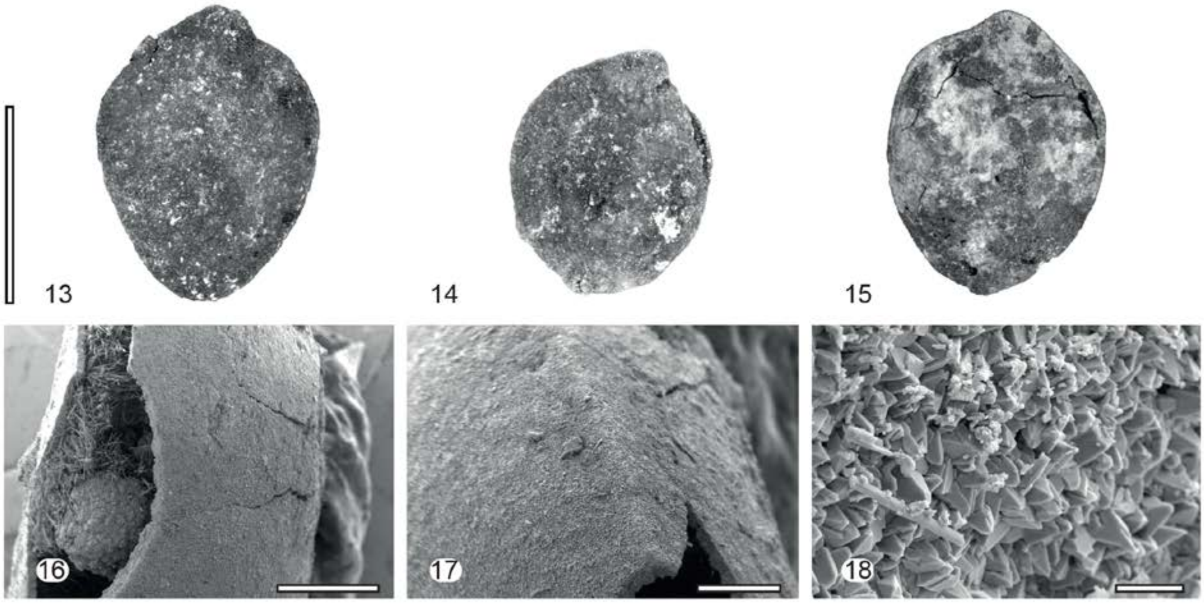
13
14
15
16
17
18

V.3. Discussion

V.3.1. Review of the *Iodes* fossil record

In the light of these new discoveries, we propose a review of *Iodes* fossil record (last summarized in Stull et al., 2016). The recognition of *Iodes* is based on three diagnostic characters: the ridges at the surface, papillae on the locule surface, and the presence of a vascular bundle inside the endocarp wall. Indeed, *Iodes* is the only genus in the family to have all three of these characters (Stull et al., 2011, Stull et al., 2016).

In North America, three species share these characters: *Iodes brownii* from Eocene localities in Wyoming, Utah, Oregon, and Colorado (Allen et al., 2015, Stull et al., 2016); *I. occidentalis* from the Eocene Bridger Formation of Wyoming (Allen et al., 2015) and *I. multireticulata* from the Eocene Clarno Formation of Oregon. *Iodes chandlerae*, from the Clarno Formation, does not have all necessary diagnostic characters to allow confident identification as *Iodes* (Stull et al., 2016); consistent with the previously cited publications, we regard this as a dubious generic identification. In addition, *Croomiocarpum missippiensis* from the early-middle Eocene Tallahatta Formation of Mississippi is very similar to *Iodes* in having a vascular bundle inside the endocarp wall and a reticulate pattern of endocarp ridges (Stull et al., 2011). It mainly differs by its thick wall (about 2 mm including ridges) and the absence of papillae, although the lack of papillae might be due to taphonomic degradation, as noted by Stull et al. (2011). The size of the endocarp wall (with ridges) is very uncommon in fossil species of *Iodes* but not aberrant: the wall thickness (including ridges) of *Iodes bilinica* reaches 1 mm (Stull et al., 2016) and 1.5 mm for *I. rivecourtensis* (Del Rio et al., 2018). In addition, we also found in modern *Iodes* species endocarp walls reaching 1 mm thick (*I. cirrhosa*, *I. balansae*, and *I. yatesii*, Tab.1). Thus, we consider it as a probable species of *Iodes* despite the lack of papillae (but also of cell preservation). The fossil genus *Iodicarpa* from the Clarno Formation (Manchester, 1994) is cited as close to, or potentially included with, *Iodes* (Allen et al., 2015, Stull et al., 2016), given that members of this fossil genus possess papillae and a vascular bundle embedded in the endocarp wall. Both diagnostic characters are only found together in *Iodes*. However, the size of the specimens (26–56 mm in length, 20–35 mm in width) and the ornamentation (or absence thereof) is unusual for the modern and fossil species of *Iodes*. Indeed, only two modern species (*I. balansae* and *I. yatesii*, Tab. 1) are as long as the species included in *Iodicarpa*. In addition, these two modern species are less than 17 mm in width. Among the current species, only *I. seguinii* has a smooth ornamentation but also a vascular bundle in a gutter and no papillae (Tab. 1). Thus, we do not have final argument to include or exclude these species in *Iodes*. Consistent with previous studies, we consider this genus as closely related to *Iodes* or included inside the clade but with extinct morphology (regarding its distinct ornamentation type, compared to described fossil and modern species of *Iodes*). An *Iodes* sp. was illustrated from the Chuckanut Formation of Washington (Pigg and Wher, 2002). However, the specimen seems to be an endocarp impression with no anatomical information available. We consider this occurrence as a dubious record of *Iodes*.

In Europe, *Iodes* is represented by 12 fossil species: *I. germanica* from Cretaceous of Eilseben and Paleocene of Gona (Germany; Knobloch and Mai, 1986, Mai, 1987), *I. multireticulata*, *I. eocenica*, *I. corniculata*, *I. hordwellensis*, and *I. acutiformis* from various sites of the well-known Eocene London Clay Formation (Reid and Chandler, 1933, Stull et al., 2016) *I. bilinica* from the Eocene Messel Biota, the Eocene of Bohemia, and from the London Clay Formation (Chandler, 1925, Kvaček and Bůžek, 1995, Collinson, 2012). Finally *Iodes tubulifera*, *I. sinuosa*, *I. rivecourtensis*, *I. reidii* and *I. parva* from the Paleocene of Rivecourt site (Del Rio et al., 2018. Tab.1). Here, we add two new species, *I. rigida* and *I. acuta*, which appear closely related to species from the Paleogene of Europe, and particularly from the Paris Basin. These species add to our understanding of the historical diversity of *Iodes* in Europe, and help establish connections among European Paleogene floras.

Palaeohosiea possesses the three major diagnostic characters of *Iodes* with no significant other distinguishing features (Allen et al., 2015). Therefore, we consider all species of this genus as members of *Iodes* and include them in our comparisons: *P. marchiaca* and *P. suleticensis* from the Paleocene and Oligocene of Bohemia (Kvaček and Bůžek, 1995). In addition, *Hosiea pterojugata* from the Paleocene of Gona, Germany (Mai, 1987), also has all key diagnostic characters of *Iodes* genus, although the specimen descriptions are relatively minimal.

Chandler (1961) attributed another fossil from Southern England to *Iodes*, as *Iodes* sp., but we consider this placement equivocal. The specimen has papillae and a reticulate pattern of ridges. It is very small, about 4.5 mm in length, which is unknown for modern members of *Iodes* (see. Tab.1), but we have described other fossil examples of small *Iodes* (Del Rio et al., 2018). However, the specimen is a locule cast, indicating that the endocarp is at least slightly larger than 4.5 mm. The position of the vascular bundle is unknown as only a locule cast remains. Because the genus *Hosiea* also possesses reticulate ridges and papillate locule linings, we hesitate to attribute this fossil to *Iodes* given the unknown condition of the vascular bundle. *Iodes* sp. from the Dormaal formation possesses a reticulation pattern “obliterated by encrustation of sand” and papillae inside the locule (Fairon-Demaret and Smith, 2002). However, the specimens are very decayed; therefore, it is difficult to decide if this specimen belongs to *Iodes* genus or other similar genera, such as *Hosiea*.

An *Iodes* from the Miocene of Yunnan (China) has been mentioned (Stull Obs. Pers.) but not formally published. A second *Iodes* species from the Miocene of Turkey seems to have been studied but not published (Duperon, com. Pers.). Therefore, there are no published records of *Iodes* from areas other than North America and Europe.

In conclusion, the *Iodes* genus has an extensive fossil record, ranging from the Cretaceous to the Miocene, with notable abundance and diversity in the Northern Hemisphere during the Paleogene. The diversity of fossil remains from the European Eocene in particular is comparable to modern diversity, distributed across tropical Africa, Madagascar, and Asia.

V.3.2 Biogeographic implication of new species

The present-day distribution of Icacinaceae is almost exclusively tropical. The presence of Icacinaceae in Le Quesnoy site and more broadly in the Eocene sites of Europe suggests a favourable paleoenvironnement for a megathermal flora. This hypothesis is corroborated for the Le Quesnoy site by the presence of Menispermaceae, a family that is also predominately tropical (with a few exceptions; Kessler, 1993). The extant genus *Iodes* comprises lianas distributed in South Asia, Africa, and Madagascar (De La Bâthie, 1952, Sleumer, 1971, Villiers, 1973). Two species of *Iodes* described here (*I. rigida* and *I. acuta*) have an apical hole, which is characteristic of the extant African species (Del Rio et al., 2018). However, the ridges of *I. rigida* are more similar to some modern Asian rather than African species in having a median channel and a rectangular shape (e.g. *Iodes ovalis*, *I. scandens*, *I. yatesii* and *I. balansae*, Fig. V.2, 1-4). Two modern species from Africa, *I. kamerounensis* and *I. seretii*, have clear channels on the ridges but not the characteristic rectangular shape (Fig. V.2, 5-6). Moreover, a third species possesses a pair of horn-like protrusions (*I. parva*), a character found only in Asian species. However, the reticulation pattern of this species is close to modern African species (Del Rio et al., 2018). Collectively, the species from Le Quesnoy show characters found today in both Africa and Asia, which may indicate that these areas represent refugia for lineages that originally diversified in the Northern Hemipshere (Wolfe, 1975).

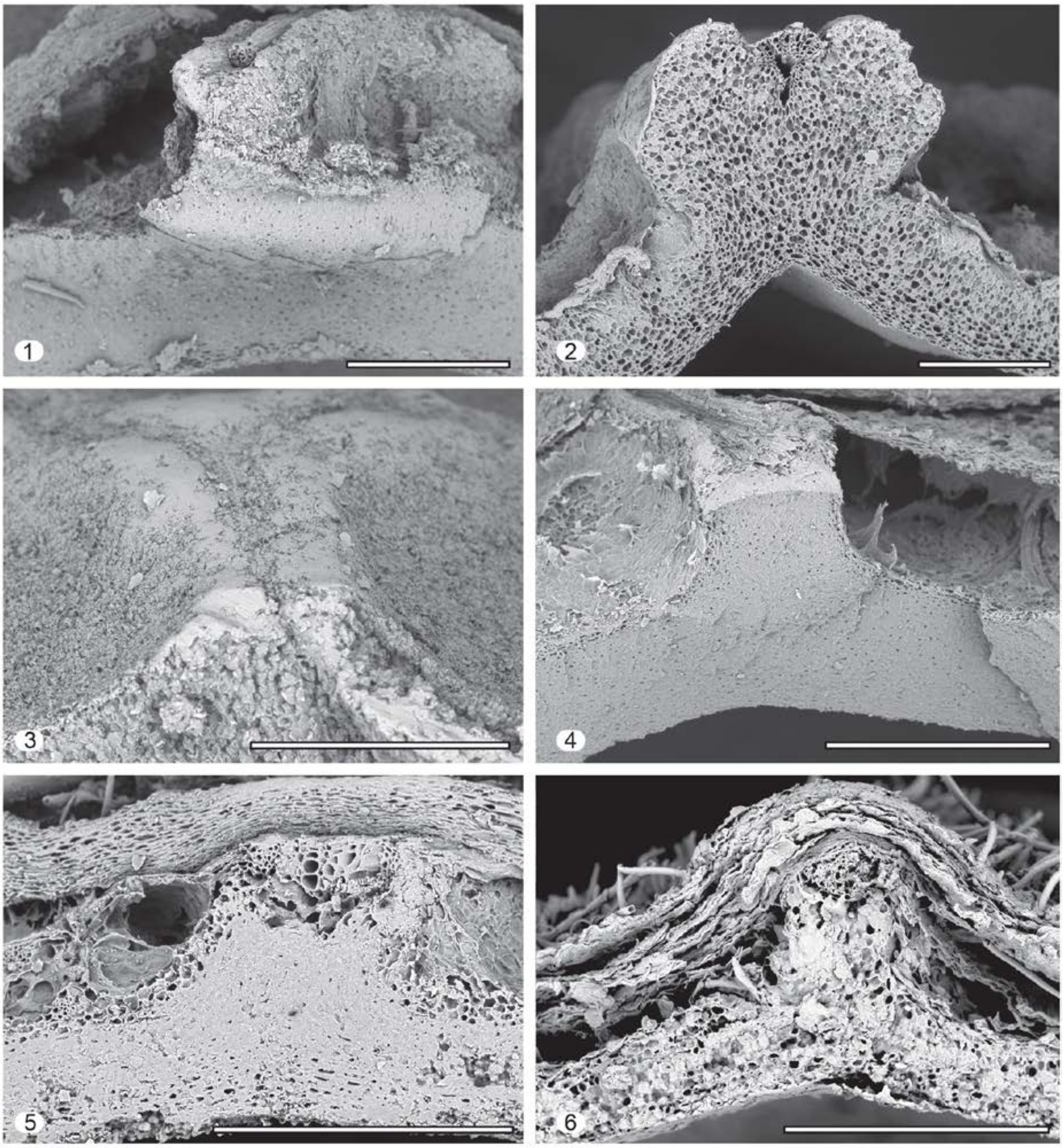

Figure. V.2. Shape of ridges of modern *Iodes* species (1) *Iodes balansae*, (2) *Iodes yatesii*, (3) *Iodes scandens*, (4) *Iodes ovalis*, (5) *Iodes seretii*, (6) *Iodes kamerounensis*. Scale bars: 500 μm.

Conclusion of the Chapter

The two news species of Icacinaceae described here increase the diversity of the family known from Eocene European sites; these species, like most of the fossil diversity known from Europe, appear to have affinities with modern floras of tropical Asia and Africa. All described specimens from Le Quesnoy are suggestive of a megathermal flora with close connections to other sites from the Paleocene of France and the Eocene of Europe more broadly. This study demonstrates the significance of the Le Quesnoy fossil assemblage for systematic, paleoecology, and paleobiogeographic research. In particular, the exceptional anatomical preservation allows detailed comparisons of the Le Quesnoy material with fossils from other European floras as well as with extant species. Others studies on this remarkable site, centered on other groups, are necessary to more fully understand the affinities of Le Quesnoy with other modern and paleofloras

Acknowledgements

The fossils were collected during fieldwork by the “amber team” of MNHN, with the help of Lafarge-Granulats Cie, and we thank the Langlois-Meurinne family for giving the authorization to work on their property. This work was supported by a grant from Agence Nationale de la Recherche under the LabEx ANR-10-LABX-0003-BCDiv, in the program “Investissements d’avenir” n_ ANR-11-IDEX-0004-02 and by the CR2P (UMR 7207).

Chapter VI

First record of an Icacinaceae Miers fossil flower from Le Quesnoy (Ypresian, France) amber

Among the diverse organisms or parts of organisms embedded in amber, angiosperm flowers are exceedingly. Only ca. 70 flowers or inflorescences have been described to date, mostly from Cretaceous (Cruickshank & Ko, 2003) Burmese amber (Poinar Jr, 2004, Poinar Jr & Chambers, 2005, Poinar Jr et al., 2007), Miocene (Iturralde-Vincent & MacPhee, 1996) Dominican amber (Poinar Jr, 1991, Poinar, 2002a, Poinar, 2002b, Poinar Jr & Judziewicz, 2005, Poinar Jr et al., 2008, Chambers et al., 2011a, 2011b, 2012b, Poinar & Columbus, 2013, Poinar Jr & Steeves, 2013, Chambers & Poinar Jr, 2014), late Oligocene-early Miocene Mexican amber (Castañeda-Posadas & Cevallos-Ferriz, 2007, Calvillo-Canadell et al., 2010, Chambers et al., 2012a), and Paleogene Baltic amber (Göppert et al., 1886, Weitschat & Wichard, 1998).

In addition, we are noticing phylogenetic disparities. The rosid clade accounts for 39% of eudicot diversity but 44% of flowers embedded in amber. In contrast, the asterid clade, which represents half of the eudicot diversity (Magallon et al., 1999), is represented in the fossil record by only 12 flowers (17%) in amber. Among these flowers, ca. 50% belong to Ericales and Cornales. Whilst five flowers belong to campanulids, only one represents the lamiid clade (in the order Gentianales), which corresponds to 26 % of the extant eudicot diversity. Nevertheless, fossil flowers embedded in amber are generally important to understand evolutionary processes and past diversity because they are often exceptionally well preserved and provide insights into the morphology of fragile structures that are not normally preserved (Poinar & Poinar, 1999).

The locality at Le Quesnoy (Houdancourt, Oise, France) was first studied in 1999 (Nel et al., 1999). This outcrop is correlated to the basal Eocene (Ypresian). This first survey highlighted the abundance of insects and the presence of at least one flower of caesalpinioid legume in amber. The pollen included in the amber was studied using a new technique of extraction (De Franceschi et al., 2000, Dejax et al., 2001), but the diversity of the floral remains had to be studied extensively.

Here we study one flower from Le Quesnoy and assign it to the lamiid clade. This flower named *Icacinanthium tainiaphorum* sp. nov. is the first known fossil occurrence of a flower from order Icacinales. The presence of this flower embedded in the resin of a tree might suggest that this species could have been a climber. This type of ecology is frequent in megathermal flora, which has developed in Europe during the Eocene global warming. This Icacinaceae flower in amber attests to the presence of an undocumented past diversity.

This study was published in Scientific reports: **Del Rio, C., Haevermans, T., & De Franceschi, D. (2017). First record of an Icacinaceae Miers fossil flower from Le Quesnoy (Ypresian, France) amber. Scientific reports, 7(1), 11099.** (Appendix 6).

VI.1. Material and Method

VI.1.1. Locality and fossil material

The fossil resin remains were collected from 1997 to 2000 from the Le Quesnoy (Houdancourt, Oise, France) lignitic clay sediments which belong to the « argiles à lignites du Soissonais » Formation. These sediments are dated to the Ypresian (± 56 Ma) according to mammal biochronology (MP7) and palynological studies (Nel et al., 1999, Cavagnetto, 2000). This corresponds to the Sparnacian facies of the lower Ypresian (lower Eocene). Several fossil resin samples contain diverse organisms, principally arthropods (mainly insects), a few plant remains, mainly represented by pollen grains (Cavagnetto, 2000, De Franceschi et al., 2000) but also a few flowers still to be studied. The fossils are kept in the collections of the Paris Muséum national d'Histoire naturelle (MNHN). The specimen studied here is a flower embedded in this fossil resin here called amber, but produced by Detarioidae trees (Leguminosae) (De Franceschi & De Ploëg, 2003, Jossang et al., 2008).

VI.1.2. Phylogenetic reconstructions

Preliminary exploratory herbarium studies (P) focusing on small pentamerous hypogynous flower with petals fused at the base and with stamens free from the petals lead to comparison of the flower in amber to those of the family Icacinaceae. We employed the most complete molecular data for the asterid clade focusing on the Icacinaceae (Stull et al., 2015). These data were composed of 73 protein-coding genes for a total of 59132 bp. We retained 51 species among the 112 accessions available (Stull et al., 2015) of which 23 species represent 21 genera of Icacinaceae. We included at least two species from other asterid orders, except for Metteniusales where we used nine species as this order includes species, which were formerly included in genera of Icacinaceae, which are morphologically close to Icacinaceae sensu stricto. All molecular characters are coded as missing for the flower in amber. In addition, we included 22 morphological floral characters corresponding to features potentially observable in the fossil flower (Appendix 7). The final matrix contains 59135 characters.

Bayesian analyses were performed using MrBayes (Ronquist et al., 2012) with a format type mixed with two partition: DNA type (with model by default, GTR+ I + G) and Standard type (equal state frequencies with all topologies equally likely a priori with unconstrained branch lengths) for morphological data. Two independent but parallel analyses were performed using flat priors, starting from random trees and consisting of four chains each. The analysis was run for 5 million generations, sampling every 1000 generations and with 20% burn-in. Analysis of output parameter using Tracer v.1.6 (Rambaut et al., 2014) confirms the convergence of chains. A 50% majority-rule consensus tree was computed with posterior probability (PP) estimates for all nodes. We generally consider as non-supported nodes those with less than 0.95 PP.

VI.1.3. Morphological studies

A morphology matrix was made using Xper 3(Ung et al., 2010) containing 22 flower and pollen characters coded for 51 taxa including the Le Quesnoy flower (Appendix 7).

The matrix was constructed from direct morphological observation of herbarium specimens (P, see Appendix 8) and from bibliographic data for flowers (Howard, 1942, De La Bâthie, 1952, Villiers, 1973, Bridson, 1975, Dahling, 1978, Ohwi, 1984, Davenport, 1988, Morat & Veillon, 1988, Peng & Howard, 2008, Gonzalez & Rudall, 2010, Santiago-Valentín & Viruet-Oquendo, 2013, Endress & Rapini, 2014) and pollen (Erdtman, 1952, Lobreau Callen, 1972, 1973, Lobreau-Callen, 1975, Dickison, 1986, Gosling et al., 2013). We observed the flower embedded in amber using a light microscope (Nikon Eclipse80i). Numerous pollen grains were found around the flower and between hairs on the adaxial surface of the petals (Fig. VI.1 DF); the vicinity and abundance of grains of the same type indicate that they probably belong to the flower. The pollen was also extracted from the amber in order to obtain a better understanding of its type (Fig. VI.2) following a previously published protocol (De Franceschi et al., 2000) and observed using the same microscope. Before extraction, we only observe the imprint left by the pollen in amber. After extraction, we show an exceptional preservation of grains with well-preserved exine wall and remains of cellular content. A darker zone could correspond to the rest of the nucleus (clearly visible on Fig. VI.1 D). Due to the presence of echinae (spines), pollen grains could not be fully separated from resin and were observed still embedded inside a small resin block. All these features were mapped into the phylogeny using Mesquite software (Maddison and Maddison, 2001) with a parsimony ancestral state reconstruction.

We conducted a qualitative study of adaxial petal hairs of *Metteniusa*, *Poraqueiba*, *Nothapodytes*, *Mappia*, *Icacina*, *Leretia*, *Mappianthus*, *Desmostachys* and *Natsiatum* using SEM (Scanning Electron Microscopy) with a Jeol JCM6000 after the specimens were coated with gold-palladium.

VI.2. Results

VI.2.1. Systematics

Order	Icacinales Tiegh.
Family	Icacinaceae Miers
Genus	*Icacinanthium* Del Rio & De Franceschi, gen. nov.
Type species	*Icacinanthium tainiaphorum* Del Rio & De Franceschi sp. nov.

Generic diagnosis: flower small, actinomorphic, hypogynous and pentamerous. Calyx cupular, Petals lanceolate curved backwards, with a straight apex, fused at base in a short cup, tomentose on adaxial surface with long, simple flattened hairs with granular ornamentation, glabrous on abaxial surface. Stamens alternate to petals, free. Pollen small, triaperturate and echinate.

Etymology: "*Icacinanthium*" refers to its appartenance to the family Icacinaceae.

Icacinanthium tainiaphorum Del Rio & De Franceschi, sp. nov. (Fig. VI.1 &2)

Holotype: Deposited in the collection of Palaeobotany of MNHN (field number PA4966)

Type Locality: Le Quesnoy, Oise, France

Stratigraphic age: Ypresian

Etymology: "*tainiaphorum*" refers to the flat "ribbon-like" hairs on the petals.

Specific diagnosis: As for the genus

Description: A single flower embedded in fossil resin, almost completely preserved. Flower particularly small, about 2.5 mm in diameter, at least unisexual male or hermaphrodite, actinomorphic pentamerous and hypogynous (Fig. VI.1 AB).

The calyx is cupulate, filmy and very short. It is composed of 5 minute sepals, which are very difficult to distinguish. Scattered single-celled hairs are visible at the margin. Aestivation of the corolla is probably valvate according to the shape and position of the petals, which are fused at the base in a short cup. The petals are lanceolate, curved backwards in apical view (Fig. VI.1 A; Fig. VI.2) and with a straight apex (Fig. VI.1 C), about 1.40 mm long and 0.7 mm broad. They are tomentose on the adaxial surface with long, simple flattened hairs with granular ornamentation, about 0.7 mm long and 0.025—0.036 mm broad; The stamens alternate with the petals and are erect but anthers were not preserved; Filaments are glabrous, about 0.15 mm in diameter, free from the petals and attached below the base of gynoecium. The globular gynoecium is free, possibly unilocular considering its shape, and glabrous. The ovary seems to be poorly developed or very small. The stigma is unknown, not preserved or not developed.

The pollen is very small (about 20-25 µm in diameter), clearly echinate (Fig. VI.1 D) and triporate (Fig. VI.1 EF). No colpus could be observed, but we cannot completely exclude the presence of faintly marked small colpi.

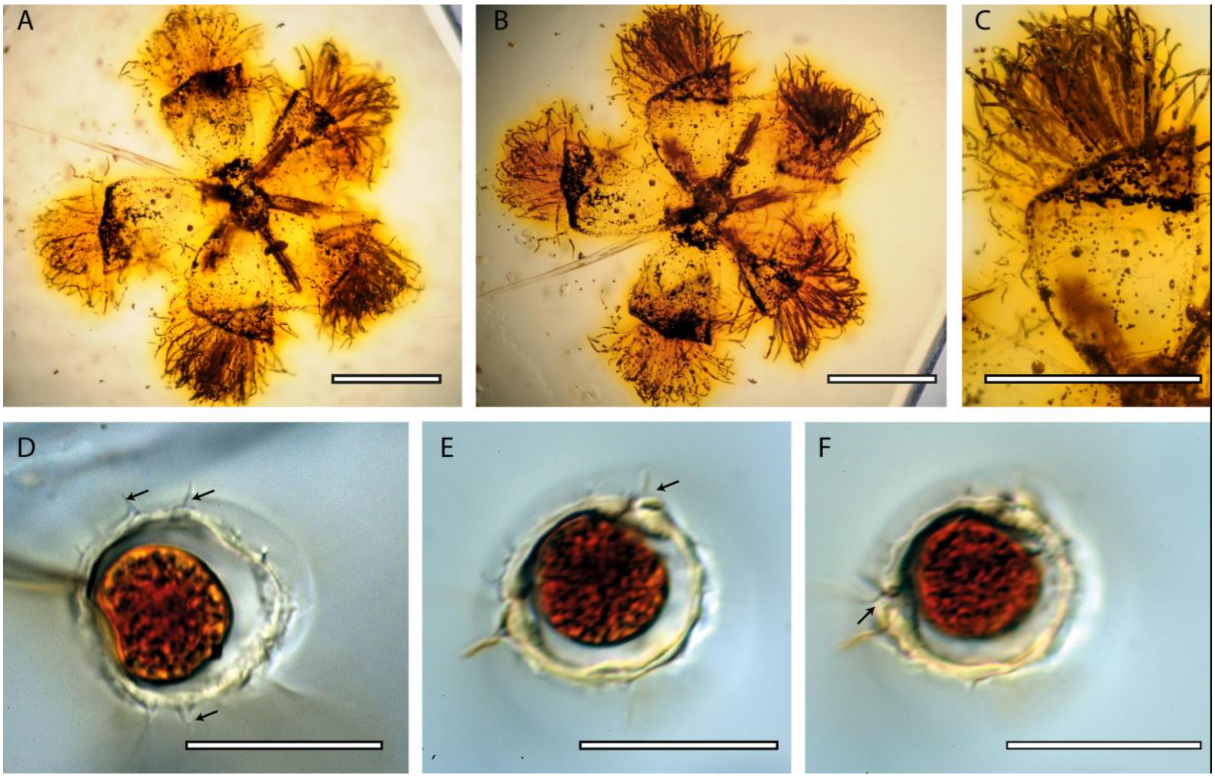

Figure VI.1: *Icacinanthium tainiaphorum* holotype, (A) flower in apical view with petals curved backwards, (B) same flower in basal view, (C) detail of petals in basal view (D) pollen grain showing echinate ornamentation (arrows) (E & F) other pollen grain showing pores (arrows). Scale: A-C = 1mm, D-F = 20 µm.

VI.2.2. Phylogenetic analysis

The Bayesian analysis 50% majority-rule consensus tree is given in Figure VI.3 (and appendix 9). As expected, we found a topology similar to the previous phylogenetic study using the same DNA data for the species included here (Stull et al., 2015). This fossil, when included in the analyses, is placed close to *Natsiatum*. However, the node with *Icacinanthium* and *Natsiatum* have very low support (PPB < 0.95). In this sense, the position of *Icacinanthium* is considered as unresolved at the base of the group IV sensu Stull et al. (2015).

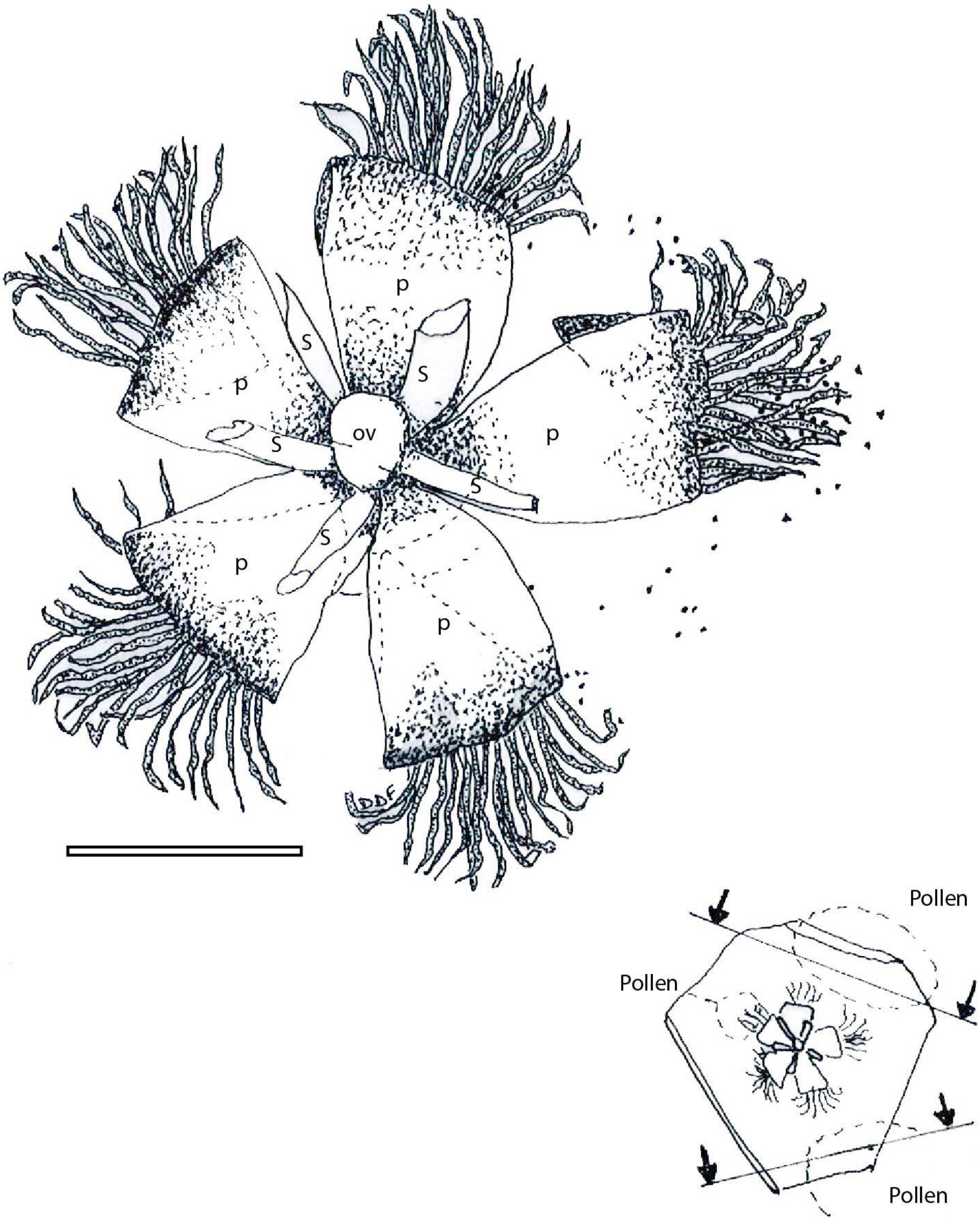

Figure VI.2: Drawing of *Icacinanthium tainiaphorum* gen. et sp. nov. in apical view ; (ov) ovary; (s) stamens; (p) petals. Arrows and lines: position of section for pollen preparation. Scale bar = 1 mm.

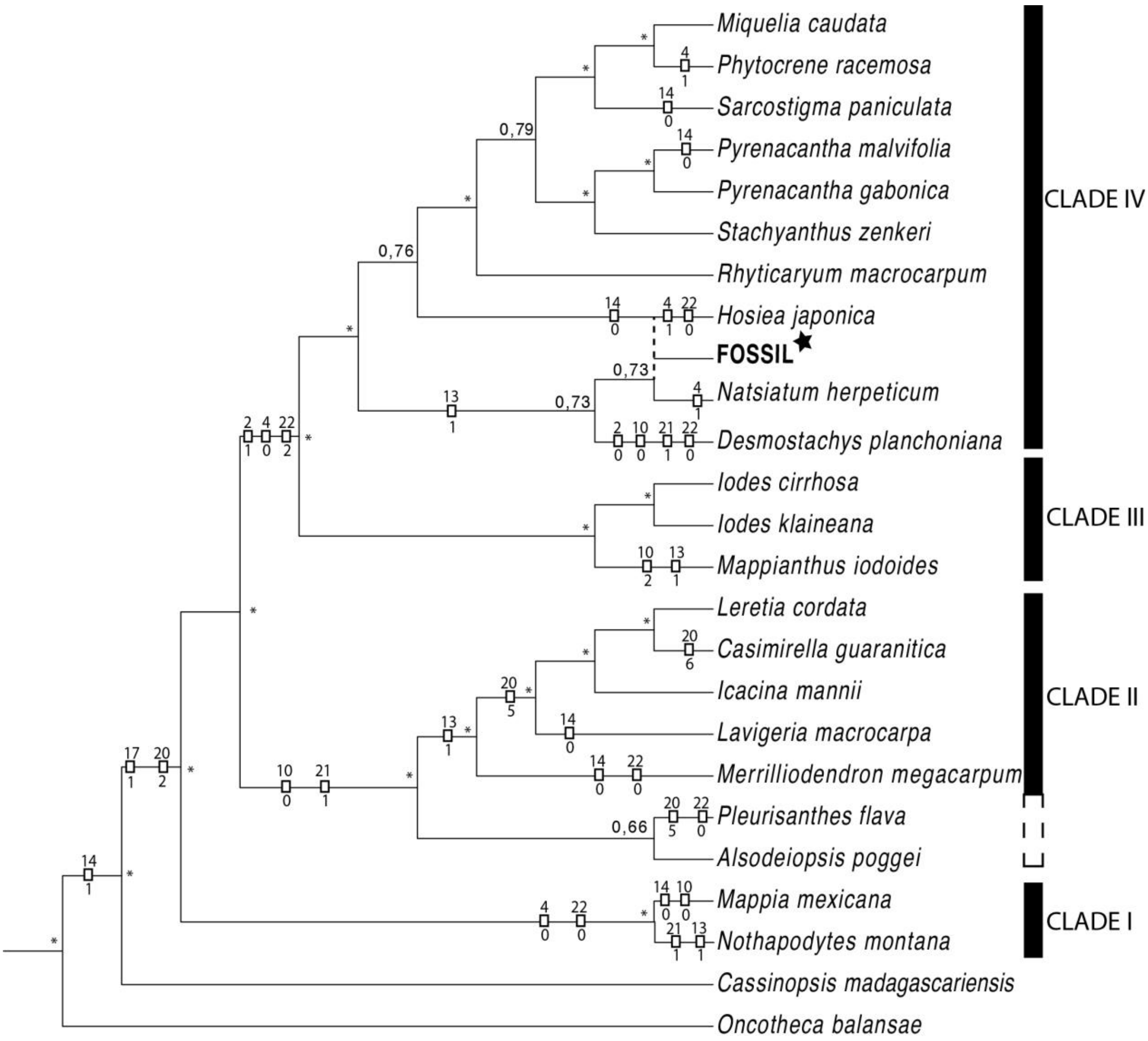

Figure VI.3: Phylogenetic relationships among asterids species focused on the family Icacinaceae based on the combined 73-plastidial genes and 22 morphological characters. The 50% majority-rule consensus tree was constructed by Bayesian inference in MrBayes. Star indicates the placement of the fossil flower close to *Natsiatum*. Dotted lines indicate another possible position for the fossil, close to *Hosiea*. Mesquite orientation of pertinent characters is shown. (*) represent strong node (>95% PP).

One hundred and ninety five steps are necessary for the reconstruction of the history based on morphological characters by Mesquite's parsimony state reconstruction (0.34 CI and 0.47 RI). The position of *Icacinanthium* close to *Natsiatum* or *Hosiea* is supported by the same number of steps. This explains why only the nodes of the clades containing *Natsiatum* and *Hosiea* are over 0.95 PP. Of the 22 morphological characters, only the stamen position [16] and the symmetry of the flower [1] are non-informative (Fig. VI.3; Appendix 7). For the fossil flower, the main informative characters are the calyx shape [4], the petal and stamen fusion [10; 17] and all pollen characters [20; 21; 22]. Positioning uncertainties correspond to both characters for presence or absence of hair adaxially and abaxially on petals [13; 14].

VI.3. Discussion

Only the presence of hairs on the outside of the petals seems to be synapomorphic for the Icacinaceae group (Fig. VI.3) according to our phylogenetic reconstruction. While *Icacinanthium* did not have hairs outside the petals, this state is also absent in four genera and some species of other genera within Icacinaceae, indicating a convergent loss of these hairs.

According to our ancestral state reconstruction, the Icacinaceae clade (excl. *Cassinopsis*) possesses small bisexual, pentamerous flowers with petal apex adaxially curved, stamen free from petals (this last state shared by all modern genera of Icacinaceae s.s, sensu Stull et al., 2015) and echinate pollen. Only the shape of the petal apex does not match with this fossil flower; however, this feature can also occurs in five genera and several species which also possess comparable straight apices.

The clade including both III and IV possesses unisexual flowers (except for *Desmostachys)*, cupular calyx, petals fused at base and small and mainly porate pollen grains (synapomorphic). Moreover, petal apex orientation of Clade IV is unresolved with a preponderance of genera with straight apices, which would be a synapomorphic character for this clade, emphasizing affinities of *I. tainiaphorum* to this clade. We therefore hypothesize that this flower is a unisexual male flower, which would explain the poorly developed ovary and make a better fit with the phylogenetic position of the fossil (rather than a poor preservation of this organ during fossilisation).

Adaxial hairs of *Emmotum nitens* (Endress & Rapini, 2014) and *Poraqueiba sericea* have an irregularly moniliform shape, and thus clearly differ from the hairs seen in other species. In fact, all adaxial hairs of Icacinaceae s.s. considered here and *Metteniusa* petals are flattened and very simple, as what is found in *Icacinanthium* (Fig. VI.4). Icacinaceae hairs however are granular, more or less longitudinally extended while in *Metteniusa* we observe nodules surrounded by longitudinal furrows (Fig. VI.4 F), very different from the Icacinaceae ornamentation. These observations corroborate the position of *I. tainiaphorum* within the family Icacinaceae. In this family, the external hairs are generally quite similar, with a tubular form, acute at the apex and with granular ornamentation (Fig. VI.4 E). The presence of these hairs seems to be homologous and synapomorphic within Icacinaceae.

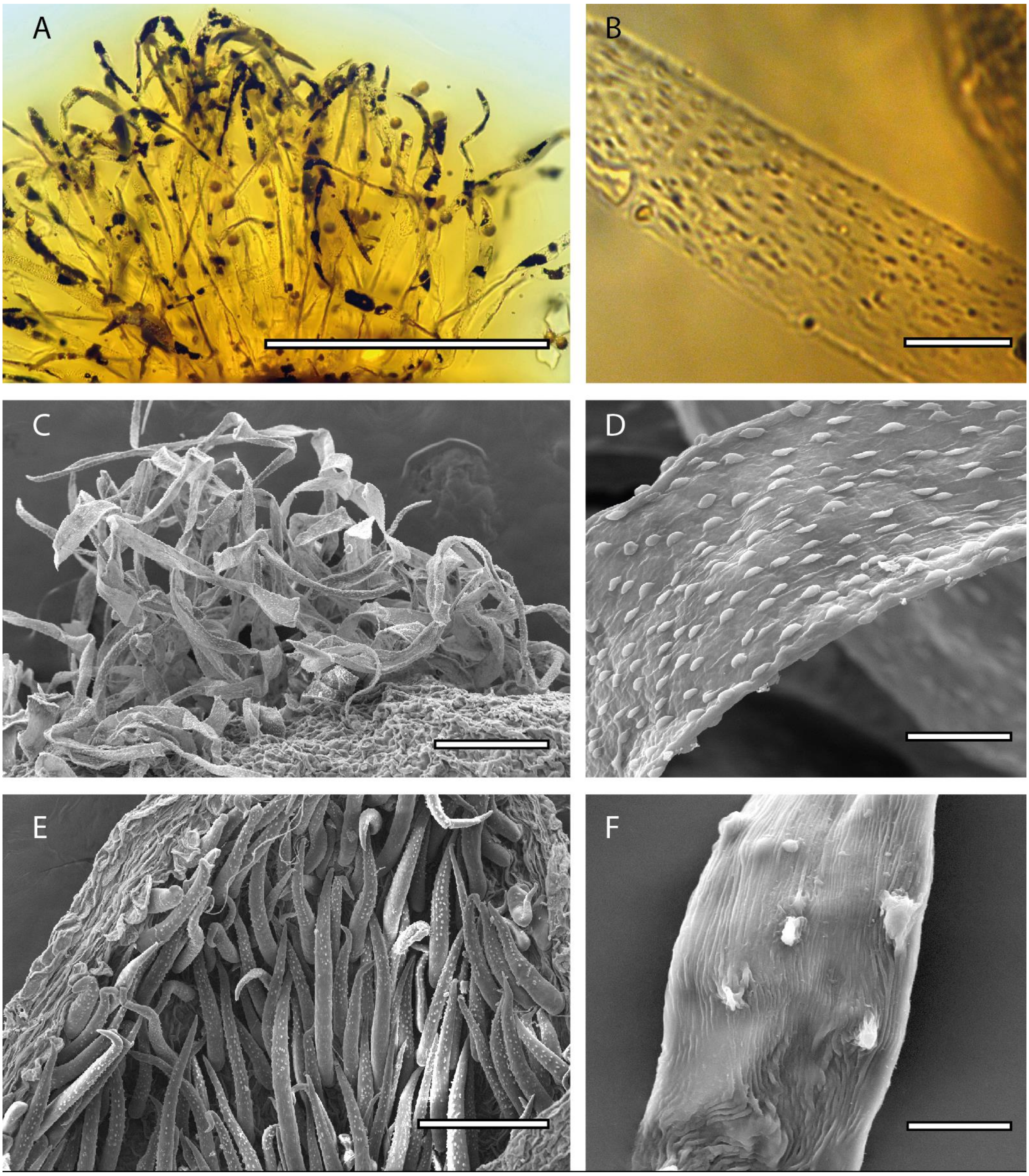

Figure VI.4: Morphological form of hairs on petals. (A) “simple” adaxial hairs from *Icacinanthium tainiaphorum*, note the presence of pollen grains between hairs (B) same, detail of ornamentation on hair surface (C) “simple” adaxial hairs from *Icacina mannii* Oliv.; (D) same, detail of ornamentation (E) tubular and acute abaxial petal hairs from *Icacina mannii*. (F) detail of ornamentation for *Metteniusa tessmaniana* Scale: A= 500 µm C & E = 100 µm; B, D & F = 20 µm.

In any case, this fossil shows a combination of characters unknown in extant Icacinaceae. Indeed, flowers of *Natsiatum herpeticum*, which have adaxial petal hairs, also have them abaxially.

In contrast, *Hosiea japonica* flowers are glabrous, and there are also flowers with adaxially hairy petals, but not adaxially in four genera of clade IV. To our knowledge, only the flower of *Merrilliodendron megacarpum*, from clade II, has adaxial petal hairs only such as what we found in our fossil flower. In clade IV this character state is unknown and new, hence our proposal to describe it as an extinct genus.

The fossil record of Icacinaceae, predominantly from the Eocene of North America and Europe, is extensive. However, no flower preserved in amber, as an imprint, lignitic or coalified were until now attributed to this family. In fact, most of these fossils consists in endocarps, in particular from modern genera *Iodes* (Reid & Chandler, 1933, Knobloch & Mai, 1986, Manchester, 1994), *Phytocrene* (Collinson et al., 2012, Stull et al., 2012) and *Pyrenacantha* (Manchester, 1994, Stull et al., 2012). Endocarp fossils of *Natsiatum* were described from the Middle Eocene of Tennessee (*Natsiatum wilcoxiana* (Berry) Stull, Moore & Manchester (Stull et al., 2011). In Europe, fossils of *Palaeohosiea,* supposed to be close to the extant genus *Hosiea*, were described (Kvaček & Bůžek, 1995). However, no character supports affinity with *Hosiea* and no feature separate the fossils from the extant genus *Iodes* (Stull et al., 2016). The presence of Icacinaceae from Le Quesnoy was only mentioned briefly and was based on what appears to be a lignitic endocarp (Nel et al., 1999), but was attributed to the genus *Iodes* (personal observation). The link between these two types of fossils is questionable, indicating an unsuspected diversity for Eocene Icacinaceae.

Extant Icacinaceae growth habits include lianas, shrubs or trees, distributed in tropical forests around the word. *Icacinanthium* is close to *Natsiatum* or *Hosiea,* both of which being Asian genera of climbing shrubs (Peng & Howard, 2008). *Icacinanthium* could testify for an Asian affinity of the Le Quesnoy Ypresian flora, as highlighted by studies on Menispermaceae (Jacques & De Franceschi, 2005) and other comparable European sites (Reid & Chandler, 1933, Cleal et al., 2001, Collinson et al., 2012). We thus hypothesize that *Icacinanthium* could be a climbing shrub, this type of ecology being frequent for megathermal flora that would have occurred in Europe during the early Eocene global warming phase (Zachos et al., 2001, 2006).

Conclusion of the chapter

This flower in amber have a combination of characters unknown in the present diversity, which argument a new genus, *Icacinanthium.* The morphological analysis of this flower and with modern species place the flower at the base of the Clade IV. This clade is mainly composed of climber now and thus we can hypothesizes that *Icacinanthium tainiaphorum* had a climb habitus. This flower is not related to the Icacinaceae endocarp found in the same site and demonstrate a greater diversity for the family during the early Eocene.

Acknowledgements

The fossil was collected during fieldwork of the “amber team” of MNHN, with the help of Lafarge-Granulat, andwe thank the Langlois-Meurinne family for giving authorization to work on their property. We thank the staff of the Paris Herbarium (MNHN P) for the loan of modern flower samples and access to herbarium sheets. We also thank Valentin Seizille de Mazancourt for the help in naming the species. We thank Martin Pickford and Steven Manchester for improving the English. This work was supported by a grant from Agence Nationale de la Recherche under the LabEx ANR-10-LABX-0003-BCDiv, in the program “Investissements d’avenir” ANR-11- IDEX-0004-02 and by the CR2P.

Author Contributions

C.D.R. and D.D.F. performed the morphological and phylogenetic analysis; C.D.R. and D.D.F. prepared the figures, D.D.F. drew Fig. VI.2; D.D.F. and T.H. designed the program; C.D.R. and D.D.F. prepared the manuscript.

Chapter VII

Review of the Icacinaceae from the Paris Basin: new remains from three Early Eocene sites

Icacinaceae Miers is a group of trees, shrubs, and climbers with a pantropical distribution. This family have an important fossil record, mainly in North America (Manchester, 1994, Pigg et al., 2008, Rankin et al., 2008, Stull et al., 2011, 2012, Allen et al., 2015) and in Europe (Reid & Chandler, 1933, Fairon-Demaret & Smith, 2002, Collinson et al., 2012) for the Paleogene.

Within the Paris Basin, some sites through the Paleogene give a view of the ancient flora via fruit, seed, pollen and flower remains. Two major sites have been partially studied, Rivecourt from the Thanetian (Smith et al., 2014, Del Rio et al., 2018) and Le Quesnoy site from the Ypresian (Nel et al., 1999, De Franceschi et al., 2000, De Franceschi & De Ploëg, 2003, Jacques & De Franceschi, 2005, Del Rio et al., 2017, Del Rio et al., submitted) mainly for the Icacinaceae group. Indeed, these two sites show a great diversity of Icacinaceae species, especially with *Iodes* endocarp remains and a flower in amber. This flower belongs to an extinct genus at the base of the clade IV sensu Stull et al. (2015). A preliminary study shows that Icacinaceae were also present in three other Paris Basin sites: Passy (MP8), Grès de Belleu (MP10) and Prémontré (MP10). These remains, younger than Le Quesnoy site, could bring a new light on the diversity of the Icacinaceae family during the Ypresian age. Moreover, recent advances in modern Icacinaceae phylogeny (Stull et al., 2015) can help to confirm our taxonomic assignation and the phylogenetic diversity inferred for the Icacinaceae during the Paleogene in France.

Therefore, our aim in this chapter is (1) to describe the Icacinaceae remains from the three localities, (2) to discuss the phylogenetic position and the diversity of Icacinaceae fossil records from the Paris Basin, (3) to propose a biogeographic insight and explore the changes that occurred for the Icacinaceae family throughout the Paleogene in this area.

VII.1. Material and method

VII.1.1. Geological settings

The Rivecourt outcrop consists in lignite beds, lignitic lacustrine marls and fluvial sands in the upper part of the Bracheux Formation (Smith et al., 2014). The age was estimated by carbon isotope data, palynology and vertebrate occurrences. The site reveals fossils of plants with abundant flowers, fruits, seed and wood remains. Among them, about 70 endocarps related to Icacinaceae family were studied (see Chapter III) as well as wood remains (see Chapter IV).

The Le Quesnoy site is part of the *argiles à lignite du Soisonnais* dated from the Early Ypresian (Nel et al., 1999). This site contains lignitic as well as amber remains. This site reveals vertebrate and plant fossils, especially endocarp remains. Especially, about 200 endocarps belong to the Icacinaceae family (see chapter V). In addition, an Icacinaceae flower in amber was published (Del Rio et al., 2017, see chapter VI).

The Passy outcrop consists in a sandy layer of three to four m called "sables d'Auteuil" resting on the "argiles plastiques" of the Sparnacian (early Ypresian) and covered by the "fausses glaises" (Ypresian). Passy is now part of the western side of Paris city, close to the Eiffel tower. In that area were found Ypersian amber and the first record of *Aulacoxylon sparnacense* Combes (1907, see De Franceschi & De Ploëg, 2003), as well as other fossils like *Cyrena cuneiformis*, *Melania inquinata*, *Melanopsis*, *Unio* and some conifer pyritized wood (Soyer, 1953) which helped to date the deposits. The "sables d'Auteuil" are then dated from middle Ypresian. The sandy layer was excavated during underground work for a building in 1999 and some sand bags were collected on the site, they were sieved and the remains sorted under a binocular microscope. The Icacinaceae fossil endocarps were discovered in that sediment.

Two fossils were collected from the Grès de Belleu (Belleu sandstone) site during the 19th century. The sediment in this site is composed of “*grain, assez grossier* (grain, quite coarse)” (Watelet, 1866) with quartz dominant (Koeniger, 1982). The Grès de Belleu was dated by Watelet (1866) as Suessonien (Ypresian) and now attributed to the Late Cuisian (Pomerol et al., 1984). This site has been studied mainly for the leaf imprints by Watelet (Watelet, 1866) and revised by Fritel (Fritel, 1908, 1924). An update of the flora diversity has been made (Furon & Soyer, 1947) and they kept only about forty species. A few fruits have been found and described (Watelet, 1866). They are mainly Fabaceae pods. Among numerous, more or less preserved, leaves and fruits, two fruits assigned to Icacinaceae were collected and kept in the MNHN collection (MNHN 8100. & MNHN 8061.).

The lower Eocene locality of Prémontré was discovered and described by Dégremont (Dégremont et al., 1985), “*à l’occasion des travaux exécutés dans l’enceinte de l’Hôpital psychiatrique de Prémontré* (during the work done on the premises of the Prémontré psychiatric Hospital)”and dated from the Cuisian. The fossils were collected in a layer of 4-5 m composed of ochreaceous weak sandstone with reddish bands due to oxidation. Prémontré (Aisne, France) outcrop provided diverse reptilian (Augé et al., 1997, Augé & Smith, 2002, Augé, 2003), mammalian (Godinot et al., 1992, Sudre & Erfurt, 1996, Escarguel, 1999, Smith, 2001) and Chondrichtyes fossils (Cappetta, 1992, Adnet & Cappetta, 2008), but also a diverse paleoflora with fruit and seed remains (Blanc-Louvel, 1985a, Blanc-Louvel, 1985b). Among them, faintly preserved, a moulding fruit was identified as part of the Icacinaceae family and described here.

VII.1.2. Method of fossil observation

All specimens were studied with the help of a binocular microscope (Wild M3Z) and imaged with a Leica DFC 420 camera (see. Chapter III and V for Rivecourt and LeQuesnoy site) Measures were taken using the ImagJ Software (Rasband, 2016).

Samples from Passy, Rivecourt and Le Quesnoy were coated with gold-palladium for examination by Scanning Electron Microscopy (SEM), using a Jeol JCM6000 instrument, facilitating observation of anatomical features, especially the endocarp wall layers and papillae.

VII.1.3. Phylogenetic reconstruction

VII.1.3.1. Sampling

We used the most complete molecular data published for the Icacinaceae family (Stull et al., 2015). These data contain 73 protein-coding genes for 59113 bp for 112 asterids species. Among them, we retained 28 species in which 23 of them represent 21 genera of Icacinaceae (two species were sampled for the *Iodes* and *Pyrenacantha* genera) and 5 species representing the outgroup (*Platea*, *Pittosporopsis*, *Emmotum*, *Apodytes* and *Oncotheca*). All molecular characters are coded as missing for all fossils. In addition, we included 31 morphological and anatomical fruit characters corresponding to features potentially observable in the fossil fruits (appendix 10) and developed from an Xper^3 database (Ung et al., 2010, see chapter II).

The morphological matrix was made via direct observations of the fruits and endocarps of species (appendix 11) except in the following cases: the fruit characters from *Mappia racemosa* (type species) were used with molecular data of *Mappia mexicana* and the fruit characters from *Nothapodytes nimmoniana* were used with molecular data of *Nothapodytes montana* (type species). In both cases, we only used the genera names in the tree. Morphological characters for *Casimirella guaranitica* and *Merrilliodendron megacarpum* were only obtained from literature (Sleumer, 1971, Howard, 1992). In addition, we added 9 fossil endocarps from the Paris Basin, with 8 *Iodes* species (including one species described in this chapter) and a *Paleophytocrene* (also described in this chapter). The final matrix contains 59 144 characters.

VII.1.3.2. Phylogenetic analysis

Two analyses were conducted. First, we conducted a maximum parsimony (MP) analysis implemented in the Paup 4.0 software. A heuristic research replicated 1000 times with a random addition of sequences in each repetition followed by a tree-bisection-reconnection (TBR) has been done. The strict consensus was compiled. The boostrap method was used in order to test the strength of nodes with a faststep research, replicated 10 000 times. Then, we made a Bayesian analysis using Mrbayes software (Ronquist et al., 2012) in CIPRES cluster V3.3 (Miller et al., 2010). The matrix format is mixed with two partitions: the DNA partition (with model by default GTR + I + G) and the standard partition using the MK model (Lewis, 2001, Nylander et al., 2004). Two independent and parallel runs were performed with 20 000 000 generations sampling every 1 000 generations and with 20% of burning, each with four chains. The outpout parameter was analysed by Tracer v.1.6 (Rambaut et al., 2014) and this analysis confirms the convergence of chains and adequate burning. A 50% majority-rule consensus tree was computed with posterior probability (PP) estimated for all nodes. Trees were visualised in Figtreev1.4 software (available at http://tree.bio.ed.ac.uk/software/figtree/).

All morphological features were mapped into the phylogeny using Mesquite software (Maddison and Maddison, 2001) and with the parsimony ancestral reconstruction option.

VII.2. Results

VII.2.1. Systematics

VII.2.1.1. Passy site

In this site, all endocarps presented here are bilateral, asymmetrical at the apex, with a reticulation pattern on the surface and a strong keel, which is characteristic of the Icacinaceae family. In addition, all species have a vascular bundle inside the endocarp wall and some of them show papillae on the surface of the locule. These characters allow us to consider these specimens as belonging to the *Iodes* genus. However, some differences lead us to describe a new species and record two new occurrences.

Family–Icacinaceae
Species –Iodes passiciensis Del Rio & De Franceschi sp. nov.
Fig. VII.1 A–I
Diagnosis. Endocarp bilaterally symmetrical, unilocular, elliptical, lenticular in transverse section; outer surface of the endocarp with a reticulate pattern of rounded and thin ridges with a channel on the median apical part, enclosing 25–29 polygonal areoles per face, with few or no free-ending ridgelets; a keel surrounds the fruit in the plane of symmetry with one part thicker containing a vascular bundle embedded in the endocarp wall. Endocarp possessing a symmetrical

and small pair of horn-like protrusions. Inner endocarp surface densely covered with regularly spaced and sessile rounded papillae. Length 6.68–7.20 mm, width 4.38–4.43 mm.

Etymology.	From the latin name of Passy where the fossil is provided, *Passicium*.
Holotype.	MNHN.F.44736.
Stratigraphy.	Early Eocene
Locality.	Passy (France)
Paratype.	MNHN.F.44739

Description. Endocarp bilaterally symmetrical, unilocular, elliptical, lenticular in transverse section; length 6.68–7.20 mm, width 4.38–4.43 mm, thickness 4.38 mm. Outer part of the endocarp with a reticulate pattern of rounded and thin ridges with a channel on the median apical part of its surface corresponding to the trace left by the outer vasculature at the boundary between endocarp and mesocarp; 4–5 irregular longitudinal ridges and some inter-ridges, enclosing 25–29 polygonal areoles per face with few or no freely ending ridgelets (Fig. VII.1 A, C); a keel surrounds the fruit in the plane of symmetry with one part thicker containing a vascular bundle embedded in the endocarp wall (Fig. VII.1 B). Endocarp possessing a symmetrical small pair of horn-like protrusions, positioned eccentrically and subapically on the apical endocarp (Fig. VII.1 F); endocarp wall 0.15–0.21 mm thick (excluding ridges, 0.34–0.44 mm thick including ridges, Fig. VII.1 G). Cell walls of the endocarp not preserved. Inner endocarp surface densely covered with regularly spaced and sessile rounded papillae, 0.011–0,019 (avg. 0.016 mm) in diameter (Fig. VII.1 H, I).

Remarks. This species is represented by only two lignitic endocarps.

Systematic affinity. *Iodes passiciensis* is unique in having 25–29 areoles with no freely ending ridgelets, small horn-like protrusions and rounded ridges. This species differs from *I. reidii* Del Rio, Thomas & De Franceschi in having a pattern of reticulation more developed and a smaller size (both not overlapping). *I. passiciensis* differs from *I. tubulifera* Del Rio, Thomas & De Franceschi in having rounded ridges and a smaller size. The horn-like protrusions are also more evident in *I. tubulifera* and protrude sub-apically whereas the horn-like protrusions are more a pore faintly apparent in this new species. This species is similar to *I. rivecourtensis* Del Rio, Thomas & De Franceschi in having rounded ridges, small horns and a reticulation pattern developed without free ending ridges. However, *I. passissiensis* is smaller, with more areoles, and with a smaller endocarp wall and ridges. This species differs from *I. sinuosa* Del Rio, Thomas & De Franceschi in having clear rounded ridges (despite the absence of cell wall preservation) and more developed reticulate pattern, but is close in other aspects. *I. parva* Del Rio, Thomas & De Franceschi is close to this species but with less areoles, horn-like protrusions that clearly protrude into the wall and is of smaller size. It also differs from *Iodes occidentalis* S.E. Allen, Stull & Manchester in having no free-ending ridges and horn-like protrusions. *I. multireticulata* Reid & Chandler has not horn-like protrusions and is bigger than *I. passiciensis*. *I. gemanica* Knobloch & Mai is slightly smaller (4–5 mm) than this new species and apparently has no horn-like protrusions. Among the species with horn-like protrusions, *Iodes bilinica* (Ettingshausen) Stull, Adams, Manchester & Collinson differs by the presence of frequent free-ending ridges. Length and width of *I. eocenica* Reid & Chandler are almost the double of those of *I. passiciensis* making it difficult to assimilate with it. *I. acutiformis* Chandler possesses acute apex not shown here, but seems to be very similar in other characters despite the most relaxed reticular pattern. *Iodes brownii* (Berry) Stull, Adams, Manchester & Collinson and *I. corniculata* Reid & Chandler show higher sizes, with close number of areoles. The channel on the median apical part of the ridges is also found in the species *I. rigida* Del Rio & De Franceschi from Le Quesnoy site. However, the ridge structures are different, *I. rigida* showing an I beam-like shape of ridges (rectangular). All these considerations allow us to describe a new species from these two specimens, close to *I. sinuosa* and *I.parva* described from the Rivecourt site.

Species - Iodes reidii Del Rio, Thomas & De Franceschi
Fig. VII.1 J–Q

Emended diagnosis. Endocarp elliptical with a reticular pattern of angular to rounded and thin ridges, delimiting 9–19 polygonal areoles per face, with few or no freely ending ridgelets. Endocarp possessing a symmetrical pair of horn-like protrusions, compressed on the keel, positioned eccentrically and subapically. Endocarp wall 0.25–0.34 mm thick (excluding ridges, 0.8–1.1 mm including ridges). Length of endocarp: 9.2–10.9 mm, width: 6.68–7.55 mm.

Stratigraphy. Late Paleocene
Additional stratigraphy. Early Eocene
Type locality. Rivecourt (Oise, France).
Additional locality. Passy (Oise, France)
Specimens. MNHN.F.44737.

Description (Passy specimen). Endocarp bilaterally symmetrical, unilocular, single-seeded, elliptical, laterally compressed in the plane of symmetry, lenticular in transverse section; length 10.9 mm, width 7.1 mm. Outer part of the endocarp with a reticulate pattern of angular to rounded and thin ridges with four longitudinal ridges and two inter-ridges, delimiting 19 polygonal areoles per face (Fig. VII.1 O), with few or no freely ending ridgelets (Fig. VII.1 J, L); a keel surrounding the endocarp in the plane of symmetry with one part thicker, containing a vascular bundle embedded in the endocarp wall (Fig. VII.1 K, Q). Presence of a symmetrical pair of horn-like protrusions compressed on the keel, positioned eccentrically and subapically on the apical endocarp faces, each with a central pit (Fig. VII.1 L); Endocarp wall 0.28-0.34 mm thick (excluding ridges, 0.83-1.1 mm including ridges, Fig. VII.1 P). Cells wall and inner endocarp surface decayed.

Systematic affinity. This unique specimen corresponds in almost all characters at the species *Iodes reidii* from the Rivecourt site. The ratio ridges thickness/wall thickness is characteristic to *I. reidii*: a small endocarp thickness with much higher ridges. The number of areoles found here is included to the variation of *I. reidii*, as for the size of the endocarp. Furthermore, the reticulation pattern and the shape of the horn-like protrusions are very similar. Unfortunately, the anatomical characters are not preserved; including papillae remains and cells preservations contrarily as it was observed in the Rivecourt specimens.

Species - Iodes tubulifera Del Rio, Thomas & De Franceschi
Fig. VII.2

Emended diagnosis. Endocarp elliptical with a reticulate pattern of sharp and thin ridges, delimiting at least 21 polygonal areoles per face, with few or no freely ending ridgelets. Endocarp possessing a symmetrical pair of horn-like protrusions prominent from the keel, positioned eccentrically and subapically. Endocarp wall about 0.2 mm thick (excluding ridges, about 0.3 mm including ridges). Inner endocarp surface densely covered with regularly spaced, minute and tubular papillae. Length of the endocarp 8.8–11.2 mm.

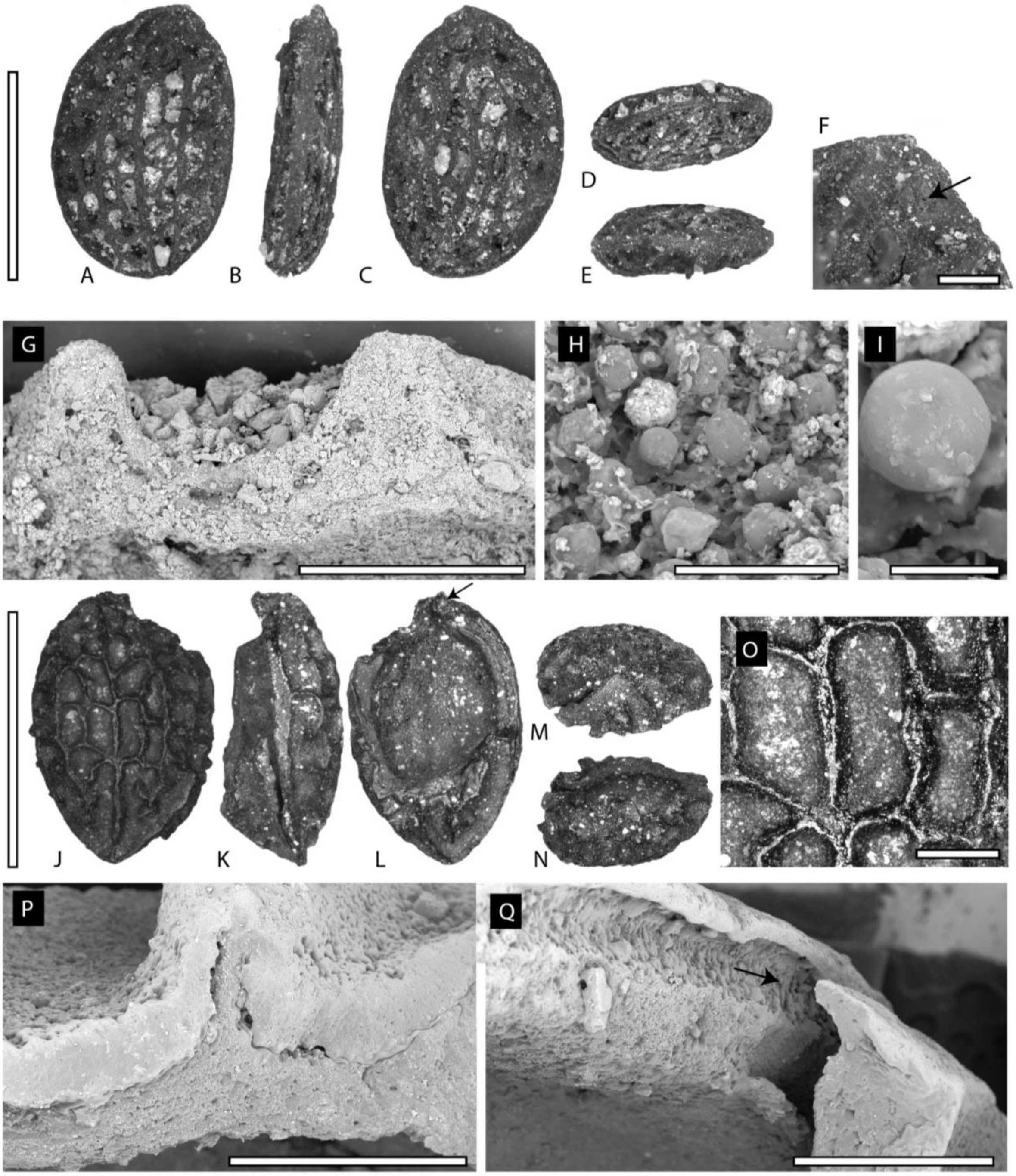

Figure VII.1. (A–I) *Iodes passiciensis* (MNHN.F.44736.), (A) lateral view of an endocarp showing the reticulum pattern of rounded and thin ridges, (B) dorsal view showing the keel, surrounding the endocarp, (C) lateral view of second face of the endocarp, (D) basal view, (E) apical view, (F) magnification showing the horn-like protrusions abraded, (G) SEM view of wall and ridges in transversal section, (H) SEM view of rounded papillae, (I) same with magnification. J–Q *Iodes reidii* (MNHN.F.44737.) (J) lateral view of endocarp showing the reticulum pattern of rounded ridges, (K) dorsal view showing the keel, surrounding the endocarp, (L) lateral view of second face of endocarp, (M) basal view, (N) apical view, (O) magnification showing the areoles from the reticulation of ridges, (P) SEM view of wall and ridges in transversal section, (Q) SEM view of the trace left by the vascular bundle embedded in the endocarp wall. Scale bar: A–E = 5 mm, O–Q = 1 mm, J–N = 10 mm, G = 500 μm, H = 50 μm I = 10 μm.

Stratigraphy. Late Paleocene

Additional stratigraphy. Early Eocene

Type locality. Rivecourt (Oise, France).

Additional locality. Passy (France)

Specimens. MNHN.F.44738.; MNHN.F.44740.

Description (Passy specimens). Endocarp bilaterally symmetrical, unilocular, single-seeded, elliptical, laterally compressed in the plane of symmetry; length 8.8-11.2 mm, width unknown (estimated about 6-7 mm), thickness 1.9 mm. Outer part of the endocarp with a reticulate pattern of sharp and thin ridges, with at least five irregular longitudinal ridges, delimiting at least 23 polygonal areoles per face with few or no freely ending ridgelets (Fig. VII.2 A,C); a keel surrounds the fruit in the plane of symmetry, with the thicker margin containing a vascular bundle embedded in the endocarp wall and the other part thin (Fig. VII.2 B). Endocarp possessing a symmetrical pair of horn-like protrusions prominent from the keel, positioned eccentrically and subapically on the apical endocarp faces, each with a central pit (Fig. VII.2 A, C, D); Endocarp wall 0.2-0.23 mm thick (excluding ridges, 0.3-0.33 mm including ridges, Fig. VII.2 G). Wall composed of four units of one or several successive cell rows, the outermost corresponds to an apical sclerotic row, cells difficult to distinguish, sometimes absent by erosion on the areoles, which show the isodiametric unistratified cell row, cells 0.034-0.053 mm diameter. The basal sclerotic row forming the major part of the endocarp wall thickness is composed of 6-8 sclerotized and periclinal cell rows 0.010-0.013 mm high, 0.030-0.041 mm wide. Inner endocarp surface densely covered with regularly spaced, minute and tubular papillae, which correspond to a cell expansion of the locule epiderma layer in one row of interdigitated cells; papillae diameter 0.018-0.020 mm, about 290 papillae per 0.25 mm^2 (Fig. VII.2 H, I).

Systematic affinity. These two specimens correspond in almost all characters to the *Iodes tubulifera* from Rivecourt site. In particular, the presence of characteristic tubular and sparse papillae is a strong argument for this affinity. Here, the density is about 290 papillae per 0.25 mm^2 whereas we have in *I. tubulifera* from Rivecourt 270 papillae per 0.25 mm^2. We think that differences of only 20 papillae per 0.25 mm^2 could be due to taphonomic process and/or the studied surface more or less plan. The sharp ridges and the size of the species comfort this assignation. In fact, the sharp ridges are very similar in shape and only slightly higher in the new specimens presented here. The endocarp wall is also very similar in all aspects. The size of the specimens presented here frames the value of the specimen from Rivecourt. Therefore, we have all the argument to attribute these specimens to *I. tubulifera*.

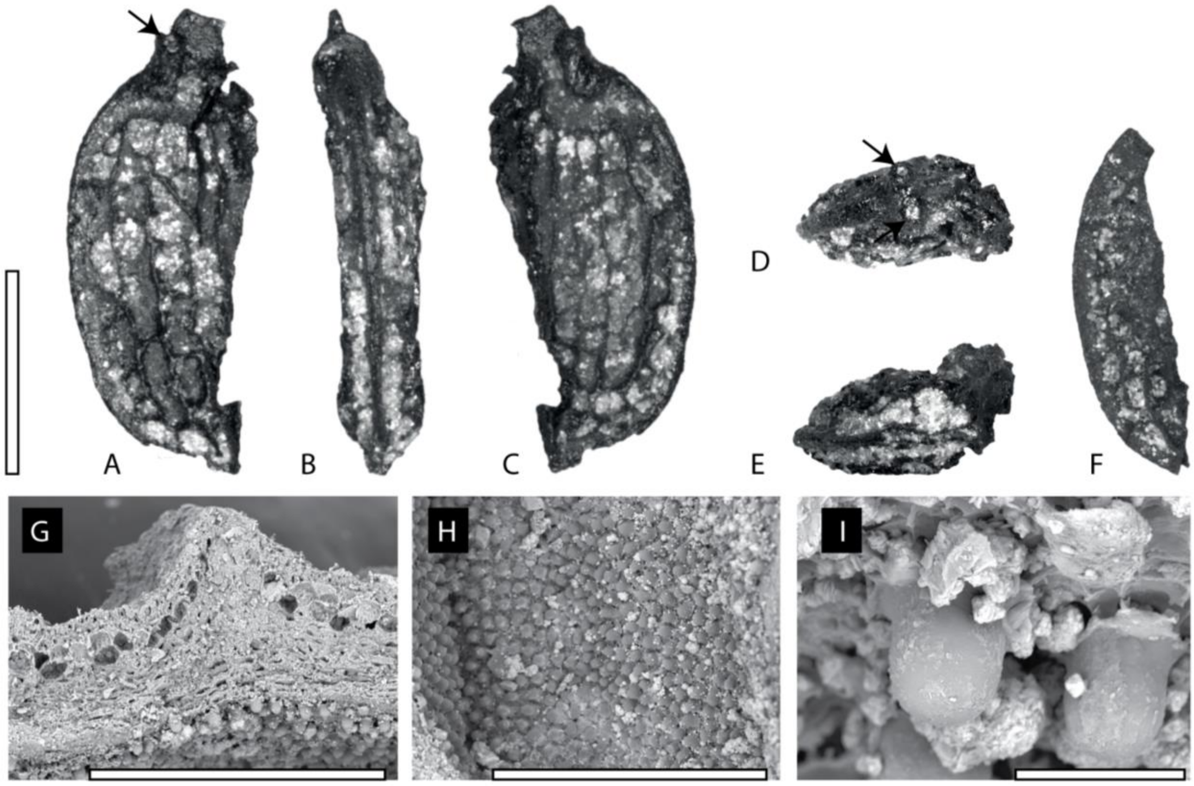

Figure VII.2. (A–E) *Iodes tubulifera* (MNHN.F.44738.), (A) lateral view of an endocarp showing the reticulum pattern of sharp ridges, (B) dorsal view showing the keel, (C) lateral view of second face of the endocarp, (D) apical view showing the small pair of horns (arrows), (E) basal view (F–I) (MNHN.F.44740.), (F) lateral view of the endocarp showing the reticulum pattern of sharp ridges, (G) SEM view of the endocarp wall units and ridges in transversal section, (H) SEM view of tubular papillae, (I) same with magnification. Scale bar A–F 5 mm, G–H 500 µm, I= 30 µm.

VII.2.1.2. Grès de Belleu site

Family–Icacinaceae

Species-*Iodes* sp.

Fig. VII.3 A, B

Locality.	Grès de Belleu
Stratigraphy.	Cuisian

Specimen. MNHN.F.8100.

Description. Endocarp elliptical, abraded in the upper right part, single-seeded with a unique locule and a lateral vascular bundle embedded in the endocarp wall (Fig. VII.3 B). Base rounded, symmetrical. Endocarp reticulate forming some polygonal areoles and with five longitudinal ridges (Fig. VII.3 A). Anatomical detail unknown. Length 13.2 mm, width 8.7 mm.

Remarks and affinities. A single specimen was found. Despite the lack of anatomical detail, especially papillae remains, we choose to assign this specimen to the *Iodes* extant genus, because it possesses a vascular bundle embedded in the endocarp wall and a reticular pattern in ornamentation. These two characters are only found in *Iodes* and *Icacina* genera (see. Chapter I & II). However, *Icacina* species are generally bigger than 13.2 mm and more globular in shape. Moreover, the lack of anatomical characters does not allow the recognition of a new species. The length and width of the specimen is close to *Iodes eocenica* (Reid & Chandler, 1933, Cleal et al., 2001) but narrower and could be close to *Iodes multireticulata*, but without enough anatomical preservation to compare it remains impossible to attribute it to a particular species.

Species-*Palaeophytocrene cf. vancouverensis*
Fig. VII.3 C

Locality. Grès de Belleu
Stratigraphy. Cuisian
Specimen. MNHN.F.8061.

Description. Endocarp oval in lateral view. Apex rounded, apparently symmetrical, base flattened, symmetrical. Outer part of endocarp pitted apparently not ridged (specimen abraded). Pits circular to elongate, about 0.58–0.86 (avg. 0.72 mm) in width, 0.82–1.02 (avg. 0.94) mm in length, randomly arranged, with 8–10 pits in length, 5–6 pits in width (about 60 pits by face). Pits associated with conical to parallel-sided protuberances. Endocarp length 21 mm, width 12 mm. Inner surface unknown.

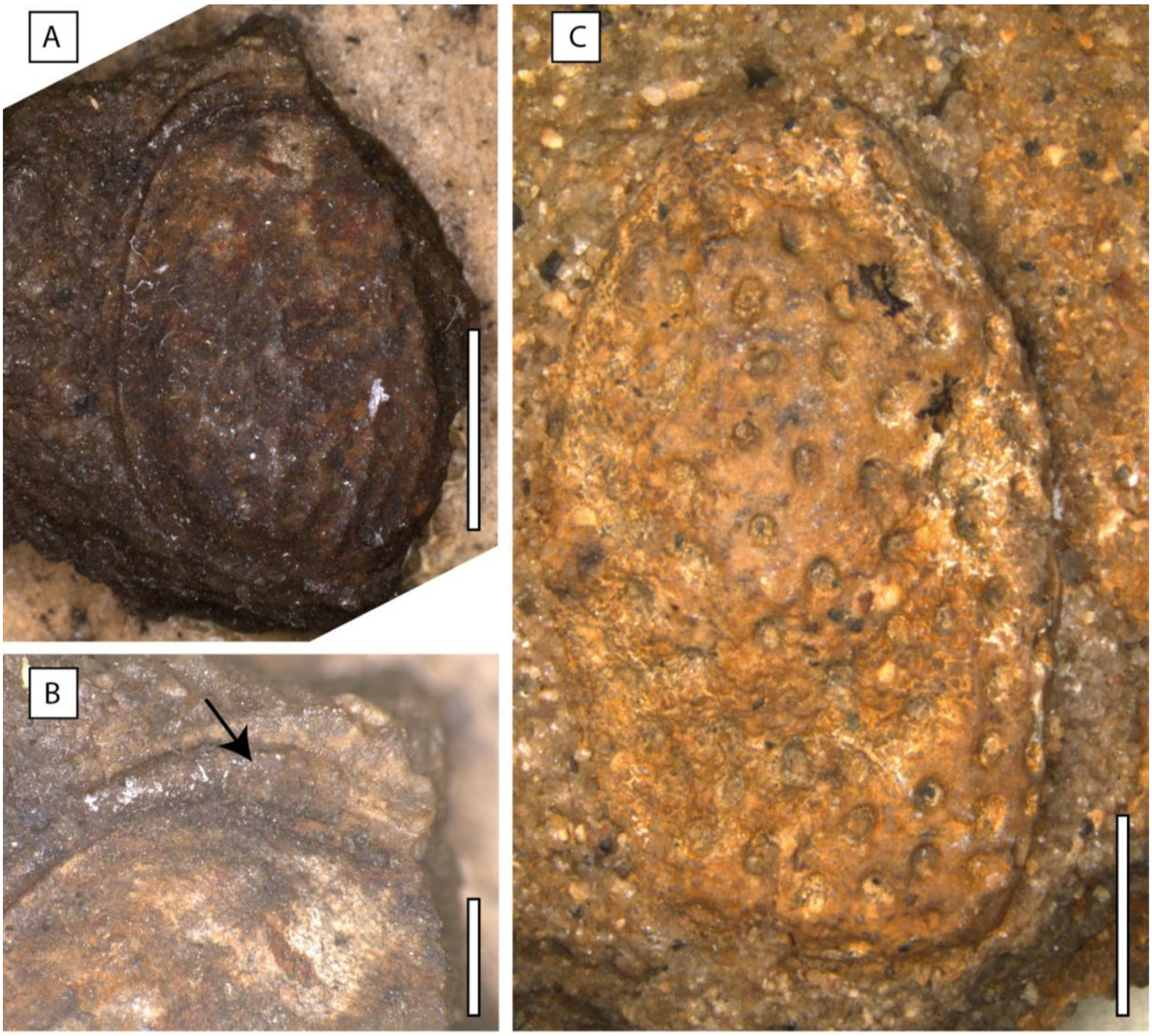

Figure VII.3. (A–B) *Iodes sp.* (MNHN.F.8100.), (A) lateral view of the endocast, (B) vascular bundle embedded on the endocarp wall (arrow); (C) *Palaeophytocrene cf. vancouverensis* (MNHN.F.8061.), lateral view. Scale bar: A–C = 5 mm, B = 1 mm.

Remarks and affinities. A single specimen represents this occurrence. The outer part of the endocarp with pits and tubercles with parallel side or conical shape (revealed by a silicone moulding of the pits) allows the attribution of this specimen to *Palaeophytocrene*. Thus, this specimen represents the first occurrence of *Palaeophytocrene* for the Paris Basin. This specimen seems to be close to the London Clay species (Reid and Chandler, 1933), *Palaeophytocrene ambigua* Reid & Chandler and *Palaeophytocrene foveolata* Reid & Chandler related to it by their size, but *Palaeophytocrene ambigua* have less and smaller pits and *Palaeophytocrene foveolata* have smaller pits too. The species from Vancouver, *Palaeophytocrene vancouverensis* Rankin & Stockey (Rankin et al., 2008) corresponds in size, diameter of pits and pits number in length and in width. However, the poor anatomical preservation of MNHN.F.8061. does not allow us to assign this fossil to any species. Further investigations as tomography studies could solve in a close future this inaccuracy.

VII.2.1.3. Prémontré site

Family–Icacinaceae
Species - Icacinicarytes sp.
Fig. VII.4

Stratigraphy. Cuisian
Locality. Prémontré (France)
Specimen. MNHN.F.44741.

Description. Fossil bilaterally symmetrical, elliptical; unilocular and single-seeded, length 8.84 mm, width 7.56 mm. Apex slightly asymmetrical, base rounded, symmetrical. Outer part of endocarp with reticulate pattern of rounded ridges; face of endocarp with 3–4 longitudinal ridges enclosing 6–9 polygonal areoles on each lateral face with few or no freely ending ridgelets; a keel surrounds the fruit in the plane of symmetry (?); cellular details unknown.

Remarks. Only one specimen represents the Icacinaceae in this outcrop. We found no thicker part on the keel that suggests that this specimen corresponds to an internal moulding. In the absence of apparent anatomical preservation, we choose to include this specimen in the genus *Icacinicarytes* without species name. This specimen could be close to *Iodes multireticulata* sensu Reid and Chandler (1933) but with less areoles. It may correspond to *Iodes rigida* from Le Quesnoy site, but the reticulation pattern is not matching. This specimen seems to have a unique morphological feature despite the lack of anatomical characters.

Figure VII.4. *Icacinicarytes* sp. (MNHN.F.44741.) (A) lateral view, (B) dorsal view showing the keel, (C) other lateral view, (D) apical view, (D) basal view. Scale bar: 5 mm

VII.2.2. Phylogeny of the Icacinaceae from the Paris basin

The phylogenetic reconstruction in MP (Fig. VII.5) is not similar to the previous study (Stull et al., 2015, see Fig. 2 in the introduction part of this thesis). The most important change in this result is that the clade II and III are sister groups. However, the position of the clade III as sister of the clade IV previously found (see. Fig. 2 of the introduction) is not well resolved with the molecular study (Stull et al., 2015). Only 5 023 characters were parsimony-informative characters (8.5%). The analysis reveals one parsimony tree with 15 556 steps, a CI (consistency index) excluding uninformative characters = 0.63 and a RI (retention index) = 0.76. Despite the completely resolved and unique parsimony tree, the Bootstrap analysis (appendix 12) shows that this result is not strongly supported. In fact, the morphological data represent 0.05 % of the matrix: the result of a random sampling analysis (as the Boostrap method) excludes *de facto* the best resolution for the fossil species, which only had missing data for the molecular part. The BI tree was less resolved than the MP tree (appendix 13). The *Paleophytocrene* specimen is very incomplete with 38% of morphological missing data. This lack of data could explain the long branch effect in this phylogeny, which could destabilize the analysis. In both analyses, the *Iodes* fossils belong to the modern *Iodes* genus (MP 100%; BI = 0.79). In the MP tree, *Paleophytocrene* is sister of *Stachyanthus* whereas it is unresolved in the BI tree. *Oncotheca balansae* Baill. is in the ingroup in the MP reconstruction (not resolved in BI), with a shift with *Cassinopsis madagascarensis* Baill. This result is not very surprising; the position of the *Cassinopsis* species was not fully resolved in the molecular analysis (Stull et al., 2015). Stull and collaborator defined Icacinoideae excluding the *Cassinopsis* genus as the well-defined clade. Indeed, the study of the flower (Del Rio et al., 2017) and fruits (in this work) raised questions about the position of this genus.

One hundred and sixty (160) steps are necessary to reconstruct the ancestral characters states via the morphological characters in Mesquite (CI= 0.56, RI = 0.47). For the fossils, the main informative characters are the ornamentation of the apex (5), the presence of pits at the surface of the endocarp (7), the presence of ridgelets inside the areoles (13), the position of the endocarp primary vascular strand (14) and the micromorphology of locule surface (16).

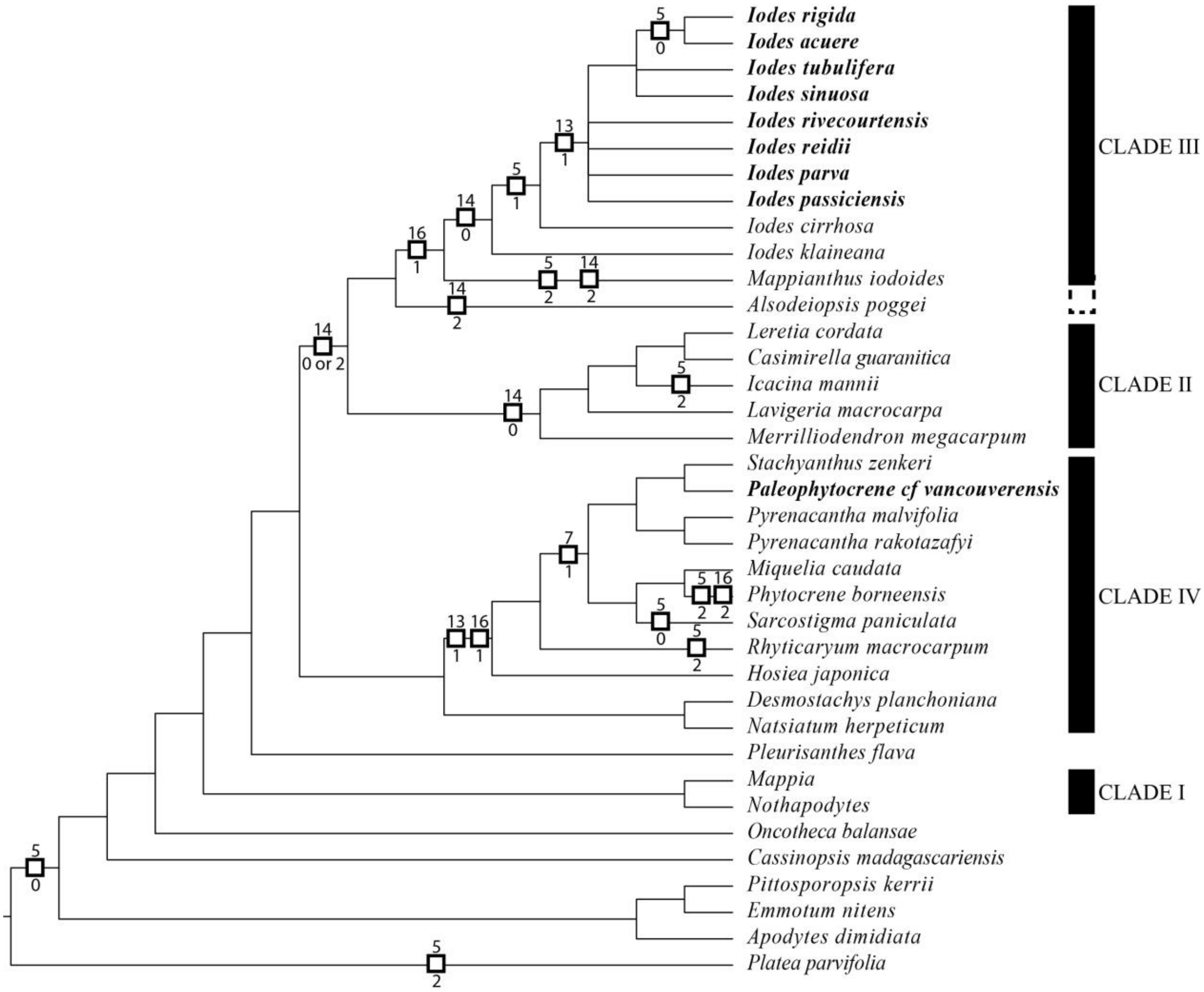

Figure VII.5. Strict consensus phylogenetic tree of the Icacinaceae family reconstructed via Paup 4.0 with a mixed molecular and morphological matrix (59 144 characters). In bold: fossils species from the Paris Basin. Mesquite orientation of pertinent characters for the fossil position is shown.

VII.3. Discussion

VII.3.1. Phylogenetic insight

A potential diagnostic endocarp character for the Icacinaceae family is the presence of digitate cells in the endocarp wall (31). The division of the endocarp wall in distinctive layers is a potential other diagnostic character of the clade. The primary vascular strand (14) which is inside the endocarp wall is a great argument in favour of the hypothesis of the Clade II sister group of the clade III. This character seems to be very constant in both clades, and completely absent in other Icacinaceae genera (except in *Cassinopsis* genus). Alternatively, Clade III as sister group of Clade

IV (as found in Stull et al. 2015) could be argued by the presence of papillae in the locule surface. However, the shape of papillae (21) and their density was not clearly related between the two clades, the papillae being rounded and uniform in the clade III whereas they are mostly large and diverse in shape in the clade IV. Therefore, the presence of papillae in clade III and IV would be rather a case of convergence.

The *Iodes* fossil species described here and in general, for the Paris Basin all belong to the *Iodes* genus. This study confirms the possibility to assign fossil species in modern *Iodes* genus with the help of endocarp characters. One character is fundamental in order to consider endocarp as associated to *Iodes* group: the vascular bundle inside the endocarp wall (14). As shown, this character was also found in the Clade II. Thus, the presence of papillae in the locule surface (16), which is present in the clade II and not in the clade III, allows the fossil assignation. The *Iodes* fossil taxa have in common a reticulation without free ending ridgelets (13). The ridgelets are present in numerous modern *Iodes* species (*Iodes africana*, Welw. Ex. Oliv. *I. balansae* Gagnep, *I. kamerounensis* Engl., *I. klaineana* Pierre, I. *ovalis* Blume, *I. scandens* (Becc.) Utteridge & Byng and *I. yatesii* Merr., see chapter I). Therefore, the *Iodes* fossil ornamentations are now restricted to some modern species (*I. seretii* (De Wild.) Boutique from Africa and *I. madagascariensis* Baill. from Madagascar).

The *Paleophytocrene* species is very incomplete (Fig. VII.3 C). However, the presence of pits at the surface (7) assigns this specimen to the Clade IV. Most precisely, this character could be diagnostic of the ancient *Phytocreneae* tribe (Engler, 1897, Sleumer, 1942).

To conclude, our phylogenetic analysis allows us to confirm the assignation of the fossils described in this study and in other related to the Paris Basin. We can now discuss about the diversity of the Icacinaceae family in the Paris Basin.

VII.3.2. Icacinaceae diversity of the Paris Basin

The Paris Basin hold a diversity comparable to other well-documented sites in Europe and North America (Reid & Chandler, 1933, Knobloch & Mai, 1986, Manchester, 1994, Collinson et al., 2012). Among the Paris Basin sites, 12 species of Icacinaceae have been determined, among them, nine species are endemic and three have no specific epithet (Table 1). These species represent only one extant genus (*Iodes*) and three extinct genera (*Palaeophytocrene*, *Icacinicarytes*, *Icacinanthium*). In comparison, in the London Clay flora (early Eocene), about 21 Icacinaceae species in seven genera were recorded, the Messel biota (middle Eocene) provided 10 species but six without specific epithet in five genera and the Clarno Formation, eight species in five genera.

However, our sites range from the Thanetian to the Ypresian, which is a greater range as other sites cited here.

TABLE 1 Stratigraphy of the Paris basin, with carpoflora sites with Icacinaceae family in bold, species from sites and mammal (MP) and pollen (NP) biochronology. Source: Schmidt-Kittler et al. 1987, Aubry et al. 2005

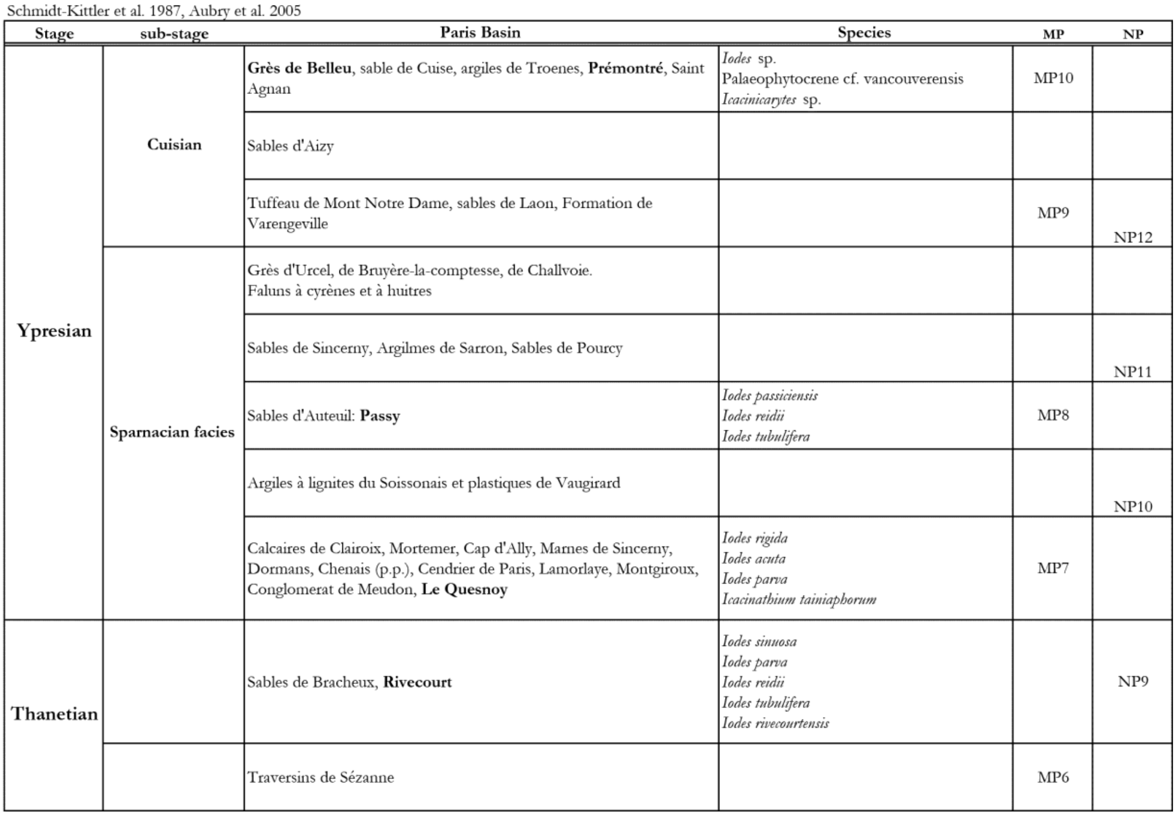

Stage	sub-stage	Paris Basin	Species	MP	NP
Ypresian	**Cuisian**	**Grès de Belleu**, sable de Cuise, argiles de Troenes, **Prémontré**, Saint Agnan	*Iodes* sp. Palaeophytocrene cf. vancouverensis *Icacinicarytes* sp.	MP10	
		Sables d'Aizy			
		Tuffeau de Mont Notre Dame, sables de Laon, Formation de Varengeville		MP9	NP12
	Sparnacian facies	Grès d'Urcel, de Bruyère-la-comptesse, de Challvoie. Faluns à cyrènes et à huitres			
		Sables de Sincerny, Argilmes de Sarron, Sables de Pourcy			NP11
		Sables d'Auteuil: **Passy**	*Iodes passiciensis* *Iodes reidii* *Iodes tubulifera*	MP8	
		Argiles à lignites du Soissonais et plastiques de Vaugirard			NP10
		Calcaires de Clairoix, Mortemer, Cap d'Ally, Marnes de Sincerny, Dormans, Chenais (p.p.), Cendrier de Paris, Lamorlaye, Montgiroux, Conglomerat de Meudon, **Le Quesnoy**	*Iodes rigida* *Iodes acuta* *Iodes parva* *Icacinathium tainiaphorum*	MP7	
Thanetian		Sables de Bracheux, **Rivecourt**	*Iodes sinuosa* *Iodes parva* *Iodes reidii* *Iodes tubulifera* *Iodes rivecourtensis*		NP9
		Traversins de Sézanne		MP6	

Within *Iodes*, nine species have been defined, in four different epochs: five in Rivecourt site (Thanetian), three in Le Quesnoy site (Ypresian), three in Passy site (middle Ypresian) and one in the Grès de Belleu site (end of Ypresian). Species from Rivecourt have been found in Le Quesnoy site (*Iodes parva*) and Passy site (*Iodes reidii* and *Iodes tubulifera*) showing a temporal link within the flora of the Paris Basin during the Paleogene. The *Iodes* sp. specimen described from the Grès de Belleu is the biggest of the Paris Basin and comparable to the London Clay specimens. However, the other sites of the Paris Basin, with Icacinaceae remains do not have the same preservation as the Grès de Belleu and should have different taphonomic process, making any size comparison difficult.

The *Palaeophytocrene* specimen from the Grès de Belleu is comparable to the species from the London Clay and from North America, but is different in some aspects. This specimen attests the presence of this common genus in the Eocene North American and European localities (Reid & Chandler, 1933, Manchester, 1994, Rankin et al., 2008, Collinson et al., 2012) in the Paris Basin during the Cuisian.

Finally, *Icacinanthium tainiaphorum*, a flower embedded in amber from Le Quesnoy, (Del Rio et al., 2017), shows an unexpected diversity for the Icacinaceae family. This flower, at the base of the Clade IV, adds a generic diversity to the lignitics remains.

The extant *Iodes* group is a genus of tropical to sub-tropical climber. *Palaeophytocrene* is an extinct genus with a probable affinity with the ancient tribe *Phytocreneae* (Engler, 1897, Sleumer, 1942) also composed of tropical to sub-tropical climbers. Moreover, *Icacinanthium* is close to tropical and sub-tropical climbing clade. All fossils remains through the Paris Basin sites seem to be related to climber species. Studies about the link between diversity of the forest and representation in the litter shows that litter represents much more the local than the regional vegetation (Burnham, 1989, Burnham et al., 1992). The climbers are abundant in the banks of the rivers or channels and the representation of only Icacinaceae climber could be a bias. On this point, the ancient Icacinaceae diversity could be underestimate. Indeed, it is not rare to find in the same area many Icacinaceae genera with many species (Sleumer, 1971, Villiers, 1973, Peng & Howard, 2008) in extant Icacinaceae diversity. *Iodes* is now represented by seven species in Malaysia (Sleumer, 1971), five species in Cameroon (Villiers, 1973) and four species in Madagascar (De La Bâthie, 1952). Our fossils found in Rivecourt, Le Quesnoy and Passy site for this genus are close to the extant diversity.

VII.3.3. Biogeographic insights

All Icacinaceae species from the Paris Basin seem to be endemic to a close area. During the Thanetian, the sea level surface was + 120 m higher than today (Scotese, 2014). The North of France had low altitudes in a great part of modern territory. The paleogeographic studies indicates that the major part of the northern France was submerged. The Paris Basin might has been isolated from the rest of the European floras. This particular geological context could favour endemism as nowadays in island cases (Whittaker & Fernández-Palacios, 2007, Kier et al., 2009). During the Paleocene-Eocene boundary, the marine level decreased (+ 80 m than today) and connected more the South and North of France with modern Eurasia. However, the Paris Basin flora exchanges with other area could be yet limited. Despite the endemism of these species, several fossils from the Paris Basin have biogeographic connections with extant and extinct species. *Palaeophytocrene cf. vancouverensis* specimen from the Grès de Belleu as well as *Iodes sp.* shows affinities with other European flora and North American vegetation, corroborating a close connexion between these two areas (Manchester, 1994, Stull et al., 2016) during the Eocene. The source of dispersion (from North America to Europe or from Europe to North America) still represents a subject of controversies in mammalian paleontology (Godinot & de Broin, 2003, Smith et al., 2006, Beard, 2008). The presence of diverse *Iodes* species with horn-like protrusions in the Paleocene Rivecourt site, close to the Eocene *Iodes brownii* from the Wyoming, suggest a dispersion during the Eocene from Europe to North America corroborating the second hypothesis (Smith et al., 2006). However, the *Paleophytocrene* species indicates a dispersion during the Eocene from North America to Europe (Stull et al., 2012) highlighted that both ways remain possible.

The Europe Eocene flora is often associated to the extant Indo-Malaysian vegetation considered as a relict of an ancient widespread flora (Reid & Chandler, 1933, Wolfe, 1975). Among Icacinaceae fossil from the Paris Basin, there are some evidences of this affinity. Only extant *Iodes* from eastern Asia possesses clear horn-like protrusions (see chapter I) as *Iodes parva* from Le Quesnoy, *Iodes passiciensis, Iodes reidii* and *Iodes tubulifera* from Passy. However, *Iodes rigida* and *Iodes acuta* do not have horn-like protrusions and are closer to the extant *Iodes* from Africa. In addition, the reticulation patterns of all *Iodes* from the Paris Basin are closer to some African modern species (as for example, *Iodes klaineana*). The fossils seem to have an extinct combination of characters now found separately in both areas.

In addition, *Icacinanthium tainiaphorum* Del Rio & De Franceschi is close to the clade IV sensu Stull (Stull et al., 2015) which contains African and Asian genera. This flower seems to be more related to *Hosiea* and *Natsiatum* which are endemic to the Asian area (Del Rio et al., 2017), but the phylogenetic position of both genera allows the flower to be considered at the base of all Clade IV genera. As discussed above, *Palaeophytocrene* belongs to Phytocrenae tribe, which is found in Asian and African areas.

In conclusion, we found that the affinity between Paleogene flora and modern floras are not as clear for the Icacinaceae family as proposed in literature. There is an uncertainty between African and Asian affinities in all cases, which could be a consequence of separated regression of the boreotropical forest during the Oligocene. These affinities are made between ancient widespread floras and extant probably refuges floras, which does not presume about the center of origin for the Icacinaceae family.

VII.3.4. Impact of the PETM in the Paris Basin

The Paleocene-Eocene thermal maximum is an abrupt global warming (Zachos et al., 2001, 2008) which affect terrestrial fauna and flora. In Europe, this event precedes the arrival of new faunas by migration (Godinot & de Broin, 2003, Smith et al., 2006, Hooker & Collinson, 2012). This event causes changes in floral composition (Wing et al., 2005, Collinson et al., 2009, Garel et al., 2013, 2014) to a thermophilic evergreen laurophyllous forest until a strongly evergreen thermophilic forest rich in climber (Collinson and Hooker, 2003). The frequency of untoothed leaf margin increases during the Eocene corresponding to a warmer flora (Traiser et al., 2018).

In the Paris Basin, differences in faunal composition through the PETM have been shown (Nel et al., 1999, Smith et al., 2014), but also in floral composition (Cavagnetto, 2000). Only two of the five species of *Iodes* from the Rivecourt Thanetian site, *Iodes rivecourtensis* and *Iodes sinuosa*, are not present in early Eocene sites (Tab. 1). It is difficult to know if it is due to local extinctions or if it is a bias in the fossil records. *Iodes reidii* and *Iodes tubulifera* are not present in Le Quesnoy site, which has only one species from Rivecourt, but these two species are present in the younger Passy site. This seems to show that the disappearance of at least these two species in Le Quesnoy site could be due to local changes. Indeed, Rivecourt site is composed of fluvial to fluvio-estuarine units (Smith et al., 2014). Contrariwise, Le Quesnoy site is formed by fluvio-lacustrine environment, probably marshy and not related to the marine environment (Nel et al., 1999). Both sites have little transport and thus characterize the local vegetation. Indeed, loss of four species from Rivecourt into Le Quesnoy sites could be due to the local record in two successive environments. In all cases (extinction or not of *I. rivecourtensis* and *I. sinuosa*), the three shared taxa between the Paleocene and the early Eocene demonstrate at least a partial continuity in the Icacinaceae species across the PETM in the Paris Basin. We show that the extinction of *Iodes* species during the PETM could be limited.

On the other hand, the number of species slightly increased during the Eocene with at least six species, with four new. Among the new species, two have no horn-like protrusions and appear just after the PETM event, whereas all species show horns in the Thanetian Rivecourt site. This new morphological disparity in *Iodes* genus for the early Eocene could be linked to an abrupt addition of vegetation following the expansion of boreotropical flora. In Europe, the PETM is linked to a decrease of marine level, which probably allows the fauna and flora from the South of France and Eurasia to disperse from the Paris Basin, which remained isolated during the Paleocene. These fauna and floras probably diversified in consequence of the PETM in others areas (Asia for the fauna). For the *Iodes* genus, we may have evidence of additional of species diversity and disparity in consequence of the global warming.

The first records of two extinct genera, *Icacinanthium* and *Palaeophytocrene* show a clear increase of genera and shape during the early Eocene. Indeed, *Icacinanthium tainiaphorum* is probably not closely related to the *Iodes* and *Paleophytocrene*. However, the presence of flowers in the lignite remains is limited, and the identification of the endocarp related to the *Icacinathium* flower could be difficult. The addition of this genus is probably only linked to the type of fossils remains. In addition, we show that the Cuisian species including *Paleophytocrene* genus from the

Paris Basin are probably not directly related to the Sparnatian and Thanetian French flora (Table 1.). In fact, no species from the Rivecourt, Le Quesnoy and Passy site are present during the Cuisian. Thus, the Sparnatian-Cuisian boundary seems to be more locally important in term of floral dynamic than the Paleocene-Eocene boundary. However, the lack of fossils during the Cusian limits the value of this observation. Despite this potential taphonomic bias, the new genera and the emergence of new disparity in the *Iodes* genus could be a clue to an early Eocene diversification of the family in Europe. This hypothesis is congruent to the development of a new evergreen thermophilic flora more diverse and favourable to climber during the PETM (Collinson & Hooker, 2003, Upchurch Jr & Wolfe, 1987).

Another emblematic family of the boreotropical flora, the Menispermaceae, was also present in Rivecourt (personal observation) and le Quesnoy site (Jacques & De Franceschi, 2005). However, only one genus is present in the Paleocene site whereas eight genera were present during the Early Eocene. Therefore, the diversification of the Menispermaceae during the Early Eocene of the Paris Basin is congruent with the Icacinaceae family. We could observe the same trend for the Vitaceae family, which are climbers too (personal observation).

To conclude, we consider that during the PETM, there is a possible rapid turnover in the Icacinaceae vegetation with an increase of diversity of the family, mainly shown by new *Iodes* shapes and no obvious extinction, due to warmer climate and decrease of sea level. This observation approves at least this event not as a catastrophic event for the vegetation in Europe. This conclusion is very similar to those made from palynological studies (Collinson et al., 2009, Garel et al., 2013, 2014).

Conclusion of the chapter

Three species were described from Passy site with one new and two from the Thanetian Rivecourt site. In addition, two specimens from the Grès de Belleu were attributed to *Iodes* and *Paleophytocrene* and a single specimen from Prémontré belongs to the non-natural *Icacinicarytes* genus. A phylogenetic study confirms these affinities. The diversity of the Icacinaceae from the Paris Basin is comparable of other great sites from Europe and North America, with 12 species and nine endemics. The endemism could be due to partial isolation of flora in consequence of the marine transgression. Affinities of these floras with Indo-Malaysian and Africa modern floras are highlighted. The changes in Icacinaceae through the PETM are limited but we showed a greater morphological disparity after the PETM, probably in response of this global warming.

Chapter VIII

Paleobiogeography of the Icacinaceae family

The fossils from the Paris Basin contain some information about the floral changes in France during the Palaeogene and in particular across the PETM. Thus, the different outcrops described in the Chapters III-VII support the idea of at least a continuity of Icacinaceae species locally and a potential rapid shift in Icacinaceae diversity through the Paleocene-Eocene boundary. In this chapter, we try to situate the Icacinaceae from the Paris Basin in a global fossil perspective.

Our main questions are: (1) what is the fossil diversity of Icacinaceae s.s. following the new circumscription of the family, (2) what is the paleogeography of this family and particularly of the *Iodes* genus, (3) what ecological and biogeography interpretations can we propose and (4) what is the contribution of the fossils from the Paris Basin in the understanding of the global paleogeography of this group.

VIII.1. Fossil occurrence of Icacinaceae s.s.

First, we compiled all the occurrences of Icacinaceae found in the literature (Table 1.). We found 178 fossil occurrences separated by differences in age, locality or country, with 99 occurrences (80 species) for fossil of endocarps divided in 12 fossil genera: *Comicilabium*, *Croomiocarpum*, *Faboidea*, *Hosiea*, *Icacinicarya*, *Icacinicaryites*, *Iodicarpa*, *Palaeohosiea*, *Paleophytocrene*, *Perforatocarpum*, *Sphaeriodes* and *Stizocarya* and four modern genera: *Iodes*, *Natsiatum*, *Phytocrene* and *Pyrenacantha*. Only one flower has been described for this family in the extinct genus *Icacinanthium*. We also compiled 13 leaf occurrences (10 species), five of them being from two extinct genera: *Goweria* and *Huziokaeae* and four of them from two extant genera: *Merrilliodendron* and *Phytocrene*. The pollen record contains 28 occurrences (seven species) in two fossil genera: *Compositoipollenites* and *Echiperiporites* and only one for the modern *Iodes* genus. Finally, we recorded 38 occurrences (14 species) in the wood fossil records, with two fossil genera: *Icacinoxylon* and *Apodytoxylon*.

VIII.2. Species and occurrences rejected or dubious for the paleogeography reconstruction

In this part, we explain the choice made in Table 1 to class the species/occurrences as rejected or dubious. In the paleogeography reconstruction (Fig. VIII.1), the rejected occurrences are not represented (considered as definitively not Icacinaceae or without certainty in age of the outcrops) whereas the dubious occurrences are presented in grey (considered as potential Icacinaceae, but without certainty). Accepted occurrences are in red (Fig. VIII.1).

VIII.2.1. Endocarp fossil

The endocarp record is the most meaningful for the Icacinaceae family, and probably the most reliable. However, some occurrences need to be revisited.

Comicilabium atkinsii was considered as belonging to Icacinaceae by its unilocular endocarp, the vascular bundle on only one side and the cellular structure of the endocarp wall. The endocarp apical structure is a bulge with a lip. The size of the endocarp and the wall thickness (2–4 mm) are surprising for a supposed Icacinaceae compared with modern species endocarps (see Chapter I). Despite the fact that the wall structure is a convincing argument for the proposed affinity, we decided to consider this species as dubious in order to consider the extreme differences in endocarp morphology.

Icacinicarya mucronata, Icacinicarya bognorensis, Icacinicarya rotundata, and *Icacinicarya sp.11* are considered as dubious in a recent revision of the London Clay fossils (Stull et al., 2016), because of the lack of some characteristic features and the bad preservation of the specimens. We also followed this opinion here. *Icacinicarya foveolata* was considered as a non-member of the Icacinaceae family in the same study because of the presence of large hexagonal secretory cells lining the outside part of the seed and the thicker endocarp wall. In the absence of alternative identification and another argument, we consider that at least the characters given by Reid and Chandler (1933); that are endocarp unilocular and wall composed with partial digitate cells, are sufficient to not totally reject the potential affinity with Icacinaceae family, so we consider it as dubious.

Icacinicarya amygdaloidea was considered as a member of Icacinaceae because of the shape, the position of the vascular bundle and the « stylar canal ». However, the specimens are smooth, which is uncommon within the Icacinaceae family. This trait is occasionally found in *Casimirella*, *Mappia* and especially in *Sarcostigma*. Additionally, the wall is composed of non-digitate cells, 10-12 µm in diameter. This kind of cells is never found in extant Icacinaceae. Consequently, we rejected this species in our study.

TABLE 1. Occurrencces of Icacinceae fossil in the fossil record. In bold species published/described in this thesis.

Species name	Organ	Occurrence (locality)	Country	Minimum Ag	Series	Stage	Status	References
Comicilabium atkinsii Manchester	Endocarp	Clarno Nut Beds (OR)	USA	43	Eocene	Lutetian	Dubious	Manchester 1994
Croomiocarpon missippiensis Stull, Manchester et Moore	Endocarp	Tallahatta Fm., Claiborne Group (MI)	USA	37	Eocene	Early-Middle	Accepted	Stull et al. 2011
Faboidea crassicutis Bowerbank	Endocarp	Herne bay, Sheppey, London Clay	United Kingdom	≈ 51– 47,8	Eocene	Ypresian	Accepted	Bowerbank 1840, Reid and Chandler 1933
Hosiea pterojugata Mai	Endocarp	Gonna, Abschnitt IV, graue Tone	Germany	56	Paleocene	Upper	Accepted	Mai 1987
Icacinicarya mucronata Chandler	Endocarp	Bognor, London Clay	United Kingdom	47,8	Eocene	Ypresian	Dubious	Chandler 1961, Cleal et al. 2001
Icacinicarya amygdaloidea Chandler	Endocarp	Herne Bay, London Clay	United Kingdom	≈ 51	Eocene	Ypresian	Rejected	Chandler 1961, Collinson 1983, Cleal et al. 2001
Icacinicarya bartonensis Chandler	Endocarp	Headon bed, London Clay	United Kingdom	41,3	Eocene	Lutetian	Accepted	Chandler 1960
Icacinicarya becktonensis Chandler	Endocarp	Hordle Cliffs, London Clay	United Kingdom	37,8	Eocene	Bartonian	Accepted	Chandler 1961
Icacinicarya bognorensis Reid and Chandler	Endocarp	Bognor, London Clay	United Kingdom	47,8	Eocene	Ypresian	Dubious	Reid and Chandler 1933, Cleal et al. 2001
Icacinicarya budvarensis Knobloch and Mai	Endocarp	České Bude˘jovice Budvar	Germany	83.6	Cretaceous	Santonian	Rejected	Knobloch and Mai 1986
Icacinicarya collinsonae Pigg, Manchester et Devore	Endocarp	Almont (ND)	USA	56,8	Paleocene	Tiffanian Ti3	Accepted	Pigg et al. 2008
Icacinicarya davisii (Chandler) Stull, Adams, Manchester et Collinson	Endocarp	Suffolk, London Clay	United Kingdom	47,8	Eocene	Ypresian	Accepted	Chandler 1961, Collinson 1983
Icacinicarya densipunctata Collinson, Manchester et Wilde	Endocarp	Messel biota	Germany	≈ 47	Eocene	Lutetian	Accepted	Collinson 2012
Icacinicarya dictyota Pigg, Manchester et Devore	Endocarp	Beicegel (ND)	USA	56,8	Paleocene	Tiffanian Ti3	Accepted	Pigg et al. 2008
Icacinicarya elegans (Bowerbank) Reid and Chandler	Endocarp	Sheppey, London Clay	United Kingdom	47,8	Eocene	Ypresian	Accepted	Reid and Chandler 1933, Cleal et al. 2001
Icacinicarya emarginata Chandler	Endocarp	Sheppey, London Clay	United Kingdom	47,8	Eocene	Ypresian	Accepted	Chandler 1961, Cleal et al. 2001
Icacinicarya forbesii Chandler	Endocarp	Sheppey, London Clay	United Kingdom	47,8	Eocene	Ypresian	Accepted	Chandler 1961, Collinson 1983, Cleal et al. 2001
Icacinicarya foveolata Reid and Chandler	Endocarp	Herne Bay, Sheppey, London Clay	United Kingdom	≈ 51–47,8	Eocene	Ypresian	Dubious	Reid and Chandler 1933, Collinson 1983, Cleal et al. 2001
Icacinicarya glabra Chandler	Endocarp	Sheppey, London Clay	United Kingdom	47,8	Eocene	Ypresian	Accepted	Chandler 1961,Cleal et al. 2001
Icacinicarya inornata Chandler	Endocarp	Lake, London Clay	United Kingdom	47,8	Eocene	Ypresian	Accepted	Chandler 1962, Cleal et al. 2001
Icacinicarya jenkinsi Reid and Chandler	Endocarp	Herne Bay, London Clay	United Kingdom	≈ 51	Eocene	Ypresian	Accepted	Reid and Chandler 1933, Cleal et al. 2001
Icacinicarya minima Reid and Chandler	Endocarp	Bognor, Sheppey, London Clay	United Kingdom	47,8	Eocene	Ypresian	Accepted	Reid and Chandler 1933, Collinson 1983, Cleal et al. 2001
Icacinicarya nodulifera Reid and Chandler	Endocarp	Herne Bay, Sheppey, London Clay	United Kingdom	≈ 51–47,8	Eocene	Ypresian	Accepted	Reid and Chandler 1933, Collinson 1983, Cleal et al. 2001
Icacinicarya ovalis Ried and Chandler	Endocarp	Sheppey, London Clay	United Kingdom	47,8	Eocene	Ypresian	Accepted	Reid and Chandler 1933
Icacinicarya ovoidea Reid and Chandler	Endocarp	Herne Bay, Sheppey, London Clay	United Kingdom	≈ 51–47,8	Eocene	Ypresian	Accepted	Reid and Chandler 1933, Cleal et al. 2001
Icacinicarya papillaris Knobloch and Mai	Endocarp	Eisleben	Germany	66	Cretaceous	Maastrichian	Dubious	Knobloch and Mai 1986
Icacinicarya platycarpa Reid and Chandler	Endocarp	Herne Bay, Bognor, Sheppey, London Clay	United Kingdom	≈ 51–47,8	Eocene	Ypresian	Accepted	Reid and Chandler 1933, Collinson 1983, Cleal et al. 2001
Icacinicarya pygmaea Chandler	Endocarp	Headon beds, London Clay	United Kingdom	41,3	Eocene	Lutetian	Accepted	Chandler 1960 , Cleal et al. 2001
Icacinicarya reticulata Chandler	Endocarp	Herne Bay, Bognor, London Clay	United Kingdom	≈ 51–47,8	Eocene	Ypresian	Accepted	Chandler 1961, Collinson 1983, Cleal et al. 2001
Icacinicarya rotundata (Bowerbank) Reid and Chandler	Endocarp	Sheppey, London Clay	United Kingdom	47,8	Eocene	Ypresian	Dubious	Reid and Chandler 1933, Cleal et al. 2001

TABLE 1. Continued.

Species name	Organ	Occurrence (locality)	Country	Minimum Ag	Series	Stage	Status	References
Icacinicarya sp.	Endocarp	Igala Division, Kabba Province	Nigeria	66?	Cretaceous?	Maastrichian?	Rejected	Chesters 1955
Icacinicarya sp11	Endocarp	Sheppey, London Clay	United Kingdom	47,8	Eocene	Ypresian	Dubious	Reid and Chandler 1933
Icacinicarya sp12	Endocarp	Sheppey, London Clay	United Kingdom	47,8	Eocene	Ypresian	Accepted	Reid and Chandler 1933
Icacinicarya youssefi Chandler	Endocarp	Gebel Atshai and Kosseir Area, Red Sea	Egypt	61,6	Paleocene	Danian	Accepted	Chandler 1954
Icacinicaryites corruga (Brown) Pigg, Manchester et Devore	Endocarp	Almy, Animas FM., Coalmont, Ferris, Fort Union (CO)	USA	56	Paleocene	?	Dubious	Pigg et al. 2008, Brown 1962
Icacinicaryites israelii (Soudry & Gregor) Del Rio, Thomas & De Franceschi	Endocarp	Har Nishpeh area, central Negev	Israel	about 72,1	Cretaceous	Early Maastrichtian	Dubious	Soudry & Gregor 1997
Icacinicaryites linchensis Pigg, Manchester et Devore	Endocarp	Linch, Sand Draw (WY), Animas Fm. (CO)	USA	56	Paleocene	Thanetian	Accepted	Pigg et al. 2008
Icacinicaryites lottii Stull, S.E. Allen, & Manchester	Endocarp	Kinsinger Lakes (WY)	USA	48,5	Eocene	Ypresian	Accepted	Allen et al. 2015
Icacinicarytes sp.	Endocarp	Prémontré	France	49	Eocene	Cuisian Sup.	Accepted	Del Rio & De Franceschi in prep.
***Iodes acuta* Del Rio & De Franceschi**	Endocarp	Le Quesnoy, Oise	France	55-56	Eocene	Basal sparnatian	Accepted	Del Rio et al. In prep
Iodes acutiformis Chandler	Endocarp	Lake, Arne, London Clay	United Kingdom	47,8	Eocene	Ypresian	Accepted	Chandler 1962, Cleal et al. 2001
Iodes bilinica (Ettingshausen) Stull, Adams, Manchester	Endocarp	Messel biota	Gremany	≈ 47	Eocene	Lutetian	Accepted	Collinson 2012
Iodes bilinica (Ettingshausen) Stull, Adams, Manchester	Endocarp	Bohemia	Czech Republic	33,9	Eocene	Upper	Accepted	Kvacek & Buzek 1995
Iodes bilinica (Ettingshausen) Stull, Adams, Manchester	Endocarp	Hordle Cliffs, London Clay	United Kingdom	47,8	Eocene	Ypresian	Accepted	Ettingshausen 1866, Chandler 1925, Kvacek & Buzek 1995, Takhjatan 1966,
Iodes brownii (Berry) Stull, Adams, Manchester et	Endocarp	Tipperary flora (WY), Kisinger Lakes (WY), Blue Rim (WY), Bonanza	USA	49,5 – 43,0	Eocene	End Ypresian - Lutetiai	Accepted	Allen et al. 2015; Stull et al. 2016, Manchester 1994
Iodes chandlerae Manchester	Endocarp	Clarno Nut Beds (OR)	USA	43	Eocene	Lutetian	Accepted	Manchester 1994
Iodes corniculata Reid and Chandler	Endocarp	Herne bay, Sheppey, London Clay	United Kingdom	≈ 51–47,8	Eocene	Ypresian	Accepted	Reid and Chandler 1933, Collinson 1983, Cleal et al. 2001
Iodes eocenica Reid and Chandler	Endocarp	Sheppey, London Clay	United Kingdom	47,8	Eocene	Ypresian	Accepted	Reid and Chandler 1933 ,Cleal et al. 2001
Iodes germanica Knobloch and Mai	Endocarp	Eisleben	Germany	66	Cretaceous	Maastrichtian	Accepted	Knobloch and Mai 1986, Mai 1987
Iodes germanica Knobloch and Mai	Endocarp	Gonna	Germany	56	Paleocene	Upper	Accepted	Mai 1987
Iodes hordwellensis ? Chandler	Endocarp	Hordle Cliffs, London Clay	United Kingdom	37,8	Eocene	Bartonian	Accepted	Chandler 1961
Iodes multireticulata Reid and Chandler	Endocarp	Sheppey, Herne bay, London Clay	United Kingdom	≈ 51–47,8	Eocene	Ypresian	Accepted	Reid and Chandler 1933, Cleal et al. 2001
Iodes multireticulata Reid and Chandler	Endocarp	Clarno Nut Beds (OR)	USA	43	Eocene	Lutetian	Accepted	Manchester 1994
Iodes multireticulata Reid and Chandler	Endocarp	Fisher/Sullivan Site (VI)	USA	55.5	Eocene	Early	Accepted	Tiffney 1999
Iodes occidentalis S.E. Allen, Stull, & Manchester	Endocarp	Blue Rim (WY)	USA	49,5	Eocene	Ypresian	Accepted	Allen et al. 2015
***Iodes parva* Del Rio, Thomas & De Franceschi**	Endocarp	Petit Pâtis, Rivecourt, Oise	France	57-56	Paleocene	Thanetian	Accepted	Del Rio et al. Accepted
***Iodes parva* Del Rio, Thomas & De Franceschi**	Endocarp	Le Quesnoy, Oise	France	55-56	Eocene	Basal sparnatian	Accepted	Del Rio et al. In prep
***Iodes passiciensis* Del Rio & De Franceschi**	Endocarp	Passy	France	about 55	Eocene	Middle sparnatian	Accepted	Del Rio & De Franceschi in prep.
***Iodes reidii* Del Rio, Thomas & De Franceschi**	Endocarp	Petit Pâtis, Rivecourt, Oise	France	57-56	Paleocene	Thanetian	Accepted	Del Rio et al. Accepted
***Iodes reidii* Del Rio, Thomas & De Franceschi**	Endocarp	Passy	France	about 55	Eocene	middle sparnatian	Accepted	Del Rio & De Franceschi in prep.

TABLE 1. Continued.

Species name	Organ	Occurrence (locality)	Country	Minimum Ag	Series	Stage	Status	References
***Iodes rigida* Del Rio & De Franceschi**	Endocarp	Le Quesnoy, Oise	France	55-56	Eocene	Basal sparnatian	Accepted	Del Rio et al. In prep
***Iodes rivecourtensis* Del Rio, Thomas & De Franceschi**	Endocarp	Petit Pâtis, Rivecourt, Oise	France	57-56	Paleocene	Thanetian	Accepted	Del Rio et al. Accepted
***Iodes rivecourtensis* Del Rio, Thomas & De Franceschi**	Endocarp	Petit Pâtis, Rivecourt, Oise	France	57-56	Paleocene	Thanetian	Accepted	Del Rio et al. Accepted
***Iodes sinuosa* Del Rio, Thomas & De Franceschi**	Endocarp	Petit Pâtis, Rivecourt	France	57-56	Paleocene	Thanetian	Accepted	Del Rio et al. Accepted
Iodes sp.	Endocarp	Chuckanut Formation (WA)	USA	33,9	Eocene	"Late"	Accepted	Pigg and Wehr 2002
Iodes sp.	Endocarp	Bognor, London Clay	United Kingdom	47,8	Eocene	Ypresian	Accepted	Chandler 1961
Iodes sp.	Endocarp	Grès de Belleu	France	49	Eocene	Cuisian Sup.	Accepted	Del Rio & De Franceschi in prep.
Iodes sp.	Endocarp	Dormaal	Belgium	55	Eocene	Ypresian	Accepted	Fairon-Demaret
***Iodes tubulifera* Del Rio, Thomas & De Franceschi**	Endocarp	Petit Pâtis, Rivecourt, Oise	France	57-56	Paleocene	Thanetian	Accepted	Del Rio et al. Accepted
***Iodes tubulifera* Del Rio, Thomas & De Franceschi**	Endocarp	Passy	France	about 55	Eocene	middle sparnatian	Accepted	Del Rio & De Franceschi in prep.
Iodicarpa ampla Manchester	Endocarp	Clarno Nut Beds (OR)	USA	43	Eocene	Lutetian	Accepted	Manchester 1994
Iodicarpa lenticularis Manchester	Endocarp	Clarno Nut Beds (OR)	USA	43	Eocene	Lutetian	Accepted	Manchester 1994
Natsiatum wilcoxiana (Bery) Stull, Moore & Manchester	Endocarp	Fayette County, Wilbanks II Clay Pits (TE)	USA	37,8	Eocene	Middle	Accepted	Stull et al. 2011
Palaeohosiea marchiaca (Mai) Kvacek & Buzek	Endocarp	Bohemia	Czech Republic	59.2	Paleocene	Middle	Accepted	Mai 1987, Kvacek & Buzek 1995
Palaeohosiea marchiaca (Mai) Kvacek & Buzek	Endocarp	Shepey, Bognor, London Clay	United Kingdom	47.8	Eocene	Lower	Accepted	Kvacek & Buzek 1995
Palaeohosiea suleticensis (Mai) Kvacek & Buzek	Endocarp	Suletice, Bohemia	Czech Republic	28.1	Oligocene	Lower	Accepted	Kvacek & Buzek 1996
Palaeophytocrene ambigua Reid and Chandler	Endocarp	Bognor, Sheppey, London Clay	United Kingdom	47,8	Eocene	Ypresian	Accepted	Read and Chandler 1933
Palaeophytocrene foveolata Reid and Chandler	Endocarp	Herne Bay, Bognor, Sheppey, London Clay	United Kingdom	≈ 51–47,8	Eocene	Ypresian	Accepted	Read and Chandler 1933
Palaeophytocrene foveolata var. minima Reid and Chandler	Endocarp	Herne Bay, Bognor, Sheppey, London Clay	United Kingdom	≈ 51–47,8	Eocene	Ypresian	Accepted	Reid and Chandler 1933
Palaeophytocrene hammenii Stull	Endocarp	Bogota fm. Checua clay pit	Colombia	58	Paleocene	Middle-Late	Accepted	Stull et al. 2012
Palaeophytocrene hancockii (Scott) Manchester	Endocarp	Clarno Nut Beds (OR)	USA	43	Eocene	Lutetian	Accepted	Scott 1954, Manchester 1994
Palaeophytocrene lacunosum (MacGinitie) Wolfe	Endocarp	Independence Hill (SN)	USA	37.8	Eocene	Middle	Accepted	MacGinitie 1941, MacGinitie 1969
Palaeophytocrene manchesteri Rankin, Stockey et Beard	Endocarp	Vancouver island	Canada	33,9	Eocene	?	Accepted	Rankin et al. 2008
Palaeophytocrene pseudopersica Scott emend Manchester	Endocarp	Clarno Nut Beds (OR)	USA	43	Eocene	Lutetian	Accepted	Scott 1954, Manchester 1994
Paleophytocrene sp.	Endocarp	Ronald, Kittitas County (WA)	USA	33.9	Eocene	Late	Accepted	Pigg & Wehr 2002
Paleophytocrene sp.	Endocarp	Almont (ND)	USA	56	Paleocene		Accepted	Crane et al. 1990
Palaeophytocrene vancouverensis Rankin, Stockey et Beard	Endocarp	Vancouver island	Canada	33,9	Eocene	?	Accepted	Rankin et al. 2008
Paleophytocrene cf. vancouverensis	Endocarp	Grès de Belleu	France	49	Eocene	Cuisian Sup.	Accepted	Del Rio & De Franceschi in prep.
Paleophytocrene elytraeformis (Holl.) Wolfe	Endocarp	Yakutat Frm.	Alaska	33,9	Eocene	Middle-Late	Accepted	Wolfe 1977, Hollick 1936, Heer 1870
Perforatocarpum echinatum (Chandler) Stull, Adams, Manchester et Collinson	Endocarp	Sheppey, London Clay	United Kingdom	47,8	Eocene	Ypresian	Accepted	Chandler 1961, Cleal et al. 2001, Stull et al. 2016

TABLE 1. Continued.

Species name	Organ	Occurrence (locality)	Country	Minimum Ag	Series	Stage	Status	References
Phytocrene densipunctata Stull, Moore et Manchester	Endocarp	Wilbanks II Clay Pits (TE)	USA	37,8	Eocene	Bartonian	Accepted	Stull et al. 2011
Phytocrene microcarpa Scott & Barghoorn	Endocarp	Androvette Pit, Kreischerville (NY)	USA	66	Cretaceous	Early-Late	Rejected	Scott & Barghoorn 1957
Phytocrene punctilinearis Collinson, Manchestet et Wilde	Endocarp	Messel biota	Gremany	≈ 47	Eocene	Lutetian	Accepted	Collinson 2012
Cf. Phytocrene sp.	Endocarp	Guajira peninsula	Colombia	58	Paleocene	Thanetian	Accepted	Stull et al. 2012
Pyrenacantha austroamericana Stull	Endocarp	Belen flora	Peru	28,5	Oligocene	Late early	Accepted	Stull et al. 2012
Pyrenacantha occidentalis Manchester	Endocarp	Clarno Nut Beds (OR)	USA	43	Eocene	Lutetian	Accepted	Manchester 1994
Sphaeriodes ventricosa (Bowerbank) Reid and Chandler	Endocarp	Sheppey, London Clay	United Kingdom	47,8	Eocene	Ypresian	Accepted	Reid and Chandler 1933
Stizocarya communis Reid and Chandler	Endocarp	Sheppey, London Clay	United Kingdom	47,8	Eocene	Ypresian	Accepted	Reid and Chandler 1933
Stizocarya oviformis Reid and Chandler	Endocarp	Sheppey, London Clay	United Kingdom	47,8	Eocene	Ypresian	Accepted	Reid and Chandler 1933
***Icacinanthium tainiaphorum* Del Rio & De Franceschi**	Flower	Le Quesnoy, Oise	France	55-56	Eocene	Basal sparnatian	Accepted	Del Rio et al. 2017
Goweria alaskana Wolfe	Leaf	Kushtaka Frm.	Alaska	33,9	Eocene	Middle-Late	Dubious	Wolfe 1977
Goweria bibaiensis Tanai	Leaf	Okuno-sawa, Bibai, Hokkaido	Japan	≈ 46	Eocene	Middle	Dubious	Tanai 1990
Goweria bluerimensis S.E. Allen, Stull, & Manchester	Leaf	Blue Rim (WY)	USA	49,5	Eocene	Ypresian	Dubious	Allen et al. 2015
Goweria dilleri (Knowlton) Wolfe	Leaf	Kushtaka Frm.	Alaska	33,9	Eocene	Middle-Late	Dubious	Wolfe 1977, Wolfe 1968
Goweria linearis Wolfe	Leaf	Green river (WA)	USA	37.8?	Eocene	Middle?	Dubious	Wolfe 1968
Huziokaeae eoutilus (Endo) Tanai	Leaf	Am-site,Shimizusawa,Yubari, Hokkai	Japan	≈ 40	Eocene	Middle	Rejected	Tanai 1990
Merrilliodendron ezoanum Tanai	Leaf	Am-site,Shimizusawa,Yubari, Hokkai	Japan	≈ 40	Eocene	Middle	Dubious	Tanai 1990
Phytocrene acutissima Wolfe	Leaf	Kushtaka Frm.	Alaska	33,9	Eocene	Middle-Late	Dubious	Wolfe 1977
Phytocrene ozakii Tanai	Leaf	Reisui-zan,Yubari, Hokkaido	Japan	≈ 40	Eocene	Middle	Dubious	Tanai 1990
Phytocrene sordida (Lesuereux.) MacGinitie	Leaf	Kulthieth Frm.	Alaska	33,9	Eocene	Middle-Late	Dubious	Wolfe 1977
Phytocrene sordida (Lesuereux.) MacGinitie	Leaf	Chalk Bluffs, Buckeye Flat, Independence hill (SN)	USA	37.8	Eocene	Middle	Dubious	Macginitie 1941
Pyrenacantha sp.	Leaf	Kulthieth Frm.	Alaska	33,9	Eocene	Middle-Late	Dubious	Wolfe 1977
Pyrenacantha sp.	Leaf	Ishikari coal field Ic-9	Japan	≈ 40	Eocene	Middle	Dubious	Tanai 1990
Compositoipollenites medius Krutzch & Vanhoorne 1977	Pollen	Houdancourt	France	56	Eocene	Ypresian	Dubious	Cavagnetto 2000
Compositoipollenites medius Krutzch & Vanhoorne 1977	Pollen	Epinois	Belgium	56	Eocene	Ypresian	Dubious	Krutzsch & Vanhoorne 1977
Compositoipollenites microechinatus Kruttzch & Vanhoorne 1977	Pollen	Epinois	Belgium	56	Eocene	Ypresian	Dubious	Krutzsch & Vanhoorne 1977
Compositoipollenites minimus Krutzch & Vanhoorne 1977	Pollen	Houdancourt	France	56	Eocene	Ypresian	Dubious	Cavagnetto 2000
Compositoipollenites minimus Krutzch & Vanhoorne 1977	Pollen	Epinois	Belgium	56	Eocene	Ypresian	Dubious	Krutzsch & Vanhoorne 1977
Compositoipollenites minimus Krutzch & Vanhoorne 1977	Pollen	Messel	Germany	≈ 47	Eocene	Middle	Dubious	Lenz et al. 2007, Thiele-Pfeiffer 1988
Compositoipollenites minimus Krutzch & Vanhoorne 1977	Pollen	Petite Pyrénées	France	61,6	Paleocene	Danian	Dubious	Cavagnetto et al. 1992

TABLE 1. Continued.

Species name	Organ	Occurrence (locality)	Country	Minimum Ag	Series	Stage	Status	References
Compositoipollenites minimus Krutzch & Vanhoorne 1977	Pollen	Nointel	France	53	Eocene	Sparnacian sup.	Dubious	Kedves 1970
Compositoipollenites minimus Krutzch & Vanhoorne 1977	Pollen	Menat	France	59,2	Paleocene	Selandian	Dubious	Kedves & Russel 1982 ,for the datation Mélanie Tanrattana com. pers.
Compositoipollenites rhizophorus burghasungensis (Murriger & Pflug 1952) Thomson & Pflug 1949	Pollen	Houdancourt	France	56	Eocene	Ypresian	Dubious	Cavagnetto 2000
Compositoipollenites rhizophorus burghasungensis (Murriger & Pflug 1952) Thomson & Pflug 1950	Pollen	Borkener	Germany	58-33,9	Paleocene-Eocen	Thanecian-Priabonian	Dubious	Thomson & Pflug 1953
Compositoipollenites rhizophorus burghasungensis (Murriger & Pflug 1952) Thomson & Pflug 1951	Pollen	Central Anatolia	Turkey	33,9	Oligocene	inf.	Dubious	Akkiraz & Akgun 2005
Compositoipollenites rhizophorus burghasungensis (Murriger & Pflug 1952) Thomson & Pflug 1952	Pollen	Messel biota	Germany	≈ 47	Eocene	Middle	Dubious	Lenz et al. 2007
Compositoipollenites rhizophorus burghasungensis (Murriger & Pflug 1952) Thomson & Pflug 1953	Pollen	Saint-Lege-en-Bois, Guitrancourt	France	56-53	Paleocene	Sparnacian	Dubious	Kedves 1970, Kedves & Pardutz 1970
Compositoipollenites rhizophorus (R. Potonié 1934) R. Potonié 1960	Pollen	Houdancourt	France	56	Eocene	Ypresian	Dubious	Cavagnetto 2000, Potonié 1960
Compositoipollenites rhizophorus (R. Potonié 1934) R. Potonié 1960	Pollen	Salaj District, Jibou	Romania	58	Paleocene	Thanetian	Dubious	Petrescu et Codrea 2004
Compositoipollenites rhizophorus (R. Potonié 1934) R. Potonié 1960	Pollen	Merseburg	Germany	56	Eocene	Ypresian	Dubious	Hofmann et al. 2011
Compositoipollenites rhizophorus (R. Potonié 1934) R. Potonié 1960	Pollen	Weißelster	Germany	33,9	Eocene	Upper	Dubious	Knobloch & Konzalova 1998
Compositoipollenites rhizophorus (R. Potonié 1934) R. Potonié 1960	Pollen	Bracklesham Beds, Surrey	United Kingdom	41,2	Eocene	Ypresian-Lutetian	Dubious	Potter 1977
Compositoipollenites rhizophorus (R. Potonié 1934) R. Potonié 1960	Pollen	Buda Marl	Hungary	33,9	Eocene	?	Dubious	Kedves & Endredi 1968
Compositoipollenites rhizophorus (R. Potonié 1934) R. Potonié 1960	Pollen	Saint-Leger-en-Bois	France	56	Eocene	Sparnacian	Dubious	Kedves 1970
Compositoipollenites rhizophorus (R. Potonié 1934) R. Potonié 1960	Pollen	Paris Austerlitz	France	41,2	Eocene	Lutetan sup.	Dubious	Kedves 1970
Compositoipollenites rhizophorus (R. Potonié 1934) R. Potonié 1960	Pollen	Borken, Kassel, Lower Hesse	Germany	47,8	Eocene	Middle	Dubious	Hofmann & Gregor 2018
Echiperiporites icacinoides Samard-Cheboldaeff 1975	Pollen	Douala	Cameroon	5,33	Miocene	inférieur	?	Salard-Cheboldaeff 1975
Echiperiporites minor Samard-Cheboldaeff 1975	Pollen	Douala	Cameroon	5,33	Miocene	inférieur	Rejected	Salard-Cheboldaeff 1975
Iodes type	Pollen	Wagon Bed Frm. (WY)	USA	46,2	Eocene	Bridgerian	Rejected	Leopold & Macginitie 1972
Apodytoxylon hamamelidoides Grambast-Fessard	Wood	Castellane	France	5,3	Miocene	Sup.	Rejected	Grambast-Fessard 1969
Icacinixylon kokubunii Takahashi & Suzuki	Wood	Rumoi County	Japan	100,5	Cretaceous	Albian	Rejected	Takashi & Suzuki 2003
***Icacinoxylon* ?**	Wood	Petit Pâtis, Rivecourt, Oise	France	57-56	Paleocene	Thanetian	Rejected	This thesis
Icacinoxylon alternipunctata Wheeler	Wood	Ilinois	USA	66	Cretaceous	Upper	Rejected	Wheeler et al. 1987
Icacinoxylon crystallophorum Greguss	Wood	Dorog	Hungrary	23,03	Oligocene		Rejected	Greguss 1969
Icacinoxylon densiporosum Petrescu	Wood	Transilvania	Romania	28,1	Oligocene	Middle	Rejected	Petrescu 1978
Icacinoxylon grambast-fessardi Petrescu & Dragastan	Wood	Telega-Prahova	Georgia	23,03	Oligocene	Upper	Rejected	Petrescu & Dragastan 1972
Icacinoxylon hotobagyii Greguss	Wood	Balaton	Hungary	11,6	Miocene	Helvetian	Rejected	Greguss 1969
Icacinoxylon laticiphorum Greguss	Wood	Dorog	Hungary	23,03	Oligocene		Rejected	Greguss 1969
Icacinoxylon nishidae Takahashi & Suzuki	Wood	Rumoi County	Japan	89,8?	Cretaceous	Turonian?	Rejected	Takahashi & Suzuki 2003
Icacinoxylon pittiense Thayn, Tidell & Stokes	Wood	Utah	USA	100,5	Cretaceous	Aptian-Albian	Rejected	Thayn et al. 1985

TABLE 1. Continued.

Species name	Organ	Occurrence (locality)	Country	Minimum Ag	Series	Stage	Status	References
Icacinoxylon platanoides Greguss	Wood	Zirc	Hungary	11,6	Miocene	Helvetian	Rejected	Greguss 1969
Icacinoxylon shilikinae Greguss	Wood	Pomaz	Hungary	11,6	Miocene	Helvetian	Rejected	Greguss 1969
Icacinoxylon sp.	Wood	Colti-Buzau	Romania	28,1	Oligocene	Lower	Rejected	Petrescu et al. 1989
Icacinoxylon sp.	Wood	Pravaleni	Romania	5,33	Miocene	Sup.	Rejected	Petrescu & Nutu 1972
Icacinoxylon sp. 1	Wood	Dorog	Hungary	23,03	Oligocene		Rejected	Greguss 1969
Icacinoxylon sp. 2	Wood	Bajna	Hungary	23,03	Oligocene		Rejected	Greguss 1969
Icacinoxylon sp. 3	Wood	Cserhathalap	Hungary	11,6	Miocene	Helvetian	Rejected	Greguss 1969
Icacinoxylon sp. 4	Wood	Varpalota	Hungary	15.9	Miocene	Lower Helvetian	Rejected	Greguss 1969
Icacinoxylon sp. 5	Wood	Cinkota	Hungary	11,6	Miocene	Helvetian	Rejected	Greguss 1969
Icacinoxylon sp. 6	Wood	Pecsszabolcs	Hungary	11,6	Miocene	Helvetian	Rejected	Greguss 1969
Icacinoxylon sp. 7	Wood	Mor	Hungary	11,6	Miocene	Helvetian	Rejected	Greguss 1969
Icacinoxylon sp. 8	Wood	Megyaszo	Hungary	11,6	Miocene	Sarmatian	Rejected	Greguss 1969
Icacinoxylon sp. 9	Wood	Budapest	Hungary	11,6	Miocene	Helvetian	Rejected	Greguss 1969
Icacinoxylon sp. 10	Wood	Harsagy	Hungary	11,6	Miocene	Helvetian	Rejected	Greguss 1969
Icacinoxylon sp. 11	Wood	Bodajk	Hungary	11,6	Miocene	Lower Helvetian	Rejected	Greguss 1969
Icacinoxylon sp. 12	Wood	Iskaszent-gyorgy	Hungary	15,9	Miocene	Helvetian	Rejected	Greguss 1969
Icacinoxylon sp. 13	Wood	Homokbodoge	Hungary	15,9	Miocene	Helvetian	Rejected	Greguss 1969
Icacinoxylon sp. 14	Wood	Solymar	Hungary	23,03	Oligocene		Rejected	Greguss 1969
Icacinoxylon sp. 15	Wood	Penzeskut	Hungary	11.6	Miocene	Helvetian	Rejected	Greguss 1969
Icacinoxylon sp. 16	Wood	Ratka	Hungary	11.6	Miocene	Samatian	Rejected	Greguss 1969
Icacinoxylon sp. 17	Wood	Nagybatony	Hungary	15,9	Miocene	Burdigalian	Rejected	Greguss 1969
Icacinoxylon sp. 18	Wood	Nograd	Hungary	11,6	Miocene	Helvetian	Rejected	Greguss 1969
Icacinoxylon sp.1	Wood	Potomac group	USA	93,9	Cretaceous	Albian-Cenomanian	Rejected	Herenden 1997
Icacinoxylon sp.2	Wood	Asen	Sweden	72,1	Cretaceous	Santonian-Campanian	Rejected	Herenden 1997
Icacinoxylon sylvaticum (Tuzon) Greguss	Wood	Ipolytarnoc	Hungary	15,97	Miocene	Burdigalian	Rejected	Tuzson 1906, Greguss 1969
Icacinoxylon aff. sylvaticum (Tuzon) Greguss	Wood	Grateloup	France	28.1	Oligocene	Stampien	Rejected	Duperon 1976
Icacninoxylon cantleyoides Gottwald	Wood	?	Belgium	83,6	Cretaceous	Santonian	Rejected	Gottwald 2000

Icacinicarya budvarensis from the Santonian of Germany has nodulose ornamentation, not common in the modern Icacinaceae family, and a shape also not found in extant species of Icacinaceae. Moreover, the description is not sufficient (e.g., the inner endocarp and the wall are partially not described). Therefore, we choose to consider this species as rejected.

Icacinicarya papillaris resembles much more to an Icacinaceae especially belonging to the *Iodes* genus, but the preservation seems to be insufficient to assign this species to a particular genus. We consider this species as dubious with regard for the rough ornamentation and the absence of the papillae on the inner endocarp surface.

Finally, *Iodes germanica*, from the Maastrichtian of Germany, seems to have all the *Iodes* diagnostic characters (reticulate ornamentation, papillae on the inner surface, vascular bundle in one side on the endocarp wall). Despite the lack of revision and a good illustration (Manchester, 2015), we decided to accept this last species as Icacinaceae member based on the initial quite complete description.

Icacinicarya sp. (Chester, 1955) is rejected for this paleogeographical reconstruction because of the doubtful age of the Nigeria outcrops. Chester writes “Maastrichtian?” for this specimen in locality and horizon part. Considering the importance of species from Cretaceous in paleogeographical reconstructions, we decided to not take the risk to include this specimen, not formerly described as a species by the author.

Icacinicarytes corruga lacks anatomical details and is based on a single unusually large specimen (38 mm x 28 mm). In addition, the morphology of this specimen seems to be difficult to interpret, in particular the ornamentation. We consider it as dubious.

Icacinicaryites israelii from the Early Maastrichtian of Israel was a controversial species. Some authors disputed the attribution of this specimen to the *Iodes* genus (Stull et al., 2016, Del Rio et al., 2018). In fact, this specimen lacks the anatomical detail needed to assign it. The potential inner cotyledon discussed in the original article (Soudry & Gregor, 1997, Figures 4, 8, 9) seems to be an internal fracture of the fossil. We decided to place this fossil in a more appropriate genus: *Icacinicarytes*. The specimen proposed is bilateral, slightly compressed laterally, asymmetrical at the apex and reticulate at the surface. All these characters could be a clue for an Icacinaceae assignment. However, the reticulation pattern seems to be very orderly. The lack of anatomical detail and internal information (Unilocular? Anatropous?) led us to consider this species as very questionable.

Phytocrene microcarpa is rejected by some authors (Stull et al., 2012, Manchester et al., 2015). This species has an anatomy that cannot matches with the Icacinaceae family (Manchester et al., 2015). The shape and the size of the endocarp do not match with this assignation (Chapt. I). For this reason, we consider it as rejected.

VIII.2.2. Fossil leaves

The leaves from modern Icacinaceae s.s. are in general simple, entire, mainly pinnatifid with secondary brochydodromous venation and tertiary percurrent venation (Sleumer, 1971, Villiers, 1973, Utteridge et al., 2007, Allen et al., 2015 and personal observation). We have some notable exceptions: leaves from *Hosiea* and *Natsiatum* are toothed with craspedodromous secondary vein; some *Phytocrene* and *Pyrenacantha* species have palmate primary vein (*Phytocrene borneensis*, *P. bracteata*, *P. palmata*, *P. hirsuta*, *Pyrenacantha malvifolia*), tertiary veins are occasionally more reticulate as some species in *Casimirella*, *Desmostachys*, *Miquelia*, *Pyrenacantha*, and *Stachyanthus* general. These examples show the great diversity of cases in Icacinaceae family, probably due to various ecological adaptation (*Hosiea* is mostly a temperate genus), but also the weak variation in the majority of species. Nevertheless, the classical type of leaves for Icacinaceae family is common in flowering tropical plants, at least the trait of entire leaves (Bailey & Sinnott, 1916, Wolfe, 1985). Thus, diagnostic characters to identify Icacinaceae fossil leaves are very hard. This probably explains the poor record for the Icacinaceae leaves (only 13 occurrences). We choose to consider the leaves as dubious if no clear diagnostic characters are given.

The *Goweria* genus, attributed to Icacinaceae family by Wolfe (1977) and primarily to Menispermaceae (Wolfe, 1968) gather oval to lanceolate leaves with palmate primarily venation (in fact pinnatifid, see discussion in Allen et al., 2015), five primaries, brochydodromous secondary venation and percurrent tertiary vein. This diagnosis could correspond to Icacinaceae family but not only. Indeed, we found a similar type of leaves for at least the Metteniusaceae family (*Emmotum*, *Dendrobangia*, *Platea*, *Apodytes*, *Pittosporopsis*, personal observation). We decided to consider all *Goweria* species as dubious. *Goweria linearis*, in particular, seems to be very ambiguous (Wolfe, 1968). In fact, the specimen has a strong asymmetrical apex, which is uncommon in Icacinaceae species. In our opinion, *Goweria bluerimensis* is the most convincing assignation (Allen et al., 2015). These specimens possess expanded petioles with a narrow, resistant vascular strand that could be a diagnostic character.

Huziokaea eoutilus partially resemble to Icacinaceae, but are closer to the *Gomphandra* genus (Tanai, 1990), which is currently in Stemonuraceae family (Kårehed, 2001). The assignation of this extinct genus to Icacinaceae s.s is here considered as wrong.

Merrilliodendron ezoanum identification seems to be based on traits now shared by several families including Icacinaceae; we consider it as dubious.

The fossil record for *Phytocrene* leaves is composed of three species. However, *Phytocrene acutissima* from Alaska is represented by a partial fossil of leaves (Wolfe, 1977, Pl. 12, 1–6). *Phytocrene sordida* seems to be more convincing (MacGinitie, 1941) but the main traits correspond to the common characters discussed above for the *Goweria* genus. The author of this species notes the similarity between the fossil species and modern *Phytocrene blancoi* and *Hyperbaena hondurensis* (Menispermaceae) showing the ambiguity of the determination at the family level. Finally, *Phytocrene ozakii* is based on partial fossil (Tanai, 1990, Pl. 6) and no diagnostic characters are clearly used.

Both descriptions of *Pyrenacantha* sp. from Alaska and Japan are based on fragmentary material and are not considered other than dubious.

The genus *Icaciniphyllum* (not shown in Table 1.) was described for simple leaves, with a non-entire margin (undulate, crenulated, and irregularly dentate) and with a craspedodromous venation (Kvaček & Bůžek, 1995). These characteristics are rare in Icacinaceae family. In fact, only *Hosiea* and *Natsiatum* could roughly correspond to this description. Other genera have entire margin and brochidodromous venation. Then the affinity is probably wrong. Indeed, the type species *Icaciniphyllum artocarpites* (Ettingshausen) Kvaček & Bůžek is now considered as a member of *Sloanea* L., (Elaeocarpaceae), with invalidate the previous assignment (Kvaček et al., 2001, Allen et al., 2015).

To conclude, all fossil leaves are considered as dubious or as rejected for our paleogeographical reconstruction. We are convinced that some occurrences (e.g. *Goweria bluerimensis*) are adequately documented, however, we shown that main traits of leaves correspond mostly to the Icacinaceae s.l. are now shared by some more or less closely related families.

VIII.2.3. Pollen record

The fossil record of potential Icacinaceous pollen is low in term of species diversity but high in occurrences, especially in Europe. To our knowledge, only one pollen was considered as "*Iodes* type" in the USA (Leopold & MacGinitie, 1972). This specimen was not represented nor described so we rejected this occurrence. The two other occurrences outside Europe are from the Miocene of Cameroon (Salard-Cheboldaeff, 1975). *Echiperiporites minor* is described as a periporate (5) pores and echinulate pollen, which is apparently close to *Phytocrene* pollen. However, a re-examination of the original material (KWI-1 lame B, W35/W36) led us to recognize about ten pores (J. Dejax com. Pers.), which allow the rejection of this species, because no modern Icacinaceae pollen have more than eight pores (Lobreau-Callen, 1972). *Echiperiporites icacinoides* is described as three (4-5?) porate with echinulate pollen and could correspond to *Stachyanthus*, *Deptaulus* (*Leptaulus*?, Aquifoliaceae) and (mostly) *Iodes*. The original material is decayed and so we are waiting for its restoration.

In the *Compositoipollenites* genus, four species were related to the Icacinaceae family. Manchester (2015) considers that "*a comprehensive comparative investigation remains to be done with attention to other families that also share echinate pollen*", in order to confidently conclude about the affinity of these pollen specimens. We decided to follow the same caution and we used the dubious status for all *Compositoipollenites* pollen.

VIII.2.4. Wood record

The wood attributed to Icacinaceae possesses a wide occurrence and stratigraphy (100.5–5.3 Ma). Unfortunately, we are convinced that all occurrences do not correspond to Icacinaceae s.s. and we rejected them all. Indeed, Icacinaceae s.s. have simple perforation plates (Lens et al., 2008) whereas *Icacinoxylon* genus has scalariform perforation plates. The initial affinity of this fossil genus was made with *Citronella* genus, which is now in Cardiopteridaceae family (Stull et al., 2015). Finally, *Apodytoxylon hamamelidoides* have *Apodytes* affinity, which is now in Metteniusaceae family.

VIII.2.5. Summary of the Icacinaceae fossil record

To sum up, we accepted 86 occurrences (mainly from endocarps), considered 46 occurrences as dubious (mainly leaves and pollen species) and rejected 44 occurrences (mainly from the wood species). In the previous parts, we tried to justify the selection made for the paleogeography reconstruction. It has to be considered that all dubious species could be a false identification. We represent them in the following part in order to provide information about the *potential* range of the family, which could be a subject of discussion, only accepted species will be used in the ecological and biogeographic discussions.

VIII.3. Paleogeography reconstruction

VIII.3.1. Icacinaceae family

In this part, we propose a reconstruction of the paleogeography of the Icacinaceae s.s. (Fig. VIII.1). In this study, we used paleoclimatic reconstruction based on lithologic indicators (Boucot et al., 2013). In fact, this climatic ancestral reconstruction was based on the presence of some lithological remains, as the evaporates, which indicate an arid climate and the coal a moister tropical climate.

The occurrences of Icacinaceae all belong to a warm temperate or boreotropical and tropical climate except for the Paleocene Egyptian occurrence, which apparently belongs to an arid climate (*Icacinicarya youssefi*). The Northern Hemisphere, in particular Europe and North America areas, has almost all confident fossil occurrences (which could be a bias, see the sampling issue). We have only one occurrence for the Cretaceous period and the most of the occurrences are from the early and middle-late Eocene. The Oligocene record is very poor. We have relatively few dubious records showed in the different map, this kind of fossils generally co-occurred with accepted fossil.

In term of (accepted) species richness (Table 2.), only one species belongs to the Cretaceous period, 14 from the Paleocene, 58 from the Eocene (38 from the early Eocene and 24 from the middle-late) and only 2 species belong to the Oligocene epoch.

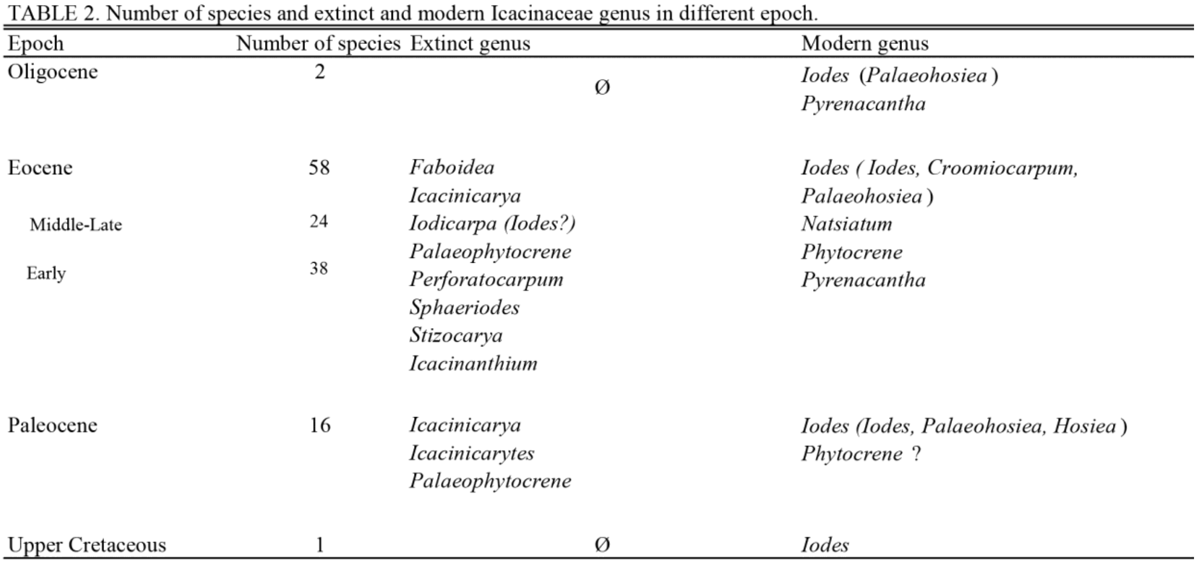

TABLE 2. Number of species and extinct and modern Icacinaceae genus in different epoch.

Epoch	Number of species	Extinct genus	Modern genus
Oligocene	2	Ø	*Iodes* (*Palaeohosiea*) *Pyrenacantha*
Eocene	58	*Faboidea* *Icacinicarya* *Iodicarpa (Iodes?)* *Palaeophytocrene* *Perforatocarpum* *Sphaeriodes* *Stizocarya* *Icacinanthium*	*Iodes (Iodes, Croomiocarpum, Palaeohosiea*) *Natsiatum* *Phytocrene* *Pyrenacantha*
Middle-Late	24		
Early	38		
Paleocene	16	*Icacinicarya* *Icacinicarytes* *Palaeophytocrene*	*Iodes (Iodes, Palaeohosiea, Hosiea*) *Phytocrene* ?
Upper Cretaceous	1	Ø	*Iodes*

We have records of *Iodes* from the Upper Cretaceous until the Oligocene. The *Phytocrene* genus appears in the fossil record during the Paleocene or during the Eocene. Some fossil of *Pyrenacantha* and *Natsiatum* were found during the Eocene, but only *Pyrenacantha* was present during the Oligocene. We have no other extant genera represented in the fossil record. No extinct genus is present during the Upper Cretaceous and during the Oligocene: All extinct records are found in the Paleogene, mainly during the Eocene epoch. Removing the unnatural genera (*Icacinicarya*, *Icacinicarytes*), we can consider only one extinct genus during the Paleocene and six genera from the Eocene.

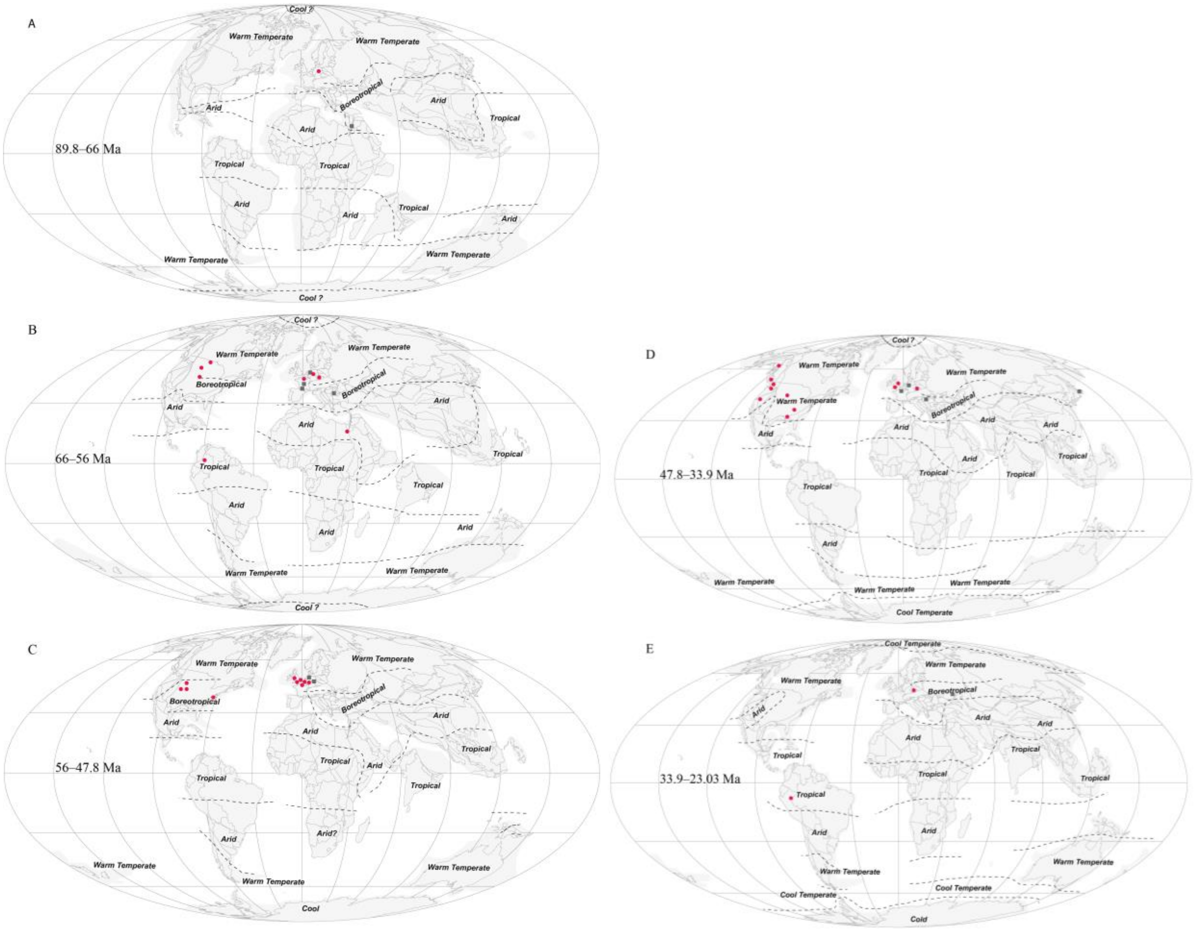

Figure VIII.1. Paleomaps showing the distribution of the Icacinaceae family in the fossil record. (A) Upper Cretaceous, (B) Paleocene, (C) early Eocene, (D) middle-late Eocene and (E) Oligocene. Red dots: accepted occurrence; grey squares: dubious occurrence. Paleomaps modified from Boucot et al., 2013.

VIII.3.2. *Iodes* genus

VIII.3.2.1. The *Iodes* record

In this part, we try to propose a reliable list of *Iodes* endocarp occurrences. In view of the number of cases with the lack of some characters, we choose to propose a decision table considering the presence or the absence of the three diagnostic characters for the *Iodes* genus (Table 3.). A review of the fossil record was made in the chapter V, which informally use this decision table. Therefore, we use the result of the chapter V here as a basis.

The *Iodes* fossil record is composed of 21 species. Four species occur in North America: *Iodes brownii*, *I. occidentalis*, *I. multireticulata*, and *Croomiocarpum missippiensis* and 17 occurs in Europe: *Iodes tubulifera*, *I. sinuosa*, *I. rivecourtensis*, *I. rigida*, *I. reidii*, *I. passiciensis*, *I. parva*, *I. multireticulata*, *I. hordwellensis*, *I. germanica, I. eocenica*, *I. corniculata*, *I. bilinica* and *I. acutiformis*, *Hosiea pterojugata*, *Paleohosiea suleticensis* and *P. marchiaca (*see Table 1. for epochs and sites considerations).

TABLE 3. Explanation of the decision in *Iodes* acceptance.

Ridges	Papillae	Vascular bundle inside the wall	Acceptation	Condition of acceptance or explanation of the reject
+	+	+	OK	Ø
+	?	+	OK*	*Potential taphonomic biais & common shape of *Iodes*
NO, other	+	+	NO	Could be close to *Iodes* the genus or inside the genus
+	+	?	NO	*Hosiea* have the same characteristics
+	?	?	NO	Other genera possible *Hosiea*, *Icacina*, *Rhyticaryum*
?	?	?	NO	Ø

Iodicarpa genus is cited as close to, or potentially included in *Iodes* (Allen et al., 2015, Stull et al., 2016) in having papillae and a vascular bundle embedded in the endocarp wall. Both diagnostic characters are only found together in *Iodes* genus. However, the size of the specimens (26–56 mm length, 20–35 mm width) and the presence/absence of ornamentation is unusual for the modern and fossil *Iodes* species. Indeed, only two modern species (*I. balansae* and *I. yatesii*) are as long as the species from *Iodicarpa*. In addition, these two modern species are less than 17 mm width. Among the current species, only *I. seguinii* has a smooth ornamentation and a vascular bundle in a gutter. We proposed that these two characters belong to the same developmental causes (see Chapter I). Thus, we do not have final evidence to include these species in *Iodes* genus. We consider -as in literature- this genus as closely related to *Iodes* or included inside with extinct ornamentation for the genus. Consequently, they are considered as dubious because the affinities are not permanently resolved.

An *Iodes* sp. from the Grès de Belleu was proposed in this thesis from a single specimen (see chapter VII). This fossil shows a clear vascular bundle inside the endocarp wall and reticulation but lacks of papillae. The specimen does not have cells preservation: the lack of papillae could be a taphonomic bias. In addition, the shape and the size of the specimen are clearly in favor of *Iodes* assignment. Thus, we consider this specimen as an accepted occurrence.

Some occurrences have been excluded from this study: an *Iodes* from the Miocene of Yunnan (China) was mentioned by Stull et al. (2014) but not formerly published; a second *Iodes* species from the Miocene of Turkey seems to have been studied but not published and not found in the MNHN collection of Paleobotany (De Franceschi & Dupéron, com. Pers.).

VIII.3.2.2. Paleogeography of the *Iodes* genus

In this part, we reconstruct the paleogeography of the genus *Iodes* (Fig. VIII.2). The occurrences all belong to a warm temperate and boreotropical climate (reconstructed from lithologic evidence, Boucot et al., 2013). The genus *Iodes* occurs during the Upper Cretaceous in Europe. During the Paleocene, only a species occurs from the European area with eight *Iodes* species in three sites (Table 4.).

TABLE 4. Number of species of the *Iodes* genus in different epoch.

Epoch	Number of species	Species with horn-like protrusions	Species without horn-like protrusions	NA
Oligocene	1	0	0	1
Eocene	17	11	6	
Middle-Late	5	3	2	Ø
Early	14	10	4	
Paleocene	8	6	0	2
Upper Cretaceous	1	0	0	1

At least, six species have horn-like protrusions whereas two are unknown. During the Eocene, especially the early Eocene, some species without horns appear in the record and the number of species significantly increases. Occurrences of *Iodes* in the USA begin during the early Eocene. A lower number of species occurs during the middle-late Eocene and only one species during the Oligocene in Europe.

VIII.4. Ecological and biogeographical interpretation

VIII.4.1. Age of the family

The age of Icacinaceae was estimated at 96.7 Ma with the help of molecular phylogeny (Magallon et al., 2009), but without using fossil or molecular data (?) from Icacinaceae. In another recent study, the estimated age was 104 Ma (Wikström et al., 2015). This analysis used 17 fossils calibration point, but from asterids and no Icacinaceae fossil record was included. In another molecular study, the estimated age is between 103 and 110 Ma with the maximum likelihood method and between 65.5 and 100.3 Ma with a Bayesian analysis (Magallon et al., 2015). This last publication used numerous fossils as calibration points and in particular three fossils attributed to Icacinaceae family: *Icacinoxylon alternipuncata*, *Icacinicarya papillaris*, and *Iodes germanica*. The *Icacinoxylon* genus was rejected in this review, and *Icacinicarya papillaris* was considered as dubious. Only *Iodes germanica* seems to be an unambiguous Icacinaceae fossil. The authors used 65.5 Ma as the age of calibration base on this record. Two reviews of the fossil record of asteridae were made (Martínez-Millán, 2010, Manchester, 2015), highlighting a Maastrichtian minimum age for the Icacinaceae family. In our review of the fossil record, 13 species belong to the Cretaceous epoch but only *Iodes germanica* is accepted. The minimum appearance age selected for the *Iodes* genus is 66 Ma (Upper Maastrichtian, following the International chronostratigraphic chart v2017/02).

According to the previous studies, we consider the Upper Maastrichtian as the minimum age given by the fossil record for the Icacinaceae family. However, the calibration point for future molecular studies could be more precise including this minimum age at the internal node *Iodes-Mappianthus* (Stull et al., 2015) rather than at the Icacinaceae divergence.

VIII.4.2. Major events

VIII.4.2.1. The Cretaceous-Paleogene extinction event

A major mass extinction occurred during the Cretaceous-Paleogene boundary probably due to meteoritic impact and volcanism that drastically changed the environment and climate (Alvarez et al., 1980, Hildebrand et al., 1991, Keller, 2012). This crisis of biodiversity mainly concerns marine (Raup & Sepkoski, 1982, Alroy et al., 2008) and terrestrial faunas (Longrich et al., 2011, 2012,). However, a rapid turnover in land plants is shown by the local extinction of dominant groups (Johnson, 2002, , Wilf & Johnson, 2004, McElwain & Punyasena, 2007, Mizukami et al. 2013, Vajda & Bercovici, 2014).

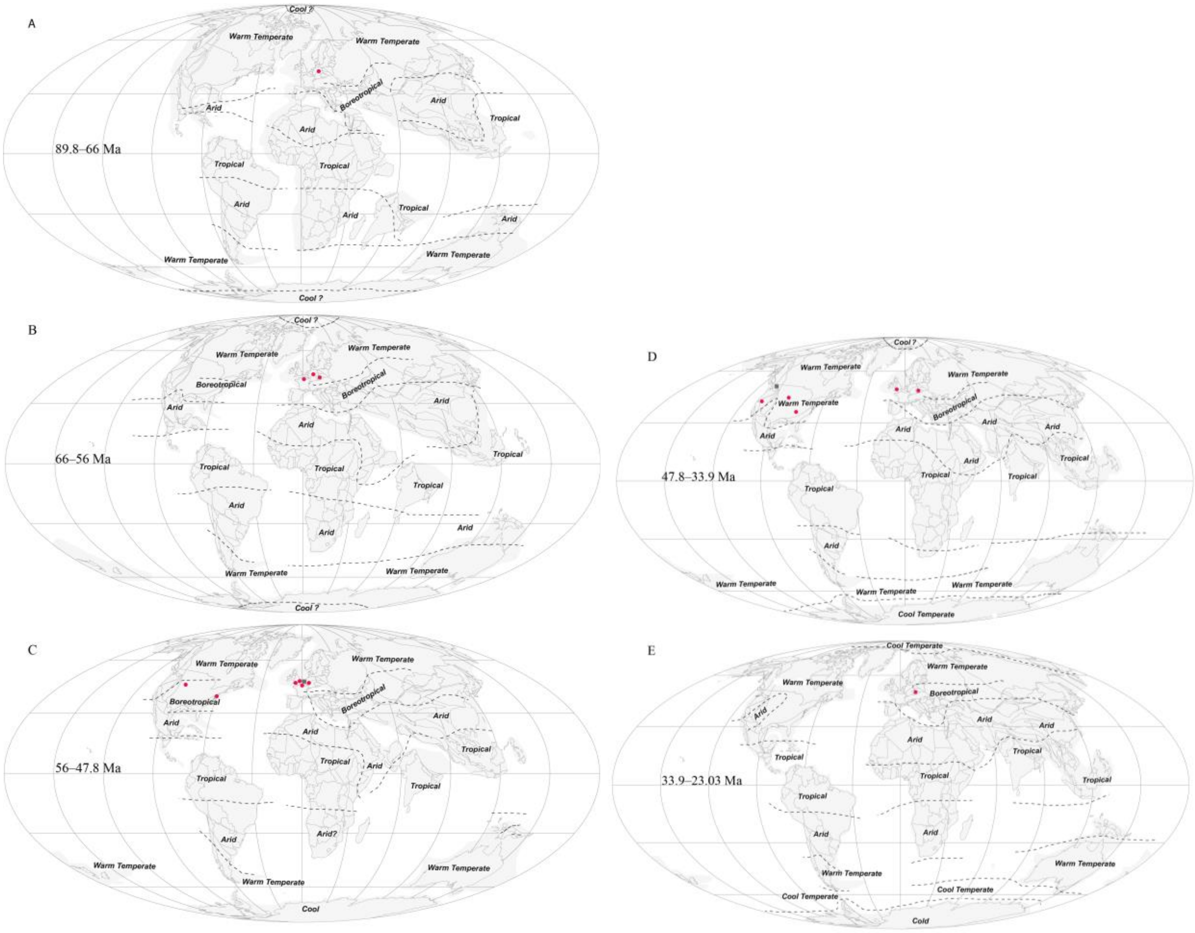

Figure VIII.2. Paleomaps showing the distribution of the *Iodes* genus in the fossil record. (A) Upper Cretaceous, (B) Paleocene, (C) early Eocene, (D) middle-late Eocene and (E) Oligocene. Red dots: accepted occurrence; grey squares: dubious occurrence. Paleomaps modified from Boucot et al., 2013.

Another study based at family level shows that the land plants did not suffer from global extinction (but local turnover) during the Cretaceous-Palaeogene boundary (Cascales-Miñana & Cleal, 2014). In Europe, the thermophilic Normapolles group dominated the flora during the Upper Cretaceous and then became extinct, and been replaced by the boreotropical or laurophyll vegetation during the Paleocene (Mai, 1989, Wolfe, 1975).

In our review, only *Iodes germanica* species from Europe occurs during the Upper Cretaceous, showing that the Icacinaceae family is present early in Europe. This species is found during the Upper Paleocene in Europe showing (if the species identification is correct) that at least this species crosses the Cretaceous-Palaeogene boundary and persists during the Paleocene in the same area. This could be a clue to the resilience of some family, which could explain the previous results (Cascales-Miñana & Cleal, 2014).

In addition, we show an increase of occurrences, genera, and species for the Icacinaceae family during the Paleocene and new occurrences out of Europe, mainly in North America, following the expansion of the boreotropical forest area. The *Iodes* genus seems to be limited to Europe as during the Upper Cretaceous, however, with seven new species described for the Paleocene epoch, we show an increase of species richness. All species of *Iodes* from Paleocene have horn-like protrusions and only differ for some precise traits. Most *Iodes* species are from the Thanetian, and it is difficult to assign this great diversity to the Cretaceous-Paleogene turn over which allow a new diversification of non-dominant families with new free ecological niches or to a subsequent global warming whose the acme will be the Paleocene-Eocene thermal maximum.

VIII.4.2.2. Paleocene-Eocene events

VIII.4.2.2.1. The Paleocene-Eocene Thermal Maximum (PETM)

The PETM was a period of increasing of temperature (Kennett & Stott, 1991, Zachos et al., 2001, 2008) due to massive and quick release of carbon in the atmosphere (McInerney & Wing, 2011, Wright & Schaller, 2013, Bowen et al., 2014). This event affected the marine fauna with at least a mass extinction of benthic foraminifera (Thomas, 2007) and perturbation of ostracodes and calcareous nannofossils (Speijer and Morsi, 2002, Gibbs et al., 2006, Agnini et al., 2007b, Bown and Pearson, 2009, Morsi et al., 2011). In terrestrial diversity, studies show less perturbation but migrations of the fauna (Godinot & de Broin, 2003, Gingerich, 2006) and rapid turnover but not catastrophic changes for plants (Cavagnetto, 2000, Wing et al., 2005, Collinson et al., 2009, Pigg & DeVore, 2009).

We show here a clear increase in Icacinaceae diversity during the early Eocene, in term of species, new genera and shapes. Among the 14 species from the Paleocene, only three species were found in the 38 early Eocene species, which show a turnover and increase of diversity in the Icacinaceae family. Two genera were more diverse, *Palaeophytocrene* and *Iodes*, which are probably climber species. This increase could be due to the new evergreen thermophilic flora highly diversified and favourable to climbers, flora that occurs during the PETM (Upchurch Jr & Wolfe, 1987, Collinson & Hooker, 2003). The *Palaeophytocrene* genus only has one species from Bogota during the Paleocene and eight species during the Eocene from North America and Europe. This could indicate a diversification and an expansion of the area of *Paleophytocrene* during the PETM, following the expansion of the megathermal vegetation. Indeed, a geological connexion between North and South America for the *Paleophytocrene* was proposed during the Paleocene (Stull et al., 2012). This connexion became possible by the renewal of the magmatic arc of the Northern Andes during the Paleocene-Eocene (Bayona et al., 2011, Cardona et al., 2011). Therefore, this genus shows a strong evidence of potential exchanges between tropical South America and boreotropical flora during this period. Changes during the PETM in North America could be partially due to flora immigration from South America followed by an immigration of these floras in Europe during the late Ypresian.

New shapes appeared during the end of early Eocene in Europe, as *Faboidea*, *Perforatocarpum*, *Sphaeriodes Stizocarya* and *Icacinanthium*, all of these genera are now extinct. Among the eight *Iodes* species from the Palaeogene, three were found from the early Eocene showing a partial but important change in Icacinaceae floristic composition. In particular, among the 14 species that occur during the early Eocene, four have no horn-like protrusions at the apex, whereas in the Paleocene, all *Iodes* species have it. In other words, we found new shapes and new endocarp organisations during the early Eocene. This new shape could be due to local diversifications or migrations of new floras from other areas.

All species from the Paleocene are in Europe, whereas at least three species of *Iodes* (one with horn-like protrusions, two without) are in North America during the early Eocene. The connexion between North America and Europe during the Paleocene and early Eocene was well-documented (Wolfe, 1975, Manchester, 1994, 1999). This connexion remains possible via the North Atlantic land bridge (McKenna, 1975, Tiffney, 1985) and following the extension of the boreotropical forest in link with the warmer climate. The migrating direction of exchanges (Asia-North America-Europe or Asia-Europe-North America) was intensively discussed in mammal palaeontology (Godinot & de Broin, 2003, Smith et al., 2006, Beard, 2008). Here, we have clues for an exchange from Europe during the early Eocene. In fact, all species with or without horn-like protrusions are older in Europe than North America. However, an *Iodes multireticulata* specimen, dated from 55.5 Ma was found in the USA, the occurrence of this species in Europe was dated to about 51 Ma (Reid & Chandler, 1933, Tiffney, 1999). Nevertheless, we suspected that the assignment of specimens from the Fisher/Sullivan site by Tiffney was probably overestimated. In fact, at least the size of the specimens from Fisher and London Clay site is clearly distinctive. We show that the size of the endocarps could be used to differentiate modern species when it exists a clear gap between the sizes within species (see Chapter I). This is here the case. With *Iodes* and *Paleophytocrene*, we have in consequence two examples of interchanges North America and Europe, showing that the dispersion of floras was bilateral.

VIII.4.2.2.2. Middle and late Eocene

Due to particularly warmer climate, the widest fossil extension of the Icacinaceae (in term of species richness and probably area) was reached during the early Eocene. However, this is from the middle-late Eocene that we found the fossil records in modern genera as *Natsiatum* (Stull et al., 2011), *Phytocrene*, at first in Europe and then in the USA (Stull et al., 2011, Collinson et al., 2012) and *Pyrenacantha* (Manchester, 1994). Therefore, this is probably during the Eocene that the main modern genera appeared and diversified. In the *Iodes* genus, we show only a slight change of proportion between endocarp specimens with or without horn-like protrusions and less species richness during the middle-late Eocene. These "species richness regression" could be attributed to the cooling climate (Collinson et al., 1981, Keller, 1983, Zachos et al., 2008), what Tiffney called a "*climatic deterioration*" (Tiffney, 1985). This climate induced a change in floral structure, less favourable to the climber species (Collinson & Hooker, 2003).

VIII.4.2.3. The Oligocene cooling

In the Oligocene-Eocene boundary, the climate was probably the coolest of the Palaeogene and remained cold throughout the Oligocene. (Zachos et al., 2001, 2008). The boreotropical flora regressed and the deciduous vegetation, with less diversity, expanded (Tiffney, 1985). In our study, only two occurrences of Icacinaceae were found during the Oligocene. This result shows an important decrease of diversity in the fossil record and is consistent with a regression of the boreotropical forest. There are only two modern genera represented, *Pyrenacantha* and *Iodes*. The species *Pyrenacantha austroamericana* was from the Oligocene of Peru (Stull et al., 2012). The oldest fossil remain of this genus is *Pyrenacantha occidentalis* of Lutetian age from North America (Manchester, 1994). Thus, these two species show a connexion between North and South America during the Eocene. In the other side, the *Iodes* species are from Europe. This species allows considering the *Iodes* genus as being present in Europe through the Palaeogene. This genus was probably part of a remain of the boreotropical forest, which is almost completely replaced in Europe by cold-tolerant species during the Neogene. (Tiffney, 1985, Wolfe, 1985, 1975).

VIII.4.3. Comparison with the history of other angiosperm families

Our results are in accordance with the boreotropical regression hypothesis (Lavin & Luckow, 1993). In particular, a study establishes a disjunction of 65 genera between North America and Asian flora, which occurs during the Miocene (Wen, 1999). This pattern could be explained by an expansion of a boreotropical flora during the Paleocene and Eocene and a high regression during the Neogene.

Some families were considered as closely associated with the boreotropical flora and in particular the Icacinaceae and Menispermaceae (Wolfe, 1975). These two families have in common a majority of species with a climber habitus and a similar present distribution. Thus, we can hypothesize that both families could have a similar history in link with the boreotropical expansion and regressions. A fossil history of the Menispermaceae was proposed (Jacques, 2009a). The Menispermaceae appears during the Paleocene in the fossil record (recorded from Cretaceous but dubiously), diversifies during the Eocene and then regresses during the Oligocene in Europe and North America. In particular, the maximum of diversity was found during the PETM event. A new species of Menispermaceae, *Sinomenium macrocarpum* Liu et Jacques, was found after this review from the Miocene of North America (Liu & Jacques, 2010). However, this is probably a late refuge of the boreotropical flora. New studies show Menispermaceae in South America during the Paleocene (Herrera et al., 2011, Jud et al., 2018). This discovery reveals a complex relationship between North and South America during the Paleocene. We found the same pattern for the Icacinaceae family during the Paleocene (Stull et al., 2011).

In the Vitaceae family, also a climber family, the oldest known fossil found is from India before the continental collision (Manchester et al., 2013), followed by a rapid widespread during the Paleocene and Eocene in Northern Hemisphere. Other routes of dispersion have been highlighted from South America (Manchester et al., 2012). In addition, a study on *Parthenocissus* (climber) genus shows a disjunction between Asia and North America in the Early Miocene, which is congruent with the boreotropical regression (Nie et al., 2010, 2012).

Some other evidence of expansion during the Paleogene and regression/extinction of tropical floras in some areas (mainly North America and Europe) during the Neogene are found for the *Paliurus* genus (Rhamnaceae), Sabiaceae family, *Canarium* (Burseraceae), *Deviacer*, Ulmaceae, *Carya* (Juglandaceae), Sapindaceae and *Anacardium* (Anacardiaceae), (McClain & Manchester, 2001, Manchester et al., 2007, Burge & Manchester, 2008, Wang et al., 2013, Zhang et al., 2013, Chen & Manchester, 2015, Jia et al., 2015, Han et al., 2018). Therefore, the results in the dynamic of flora on the Menispermaceae and other families are very congruent with what we found in the Icacinaceae family.

VIII.4.4. Sampling issue

The fossil record depends on available outcrops, search efforts, and findings. Here we took into consideration a majority of species from North America and Europe. This is probably due to a most important search effort in this area than others in palaeobotanical history (Morley & Dick, 2003). Indeed, Icacinaceae fossils were recently found from Paleocene-Miocene range in South-America (Stull et al., 2012). The palaeobotanical studies of the South-America area were in general intensive in the last ten years (Herrera et al., 2011, 2014, Jud et al., 2016, Pérez-Consuegra et al., 2017, 2018), and reveal a new diversity, and new biogeographical hypotheses. The number of outcrops with Icacinaceae for each epoch is also different. For example, only one locality is known for the Cretaceous, nine localities for the Paleocene, 25 localities for the Eocene (16 for the early Eocene, 10 for the middle-late Eocene) and two localities for the Oligocene. It is difficult to see if this result is due to a lack of Icacinaceae species in some localities during some epochs (the Icacinaceae family would then be clearly rare or absent) or if it is a lack of outcrops available or directly connected/linked to the search effort. We cannot exclude that the differences in a number of species across the Paleocene-Eocene period could be partially due to a bias in the number of localities. However, this conclusion does not change the remarkable diversity of shapes and genera of Icacinaceae in the Eocene rather than Paleocene.

Another issue for Icacinaceae family is the dominance in the fossil record of the climbing genera. This kind of habitus is well developed in the banks of the rivers or in the channels. We know that the litter represents much more a local than the regional vegetation (Burnham, 1989, Burnham et al., 1992). For this reason, climber abundance could be a taphonomic bias.

VIII.5. The contribution of Icacinaceae from the Paris Basin

With nine new species, the Icacinaceae from the Paris Basin significantly increase the fossil record: + 8.2 % of Icacinaceae fossil species (+ 9.5 % if we removed the rejected species) and + 44.4 % for *Iodes* fossil species. This new fossil diversity approves the recognition of a partial continuity in the Paleocene-Eocene vegetation in Europe, which were not clearly shown before. In fact, the shared taxa between two epochs are scarce in the fossil record. In the Paris Basin, *Iodes parva*, *I. reidii* and *I. tubulifera* are present in the Paleocene and early Eocene epochs. This could be due to the proximity of the deposits and age of the sites that are close. The *Iodes* history presented here considers the presence or absence of the horn-like protrusions. In the Paris Basin, we probably have the oldest *Iodes* fossil carrying these horns, which indicates the likely movement of the *Iodes* genus during the PETM. Finally, the flower in amber, *Icacinanthium tainiaphorum*, adds for the early Eocene an extinct genus and contributes to the hypothesis that the early Eocene was a key period for the diversification of the Icacinaceae.

Conclusion of the chapter

Among the 178 occurrences previously described as Icacinaceae, only 86 were accepted as belonging to this family in this study and are mainly from endocarp remains. We consider four species from North America and 17 from Europe as belonging to the *Iodes* genus. With this sampling, we show an increase of the species richness during the Paleocene, but it is difficult to consider this increase as linked to the recovery after the Cretaceous-Paleogene or to the increase of temperature during the Thanetian. A great increase of diversity in term of genera, species, and morphology is shown through the Paleocene-Eocene boundary and during the Ypresian. Exchanges were shown between North America and Europe during the PETM in both ways. This is during the middle and late Eocene that most of the modern genera appear in the fossil record as *Natsiatum*, *Phytocrene*, and *Pyrenacantha*. Finally, the cooling period during the Oligocene, less favourable to climbers, could explain the decrease in the diversity of the Icacinaceae in the fossil record. We show the same pattern of diversification and regression in other megathermal families (Menispermaceae, Vitaceae…) showing that the Icacinaceae fit with the dynamic of the North Hemisphere forest (boreotropical sensu. Wolfe, 1975) during the Paleogene. The fossils studied in the Paris Basin add new diversity to the *Iodes* genus. In particular, this new fossil diversity agrees with the recognition of a partial continuity in the Paleocene-Eocene vegetation in Europe in species level, which was no clearly shown before.

Chapter IX

Age and biogeography of extant Icacinaceae

Icacinaceae Miers is an angiosperm family, with a pantropical distribution (Perrier De La Bâthie, 1952, Villiers, 1973, De Roon, 1994, Peng & Howard, 2008). This family, which contained 58 genera in its greatest extension (Sleumer, 1942), was the subject of intensive phylogenetic works in the past decades. It has been shown in particular that the Icacinaceae Miers family sensu Sleumer was not monophyletic (Kårehed, 2001). New studies including molecular and morphological data (Lens et al., 2008) or molecular data alone (Byng et al., 2014) precise the delimitation of this family. Recently, a new molecular phylogeny of the basal lamiids led to new limits and position of the Icacinaceae family and defined the Icacinaceae s.s. as including four major clades and 23 genera (Stull et al., 2015). This study was included in the update of the Angiosperm Phylogeny Group (APG, 2016).

The Icacinaceae were also intensively studied by paleobotanists. Indeed, occurrences of Icacinaceae during the Palaeogene are abundant, especially in North America (Manchester, 1994, Pigg et al., 2008, Rankin et al., 2008, Stull et al., 2011) and Europe (Reid & Chandler, 1933, Chandler, 1954, 1961a, 1961b, 1962, Knobloch & Mai, 1986, Collinson et al., 2012, Del Rio et al., 2017). This family was used in order to characterise the boreotropical forest (Wolfe, 1975), which corresponds to an ancient widespread flora that occurred during the Paleocene and Eocene periods in the Northern Hemisphere. Some groups of this ancient flora can be still found in modern tropical areas, like the Indomalayan realm, considered as refuge during the Oligocene and Neogene cooling.

Therefore, the Icacinaceae biogeography seems to be linked to the biogeography of the boreotropical flora. Recent fossil studies of this family (see Chapt. VIII) attempt to reconstruct this history in the light of recent fossil findings and new considerations on the phylogenetic circumscription of the family. These previous works select the fossils with a correct assignation (rejecting all fossil wood, for example, Lens et al., 2008). Nevertheless, no attempt at a biogeographic analysis was made using the molecular data.

In this work, we try to (1) date the Icacinaceae family, using relevant fossils, (2) propose a biogeographic reconstruction and interpretation of this group and (3) study the impact of the PETM on this biogeographic history.

IX.1. Material and method

IX.1.1. Molecular dating

We used the most complete molecular data for asterids clade focusing on the Icacinaceae (Stull et al., 2015). For this analysis, we removed Icacinaceae outgroups except for *Platea latifolia*, *Garrya flavescens* and *Oncotheca balansae*. Furthermore, we kept only two species for genera *Pyrenacantha* and *Iodes*, leading to a total of 26 accessions. Only 11 partitions were retained to favour a rapid convergent analysis corresponding to the following gene units: accD, atpA, atpH, matK, ndhB, psaB, psbEn rbcL, rpl14, rpl2 and rpl20 for a total of 11149 pb. These partitions were selected for the completeness of each gene and the presence of these genes in the sequences used here. Indeed, the reductions of partitions do not change significantly the result (Foster et al., 2016).

Molecular dating was based on five fossils calibration points: 66 Ma for *Iodes* node with *Iodes germanica* Knobloch and Mai fossil (Knobloch & Mai, 1986; Mai, 1987), 56 Ma for the clade IV with *Icacinanthium tainiaphorum* Del Rio and De Franceschi (Del Rio et al., 2017), 47 Ma for the *Phytocrene* node with *Phytocrene punctilinearis* Collinson, Manchester and Wilde (Collinson et al., 2012), 43 Ma for the *Pyrenacantha* node with *Pyrenacantha occidentalis* Manchester (Manchester, 1994) and 38 Ma for the *Natsiatum* node with *Natsiatum wilcoxiana* (berry) Stull, Moore and Manchester (Stull et al., 2011).

We modelled the ages of the corresponding node by a uniform prior (Sauquet, 2013) with a lower range corresponding to the fossil dating and the maximum age corresponding to 128 Ma, the first occurrence of tricolpate pollen, commonly used to justify the maximum age inside eudicots (Bell et al., 2005, Magallón & Sanderson, 2005, Magallón & Castillo, 2009, Wikström et al., 2015). We used the software BEAST v.1.8.3 (Drummond et al., 2012) with an uncorrelated lognormal relaxed clock approach, a substitution model GTR+ I+ G and a speciation as Birth-Death Process was employed as tree prior (Gernhard, 2008). Two analyses with four Markov Chain Monte Carlo (MCMC) analyses were run for 40 million generations and sampled every 1000 generations. The convergences of chains were confirmed with the software Tracer v. 1.6 and the adequate Effective Sample Sizes (ESS>200) were verified. All chains were combined using the software LogCombiner v1.8.3, after discarding the first 20% generations as burn-in. The maximum clade credibility tree was used to combine trees by the software TreeAnnotator v1.8.3 and visualized with the software FigTree 1.4.2. Error bar corresponds to 95% Highest Posterior Densities (HPD).

IX.1.2. Biogeographic analyses

Five biogeographic areas have been delimited as following (Fig. IX.1): (A) Africa, (B) Madagascar, (C) Asia, (D) South America, (E) Oceania (New Caledonia) and (F) North America. In our Icacinaceae sampling, 11 (45.8%) species belong to Asia, seven (29.2%) to Africa, three to South America (12.5%), two to Madagascar (8.3%) and one to North America (4.1%). The representativeness of our sampling is consistent with the distribution of the Icacinaceae family. Africa, as well as Madagascar is slightly less represented.

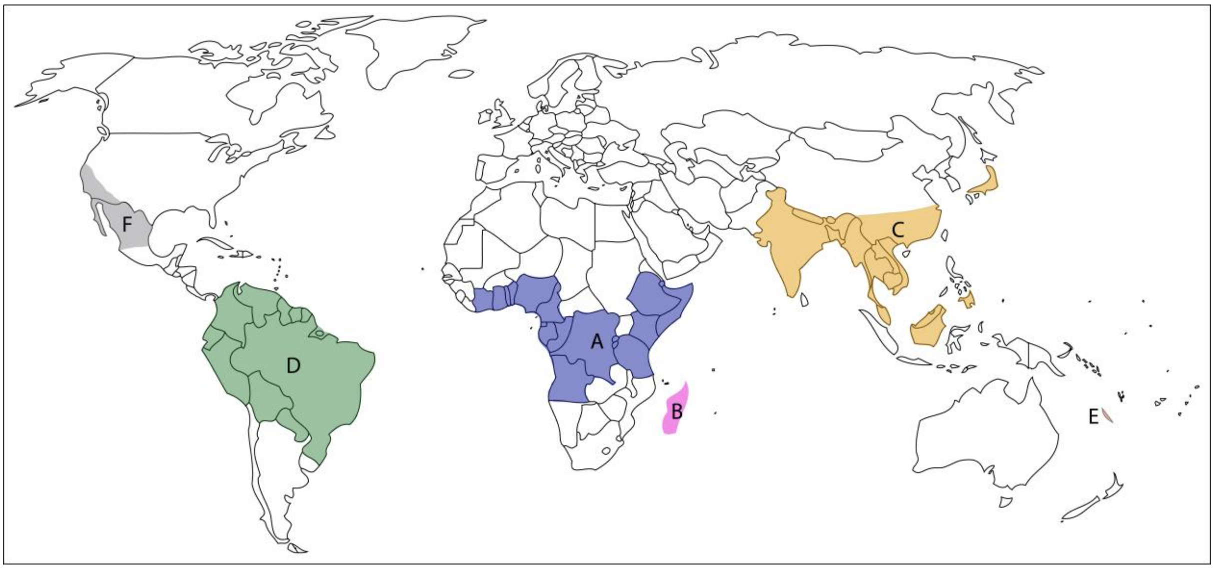

Figure IX.1. Distribution of species and biogeographic area defined for this study (A) Africa, (B) Madagascar, (C) Asia, (D) South America, (E) Oceania, (F) North America.

We implemented two methods of biogeographic reconstruction. The Statistical-Dispersal Vicariance analysis (S-DIVA, Yu et al., 2010) is a method developed from DIVA (Ronquist, 1997), it allows us to use the trees made by BEAST (in our case, 7000 random trees) and to consider the phylogenetic uncertainty. We authorized the reconstruction for up to three areas occupied by a species, in order to limit the reconstruction of large areas. Indeed, no modern species occur in three areas. The second method, Dispersal, Extinction, and Cladogenesis (Ree and Smith, 2008) was used to reconstruct the ancestral areas. This method infers fewer vicariances compared to S-DIVA. We also allowed the reconstruction of three areas occupied by these species. It is interesting to compare these two methods in order to increase the strength of the biogeographic hypothesis (Kodandaramaiah, 2009). These two methods were implemented in the software Rasp 4.0 (Yu et al., 2015).

IX.2. Results

IX.2.1. Temporal origin

The resulting topology is similar to the tree previously reconstructed (Stull et al., 2015). The topology is, however, better resolved in the BEAST analysis for *Alsodeiopsis* and *Pleurisanthes* genera (sister group of the Clade II), but it is rather a constraint of the method used than a better resolution result.

The divergence of the Icacinaceae family is dated from about 122.3 Ma (112.1-128), during the end of the Lower Cretaceous (Fig. IX.2). *Cassinopsis* might have diverged from the rest of the Icacinaceae family early, from 116.6 Ma (105.2-126.2), whereas the Icacinoideae group (Icacinaceae excl. *Cassinopsis*) first diversified during the Early Upper Cretaceous (96.3 Ma, 83.9-108.9). The four major clades seem to diversify during the Campanian and Maastrichtian (Upper Cretaceous) except the clade I, which diversifies during the Oligocene (32.5 Ma, 6.8-64.3).

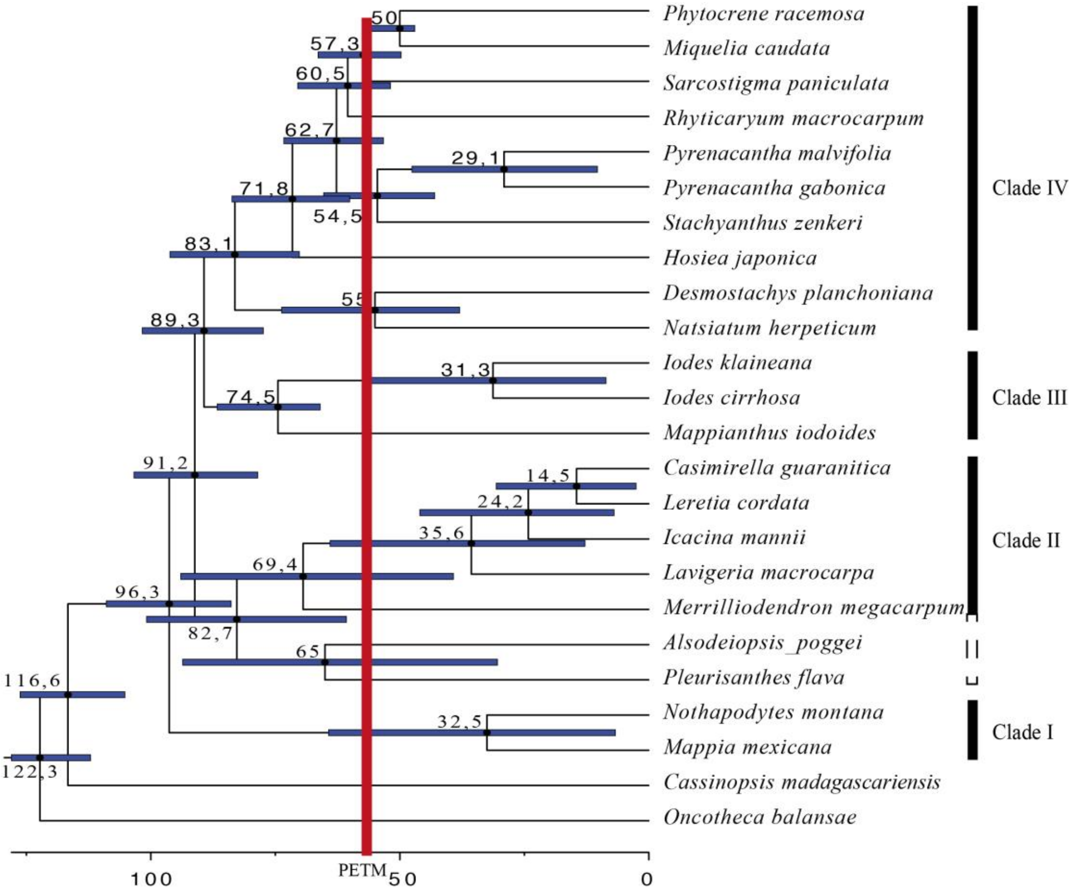

Figure IX.2. Chronogram of the Icacinaceae family made by BEAST 1.8.3 with five fossils calibrations and using a molecular matrix with 11 partitioned genes (accD, atpA, atpH, matK, ndhB, psaB, psbEn rbcL, rpl14, rpl2 and rpl20). Node value = Mean age. Bar= 95% HPD.

The mean age of divergence estimated for the genera are as following: end of Cretaceous for four genera (*Hosiea*, *Iodes*, *Mappianthus* and *Merrilliodendron*), Paleocene for four genera (*Sarcostigma*, *Rhyticaryum*, *Alsodeiopsis* and *Pleurisanthes*), Eocene for seven genera with six from the Ypresian (*Phytocrene*, *Miquelia*, *Pyrenacantha*, *Stachyanthus*, *Desmostachys*, *Natsiatum*) and one for the Priabonian (*Lavigeria*), Oligocene for three genera (*Icacina*, *Nothapodytes*, *Mappia*) and finally Miocene for two genera (*Casimirella*, *Leretia*). Nine nodes are compatible with the PETM event including the ancient Phytocrenae tribe and the Clade II.

IX.2.2. Spatial origin

The reconstruction of ancestral areas, performed with S-DIVA (Fig. IX.3) and DEC (Fig. IX.3 in red when different) are shown. First, we highlight that the S-DIVA and DEC methods give the same result except in four cases (Fig. IX.3). This global congruence in both methods increases the confidence in the ancestral reconstruction result. S-DIVA method reconstructs 10 dispersions and 10 vicariances whereas DEC method reconstructs 13 dispersions and 10 vicariances.

The reconstruction of the ancestral area (Table 1.) of the Icacinaceae family is located in Asia-Madagascar, (according to S-DIVA) but located only in Asia according to DEC. The Icacinoideae group area reconstruction ends in Asia. In this group, the reconstruction of the ancestral area for the Clade I is Asia and North America, the Clade II is Africa and Asia, the Clade III and IV are both Asia. The reconstruction of the ancestral area for the ancient Phytocreneae tribe (*Rhyticaryum*, *Phytocrene*, *Miquelia*, *Sarcostigma*, *Pyrenacantha* and *Stachyanthus*) is Asia and Africa.

Table 1. Molecular dating of Icacinaceae infered by beast and ancestral area estimation from S-DIVA and DEC model implemented by RASP 4.0.

Taxon of interest	Mean estimated date (95% HPD)	S-DIVA	DEC
Icacinaceae	116.5 (112.1-128)	BC (1)	C (0.62), BC (0.38)
Icacinoideae	96.3 (83.9-108.9)	C (1)	C (0.87), CF (0.13)
Clade I	32.5 (6.7-64.3)	CF (1)	CF (1)
Clade II	69.4 (39.3-94)	AC (1)	AC (0.64), CD (0.19), ACD (0.17)
Clade III	74.5 (66-86.7)	C (1)	C (1)
Clade IV	83.1 (78.5-103.3)	C (1)	C (1)
Phytocreneae	62.7 (53.3-73.3)	AC (0.6), C (0.4)	AC (0.86), C (0.14)

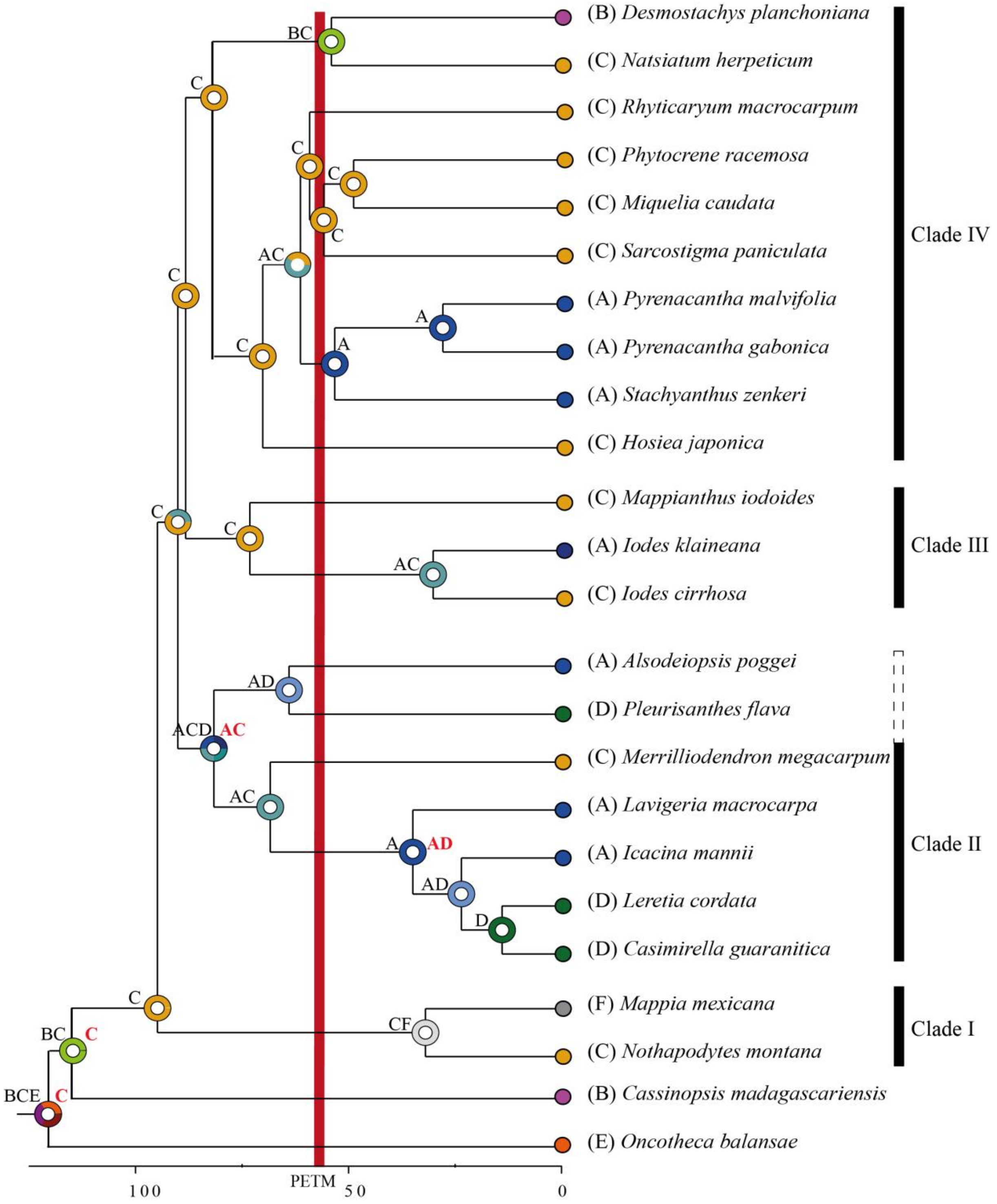

Figure IX.3. Ancestral areas estimations for Icacinaceae family. The geographic distribution of species as coded in Rasp4.0 is bracketed before the species names. Each geographic reconstructed area is indicated by a coloured circle and a letter showing the most likely ancestral state: (A) Africa, (B) Madagascar, (C) Asia, (D) South America, (E) New Caledonia and (F) North America. Ancestral areas were estimated using S-DIVA (result presented here) and DEC models (in red when the reconstruction is different), both implemented in Rasp 4.0.

IX.3. Discussion

IX.3.1. Temporal datation

The temporal datation of the Icacinaceae emergence was attempted before, but in analyses at the angiosperm and asterid levels. Indeed, the Icacinaceae stem was dated to 96.7 Ma in a study on the diversification of the angiosperms (Magallón & Castillo, 2009). Another recent study centred in the asterid reconstructs the date of the stem Icacinaceae at 104 Ma (93-114) (Wikström et al., 2015). There is however no mention of fossil constraints for the Icacinaceae group in these studies. An update of the time calibrate of the angiosperm group gives a mean stem age at 69.3 Ma (65.5-100.3) (Magallón et al., 2015). This study uses three fossils of Icacinaceae with only one remain accepted (*Iodes germanica*, see Chapt. VIII).

Our results based on five fossils for the calibration show a stem age older than in other studies (122.3 Ma, 112.1-128), but compatible with Wikström et al.'s (2015) reconstruction. The result of the different analysis converges to an end of the Lower Cretaceous-begin of the Upper Cretaceous age for the divergence of main clades. The Icacinaceae is now sister to all other Lamiidae (Stull et al., 2015, APG, 2016). This new phylogenetic assignation is congruent with an old age of the Icacinaceae family, close to the early diversification of the eudicots.

The divergence of the Icacinaceae occurs early with the *Cassinopsis* genus that seems to diverge from the end of the Lower Cretaceous. This early divergence could explain the difficulties to resolve the position of this genus (Stull et al., 2015). In addition, this age could explain the differences in morphological characters between this genus and other Icacinaceae genera: the *Cassinopsis* genus alone has scalariform perforation plates (Lens et al., 2008) in the wood, a flower with stamens adnate to the petals (Del Rio et al., 2017) and the endocarp wall with homogeneous isodiametric cells (see Chapter I.). The diversification of Icacinoideae and other major clades occurs during the Upper Cretaceous, which is in accordance with the rapid radiation of the angiosperm group during this warmer period (Niklas et al., 1983, Knoll, 1986, Friis et al., 1987, Wang et al., 2013).

Nevertheless, the divergence of main modern genera is dated from the Cenozoic period. In particular, six genera diverge during the Ypresian period, which seems to be the peak of diversification for the Icacinaceae genera. This result is in accordance with fossil finding. Indeed, the fossils remains from the Ypresian period are the most abundant in term of species and genera's richness. The Paleocene-Eocene Thermal Maximum, a time period of sudden increase of temperature (Zachos et al., 2001, McInerney & Wing, 2011), favours the development of a thermophilic flora rich in climbers (Upchurch Jr & Wolfe, 1987, Collinson & Hooker, 2003). It is noteworthy that all genera, which diverged during the Ypresian, are now climbers or scrambling shrubs.

IX.3.2. Spatial origin

The Icacinaceae family has an Asian origin during the end of the Lower Cretaceous. However, this area, defined as in Fig. IX.1 has no sense during the Cretaceous period, the lower Asian latitude being arid. Actually, the climate was warm temperate to boreotropical (Boucot et al., 2013) in Eurasia, favourable to the development of this family. Therefore, there is no reason to consider the Icacinaceae as restricted to the "North" Asia zone, but rather that this family followed the climatic zone reconstructed by lignitic evidence, which covered Eurasia. In addition, we have evidence of the presence of Icacinaceae during the Upper Cretaceous in Europe (Knobloch & Mai, 1986), which add a strong evidence of Eurasian origin area for the Icacinaceae.

During the beginning of the Upper Cretaceous, a group containing the clade III and IV diversified, probably in this Eurasian area whereas another group with the Clade II disperse from Eurasia to Africa. The increase of warm climate in Eurasia (Niklas et al., 1983) could be at the origin of diversification of habitus and in particular to the radiation of the climber group in situ (Clade III and IV). A connection between Eurasia and Africa is yet possible during the Upper Cretaceous, with a subsequent separation of the two areas during the early Cainozoic probably following the expansion of the Tethysian Ocean (Morley, 2000, 2011, Gheerbrant & Rage, 2006).

During the Paleocene, but more intensively during the early Eocene, the Icacinaceae diversification results from a radiation in situ, with a strong diversification of the climber Clade IV in parallel in Africa and in Eurasia. However, there are some evidence of the expansion of the boreotropical flora, including Icacinaceae, in North America during the Paleocene and Eocene (Reid & Chandler, 1933, Knobloch & Mai, 1986, Manchester, 1994, Collinson et al., 2012). This connection with North America remains possible by the North Atlantic land bridge (McKenna, 1975, Tiffney, 1985). Therefore, what we named Eurasia could be more related to a North Hemisphere area during the Palaeogene. We can conclude that the rapid diversification occurred more in the North Hemisphere and Africa during the Paleocene and Eocene, which concurred with the diversification of fossils (see Chapter VIII). This is congruent with the hypothesis of a new thermophilic flora more diverse and containing more climbers during the PETM (Collinson & Hooker, 2003, Upchurch Jr & Wolfe, 1987).

The North African area was arid during the Paleocene-Eocene, and the absence of interchange between North Hemisphere and Africa could be due to this climatic dispersal barrier first, in addition of the Thetys' expansion.

Desmostachys seems to disperse from Asia to Madagascar in our reconstruction during the Early Eocene. This may be linked to the Indian drift during the Cretaceous-Early Eocene (Chatterjee & Bajpai, 2016). However, we have no strong hypothesis about this case.

Finally, we do not reconstruct a diversification in South America during the Palaeogene, despite the recorded fossils (Stull et al., 2012). In fact, the fossil record shows potential interchanges between North and South America during the Paleocene and Eocene. In particular, the modern genus *Phytocrene*, which is now endemic to the Asian area, is probably found in the Columbian Paleocene (Stull et al., 2012). Other *Phytocrene* fossils were found during the Eocene in the USA and in Germany (Stull et al., 2011, Collinson et al., 2012). This genus has a Northern Hemisphere and South American areas during the Paleocene-Eocene and then became extinct, except for the Asian area (sensu. Fig. IX.1)

During the Oligocene, a vicariance event was shown between Asia and South America (*Icacina* (*Leretia-Casimirella*)), between the Asia and Africa in the *Iodes* genus and between Asia and North America (*Mappia-Nothapodytes*). *Mappia mexicana* is sister to the three others *Mappia*, which are South American (Angulo et al. 2013). The distribution of this specimen (Fig. IX.1) could be in an intermediate position, between the Northern Hemisphere and South America. The regression of the boreotropical flora during the Oligocene cooling could explain the different vicariances found in this study between all areas. In fact, the European and North American boreotropical vegetation, which ensured the continuity of all areas during the Paleocene and Eocene, became reduced during the Oligocene. The loss of these floras, widespread in Europe and North America, gave rise to the isolate tropical floras in regions, which became refugees (Asia, Africa, South America). This pattern was found in some other families and genera as Sabiaceae, Menispermaceae, *Carya*, *Anacardium* etc. (Wen, 1999, Manchester et al., 2007, Jacques, 2009, Zhang et al., 2013, Yang et al., 2018).

Only two Icacinaceae fossil species were found during the Oligocene, a species of *Iodes* in Europe (Knobloch & Mai, 1986) and a *Pyrenacantha* in South America. This last case is interesting because the genus *Pyrenacantha* now only occurs in Africa and have a few species in Asia (Sleumer, 1971, Villiers, 1973). The extinction of this genus in South America area may occur during the Neogene and could result in a recent remodelling of the composition of the flora.

Finally, *Leretia* + *Casimirella* clade (part of the Clade II, Fig. IX.3) is the unique example of a new diversification in the refugee's zones during the Miocene, which may be linked to the middle-Miocene climatic optimum (Zachos et al., 2008).

IX.3.3. The incorporation of fossils in biogeographic study

Taking in to account the modern distribution of a family alone conduces to a misleading interpretation of the biogeographic history (Manchester & Tiffney, 2001). We show, with the help of the fossil record and geological climatic reconstruction of zones, that considering extinct areas for genera could change the patterns in the reconstruction events and the extent of ancestral areas. The fossil record allows dating major clades in the calibration of molecular studies based on modern species. In addition, the fossils also gave biogeographic information by their finding locations. Sometimes, as for *Pyrenacantha*, we lost, in the modern distribution, a great part of the historical area, probably not far ago, and this could introduce a significant bias in our analysis.

On the other hand, the fossils alone are insufficient to understand the historical pattern of diversification. The Icacinaceae were probably in African, Asian and South American areas during the Paleogene as shown by this study. New studies show Icacinaceae fossils in Paleocene of South America (Stull et al., 2012), but the search effort remains unbalanced between areas.

The congruence of the location of fossils with the reconstruction of past events using modern distributions is a good way to improve our hypothesis' strength and our understanding of biogeography. The addition of fossils directly in the biogeographic reconstruction together with modern species could give more confident results. In order to make possible this kind of studies, new methods of analysis have been developed. The use of molecular and morphological data together in a Bayesian analysis was implemented (Nylander et al., 2004) using the MK model for the morphological part (Lewis, 2001). A first test of time estimate using fossil as terminal taxa has been made by Pyron (2011). The development of a total-evidence approach (or tip-dating) in order to include the fossils with extant species together in a Bayesian analysis has been made by Ronquist (Ronquist et al., 2012). In these new studies, the authors used all fossils with a good preservation in an analysis of temporal calibration and not only the oldest one in a particular node. This approach needs an appropriate evolutive model, which considers the fossil data. The fossilized birth-death model (FDB) was developed (Stadler, 2010, Didier et al., 2012) and used for this purpose (Heath et al., 2014). Despite a potential overestimated age of divergence, estimated by the tip-dating method, (Arcila et al., 2015) this method increases the estimated time of divergence when it uses important fossil data (Ronquist et al., 2016). Thus, this method was widely used these last years (Cannatella, 2015, Gavryushkina et al., 2016, Renner et al., 2016, Vinther et al., 2017, Wright & Toom, 2017). This approach could be used in our context in order to improve the reliability of the dating and biogeographic results.

Conclusion of the chapter

The age of the divergence of Icacinaceae clade given by the present analysis, (122.3; 112.1-128 Ma) is older than in the main previous studies including Icacinaceae. Nine nodes are compatibles with a divergence during the PETM. The spatial reconstruction is compatible between the two methods used (S-DIVA and DEC) with 10 (13 DEC) dispersions and 10 vicariance events reconstructed. Asia seems to correspond to the ancestral area of Icacinaceae. However, the climate was arid in a greater part of Asia during the Cretaceous period. Moreover, the fossils findings for the Icacinaceae show that this family was present in Europe in the Upper Cretaceous. Therefore, the ancestral area of Icacinaceae could be Eurasia. The diversification of Icacinaceae, which begins during the Upper Cretaceous, increases during the Paleogene and particularly during the early Eocene. The Eurasian area became a Northern Hemisphere area, with exchanges between Europe and Nord America during the PETM. An increase of the diversity of climber clade IV during the PETM is shown and is congruent with the hypothesis of the presence of a new thermophilic vegetation favourable to climbers in response to the global warming. Exchanges between South and North America were shown. During the Oligocene, vicariance events were reconstructed between Northern Hemisphere, South America and Africa. The loss of the North American and European area for the boreotropical flora, reduced the Northern Hemisphere area to only the Asian area. Therefore, all extant tropical area (Asia, Africa, and South America) were separated by this event, and became refuges for ancient floras. The presence of a *Pyrenacantha* fossil in South America during the Oligocene, genus only present in Africa and residual in Asia, now shows that the view of biogeography with extant species could be wrong due to late changes. It is necessary to use living species and fossil data together in order to understand the biogeography of a group. New methods using all data together exist and could be the next step of this preliminary study.

Conclusions and perspectives

The present study aims at understanding the changes in Icacinaceae during the Paleogene, particularly during the Paleocene-Eocene Thermal Maximum (PETM), in the Paris Basin and to expand the observations from a global perspective.

A reference from extant fruits and endocarps of Icacinaceae species has been done and shows the great morphological, anatomical diversity and in particular in term of hairs shapes, ornamentation of the endocarps, the shape of tubercles (if present), the apex structure and the vascularization. Those characters allow the recognition of species and major clades and to discriminate Icacinaceae s.s. from Icacinaceae s.l. (now mainly belonging to the Metteniusaceae family). In particular, the *Iodes* species have ridges at the endocarp surface, a vascular bundle inside the endocarp wall and papillae on the locule surface. Therefore, this work confirms the fossil recognition of genus *Iodes* and permits the species delimitation from endocarp differences within the fossil record. In addition of this work, we propose an identification key built with the software Xper^3's database in order to respond to the availability need of the raw data, the standardization of the descriptions and the understanding by all of the descriptors used. This base is linked to a computer-assisted key. In addition, it can generate a natural key and a Nexus format file for phylogenetic studies.

With this reference and tools, we conducted studies of Icacinaceae remains in the Paris Basin. We first studied the Rivecourt site remains from the Thanetian. We described five *Iodes* species from 70 anatomically well-preserved lignitic specimens. All species have horn-like protrusions sub-apically, now characteristic to the Asian *Iodes* species. Abnormal specimens confirm the assignation of the fossils to the family Icacinaceae in having two pendulous ovules, which only one generally become mature.

Then, we studied lignitic remains from Le Quesnoy site (Ypresian, MP7) as well as a flower embedded in amber. We described two new *Iodes* species from lignitic endocarps and a new occurrence of a species described from Rivecourt. The new species do not have horn-like protrusions, showing a new morphological disparity for *Iodes*. Regarding the flower in amber, we document an unknown combination of characters in extant diversity, which led to the description of a new genus, *Icacinanthium*. The morphological analysis of this flower along with modern species locate the flower at the base of the Clade IV, not directly related to the endocarps. Therefore, this flower demonstrates a greater diversity for the family during the Early Eocene than revealed by the fruits.

We described three species from the Passy (Paris) site, with one new and two already known from Rivecourt. In addition, two specimens from the Grès de Belleu were attributed to *Iodes* and *Paleophytocrene*. Finally, a single specimen from Prémontré belongs to the unnatural

Icacinicarytes genus. The review of all sites shows that we have 12 species attributed to Icacinaceae in the Paris Basin, with nine endemics. A phylogenetic analysis was done using morphological data from fossils of the Paris Basin and morpho-molecular data for modern species. The result confirms the taxonomic assignation of the fossils. The endemism could be due to the partial isolation of floras in consequence of the marine transgression. Affinities of these floras with Indo-Malayan and African modern floras are highlighted, which probably correspond to refuges' area. The changes of flora through the PETM appear to be limited: three of the five species from Rivecourt cross the Paleocene-Eocene boundary. However, we showed a greater morphological disparity after the PETM especially in the *Iodes* genus, probably in response to the global warming.

In order to place the observations made in the Paris Basin from a global perspective, we used all the fossil record of Icacinaceae in a paleobiogeographic study. Among 179 occurrences of Icacinaceae, we only accepted 86 of them, mainly from endocarp remains. In fact, the leaves and pollen remains, attributed to Icacinaceae, appeared to be more common than expected (in the present asterid diversity), and the wood affinity is based on genera now placed in groups other than Icacinaceae (and are excluded). For the *Iodes* genus, we considered four species from North America and 17 from Europe.

Only with accepted occurrences, we showed an increase of the species richness during the Paleogene and more during the Eocene. In particular, the greater species richness and morphological shape are found during the early Eocene (or Ypresian) period showing a diversification event for the family linked to the PETM. Exchanges were shown between North America and Europe during the PETM, in both ways. This is during the middle and late Eocene that most of the modern genera appear in the fossil record as *Natsiatum*, *Phytocrene*, and *Pyrenacantha*. Finally, the Oligocene period, less favourable to Icacinaceae family (cooling period), shows a decrease of species richness in North America and Europe. In this review, the fossils studied in the Paris Basin add new diversity to the genus *Iodes*. In particular, this new fossil diversity agrees with the recognition of a partial continuity in the Paleocene-Eocene vegetation in Europe, never clearly shown before in macrorest studies.

With the help of this review and molecular data available in the literature, we tried a phylogenetic dating and biogeographic reconstruction. The divergence age of Icacinaceae (122.3; 112.1-128 Ma) confirms that this family is ancient. We show a diversification of major clades during the Upper Cretaceous and diversification inside the clades during the Paleogene. In particular, nine nodes are compatible with the PETM event. The biogeographic reconstruction shows about 10 dispersions and 10 vicariances necessary to explain the global pattern. The ancestral area of core-Icacinaceae is Eurasia, in the light of the fossil record and geological climatic zone reconstruction. This Eurasian area became a Northern Hemisphere area during the Paleogene and especially during the PETM with the expansion of Icacinaceae probably using the North Atlantic land bridge. The climber clade IV (sensu Stull et al., 2015) increased in diversity through the PETM, showing the development of a new thermophilic flora more favourable to climbers. During the Oligocene, vicariances event were shown between Asia, South America, and Africa. This reconstruction could be explained by the regression and extinction of the megathermal flora in North America and Europe, which isolated the tropical floras.

In conclusion on the impact of the PETM in Icacinaceae changes, the study of the Paris Basin shows at least a partial continuity of Icacinaceae floras throughout the PETM, but with probably an enrichment of Icacinaceae species and shapes. Using all the fossil record, we also found a partial continuity of Icacinaceae at the genus level with a diversification of Icacinaceae species and an increase of endocarp shape through the Ypresian. In addition, we show migrations of Icacinaceae between North America and Europe areas. Finally, the phylogenetic dating and biogeographic studies show a diversification of a climber clade in Northern Hemisphere and Africa during the PETM. Therefore, all the level of Icacinaceae studies are congruent and show that the PETM appears to be a non-catastrophic event but rather an event of vegetation enrichment especially for climber's species and to intensive migrations throughout the Northern Hemisphere.

We would like to propose some perspectives on this thesis.

First, the work made with the Xper^3 database could be the starting point of two different works: (1) create a modern fruit and endocarp database for the use of carpologists and paleocarpologists, (2) develop a modern Icacinaceae database adding information about other organs for the use of Icacinaceae fossils and phylogenetic studies. Both are compatible and could be a project in a long-term perspective, in order to propose a reference in both studies areas.

The Rivecourt and Le Quesnoy sites contain thousands of endocarps and seeds from dozens of families. Studying remains from these two sites could be a good opportunity to have a better understanding of the effect of the PETM in the Paris Basin at a species level. Indeed, some families are shared by these two sites but with changes in species and genera. Results found for Icacinaceae family need to be confronted with others family changes. For example, Metteniusaceae family remains are published for Le Quesnoy, but not yet for the Rivecourt site. Preliminary studies show the same patterns than Icacinaceae and we can expect a global evolutionary congruence for floras throughout the Paleogene in the Paris Basin.

Finally, other new phylogenetic methods of investigation exist, which were not used in this thesis, using fossils as terminal taxa to perform the phylogenetic dating. This total evidence study could be more accurate than the method used here: *i.e.* using fossil information as a correction patch of the ancestral area reconstruction. The fossil birth-death model (FDB) was developed in order to incorporate the fossil data directly in the analysis. Becoming more and more popular these last couple of years, this method seems to be more accurate and able to increase the reliability of our datings as well as our biogeographic results.

Résumé étendu en français

Introduction

En 1823, Adrien de Jussieu (1797 – 1853) décrit un nouveau genre nommé « *Icacina* ». C'est en 1852 que la famille des Icacinacées apparait dans la littérature (Miers, 1852) et contenant 14 genres. La plus large acceptation de la famille est donnée par Hermzann Sleumer (1906-1993) avec quatre tribus et 58 genres. Puis, dans les années 2000, un certain nombre d'études utilisant des données morphologiques et moléculaires remettent en question la monophylie de la famille. En 2016, la nouvelle phylogénie de l'Angiosperm Phylogeny Group (APG), qui fait la synthèse des travaux antérieurs, n'inclut plus que 23 genres dans la famille des Icacinaceae. Cette famille est placée en groupe frère des Oncothecaceae dans l'ordre des Icacinales, lui-même groupe frère des autres ordres des Lamiidae.

La famille des Icacinaceae, telle qu'elle est actuellement définie, contient environ 160 espèces d'arbres, d'arbustes et de lianes. La famille est tropicale à sub-tropicale avec quelques exceptions, comme le genre *Hosiea* (deux espèces), qui sont plus tempérées. Les Icacinaceae sont répartis en Afrique, Asie, Madagascar et Amérique du Sud.

Il n'existe pas vraiment de caractère diagnostique pour reconnaitre la famille mais plutôt un ensemble de caractères. Les feuilles sont généralement alternes simples et entières, avec des nervures primaires pennées et des nervures secondaires brochidodromes. Des domaties, cristaux et vrilles sont trouvés dans certaines espèces et genres. L'inflorescence est très diversifiée et caractérise plus les genres que la famille. Les fleurs sont généralement actinomorphes, très petites (inférieure à 10 mm de diamètre) et hermaphrodites. Les pétales sont à préfloraison valvaire et les étamines ont une insertion libre. Le pollen est généralement petit, tri(col)pore ou à plusieurs ouvertures germinatives et d'ornementation très variée. Le fruit est peut-être l'organe le plus déterminant pour reconnaître les Icacinaceae. En effet, le fruit est une drupe contenant deux ovules anatropes et pendants, dont seulement un arrive à maturité. L'apex est généralement asymétrique. Il existe une variété assez importante en termes d'ornementation externe et interne de l'endocarpe. Cependant, deux tendances se révèlent : les endocarpes avec des crêtes et ceux avec des trous. Ces trous sont souvent associés à des tubercules internes qui entrent en contact avec les tissus de la graine.

Les Icacinaceae sont abondamment utilisées en médecine traditionnelle et chimique. Les racines, feuilles et fruits sont utilisés. Cet usage semble universel, en effet des cas d'utilisation sont connus dans l'ensemble des aires de répartition des Icacinaceae. En médecine chimique, ce sont les propriétés anti-cancéreuses et anti-malarienne de certains alcaloïdes produits par des Icacinaceae qui sont mises en avant.

Mais cette famille est également importante pour les paléobotanistes. En effet, on retrouve un grand nombre de fossiles attribués aux Icacinaceae durant le Paléogène, principalement en Europe et en Amérique du Nord. Au niveau du bassin de Paris, qui est un des plus grands bassins sédimentaires français, on retrouve des restes d'Icacinaceae dans cinq sites datés du Paléogène comme suit : Grès de Belleu, Prémontré, Passy (Paris), Le Quesnoy (Houdancourt) et Rivecourt. En particulier, les sites de Rivecourt et de Le Quesnoy ont montrés des restes de nombreux endocarpes sous forme de lignite. Ces deux sites ont également l'avantage d'être très proches géographiquement (moins de 4 km) et de représenter des âges successifs encadrant la limite Paléocène-Eocène. Ces sites sont donc une bonne opportunité d'étudier les changements de flores locales suite au maximum thermique de la limite Paléocène-Eocène (PETM).

Le PETM correspond à une augmentation de température de l'ordre de 5 à 8 degrés en une très courte période. Elle est liée à une augmentation de carbone dans l'atmosphère. La source primaire de cette perturbation reste irrésolue : volcanisme ? Impact météoritique ? Forçage orbital ? En revanche, il semblerait que l'augmentation de température initiale ait été amplifiée par la déstabilisation des clathrates de méthane. Les conséquences pour les organismes tant marins que terrestres sont variables. La composition floristique bascule vers une flore plus tropicale qui se met en place en Hémisphère Nord.

La thèse se propose donc de répondre aux questions suivantes :

(1) Quel est l'impact du PETM sur les Icacinaceae du Bassin de Paris ?
(2) Quelles inférences peut-on faire au sujet de l'évolution des Icacinaceae durant le Paléogène ?

Pour cela, nous avons divisé notre étude en trois grandes parties. La première s'intéresse à la diversité actuelle des fruits et endocarpes de la famille afin de proposer un référentiel pour les fossiles (Chapitre I et II). La seconde partie traite des fossiles d'Icacinaceae du Bassin de Paris (Chapitre III à VII). Enfin, une troisième partie tente de mettre les Icacinaceae du Bassin de Paris dans une perspective globale, en intégrant l'ensemble des fossiles reconnus valides dans une étude paléobiogéographique et en proposant une datation ainsi qu'une biogéographie de la famille à partir des espèces actuelles (Chapitre VIII et IX).

Chapitre I. Les fruits et endocarpes des espèces modernes d'Icacinaceae

Dans cette partie, 88 fruits d'Icacinaceae et six fruits de groupes externes ont été étudiés morpho-anatomiquement. Une clé naturelle est proposée en accompagnement des descriptions des fruits.

Cette étude a permis de montrer la grande diversité des fruits et endocarpes chez les Icacinaceae, en particulier en ce qui concerne la forme des poils sur le fruit, l'épaisseur du mésocarpe, l'ornementation de l'endocarpe et la forme des tubercules lorsqu' ils sont présents. Ces caractères et d'autres encore permettent de différencier dans la plupart des cas une espèce actuelle d'une autre. La forme des cellules de la paroi des endocarpes semble être un bon caractère pour différencier les Icacinaceae sens strict des Icacinaceae sens large, parmi ces dernières, celles aujourd'hui exclues de la famille s.s. sont majoritairement rassemblées dans la famille des Metteniusaceae.

Certaines particularités sont notées, comme des poils à la surface de la loge pour les genres *Leretia*, *Lavigeria* et *Cassinopsis,* un capuchon issu de l'accrescence de l'ovaire sur le fruit pour certaines espèces du genre *Pyrenacantha*, des poils à la surface de l'endocarpe pour le genre *Pleurisanthes* et la présence de gynophores dans les genres *Miquelia* et *Pyrenacantha.*

Les espèces du genre *Iodes* sont généralement reconnaissables par leurs crêtes à la surface de l'endocarpe, la présence d'un faisceau vasculaire à l'intérieur de la paroi de l'endocarpe et la présence de papilles arrondies à la surface de la loge. D'autres genres partagent un ou deux de ses caractères, la présence des trois semble être la seule manière de confirmer l'identification. Cependant, la forme globale du spécimen peut également orienter l'identification en cas de dégradation.

Des stomates ont été trouvés à la surface de la loge, souvent situés entre les papilles ou sur des tubercules. Ces trois structures semblent partager un même rôle : assurer les échanges gazeux entre l'extérieur et l'intérieur de la loge.

Par ailleurs, un certain nombre de spécimens étudiés dans cette étude ont été partiellement dégradés par des attaques de champignon. Il est peut-être envisageable de reconsidérer l'échantillonnage de fruits sur le terrain en utilisant un protocole évitant les contaminations par des champignons, à l'image des protocoles utilisés pour la récolte de spécimens pour l'étude ADN.

Chapitre II. E-identification des fruits et des endocarpes des Icacinaceae modernes

Parmi tous les défis des études taxonomiques, les plus important pourrait être la disponibilité des données brutes, la standardisation des descriptions et la compréhension des caractères utilisés. Un logiciel libre, maintenant disponible sur internet, Xper^3 (Ung et al. 2010) permet de produire des bases de connaissances adaptées à ces besoins. Dans notre cas, une base Xper a été produite, disponible dans le lien suivant : http://www.xper3.fr/xper3GeneratedFiles/publish/identification/-8704055676548069962/mkey.html

Elle contient les 94 espèces étudiées au chapitre I caractérisées par 56 descripteurs dont 18 sont numériques et 38 sont catégoriques. La base est complète à 95.5% et présente 652 illustrations, pour renseigner à la fois les espèces ainsi que les caractères.

On remarque qu'aucune espèce n'a de description recouvrante, ce qui montre que les fruits et endocarpes sont de bons organes pour identifier les espèces. Cependant, le manque de diversité intra-spécifique rend les caractères discrets les plus discriminants, c'est-à-dire les caractères numériques, peu utilisables.

Cette base peut être utilisée comme point de départ d'une base de données complète sur les fruits et noyaux et/ou pour la description standardisée des Icacinaceae en ajoutant d'autres organes. Nous pouvons également envisager de produire une autre base adaptée à des études phylogénétiques, car Xper^3 peut facilement générer un fichier Nexus à partir de la base de données produite. Enfin, elle permet une comparaison rapide et efficace avec le registre fossile des Icacinaceae.

Chapitre III. Etude des fruits d'Icacinaceae du Paléocène du Bassin de Paris

Dans cette partie, nous décrivons cinq nouvelles espèces d'Icacinaceae à partir des 70 spécimens d'endocarpes ligniteux provenant du site Thanétien de Rivecourt. Ces espèces ont en commun un faisceau vasculaire à l'intérieur de la paroi de l'endocarpe, des papilles à l'intérieur de la loge, des crêtes à la surface de l'endocarpe ainsi qu'une corne subapicale sur chaque face. La taille de l'endocarpe, la forme des crêtes, l'épaisseur des parois ainsi que la forme et la densité des papilles sont les caractères pertinents pour différencier les cinq espèces entre elles ainsi qu'avec les espèces de la littérature. Une clé d'identification des espèces fossiles de *Iodes* est proposée. Par ailleurs, l'espèce *Iodes israelii* a été exclue de l'analyse car elle est basée sur un seul spécimen qui ne présente pas les caractères clés du genre *Iodes*. Nous décidons de changer la combinaison de cette espèce en *Icacinicaryites israelii*.

Nous proposons une standardisation des mesures de la densité des papilles en utilisant la première unité proposée dans la littérature par Reid et Chandler (1933), soit le nombre de papilles par 0.25 mm^2. Nous proposons également une standardisation de la terminologie de la forme des papilles. On trouve en effet de nombreuses appellations pour la même forme : « buble-like », « balloon-like » ou « rounded » (Chandler, 1961, Manchester, 1994). Nous préférons le terme de « sessile arrondi » pour désigner les papilles de cette forme.

Les cornes subapicales ne sont retrouvées actuellement que pour les espèces asiatiques de *Iodes*. Nous postulons donc une affinité entre les flores paléocène d'Europe et celles retrouvées en Indo-Malaisie actuellement. Cette flore semble correspondre à une aire refuge de l'ancienne flore boréotropicale.

Parmi les spécimens examinés, l'un d'entre eux a particulièrement attiré notre attention. En effet, le spécimen Riv. PPB19 est divisé en deux parties latérales avec deux cornes sur chaque face (au lieu d'une seule pour les spécimens habituels). Icacinaceae Miers est une famille avec deux ovules pendants où un seul atteint la maturité, ici nous avons le cas où les deux ovules sont fécondés et deviennent des graines. Le développement des deux ovules en graines induit le développement de deux unités symétriques d'endocarpe reliées par une paroi. Ce spécimen anormal suggère que les espèces d'*Iodes* de Rivecourt avaient deux ovules pendants, où habituellement un seul mûrit. Cette observation corrobore le fait que ces espèces fossiles possèdent tous les caractères des membres de la famille des Icacinaceae.

Certains spécimens possèdent des graines de couleur crème et de texture qui dénote dans le gisement à lignite de Rivecourt. Des études chimiques ont été tentées pour essayer d'expliquer ces différences. Un test de combustion préliminaire montre que ces graines sont composées de molécules organiques. Cependant, nos investigations n'ont pas permis d'aller plus loin dans la caractérisation de ces molécules dont certaines appartiennent au groupe des lipides.

Chapitre IV. Recherche de bois d'Icacinaceae pour le site de Rivecourt et affinité du genre *Icacinoxylon* Shilk.

Beaucoup de fragments de bois sous forme de lignite ont été retrouvés sur le site Thanétien de Rivecourt. Parmi ceux-ci, une étude préliminaire a permis d'identifier trois bois correspondants potentiellement à des espèces d'Icacinaceae. Une nouvelle description de ces bois a permis de mettre en évidence leurs caractères communs : un bois diffus avec des vaisseaux solitaires, des perforations scalariformes avec 20 à 40 barres et des rayons hétérocellulaires et communément 4 à 10 sériés. Ces caractères sont cohérents avec une identification avec le genre *Icacinoxylon*. Cependant, ce genre est probablement défini via des caractères plésiomorphes pour la famille des Icacinaceae. En effet, l'affinité de ce genre fossile avec la famille des Icacinaceae est basée sur une ancienne classification comprenant des genres maintenant distribués parmi les asterids. Les Icacinaceae sens strict (excl. *Cassinopsis*, groupe à la base de la famille) ont tous des perforations simples. Nous considérons donc ces fossiles comme n'appartenant probablement pas à la famille des Icacinaceae. Cependant, ces bois ne possèdent pas de cercles d'accroissement marqués, ce qui nous permet de penser que la saisonnalité à Rivecourt était faible durant le Paléocène.

Chapitre V. Deux nouvelles espèces d'*Iodes* (Icacinaceae) provenant du site du Quesnoy (Yprésien, Oise, France)

Le site à lignite et ambre du Quesnoy est encore très peu étudié en ce qui concerne les restes floristiques. En particulier, 185 endocarpes ont été identifiés comme appartenant à la famille des Icacinaceae. Dans ce chapitre, nous décrivons deux nouvelles espèces et une nouvelle occurrence d'une espèce décrite pour le site paléocène de Rivecourt, toutes associées au genre *Iodes*. Les nouvelles espèces ne possèdent pas de cornes subapicales, ce qui dénote d'une nouvelle disparité morphologique pour le genre en comparaison avec le site de Rivecourt. Une revue du registre fossile des *Iodes* montre la diversité des formes ayant existé, en particulier en Europe. Ces nouvelles espèces ont des affinités avec les flores modernes d'Asie et d'Afrique comme le montrent le patron de réticulation et la forme des crêtes. Ces aires semblent correspondre à des aires refuges de la forêt boréotropicale, qui atteint son extension maximale durant l'Yprésien. Enfin, la présence d'espèces de *Iodes*, genre lianescent, est un argument pour considérer la flore comme étant mégathermale au Quesnoy durant l'Yprésien. L'étude du site du Quesnoy n'est qu'à ses débuts et il est important de continuer à étudier d'autres familles également bien représentées dans le gisement.

Chapitre VI. Première fleur fossile d'Icacinaceae provenant du site à ambre du Quesnoy (Yprésien, France)

L'ambre du Quesnoy a révélé de nombreux insectes mais également quelques fleurs et du pollen (Nel et al., 1999). Dans ce chapitre, nous étudions une fleur dans l'ambre attribuée à la famille des Icacinaceae. La fleur est petite (inférieur à 2.5 mm de diamètre), actinomorphe, hypogyne et pentamère. Le calice est cupulaire, les pétales sont lancéolés, courbés vers l'extérieur, attachés à la base, tomenteux sur la face adaxiale avec des poils longs, simples et granuleux. Les étamines sont libres et alternes avec les pétales. Le pollen est petit (environs 20 µm), triaperturé et échiné. Cette combinaison de caractère n'existe pas dans l'actuel, nous avons donc décrit un nouveau genre éteint, nommé *Icacinanthium* comprenant l'espèce *Icacinanthium tainiaphorum* (Del Rio et al., 2017). Ces données morphologiques ont été utilisées afin d'inclure le fossile dans une phylogénie bayésienne mêlant données morphologiques et moléculaires pour 51 espèces actuelles. Cette phylogénie associe ce fossile au Clade IV sensu Stull et collaborateurs (2015) au sein des Icacinaceae. Cette fleur n'est donc pas associée aux endocarpes retrouvés sur le même gisement, endocarpes faisant partie du genre *Iodes* (Clade III, Stull et al., 2015) et démontre une diversité insoupçonnée pour les Icacinaceae au début de l'Eocène.

Chapitre VII. Revue des Icacinaceae du Basin de Paris : nouveaux restes provenant de trois sites du début Eocène.

Deux sites du Bassin de Paris, Rivecourt et Le Quesnoy, ont révélés une grande diversité de formes et d'espèces pour le genre *Iodes*. Des études préliminaires ont montré que les Icacinaceae étaient également présents sur trois autres sites : Passy (MP8), Grès de Belleu (MP10) et Prémontré (MP10). De plus, de nouvelles données moléculaires (Stull et al., 2015) permettent de proposer une phylogénie intégrant fossiles et actuels et ainsi permettre de confirmer les identifications proposées. Dans cette étude, nous décrivons trois espèces pour le site de Passy, dont une nouvelle et deux correspondant à des espèces déjà décrites dans le site de Rivecourt ; deux spécimens provenant du Grès de Belleu, l'un attribué à *Iodes* sans épithète spécifique et l'autre associé au genre fossile *Paleophytocrene* proche de l'espèce *P. vancouverensis* (Rankin et al., 2008) ; enfin un moulage d'endocarpe attribué au genre non naturel *Icacinicarytes* a été trouvé dans le site de Prémontré.

Une étude phylogénétique via les logiciels Paup 4.0 et MrBayes confirme l'assignation des espèces du Bassin de Paris au genre *Iodes*. Le spécimen attribué à *Paleophytocrene* semble s'intégrer au Clade IV, caractérisé par la présence de trous à la surface de l'endocarpe, mais le spécimen reste très incomplet et la fiabilité des nœuds sont faibles.

La diversité des Icacinaceae au niveau du Bassin de Paris est comparable aux autres grands sites en Europe et Amérique du Nord (Reid & Chandler, 1933, Knobloch & Mai, 1986, Manchester, 1994, Collinson et al., 2012) avec 12 espèces décrites dont 9 endémiques. Les espèces sont apparentées à des groupes lianescents, très présentes sur les rives des rivières favorables à la fossilisation. Ainsi, la diversité des Icacinaceae est potentiellement sous-estimée, comme l'atteste la découverte de cette fleur dans l'ambre *Icacinathium tainiaphorum*.

En dépit des ressemblances des espèces d'Icacinaceae du Bassin de Paris avec d'autres espèces de grands gisements, nous les considérons endémiques d'une aire assez restreinte. Cet endémisme peut s'expliquer par l'immersion partielle du Nord de la France durant le Paléocène et l'Eocène formant une série d'îlots. Une baisse du niveau marin durant le PETM peut d'ailleurs expliquer l'arrivée de nouvelles faunes et flores qui se sont ensuite diversifiées dans d'autres aires. Les affinités les plus évidentes des fossiles du Bassin de Paris sont avec les flores actuelles Indo-malaise et Africaine. Cette affinité résulte sans doute d'une régression de la flore boreotropicale durant l'Oligocène et le Néogène.

Les flores pré-PETM et post-PETM sont liées par la présence de certaines espèces du genre *Iodes*. Cependant, de nouvelles disparités morphologiques et de nouveaux genres apparaissent au cours de l'Yprésien et montrent une augmentation de diversité, probablement en réponse au réchauffement global. Cette dernière observation peut être toutefois liée à des biais taphonomiques : nombre de spécimens différents par sites, conditions environnementales de dépôts différentes, faible couverture du Bassin de Paris pour le Paléocène, etc. Cette observation est cependant en accord avec les observations faites sur les Menispermaceae et Vitaceae (observation personnelle). Nous proposons donc comme hypothèse un changement plutôt rapide mais non catastrophique durant le PETM avec une augmentation de diversité pour les Icacinaceae.

Chapitre VIII. Paléobiogéographie de la famille des Icacinaceae

Les fossiles étudiés au niveau du Bassin de Paris dressent un portrait des changements de flores locales durant le PETM. Les flores se modifient avec un enrichissement notable des flores probablement liées au réchauffement global. Le but de ce chapitre est de généraliser à partir de l'ensemble des occurrences d'Icacinaceae fossiles nos observations locales ainsi que d'augmenter la temporalité étudiée.

Dans une première approche, nous avons revu les occurrences d'Icacinaceae existantes en utilisant la circonscription actuelle des Icacinaceae. Ainsi, sur 179 occurrences, 86 sont acceptées (principalement des endocarpes), 46 occurrences sont considérées comme douteuses (principalement les feuilles et le pollen) et 44 occurrences sont rejetées (principalement le bois, cf. Chapitre IV). Seules les occurrences acceptées ont été utilisées par la suite dans la localisation et la stratigraphie de la famille. Une attention particulière a été accordée au genre *Iodes* : *Iodes* *chandlerae* a été exclus du genre *Iodes* pour cette étude et nous y avons ajouté *Croomiocarpum missippiensis*, *Hosiea pterojugata*, *P. suleticensis* et *P. marchiaca*. Au total, nous reconnaissons quatre espèces d'Amérique du Nord et 17 d'Europe (conformément à la revue proposée en Chapitre V).

Nous montrons que la seule espèce connue d'Icacinaceae du Crétacé, *Iodes germanica*, traverse la crise Crétacé-Paléogène. Il y a une augmentation de la richesse spécifique chez les Icacinaceae dès le Paléocène, mais la plupart des nouvelles espèces datent de la fin du Paléogène ; il est donc difficile d'attribuer ces changements à une diversification post-crise ou liés à l'augmentation de température pré-PETM.

Une grande augmentation de la diversité en termes générique, spécifique et morphologique est montrée à la transition Paléocène-Eocène. Les genres existants au Paléocène se diversifient tandis que de nouveaux genres apparaissent à la fin de l'Yprésien durant l'optimum climatique. La connexion Europe-Amérique du Nord est effective durant le PETM. L'Yprésien est la période la plus riche en terme spécifique ; cependant c'est durant le milieu et la fin de l'Eocène qu'apparaissent dans le registre fossile les genres modernes tel que *Natsiatum*, *Phytocrene* et *Pyrenacantha*. Finalement, le refroidissement climatique durant l'Oligocène, moins favorable aux formes lianescentes, pourrait expliquer la chute de diversité brutale d'Icacinaceae dans le registre fossile.

Chapitre IX. Âge et biogéographie des Icacinaceae actuelles.

Dans ce chapitre, nous proposons une datation pour les Icacinaceae ainsi qu'une reconstruction biogéographique à partir de données moléculaires précédemment publiées (Stull et al., 2015). La datation moléculaire est menée via BEAST v.1.8.3 en utilisant une sélection de 11 partitions (11 149 pb) et cinq calibrations fossiles internes à la famille. L'analyse biogéographique est menée via les méthodes S-DIVA et DEC utilisant six distributions biogéographiques : Afrique, Madagascar, Asie, Amérique du Sud, Océanie et Amérique du Nord.

L'étude de datation donne un âge de divergence de 122.3 Ma (112.1-128) pour les Icacinaceae, ainsi que des âges de divergence des principaux clades au cours du Crétacé supérieur. Neuf nœuds sont compatibles avec une divergence durant le PETM. L'âge de divergence des Icacinaceae est plus ancien que les principales reconstructions précédentes. Cependant, l'assignation nouvelle des Icacinaceae à la base des Lamideae semble en accord avec une divergence du groupe très ancienne.

La reconstruction spatiale est comparable entre les deux méthodes usitées. Le patron biogéographique est expliqué par 10 (13 en DEC) dispersions et 10 vicariances. L'Asie semble être la répartition ancestrale de la famille. Cependant, les données climatiques montrent qu'une partie de l'Asie est touchée par l'aridité durant le Crétacé. Si nous suivons la zone climatique reconstruites via des indices géologiques et la répartition des fossiles, nous pouvons en déduire que la répartition ancestrale est plutôt Eurasienne. Durant le Crétacé supérieur, le Clade II (sensu. Stull et al., 2015) se disperse d'Eurasie en Afrique tandis que les autres clades (III et IV) se diversifient in situ. Des restrictions au niveau des échanges entre l'Afrique et l'Eurasie se mettent en place dès la fin du Crétacé. La diversification des Icacinaceae se poursuit durant le Paléocène et plus encore durant le début de l'Eocène, issue de diversification in situ. L'aire eurasienne se transforme en aire nord hémisphérique avec la connexion qui s'installe durant le PETM entre l'Europe et l'Amérique du Nord (argumenté par la position et les affinités des fossiles). Des échanges entre l'Amérique du Nord et du Sud sont montrés dès le Paléocène. Durant l'Oligocène, des événements de vicariance sont reconstruits entre l'Asie et l'Amérique du Sud, ainsi qu'avec l'Afrique. Ceci peut s'expliquer par la régression des flores mégathermales d'Amérique du Nord et d'Europe qui isolent les flores tropicales. La présence d'un fossile de *Pyrenacantha* en Amérique du Sud durant l'Oligocène, genre actuellement absent de l'aire, montre que la répartition des espèces a changé très récemment ce qui peut donner une vision faussée de la biogéographie du groupe. Il est donc nécessaire d'utiliser à la fois les données issues des espèces actuelles, mais également les fossiles, comme moyen de calibration et également d'orientation de l'interprétation du patron général.

De nouvelles méthodes utilisant la totalité des informations disponibles dans une seule analyse, « total evidence approach » semble prometteur pour l'étude des Icacinaceae.

Conclusion générale et perspectives

En conclusion, cette thèse a permis de montrer une continuité au moins partielle des Icacinaceae avant et après le PETM, avec probablement un enrichissement des Icacinaceae en terme spécifique et morphologique. Le registre fossile de la famille montre également une continuité partielle des Icacinaceae au niveau générique avec un enrichissement des flores et des migrations entre l'Europe et l'Amérique du Nord. Enfin, les analyses phylogénétiques de datation et les analyses biogéographiques montrent une diversification des Icacinaceae grimpantes-lianescentes dans hémisphère nord et en Afrique durant le PETM. Ainsi, tous les niveaux d'études montrent que le PETM est un évènement non catastrophique, mais plutôt un évènement lié à un enrichissement des flores mégathermales, favorisant les modes de vie grimpant et de migrations intensives dans l'hémisphère nord.

La base Xper^3 produite durant cette thèse pourrait être enrichie. Rivecourt et Le Quesnoy contiennent de nombreuses familles dont certaines sont partagées sur les deux sites. L'étude des groupes majoritaires pourrait permettre de tester les hypothèses développées dans cette thèse Enfin, de nouvelles méthodes d'investigations phylogénétiques existent, (« Fossil Birth Death model » par exemple) et pourraient être utilisées dans le cas des Icacinaceae.

References

Adnet, S., Cappetta, H., 2008. New fossil triakid sharks from the early Eocene of Prémontré, France, and comments on fossil record of the family. Acta Palaeontol. Pol. 53(3), 433–448.

Agnini, C., Fornaciari, E., Raffi, I., Rio, D., Röhl, U., Westerhold, T., 2007a. High-resolution nannofossil biochronology of middle Paleocene to early Eocene at ODP Site 1262: Implications for calcareous nannoplankton evolution. Mar. Micropaleontol. 64(3), 215–248.

Agnini, C., Fornaciari, E., Rio, D., Tateo, F., Backman, J., Giusberti, L., 2007b. Responses of calcareous nannofossil assemblages, mineralogy and geochemistry to the environmental perturbations across the Paleocene/Eocene boundary in the Venetian Pre-Alps. Mar. Micropaleontol. 63(1-2), 19–38.

Akkiraz, M.S., Kayseri, M.S., Akgün, F., 2008. Palaeoecology of coal-bearing Eocene sediments in Central Anatolia (Turkey) based on quantitative palynological data. Turk. J. Earth Sci. 17(2), 317–360.

Allen, S.E., Stull, G.W., Manchester, S.R., 2015. Icacinaceae from the Eocene of western North America. Am. J. Bot. 102(5), 725–744.

Alroy, J., Aberhan, M., Bottjer, D.J., Foote, M., Fürsich, F.T., Harries, P.J., Hendy, A.J.W., Holland, S.M., Ivany, L.C., Kiessling, W., Kosnik, M.A., Marshall, C.R., McGowan, A.J., Miller, A.I., Olszewski, T.D., Patzkowsky, M.E., Peters, S.E., Villier, L., Wagner, P.J., Bonuso, N., Borkow, P.S., Brenneis, B., Clapham, M.E., Fall, L.M., Ferguson, C.A., Hanson, V.L., Krug, A.Z., Layou, K.M., Leckey, E.H., Nürnberg, S., Powers, C.M., Sessa, J.A., Simpson, C., Tomašových, A., Visaggi, C.C., 2008. Phanerozoic trends in the global diversity of marine invertebrates. Science 321(5885), 97–100.

Alvarez, L.W., Alvarez, W., Asaro, F., Michel, H.V., 1980. Extraterrestrial cause for the Cretaceous-Tertiary extinction. Science 208(4448), 1095–1108.

Angulo, D.F., De Stefano, R..D., & Stull, G.W., 2013. Systematics of Mappia (Icacinaceae), an endemic genus of tropical America. Phytotaxa, 116(1), 1–18.

APG, 1998. An ordinal classification for the families of flowering plants. Ann. Mo. Bot. Gard. 85(4), 531–553.

APG, 2016. An update of the Angiosperm Phylogeny Group classification for the orders and families of flowering plants: APG IV. Bot. J. Linn. Soc. 141(4), 399–436.

Arcila, D., Alexander Pyron, R., Tyler, J.C., Ortí, G., Betancur-R.R., 2015. An evaluation of fossil tip-dating versus node-age calibrations in tetraodontiform fishes (Teleostei:

Percomorphaceae). Mol. Phylogenet. Evol. 82(A), 131–145.

Aria, C., Perrichot, V., Nel, A., 2011. Fossil Ponerinae (Hymenoptera: Formicidae) in Early Eocene amber of France. Zootaxa 2870(1), 53–62.

Arisawa, M., Gunasekera, S., Cordell, G., Farnsworth, N., 1981. Plant anticancer agents XXI. Constituents of *Merrilliodendron megacarpum*. Planta Med. 43(4), 404–407.

Aubry, M.-P., Thiry, M., Dupuis, C., Berggren, W.A., 2005. The Sparnacian deposits of the Paris Basin: A lithostratigraphic classification. Stratigraphy 2(1), 65–100.

Augé, M., 2003. La faune de Lacertilia (Reptilia, Squamata) de l'Éocène inférieur de Prémontré (Bassin de Paris, France). Geodiversitas 25(3), 539–574.

Augé, M., Smith, R., 2002. Nouveaux Lacertidae (Reptilia, Squamata) de l'Eocène inférieur européen. Belg. J. Zool. 132(1), 3–15.

Augé, M., Duffaud, S., Lapparent de Broin, F. de, Rage, J.C., Vasse, D., 1997. Les amphibiens et les reptiles de Prémontré (Cuisien, Bassin parisien) : une herpétofaune de référence pour l'Eocène inférieur. Géologie Fr. 1, 23–33.

Aziz, H.A., Hilgen, F.J., van Luijk, G.M., Sluijs, A., Kraus, M.J., Pares, J.M., Gingerich, P.D., 2008. Astronomical climate control on paleosol stacking patterns in the upper Paleocene–lower Eocene Willwood Formation, Bighorn Basin, Wyoming. Geology 36(7), 531–534.

Baas, P., 1974. Stomatal types in Icacinaceae. Additional observations on genera outside Malesia. Acta Bot. Neerlandica 23(3), 193–200.

Bailey, I.W., Sinnott, E.W., 1916. The Climatic distribution of certain types of angiosperm leaves. Am. J. Bot. 3(1), 24–39.

Bailey, I.W., Howard, R.A., 1941a. The comparative morphology of the Icacinaceae I. Anatomy of the node and internode. J. Arnold Arbor. 22(1), 125–132.

Bailey, I.W., Howard, R.A., 1941b. The comparative morphology of the Icacinaceae II. Vessels. J. Arnold Arbor. 22(2), 171–184.

Bailey, I.W., Howard, R.A., 1941c. The comparative morphology of the Icacinaceae IV. Rays of the secondary Xylem. J. Arnold Arbor. 22(4), 556–568.

Baillon, H. E., 1874. Deuxième étude sur les Mappiées (cont.). Adansonia 11, 187–203.

Bande, M., Khatri, S., 1980. Some more fossil woods from the Deccan Intertrappean beds of Mandla District, Madhya Pradesh, India. Palaeontogr. Abt. B. 147–165.

Bayona, G., Montes, C., Cardona, A., Jaramillo, C., Ojeda, G., Valencia, V., Ayala-Calvo, C., 2011. Intraplate subsidence and basin filling adjacent to an oceanic arc-continent collision: a case from the southern Caribbean-South America plate margin: Intraplate subsidence and basin filling adjacent to an oceanic arc-continent collision. Basin Res. 23(4), 403–422.

Beard, K.C., 2008. The oldest North American primate and mammalian biogeography during the Paleocene–Eocene Thermal Maximum. Proc. Natl. Acad. Sci. 105(10), 3815–3818.

Bell, C.D., Soltis, D.E., Soltis, P.S., 2005. The age of the angiosperms: a molecular timescale without a clock. Evolution 59(6), 1245–1258.

Bentham, G., 1841. XLIII. Account of two new genera allied to Olacineae. Trans. Linn. Soc. Lond. 18(4), 671–685.

Blanc-Louvel, C., 1985a. Paléoflore du gisement Éocène de Prémontré dans l'Aisne: étude de deux fruits. Act. Du 110^{e} Cong. Des Soc. Sav. V, 149–161.

Blanc-Louvel, C., 1985b. Paléoflore du gisement Éocène de Prémontré dans l'Aisne: Vitaceae. Act. Du 110e Cong. Des Soc. Sav. V.

Bodmer, R.E., 1991. Strategies of seed dispersal and seed predation in Amazonian ungulates. Biotropica 23(3), 255–261.

Boucot, A.J., Xu, C., Scotese, C.R., Morley, R.J., 2013. Phanerozoic paleoclimate: an atlas of lithologic indicators of climate. SEPM (Society for Sedimentary Geology). 11, 1–30.

Boutique, R., 1960. Icacinaceae, in: Flore Du Congo Belge et Du Ruanda-Urundi. Bruxelles. 237–278.

Bowen, G.J., Maibauer, B.J., Kraus, M.J., Röhl, U., Westerhold, T., Steimke, A., Gingerich, P.D., Wing, S.L., Clyde, W.C., 2014. Two massive, rapid releases of carbon during the onset of the Palaeocene–Eocene thermal maximum. Nat. Geosci. 8(1), 44–47.

Bowerbank, J.-S., 1840. A history of the fossil fruits and seeds of the London Clay. The Zoological society, London. 144 pp.

Bown, P., Pearson, P., 2009. Calcareous plankton evolution and the Paleocene/Eocene thermal maximum event: New evidence from Tanzania. Mar. Micropaleontol. 71(1-2), 60–70.

Bralower, T.J., Thomas, D.J., Zachos, J.C., Hirschmann, M.M., Rohl, U., Sigurdsson, H., Thomas, E., Whitney, D.L., 1997. High-resolution records of the late Paleocene thermal maximum and circum-Caribbean volcanism: Is there a causal link? Geology 25(11), 963–966.

Brasero, N., Nel, A., Michez, D., 2009. Insects from the early Eocene amber of Oise (France): diversity and palaeontological significance. Denisia 26(86), 41–52.

Bridson, D.M., 1975. A revision of the family Vahliaceae. Kew Bull. 30(1), 163–182.

Briggs, D.E.G., Summons, R.E., 2014. Ancient biomolecules: their origins, fossilization, and role in revealing the history of life. BioEssays 36(5), 482–490.

Bronnert, C., Gheerbrant, E., Godinot, M., Métais, G., 2017. A primitive perissodactyl (Mammalia) from the early Eocene of Le Quesnoy (MP7, France). Hist. Biol. 30(1-2), 237–250.

Brown, R.W., 1962. Paleocene flora of the Rocky Mountains and Great Plains. US Government Printing Office, Washington. 375, 179 pp.

Burge, D.O., Manchester, S.R., 2008. Fruit morphology, fossil history, and biogeography of *Paliurus* (Rhamnaceae). Int. J. Plant Sci. 169(8), 1066–1085.

Burguiere, T., Causse, F., Ung, V., Vignes-Lebbe, R., 2012. IKey+: a new single-access key generation web service. Systematic biology, 62(1), 157-161.

Burnham, R.J., 1989. Relationships between standing vegetation and leaf litter in a paratropical forest: implications for paleobotany. Rev. Palaeobot. Palynol. 58(1), 5–32.

Burnham, R.J., Wing, S.L., Parker, G.G., 1992. The reflection of deciduous forest communities in leaf litter: implications for autochthonous litter assemblages from the fossil record. Paleobiology 18(1), 30–49.

Byng, J.W., Bernardini, B., Joseph, J.A., Chase, M.W., Utteridge, T., 2014. Phylogenetic relationships of Icacinaceae focusing on the vining genera. Bot. J. Linn. Soc. 176(3), 277–294.

Calvillo-Canadell, L., Cevallos-Ferriz, S.R.S., Rico-Arce, L., 2010. Miocene *Hymenaea* flowers preserved in amber from Simojovel de Allende, Chiapas, Mexico. Rev. Palaeobot. Palynol. 160(3-4), 126–134.

Cannatella, D., 2015. *Xenopus* in space and time: fossils, node calibrations, tip-dating, and paleobiogeography. Cytogenet. Genome Res. 145(3-4), 283–301.

Cappetta, H., 1992. Carcharhiniformes nouveaux (Chondrichthyes, Neoselachii) de l'Yprésien du Bassin de Paris. Geobios 25(5), 639–646.

Cardona, A., Valencia, V.A., Bayona, G., Duque, J., Ducea, M., Gehrels, G., Jaramillo, C., Montes, C., Ojeda, G., Ruiz, J., 2011. Early-subduction-related orogeny in the northern Andes: Turonian to Eocene magmatic and provenance record in the Santa Marta Massif and Rancheria Basin, northern Colombia: Palaeogene subduction in the northern Andes. Terra Nova 23(1), 26–34.

Cascales-Miñana, B., Cleal, C.J., 2014. The plant fossil record reflects just two great extinction events. Terra Nova 26(3), 195–200.

Castañeda-Posadas, C., Cevallos-Ferriz, S.R., 2007. *Swietenia* (Meliaceae) flower in Late Oligocene–Early Miocene amber from Simojovel de Allende, Chiapas, Mexico. Am. J.

Bot. 94(11), 1821–1827.

Catarino, L., Havik, P.J., Romeiras, M.M., 2016. Medicinal plants of Guinea-Bissau: Therapeutic applications, ethnic diversity and knowledge transfer. J. Ethnopharmacol. 183, 71–94.

Cavagnetto, C.G., 1967. Complexes sporo-polliniques du Sparnacien du Bassin de Paris. Rev. Palaeobot. Palynol. 5(1-4), 243–261.

Cavagnetto, C.G., 2000. La palynoflore d'un gisement d'ambre de l'Eocène basal du Bassin Parisien (Le Quesnoy, France). Palaeontographica Abteilung B 255(4-6), 147–171.

Chambers, K.L., Poinar Jr, G.O., 2014. *Ticodendron Palaios* Sp. Nov. (Ticodendraceae), a Mid-Tertiary Fossil Flower in Dominican Amber. J. Bot. Res. Inst. Tex. 8(2), 559–564.

Chambers, K.L., Poinar Jr, G.O., Brown, A.E., 2011a. Two fossil flowers of *Trichilia* (Meliaceae) in Dominican amber. J. Bot. Res. Inst. Tex. 5(2), 463–468.

Chambers, K.L., Poinar Jr, G.O., Brown, A.E., 2011b. A fossil flower of *Persea* (Lauraceae) in Tertiary Dominican amber. J. Bot. Res. Inst. Tex. 5(2), 457–462.

Chambers, K.L., Poinar Jr, G.O., Brown, A.E., 2012a. A new fossil species of *Colpothrinax* (Arecaceae) from Mid-Tertiary Mexican amber. J. Bot. Res. Inst. Tex. 6(2), 557–560.

Chambers, K.L., Poinar Jr, G.O., Chanderbali, A.S., 2012b. *Treptostemon* (Lauraceae), a new genus of fossil flower from Mid-Tertiary Dominican amber. J. Bot. Res. Inst. Tex. 6(2), 551–556.

Chandler, M.E.J., 1925. The Upper Eocene flora of Hordle, Hants, Palaeontographical Society monographs, London. 52 pp.

Chandler, M.E.J., 1954. Some Upper Cretaceous and Eocene fruits from Egypt (with appendices by M.Y. Hassan & M. I. Youssef. Br. Mus. Nat. Hist. Bull. Geol. 2, 149–187.

Chandler, M.E.J. 1961a. Plant remains of the Hengistbury and Barton Beds. British Museum of Natural History, London. 238 pp.

Chandler, M.E.J., 1961b. The Lower Tertiary floras of Southern England. I. British Museum of Natural History, London. 354 pp.

Chandler, M.E.J., 1962. The Lower Tertiary floras of Southern England. II. Flora of the Pipe-Clay Series of Dorset (Lower Bagshot). British Museum of Natural History, London. 176 pp.

Chase, M.W., Hills, H.H., 1991. Silica Gel: An Ideal Material for Field Preservation of Leaf Samples for DNA Studies. Taxon 40(2), 215–220.

Chatterjee, S., Bajpai, S., 2016. India's Northward Drift from Gondwana to Asia during the Late Cretaceous-Eocene. Proc. Indian Natl. Sci. Acad. 82(3), 479–487.

Chen, Y., Manchester, S.R., 2015. Winged Fruits of *Deviacer* in the Oligocene from the Ningming

Basin in Guangxi, South China. PloS one 10(12), e0144009.

Chen, S.-Y., Tsai, Y.-H., Baskin, C.C., Baskin, J.M., Chien, C.-T., 2015. Seed dormancy and germination of the three tropical medicinal species *Gomphandra luzoniensis* (Stemonuraceae), *Nothapodytes nimmoniana* (Icacinaceae) and *Goniothalamus amuyon* (Annonaceae). Seed Sci. Res. 25(1), 57–63.

Chester, K., I., M., 1955. Some plant remains from the Upper Cretaceous and Tertiary of West Africa. Ann Mag Nat Hist 8(91), 498–504.

Cisse, A., Gueye, M., Ka, A., Ndiaye, F., Koma, S., Akpo, L.E., 2016. Ethnobotanique des plantes médicinales chez les bergers peuls de Widou Thiengoly de la commune de Téssékéré (Ferlo-Nord Sénégal). J. Appl. Biosci. 98, 9301–9308.

Cleal, C.J., Thomas, B.A., Batten, D.J., Collinson, M., E., 2001. Mesozoic and Tertiary paleobotany of Great Britain. Peterborough: Geological Conserv. Rev. Ser. 22, 335 pp.

Collinson, M.E., 1983. Fossil Plants of the London Clay. The Paleaeontological association, London. 121 pp.

Collinson, M.E., Cleal, C.J., 1995. Early and early middle Eocene (Ypresian-Lutetian) Palaeobotany of Great Britain, in: Palaeozoic Palaeobotany of Great Britain, Geological Conservation Review Series, London. 187–226.

Collinson, M.E., Hooker, J.J., 2003. Paleogene vegetation of Eurasia: framework for mammalian faunas. Deinsea 10(1), 41–84.

Collinson, M.E., Fowler, K., Boulter, M., 1981. Floristic changes indicate a cooling climate in the Eocene of southern England. Nature 291(5813), 315–317.

Collinson, M.E., Steart, D.C., Harrington, G.J., Hooker, J.J., Scott, A.C., Allen, L.O., Glasspool, I.J., Gibbons, S.J., 2009. Palynological evidence of vegetation dynamics in response to palaeoenvironmental change across the onset of the Paleocene ‐ Eocene Thermal Maximum at Cobham, Southern England. Grana 48(1), 38–66.

Collinson, M.E., Manchester, S.R., Wilde, V., 2012. Fossil fruit and seeds of the Middle Eocene Messel biota, Germany, Abh. Senckenb. Ges. Naturforsch, Stuttgart. 251 pp.

Corner, E.J.H., 1976. The Seeds of Dicotyledon, Cambridge University Press, New York. 311 pp.

Crane, P.R., Manchester, S.R., Dilcher, D.L., 1990. A preliminary survey of fossil leaves and well-preserved reproductive structures from the Sentinel Butte Formation (Paleocene) near Almont, North Dakota. Geology 20, 1–63.

Cruickshank, R.D., Ko, K., 2003. Geology of an amber locality in the Hukawng Valley, northern Myanmar. J. Asian Earth Sci. 21(5), 441–455.

Currano, E.D., 2008. Variations in insect herbivory on angiosperm leaves through the Late

Paleocene and Early Eocene in the Bighorn Basin, Wyoming, USA. PNAS 105, 1960–1964.

Cuvier, G., Brongniart, A., 1811. Essai sur la géographie minéralogique des environs de Paris. Baudouin, Paris. 278 pp.

Dahl, A.O., 1952. The comparative morphology of the Icacinaceae, VI. The pollen. J. Arnold Arbor. 33(3), 252–295.

Dahling, G.V., 1978. Systematics and evolution of *Garrya*. Contrib. Gray Herb. Harv. Univ. 209, 1–104.

Datkhile, K.D., Durgavale, P.P., Patil, M.N., 2017. Biogenic silver nanoparticles from *Nothapodytes foetida* kills human cancer cells in vitro through inhibition of cell proliferation and induction of apoptosis. J. Bionanoscience 11(5), 416–427.

Davenport, L.J., 1988. A monograph of *Hydrolea* (Hydrophyllaceae). Rhodora 90(892), 169–208.

David-Oku, E., Obiajunwa-Otteh, J.I., 2015. A combination of the leaves and tuber of *Icacina senegalensis* A. Juss (Icacinaceae) improves the antimalarial activity of the plant in mice. J. Coast. Life Med. 3(10), 821–825.

David-Oku, E., Ifeoma, O.-O.J., Christian, A.G., Dick, E.A., 2014. Evaluation of the antimalarial potential of *Icacina senegalensis* Juss (Icacinaceae). Asian Pac. J. Trop. Med. 7, S469–S472.

David-Oku, E., Akuodor, G., Edet, E., Ogbuji, G., Obiajunwa-Otteh, J., Aja, D., 2016. Antinociceptive, anti-inflammatory and antipyretic effects of ethanolic root bark extract of *Icacina senegalensis* in rodents. J. Appl. Pharm. Sci. 6(2), 104–108.

De Franceschi, D., De Ploëg, G., 2003. Origine de l'ambre des faciès sparnaciens (Éocène inférieur) du Bassin de Paris : le bois de l'arbre producteur. Geodiversitas 25(4), 633–647.

De Franceschi, D., Dejax, J., De Ploëg, G., 2000. Extraction du pollen inclus dans l'ambre [Sparnacien du Quesnoy (Oise), bassin de Paris] : vers une nouvelle spécialité de la paléo-palynologie. Comptes Rendus Académie Sci.-Ser. IIA-Earth Planet. Sci. 330(3), 227–233.

De Roon, A.C., 1994. Icacinaceae, in: Flora of the Guianas. Goerq-Van Rijn, Czech Republic. 82–109.

De Roon, A.C., 2003. Icacinaceae, in: Guide to the vascular plants of Central French Guiana, Memoirs of The New York Botanical Garden. The New York Botanical Press, New York. 358–362.

De Wever, P., Guillocheau, F., Reynaud, J.-Y., Vennin, E., Robin, C., Cornée, A., Rouby, D., 2002. Deux siècles de stratigraphie dans le bassin de Paris. Comptes Rendus Palevol

1(6), 399–414.

DeConto, R., Galeotti, S., Pagani, M., Tracy, D., Pollard, D., Beerling, D., 2010. Hyperthermals and orbitally paced permafrost soil organic carbon dynamics, in: AGU Fall Meeting Abstracts.

Dégremont, E., Duchaussois, F., Hautefeuille, F., Laurain, M., Louis, P., Têtu, R., 1985. Paléontologie: Découverte d'un gisement du Cuisien tardif à Prémontré. Bull. Inf. Géol. Bass. Paris 22(2), 11–18.

Dei, H.K., Ajigepungu, W.T., Mohammed, A., 2015. Growth performance of broilers fed varying levels of soaked false yam (*Icacina oliviformis*) tuber meal. Ghana Jour. Of Sc., Tech. And Dev. 3(1), 72–76.

Dejax, J., De Franceschi, D., Lugardon, B., De Ploëg, G., Arnold, V., 2001. Le contenu cellulaire du pollen fossilisé dans l'ambre, préservé à l'état organique. Comptes Rendus Académie Sci.-Ser. IIA-Earth Planet. Sci. 332(5), 339–344.

Del Rio, C., Haevermans, T., De Franceschi, D., 2017. First record of an Icacinaceae Miers fossil flower from Le Quesnoy (Ypresian, France) amber. Sci. Rep. 7(1), 11099.

Del Rio, C., Thomas, R., De Franceschi, D., 2018. Fruits of Icacinaceae Miers from the Paleocene of the Paris Basin (Oise, France). Earth Environ. Sci. Trans. R. Soc. Edinb. Accepted.

Dickens, G.R., O'Neil, J.R., Rea, D.K., Owen, R.M., 1995. Dissociation of oceanic methane hydrate as a cause of the carbon isotope excursion at the end of the Paleocene. Paleoceanography 10(6), 965–971.

Dickens, G.R., Castillo, M.M., Walker, J.C., 1997. A blast of gas in the latest Paleocene: Simulating first-order effects of massive dissociation of oceanic methane hydrate. Geology 25(3), 259–262.

Dickison, W.C., 1986. Further observations on the floral anatomy and pollen morphology of *Oncotheca* (Oncothecaceae). Brittonia 38(3), 249–259.

Didier, G., Royer-Carenzi, M., Laurin, M., 2012. The reconstructed evolutionary process with the fossil record. J. Theor. Biol. 315, 26–37.

Dollfus, F.G., 1880. Essai sur l'étendue des terrains tertiaires dans le bassin anglo-parisien. Bull. de la Soc. géol. De Norm. 6, 584–-605.

Duno de Stephano, R., 2013. Icacinaceae, in: Flora of Ecuador. Claes Persson and Bertil Stahl, Mexico. 6–43.

Duperon, J., 1976. A propos de quelques bois fossiles du Sud-Ouest de la France. Bull. Société Bot. Fr. 123(9), 533–540.

Drummond, A.J., Suchard, M.A., Xie, D., Rambaut, A., 2012. Bayesian Phylogenetics with BEAUti and the BEAST 1.7. Mol. Biol. Evol. 29, 1969–1973.

Endress, P.K., Rapini, A., 2014. Floral structure of *Emmotum* (Icacinaceae sensu stricto or Emmotaceae), a phylogenetically isolated genus of lamiids with a unique pseudotrimerous gynoecium, bitegmic ovules and monosporangiate thecae. Ann. Bot. 114(5), 945–959.

Engler, A., 1897. Icacinaceae, in: Die Natürlichen Pflanzenfamilien. Engelmann, Leipzig, Germany, 3, 233–257.

Erdtman, G., 1952. Pollen morphology and plant taxonomy. GFF 74, 526–527.

Escarguel, G.E., 1999. Les rongeurs de l'Éocène inférieur et moyen d'Europe Occidentale. Systematique, phylogénie, biochronologie et paléobiogéographie des niveaux-repères MP 7 a MP 14. Palaeovertebrata 28(2-4), 89–351.

Fairon-Demaret, M., Smith, T., 2002. Fruits and seeds from the Tienen Formation at Dormaal, Palaeocene–Eocene transition in eastern Belgium. Rev. Palaeobot. Palynol. 122(1-2), 47–62.

Fay, J.M., 1987. *Icacina oliviformis* (Icacinaceae): A close look at an underexploited crop. I. Overview and ethnobotany. Econ. Bot. 41(4), 512–522.

Fay, J.M., 1993. *Icacina oliviformis* (Icacinaceae): A close look at an underexploited food plant. III. Ecology and production. Econ. Bot. 47(2), 163–170.

Feiz Haddad, M.H., Mahbodfar, H., Zamani, Z., Ramazani, A., 2017. Antimalarial evaluation of selected medicinal plant extracts used in Iranian traditional medicine. Iranian J. Basic Med. Sci. 20(4), 415–422.

Foster, C.S.P., Sauquet, H., van der Merwe, M., McPherson, H., Rossetto, M., Ho, S.Y.W., 2016. Evaluating the impact of genomic data and priors on bayesian estimates of the Angiosperm evolutionary timescale. Syst. Biol. 66(3), 338–351.

Fricke, H.C., Clyde, W.C., O'Neil, J.R., Gingerich, P.D., 1998. Evidence for rapid climate change in North America during the latest Paleocene thermal maximum: oxygen isotope compositions of biogenic phosphate from the Bighorn Basin (Wyoming). Earth Planet. Sci. Lett. 160(1-2), 193–208.

Friis, E.M., Chaloner, W.G., Crane, P.R., 1987. The origins of angiosperms and their biological consequences. Cambridge university Press, 339 pp.

Fritel, P.H., 1908. Révision des Myricacées fossiles du grès de Belleu. Bull. Soc. Géol. France 4(8), 274–280.

Fritel, P.H., 1924. Suite et additions à la révision de la flore cuisienne des grès de Belleu. Bull.

Soc. Géol. France 4(24), 150–175.

Furon, R., Soyer, R., 1947. Catalogue des fossiles tertiaires du Bassin de Paris. P. Lechevalier. Paris. 6, 240 pp.

Gabaix-Hiale, R., 2014. La paléoflores du gisement de Rivecourt (Oise) : étude paléoxylologique. Mémoire du Master SEP du Muséum national d'Histoire naturelle (Paris, France), unpublished.

Ganesh, T., Davidar, P., 2001. Dispersal modes of tree species in the wet forests of southern Western Ghats. Curr. Sci. 80(3), 394–399.

Garel, S., Schnyder, J., Jacob, J., Dupuis, C., Boussafir, M., Le Milbeau, C., Storme, J.-Y., Iakovleva, A.I., Yans, J., Baudin, F., Fléhoc, C., Quesnel, F., 2013. Paleohydrological and paleoenvironmental changes recorded in terrestrial sediments of the Paleocene–Eocene boundary (Normandy, France). Palaeogeogr. Palaeoclimatol. Palaeoecol. 376, 184–199.

Garel, S., Quesnel, F., Jacob, J., Roche, E., Le Milbeau, C., Dupuis, C., Boussafir, M., Baudin, F., Schnyder, J., 2014. High frequency floral changes at the Paleocene–Eocene boundary revealed by comparative biomarker and palynological studies. Org. Geochem. 77, 43–58.

Gaudeul, M., Rouhan, G., 2013. A plea for modern botanical collections to include DNA-friendly material. Trends Plant Sci. 18(4), 184–185.

Gavryushkina, A., Heath, T.A., Ksepka, D.T., Stadler, T., Welch, D., Drummond, A.J., 2016. Bayesian total-evidence dating reveals the recent crown radiation of penguins. Syst. Biol. 66(1), 57–73.

Gehler, A., Gingerich, P.D., Pack, A., 2016. Temperature and atmospheric CO_2 concentration estimates through the PETM using triple oxygen isotope analysis of mammalian bioapatite. Proc. Natl. Acad. Sci. 113(28), 7739–7744.

Gély, J.-P., Hanot, F., Amédro, F., Bergerat, F., Debeglia, N., Delmas, J., Deroin, J.-P., Doligez, B., Dugué, O., Durand, M., Edel, J.-B., Gaudant, J., Hanzo, M., Houel, P., Lorenz, J., Robaszynski, F., Robelin, C., Thierry, J., Vicelli, J., Violette, S., Vrielynck, B., Wyns, R., et coll., 2014. Le Bassin parisien : Un nouveau regard sur la géologie, Bull. Inf. Géol. Bass. Paris. ed, Mémoire hors-série n' 9. Association des géologues du Bassin de Paris, France. 278 pp.

Gernhard, T., 2008. The conditioned reconstructed process. J. Theor. Biol. 253(4), 769–778.

Gheerbrant, E., Rage, J.-C., 2006. Paleobiogeography of Africa: How distinct from Gondwana and Laurasia? Palaeogeogr. Palaeoclimatol. Palaeoecol. 241(2), 224–246.

Gibbs, S.J., Bown, P.R., Sessa, J.A., Bralower, T.J., Wilson, P.A., 2006. Nannoplankton extinction and origination across the Paleocene-Eocene Thermal Maximum. Science 314(5806), 1770–1773.

Gingerich, P.D., 2000. Paleocene/Eocene boundary and continental vertebrate faunas of Europe and North America. GFF. 122(1), 57-59.

Gingerich, P.D., 2003. Mammalian responses to climate change at the Paleocene-Eocene boundary: Polecat Bench record in the northern Bighorn Basin, Wyoming. Spec. Pap.-Geol. Soc. Am. 463–478.

Gingerich, P.D., 2006. Environment and evolution through the Paleocene–Eocene thermal maximum. Trends Ecol. Evol. 21(5), 246–253.

Godinot, M., de Broin, F. de L., 2003. Arguments for a mammalian and reptilian dispersal from Asia to Europe during the Paleocene-Eocene boundary interval. Deinsea 10(1), 255–276.

Godinot, M., Russel, D.E., Louis, P., 1992. Oldest known *Nannopithex* (Primates, Omomyiformes) from the early Eocene of France. Folia Primatol 58(1), 32–40.

Gonzalez, F.A., Rudall, P.J., 2010. Flower and fruit characters in the early-divergent lamiid family Metteniusaceae, with particular reference to the evolution of pseudomonomery. Am. J. Bot. 97(2), 191–206.

Göppert, J.H.R., Menge, A., Conwentz, H.W., 1886. Die Flora des Bernsteins, und ihre Beziehungen zur Flora der Tortiärformation und der Gegenwart. Commissions-verlag von W. Engelmann in Leipzig. 63 pp.

Gosling, W.D., Miller, C.S., Livingstone, D.A., 2013. Atlas of the tropical West African pollen flora. Rev. Palaeobot. Palynol. 199, 1–135.

Gottwald, H.P., 2000. Gymnosperme und dicotyle Hölzer (67) aus dem" Aachener Sanden" der Oberen Kreide von NO-Belgien und NW-Deutschland: mit anatomischer Bestimmung der Arten, Kommentaren, Tafeln und 96 Mikrofotos. Verlag Documenta Naturae 131, 1–44.

Grambast Fessard, N., 1969. Contribution à l'étude des flores tertiaires des régions provençales et alpines. V. Deux bois de dicotylédones à caractères primitifs du Miocène supérieur de Castellane. Nat. Monspel. 20, 105–118.

Greguss, P., 1969. Tertiary angiosperm woods in Hungary. Bp. Akad. Kiado. 151 pp.

Gruas-Cavagnetto, C., 1967a. Complexes sporo-polliniques du Sparnacien du Bassin de Paris.

Rev. Palaeobot. Palynol. 5(1-4), 243–261.

Gruas-Cavagnetto, C., 1967b. Quelques nouvelles espèces sparnaciennes de pollens et spores. Bull. Société Géologique France 7(1), 57–62.

Gruas-Cavagnetto, C., 1968. Étude palynologique des divers gisements du Sparnacien du Bassin de Paris. Société géologique de France 110, 1–144.

Gruas-Cavagnetto, C., 1974. Associations sporopolliniques et microplanctoniques de l'Éocène et de l'Oligocène inférieur du Bassin de Paris. Paléobiologie Continentale, 5(2), 1–20.

Gruas-Cavagnetto, C., 1976. Étude palynologique du sondage de la Défense (Paris). Rev. Micropaleontol. 19(1), 27–46.

Gruas-Cavagnetto, C., 1978. Étude palynologique de L'Éocène du bassin Anglo-Parisien. Soc. Géol. France. 131, 1–64.

Gruas-Cavagnetto, C., 1987. Nouveaux éléments mégathermes dans la palynoflore Éocène du Bassin Parisien. Mém. Trav. Inst. Montp. 17, 207–233.

Gruas-Cavagnetto, C., Bui, N.-S., 1976. Présence de pollen d'Araliacées dans le Paléogène Anglais et Francais. Rev. Palaeobot. Palynol. 22, 61–72.

Gruas-Cavagnetto, C., Cerceau-Larrival, M.-T., 1982. Présence de pollens d'Ombellifères fossiles dans le Paléogène du Bassin Anglo-Parisien: premiers résultats. Monogr. Syst. Bot. Mo. Bot. Gard. 6, 255-267.

Gruas-Cavagnetto, C., Tambareau, Y., Villatte, J., 1992. Découverte de pollens, Dinoflagellés et Forminifères dans le Danien des Petites Pyrénées : Implications sur la position de La Limite Crétacé/Tertiaire. Geobios 25, 19–28.

Gutjahr, M., Ridgwell, A., Sexton, P.F., Anagnostou, E., Pearson, P.N., Pälike, H., Norris, R.D., Thomas, E., Foster, G.L., 2017. Very large release of mostly volcanic carbon during the Palaeocene–Eocene Thermal Maximum. Nature 548(7669), 573.

Han, M., Manchester, S.R., Wu, Y., Jin, J., Quan, C., 2018. Fossil fruits of *Canarium* (Burseraceae) from Eastern Asia and their implications for phytogeographical history. J. Syst. Palaeontol. 16(10), 841–852.

Hass, H., Rowe, N., 1999. Thin sections and wafering. Foss. Plants Spores Mod. Tech. 76–81.

Heath, T.A., Huelsenbeck, J.P., Stadler, T., 2014. The fossilized birth-death process for coherent calibration of divergence-time estimates. Proc. Natl. Acad. Sci. 111(29), E2957–E2966.

Heer, O., 1870. Die Miocene flora und fauna Spitzbergens. PA Norstedt & söner, Stockholm. 98 pp.

Heintzelman, C.E., Howard, R.A., 1948. The comparative morphology of the Icacinaceae. V. The pubescence and the crystals. Am. J. Bot. 35(1), 42–52.

Herendeen, P.S., 1991. Charcoalified angiosperm wood from the Cretaceous of eastern North America and Europe. Rev. Palaeobot. Palynol. 70(3), 225–239.

Herrera, F., Manchester, S.R., Hoot, S.B., Wefferling, K.M., Carvalho, M.R., Jaramillo, C., 2011. Phytogeographic implications of fossil endocarps of Menispermaceae from the Paleocene of Colombia. Am. J. Bot. 98(12), 2004–2017.

Herrera, F., Manchester, S.R., Carvalho, M.R., Jaramillo, C., Wing, S.L., 2014. Paleocene wind-dispersed fruits and seeds from Colombia and their implications for early Neotropical rainforests. Acta Palaeobot. 54(2), 197–229.

Hervet, S., 2006. The oldest European ptychogasterid turtle (Testudinoidea) from the lowermost Eocene amber locality of Le Quesnoy (France, Ypresian, MP7). J. Vertebr. Paleontol. 26(4), 839–848.

Higgins, J.A., Schrag, D.P., 2006. Beyond methane: Towards a theory for the Paleocene–Eocene Thermal Maximum. Earth Planet. Sci. Lett. 245(3-4), 523–537.

Hildebrand, A.R., Penfield, G.T., Kring, D.A., Pilkington, M., Camargo Z.A., Jacobsen, S.B., Boynton, W.V., 1991. Chicxulub crater: a possible Cretaceous/Tertiary boundary impact crater on the Yucatan Peninsula, Mexico. Geology 19(9), 867–871.

Hofmann, C.-C., Gregor, H.-J., 2018. Scanning electron microscope and light microscope investigations of pollen from an atypical mid-Eocene coal facies in Stolzenbach mine (Preu\s senElektra) near Borken (Kassel, Lower Hesse, Germany). Rev. Palaeobot. Palynol. 252, 41–63.

Hofmann, C.-C., Mohamed, O., Egger, H., 2011. A new terrestrial palynoflora from the Palaeocene/Eocene boundary in the northwestern Tethyan realm (St. Pankraz, Austria). Rev. Palaeobot. Palynol. 166(3-4), 295–310.

Hollick, C.A., 1936. The tertiary floras of Alaska. US Gov't. Print. Off. 182, 185 pp.

Holmgren, P., Holmgren, N., Barnett, L., 1990. Index Herbariorum, Part I: The herbaria of the world, New York Botanical Garden, New York.

Hooker, J.J., 2015. A two-phase Mammalian Dispersal Event across the Paleocene–Eocene transition. Newsl. Stratigr. 48(2), 201–220.

Hooker, J.J., Collinson, M.E., 2012. Mammalian faunal turnover across the Palaeocene-Eocene boundary in NW Europe: the roles of displacement, community evolution and environment. Austrian J. Earth Sci. 105(1), 17–28.

Howard, R.A., 1940. Study of the Icacinaceae I. Preliminary taxonomic notes. J. Arnold Arbor. 21(4), 461–488.

Howard, R.A., 1942a. Study of the Icacinaceae II. *Humirianthera*, *Leratia*, *Mappia* and *Nothapodytes*, valid genera of the Icacineae. J. Arnold Arbor. 23(1), 55–78.

Howard, R.A., 1942b. Study of the Icacinaceae III. A revision of *Emmotum*. J. Arnold Arbor. 23(4), 479–494.

Howard, R.A., 1942c. Study of the Icacinaceae IV. Considerations of the new world genera. Harv. Univ. Herb. 142, 3–60.

Howard, R.A., 1942d. Study of the Icacinaceae V. A revision of the genus *Citronella* D. Don. Harv. Univ. Herb. 142, 60–89.

Howard, R.A., 1943. Studies of the Icacinaceae-VI. *Irvingbaileya* and *Codiocarpus*, Two New Genera of the Icacineae. Brittonia 5(1), 47–57.

Howard, R.A., 1992. A Revision of *Casimirella*, Including *Humirianthera* (Icacinaceae). Brittonia 44(2), 166–172.

Iturralde-Vincent, M.A., MacPhee, R.D.E., 1996. Age and Paleogeographical Origin of Dominican Amber. Science 273(5283), 1850–1852.

Jacques, F.M.B., 2009a. Fossil history of the Menispermaceae (Ranunculales). Ann. Paléontol. 95(2), 53–69.

Jacques, F.M.B., 2009b. Survey of the Menispermaceae endocarps. Adansonia 31(1), 47–87.

Jacques, F.M.B., De Franceschi, D., 2005. Endocarps of Menispermaceae from Le Quesnoy outcrop (Sparnacian facies, Lower Eocene, Paris Basin). Rev. Palaeobot. Palynol. 135(1-2), 61–70.

Jain, S.K., Dam, N., 1979. Some ethnobotanical notes from Northeastern India. Econ. Bot. 33(1), 52–56.

Jansen-Jacobs, M.J., 1979. Icacinaceae, in: Flora of Suriname. A.L. Stoffers and J.C. Lindeman, Leiden, 344–355.

Jaramillo, C., Ochoa, D., Contreras, L., Pagani, M., Carvajal-Ortiz, H., Pratt, L.M., Krishnan, S., Cardona, A., Romero, M., Quiroz, L., et coll., 2010. Effects of rapid global warming at the Paleocene-Eocene boundary on Neotropical vegetation. Science 330(6006), 957–961.

Jia, L.-B., Manchester, S.R., Su, T., Xing, Y.-W., Chen, W.-Y., Huang, Y.-J., Zhou, Z.-K., 2015. First occurrence of *Cedrelospermum* (Ulmaceae) in Asia and its biogeographic implications. J. Plant Res. 128(5), 747–761.

Jiang, Z.-H., Chai, L., Liu, Y.-P., Qiu, H.-C., Wang, T.-T., Feng, X.-Y., Wang, Y.-T., Huang, Z.-H., Liu, B.-M., Fu, Y.-H., 2017. Bioactive lignans from the stems of *Mappianthus iodoides*. Phytochem. Lett. 22, 194–198.

Jiofack, T., Fokunang, C., Guedje, N., Kemeuze, V., Fongnzossie, E., Nkongmeneck, B.A., Mapongmetsem, P.M., Tsabang, N., 2010. Ethnobotanical uses of medicinal plants of two ethnoecological regions of Cameroon. Int. J. Med. Med. Sci. 2(3), 60–79.

Johnson, K.R., 2002. Megaflora of the Hell Creek and lower Fort Union Formations in the western Dakotas: Vegetational response to climate change, the Cretaceous-Tertiary boundary event, and rapid marine transgression. Geol. Soc. Am. Spec. Pap. 361, 329–391.

Jossang, J., Bel-Kassaoui, H., Jossang, A., Seuleiman, M., Nel, A., 2008. Quesnoin, a novel pentacyclic ent-diterpene from 55 million years old Oise amber. J. Org. Chem. 73(2), 412–417.

Jud, N.A., Nelson, C.W., Herrera, F., 2016. Fruits and wood of Parinari from the early Miocene of Panama and the fossil record of Chrysobalanaceae. Am. J. Bot. 103(2), 277–289.

Jud, N.A., Iglesias, A., Wilf, P., Gandolfo, M.A., 2018. Fossil moonseeds from the Paleogene of West Gondwana (Patagonia, Argentina). Am. J. Bot. 105(5), 927–942

Jussieu, A. (de), 1823. Description d'un genre nouveau nommé Icacina, in: Mémoires de La Société d'Histoire Naturelle de Paris, Paris. 1, 174-178.

Kaplan, M.A.C., Ribeiro, J., Gottlieb, O.R., 1991. Chemogeographical evolution of terpenoids in Icacinaceae. Phytochemistry 30(8), 2671–2676.

Kårehed, J., 2001. Multiple origin of the tropical forest tree family Icacinaceae. Am. J. Bot. 88(12), 2259–2274.

Kedves, M., 1967a. Sur quelques problèmes de stratigraphie palynologique appliquée au Tertiaire inférieur en Europe. Pollen & Spores 9, 321–334.

Kedves, M., 1967b. Études palynologiques des couches du Tertiaire inférieur de la région Parisienne. I. Spores. Pollen & Spores 9, 521–552.

Kedves, M., 1968a. Études palynologiques des couches du Tertiaire inférieur de la région Parisienne. II. Tableau de quelques espèces et types sporomorphes. Pollen & Spores 117–128.

Kedves, M., 1968b. Études palynologiques des couches du Tertiaire inférieur de la région Parisienne. III. Pollen inaperturé, à ballonnets, polypliqués, monocolpé, disulqué, trichotomosulqué et proxaperturés. Pollen & Spores 315–334.

Kedves, M., 1969. Études palynologiques des couches du Tertiaire inférieur de la région Parisienne. IV. Pollen des Normapolles. Pollen & Spores 11(2), 385–396.

Kedves, M., 1970. Études palynologiques des couches du Tertiaire inférieur de la région Parisienne.V. Pollen triporés, subtriporés et intratriporés. Pollen Spores 12(1), 83–97.

Kedves, M., 1992. Études palynologiques des couches du Tertiaire inférieur de la région Parisienne.VII. Acta Biol 38, 33–46.

Kedves, M., 1997. Études palynologiques des couches du Tertiaire inférieur de la région Parisienne. VIII. Plant Cell Biol. Dev. 34–43.

Kedves, M., 1998. Études palynologiques des couches du Tertiaire inférieur de la région Parisienne. IX. Plant Cell Biol. Dev. 28–42.

Kedves, M., 1999. Études palynologiques des couches du Tertiaire inférieur de la région Parisienne. X. Plant Cell Biol. Dev. 30–38.

Kedves, M., Endredi, L., 1968. Palynologie investigations in the strata of «Buda Marl» with plantremains. Acta Biol 14, 1–4.

Kedves, M., Pradutz, A., 1970. Études palynologiques des couches du tertiaire inférieur de la région Parisienne. VI. Ultrastructure de quelques pollens d'Angiospermes de l'Éocène inférieur (Sparnacien). Pollen & Spores 12(4), 553–575.

Kedves, M., Russell, D.E., 1982. Palynology of the Thanetian layers of Menat. The geology of the Menat Basin, France. Palaeontogr. Abt. B 182(4-6), 87–150.

Keller, G., 1983. Paleoclimatic analyses of middle Eocene through Oligocene planktic foraminiferal faunas. Palaeogeogr. Palaeoclimatol. Palaeoecol. 43(1-2), 73–94.

Keller, G., 2012. The Cretaceous–Tertiary Mass Extinction, Chicxulub Impact, and Deccan Volcanism, in: Talent, J.A. (Ed.), Earth and Life. Springer Netherlands, Dordrecht, 759–793.

Kelly, D.C., Bralower, T.J., Zachos, J.C., 1998. Evolutionary consequences of the latest Paleocene thermal maximum for tropical planktonic foraminifera. Palaeogeogr. Palaeoclimatol. Palaeoecol. 141(1-2), 139–161.

Kennett, J.P., Stott, L.D., 1991. Abrupt deep-sea warming, palaeoceanographic changes and benthic extinctions at the end of the Palaeocene. Nature 353(6341), 225–229.

Kent, D.V., Cramer, B.S., Lanci, L., Wang, D., Wright, J.D., van der Voo, R., 2003. A case for a comet impact trigger for the Paleocene/Eocene thermal maximum and carbon isotope excursion. Earth Planet. Sci. Lett. 211(1-2), 13–26.

Kerr, A.F.G., 1911. Contributions to the Flora of Siam. I.: Sketch of the Vegetation of Chiengmai. Bull. Misc. Inf. R. Gard. Kew 1911(1), 1–60.

Kessler, P.J.A., 1993. Menispermaceae, in: Kubitzki, K., Rohwer, J.G., Bittrich, V. (Eds.), Flowering Plants • Dicotyledons: Magnoliid, Hamamelid and Caryophyllid Families. Springer Berlin Heidelberg, Berlin, Heidelberg. 402–418.

Kier, G., Kreft, H., Lee, T.M., Jetz, W., Ibisch, P.L., Nowicki, C., Mutke, J., Barthlott, W., 2009.

A global assessment of endemism and species richness across island and mainland regions. Proceedings of the National Academy of Sciences 106(23), 9322–9327.

Kipre, G.R., Offoumou, M.R., Silue, K.D., Bouabre, G.M., Zirihi, G.N., Djaman, A.J., 2017. Enquête ethnopharmacologique des plantes antipaludiques dans le département d'Agboville, sudest de la Cote d'Ivoire. J. Appl. Biosci. 109(1), 10618–10629.

Knobloch, E., Mai, D.H., 1986. Monographie der Fruchte und Samen in der Kreide von Mitteleuropa. Vydal Ustredni ustav geologicky, Praha. 219 pp.

Knobloch, E., Konzalova, M., 1998. Comparison of the Eocene plant assemblages of Bohemia (Czech Republic) and Saxony (Germany). Rev. Palaeobot. Palynol. 101(1-4), 29–41.

Knoll, A.H., 1986. Patterns of change in plant communities through geological time. Community Ecol. 126–141.

Koch, P.L., Clyde, W.C., Hepple, R.P., Fogel, M.L., Wing, S.L., Zachos, J.C., 2003. Carbon and oxygen isotope records from paleosols spanning the Paleocene-Eocene boundary, Bighorn Basin, Wyoming. Spec. Pap.-Geol. Soc. Am. 369, 49–64.

Kodandaramaiah, U., 2009. Use of dispersal-vicariance analysis in biogeography - a critique: A critique of dispersal-vicariance analysis. J. Biogeogr. 37(1), 3–11.

Koeniger, J. C., 1982. Un site à bois et empreintes dans les grès de Belleu (Cuisien) du Tardenois. Congrès national des sociétés savantes. 1, 97-107.

Krutzsch, W., Vanhoorne, R., 1977. Die Pollenflora von Epinois und Loksbergen in Belgien. Palaeontogr. Abt. B 163, 1–110.

Kuhlmann, M., Ribeiro, J.F., 2016. Fruits and frugivores of the Brazilian Cerrado: ecological and phylogenetic considerations. Acta Bot. Bras. 30(3), 495–507.

Kurtz, A.C., Kump, L.R., Arthur, M.A., Zachos, J.C., Paytan, A., 2003. Early Cenozoic decoupling of the global carbon and sulfur cycles. Paleoceanography 18(4), 1–14.

Kvaček, Z., Bůžek, Č., 1995. Endocarps and foliage of the flowering plant family Icacinaceae from the Tertiary of Europe. Tert. Res. 15(3), 121–138.

Kvaček, Z., Hably, L., Manchester, S.R., 2001. *Sloanea* (Elaeocarpaceae) fruits and foliage from the Early Oligocene of Hungary and Slovenia. Palaeontogr. B 259(1-6), 113–124.

Labat, J. N., El-Achkar, E., Rabevohitra, R., 2006. Révision synoptique du genre *Pyrenacantha* (Icacinaceae) à Madagascar. Adansonia, 28(2), 389-404.

Lacau, S., Nel, A., Villemant, C., Menier, J.-J., Orliac, M.J., De Plöeg, G., 2000. A Fossil Scolebythidae from the Lowermost Eocene Amber of France (Insecta: Hymenoptera). Ann. Entomol. Soc. Am. 93(4), 701–706.

Lavin, M., & Luckow, M, 1993. Origins and relationships of tropical North America in the context of the boreotropics hypothesis. Am. Jour. of Botany, 80(1), 1–14.

Leaf Architecture Working Group. (1999). Manual of leaf architecture: - morphological description and categorization of dicotyledonous and net-veined monocotyledonous angiosperms. Smithsonian Institute: Washington, DC. 580, 67 pp.

Lemoine, P., 1911. Géologie du Bassin de Paris. A. Hermann et fils, Paris. 408 pp.

Lens, F., Kårehed, J., Baas, P., Jansen, S., Rabaey, D., Huysmans, S., Hamann, T., Smets, E., 2008. The wood anatomy of the polyphyletic Icacinaceae s.l., and their relationships within asterids. Taxon 57(2), 525–552.

Lenz, O.K., Wilde, V., Riegel, W., 2007. Recolonization of a Middle Eocene volcanic site: quantitative palynology of the initial phase of the maar lake of Messel (Germany). Rev. Palaeobot. Palynol. 145(3-4), 217–242.

Leopold, E.B., MacGinitie, H.D., 1972. Development and affinities of Tertiary floras in the Rocky Mountains. In A. Graham, ed., Floristics and paleofloristics of Asia and eastern North America. Elsevier Pubi. Co., Amsterdam. 147–200.

Lewis, P.O., 2001. A likelihood approach to estimating phylogeny from discrete morphological character data. Syst. Biol. 50(6), 913–925.

Liu, Y.-S. (Christopher), Jacques, F.M.B., 2010. Sinomenium macrocarpum sp. nov. (Menispermaceae) from the Miocene–Pliocene transition of Gray, northeast Tennessee, USA. Rev. Palaeobot. Palynol. 159(1-2), 112–122.

Lobreau-Callen, D., 1972. Pollen des Icacinaceae: 1. Atlas (1). Pollen & Spores 14(4), 345–388.

Lobreau-Callen, D., 1973. Le pollen des Icacinaceae: 2. Observations en microscopie électronique, corrélations, conclusions. Pollen & Spores 15(1), 47–89.

Lobreau-Callen, D., 1975. Les variations dimensionnelles du pollen du genre *Ilex* (Aquifoliaceae) et leurs rapports avec le climat. Bull. Société Bot. Fr. 122(sup1), 179–199.

Longrich, N.R., Tokaryk, T., Field, D.J., 2011. Mass extinction of birds at the Cretaceous–Paleogene (K–Pg) boundary. Proc. Natl. Acad. Sci. 108(37), 15253–15257.

Longrich, N.R., Bhullar, B.-A.S., Gauthier, J.A., 2012. Mass extinction of lizards and snakes at the Cretaceous–Paleogene boundary. Proc. Natl. Acad. Sci. 109(52), 21396–21401.

Lorence, A., Nessler, C.L., 2004. Camptothecin, over four decades of surprising findings. Phytochemistry 65(20), 2735–2749.

Louis, P., 1996. Recherches de mammifères paléogènes dans les départements de l'Aisne et de la Marne pendant la deuxième moitié du vingtième siècle. Palaeovertebrata 25, 83–113.

Lourens, L.J., Sluijs, A., Kroon, D., Zachos, J.C., Thomas, E., Röhl, U., Bowles, J., Raffi, I., 2005. Astronomical pacing of late Palaeocene to early Eocene global warming events. Nature

435(7045), 1083–1087.

Luterbacher, H., Hardenbol, J., Schmitz, B., 2000. Decision of the voting members of the International Subcommission on Paleogene Stratigraphy on the criterion for the recognition of the Paleocene/Eocene boundary. Newsl. Int. Subcomm. Paleogene Stratigr. 9, 13.

MacGinitie, H.D., 1941. Middle Eocene flora from the central Sierra Nevada. Publ. Carnegie Inst. Washington 534, 1-178.

MacGinitie, H.D., 1969. The Eocene Green River flora of northwestern Colorado and northeastern Utah. University of California Press. 83, 1-202.

Maddison, W.P., Maddison, D.R., 2001. Mesquite: a modular system for evolutionary analysis.

Magallón, S.A., Sanderson, M.J., 2005. Angiosperm divergence times: the effect of genes, codon positions, and time constraints. Evolution 59(8), 1653–1670.

Magallón, S., Castillo, A., 2009. Angiosperm diversification through time. Am. J. Bot. 96(1), 349–365.

Magallón, S., Crane, P.R., Herendeen, P.S., 1999. Phylogenetic pattern, diversity, and diversification of Eudicots. Ann. Mo. Bot. Gard. 86(2), 297–372.

Magallón, S., Gómez-Acevedo, S., Sánchez-Reyes, L.L., Hernández-Hernández, T., 2015. A metacalibrated time-tree documents the early rise of flowering plant phylogenetic diversity. New Phytol. 207(2), 437–453.

Mai, D.H., 1987. Neue Fruchte und Samen aus palaozanen Ablagerungen Mitteleuropas. Feddes Repert. 98, 197–229.

Mai, D.H., 1989. Development and regional differentiation of the European vegetation during the Tertiary, in: Woody Plants evolution and Distribution since the Tertiary. Springer, Vienna. 79–91.

Manchester, S.R., 1994. Fruits and seeds of the Middle Eocene nut beds flora, Clarno Formation, Oregon, Palaeontolographica Americana. Paleontological Research Institution, New York. 205 pp.

Manchester, S.R. 1999. Biogeographical relationships of North American tertiary floras. Annals of the Missouri Botanical Garden 86(2), 472–522.

Manchester, S.R., Tiffney, B.H., 1993. Fossil fruits of *Pyrenacantha* and related Phytocreneae (Icacinaceae) in the Paleogene of North America, Europe, and Africa. In American Journal of Botany Abstracts 80, 91.

Manchester, S.R., Tiffney, B.H., 2001. Integration of paleobotanical and neobotanical data in the assessment of phytogeographic history of Holarctic Angiosperm clades. Int. J. Plant Sci.

162(S6), S19–S27.

Manchester, S.R., Wilde, V., Collinson, M.E., 2007. Fossil cashew nuts from the Eocene of Europe: biogeographic links between Africa and South America. Int. J. Plant Sci. 168(8), 1199–1206.

Manchester, S.R., Chen, I., Lott, T.A., 2012. Seeds of *Ampelocissus*, *Cissus*, and *Leea* (Vitales) from the Paleogene of Western Peru and their biogeographic significance. Int. J. Plant Sci. 173(8), 933–943.

Manchester, S.R., Kapgate, D.K., Wen, J., 2013. Oldest fruits of the grape family (Vitaceae) from the Late Cretaceous Deccan Cherts of India. Am. J. Bot. 100(9) 1849–1859.

Manchester, S.R., Grímsson, F., Zetter, R., 2015. Assessing the fossil record of Asterids in the context of our current phylogenetic framework 1. Ann. Mo. Bot. Gard. 100(4), 329–363.

Marandat, B., Adnet, S., Marivaux, L., Martinez, A., Vianey-Liaud, M., Tabuce, R., 2012. A new mammalian fauna from the earliest Eocene (Ilerdian) of the Corbières (Southern France): palaeobiogeographical implications. Swiss J. Geosci. 105(3), 417–434.

Martínez-Millán, M., 2010. Fossil record and age of the Asteridae. Bot. Rev. 76(1), 83–135.

Marynowski, L., Otto, A., Zatoń, M., Philippe, M., Simoneit, B.R.T., 2007. Biomolecules preserved in ca. 168 million year old fossil conifer wood. Naturwissenschaften 94(3), 228–236.

McClain, A.M., Manchester, S.R., 2001. *Dipteronia* (Sapindaceae) from the tertiary of North America and implications for the phytogeographic history of the Aceroideae. Am. J. Bot. 88(7), 1316–1325.

McElwain, J.C., Punyasena, S.W., 2007. Mass extinction events and the plant fossil record. Trends Ecol. Evol. 22(10), 548–557.

McInerney, F.A., Wing, S.L., 2011. The Paleocene-Eocene Thermal Maximum: A Perturbation of Carbon Cycle, Climate, and Biosphere with Implications for the Future. Annu. Rev. Earth Planet. Sci. 39, 489–516.

McKenna, M.C., 1975. Fossil mammals and early Eocene North Atlantic land continuity. Ann. Mo. Bot. Gard. 62(2), 335–353.

Megnien, C., 1980a. Tectogenese du Bassin de Paris; etapes de l'evolution du bassin. Bulletin de la Société géologique de France, 7(4), 669-680.

Mégnien, C., 1980b. Synthèse géologique du Bassin de Paris (No. 101-103). Édition du BRGM.

Menier, J.-J., Nel, A., Waller, A., De Ploëg, G., 2004. A new fossil ichneumon wasp from the Lowermost Eocene amber of Paris Basin (France), with a checklist of fossil

Ichneumonoidea sl. (Insecta: Hymenoptera: Ichneumonidae: Metopiinae). Geol. Acta 2(1), 83–94.

Michez, D., Nel, A., Menier, J.-J., Rasmont, P., 2007. The oldest fossil of a melittid bee (Hymenoptera: Apiformes) from the early Eocene of Oise (France). Zool. J. Linn. Soc. 150(4), 701–709.

Miers, J., 1851. Observations on the affinities of the Olacaceae. Ann. Mag. Nat. Hist. 8(45), 161–184.

Miers, J., 1852. On some genera of the Icacinaceae. Ann. Mag. Nat. Hist. 10, 30–44.

Miller, M.A., Pfeiffer, W., Schwartz, T., 2010. Creating the CIPRES Science Gateway for inference of large phylogenetic trees, in: Gateway Computing Environments Workshop (GCE), 2010. Ieee, 1–8.

Mizukami, T., Kaiho, K., Oba, M., 2013. Significant changes in land vegetation and oceanic redox across the Cretaceous/Paleogene boundary. Palaeogeogr. Palaeoclimatol. Palaeoecol. 369, 41–47.

Moore, E.A., Kurtz, A.C., 2008. Black carbon in Paleocene–Eocene boundary sediments: A test of biomass combustion as the PETM trigger. Palaeogeogr. Palaeoclimatol. Palaeoecol. 267(1-2), 147–152.

Morat, P., Veillon, J.M., 1988. Oncothécacées, in: Flore de La Nouvelle-Calédonie et Dépendances. Muséum national d'Histoire naturelle, Paris 15, 90–98.

Morley, R.J., 2000. Origin and Evolution of Tropical Forest. Willey & Son, Chichester. 362 pp.

Morley, R.J., 2011. Cretaceous and Tertiary climate change and the past distribution of megathermal rainforests. Wiley, New-York. 362 pp.

Morley, R.J., Dick, C.W., 2003. Missing fossils, molecular clocks, and the origin of the Melastomataceae. Am. J. Bot. 90(11), 1638–1644.

Morsi, A.-M.M., Speijer, R.P., Stassen, P., Steurbaut, E., 2011. Shallow marine ostracode turnover in response to environmental change during the Paleocene–Eocene thermal maximum in northwest Tunisia. J. Afr. Earth Sci. 59(2-3), 243–268.

Mouton, J.A., 1970. Florule élémentaire du Thanétien de Sézanne, in: Comptes Rendus Du Congrès National Des Sociétés Savantes: Section Des Sciences. Bibliothèque nationale, Reims. 213–225.

Murphy, B., Farley, K., Zachos, J., 2010. An extraterrestrial ^{3}He-based timescale for the Paleocene–Eocene thermal maximum (PETM) from Walvis Ridge, IODP Site 1266. Geochim. Cosmochim. Acta 74(17), 5098–5108.

Nagamasu, H., Kato, M., 2004. *Nothapodytes amamianus* (Icacinaceae), a new species from the

Ryukyu Islands. Acta Phytotax. Geobot. 55(2), 75–78.

Nel, A., Prokop, J., 2006. New fossil gall midges from the earliest Eocene French amber (Insecta, Diptera, Cecidomyiidae). Geodiversitas 28(1), 37–54.

Nel, A., de Plöeg, G., Dejax, J., Dutheil, D., De Franceschi, D., Gheerbrant, E., Godinot, M., Hervet, S., Menier, J.-J., Augé, M., Bignot, G., Cavagnetto, C., Duffaud, S., Gaudant, J., Hua, S., Jpssang, A., de Lapparent de Broin, F., Pozzi, J.-P., Paicheler, J.-C., Beuchet, F., Rage, J.-C., 1999. Un gisement sparnacien exceptionnel à plantes, arthropodes et vertébrés (Éocène basal, MP7) : Le Quesnoy (Oise, France). Comptes Rendus Académie Sci. - Ser. IIA - Earth Planet. Sci. 329, 65–72.

Nel, A., Waller, A., Albouy, V., Menier, J.-J., De Ploëg, G., 2003. New fossil earwigs from the lowermost Eocene amber of Paris basin (France) (Insecta, Dermaptera, family incertaesedis). Geodiversitas 25, (1) 119–129.

Nel, A., De Ploëg, G., Milliet, J., Menier, J.-J., Waller, A., 2004a. The French ambers: a general conspectus and the Lowermost Eocene amber deposit of Le Quesnoy in the Paris Basin. Geologica Acta 2(1), 3–8.

Nel, A., Waller, A., De Ploëg, G., 2004b. The oldest fossil piesmatid bug in the Lowermost Eocene amber of the Paris Basin (Heteroptera: Lygaeoidea: Piesmatidae). Geologica Acta 2(1), 45–50.

Nel, P., Schmidt, A. R., Bässler, C., Nel, A., 2011. Fossil thrips of the family Uzelothripidae suggest 53 million years of morphological and ecological stability. Acta Palaeontologica Polonica, 58(3), 609-614.

Nie, Z.-L., Sun, H., Chen, Z.-D., Meng, Y., Manchester, S.R., Wen, J., 2010. Molecular phylogeny and biogeographic diversification of *Parthenocissus* (Vitaceae) disjunct between Asia and North America. Am. J. Bot. 97(8), 1342–1353.

Nie, Z.-L., Sun, H., Manchester, S.R., Meng, Y., Luke, Q., Wen, J., 2012. Evolution of the intercontinental disjunctions in six continents in the *Ampelopsis* clade of the grape family (Vitaceae). BMC Evol. Biol. 12(17), 1–13.

Niklas, K.J., 1982. Preservation of unsaturated fatty acids in Palaeogene angiosperm fruits and seeds. Nature 296(5852), 63–64.

Niklas, K.J., Tiffney, B.H., Knoll, A.H., 1983. Patterns in vascular land plant diversification. Nature 303(5918), 614–616.

Nylander, J.A.A., Ronquist, F., Huelsenbeck, J.P., Nieves-Aldrey, J., 2004. Bayesian phylogenetic analysis of combined data. Syst. Biol. 53(1), 47–67.

Odonne, G., Valadeau, C., Alban-Castillo, J., Stien, D., Sauvain, M., Bourdy, G., 2013. Medical ethnobotany of the Chayahuita of the Paranapura basin (Peruvian Amazon). J. Ethnopharmacol. 146(1), 127–153.

Ohwi, J., 1984. A combined, much revised, and extended translation by the author of his Flora of Japan (1953) and Flora of Japan-Pteridophyta (1957). In: Meyer FG, Walker EH (eds) Flora of Japan. Smithsonian Inst, Washington, 461 pp.

Okieimen, F. E., Owolabi, J. O., Iyekowa, O., Jonathan, J. E., 2018. Uterine contractile activity of extract of *Icacina trichantha* on albino non-pregnant rat uterus. Trop. J. Nat. Prod. Res. 2(2), 118-121.

Omalius d'Halloy, J.-B., 1816. Mémoire sur l'étendue géographique du terrain des environs de Paris. Ann. Mines 1, 231–266.

Otun, K.O., Onikosi, D.B., Ajiboye, A.A., Jimoh, A.A., 2015. Chemical composition, antioxidant and antimicrobial potentials of *Icacina trichantha* Oliv. Leaf extracts. Inter. J. of Trop. Med. 10(4-6), 21–29.

Panchuk, K., Ridgwell, A., Kump, L., 2008. Sedimentary response to Paleocene-Eocene Thermal Maximum carbon release: A model-data comparison. Geology 36(4), 315–318.

Peng, H., Howard, R.A., 2008. Icacinaceae, in: Flora of China. W.Zhengyi, P.H.Raven, Science Press. Beijing -- Missouri Botanical Garden. St. Louis, 505–513.

Pérez-Consuegra, N., Cuervo-Gómez, A., Martínez, C., Montes, C., Herrera, F., Madriñán, S., Jaramillo, C., 2017. Paleogene *Salvinia* (Salviniaceae) from Colombia and their paleobiogeographic implications. Rev. Palaeobot. Palynol. 246, 85–108.

Pérez-Consuegra, N., Góngora, D.E., Herrera, F., Jaramillo, C., Montes, C., Cuervo-Gómez, A.M., Hendy, A., Machado, A., Cárdenas, D., Bayona, G., 2018. New records of Humiriaceae fossil fruits from the Oligocene and Early Miocene of the western Azuero Peninsula, Panamá. Bol. Soc. Geológica Mex. 70(1), 223–239.

Perrier De La Bâthie, H.H., 1944. Révision des Icacinacées de Madagascar et des Comores. Mémoires du Muséum national d'Histoire naturelle, Paris. 18(9), 289–308.

Perrier De La Bâthie, H.H., 1952. Icacinacées (Icacinaceae), in: Flore de Madagascar et Des Comores 119. H. Humbert, Paris. 1–45.

Perrodon, A., Zabek, J., 1991, Paris Basin, in Leighton, M.W., et al., eds., Selected analog interior cratonic basins: American Association of Petroleum Geologists Memoir 51, 633-680.

Petrescu, J., Dragastan, O., 1972. Asupra unor lemne de *Icacinoxylon* Shilkina din oligocenul de la Telega-Prahova. Stud. Cerc Geol Geofiz Geog Ser Geol 17, 445–451.

Petrescu, I., Nutu, A., 1972. Asupra unui lemn de *Icacinoxylon* Sh. in micenul superior de la Pravaleni. Brad. Sargetia Ser Sc 9, 77–79.

Petrescu, I., Codrea, V., 2004. The signification of the Paleocene microflora from Jibou (Sălaj District) for the Paleogene palinological heritage of Romania. Acta Palaeontol. Romaniae 4, 351–360.

Petrescu, I., Ghiurca, V., Nica, V., 1989. Paleobotanical and palynological researches on the lower-Oligocene amber and amber-bearing formation at Colti–Buzau. Oligocene Transylv. Basin 183–198.

Pigg, K.B., Wher, W.C., 2002. Tertiary flowers, fruits, and seeds of Washington State and adjacent area-Part III. Washington Geology 30(3/4), 3–16.

Pigg, K.B., DeVore, M.L., 2009. Floristic composition and variation in late Paleocene to early Eocene floras in North America. Bull. Geosci. 85(1), 135–154.

Pigg, K.B., Manchester, S.R., DeVore, M.L., 2008. Fruits of Icacinaceae (Tribe Iodeae) from the Late Paleocene of western North America. Am. J. Bot. 95(7), 824–832.

Poinar Jr, G.O., 1991. *Hymenaea protera* sp. n. (Leguminosae, Caesalpinioideae) from Dominican amber has African affinities. Experientia 47(10), 1075–1082.

Poinar Jr, G.O., 2002a. Fossil palm flowers in Dominican and Mexican amber. Bot. J. Linn. Soc. 138(1), 57–61.

Poinar Jr, G.O., 2002b. Fossil palm flowers in Dominican and Baltic amber. Bot. J. Linn. Soc. 139(4), 361–367.

Poinar Jr, G.O., 2004. *Programinis burmitis* gen. et sp. nov., and *P. laminatus* sp. nov., Early Cretaceous grass-like monocots in Burmese amber. Aust. Syst. Bot. 17(5), 497–504.

Poinar Jr, G.O., Poinar, R., 1999. The amber forest: a reconstruction of a vanished world. Princeton University Press, New Jersey. 229 pp.

Poinar Jr, G.O, Chambers, K.L., 2005. *Palaeoanthella huangii* gen. and sp. nov., an early Cretaceous flower (Angiospermae) in Burmese amber. SIDA Contrib. Bot. 21(4), 2087–2092.

Poinar Jr, G.O., Judziewicz, E.J., 2005. *Pharus primuncinatus* (Poacae: Pharoideae: Phareae) from Dominican amber. SIDA Contrib. Bot. 21(4), 2095–2103.

Poinar Jr, G.O., Columbus, J.T., 2013. *Alarista succina* gen. et sp. nov. (Poaceae: Bambusoideae) in Dominican amber. Hist. Biol. 25(5-6), 691–696.

Poinar Jr, G.O, Steeves, R., 2013. *Virola dominicana* sp. nov. (Myristicaceae) from Dominican amber. Botany 91(8), 530–534.

Poinar Jr, G.O., Chambers, K.L., Buckley, R., 2007. *Eoëpigynia burmensis* gen. and sp. nov., an Early Cretaceous eudicot flower (Angiospermae) in Burmese amber. J. Bot. Res. Inst.

Tex. 1(1), 91–96.

Poinar Jr, G.O., Chambers, K.L., Brown, A.E., 2008. *Trochanthera lepidota* gen. and sp. nov., a fossil angiosperm inflorescence in Dominican amber. J. Bot. Res. Inst. Tex. 2(2), 1167–1173.

Pomerol, C., Boureaux, M., Bournérias, M., Dorigny, A., Solau, J.-L., Vantinel, M., 1984. Notice explicative de la feuille soissons a 1/50 000 5–46.

Potgieter, M.J., van Wyk, A.E., 1993. Fruit structure of the genus *Cassinopsis* Sond. (Icacinaceae) in Africa. S. Afr. J. Bot. 60(2), 117–122.

Potgieter, M.J., van Wyk, A.E., 1994. Fruit structure of the genus *Pyrenacantha* Hook. (Icacinaceae) in southern Africa. Bot. Bull. Acad. Sin. 35, 105–113.

Potgieter, M.J., Duno, R., 2016. Icacinaceae, in: Kadereit, J.W., Bittrich, V. (Eds.), Flowering Plants. Eudicots. Springer International Publishing, Cham. 239–256.

Potonié, R., 1960. Synopsis der Gattungen der Sporae dispersae: III. Beib. Geol. Jahrb. 39, 1--189.

Potter, J.F., 1977. Eocene, lower Bracklesham Beds, iron workings in Surrey. Proc. Geol. Assoc. 88(4), 229–241.

Prashanth Kumar, G.M., Shiddamallayya, N., 2016. Survey of wild medicinal plants of Hassan district, Karnataka. J. Med. Plants 4(1), 91–102.

Pujalte, V., Schmitz, B., Baceta, J.I., Orue-Etxebarria, X., Bernaola, G., Dinarès-Turell, J., Payros, A., Apellaniz, E., Caballero, F., 2009. Correlation of the Thanetian-Ilerdian turnover of larger foraminifera and the Paleocene-Eocene thermal maximum: confirming evidence from the Campo area (Pyrenees, Spain). Geol. Acta Int. Earth Sci. J. 7(1), 161–175.

Pyron, R.A., 2011. Divergence time estimation using fossils as terminal taxa and the origins of Lissamphibia. Syst. Biol. 60(4), 466–481.

Rambaut, A., Suchard, M.A., Xie, D., Drummond, A.J., 2014. Tracer v1. 6.

Ramesha, B.T., Suma, H.K., Senthilkumar, U., Priti, V., Ravikanth, G., Vasudeva, R., Kumar, T.R.S., Ganeshaiah, K.N., Shaanker, R.U., 2013. New plant sources of the anti-cancer alkaloid, camptothecine from the Icacinaceae taxa, India. Phytomedicine 20(6), 521–527.

Rampino, M.R., 2013. Peraluminous igneous rocks as an indicator of thermogenic methane release from the North Atlantic Volcanic Province at the time of the Paleocene–Eocene Thermal Maximum (PETM). Bull. Volcanol. 75(1), 678.

Rankin, B.D., Stockey, R.A., Beard, G., 2008. Fruits of Icacinaceae from the Eocene Appian Way Locality of Vancouver Island, British Columbia. Int. J. Plant Sci. 169(2), 305–314.

Rasband, W. S. 2016. “ImageJ Website.” https://imagej.nih.gov/ij/.

Rasoanaivo, P., Ratsimamanga-Urverg, S., Messana, I., De Vincente, Y., Galeffi, C., 1990. Cassinopin, a kaempferal trirhamnoside from *Cassinopsis madagascariensis*. Phytochemistry 29(6), 2040–2043.

Raup, D.M., Sepkoski, J.J., 1982. Mass extinctions in the marine fossil record. Science 215(4539), 1501–1503.

Ree, R.H., Smith, S.A., 2008. Maximum likelihood inference of geographic range evolution by dispersal, local extinction, and cladogenesis. Syst. Biol. 57(1), 4–14.

Reid, E.M., Chandler, M.E., 1933. The London Clay Flora. The British Museum (Natural History), London. 561 pp.

Renner, S.S., Grimm, G.W., Kapli, P., Denk, T., 2016. Species relationships and divergence times in beeches: new insights from the inclusion of 53 young and old fossils in a birth–death clock model. Philos. Trans. R. Soc. B Biol. Sci. 371(1699), 20150135.

Robin, N., Foldi, I., Godinot, M., Petit, G., 2016. Scale insect larvae preserved in vertebrate coprolites (Le Quesnoy, France, Lower Eocene): paleoecological insights. Sci. Nat. 103(9-10), 85.

Roessler, R., Amprako, L., Sayibu, A.R., Mohammed, A., Menezes, R.C., Hölscher, D., Alenyorege, B., Dei, H.K., Steiner, C., 2017. Effects of false yam tuber meals and charcoal on broiler chicken production and blood parameters. South Afr. J. Anim. Sci. 47(6), 843–853.

Röhl, U., Westerhold, T., Bralower, T.J., Zachos, J.C., 2007. On the duration of the Paleocene-Eocene thermal maximum (PETM). Geochem. Geophys. Geosystems 8(12), 1–13.

Roja, G., Heble, M.R., 1994. The quinoline alkaloids Camptothecin and 9-methoxycamptothecin from tissue cultures and mature trees of *Nothapodytes foetida*. Phytochemestry 36(1), 65–66.

Ronquist, F., 1997. Dispersal-vicariance analysis: a new approach to the quantification of historical biogeography. Syst. Biol. 46(1), 195–203.

Ronquist, F., Klopfstein, S., Vilhelmsen, L., Schulmeister, S., Murray, D.L., Rasnitsyn, A.P., 2012. A total-evidence approach to dating with fossils, applied to the early radiation of the Hymenoptera. Syst. Biol. 61(6), 973–999.

Ronquist, F., Teslenko, M., van der Mark, P., Ayres, D.L., Darling, A., Hohna, S., Larget, B., Liu, L., Suchard, M.A., Huelsenbeck, J.P., 2012. MrBayes 3.2: efficient Bayesian phylogenetic inference and model choice across a large model space. Syst. Biol. 61(3), 539–542.

Ronquist, F., Lartillot, N., Phillips, M.J., 2016. Closing the gap between rocks and clocks using total-evidence dating. Philos. Trans. R. Soc. B Biol. Sci. 371(1699), 20150136.

Rouhan, G., Gaudeul, M., 2014. Plant taxonomy: a historical perspective, current challenges, and perspectives, in: Besse, P. (Ed.), Molecular Plant Taxonomy. Humana Press, Totowa. 1–37.

Saganuwan, S., 2017. Ethnoveterinary Values of Nigerian Medicinal Plants: An Overview. Eur. J. Med. Plants 18(4), 1–35.

Salard-Cheboldaeff, M., 1975. Quelques grains de pollen périporés tertiaires du Cameroun. Rev. Micropaleontol. 17(4), 182–190.

Santiago-Valentín, E., Viruet-Oquendo, E., 2013. Notes on the flower, fruit, and the reproductive phenology of the elusive *Ottoschulzia rhodoxylon*. Harv. Pap. Bot. 18(1), 61–65.

Saporta (De), G., 1868. Prodrome d'une flore fossile des traversins anciens de Sézanne, Société Géologique, Paris. 8, 289–438.

Sarkar, A.K., Dey, M., Mazumder, M., 2017. Ecological status of medicinal plants of Chalsa forest range under Jalpaiguri division, West Bengal, India. Intern. J. Herb. Med. 5(5), 196–215.

Sarmiento, C., Détienne, P., Heinz, C., Molino, J.F., Grard, P., Bonnet, P., 2011. Pl@ntWood: a computer-assisted identification tool for 110 species of amazon trees based on wood anatomical features. Iawa Journal 32(2), 221–232.

Sarr, S.O., Perrotey, S., Fall, I., Ennahar, S., Zhao, M., Diop, Y.M., Candolfi, E., Marchioni, E., 2011. *Icacina senegalensis* (Icacinaceae), traditionally used for the treatment of malaria, inhibits in vitro *Plasmodium falciparum* growth without host cell toxicity. Malar. J. 10(1), 85.

Sauquet, H., 2013. A practical guide to molecular dating. Comptes Rendus Palevol 12(6), 355–367.

Schaller, M.F., Fung, M.K., Wright, J.D., Katz, M.E., Kent, D.V., 2016. Impact ejecta at the Paleocene-Eocene boundary. Science 354, 225–229.

Schmidt-Kittler, N., Brunet, M., Godinot, M., Franzen, J.L., Hooker, J.J., Legendre, S., 1987. European reference levels and correlation tables. Münch. Geowiss. Abh. A 10, 15–31.

Scotese, C.R., 2014. Atlas of Paleogene Paleogeographic Maps (Mollweide Projection), Maps 8-15, Volume 1, The Cenozoic, PALEOMAP Atlas for ArcGIS, PALEOMAP Project, Evanston, Illinois.

Scott, R.A., 1954. Fossil fruits and seeds from the Eocene Clarno Formation of Oregon. Palaeontogr. Abt. B 66–97.

Scott, R.A., Barghoorn, E.S., 1957. *Phytocrene microcarpa*-a new species of Icacinaceae based on Cretaceous fruits from Kreischerville, New York. The Paleobotanist. 25–28.

Sharma, M.V., Uma Shaanker, R., Leather, S.R., Vasudeva, R., Shivanna, K.R., 2011. Floral resources, pollinators and fruiting in a threatened tropical deciduous tree. J. Plant Ecol. 4(4), 259–267.

Shilkina, A.I., 1956. *Icacinoxylon*, in: kjpariaova, B. P. Markovski, and G. P. Radchenko (ed) New families and genera, records of palaeontology. Ministerstvo Geologii I Ochrany Nedr, SSSR, Vses. Nauchno-Issled. Geol. Inst. (VSEGEI), Palaeontologiia, 12.

Sleumer, H., 1942. Icacinaceae. In Engler, A. (ed) Die Natürlichen Pflanzenfamilien, Leipzig: Engelmann 20b, 322–396.

Sleumer, H., 1969. Materials towards the knowledge of the Icacinaceae of Asia, Malesia, and adjacent areas. Blumea-Biodiv. Evol. and Biogeo. of Plants, 17(1), 181–264.

Sleumer, H., 1971. Icacinaceae, in: Flora Malesiana. CGGJ van Steenis, Noordhoff, Leiden. 7(1), 1–87.

Soyer R., 1953. Carte géologique à 1/50 000, N° 183 – Notice. Paris BRGM. 8 pp.

Sluijs, A., Schouten, S., Pagani, M., Woltering, M., Brinkhuis, H., Damsté, J.S.S., Dickens, G.R., Huber, M., Reichart, G.-J., Stein, R., Matthiessen, J., Lourens, L.J., Pedentchouk, N., Backman, J., Moran, K., the Expedition 302 Scientists, 2006. Subtropical Arctic Ocean temperatures during the Palaeocene/Eocene thermal maximum. Nature 441(7093), 610–613.

Smith, R., 2001. Les pantolestides (Mammalia, Pantolesta) de l'Éocene inférieur de Prémontré (Aisne, France). Palaeovertebrata 30(1-2), 11–35.

Smith, K.T., 2009. A new lizard assemblage from the earliest Eocene (Zone Wa0) of the Bighorn Basin, Wyoming, USA: biogeography during the warmest interval of the Cenozoic. J. Syst. Palaeontol. 7(3), 299–358.

Smith, T., Rose, K.D., Gingerich, P.D., 2006. Rapid Asia–Europe–North America geographic dispersal of earliest Eocene primate *Teilhardina* during the Paleocene–Eocene thermal maximum. Proc. Natl. Acad. Sci. 103(30), 11223–11227.

Smith, T., Quesnel, F., De Plöeg, G., De Franceschi, D., Métais, G., De Bast, E., Solé, F., Folie, A., Boura, A., Claude, J., Dupuis, C., Gagnaison, C., Iakovleva, A., Martin, J., Maubert, F., Prieur, J., Roche, E., Storme, J.-Y., Thomas, R., Tong, H., Yans, J., Buffetaut, E., 2014. First Clarkforkian Equivalent Land Mammal Age in the Latest Paleocene Basal Sparnacian Facies of Europe: Fauna, Flora, Paleoenvironment and (Bio)stratigraphy. PLoS ONE 9(1), 1–20.

Soladoye, M.O., Amusa, N., Raji-Esan, S., Chukwuma, E., Taiwo, A., 2010. Ethnobotanical survey of anti-cancer plants in Ogun State, Nigeria. Ann. Biol. Res. 1(4), 261–273.

Soltis, D., 2000. Angiosperm phylogeny inferred from 18S rDNA, rbcL, and atpB Sequences. Botanical Journal of the Linnean Society 133 (4), 381–461.

Soudry, D., Gregor, H.-J., 1997. *Jodes israelii* sp. nov.: a huge phosphate-mineralized icacinacean fructification from the Late Cretaceous of the Negev, southern Israel. Cretac. Res. 18(2), 161–178.

Soujanya, K.N., Siva, R., Mohana Kumara, P., Srimany, A., Ravikanth, G., Mulani, F.A., Aarthy, T., Thulasiram, H.V., Santhoshkumar, T.R., Nataraja, K.N., Uma Shaanker, R., 2017. Camptothecin-producing endophytic bacteria from *Pyrenacantha volubilis* Hook. (Icacinaceae): A possible role of a plasmid in the production of camptothecin. Phytomedicine 36, 160–167.

Speijer, R.P., Morsi, A.-M.M., 2002. Ostracode turnover and sea-level changes associated with the Paleocene-Eocene thermal maximum. Geology 30(1), 23–26.

Stadler, T., 2010. Sampling-through-time in birth–death trees. J. Theor. Biol. 267(3), 396–404.

Steineck, P., Thomas, E., 1996. The latest Paleocene crisis in the deep sea: Ostracode succession at Maud Rise, Southern Ocean. Geology 24(7), 583–586.

Storey, M., Duncan, R.A., Swisher, C.C., 2007. Paleocene-Eocene thermal maximum and the opening of the northeast Atlantic. Science 316(5824), 587–589.

Stull, G.W., Moore, B.R., Manchester, S.R., 2011. Fruits of Icacinaceae from the Eocene of southeastern North America and their biogeographic implications. Int. J. Plant Sci. 172(7), 935–947.

Stull, G.W., Herrera, F., Manchester, S.R., Jaramillo, C., Tiffney, B.H., 2012. Fruits of an "Old World" tribe (Phytocreneae; Icacinaceae) from the Paleogene of North and South America. Syst. Bot. 37(3), 784–794.

Stull, G.W., Duno de Stefano, R., Soltis, D.E., Soltis, P.S., 2015. Resolving basal lamiid phylogeny and the circumscription of Icacinaceae with a plastome-scale data set. Am. J. Bot. 102(11), 1794–1813.

Stull, G.W., Adams, N.F., Manchester, S.R., Sykes, D., Collinson, M.E., 2016. Revision of Icacinaceae from the Early Eocene London Clay flora based on X-ray micro-CT. Botany 94(9), 713–745.

Sudre, J., Erfurt, J., 1996. Les artiodactyles du gisement yprésien terminal de Prémontré (Aisne, France). Palaeovertebrata 25(2-4), 391–414.

Suma, H.K., Kumar, V., Patel, M.K., Srimany, A., Ravikanth, G., Umapathy, S.K., Vasudeva, R., Uma Shaanker, R., 2017. Spatial and temporal distribution pattern of camptothecin in seeds and fruits of *Pyrenacantha volubilis* Hook. (Icacinaceae) during different fruit developmental stages. Curr. Sci. 110(5), 1034–1038.

Süss, H., 2007. Holzfossilien der Morphogattung *Spiroplatanoxylon* gen. nov. aus dem Tertiär von Europa und Vorderasien. Feddes Repert. 118(1-2), 1–19.

Svensen, H., Planke, S., Malthe-Sørenssen, A., Jamtveit, B., Myklebust, R., Eidem, T.R., Rey, S.S., 2004. Release of methane from a volcanic basin as a mechanism for initial Eocene global warming. Nature 429(6991), 542–545.

Takahashi, K., Suzuki, M., 2003. Dicotyledonous fossil wood flora and early evolution of wood characters in the Cretaceous of Hokkaido, Japan. Iawa Journal 24(3), 269–309.

Takhtajan, A., 1966. Major phytochoria of the Late Cretaceous and the Early Tertiary on the territory of the USSR and adjacent countries. Bot. Zh. 51, 1217–1230.

Takhtajan, A., 1997. Diversity and classification of flowering plants. Columbia University Press, New York. 620 pp.

Tanai, T., 1990. Euphorbiaceae and Icacinaceae from the Paleogene of Hokkaido, Japan. Bull. Natn. Sci. Mus. Tokyo Ser C. 16(3), 91–118.

Thayn, G.F., Tidwell, W.D., Stokes, W.L., 1985. Flora of the Lower Cretaceous Cedar Mountain Formation of Utah and Colorado. Part III: *Icacinoxylon pittiense* n. sp. Am. J. Bot. 72(2), 175.

Thiele-Pfeiffer, H., 1988. Die Mikroflora aus dem mitteleozänen Ölschiefer von Messel bei Darmstadt. Palaeontogr. Abt. B 211(1-3), 1–86.

Thomas, E., 2007. Cenozoic mass extinctions in the deep sea: What perturbs the largest habitat on Earth? in: Special Paper 424: Large Ecosystem Perturbations: Causes and Consequences. Geological Society of America. 1–23.

Thomas, R., 2011. Palm-ID, a database to identify the palm stem anatomy with an expert system (Xper2). Paris: Université Paris, 6.

Thomas, R., De Franceschi, D., 2013. Palm stem anatomy and computer-aided identification: The Coryphoideae (Arecaceae). American Journal of Botany, 100(2), 289-313.

Thomson, P.W., Pflug, H.D., 1953. Pollen und Sporen des mitteleuropäischen Tertiärs. Palaeontogr. Abt. B 1–138.

Tiffney, B.H., 1984. Seed size, dispersal syndromes, and the rise of the angiosperms: evidence and hypothesis. Ann. Mo. Bot. Gard. 71(2), 551–576.

Tiffney, B.H., 1985. The Eocene North Atlantic land bridge: its importance in Tertiary and modern phytogeography of the Northern Hemisphere. J. Arnold Arbor. 66(2), 243–273.

Tiffney, B.H., 1999. Fossil fruit and seed flora from the early Eocene fisher/sullivan site, in: Early Eocene Vertebrates and Plants from the Fisher/Sullivan Site (Nanjemoy

Formation) Stafford County, Virginia. Virginial Division of Mineral Ressources. 139–159.

Traiser, C., Roth-Nebelsick, A., Grein, M., Kovar-Eder, J., Kunzmann, L., Moraweck, K., Lange, J., Kvaček, J., Neinhuis, C., Folie, A., De Franceschi, D., Kroh, A., Prestianni, C., Poschmann, M., Wuttke, M., 2018. MORPHYLL: A database of fossil leaves and their morphological traits. Palaeontol. Electron. 21(1), 1–17.

Tuzson, J., 1906. A balatoni fossilis fak monografiaja. [A monograph of the fossil plant remains from the Balaton region.]. Bal. Tud Tanulmanyozasanak Eredmenyei 1, 1–56.

Ung, V., Dubus, G., Zaragueta-Bagils, R., Vignes-Lebbe, R., 2010. Xper2: introducing e-taxonomy. Bioinformatics 26(5), 703–704.

Upchurch Jr, G., Wolfe, J., 1987. Mid-Cretaceous to Early Tertiary vegetation and climate: evidence from fossil leaves and woods, in: The Origins of Angiosperms and Their Biological Consequences, EM Friis, WG Chaloner, and PR Crane (ed), England. 75–105.

Utteridge, T., Nagamasu, H., Teo, S., White, L., Gasson, P., Brummitt, R., 2007. Icacinaceae. Flower. Plant Fam. World 173.

Vajda, V., Bercovici, A., 2014. The global vegetation pattern across the Cretaceous–Paleogene mass extinction interval: A template for other extinction events. Glob. Planet. Change 122, 29–49.

Van Staveren, M.G.C., Baas, P., 1973. Epidermal leaf characters of the Malesian Icacinaceae. Acta Bot. Neerlandica 22(4), 329–359.

Villiers, J. F., 1971. Origine et développement de l'accrescence dans les genres *Chlamydocarya* Baill. et *Polycephalium* Engl.(Icacinacées). Bulletin de la Société Botanique de France, 118(9), 659-666.

Villiers, J.-F., 1973. Icacinaceae, in: Flore Du Cameroun. A. Aubréville et J-F. Leroy (ed), Paris, France. 3–100.

Vinther, J., Parry, L., Briggs, D.E.G., Van Roy, P., 2017. Ancestral morphology of crown-group molluscs revealed by a new Ordovician stem aculiferan. Nature 542(7642), 471–474.

Von Ettingshausen, C., 1869. Die fossile flora des Tertiär-Beckens von Bilin. K. Gerold's Sohn. 110 pp.

Wang, Q., Manchester, S.R., Gregor, H.-J., Shen, S., Li, Z.-Y., 2013. Fruits of *Koelreuteria* (Sapindaceae) from the Cenozoic throughout the northern hemisphere: Their ecological, evolutionary, and biogeographic implications. Am. J. Bot. 100(2), 422–449.

Watelet, A., 1866. Description des plantes fossiles du Bassin de Paris. J-B. Baillière et Fils, Paris.

256 pp.

Webb, A.E., Leighton, L.R., Schellenberg, S.A., Landau, E.A., Thomas, E., 2009. Impact of the Paleocene-Eocene thermal maximum on deep-ocean microbenthic community structure: Using rank-abundance curves to quantify paleoecological response. Geology 37(9), 783–786.

Wei, J.-J., Wang, W.-Q., Song, W.-B., Li, J., Xuan, L., 2018. Three new indole alkaloids from *Mappianthus iodoides*. Phytochem. Lett. 23, 1–4.

Weijers, J.W., Schouten, S., Sluijs, A., Brinkhuis, H., Damsté, J.S.S., 2007. Warm arctic continents during the Palaeocene–Eocene thermal maximum. Earth Planet. Sci. Lett. 261(1), 230–238.

Weitschat, W., Wichard, W., 1998. Atlas der Pflanzen und Tiere im baltischen Bernstein. F. Pfeil. 256 pp.

Wen, J., 1999. Evolution of eastern Asian and eastern North American disjunct distributions in flowering plants. Annu. Rev. Ecol. Syst. 30(1), 421–455.

Wheeler, E.A., 2011. Inside Wood–A web resource for hardwood anatomy. Iawa Journal, 32(2), 199-211.

Wheeler, E.A., Lee, M., Matten, L.C., 1987. Dicotyledonous woods from the Upper Cretaceous of southern Illinois. Bot. J. Linn. Soc. 95(2), 77–100.

Wheeler, E.A., Baas, P., Gasson, P.E., 1989. IAWA list of microscopic features for hardwood identification. IAWA Bulletin.

Wikström, N., Kainulainen, K., Razafimandimbison, S.G., Smedmark, J.E.E., Bremer, B., 2015. A revised time tree of the asterids: establishing a temporal framework for evolutionary studies of the coffee family (Rubiaceae). PLoS ONE 10(5), 1–26, e0157206.

Wilf, P., Johnson, K.R., 2004. Land plant extinction at the end of the Cretaceous: a quantitative analysis of the North Dakota megafloral record. Paleobiology 30(3), 347–368.

Wing, S.L., Harrington, G.J., Smith, F.A., Bloch, J.I., Boyer, D.M., Freeman, K.H., 2005. Transient floral change and rapid global warming at the Paleocene-Eocene boundary. Science 310(5750), 993–995.

Whittaker, R.J., Fernández-Palacios, J.M., 2007. Island biogeography: ecology, evolution, and conservation. Oxford University Press. 383 pp.

Wolfe, J.A., 1968. Paleogene biostratigraphy of nonmarine rocks in King County, Washington. U.S. Geol. Surv.Prof. Paper 571.

Wolfe, J.A., 1975. Some aspects of plant geography of the Northern Hemisphere during the late Cretaceous and Tertiary. Ann. Mo. Bot. Gard. 62(2), 264–279.

Wolfe, J.A., 1977. Paleogene floras from the Gulf of Alaska region. U.S.GS. Prof. Paper 997.

Wolfe, J.A., 1985. Distribution of major vegetational types during the Tertiary. The carbon cycle and atmospheric CO_2. Nat. Var. Archean Present 32, 357–375.

Wright, J.D., Schaller, M.F., 2013. Evidence for a rapid release of carbon at the Paleocene-Eocene thermal maximum. Proc. Natl. Acad. Sci. 110(40), 15908–15913.

Wright, D.F., Toom, U., 2017. New crinoids from the Baltic region (Estonia): fossil tip-dating phylogenetics constrains the origin and Ordovician-Silurian diversification of the *Flexibilia* (Echinodermata). Palaeontology 60(6), 893–910.

Wu, S.-F., Hsieh, P.-W., Wu, C.-C., Lee, C.-L., Chen, S.-L., Lu, C.-Y., Wu, T.-S., Chang, F.-R., Wu, Y.-C., 2008. Camptothecinoids from the seeds of Taiwanese *Nothapodytes foetida*. Molecules 13(6), 1361–1371.

Yang, T., Lu, L.-M., Wang, W., Li, J.-H., Manchester, S.R., Wen, J., Chen, Z.-D., 2018. Boreotropical range expansion and long-distance dispersal explain two amphi-Pacific tropical disjunctions in Sabiaceae. Mol. Phylogenet. Evol. 124, 181–191.

Yu, Y., Harris, A.J., He, X., 2010. S-DIVA (Statistical Dispersal-Vicariance Analysis): A tool for inferring biogeographic histories. Mol. Phylogenet. Evol. 56(2), 848–850.

Yu, Y., Harris, A.J., Blair, C., He, X., 2015. RASP (Reconstruct Ancestral State in Phylogenies): A tool for historical biogeography. Mol. Phylogenet. Evol. 87, 46–49.

Zachos, J.C., 2005. Rapid acidification of the ocean during the Paleocene-Eocene thermal maximum. Science 308(5728), 1611–1614.

Zachos, J.C., Pagani, M., Sloan, L., Thomas, E., Billups, K., 2001. Trends, rhythms, and aberrations in global climate 64 Ma to Present. Science 292(5517), 686–693.

Zachos, J.C., Schouten, S., Bohaty, S., Quattlebaum, T., Sluijs, A., Brinkhuis, H., Gibbs, S.J., Bralower, T.J., 2006. Extreme warming of mid-latitude coastal ocean during the Paleocene-Eocene Thermal Maximum: Inferences from TEX86 and isotope data. Geology 34(9), 737–740.

Zachos, J.C., Dickens, G.R., Zeebe, R.E., 2008. An early Cenozoic perspective on greenhouse warming and carbon-cycle dynamics. Nature 451(7176), 279–283.

Zeebe, R.E., Zachos, J.C., Dickens, G.R., 2009. Carbon dioxide forcing alone insufficient to explain Palaeocene–Eocene Thermal Maximum warming. Nat. Geosci. 2(8), 576–580.

Zhang, J.-B., Li, R.-Q., Xiang, X.-G., Manchester, S.R., Lin, L., Wang, W., Wen, J., Chen, Z.-D., 2013. Integrated fossil and molecular data reveal the biogeographic diversification of the Eastern Asian-Eastern North American disjunct *Hickory* Genus (*Carya* Nutt.). PLoS ONE 8, e70449.

Zhang, K., Sun, P., Liu, H., Shang, S., Song, J., Wang, D., 2016. Extraction and comparison of carboxylated cellulose nanocrystals from bleached sugarcane bagasse pulp using two different oxidation methods. Carbohydr. Polym. 138, 237–243.

Zhang, G.-J., Hu, F., Jiang, H., Dai, L.-M., Liao, H.-B., Li, N., Wang, H.-S., Pan, Y.-M., Liang, D., 2018. Mappianines A−E, structurally diverse monoterpenoid indole alkaloids from *Mappianthus iodoides*. Phytochemistry 145, 68–76.

Zheng, X., Xing, F., 2009. Ethnobotanical study on medicinal plants around Mt.Yinggeling, Hainan Island, China. J. Ethnopharmacol. 124(2), 197–210.

Zhou, B.-N., Hoch, J.M., Johnson, R.K., Mattern, M.R., Eng, W.-K., Ma, J., Hecht, S.M., Newman, D.J., Kingston, D.G., 2000. Use of compare analysis to discover new natural product drugs: isolation of camptothecin and 9-methoxycamptothecin from a new source. J. Nat. Prod. 63(9), 1273–1276.

Zuquim, G, Tuomisto, H, Prado, J., 2017. A free-access online key to identify Amazonian ferns. PhytoKeys. 78, 1–15.

Appendices

Appendix 1

Synonymy of the modern Icacinaceae

ICACINACEAE Miers, Ann. Mag. Nat. Hist., ser. 2 8: 174 (1851).

= **Emmotacaceae** Tiegh.,Bot. Jahresber. 25(2): 406 (1899).

Genus – *Alsodeiopsis* Oliv. In Benth., Gen. Pl. 1: 996 (1867).

Alsodeiopsis chippii Hutch, Bull. Misc. Inform. Kew 1912: 224 (1912).

≡ ***Alsodeiopsis chippii*** subsp ***chippii***

Alsodeiopsis chippii subsp. ***rubra*** (Engl.) Govaerts, World Checkl. Seed Pl. 1(1): 6 (1995).

≡ ***Alsodeiopsis rubra*** Engl., pfl a 3(2): 254 (1921).

Alsodeiopsis chippii subsp. ***villosa*** (Keay) Govaerts, World Checkl. Seed Pl.1 (1): 6 (1995).

≡ ***Alsodeiopsis villosa*** Key., Bull. Jard. Bot. État Bruxelles 26: 185 (1956).

Alsodeiopsis mannii Oliv., J. Linn. Soc., Bot. 10: 43 (1867).

=***Alsodeiopsis weissenborniana*** J.Braun & K.Schum., Mitt. Deutsch. Schutzgeb. 2: 165 (1889).

Alsodeiopsis poggei Engl., Bot. Jahrb. Syst. 17: 71 (1893).

Alsodeiopsis rowlandii Engl., Bot. Jahrb. Syst. 24: 479 (1898).

= ***Alsodeiopsis bequaertii*** De Wild., Rev. Zool. Bot. Africaines 10(1) Suppl. Bot. p. 9 (1922).

Alsodeiopsis schumannii (Engl.) Engl., Nat. Pflanzenfam. Nachtr. zu III. 5: 226 (1897).

≡ ***Alsodeiidium schumannii*** Engl. Pflanzenw. Ost-Afrikas C: 248 (1895).

Alsodeiopsis staudtii Engl., Bot. Jahrb. Syst. 24: 479 (1898).

Alsodeiopsis tessmannii Engl., Veg. Erde 9(III 2): 254 (1921).

Alsodeiopsis zenkeri Engl., Bot. Jahrb. Syst. 24: 478 (1898).

Genus – *Casimirella* Hassl., Repert. Spec. Nov. Reg. Veg. 12(322/324): 249 (1913).

= ***Humirianthera*** Huber**,** Bull. Soc. Bot. Genève, Sér. 2 6 (7-8): 184 (1914).

Casimirella ampla (Miers) R.A.Howard, Brittonia 44(2): 168 (1992).

≡ ***Leretia ampla*** Miers, Ann. Mag. Nat. Hist. 4 (23): 364 (1859) ≡ ***Mappia ampla*** (Miers) Engl., Fl. Bras. 12(2): 51 (1872) ≡ ***Humirianthera ampla*** (Miers) Baehni, Candollea 7: 182 (1936).

= ***Humirianthera duckei*** Huber**,** Bull. Soc. Bot. Gen., Sér. 2 6 (7-8): 184-185, f. 2 (1914).

Casimirella beckii (Fern.Casas) Breteler, Taxon 40(1): 112 (1991).

≡ ***Dichapetalum beckii*** Fern. Casas, Fontqueria 2: 15, f. 3 (1982).

Casimirella crispula (R.A.Howard) R.A.Howard, Brittonia 44(2): 169 (1992).

≡ ***Humirianthera crispula*** R.A. Howard, J. Arnold Arbor. 23 (1): 77, t.4 (1942).

Casimirella diversifolia R.A.Howard, Brittonia 44(2): 169, f. 1C. (1992).

Casimirella guaranitica Hassl., Repert. Spec. Nov. Regni Veg. 12: 249 (1913).

= ***Casimirella guaranitica*** fo. *calvata* Hassl. Repert. Spec. Nov. Regni Veg. 12: 252 (1913).

= ***Dichapetalum prancei*** Fern. Casas, Fontqueria 2: 15–17, f. 1–2 (1982).

Casimirella lanata R.A.Howard, Brittonia 44(2): 171, f. 1A–B (1992).

Casimirella rupestris (Ducke) R.A.Howard, Brittonia 44(2): 171 (1992).

≡ ***Humirianthera rupestris*** Ducke, Arch. Jard. Bot. Rio de Jan., 4 : 118 (1925).

Genus – *Cassinopsis* Sond., Fl. Cap. 1: 473 (1860).

Cassinopsis chapelieri (Baill.) H.Perrier, Mém. Mus. Natl. Hist. Nat. n.s., 18: 291 (1944).

≡ ***Tridianisia chapelieri*** Baill. Bull. Mens. Soc. Linn. Paris 1: 197 (1879).

Cassinopsis ciliata Baker, J. Linn. Soc., Bot. 20: 118 (1883).

Cassinopsis ilicifolia (Hochst.) Sleumer, Notizbl. Bot. Gart. Berlin-Dahlem 15: 228 (1940).

≡ ***Hartogia ilicifolia*** Hochst., Flora 27: 305 (1844) ≡ ***Cassine ilicifolia*** Hochst. ex Sond., Fl. Cap. 1: 474 (1860).

= ***Cassinopsis mucronata*** Turcz., Bull. Soc. Imp. Naturalistes Moscou 31(1): 455 (1858).

= ***Cassinopsis capensis*** Harv. & Sond., Fl. Cap. 1: 474 (1860).

Cassinopsis madagascariensis Baill., Adansonia 11: 180 (1875).

= ***Nuxia brachyscypha*** Baker, J. Linn. Soc., Bot. 25: 334 (1890).

Cassinopsis tinifolia Harv., Thes. Cap. 2: 44 (1863).

Cassinopsis tomentosa H.Perrier, Mém. Mus. Natl. Hist. Nat. n.s., 18: 291 (1944).

Genus – *Desmostachys* Planch. ex Miers, Ann. Mag. Nat. Hist., ser. 2 9: 398-399 (1852).

Desmostachys brevipes (Engl.) Sleumer, Notizbl. Bot. Gart. Berlin–Dahlem 15: 359 (1941).

≡ ***Pyrenacantha brevipes*** Engl., Bot. Jahrb. Syst. 43: 187 (1909).

Desmostachys oblongifolius (Engl.) Villiers, in Fl. Cameroun 15: 48. (1973).

≡ ***Alsodeiopsis oblongifolia*** Engl., Nat. Pflanzenfam. Nachtr. [Engler & Prantl] I. 226, nomen; et in Engl. Jahrb. xxiv. 480 (?).

Desmostachys planchonianus Miers, Ann. Mag. Nat. Hist. II, 9: 399 (1852).

= ***Desmostachys renschii*** O.Hoffm. & Hildebr. Sert. Pl. Madagasc. 11-12 (1881) ≡ ***Desmostachys planchonianus*** fo. ***renschii*** (O.Hoffm. & Hildebr.) H.Hubert, Fl. Madag. 119: 25 (1952).

= ***Desmostachys acuminatus*** Baker, J. Linn. Soc., Bot. 21: 332 (1884) ≡ ***Desmostachys planchonianus*** fo. ***acuminatus*** (Baker) H.Hubert, Fl. Madagasc. et des Com. 119: 25 (1952).

= ***Desmostachys deltoideus*** Baker, J. Linn. Soc., Bot. 21: 332 (1884) ≡ ***Desmostachys planchoniana*** fo. ***deltoides*** (Baker) H. Perrier, Fl. Madagasc. et des Com. 119: 23 (1952).

= ***Desmostachys nitidus*** Planch., ex Valeton Crit. Overz. Olacin. 205 (1886).

= ***Desmostachys planchoniana*** fo. ***angustisepala*** H. Perrier , Mem. Mus. 18: 301. (1944).

= ***Desmostachys planchoniana*** fo. ***cuspidata*** H. Perrier, Mem. Mus. 18: 301 (1944).

= ***Desmostachys planchoniana*** fo. ***glabrescens*** H. Perrier, Mem. Mus. 18: 300 (1944).

= ***Desmostachys planchoniana*** fo. ***glabriflora*** H. Perrier, Mem. Mus. 18: 302 (1944).

= ***Desmostachys planchoniana*** fo. ***glaucifolia*** H. Perrier, Mem. Mus. 18: 300 (1944).

= ***Desmostachys planchoniana*** fo. ***intermedia*** H. Perrier, Mem. Mus. 18: 301 (1944).

= ***Desmostachys planchoniana*** fo. ***lanceolata*** H. Perrier, Mem. Mus. 18: 300 (1944).

= ***Desmostachys planchoniana*** fo. ***mayottensis*** H. Perrier, Mem. Mus. 18: 302 (1944).

= ***Desmostachys planchoniana*** fo. ***nervosa*** H. Perrier, Mem. Mus. 18: 301 (1944).

= ***Desmostachys planchoniana*** fo. ***oblanceolata*** H. Perrier, Mem. Mus. 18: 301 (1944).

= ***Desmostachys planchoniana*** fo. ***oblongifolia*** H. Perrier, Mem. Mus. 18: 30. (1944).

= ***Desmostachys planchoniana*** fo. ***ovatolanceolata*** H. Perrier, Mem. Mus. 18: 301 (1944).

= ***Desmostachys planchoniana*** fo. ***subrotundata*** H. Perrier, Mem. Mus. 18: 302 (1944).

Desmostachys tenuifolius Oliv. Fl. Trop. Afr. 1: 353 (1868).

= ***Desmostachys preussii*** Engl.**,** Bot. Jahrb. Syst. (1893).

Desmostachys vogelii (Miers) Stapf Pl. Liberia 2: 587 (1906).

≡ ***Sarcostigma vogelii*** Miers, Mag. Nat. Hist. 10: 117 (1852).

Genus – *Hosiea* Hemsl. & E.H. Wilson, Bull. Misc. Inform. Kew (1906).

Hosiea sinensis (Oliv.) Hemsl. & E.H. Wilson, Bull. Mis. Infor. Kew 1906(5): 154 (1906).

≡ ***Natsiatum sinense*** Oliv., Hooker's Icon. Pl. 19(4) pl. 1900 (1889).

Hosiea japonica Makino, J. Jap. Bot. 6: 28 (1929).

Genus – *Icacina* A. Juss., Mém. Soc. Hist. Nat. Paris 1: 174 (1823).

Icacina claessensi De Wild., Pl. Bequaert. 1 (2): 237 (1922).

Icacina guessfeldtii Asch. Nat. Pflanzenfam. 3(5): 250 (1893).

Icacina mannii Oliv., Fl. Trop. Afr. 1: 357 (1868).

Icacina oliviformis (Poir.) J.Raynal Adansonia, n.s. 15: 193 (1975).

≡ ***Hirtella oliviformis*** Poir., Encycl., Suppl. 3: 53 (1813).

= ***Icacina senegalensis*** A. Juss., Mém. Soc. Hist. Nat. Paris 1: 174 (1823) ≡ ***Mappia senegalensis*** (Juss.) Baill. Hist. Pl. (Baillon) 5: 277 (1874).

= ***Icacina senegalensis*** var. ***pubescens*** Boutique, Bull. Jard. Bot. Ét. Brux. 26: 347 (1956) B ≡ ***Icacina oliviformis*** var**. *pubescens*** (Boutique) J.M. Fay, Kew Bull. 42(2): 46 (1987).

Icacina trichantha Oliv. Fl. Trop. Afr. 1: 358 (1868).

Genus – Iodes Blume, Bijdr. Fl. Ned. Ind. 29 (1825).

Iodes africana Welw. ex Oliv., Fl. Trop. Afr. 1: 358 (1868).

Iodes cirrhosa Turcz., Bjull. Moskovsk. Obač. Isp. Prir., Otd. Biol. 27(II): 281 (1854).

= ***Natsiatum oppositifolium*** Planch. London J. Bot. 5: 247 (1846) [Invalid].

= ***Iodes tomentella*** Miq., Fl. Ned. Ind. 1(1): 796 (1856).

= ***Iodes brandisii*** Kurz, J. Asiat. Soc. Bengal, Pt. 2, Nat. Hist. 41(4): 298 (1872).

= ***Iodes ovalis*** var. ***miquelii*** Baill., Prodr. 17: 23 (1873).

= ***Iodes ovalis*** var. ***cochinchinensis*** Pierre ex Gagnep, Fl. Indo-Chine 1: 845 (1911).

= ***Iodes floribunda*** Merr., Pap. Michigan Acad. Sci. 1933, xix. 166 (1934).

Iodes kamerunensis Engl., Bot. Jahrb. Syst. 24: 481 (1898).

Iodes klaineana Pierre, Bull. Mens. Soc. Linn. Paris 1321(1897).

Iodes liberica Stapf, Pl. Liberia 2: 588 (1906).

Iodes madagascariensis Baill., Adansonia 9: 146 (1868).

Iodes ovalis Blume, Bijdr. Fl. Ned. Ind. 30 (1825).

= ***Iodes horsfieldii*** Baill., Adansonia 10: 267 (1872).

= ***Iodes oblonga*** Planch. ex Mast., Fl. Brit. India 1: 597 (1875).

= ***Polyporandra junghuhnii*** Koord., Proc. Sect. Sci. Kon. Akad. Wetensch. Ams. 11: 763 (1909).

Iodes philippinensis Merr., Philipp. J. Sci. 3: 241 (1908).

= ***Iodes oblonga*** var. ***moluccana*** Hochr., Pl. Bogor. Exs. 18 (1904).

Iodes reticulata King, J. Asiat. Soc. Bengal, Pt. 2, Nat. Hist. 64(2): 126 (1895).

Iodes scandens (Becc.) Utteridge & Byng, Bot. J. Linn. Soc. 176(3): 292 (2014).

≡ ***Polyporandra scandens*** Becc., Malesia 1: 125 (1877).

= ***Polyporandra hansemannii*** Engl., Bot. Jahrb. Syst. 16(39): 13 (1893).

= ***Iodes sogerensis*** Baker f., J. Bot. 61(Suppl.): 10 (1923).

Iodes seguinii (H.Lév.) Rehder, J. Arnold Arbor. 15(1): 3 (1934).

≡ ***Vitis seguinii*** H. Lév., Repert. Spec. Nov. Regni Veg. 4(73–74): 331 (1907).

= ***Iodes vitiginea*** var. ***levitestis*** Hand.-Mazz. Sitzung. Kaiserl. Akad. Wiss., Math.- Natur. Cl., Abt. 1 58: 150 (1876).

= ***Iodes balansae*** Gagnep, Notul. Syst. (Paris) 1: 200 (1910).

= ***Iodes rugosa*** Gagnep, Notul. Syst. (Paris) 1: 200 (1910).

Iodes seretii (De Wild.) Boutique, Fl. Congo Belge 9: 243 (1960).

≡ ***Lasiodiscus seretii*** De Wild., Bull. Jard. Bot. État 3: 271 (1911).

= ***Iodes trichocarpa*** Mildbr. Repert. Spec. Nov. Regni Veg. 18: 97 (1922).

Iodes velutina King, J. Asiat. Soc. Bengal, Pt. 2, Nat. Hist. 64(2): 127 (1895).

Iodes vitiginea (Hance) Hance, J. Bot. 184 (1874).

≡ ***Erythrostaphyle vitiginea*** Hance, J. Bot. 184 (1874) ≡ ***Iodes vitiginea*** (Hance) Hemsl., J. Linn. Soc., Bot. 23(153): 115 (1886) ≡ ***Iodes ovalis*** var. ***vitiginea*** (Hance) Gagnep., Fl. Indo-Chine 1: 845 (1911).

= ***Vitis chrysobotrys*** H.Lév. & Vaniot, Repert. Spec. Nov. Regni Veg. 3: 350 (1907).

= ***Sabia edulis*** H.Lév. [Invalid], Fl. Kouy-Tchéou 379 (1915).

Iodes yangambiensis Louis ex Boutique, Bull. Jard. Bot. État 26: 345 (1956).

Iodes yatesii Merr., Pap. Michigan Acad. Sci. 19: 165 (1934).
Iodes yatesii var. ***glabrescens*** (Ridl.) Sleumer, Blume 17: 221 (1969).

≡ ***Iodes reticulata*** var. ***glabrescens*** Ridl. Bull. Misc. Inform. Kew 1931: 35 (1931).

Iodes globulifera H. Perrier, Mem. Mus. 18: 305 (1944).

Iodes laurentii De Wild., Miss. Ém. Laurent 1: 381 (1907).

Iodes nectarifera H. Perrier, Mem. Mus. 18: 304 (1944).

Iodes perrieri Sleumer, Notizbl. Bot. Gart. Berlin–Dahlem 15: 251 (1940).

Iodes talbotii Baker f. ex Hutch. & Dalziel, Fl. W. Trop. Afr. 1(1): 457 (1928).

Iodes usambarensis Sleumer Notizbl. Bot. Gart. Berlin–Dahlem 15: 251(1940).

Genus – ***Lavigeria*** Pierre, Fl. Forest. Cochinch. ad t. 267 (1892).

Lavigeria macrocarpa (Oliv.) Pierre, Fl. Forest. Cochinch. fasc. 17: 267 (1892).
≡ ***Icacina macrocarpa*** Oliv., Fl. Trop. Afr. 1: 357 (1868).

Lavigeria salutaris Pierre, Fl. Forest. Cochinch. fasc. 17: 267 (1892).

Genus – ***Leretia*** Vell., Fl. Flumin. 99 (1829).

Leretia cordata Vell., Fl. Flumin. 99 (1829).
≡ ***Mappia cordata*** (Vell.) Engl., Fl. Bras. 12(2): 50 (1872).
= ***Leretia vellozoi*** Miers, Ann. Mag. Nat. Hist. II, 9: 392 (1852).
= ***Leretia nitida*** Miers, Ann. Mag. Nat. Hist. III, 4: 365 (1859) ≡ ***Mappia nitida*** (Miers) Engl., Fl. Bras. 12(2): 51 (1872).
= ***Mappia poeppigiana*** Baill., Adansonia 11: 175 (1874) ≡ ***Icacina poeppigiana*** (Baill.) Valeton, Crit. Overz. Olacin. 187 (1886) ≡ ***Leretia poeppigiana*** (Baill.) Sleumer, Notizbl. Bot. Gart. Berlin-Dahlem 15: 245 (1940).
= ***Leretia glabrata*** Sleumer, Notizbl. Bot. Gart. Berlin-Dahlem 15: 245 (1940).

Genus – ***Mappia*** Jacq., Pl. Hort. Schoenbr. 1: 22, pl. 47 (1797).

Mappia angustifolia Griseb. Cat. Pl. Cub. 119 (1866).
≡ ***Leretia angustifolia*** (Griseb.) House, Amer. Midl. Naturalist 8: 62 (1922).

Mappia longipes Lundell, Contr. Univ. Michigan Herb. 7: 26 (1942).

Mappia mexicana B.L. Rob. & Greenm., Amer. J. Sci., ser. 4 50: 150 (1895).
≡ ***Leretia mexicana*** (B.L. Rob. & Greenm.) Sleumer, Notizbl. Bot. Gart. Berlin Dahlem 15: 245 (1940).

Mappia multiflora Lundell Wrightia 4(4): 139–140 (1970).
Mappia racemosa Jacq., Pl. Hort. Schoenbr. 1: 22, pl. 47 (1797).

≡ ***Leretia racemosa*** (Jacq.) House, Amer. Midl. Naturalist 8: 62 (1922).

= ***Icacina dubia*** Macfad. Fl. Jamaica 1: 122 (1837).

= ***Mappia affinis*** Miers, Ann. Mag. Nat. Hist., ser. 2 9: 394 (1852).

= ***Mappia angustifolia*** Griseb. Cat. Pl. Cub. 119 (1866) ≡ ***Leretia angustifolia*** (Griseb.) House, Amer. Midl. Naturalist 8: 62 (1922).

= ***Mappia racemosa*** var. ***brachycarpa*** Griseb. , Cat. Pl. Cub. 119 (1866) ≡ ***Mappia racemosa*** subsp. ***brachycarpa*** (Griseb.), Borhidi 29(1–4): 185 (1983).

= ***Mappia racemosa*** var**.** ***typica*** R.A. Howard, J. Arnold Arbor. 23: 64 (1942).

Mappia oppositifolia Merr., Lingnan Sci. J. 14(1): 28, f. 9 (1935).

Genus – ***Mappianthus*** Hand.-Mazz., Kaiserl. Akad. Wiss. Wien, Math.-Naturwiss. Kl., Anz. 58: 150 (1921).

Mappianthus hookeranus (Bail.) Sleumer, Blumea 17(1): 225-226 (1969).

≡ ***Iodes hookeriana*** Baill., Adansonia 10: 268 (1872).

= ***Iodes thomsoniana*** Baill. Adansonia 10: 270 (1872).

= ***Mappianthus borneensis*** Merr., Webbia 7: 317 (1950).

Mappianthus iodoides Hand.-Mazz., Kaiserl. Akad. Wiss. Wien, Math.-Naturwiss. Kl., Anz. 58: 150 (1921).

= ***Mappianthus tomentosus*** D. Fang, Acta Bot. Yunnan. (2002).

Genus – ***Merrilliodendron*** Kanehira, Bot. Mag. (Tokyo) 48: 920 (1934).

Merrilliodendron megacarpum Notizbl., Bot. Gart. Berlin-Dahlem 15: 243 (1940).

= ***Stemonurus megacarpus*** Hemsl., Bull. Misc. Inform. Kew 1895: 133 (1895).

= ***Merrilliodendron rotense*** Kaneh, Bot. Mag. (Tokyo) 48: 920 (1934).

= ***Peekeliodendron missionariorum*** Sleumer, Notizbl. Bot. Gart. Berlin-Dahlem 13: 510 (1937).

Genus – ***Miquelia*** Meisn. Pl. Vasc. Gen. 1: 152 (1838).

Miquelia assamica (Griff.) Mast. ex B.D.Jacks, Index Kew. 2: 247 (1894).

≡ ***Jenkinsia assamica*** Griff., Calcutta J. Nat. Hist. 4: 231 (1843) ≡ ***Miquelia assamica*** (Griff.) D.G. Long Edinburgh J. Bot. 47(3): 353 (1990).

Miquelia caudata King, J. Asiat. Soc. Bengal, Pt. 2, Nat. Hist. 64(2): 124 (1895).

Miquelia celebica Blume, Rumphia 4: 37 (1849).

= ***Miquelia cumingii*** Baill., Adansonia 10: 278 (1872).

= ***Miquelia rostrata*** Merr. Univ. Calif. Publ. Bot. 15: 172 (1929).

Miquelia kleinii Meisn., Pl. Vasc. Gen. 1: 152 (1838).

Miquelia philippinensis Merr., Philipp. J. Sci. 14: 416 (1919).

Miquelia reticulata Merr., Philipp. J. Sci., C 9: 312 (1914).

Miquelia thorelii Gagnep., Notul. Syst. (Paris) 1: 204 (1910).

Miquelia dentata Bedd., Madras J. Lit. Sci. III, 1: 38 (1864).

Miquelia gibba Baill., Adansonia 10: 278 (1872).

Genus – *Natsiatopsis* Kurz, J. Asiat. Soc. Bengal 44(2): 201, pl. 15, f. 8–9 (1876).

Natsiatopsis thunbergiifolia Kurz, J. Asiat. Soc. Bengal 44(2): 201 (1875).

Genus – *Natsiatum* Buch.-Ham. ex Arn., Edinburgh New Philos. J. 16: 314 (1834).

Natsiatum herpeticum, Buch.-Ham. ex Arn. Edinburgh New Philos. J. 16: 314 (1834).

= ***Sicyos pentandrus*** Wall. Numer. List 6682 (1832) [Invalid].

= ***Natsiatum tonkinense*** Gagnep., Notul. Syst. (Paris) 1: 205 (1910).

Genus – *Nothapodytes* Blume, Mus. Bot. 1: 248 (1850).

= ***Mappia*** sect. ***Trichocrater*** Miers, Ann. Mag. Nat. Hist., ser. 2 9: 395 (1852).

= ***Neoleretia*** Baehni, Compt. Rend. Seances Soc. Phys. Geneve 53: 35 (1936).

Nothapodytes collina C.Y. Wu, Fl. Yunnan. 1: 169, pl. 40, f. 10 (1977).

Nothapodytes montana Blume, Mus. Bot. 1: 248 (1850).

≡ ***Mappia montana*** (Blume) Miers, Ann. Mag. Nat. Hist. II, 9: 398 (1852).

Nothapodytes nimmoniana (J. Graham) Mabb., Bot. Hist. Hort. Malab. 88 (1980).

≡ ***Premna nimmoniana*** J.Graham, Cat. Pl. Bombay 155 (1839).

= ***Stemonurus foetidus*** Wight, Icon. Pl. Ind. Orient. 3: 955 (1845) ≡ ***Mappia foetida*** (Wight) Miers, Ann. Mag. Nat. Hist. II, 9: 395 (1852) ≡ ***Neoleretia foetida*** (Wight) Baehni, Candollea 7: 179 (1936) ≡ ***Nothapodytes foetida*** (Wight) Sleumer, Notizbl. Bot. Gart. Berlin-Dahlem 15: 247 (1940).

= ***Mappia tomentella*** Miers ex Valeton, Crit. Overz. Olacin. 183 (1836).

= ***Mappia tomentosa*** Miers, Ann. Mag. Nat. Hist. II, 9: 397 (1852).

= ***Mappia wightiana*** Miers, Ann. Mag. Nat. Hist. II, 9: 397 (1852).

= ***Mappia oblonga*** Miers, Ann. Mag. Nat. Hist. II, 9: 396 (1852).

= ***Mappia ovata*** Miers, Ann. Mag. Nat. Hist. II, 9: 396 (1852).

= ***Mappia gardneriana*** Miers, Ann. Mag. Nat. Hist. II, 9: 396 (1852) ≡ ***Mappia foetida*** var. ***gardneriana*** (Miers) Thwaites, Enum. Pl. Zeyl. 43 (1858).

= ***Mappia championiana*** Miers, Ann. Mag. Nat. Hist. II, 9: 397 (1852) ≡ ***Mappia foetida*** var. ***championiana*** (Miers) Thwaites, Handb. Fl. Ceyl. 1: 263 (1893) ≡ ***Mappia ovata*** var. ***championiana*** (Miers) Trimen, Handb. Fl. Ceyl. 1: 263 (1893).

= ***Mappia gardneriana*** Miers, Ann. Mag. Nat. Hist. II, 9: 396 (1852) ≡ ***Nothapodytes gardneriana*** (Miers) Kosterm., Acta Bot. Neerl. 31: 127 (1982).

= ***Mappia cambodiana*** Pierre, Fl. Forest. Cochinch. t. 267b (1892).

= ***Mappia insularis*** (Matsum.) Hatus. ≡ ***Mappia ovata*** var. ***insularis*** Matsum., Bot. Mag. (Tokyo) 15: 55 (1901).

= ***Mappia dimorpha*** Craib, Bull. Misc. Inform. Kew 1926: 347 (1926) ≡ ***Neoleretia dimorpha*** (Craib) Baehni, Candollea 7: 178 (1936) ≡ ***Nothapodytes dimorpha*** (W. G. Craib) Sleumer, Notizbl. Bot. Gart. Berlin-Dahlem 15(2): 247 (1940).

Nothapodytes obscura C.Y. Wu, Fl. Yunnan. 1: 170, pl. 40, f. 8–9 (1977).

Nothapodytes obtusifolia (Merr.) R.A.Howard, J. Arnold Arbor. 23(1): 70 (1942).

≡ ***Mappia obtusifolia*** Merr., Lingnan Sci. J. 14: 28 (1935).

Nothapodytes pittosporoides (Oliv.) Sleumer, Notizbl. Bot. Gart. Berlin–Dahlem 15(2): 247

(1940).

≡ ***Mappia pittosporoides*** Oliv., Hooker's Icon. Pl. 18: t. 1762 (1888) ≡ ***Neoleretia pittosporoides*** (Oliv.) Baehni, Candollea 7: 178 (1936).

Nothapodytes tomentosa C.Y. Wu, Fl. Yunnan. 1: 169, pl. 40, f. 6–7 (1977).

Genus – *Phytocrene* Wall., Pl. Asiat. Rar. 3: 11 (1831).

Phytocrene anomala Merr., J. Straits Branch Roy. Asiat. Soc. 86: 325 (1922).

Phytocrene borneensis Becc., Malesia 1: 128 (1877).

=***Phytocrene porphyrea*** Stapf, Bull. Misc. Inform. Kew 1906: 72 (1906).

Phytocrene bracteata Wall., Pl. Asiat. Rar. 3: 12 (1832).

≡ ***Gynocephalum bracteatum*** (Wall.) Trécul, Ann. Sci. Nat., Bot. III, 8: 149 (1847).

= ***Phytocrene macrocarpa*** Griff., Not. Pl. Asiat. 4: 322 (1854).

Phytocrene hirsuta Blume, Rumphia 4: 37 (1849).

= ***Boehmeria racemiflora*** J.R.Forst. ex Blume, Rumphia 4: 37 (1849).

= ***Phytocrene crinipes*** Baill. ex Bureau, Monogr. Bignon. 146 (1864) [Invalid].

= ***Phytocrene minahassae*** Koord., Meded. Lands Plantentuin 19: 629 (1898) [Invalid].

Phytocrene interrupta Sleumer, Notizbl. Bot. Gart. Berlin-Dahlem 15: 252 (1940).

Phytocrene macrophylla (Blume) Blume, Rumphia 4: 36 (1849).

Phytocrene macrophylla var. ***macrophylla***

≡ ***Gynocephalum macrophyllum*** Blume, Bijdr. 483 (1825).

= ***Phytocrene gigantea*** Wall., Pl. Asiat. Rar. 3: 11 (1832) ≡ ***Gynocephalum giganteum*** (Wall.) Trécul, Ann. Sci. Nat., Bot. III, 8: 149 (1847).

= ***Kadsura blancoi*** Blanco, Fl. Filip., ed. 2: 594 (1845) ≡ ***Phytocrene blancoi*** (Blanco) Merr., Philipp. J. Sci., C 2: 432 (1907).

= ***Phytocrene calicarpa*** Griff., Not. Pl. Asiat. 4: 327 (1854).

= ***Gynocephalum luzoniense*** Llanos, Revista Progr. Ci. Exact. 15: 55 (1865) ≡ ***Phytocrene luzoniensis*** (Llanos) Baill. Adansonia 10: 281 (1872).

= ***Phytocrene loheri*** Merr., Philipp. J. Sci., C 7: 293 (1912).

= ***Phytocrene tinosporifolia*** Koord.-Schum., Syst. Verz. 3: 74 (1914).

= ***Phytocrene obovoidea*** Merr., Philipp. J. Sci., C 10: 322 (1915).

= ***Phytocrene forbesii*** Baker f., J. Bot. 62(Suppl.): 21 (1924).

Phytocrene macrophylla var. ***caudigera*** (Sleumer) Sleumer, Blumea 17: 240 (1969).

≡ ***Phytocrene caudigera*** Sleumer, Notizbl. Bot. Gart. Berlin-Dahlem 15: 253 (1940).

Phytocrene macrophylla var. ***dasycarpa*** (Miq.) Sleumer, Blumea 17: 240 (1969).

≡ ***Phytocrene dasycarpa*** Miq., Ann. Mus. Bot. Lugduno-Batavi 3: 248 (1868).

= ***Phytocrene ovalifolia*** Koord.-Schum., Syst. Verz. 3: 74 (1914).

Phytocrene malacothrix Sleumer, Notizbl. Bot. Gart. Berlin-Dahlem 15: 361 (1941).

Phytocrene oblonga Wall., Pl. Asiat. Rar. 3: 12 (1832).

≡ ***Gynocephalum oblongum*** (Wall.) Trécul, Ann. Sci. Nat., Bot. III, 8: 149 (1847).

= ***Miquelia cancellata*** Kurz, J. Asiat. Soc. Bengal, Pt. 2, Nat. Hist. 44: 201 (1875).

Phytocrene palmata Wall., Pl. Asiat. Rar. 3: 12 (1832).

≡ ***Gynocephalum palmatum*** (Wall.) Trécul, Ann. Sci. Nat., Bot. III, 8: 149 (1847).

= ***Phytocrene stylocarpa*** Griff., Not. Pl. Asiat. 4: 320 (1854).

Phytocrene racemosa Sleumer, Blumea 17: 236 (1969).

Phytocrene trichura Ridl., Fl. Malay Penins. 1: 433 (1922).

Genus – ***Pleurisanthes*** Baill., Adansonia 11: 201 (1874).

= ***Martia*** Valeton, Crit. Overz. Olacin. 259 (1886).

= ***Valetonia*** T. Durand, Index Gen. Phan. ix, 64 (1888).

Pleurisanthes artocarpi Baill., Adansonia 11: 201 (1874).

Pleurisanthes brasiliensis (Valeton) Tiegh., Bull. Soc. Bot. France 44: 117 (1897).

≡ ***Martia brasiliensis*** Valeton, Crit. Overz. Olacin. 261 (1886) ≡ ***Valetonia brasiliensis*** (Valeton) T. Durand, Index Gen. Phan. 64 (1886).

Pleurisanthes emarginata Tiegh., Bull. Soc. Bot. France 44: 117 (1897).

Pleurisanthes flava Sandwith, Kew Bull. 1931: 467 (1931).

Pleurisanthes howardii R. Duno, Riina & P.E. Berry, Harvard Pap. Bot. 7(1): 13–15, f. 1, 2A (2002).

Pleurisanthes parviflora (Ducke) R.A. Howard, J. Arnold Arbor. 21(4): 482–483 (1940).

≡ ***Leretia parviflora*** Ducke, Arch. Jard. Bot. Rio de Janeiro 4: 119 (1925) ≡ ***Mappia parviflora*** (Ducke) Baehni, Candollea 7: 174 (1936).

Pleurisanthes simpliciflora Sleumer, Notizbl. Bot. Gart. Berlin–Dahlem 15: 256 (1940).

Genus – ***Pyrenacantha*** Hook. Bot. Misc. 2(4): 107 (1830).

= ***Cavanilla*** Thunb., Nov. Gen. Pl. [105]. (1792).
= ***Moldenhauera*** Spreng., Syst. Veg. 1: 373 (1825).
= ***Adelanthus*** Endl., Gen. Pl. 1327(1840).
= ***Endacanthus*** Baill., Hist. Phys. Madagascar (1892).
= ***Freeria*** Merr., Philipp. J. Sci. 7: 292 (1912).
= ***Monocephalium*** S. Moore, J. Bot. 58: 221 (1920).

Pyrenacantha acuminata Engl., Bot. Jahrb. Syst. 24: 483 (1898).

= ***Chlamydocarya tenuis*** Engl., Bot. Jahrb. Syst. 24: 486 (1898).
= ***Chlamydocarya tessmannii*** Engl., Veg. Erde 9(III 2): 263 (1921).

Pyrenacantha anhydathoda Utteridge & Byng, Bot. J. Linn. Soc. 176(3): 292 (2014).

≡ ***Chlamydocarya anhydathoda*** Villiers, Adansonia n.s., 10: 429 (1971).

Pyrenacantha chlorantha Baker, J. Linn. Soc., Bot. 21: 331 (1884).

Pyrenacantha cordicula Villiers, Fl. Cameroun 15: 86 (1973).

= ***Pyrenacantha cordata*** Villiers, Adansonia n.s., 12: 285 (1972) [Illégitime].
= ***Pyrenacantha villiersii*** Breteler, Syst. & Geogr. Pl. 78: 131 (2008) [Illégitime].

Pyrenacantha gabonica Breteler & Villiers, Adansonia III, 22: 201 (2000).

Pyrenacantha glabrescens (Engl.) Engl., Bot. Jahrb. Syst. 43: 187 (1909).

≡ ***Chlamydocarya glabrescens*** Engl., Bot. Jahrb. Syst. 24: 485 (1898).

Pyrenacantha gossweileri (Exell) Utteridge & Byng, Bot. J. Linn. Soc. 176(3): 292 (2014).

≡ ***Chlamydocarya gossweileri*** Exell., Bot. 70(Suppl. 1): 224 (1932).

Pyrenacantha grandifolia Engl., Bot. Jahrb. Syst. 43: 187 (1909).

Pyrenacantha humblotii (Baill. ex Grandid.) Sleumer, Notizbl. Bot. Gart. Berlin-Dahlem 15: 254 (1940).

≡ ***Endacanthus humblotii*** Baill. ex Grandid., Hist. Nat. Madag., Bot. Atlas 4: 241 (1892).

Pyrenacantha kaurabassana Baill., Adansonia 10: 272 (1872).

= ***Pyrenacantha kamassana*** Baill., Acta Hydrobiol. 10: 272 (1872).

Pyrenacantha klaineana Pierre ex Exell & Mendonça, Consp. Fl. Angol. 1: 345 (1951).

Pyrenacantha laetevirens Sleumer, Notizbl. Bot. Gart. Berlin-Dahlem 15: 254 (1940).

= ***Pyrenacantha fissistigma*** Sleumer, Notizbl. Bot. Gart. Berlin-Dahlem 15: 254 (1940).

Pyrenacantha lebrunii Boutique, Bull. Jard. Bot. État 29: 426 (1959).

Pyrenacantha lobata (Pierre) Byng & Utteridge, Bot. J. Linn. Soc. 176(3): 292 (2014).

≡ ***Chlamydocarya lobata*** Pierre, Bull. Mens. Soc. Linn. Paris 2: 1316 (1896), ≡ ***Polycephalium lobatum*** (Pierre) Pierre ex Engl., Bot. Jahrb. Syst. 24: 485 (1898).

Pyrenacantha longirostrata Villiers, Adansonia n.s., 12: 283 (1972).

Pyrenacantha macrocarpa (A.Chev. ex Hutch. & Dalziel) Byng & Hutteridge, Bot. J. Linn. Soc. 176(3): 292 (2014).

≡ ***Chlamydocarya macrocarpa*** A.Chev. ex Hutch. & Dalziel, Fl. W. Trop. Afr. 1: 456 (1928).

Pyrenacantha malvifolia Engl., Sitzungsber. Kaiserl. Akad. Wiss., Math.-Naturwiss. Cl., Abt. 1 18: 268 (1893).

≡ ***Pyrenacantha malvifolia*** var. ***malvifolia***

Pyrenacantha occidentalis Byng & Utteridge, Bot. J. Linn. Soc. 176(3): 292 (2014).

= ***Polycephalium capitatum*** (Baill.) Keay, Bull. Jard. Bot. État Bruxelles 26: 184 (1956).

Pyrenacantha perrieri Labat, El-Achkar & R. Rabev., Adansonia, sér. 3, 28(2): 399–400, f. 5 (2006).

= ***Pyrenacantha chlorantha*** f. ***opulenta*** H. Perrier, Mem. Mus. 18: 305 (1944).

= ***Pyrenacantha chlorantha*** var. ***sambiranensis*** H. Perrier, Mem. Mus. 18: 305 (1944).

Pyrenacantha puberula Boutique, Bull. Jard. Bot. État 29: 429 (1959).

Pyrenacantha repanda (Merr.) Merr., Enum. Philipp. Fl. Pl. 2: 492 (1923).

≡ ***Freeria repanda*** Merr., Philipp. J. Sci., C 7: 292 (1912).

= ***Tragia luzoniensis*** Merr., Philipp. J. Sci. 16: 564 (1920).

Pyrenacantha rostra (Bullick) Byng & Utteridge, Bot. J. Linn. Soc. 176(3): 292 (2014).

≡ ***Chlamydocarya rostrata*** Bullock, Bull. Misc. Inform. Kew 1933: 469 (1933).

Pyrenacantha scandens (Thunb.) Planch. Ex Harv., Thes. Cap. 1(1): 14 (1859).

≡ ***Cavanilla scandens*** Thunb., Nov. Gen. Pl. [Thunberg] 7: 105 (1792).

Pyrenacantha soyauxii (Engl.) Byng & Utteridge, Bot. J. Linn. Soc. 176(3): 292 (2014).

≡ ***Chlamydocarya soyauxii*** Engl., Bot. Jahrb. Syst. 22: 73 (1895).

Pyrenacantha staudtii (Engl.) Engl., Veg. Erde 9(III 2): 262 (1921).

≡ ***Chlamydocarya staudtii*** Engl., Bot. Jahrb. Syst. 24: 486 (1898).

Pyrenacantha sylvestris S.Moore, J. Bot. 58: 223 (1920).

Pyrenacantha thomsoniana (Bail.) Byng & Utteridge, Bot. J. Linn. Soc. 176(3): 292 (2014).

≡ ***Chlamydocarya thomsoniana*** Baill., Adansonia 10: 276 (1872).

Pyrenacantha tropophila Labat, El-Achkar & R. Rabev., Adansonia, sér. 3, 28(2): 400, 402–403, f. 6 (2006).

≡ ***Pyrenacantha laetevirens*** var. ***tropophila*** H. Perrier, Mem. Mus. 18: 308 (1944).

Pyrenacantha undulata Engl. Veg. Erde 3(2): 262 (1921).

Pyrenacantha vogeliana Baill., Adansonia 10: 271 (1872).

≡ ***Cavanilla vogeliana*** (Baill.) Kuntze, Revis. Gen. Pl. 1: 111 (1891).

Pyrenacantha volubilis Hook., Bot. Misc. 2: 107 (1830).

Genus – ***Rhyticaryum*** Becc., Malesia (1878).

Rhyticaryum elegans G.Schellenb., Bot. Jahrb. Syst. 58: 174 (1923).

Rhyticaryum fasciculatum Becc., Malesia 1: 121 (1877).

Rhyticaryum gracile G.Schellenb., Bot. Jahrb. Syst. 58: 170 (1923).

Rhyticaryum longifolium K.Schum. & Lauterb., Fl. Schutzgeb. Südsee 415 (1900).
= ***Rhyticaryum oncocarpum*** K.Schum. & Lauterb., Fl. Schutzgeb. Südsee 416 (1900).
= ***Pocillaria pubescens*** Ridl., Trans. Linn. Soc. London, Bot. 9: 28 (1916) ≡ ***Rhyticaryum pubescens*** (Ridl.) Sleumer, Notizbl. Bot. Gart. Berlin-Dahlem 15: 250 (1940).
= ***Antidesma megalocarpum*** S.Moore, J. Bot. 61(Suppl.): 46 (1923).
= ***Rhyticaryum bullatum*** G.Schellenb., Bot. Jahrb. Syst. 58: 169 (1923).
= ***Rhyticaryum elongatum*** G.Schellenb., Bot. Jahrb. Syst. 58: 170 (1923).
= ***Rhyticaryum oblongum*** G.Schellenb., Bot. Jahrb. Syst. 58: 169 (1923).
= ***Rhyticaryum ovale*** G.Schellenb., Bot. Jahrb. Syst. 58: 171 (1923).

Rhyticaryum lucidum G.Schellenb., Bot. Jahrb. Syst. 58: 175 (1923).

Rhyticaryum macrocarpum Becc., Malesia 1: 256 (1878).

Rhyticaryum novoguineense (Warb.) Sleumer, Blumea 17: 250 (1969).
≡ ***Buchanania novoguineensis*** Warb., Bot. Jahrb. Syst. 13: 363 (1891).

Rhyticaryum oleraceum Becc., Malesia 1: 121 (1877).
= ***Rhyticaryum parviflorum*** Pulle, Nova Guinea 8: 659 (1912).

Rhyticaryum oxycarpum K.Schum. & Lauterb., Fl. Schutzgeb. Südsee 416 (1900).
= ***Rhyticaryum pulchrum*** G.Schellenb., Bot. Jahrb. Syst. 58: 173 (1923).
= ***Rhyticaryum urophyllum*** G.Schellenb., Bot. Jahrb. Syst. 58: 174 (1923).

Rhyticaryum purpurascens G.Schellenb., Bot. Jahrb. Syst. 58: 172 (1923).

Rhyticaryum racemosum Becc., Malesia 1: 121 (1877).

Rhyticaryum rotundatum G.Schellenb., Bot. Jahrb. Syst. 58: 172 (1923).

Genus – ***Sarcostigma*** Wight & Arn., Edinburgh New Philos. J. 14: 299 (1833).

Sarcostigma kleinii Wight & Arn., Edinburgh New Philos. J. 14: 299 (1833).
= ***Sarcostigma horsfieldii*** R.Br, Pl. Jav. Rar. 241 (1844).
= ***Sarcostigma edule*** Kurz, J. Asiat. Soc. Bengal, Pt. 2, Nat. Hist. 41: 298 (1872) ≡ ***Chailletia edulis*** Kurz, J. Asiat. Soc. Bengal, Pt. 2, Nat. Hist. 41(2): 298 (1872).
= ***Sarcostigma wallichii*** Baill., Adansonia 10: 282 (1872).

Sarcostigma paniculata Pierre, Bull. Mens. Soc. Linn. Paris 2: 1319 (1897).
= ***Sarcostigma angustifolia*** Pierre, Bull. Mens. Soc. Linn. Paris 2: 1320 (1897) ≡ ***Sarcostigma paniculata*** var. ***angustifolia*** (Pierre) Gagnep., Fl. Indo-Chine 1: 842 (1911).
= ***Sarcostigma philippinense*** Merr., Philipp. J. Sci., C 10: 276 (1915).
= ***Sarcostigma surigaoense*** Elmer, Leafl. Philipp. Bot. 10: 3749 (1939) [Invalid].

Genus – ***Sleumeria*** Utteridge, Nagam. & Teo, Syst. Bot. 30 (3): 635-643 (2005).

Sleumaria auriculata Utteridge, Nagam. & Teo, Syst. Bot. 30 (3): 635-643 (2005).

Genus – ***Stachyanthus*** Engl., Nat. Pflanzenfam. Nachtr. 1: 227 (1897).

Stachyanthus cuneatus Engl., Veg. Erde 9(III 2): 263 (1921).
≡ ***Neostachyanthus cuneatus*** (Engl.) Exell & Mendonça, Bol. Soc. Brot. II, 25: 112 (1951).

Stachyanthus donisii (Boutique) Boutique, Fl. Congo Belge 9: 259 (1960).
≡ ***Neostachyanthus donisii*** Boutique, Bull. Jard. Bot. État 26: 346 (1956).

Stachyanthus occidentalis (Keay & É. Miège) Boutique, Bull. Jard. Bot. État. Brux. 29: 431 (1959).

≡ ***Neostachyanthus occidentalis*** Keay & J.Miège, Bull. Jard. Bot. État. Brux. 25: 271 (1955).

Stachyanthus zenkeri Engl., Nat. Pflanzenfam. Nachtr. 1: 227 (1897).

≡ ***Neostachyanthus zenkeri*** (Engl.) Exell & Mendonça, Bol. Soc. Brot., sér. 2, 25: 111 (1951).

= ***Stachyanthus obovatus*** S.Moore, J. Bot. 58: 222 (1920).

Total 152 species and 23 genera.

Appendix 2

Power of discrimination of the characters used in the Xper^3 database

Taxon	Number of paths leading to taxon	Length of the shortest path leading to taxon	Average length of paths leading to taxon	Length of the longest path leading to taxon
Alsodeiopsis mannii Oliv.	1	7	7.0	7
Alsodeiopsis poggei Engl.	1	5	5.0	5
Alsodeiopsis staudtii Engl.	1	6	6.0	6
Alsodeiopsis zenkeri Engl.	1	5	5.0	5
Cassinopsis ciliata Baker	1	8	8.0	8
Cassinopsis ilicifolia (Hochst.) Sleumer	1	5	5.0	5
Cassinopsis madagascariensis Baill.	1	4	4.0	4
Desmostachys oblongifolius (Engl.) Villiers	2	7	7.0	7
Desmostachys planchonianus Miers	1	7	7.0	7
Desmostachys tenuifolius Oliv.	1	3	3.0	3
Desmostachys vogelii (Miers) Stapf	2	6	6.5	7
Hosiea japonica Makino	3	6	7.667	10
Hosiea sinensis (Oliv.) Hemsl. & E.H. Wilson	1	8	8.0	8
Icacina claessensii De Wild.	1	5	5.0	5
Icacina guessfeldtii Asch.	2	5	6.0	7
Icacina mannii Oliv.	1	7	7.0	7
Icacina oliviformis (Poir.) J.Raynal	1	7	7.0	7
Icacina trichantha Oliv.	1	7	7.0	7
Iodes africana Welw. ex Oliv.	1	6	6.0	6
Iodes balansae Gagnep.	1	7	7.0	7
Iodes cirrhosa Turcz.	2	6	6.5	7
Iodes kamerunensis Engl.	1	6	6.0	6
Iodes klaineana Pierre	1	6	6.0	6
Iodes liberica Stapf	1	6	6.0	6
Iodes madagascariensis Baill.	1	5	5.0	5
Iodes ovalis Blume	2	5	6.0	7
Iodes perrieri Sleumer	1	5	5.0	5
Iodes philippinensis Merr.	1	6	6.0	6
Iodes scandens (Becc.) Utteridge & Byng	1	7	7.0	7
Iodes seguinii (H.Lév.) Rehder	1	4	4.0	4
Iodes seretii (De Wild.) Boutique	1	5	5.0	5
Iodes yatesii Merr.	1	5	5.0	5
Lavigeria macrocarpa (Oliv.) Pierre	2	4	4.0	4
Leretia cordata Vell.	1	3	3.0	3
Mappia longipes Lundell	1	5	5.0	5
Mappia multiflora Lundell	1	8	8.0	8
Mappia racemosa Jacq.	1	8	8.0	8
Mappianthus iodoides Hand.-Mazz.	1	4	4.0	4
Miquelia assamica (Griff.) Mast. ex B.D.Jacks.	5	4	6.6	10
Miquelia caudata King	7	3	6.286	9
Miquelia celebica Blume	2	4	6.5	9
Natsiatum herpeticum Buch.-Ham. ex Arn.	2	4	6.0	8
Nothapodytes nimmoniana (J.Graham) Mabb.	1	7	7.0	7
Nothapodytes pittosporoides (Oliv.) Sleumer	1	4	4.0	4
Phytocrene anomala Merr.	1	5	5.0	5
Phytocrene borneensis Becc.	1	5	5.0	5
Phytocrene bracteata Wall.	2	6	6.5	7
Phytocrene hirsuta Blume	2	6	6.5	7
Phytocrene macrophylla (Blume) Blume	1	4	4.0	4
Phytocrene oblonga Wall.	1	5	5.0	5
Phytocrene palmata Wall.	1	4	4.0	4
Pleurisanthes flava Sandwith	1	4	4.0	4
Pyrenacantha acuminata Engl.	2	6	6.0	6
Pyrenacantha ambrensis Labat, El-Achkar & R.Rabev.	1	7	7.0	7
Pyrenacantha andapensis Labat, El-Achkar & R.Rabev.	1	7	7.0	7

Pyrenacantha anhydathoda (Villiers) Byng & Utteridge	2	4	6.0	8
Pyrenacantha capitata H.Perrier	1	4	4.0	4
Pyrenacantha cordicula Villiers	2	4	6.0	8
Pyrenacantha glabrescens (Engl.) Engl.	1	5	5.0	5
Pyrenacantha gossweileri (Exell) Byng & Utteridge	2	4	5.0	6
Pyrenacantha humblotii (Baill. ex Grandid.) Sleumer	2	4	5.0	6
Pyrenacantha kaurabassana Baill.	2	4	5.5	7
Pyrenacantha klaineana Pierre ex Exell & Mendonça	1	4	4.0	4
Pyrenacantha laetevirens Sleumer	2	4	6.0	8
Pyrenacantha lebrunii Boutique	2	6	7.5	9
Pyrenacantha longirostrata Villiers	1	10	10.0	10
Pyrenacantha macrocarpa (A. Chev. ex Hutch. & Dalziel) Byng & Utteridge	3	3	5.0	6
Pyrenacantha malvifolia Engl.	1	5	5.0	5
Pyrenacantha puberula Boutique	2	6	7.0	8
Pyrenacantha rakotozafyi Labat, El-Achkar & R.Rabev.	2	4	6.5	9
Pyrenacantha soyauxii (Engl.) Byng & Utteridge	2	3	4.5	6
Pyrenacantha staudtii (Engl.) Engl.	2	4	6.0	8
Pyrenacantha sylvestris S.Moore	2	4	6.0	8
Pyrenacantha thomsoniana (Bail.) Byng & Utteridge	2	3	4.5	6
Pyrenacantha tropophila Labat, El-Achkar & R. Rabev.	1	6	6.0	6
Pyrenacantha vogeliana Baill.	1	8	8.0	8
Rhyticaryum elegans G.Schellenb.	1	9	9.0	9
Rhyticaryum fasciculatum Becc.	1	9	9.0	9
Rhyticaryum longifolium K.Schum. & Lauterb.	1	10	10.0	10
Rhyticaryum macrocarpum Becc.	3	6	7.667	9
Rhyticaryum novoguineense (Warb.) Sleumer	1	3	3.0	3
Rhyticaryum oleraceum Becc.	1	9	9.0	9
Rhyticaryum racemosum Becc.	1	7	7.0	7
Sarcostigma kleinii Wight & Arn.	2	4	4.0	4
Sarcostigma paniculata Pierre	2	5	5.5	6
Stachyanthus donisii (Boutique) Boutique	2	4	5.5	7
Stachyanthus occidentalis (Keay & É. Miège) Boutique	2	3	4.5	6
Stachyanthus zenkeri Engl.	2	4	5.5	7
Apodytes dimidiata E.Mey. ex Arn.	1	3	3.0	3
Dendrobangia boliviana Rusby	2	5	6.5	8
Emmotum nitens (Benth.) Miers	1	2	2.0	2
Pittosporopsis kerrii Craib	1	6	6.0	6
Platea parvifolia Merr. & Chun	1	6	6.0	6
Oncotheca balansae Baill.	1	2	2.0	2
AVERAGE	1.489	5.319	5.827	6.33

Appendix 3

Xper key generated by IKEY+

1 Endocarp : surface structures (?):

Ridged => 2

Pitted => 3

Rugose, irregular => 4

Smooth => 5

2 Endocarp primary vascular strand : position (?):

Outside endocarp wall => 6

In a gutter or channel => 7

Inside endocarp wall => 8

3 Tubercles : morphology (?):

Conical => 9

Elongate.-flattened => 10

Peg shaped => 11

Cylindrical => 12

Spiny => 13

"Shallow mound" not protrude beyond wall => 14

4 Locule : number (?):

One => 15

Three => *Emmotum nitens (Benth.) Miers*

5 Locule : number (?):

One => 16

Five => *Oncotheca balansae Baill.*

6 Fruit: fleshy appendage (?):

Yes => *Apodytes dimidiata E.Mey. ex Arn.*

No => 17

7 Endocarp: Apex structure (?):

Absent => 18

Pores => *Rhyticaryum novoguineense (Warb.) Sleumer*

Bulge => *Desmostachys tenuifolius Oliv.*

8 Locule : hairs (?):

- Yes => *19*
- No => *20*

9 Ridges : number reaching the base (?):

- 0 => *21*
- 1 => *Stachyanthus occidentalis (Keay & É. Miège) Boutique*
- 2 => *22*
- 4 => *Miquelia caudata King*

10 Endocarp : shape in lateral view (?):

- Elliptical => *Pyrenacantha thomsoniana (Bail.) Byng & Utteridge*
- Globulose => *23*
- Obovoid => *Pyrenacantha soyauxii (Engl.) Byng & Utteridge*
- Triangular => *Pyrenacantha macrocarpa (A. Chev. ex Hutch. & Dalziel) Byng & Utteridge*

11 Fruit: gynophore (?):

- Yes => *24*
- No => *25*

12 Fruit: gynophore (?):

- Yes => *26*
- No => *27*

13 Epicarp : indumentum type (?):

- Pilose => *28*
- Pubescent => *29*

14 Pits : arrangement (?):

- In longitudinal lines => *30*
- Random => *31*

15 Endocarp primary vascular strand : position (?):

- Outside endocarp wall => *32*
- In a gutter or channel => *33*
- Inside endocarp wall => *34*

16 Endocarp primary vascular strand : position (?):

- Outside endocarp wall => *35*
- In a gutter or channel => *36*
- Inside endocarp wall => *Leretia cordata Vell.*

17 Epicarp : indumentum type (?):

Glabrous => *37*

Pilose => *38*

Pubescent => *39*

Strigose => *40*

18 Endocarp wall : layers (?):

Divided into distinctive units => *41*

Homogeneous => *Natsiatum herpeticum Buch.-Ham. ex Arn.*

19 Endocarp wall : layers (?):

Divided into distinctive units => *Lavigeria macrocarpa (Oliv.) Pierre*

Homogeneous => *Cassinopsis madagascariensis Baill.*

20 Endocarp : Apex structure (?):

Absent => *42*

Horns => *43*

Pores => *44*

21 Endocarp : Apex structure (?):

Absent => *Stachyanthus donisii (Boutique) Boutique*

Horns => *Miquelia assamica (Griff.) Mast. ex B.D.Jacks.*

Pores => *Miquelia celebica Blume*

22 Epicarp : indumentum type (?):

Pubescent => *Stachyanthus zenkeri Engl.*

Strigose => *Miquelia caudata King*

23 Epicarp : additionnal structure (?):

Apex elongate => *Pyrenacantha anhydathoda (Villiers) Byng & Utteridge*

Cap at the apex inflated => *Pyrenacantha gossweileri (Exell) Byng & Utteridge*

24 Epicarp : indumentum type (?):

Pubescent => *Pyrenacantha klaineana Pierre ex Exell & Mendonça*

Strigose => *Pyrenacantha kaurabassana Baill.*

25 Epicarp : indumentum type (?):

Pubescent => *Pyrenacantha rakotozafyi Labat, El-Achkar & R.Rabev.*

Strigose => *45*

26 Pits : arrangement (?):

In longitudinal lines => *Pyrenacantha cordicula Villiers*

Random => *Pyrenacantha laetevirens Sleumer*

27 Locule : microtomography (?):

Smooth => *Pyrenacantha staudtii (Engl.) Engl.*

Papillate => *Pyrenacantha sylvestris S.Moore*

28 Tubercle apex : morphology (?):

Not elaborated (more or less rounded or pointed) => *Pyrenacantha capitata H.Perrier*

Capitate (Swollen head) => *Pyrenacantha humblotii (Baill. ex Grandid.) Sleumer*

29 Endocarp : Presence of a keel (?):

Yes => *46*

No => *47*

30 Shallow mound invagination : shape (?):

Spiny => *Phytocrene macrophylla (Blume) Blume*

Areoles type => *48*

31 Endocarp : Apex structure (?):

Horns => *Phytocrene palmata Wall.*

Pores => *49*

32 Endocarp: hairs (?):

Yes => *Pleurisanthes flava Sandwith*

No => *50*

33 Endocarp : Apex structure (?):

Horns => *Sarcostigma kleinii Wight & Arn.*

Pores => *Mappianthus iodoides Hand.-Mazz.*

Bulge => *Nothapodytes pittosporoides (Oliv.) Sleumer*

34 Locule : hairs (?):

Yes => *Lavigeria macrocarpa (Oliv.) Pierre*

No => *51*

35 Endocarp wall cells : orientation (?):

Periclinal OR Anticlinal => *52*

Isodiametric => *53*

36 Endocarp wall : layers (?):

Divided into distinctive units => *Sarcostigma kleinii Wight & Arn.*

Homogeneous => *Iodes seguinii (H.Lév.) Rehder*

37 Ridges : number reaching the base (?):

0 => *54*

2 => *55*

4 => *Icacina claessensii De Wild.*

38 Epicarp : additionnal structure (?):

None => *56*

Apex elongate => *57*

Cap at the apex elongate => *58*

Cap at the apex inflated => *59*

39 Ridges : number reaching the base (?):

0 => *60*

1 => *61*

2 => *62*

40 Ridges : number reaching the base (?):

0 => *63*

2 => *64*

4 => *65*

41 Ridges : number reaching the base (?):

2 => *Alsodeiopsis poggei Engl.*

4 => *Alsodeiopsis zenkeri Engl.*

42 Epicarp : indumentum type (?):

Glabrous => *Iodes madagascariensis Baill.*

Pilose => *Iodes seretii (De Wild.) Boutique*

Pubescent => *66*

Strigose => *67*

43 Endocarp : width :

[6.0, 12.9[=> *68*

[12.9, 17.0] => *69*

44 Ridges : number reaching the base (?):

2 => *Iodes yatesii Merr.*

4 => *Iodes perrieri Sleumer*

45 Locule : microtomography (?):

Papillate => *Pyrenacantha malvifolia Engl.*

46 Epicarp hair : type (?):

Uncinate => *70*

Simple => *71*

47 Tubercle apex : morphology (**?**):

Not elaborated (more or less rounded or pointed) => *Pyrenacantha glabrescens (Engl.) Engl.*

Capitate (Swollen head) => *72*

48 Epicarp hair : type (**?**):

Long and thin => *Phytocrene oblonga Wall.*

Cluster of hairs => *Phytocrene anomala Merr.*

49 Endocarp : shape in lateral view (**?**):

Elliptical => *73*

Obovoid => *Phytocrene borneensis Becc.*

50 Locule : microtomography (**?**):

Smooth => *74*

Papillate => *75*

51 Epicarp : indumentum type (**?**):

Glabrous => *Icacina guessfeldtii Asch.*

Pubescent => *76*

Strigose => *Iodes ovalis Blume*

52 Locule : microtomography (**?**):

Smooth => *Mappia longipes Lundell*

Papillate => *Sarcostigma paniculata Pierre*

53 Endocarp wall : layers (**?**):

Divided into distinctive units => *Dendrobangia boliviana Rusby*

Homogeneous => *Cassinopsis ilicifolia (Hochst.) Sleumer*

54 Fruit: gynophore (**?**):

Yes => *Miquelia assamica (Griff.) Mast. ex B.D.Jacks.*

No => *Pittosporopsis kerrii Craib*

55 Ridges : shape (**?**):

Rounded => *77*

Sharp => *78*

56 Fruit: gynophore (**?**):

Yes => *Miquelia assamica (Griff.) Mast. ex B.D.Jacks.*

No => *Hosiea japonica Makino*

57 Fruit: gynophore (**?**):

Yes => *Pyrenacantha humblotii (Baill. ex Grandid.) Sleumer*

No => 79

58 Ridges : secondary (?):

Yes => *Pyrenacantha thomsoniana (Bail.) Byng & Utteridge*

No => *Pyrenacantha macrocarpa (A. Chev. ex Hutch. & Dalziel) Byng & Utteridge*

59 Ridges : secondary (?):

Yes => *Pyrenacantha soyauxii (Engl.) Byng & Utteridge*

No => *Pyrenacantha macrocarpa (A. Chev. ex Hutch. & Dalziel) Byng & Utteridge*

60 Endocarp : width :

[7.2, 8.9[=> 80

[8.9, 15.0] => 81

61 Locule : microtomography (?):

Smooth => *Stachyanthus occidentalis (Keay & É. Miège) Boutique*

Papillate => *Pyrenacantha acuminata Engl.*

62 Endocarp : ridging pattern (?):

Reticulate => 82

Diffuse => 83

63 Epicarp : additionnal structure (?):

None => 84

Apex elongate => 85

Cap at the apex inflated => *Pyrenacantha gossweileri (Exell) Byng & Utteridge*

64 Ridges : shape (?):

Rounded => 86

Sharp => 87

Angular => *Alsodeiopsis staudtii Engl.*

65 Endocarp : ridging pattern (?):

Reticulate => 88

Diffuse => *Miquelia caudata King*

66 Endocarp wall : layers (?):

Divided into distinctive units => *Iodes klaineana Pierre*

Homogeneous => *Iodes kamerunensis Engl.*

67 Ridges : number reaching the base (?):

2 => *Iodes liberica Stapf*

6 => *Iodes africana Welw. ex Oliv.*

68 Ridges : secondary (?):

Yes => *Iodes philippinensis Merr.*

No => *89*

69 Locule : microtomography (?):

Smooth => *90*

Papillate => *91*

70 Locule : microtomography (?):

Papillate => *Pyrenacantha puberula Boutique*

71 Fruit: gynophore (?):

Yes => *Pyrenacantha lebrunii Boutique*

No => *Pyrenacantha acuminata Engl.*

72 Papillae : shape (?):

Rounded => *92*

Large => *Pyrenacantha tropophila Labat, El-Achkar & R. Rabev.*

73 Vertical ridges : number (?):

0 => *Phytocrene bracteata Wall.*

3 => *Phytocrene hirsuta Blume*

74 Endocarp : Apex structure (?):

Absent => *93*

Horns => *Desmostachys vogelii (Miers) Stapf*

Pores => *Platea parvifolia Merr. & Chun*

Bulge => *94*

75 Papillae : shape (?):

Rounded => *Sarcostigma paniculata Pierre*

Large => *Rhyticaryum macrocarpum Becc.*

76 Locule : microtomography (?):

Smooth => *95*

Papillate => *Iodes cirrhosa Turcz.*

77 Endocarp : ridging pattern (?):

Reticulate => *96*

Diffuse => *97*

78 Endocarp : ridging pattern (?):

Reticulate => *Rhyticaryum racemosum Becc.*

79 Ridges : secondary (?):

Yes => *Phytocrene hirsuta Blume*

No => *Phytocrene bracteata Wall.*

80 Endocarp : ridging pattern (?):

Reticulate => *98*

Diffuse => *99*

81 Locule : microtomography (?):

Smooth => *100*

Papillate => *101*

82 Endocarp wall : layers (?):

Divided into distinctive units => *Hosiea japonica Makino*

Homogeneous => *Desmostachys oblongifolius (Engl.) Villiers*

83 Ridges : secondary (?):

Yes => *Stachyanthus zenkeri Engl.*

No => *Desmostachys vogelii (Miers) Stapf*

84 Fruit: gynophore (?):

Yes => *Miquelia assamica (Griff.) Mast. ex B.D.Jacks.*

No => *Stachyanthus donisii (Boutique) Boutique*

85 Fruit: gynophore (?):

Yes => *Pyrenacantha kaurabassana Baill.*

No => *102*

86 Fruit: gynophore (?):

Yes => *Miquelia caudata King*

No => *103*

87 Locule : microtomography (?):

Smooth => *Desmostachys oblongifolius (Engl.) Villiers*

Papillate => *104*

88 Fruit: gynophore (?):

Yes => *Miquelia caudata King*

No => *Alsodeiopsis mannii Oliv.*

89 Epicarp : indumentum type (?):

Pubescent => *Iodes cirrhosa Turcz.*

Strigose => *Iodes ovalis Blume*

90 Endocarp wall : layers (?):

Divided into distinctive units => *Icacina trichantha Oliv.*

Homogeneous => *Icacina guessfeldtii Asch.*

91 Ridges : secondary (?):

Yes => *Iodes balansae Gagnep.*

No => *Iodes scandens (Becc.) Utteridge & Byng*

92 Endocarp : shape in lateral view (?):

Elliptical => *Pyrenacantha ambrensis Labat, El-Achkar & R.Rabev.*

Globulose => *Pyrenacantha andapensis Labat, El-Achkar & R.Rabev.*

93 Endocarp : Presence of a keel (?):

Yes => *105*

No => *106*

94 Endocarp wall : layers (?):

Divided into distinctive units => *Desmostachys planchonianus Miers*

Homogeneous => *Nothapodytes nimmoniana (J.Graham) Mabb.*

95 Endocarp : Apex structure (?):

Horns => *Icacina oliviformis (Poir.) J.Raynal*

Pores => *Icacina mannii Oliv.*

96 Areoles : freely ending ridgelets (?):

Yes => *Hosiea sinensis (Oliv.) Hemsl. & E.H. Wilson*

Rare or No => *Rhyticaryum macrocarpum Becc.*

97 Endocarp: thicker than wide (?):

Yes => *Cassinopsis ciliata Baker*

No => *107*

98 Locule : microtomography (?):

Smooth => *Pyrenacantha cordicula Villiers*

Papillate => *108*

99 Fruit: gynophore (?):

Yes => *Pyrenacantha puberula Boutique*

No => *Pyrenacantha sylvestris S.Moore*

100 Fruit: gynophore (?):

Yes => *Pyrenacantha laetevirens Sleumer*

No => *Pyrenacantha staudtii (Engl.) Engl.*

101 Ridges : secondary (?):

Yes => *Pyrenacantha anhydathoda (Villiers) Byng & Utteridge*

No => *109*

102 Endocarp : ridging pattern (?):

Diffuse => *Pyrenacantha vogeliana Baill.*

103 Endocarp wall : layers (?):

Divided into distinctive units => *110*

Homogeneous => *Natsiatum herpeticum Buch.-Ham. ex Arn.*

104 Endocarp : ridging pattern (?):

Reticulate => *111*

Diffuse => *Miquelia caudata King*

105 Epicarp : indumentum type (?):

Glabrous => *Mappia racemosa Jacq.*

106 Endocarp : shape in transverse section (?):

Lenticular => *Mappia multiflora Lundell*

Triangular => *Dendrobangia boliviana Rusby*

107 Endocarp : Apex structure (?):

Absent => *Rhyticaryum oleraceum Becc.*

Pores => *Rhyticaryum macrocarpum Becc.*

108 Endocarp : Apex structure (?):

Absent => *Pyrenacantha lebrunii Boutique*

Pores => *Miquelia celebica Blume*

109 Papillae : shape (?):

Rounded => *112*

Large => *Pyrenacantha rakotozafyi Labat, El-Achkar & R.Rabev.*

110 Endocarp : Apex structure (?):

Absent => *Rhyticaryum fasciculatum Becc.*

Pores => *Rhyticaryum elegans G.Schellenb.*

111 Fruit: gynophore (?):

Yes => *Miquelia caudata King*

No => *113*

112 Endocarp : Apex structure (?):

Absent => *Pyrenacantha longirostrata Villiers*

Horns => *Miquelia assamica (Griff.) Mast. ex B.D.Jacks.*

113 Papillae : shape (?):

Rounded => *Rhyticaryum longifolium K.Schum. & Lauterb.*

Large => *Hosiea japonica Makino*

Appendix 4

Modern fruit material examined for this study

Herbarium samples examined for comparison are listed below, including the following information: voucher number, locality, and date of collection and bar code of herbarium (P).
Iodes. ***I. africana*** Welw. Ex Oliv., A. Bouquet 833, Massia (Congo), 1964, P03951922; ***I. cirrhosa*** Turcz., B. Hayata 672, unknown, 1921, P06672331; ***I. klaineana*** Pierre, R.P. Klaine 3064, environs de Libreville (Gabon), 1902, P04472306.

Appendix 5

Modern fruit material examined for this study

Herbarium samples examined for comparison are listed below, including the following information: voucher number, locality, and date of collection and bar code of herbarium.
Iodes africana **Welw. ex Oliv.**_R.P. Tisserant s.n., Oubangui, 1948, MNHN-P-P03951984; R.P. Klaine 3505, Gabon, 1904, MNHN-P-P03951995. ***Iodes balansae*** **Gagnep.** KUN 0647593 (KUN). ***Iodes cirrhosa*** **Turcz.** B. Hayata 672, "Indo-chine", 1921, MNHN-P-P06672331. ***Iodes kamerunensis*** **Engl.** G.A. Zenker 2032, Cameroon, 1899, MNHN-P-P03951972. ***Iodes klaineana*** **Pierre** R.P. Klaine 3064, Gabon, 1902, MNHN-P-P04472306**.** ***Iodes liberica*** **Stapf** J.G. Adam 3833, Guinea, 1949, MNHN-P-P04472332. ***Iodes madagascariensis*** **Baill.** Chapelier s.n., Madagascar, s.d., MNHN-P-P04472113; McPherson 18809 (MO). ***Iodes ovalis*** **Blume** Hiep HLF 203 (MO). ***Iodes perrieri*** **Sleumer** Perrier De La Bâthie 17843, Madagascar, 1926, MNHN-P-P04472108. ***Iodes philippinensis*** **Merr.** A.D.E. Elmer 16418, Phillipines, 1916, MNHN-P-P04504850. ***Iodes scandens*** **(Becc.) Utteridge and Byng** No voucher (MO). ***Iodes seguinii*** **(H.Lév.) Rehder** Abbé Cavalerie 3932, Chine, 1913, MNHN-P-P05279333. ***Iodes seretii*** **(De Wild.) Boutique** D. Thomas and M. Etuge 63, Cameroon, s.d., BR0000015596772 (BR). ***Iodes yatesii*** **Merr.** Burley 1577 (K).

Appendix 6

www.nature.com/scientificreports

SCIENTIFIC REPORTS

OPEN

First record of an Icacinaceae Miers fossil flower from Le Quesnoy (Ypresian, France) amber

Received: 6 March 2017
Accepted: 22 August 2017

Cédric Del Rio[1,2], Thomas Haevermans[2] & Dario De Franceschi[1]

Flowers embedded in amber are rare. Only about 70 flowers or inflorescences have been described among which only one lamiid is known. Nevertheless, these fossils are important to our understanding of evolutionary process and past diversity due to the exceptional preservation of fragile structures not normally preserved. In this work, a new flower named *Icacinanthium tainiaphorum* sp. nov. from Le Quesnoy (Houdancourt, Oise, France) is described. Our phylogenetic analysis with extant species suggests that the affinity of this flower lies with the family Icacinaceae, close to *Natsiatum* or *Hosiea*. The fossil shows a combination of features unknown in extant Icacinaceae and we thus propose the description of a new fossil genus. It reveals a previously unknown diversity in the family and demonstrates the complementarity of different types of fossil preservation for a better understanding of past floral diversity.

Among the diverse organisms or parts of organisms embedded in amber, angiosperm flowers are exceedingly rare. Only ca. 70 flowers or inflorescences have been described to date, mostly from Cretaceous[1] Burmese amber[2–4], Paleogene Baltic amber[5,6] Miocene[7] Dominican amber[8–18] and Late Oligocene-Early Miocene Mexican amber[19–21].

In addition, we are noticing phylogenetic disparities. The rosid clade accounts for 39% of eudicot diversity but 44% of flowers embedded in amber. In contrast, the asterid clade, which represents half of the eudicot diversity[22], is represented in the fossil record by only 12 flowers (17%) in amber. Among these flowers, ca. 50% belong to Ericales and Cornales. Whilst five flowers belong to campanulids, only one represents the lamiid clade (in the order Gentianales), which corresponds to 26% of the extant eudicot diversity. Nevertheless, fossil flowers embedded in amber are generally important to understand evolutionary processes and past diversity because they are often exceptionally well preserved and provide insights into the morphology of fragile structures that are not normally preserved[23].

The locality at Le Quesnoy (Houdancourt, Oise, France), considered to be basal Eocene (Ypresian) was first studied in 1999[24]. This first survey highlighted the abundance of insects and the presence of at least one flower of caesalpinioid legume in amber. The pollen included in the amber was studied using a new technique of extraction[25,26], but the diversity of the floral remains had to be studied extensively.

Here we study one flower from Le Quesnoy and assign it to the lamiid clade. This flower named *Icacinanthium tainiaphorum* sp. nov. is the first known fossil occurrence of a flower from order Icacinales. The affinity of this flower embedded in the resin of a tree might suggest that this species could have been a climber. This type of ecology is frequent in megathermal flora, which has developed in Europe during the Eocene global warming. This Icacinaceae flower in amber attests to the presence of an undocumented past diversity.

Results

Systematics.

Order Icacinales Tiegh.
Family Icacinaceae Miers.
Genus *Icacinanthium* Del Rio & De Franceschi, gen. nov.
Type species *Icacinanthium tainiaphorum* Del Rio & De Franceschi, sp. nov.

[1] Centre de Recherche sur la Paléobiodiversité et les Paléoenvironnements, CR2P- UMR 7207, CNRS, MNHN, UPMC, Muséum National d'Histoire Naturelle, Sorbonne-Universités, CP38, 57 rue Cuvier, 75231, Paris Cedex 05, France. [2] Institut de Systématique, Évolution, Biodiversité, ISYEB- UMR 7205, CNRS, MNHN, UPMC, EPHE, Muséum National d'Histoire Naturelle, Sorbonne-Universités, CP39, 57 rue Cuvier, 75231, Paris Cedex 05, France. Correspondence and requests for materials should be addressed to C.D.R. (email: cedric.del-rio@edu.mnhn.fr)

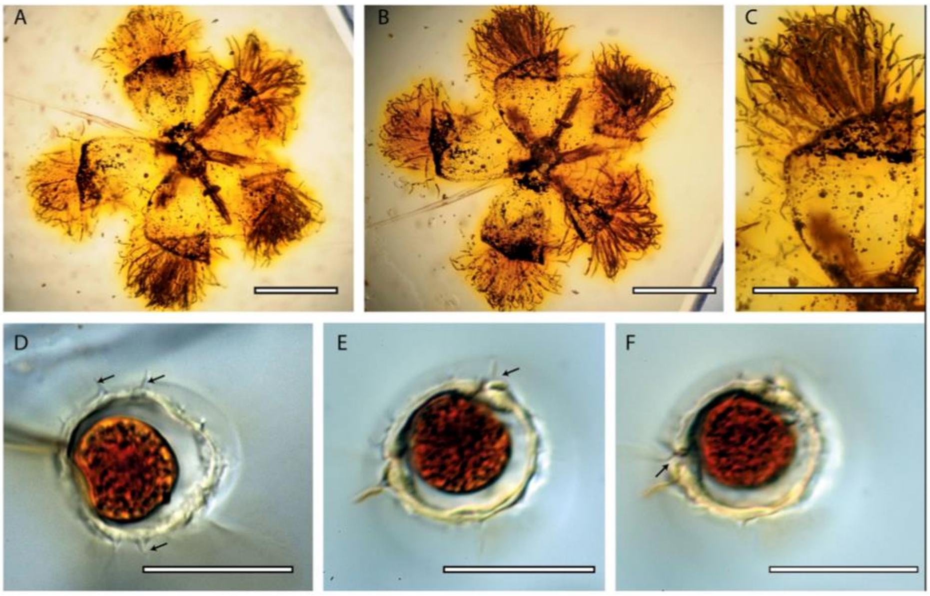

Figure 1. *Icacinanthium tainiaphorum* holotype, (**A**) flower in apical view with petals curved backwards, (**B**) same flower in basal view, (**C**) detail of petals in basal view (**D**) pollen grain showing echinate ornamentation (arrows) (**E** and **F**) other pollen grain showing pores (arrows). Scale: (**A–C**) = 1mm, (**D–F**) = 20 µm.

Generic diagnosis: Flower small, actinomorphic, hypogynous and pentamerous. Calyx cupular, Petals lanceolate curved backwards, with a straight apex, fused at base in a short cup, tomentose on adaxial surface with long, simple flattened hairs with granular ornamentation, glabrous on abaxial surface. Stamens alternate to petals, free. Pollen small, triaperturate and echinate.

Etymology: "*Icacinanthium*" indicates the familial affinity to Icacinaceae (Icaci-) and that it is a flower (L = Anthos, flower).

Icacinanthium tainiaphorum Del Rio & De Franceschi, sp. nov. (Figs 1 and 2)

Holotype: Deposited in the collection of Palaeobotany of MNHN (MNHN.F.44051.)

Type Locality: Le Quesnoy, Oise, France

Stratigraphic age: Ypresian

Etymology: "*tainiaphorum*" refers to the flat "ribbon-like" (L = tainia, ribbon) hairs borne (L = phor, bearing) on the petals.

Specific diagnosis: As for the genus

Description: A single flower embedded in amber, almost completely preserved. Flower small, about 2.5 mm in diameter, at least unisexual male or hermaphrodite, actinomorphic pentamerous and hypogynous (Fig. 1A,B).

The calyx is cupulate, filmy and very short. It is composed of 5 minute sepals, which are very difficult to distinguish. Scattered single-celled hairs are visible at the margin. Aestivation of the corolla is probably valvate according to the shape and position of the petals, which are fused at the base in a short cup. The petals are lanceolate, curved backwards in apical view (Figs 1A and 2) and with a straight apex (Fig. 1C), about 1.40 mm long and 0.7 mm broad. They are tomentose on the adaxial surface with long, simple flattened hairs with granular ornamentation, about 0.7 mm long and 0.025–0.036 mm broad; The stamens alternate with the petals and are erect but anthers were not preserved; Filaments are glabrous, about 0.15 mm in diameter, free from the petals and attached below the base of gynoecium. The globular gynoecium is free, possibly unilocular considering its shape, and glabrous. The ovary seems to be poorly developed or very small. The stigma is unknown, not preserved or not developed.

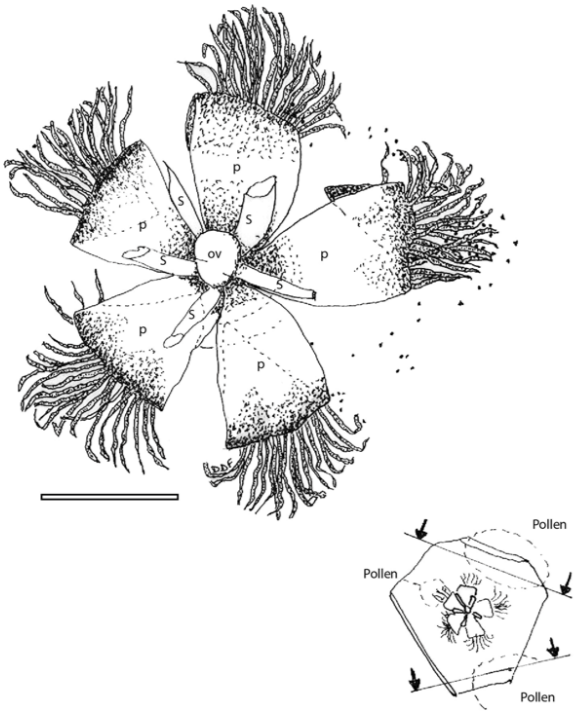

Figure 2. Drawing of *Icacinanthium tainiaphorum* gen. et sp. nov. in apical view; (ov) ovary; (s) stamens; (p) petals. Arrows and lines: position of section for pollen preparation. Scale bar = 1mm.

The pollen is very small (about 20–25 µm in diameter), clearly echinate (Fig. 1D) and triporate (Fig. 1E,F). No colpus could be observed, but we cannot completely exclude the presence of faintly marked small colpi.

Phylogenetic analysis. The Bayesian analysis 50% majority-rule consensus tree is given in Fig. 3 (and Supplementary 1). We included 51 species whose 23 species represent 21 genera of Icacinaceae and 27 species represent all other groups of the asterid. We used a combined morphological and molecular data with 73 protein-coding genes for a total of 59132 bp and 22 morphological characters (see the material and method for more precisions). As expected, we found a topology similar to the previous phylogenetic study using the same DNA data for the species included here[27]. This fossil, when included in the analyses, is placed close to *Natsiatum*. However the node with *Icacinanthium* and *Natsiatum* have very low support (PPB < 0.95). In this sense, the position of *Icacinanthium* is considered as unresolved at the base of the group IV sensu Stull *et al.*[27].

One hundred and ninety five (195) steps are necessary for the reconstruction of the history based on morphological characters by Mesquite's parsimony state reconstruction (0.34 CI and 0.47 RI). The position of *Icacinanthium* close to *Natsiatum* or *Hosiea* is supported by the same number of steps. This explains why only the nodes of the clades containing *Natsiatum* and *Hosiea* are over 0.95 PP. Of the 22 morphological characters, only the stamen position [16] and the symmetry of the flower [1] are non informative (Fig. 3; Supplementary 2). For the fossil flower, the main informative characters are the calyx shape [4], the petal and stamen fusion [10; 17] and all pollen characters [20; 21; 22]. Positioning uncertainties correspond to both characters for presence or absence of hair adaxially and abaxially on petals [13; 14].

Discussion

Only the presence of hairs on the outside of the petals seems to be synapomorphic for the Icacinaceae group (Fig. 3) according to our phylogenetic reconstruction. While *Icacinanthium* did not have hairs outside the petals, this state is also absent in four genera and some species of other genera within Icacinaceae, indicating a convergent loss of these hairs.

According to our ancestral state reconstruction, the Icacinaceae clade (excl. *Cassinopsis*) possesses small bisexual, pentamerous flowers with petal apex adaxially curved, stamen free from petals (this last state shared by all modern genera of Icacinaceae s.s, sensu Stull *et al.*[27]) and echinate pollen. Only the shape of the petal apex does

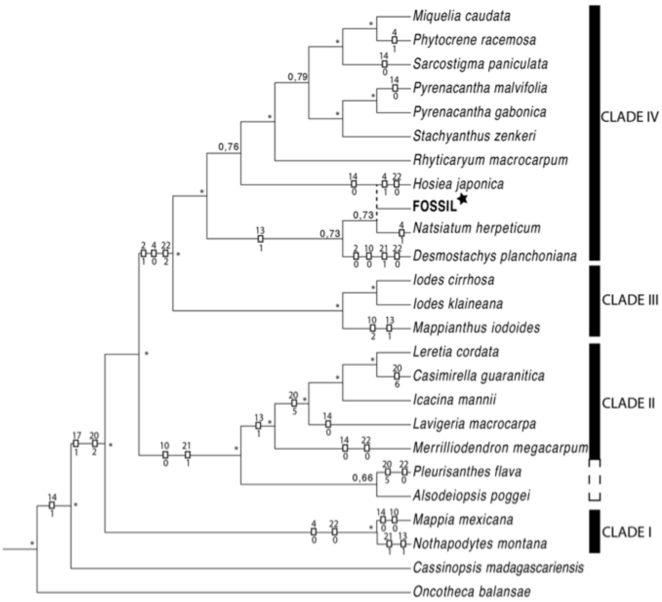

Figure 3. Phylogenetic relationships among asterid species focused on the family Icacinaceae based on the combined 73-plastidial genes and 22 morphological characters. The 50% majority-rule consensus tree was constructed by Bayesian inference in MrBayes. Star indicates the placement of the fossil flower close to *Natsiatum*. Dotted lines indicate another possible position for the fossil, close to *Hosiea*. Mesquite orientation of pertinent characters is shown. (*) represent strong node (>95% PP).

not match with this fossil flower; however, this feature also occurs in five extant genera of Icacinaceae and several species which also possess comparable straight apices.

The clade including both III and IV possesses unisexual flowers (except for *Desmostachys*), cupular calyx, petals fused at base and small and mainly porate pollen grains (synapomorphic). Moreover, petal apex orientation of Clade IV is unresolved with a preponderance of genera with straight apices, which would be a synapomorphic character for this clade, emphasizing affinities of *I. tainiaphorum* to this clade. We therefore hypothesize that this flower is a unisexual male flower, which would explain the poorly developed ovary and make a better fit with the phylogenetic position of the fossil (rather than a poor preservation of this organ during fossilisation).

Adaxial hairs of *Emmotum nitens*[28] and *Poraqueiba sericea* have an irregularly moniliform shape, and thus clearly differ from the hairs seen in other species. In fact, all adaxial hairs of Icacinaceae s.s. considered here and *Metteniusa* petals are flattened and very simple, as what is found in *Icacinanthium* (Fig. 4). Icacinaceae hairs however are granular, more or less longitudinally extended while in *Metteniusa* we observe nodules surrounded by longitudinal furrows (Fig. 4F), very different from the Icacinaceae ornamentation. These observations corroborate the position of *I. tainiaphorum* within the family Icacinaceae. In this family, the external hairs are generally quite similar, with a tubular form, acute at the apex and with granular ornamentation (Fig. 4E). The hairs in the fossil appear to be homologous and the presence of these hairs is interpreted to be synapomorphic for Icacinaceae.

In any case this fossil shows a combination of characters unknown in extant Icacinaceae. Indeed, flowers of *Natsiatum herpeticum*, which have adaxial petal hairs, also have them abaxially. In contrast, *Hosiea japonica* flowers are glabrous, and there are also flowers with abaxially hairy petals, but not adaxially in four genera of clade IV. To our knowledge, only the flower of *Merrilliodendron megacarpum*, from clade II, has adaxial petal hairs only such as what we found in our fossil flower. In clade IV this character state is unknown and new, hence our proposal to treat it as an extinct genus.

The fossil record of Icacinaceae, predominantly from the Eocene of North America and Europe, is extensive. However no fossil flowers were until now attributed to this family. In fact, most of these fossils are endocarps, in particular from the modern genera *Iodes*[29–31], *Phytocrene*[32,33] and *Pyrenacantha*[30,33]. Endocarp fossils of *Natsiatum* were described from the Middle Eocene of Tennessee (*Natsiatum wilcoxiana* (Berry) Stull, Moore & Manchester[34]). In Europe, fossils of *Palaeohosiea*, supposed to be close to the extant genus *Hosiea*, were described[35]. However, no character supports affinity with *Hosiea* and no feature separates the fossils from the extant genus *Iodes*[36]. The presence of Icacinaceae from Le Quesnoy was only mentioned briefly and was based on what appears to be a lignitic endocarp[24], but was attributed to the genus *Iodes* (personal observation). The link between these two types of fossils is questionable, thus indicating an unsuspected diversity for Eocene Icacinaceae.

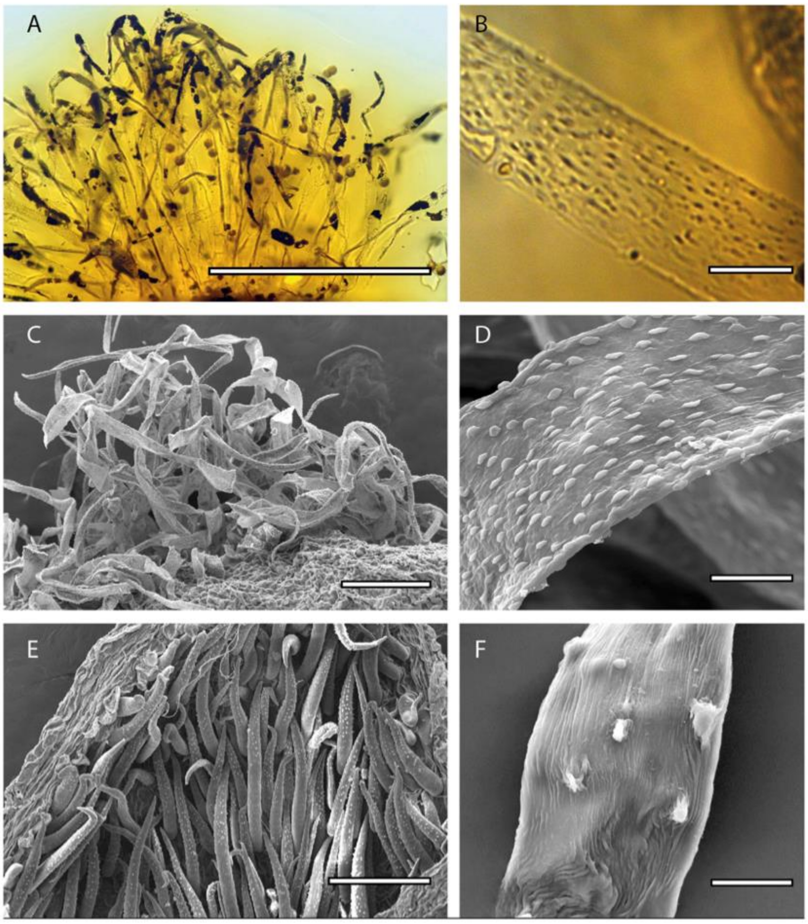

Figure 4. Morphological form of hairs on petals. (**A**) "simple" adaxial hairs from *Icacinanthium tainiaphorum*, note the presence of pollen grains between hairs (**B**) same, detail of ornamentation on hair surface (**C**) "simple" adaxial hairs from *Icacina mannii* Oliv.; (**D**) same, detail of ornamentation (**E**) tubular and acute abaxial petal hairs from *Icacina mannii*. (**F**) detail of ornamentation for *Metteniusa tessmaniana* Scale: (**A**) = 500 µm (**C** and **E**) = 100 µm; (**B**,**D** and **F**) = 20 µm.

Growth habits of extant Icacinaceae include lianas, shrubs or trees, distributed in tropical forests around the word. *Icacinanthium* is close to *Natsiatum* or *Hosiea*, both of which being Asian genera of climbing shrubs[37]. *Icacinanthium* could testify for an Asian affinity of the Le Quesnoy Ypresian flora, as highlighted by studies on Menispermaceae[38] and other comparable European sites[31, 32, 39]. We thus hypothesize that *Icacinanthium* could be a climbing shrub, this type of ecology being frequent for megathermal flora that would have occurred in Europe during the early Eocene global warming phase[40, 41].

Material and Method

Locality and fossil material.

The fossil resin remains were collected from 1997 to 2000 from the Le Quesnoy (Houdancourt, Oise, France) lignitic clay sediments which belong to the ≪ argiles à lignites du Soissonais ≫ Formation. These sediments are dated to the Ypresian (±56 Ma) according to mammal biochronology (MP7) and palynological studies[24, 42]. This corresponds to the Sparnacian facies of the lower Ypresian (lower Eocene). Several fossil resin samples contain diverse organisms, principally arthropods (mainly insects), a few plant remains, mainly represented by pollen grains[25, 42] but also a few flowers still to be studied. The fossils are kept in the collections of the Paris Muséum national d'histoire naturelle (MNHN). The specimen studied here is a flower embedded in this fossil resin here called amber, but produced by Detarioidae trees (Leguminosae)[43,44].

Phylogenetic reconstructions. Preliminary exploratory herbarium studies (P) focusing on small pentamerous hypogynous flower with petals fused at the base and with stamens free from the petals lead to comparison of the flower in amber to those of the family Icacinaceae. We employed the most complete molecular data for the asterid clade focusing on the Icacinaceae[27]. Theses data were composed of 73 protein-coding genes for a total of 59132 bp. We retained 51 species among the 112 accessions available[27] of which 23 species represent 21 genera of Icacinaceae. We included at least 2 species from other asterid orders, except for Metteniusales where we used 9 species as this order includes species which were formerly included in genera of Icacinaceae, which are morphologically close to Icacinaceae sensu stricto. All molecular characters are coded as missing for the flower in amber. In addition, we included 22 morphological floral characters corresponding to features potentially observable in the fossil flower (Supplementary 2). The final matrix contains 59135 characters.

Bayesian analyses were performed using MrBayes[45] with a format type mixed with two partition: DNA type (with model by default, GTR + I + G) and Standard type (equal state frequencies with all topologies equally likely a priori with unconstrained branch lengths) for morphological data. Two independent but parallel analyses were performed using flat priors, starting from random trees and consisting of four chains each. The analysis was run for 5 million generations, sampling every 1000 generations and with 20% burn-in. Analysis of output parameter using Tracer v.1.6[46] confirms the convergence of chains. A 50% majority-rule consensus tree was computed with posterior probability (PP) estimates for all nodes. We generally consider as non-supported nodes those with less than 0.95 PP.

Morphological studies. A morphology matrix was made using Xper 3[47] containing 22 flower and pollen characters coded for 51 taxa including the Le Quesnoy flower (Supplementary 2)

The matrix was constructed from direct morphological observation of herbarium specimens (P, see Supplementary 3) and from bibliographic data for flowers[28,37,48–57] and pollen[58–63]. We observed the flower embedded in amber using a light microscope (Nikon Eclipse80i). Numerous pollen grains were found around the flower and between hairs on the adaxial surface of the petals (Fig. 1D,F); the vicinity and abundance of grains of the same type indicate that they probably belong to the flower. The pollen was also extracted from the amber in order to obtain a better understanding of its type (Fig. 2) following a previously published protocol[25] and observed using the same microscope. Before extraction we only observe the imprint left by the pollen in amber. After extraction, we show an exceptional preservation of grains with well-preserved exine wall and remains of cellular content. A darker zone could correspond to the rest of the nucleus (clearly visible on Fig. 1D). Due to the presence of echinae (spines), pollen grains could not be fully separated from resin and were observed still embedded inside a small resin block. All these features were mapped into the phylogeny using Mesquite software[64] with a parsimony ancestral state reconstruction.

We conducted a qualitative study of adaxial petal hairs of *Metteniusa*, *Poraqueiba*, *Nothapodytes*, *Mappia*, *Icacina*, *Leretia*, *Mappianthus*, *Desmostachys* and *Natsiatum* using SEM (Scanning Electron Microscopy) with a Jeol JCM6000 after the specimens were coated with gold-palladium.

References

1. Cruickshank, R. D. & Ko, K. Geology of an amber locality in the Hukawng Valley, northern Myanmar. *J. Asian Earth Sci.* **21**, 441–455 (2003).
2. Poinar, G. Jr., Chambers, K. L. & Buckley, R. *Eoepigynia burmensis* gen. and sp. nov., an Early Cretaceous eudicot flower (Angiospermae) in Burmese amber. *J. Bot. Res. Inst. Tex.* **1**, 91–96 (2007).
3. Poinar, G. Jr. & Chambers, K. L. *Palaeoanthella huangii* gen. and sp. nov., an early Cretaceous flower (Angiospermae) in Burmese amber. *SIDA Contrib. Bot.* **21**, 2087–2092 (2005).
4. Poinar, G. O. Jr. *Programinis burmitis* gen. et sp. nov., and *P. laminatus* sp. nov., Early Cretaceous grass-like monocots in Burmese amber. *Aust. Syst. Bot.* **17**, 497–504 (2004).
5. Göppert, J. H. R., Menge, A. & Conwentz, H. W. *Die Flora des Bernsteins, und ihre Beziehungen zur Flora der Tertiärformation und der Gegenwart* (Engelmann, Leipzig, 1886).
6. Weitschat, W. & Wichard, W. *Atlas der Pflanzen und Tiere im baltischen Bernstein* (F. Pfeil, München, 1998).
7. Iturralde-Vincent, M. A. & MacPhee, R. D. E. Age and paleogeographical origin of Dominican amber. *Science* **273**, 1850 (1996).
8. Chambers, K. L., Poinar, G. O. Jr. & Chanderbali, A. S. *Treptostemon* (Lauraceae), a new genus of fossil flower from Mid-Tertiary Dominican amber. *J. Bot. Res. Inst. Tex.* **6**, 551–556 (2012).
9. Chambers, K. L., Poinar, G. O. Jr. & Brown, A. E. Two fossil flowers of *Trichilia* (Meliaceae) in Dominican amber. *J. Bot. Res. Inst. Tex.* **5**, 463–468 (2011).
10. Chambers, K. L., Poinar, G. O. Jr. & Brown, A. E. A fossil flower of *Persea* (Lauraceae) in Tertiary Dominican amber. *J. Bot. Res. Inst. Tex.* **5**, 457–462 (2011).
11. Chambers, K. L. & Poinar, G. O. Jr. *Ticodendron palaios* sp. nov. (Ticodendraceae), a Mid-Tertiary Fossil Flower in Dominican Amber. *J. Bot. Res. Inst. Tex.* **8**, 559–564 (2014).
12. Poinar, G. Fossil palm flowers in Dominican and Baltic amber. *Bot. J. Linn. Soc.* **139**, 361–367 (2002).
13. Poinar, G. Fossil palm flowers in Dominican and Mexican amber. *Bot. J. Linn. Soc.* **138**, 57–61 (2002).
14. Poinar, G. & Columbus, J. T. *Alarista succina* gen. et sp. nov. (Poaceae: Bambusoideae) in Dominican amber. *Hist. Biol.* **25**, 691–696 (2013).
15. Poinar, G. Jr. & Judziewicz, E. J. *Pharus primuncinatus* (Poacae: Pharoideae: Phareae) from Dominican amber. *SIDA Contrib. Bot.* **21**, 2095–2103 (2005).
16. Poinar, G. Jr. & Steeves, R. *Virola dominicana* sp. nov. (Myristicaceae) from Dominican amber. *Botany* **91**, 530–534 (2013).
17. Poinar, G. O. Jr. *Hymenaea protera* sp. n. (Leguminosae, Caesalpinioideae) from Dominican amber has African affinities. *Experientia* **47**, 1075–1082 (1991).
18. Poinar, G. O. Jr., Chambers, K. L. & Brown, A. E. *Trochanthera lepidota* gen. and sp. nov., a fossil angiosperm inflorescence in Dominican amber. *J. Bot. Res. Inst. Tex.* **2**, 1167–1173 (2008).
19. Calvillo-Canadell, L., Cevallos-Ferriz, S. R. S. & Rico-Arce, L. Miocene *Hymenaea* flowers preserved in amber from Simojovel de Allende, Chiapas, Mexico. *Rev. Palaeobot. Palynol.* **160**, 126–134 (2010).

20. Castañeda-Posadas, C. & Cevallos-Ferriz, S. R. *Swietenia* (Meliaceae) flower in Late Oligocene–Early Miocene amber from Simojovel de Allende, Chiapas, Mexico. *Am. J. Bot.* **94**, 1821–1827 (2007).
21. Chambers, K. L., Poinar, G. O. Jr. & Brown, A. E. A new fossil species of *Colpothrinax* (Arecaceae) from Mid-Tertiary Mexican amber. *J. Bot. Res. Inst. Tex.* **6**, 557–560 (2012).
22. Magallón, S., Crane, P. R. & Herendeen, P. S. Phylogenetic pattern, diversity, and diversification of eudicots. *Ann. Mo. Bot. Gard.* **86**, 297–372 (1999).
23. Poinar, G. O. & Poinar, R. *The amber forest: a reconstruction of a vanished world* (Princeton University Press, 1999).
24. Nel, A. *et al.* Un gisement sparnacien exceptionnel à plantes, arthropodes et vertébrés (Éocène basal, MP7): Le Quesnoy (Oise, France). *Comptes Rendus de l'Académie de Sci. - Ser. IIA - Earth Planet. Sci.* **329**, 65–72 (1999).
25. De Franceschi, D., Dejax, J. & De Ploëg, G. Extraction du pollen inclus dans l'ambre [Sparnacien du Quesnoy (Oise), bassin de Paris]: vers une nouvelle spécialité de la paléo-palynologie. *Comptes Rendus de l'Académie des Sci.-Ser. IIA-Earth Planet. Sci.* **330**, 227–233 (2000).
26. Dejax, J., De Franceschi, D., Lugardon, B., De Ploëg, G. & Arnold, V. Le contenu cellulaire du pollen fossilisé dans l'ambre, préservé à l'état organique. *Comptes Rendus de l'Académie des Sci.-Ser. IIA-Earth Planet. Sci.* **332**, 339–344 (2001).
27. Stull, G. W., Duno de Stefano, R., Soltis, D. E. & Soltis, P. S. Resolving basal lamiid phylogeny and the circumscription of Icacinaceae with a plastome-scale data set. *Am. J. Bot.* **102**, 1794–1813 (2015).
28. Endress, P. K. & Rapini, A. Floral structure of *Emmotum* (Icacinaceae sensu stricto or Emmotaceae), a phylogenetically isolated genus of lamiids with a unique pseudotrimerous gynoecium, bitegmic ovules and monosporangiate thecae. *Ann. Bot.* **114**, 945–959 (2014).
29. Knobloch, E. & Mai, D. H. *Monographie der Früchte und Samen in der Kreide von Mitteleuropa* (Vydal Ustredni ustav geologicky, Praha, 1986).
30. Manchester, S. R. *Fruits and seeds of the Middle Eocene nut beds flora, Clarno Formation, Oregon* (Paleontological Research Institution, New York, 1994).
31. Reid, E. M. & Chandler, M. E. *The London Clay Flora* (The British Museum (Natural History), London, 1933).
32. Collinson, M. E., Manchester, S. R. & Wilde, V. *Fossil fruit and seeds of the Middle Eocene Messel biota, Germany* (Abh. Senckenb. Ges. Naturforsch., Stuttgart, 2012).
33. Stull, G. W., Herrera, F., Manchester, S. R., Jaramillo, C. & Tiffney, B. H. Fruits of an 'Old World' tribe (Phytocreneae; Icacinaceae) from the Paleogene of North and South America. *Syst. Bot.* **37**, 784–794 (2012).
34. Stull, G. W., Moore, B. R. & Manchester, S. R. Fruits of Icacinaceae from the Eocene of Southeastern North America and their biogeographic implications. *Int. J. Plant Sci.* **172**, 935–947 (2011).
35. Kvaček, Z. & Bůžek, Č. Endocarps and foliage of the flowering plant family Icacinaceae from the Tertiary of Europe. *Tert. Res.* **15**, 121–138 (1995).
36. Stull, G. W., Adams, N. F., Manchester, S. R., Sykes, D. & Collinson, M. E. Revision of Icacinaceae from the Early Eocene London Clay flora based on X-ray micro-CT. *Botany* **94**, 713–745 (2016).
37. Peng, H. & Howard, R. A. In *Flora of* China **11** (ed. Wu, Z. Y., Raven, P. H., Hong) 505–513 (Sc. Press. Beijing- Missouri Botanical Garden. St. Louis, 2008).
38. Jacques, F. M. B. & De Franceschi, D. Endocarps of Menispermaceae from Le Quesnoy outcrop (Sparnacian facies, Lower Eocene, Paris Basin). *Rev. Palaeobot. Palynol.* **135**, 61–70 (2005).
39. Cleal, C. J., Thomas, B. A., Batten, D. J. & Collinson, M. E. *Mesozoic and Tertiary palaeobotany of Great Britain* (Geological conservation review series, Peterborough, 2001).
40. Zachos, J., Pagani, M., Sloan, L., Thomas, E. & Billups, K. Trends, rhythms, and aberrations in global climate 64 Ma to present. *Science* **292**, 686–693 (2001).
41. Zachos, J. C. *et al.* Extreme warming of mid-latitude coastal ocean during the Paleocene-Eocene Thermal Maximum: inferences from TEX86 and isotope data. *Geology* **34**, 737–740 (2006).
42. Cavagnetto, C. La palynoflore d'un gisement d'ambre de l'Eocène basal du Bassin Parisien (Le Quesnoy, France). *Palaeontogr. Abt. B* **255**, 147–171 (2000).
43. De Franceschi, D. & De Ploëg, G. Origine de l'ambre des faciès sparnaciens (Éocène inférieur) du Bassin de Paris: le bois de l'arbre producteur. *Geodiversitas* **25**, 633–647 (2003).
44. Jossang, J., Bel-Kassaoui, H., Jossang, A., Seuleiman, M. & Nel, A. Quesnoin, a novel pentacyclic ent-diterpene from 55 million years old Oise amber. *J. Org. Chem.* **73**, 412–417 (2008).
45. Ronquist, F. *et al.* MrBayes 3.2: efficient bayesian phylogenetic inference and model choice across a large model space. *Syst. Biol.* **61**, 539–542 (2012).
46. Rambaut, A., Suchard, M. A., Xie, D. & Drummond, A. J. *Tracer v1. 6* (2014).
47. Ung, V., Dubus, G., Zaragueta-Bagils, R. & Vignes-Lebbe, R. Xper2: introducing e-taxonomy. *Bioinformatics* **26**, 703–704 (2010).
48. Bridson, D. M. A Revision of the family Vahliaceae. *Kew Bull.* **30**, 163–182 (1975).
49. Dahling, G. V. Systematics and evolution of *Garrya. Contrib. Gray Herb. Harv. Univ.* **209**, 1–104 (1978).
50. Davenport, L. J. A monograph of *Hydrolea* (Hydrophyllaceae). *Rhodora* 169–208 (1988).
51. De la Bâthie, P. In: *Flore de Madagascar et des* Comores **119** (ed. H. Humbert) 1–45 (Firmin-Didot et Cie, 1952).
52. Gonzalez, F. A. & Rudall, P. J. Flower and fruit characters in the early-divergent lamiid family Metteniusaceae, with particular reference to the evolution of pseudomonomery. *Am. J. Bot.* **97**, 191–206 (2010).
53. Howard, R. A. Study o the Icacinaceae IV. Considerations of the new world genera. *Contrib. Gray. Herb. Harvard Univ.* **142**, 3–60 (1942).
54. Morat, P. & Veillon, J. M. In: *Flore de la Nouvelle-Calédonie et* Dépendances **15** (ed. A. Aubréville et J-F. Leroy) 90–99 (Museum National d'Histoire Naturelle, Paris, 1988).
55. Ohwi, J. *Flora of Japan. A combined, much revised, and extended translation by the author of his Flora of Japan* (*1953*) *and Flora of Japan-Pteridophyta* (1957) (Washington. DC Smithson. Inst. 1984).
56. Santiago-Valentín, E. & Viruet-Oquendo, E. Notes on the flower, fruit, and the reproductive phenology of the elusive *Ottoschulzia rhodoxylon. Harv. Pap. Bot.* **18**, 61–65 (2013).
57. Villiers, J.-F. in: *Flore du Cameroun* (ed. A. Aubréville et J-F. Leroy) (15) 3–100 (Museum National d'Histoire Naturelle, Paris 1973).
58. Dickison, W. C. Further observations on the floral anatomy and pollen morphology of *Oncotheca* (Oncothecaceae). *Brittonia* **38**, 249–259 (1986).
59. Erdtman, G. Pollen morphology and plant taxonomy. *Geol Fören. i Stockholm Förhand.* **74**, 526–527 (1952).
60. Gosling, W. D., Miller, C. S. & Livingstone, D. A. Atlas of the tropical West African pollen flora. *Rev. Palaeobot. Palynol.* **199**, 1–135 (2013).
61. Lobreau-Callen, D. Le pollen des Icacinaceae: 2. Observations en microscopie electronique, correlations, conclusions. *Pollen Spores* **15**, 47–89 (1973).
62. Lobreau-Callen, D. Pollen des Icacinaceae: 1. Atlas (1). *Pollen Spores* **14**, 345–388 (1972).
63. Lobreau-Callen, D. Les variations dimensionnelles du pollen du genre *Ilex* (Aquifoliaceae) et leurs rapports avec le climat. *Bull. Société Bot. Fr.* **122**, 179–199 (1975).
64. Maddison, W. P. & Maddison, D. R. Mesquite: a modular system for evolutionary analysis (2001).

Acknowledgements

The fossil was collected during field work of the "amber team" of MNHN, with the help of Lafarge-Granulat, and we thank the Langlois-Meurinne family for giving authorization to work on their property. We thank the staff of the Paris Herbarium (MNHN P) for the loan of modern flower samples and access to herbarium sheets. We also thank Valentin Seizille de Mazancourt for the help in naming the species. We thank Martin Pickford and Steven Manchester for improving the English. This work was supported by a grant from Agence Nationale de la Recherche under the LabEx ANR-10-LABX-0003-BCDiv, in the program "Investissements d'avenir" ANR-11-IDEX-0004-02 and by the CR2P.

Author Contributions

C.D.R. and D.D.F. performed the morphological and phylogenetic analysis; C.D.R. and D.D.F. prepared the figures, D.D.F. drew Fig. 2; D.D.F. and T.H. designed the program; C.D.R. and D.D.F. prepared the manuscript.

Additional Information

Supplementary information accompanies this paper at doi:10.1038/s41598-017-11536-y

Competing Interests: The authors declare that they have no competing interests.

Appendix 7

Flower and pollen morphological matrix.

1 Flower symmetry/ Bilateral; Radial,

2 Flower sex/ Bisexual; Unisexual,

3 Flower size/ Small; Tall,

4 Calyx form/ Cupular; Divided,

5 Sepal number of pieces/ 0; 4; 5; 6; 8,

6 Sepals hair on margin/ Yes; No,

7 Petal number/ 4; 5; 6; 8,

8 Petal aestivation/ Imbricate; Twisted; Valvate,

9 Petal shape/ Circular; Lanceolate; Oblong to linear; Spatulate; Triangular,

10 Petals welding/ Free; Gamopetal at base; Gamopetal in tube,

11 Petal apex orientation/ Curved adaxially; Straight,

12 Petals orientation in flower/ Curved abaxially; Straight,

13 Petals hair inside/ Absent; Present,

14 Petal hair outside/ Absent; Present,

15 Stamen number of pieces/ 2; 4; 5; 6; 8; 10,

16 Stamen position/ Alternate with petals; Opposite with petals,

17 Stamen fusion/ Adnate to petals; Free,

18 Ovary hair/ Absent; Present,

19 Ovary locule/ Plurilocular; Unilocular,

20 Pollen ornamentation/ Baculate; Clavate; Echinate; Gemmate; Granulate; Reticulate; Scabrate; Verrucate,

21 Pollen size/ Small; Tall,

22 Pollen aperture/ Colpate; Colporate; Porate

Character number	1	2	3	4	5	6	7	8	9	10	11	12	13	14	15	16	17	18	19	20	21	22
Garrya_flavescens	1	1	0	?	0	1	0	2	(12)	1	1	?	0	1	?	0	1	1	0	5	1	1
Gentiana_acaulis	1	0	1	1	2	1	1	1	2	2	1	0	0	0	2	0	0	0	1	5	0	1
Convolvulus_arvensis	1	0	1	1	2	1	1	0	2	2	1	1	0	0	2	0	0	0	0	4	1	0
Solanum_lycopersicum	1	0	1	1	2	1	1	2	2	1	1	0	0	0	2	0	0	0	0	?	0	1
Vahlia_capensis	1	0	1	1	2	0	1	2	(01)	1	1	1	1	0	2	0	1	0	1	5	?	1
Borago_officinalis	1	0	1	1	2	0	1	2	4	1	1	1	0	0	2	0	0	0	0	3	1	1
Coffea_arabica	1	0	1	0	(123)	1	1	1	2	2	1	1	0	0	2	0	0	?	1	4	(01)	1
Metteniusa_tessmanniana	1	0	1	1	2	0	1	0	2	1	1	0	1	0	2	0	0	1	1	?	?	1
Hydrolea_corymbosa	1	0	1	1	2	0	1	0	2	1	1	1	0	0	2	0	1	1	0	5	?	1
Jasminum_nudiflorum	1	0	1	1	(23)	1	(12)	0	2	2	1	1	0	0	0	0	0	0	0	5	1	0
Thymus_vulgaris	0	0	1	1	2	0	1	?	(02)	2	1	1	0	1	1	0	0	0	0	5	1	0
Calatola_mollis	1	1	0	0	1	?	0	2	2	0	?	?	?	1	1	0	0	1	1	6	0	1
Oncotheca_balansa	1	0	0	1	2	1	1	0	0	1	1	1	0	0	2	0	0	0	0	5	0	1
Ilex_cornuta	1	1	0	1	1	0	0	0	2	1	1	1	0	0	1	0	1	0	0	1	0	1
Pleurisanthes_flava	1	0	0	1	2	0	1	2	(12)	0	0	1	0	1	2	0	1	1	1	5	1	0
Merrilliodendron_megacarpum	1	0	0	1	2	1	1	2	2	0	0	?	1	0	2	0	1	0	1	2	1	0
Daucus_carota	(01)	0	0	0	(02)	1	1	?	2	0	0	1	0	0	2	0	1	0	0	4	0	1
Mappia_mexicana	1	0	0	0	2	0	1	2	1	0	0	1	0	0	2	0	1	0	1	2	0	0
Cornus_florida	1	0	0	0	0	0	0	2	2	1	0	1	0	1	1	0	1	?	0	?	?	1
Nothapodytres_montana	1	0	0	0	2	0	1	2	2	1	0	0	1	1	2	0	1	1	1	2	1	0
Rhododendron_simsii	1	0	1	1	2	0	1	0	2	2	1	1	0	1	5	0	1	1	0	4	1	1
Alsodeiopsis_poggei	1	0	0	1	2	0	1	2	1	0	0	1	0	1	2	0	1	1	1	2	1	1
Cassinopsis_madagascariensis	1	0	0	1	2	0	1	2	2	1	1	1	0	1	2	0	0	1	1	5	0	1
Leretia_cordata	1	0	0	1	2	0	1	2	(12)	0	0	1	1	1	2	0	1	1	1	5	1	1
Iodes_klaineana	1	1	0	0	2	0	1	2	1	0	1	1	0	1	2	0	1	1	1	2	0	2
Icacina_mannii	1	0	0	1	2	0	1	2	2	0	0	1	1	1	2	0	1	1	1	5	1	1
Lavigeria_macrocarpa	1	0	0	1	2	0	1	2	1	0	0	1	0	0	2	0	1	1	1	5	1	1
Hosiea_japonica	1	1	0	1	2	?	1	2	1	1	1	0	0	0	2	0	1	0	1	2	(01)	0
Desmostachys_planchoniana	1	0	0	0	2	0	1	2	2	0	1	?	1	1	2	0	1	1	1	2	1	0
Casimirella_guaranitica	1	0	0	1	(23)	0	(12)	2	(12)	0	1	1	1	1	(23)	?	1	1	1	6	0	1
Sarcostigma_paniculata	1	1	0	0	2	0	1	2	2	1	0	1	0	0	2	0	1	1	1	2	(01)	2
Rhyticaryum_macrocarpum	1	1	0	0	2	?	1	2	(12)	1	0	1	0	1	2	0	1	1	1	2	0	2
Iodes_cirrhosa	1	1	0	(01)	2	0	1	2	(12)	1	0	1	0	1	2	0	1	1	1	2	0	2
Mappianthus_iodoides	1	1	0	0	2	0	1	2	2	2	0	1	1	1	2	0	1	1	1	2	(01)	2
Natsiatum_herpeticum	1	1	0	1	2	0	1	2	1	1	1	0	1	1	2	0	1	0	1	2	0	2
Miquelia_caudata	1	1	0	0	(12)	?	(01)	2	?	1	0	?	?	?	(12)	?	?	1	1	2	0	2
Pyrenacantha_gabonica	1	1	0	?	?	?	0	2	2	1	1	1	0	1	1	0	1	?	?	2	0	2
Stachyanthus_zenkeri	1	1	0	0	3	0	2	2	2	?	0	1	0	1	3	?	?	?	1	2	0	2
Le_Quesnoy	1	?	0	0	2	0	1	2	1	1	1	0	1	0	2	0	1	?	?	2	0	2
Pyrenacantha_malvifolia	1	1	0	?	?	?	(01)	2	4	1	1	1	0	0	(12)	0	1	1	1	2	0	2
Phytocrene_racemosa	1	1	0	1	2	0	0	2	(12)	1	1	1	0	1	1	0	1	1	1	2	0	2
Pittosporopsis_kerrii	1	0	0	1	2	0	1	2	3	0	1	1	0	1	2	0	0	0	1	5	0	1
Platea_latifolia	1	1	0	1	2	0	1	2	2	1	1	1	0	0	2	0	0	0	1	5	0	1
Aucuba_japonica	1	1	0	0	1	1	0	2	2	0	1	1	0	0	1	0	1	1	1	0	(01)	1
Ehretia_acuminata	1	0	0	1	2	0	1	0	2	2	1	1	0	0	2	0	0	0	0	?	0	1

Appendix 8

Modern flowers examined for this study (chapter VI).

Herbarium samples examined for comparison are listed below, including the following information: voucher number, locality, date of collection and bar code of herbarium (P). The specimens used for hair comparison are in bold.

Boraginales. *Borago officinalis* L., Bosserdet SN, France, 1937, P04026682; *Ehretia acuminata* R. Br., Desvaux SN, Nouvelle-Zelande, *, P03860204. **Cornales.** *Cornus florida* L., Vaillant SN, *, 1945, P04556278. **Ericales.** *Rhododendron simsii* Planch., Poilane 29733, Indochine, 1939, P04505977. **Garryales**. *Aucuba japonica* Thunb., Savatier 531, Japan, *, P00545427; *Garrya flavescens* S. Watson, Purpus 841, California, 1894, P04472060.

Gentianales. *Coffea arabica* L., Meyer 781, Ethiopia, 1961, P03826715 ; *Gentiana acaulis* L., *, France, 1962, P05039952. **Icacinales.** *Alsodeiopsis poggei* Engl., Letouzey 11516, Cameroun, 1972, P04495898 ; *Cassinopsis madagascariensis* Bail., Phillipson et al. 5643, Madagascar, 2003, P04472155 ; *Desmostachys planchoniana* Miers, Randrianarivelo et al. 62, Madagascar, 2004, P00692577 ; *Desmostachys tenuifolius* Oliv., Endengle 141, Cameroun, 1960, P04495143 ; *Icacina manii* Oliv., *, Afrique occidentale, *, P04495581 ; *Iodes cirrhosa* Turcz., *, Sud Vietnam, 1960, P06672326 ; *Iodes cirrhosa* Turcz., Poilane 9956, « Indochine », 1924, P06672329 ; *Iodes klaineana* Pierre, Sita 2571, Congo, 1968, P04472290 ; *Lavigeria macrocarpa* (Oliv.) Pierre, Le Testu 4487, Yalinga, 1923, P04494816; *Lavigeria macrocarpa* (Oliv.) Pierre, Tisserant 2354, Bouhko, 1976, P04494814; *Leretia cordata* Vell., B. 4445, Guyane, 1972, P06672311; *Mappia mexicana* B.L. Rob. & Greenm, *, Tampico, 1897, P04513549; *Mappia racemosa* Jacq., Manriquez 3472, Mexico, 1990, P04513546 ; *Mappianthus iodoides* Hand.-Mazz, *, Tonkin, 1944, P04513536 ; *Mappianthus iodoides* Hand.-Mazz, Petelot 8750, Tonkin, 1943, P04513537 ; *Natsiatum herpeticum* Buch.-Ham. ex Arn., Bena 1142, Guadeloupe, *, P04519509 ; *Natsiatum herpeticum* Buch.-Ham. ex Arn., Griffith 170, Inde, 1850, P04513508 ; *Nothapodytes montana* Blume, Beusekom & Phengkhlai 48, Thailand, 1968, P04513563 ; *Nothapodytes pittosporoides* (Oliv.) Sleumer, *,*,*, P04513555 ; *Oncotheca balansae* Bail., Suprin 1601, Nouvelle-Calédonie,1981, P00181264 ; *Pleurisanthes flava* Sandwith, Werff & Vasquez 13898, Peru, 1995, P05279709 ; *Sarcostigma paniculata* Pierre, Pierre 1644, Vietnam, 1877, P00834244 ; *Stachyanthus zenkeri* Engl., Zenker 4914, Cameroun, 1913, P05030980. **Lamiales.** *Thymus vulgaris* L., Didier 1016, France, 1949, P04436090; **Metteniusales.** *Emmotum nitens* (Benth,) Miers, Irwin et al. 27399, Brasil, 1970, P04513263; *Metteniusa tessmanniana* (Sleumer)

Sleumer, Asplund 10211, Equator, 1940, P06590944; *Pittosporopsis kerrii* Craib, Poilane 20731, Laos, 1969, P04464735; *Platea latifolia* Blume, Liang 65285, Hainan, 1934, P06669774. *Poraqueiba sericea* Tul., Sastre 2476, Colombie, 1973, P05279040; Solanales**.** *Hydrolea corymbosa* Elliott, Howard 12951, Florida, 1952, P04054102; *Solanum lycopersicum* L., Fosberg et al. 28204, Peru, 1947, P03961429.

Appendix 9

Phylogenetic relationships among asterid species focused on the family Icacinaceae based on the combined 73-plastidial genes and 22 morphological characters. The 50% majority-rule consensus tree was constructed by Bayesian inference in MrBayes.

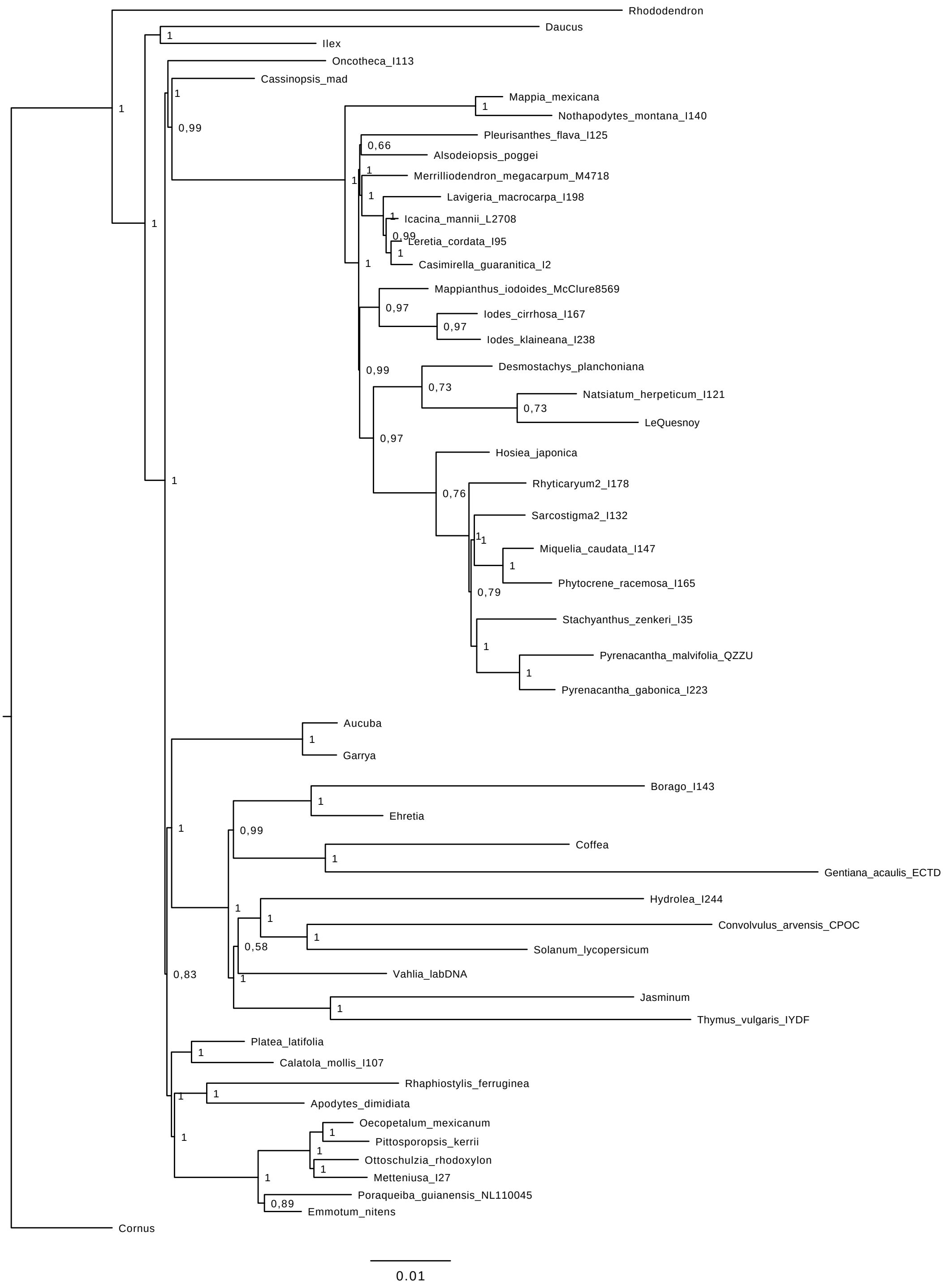

Appendix 10

Morphological characters and Matrix

1 Fruit: type – (0)Drupe (1)Berry (2)Samara

2 Endocarp: presence of the keel – (0)Yes (1)No

3 Endocarp: shape in lateral view – (0)Elliptical (1)Globulose (2)Ovoid (3)Obovoid (4)Triangular (5)Oblong

4 Endocarp: shape in transverse section – (0) Elliptical (1) Lenticular (2)Globulose (3)Triangular

5 Endocarp: apex structure– (0)Absent (1)Horns (2)Pores (3)Bulge

6 Endocarp: base morphology – (0)Cleft on one side (1)Symmetrical no basal cleft

7 Endocarp surface: pits – (0)Absent(1)Present

8 Endocarp surface: ridges – (0)Absent (1)Present

9Endocarp: rugosities– (0)Absent (1)Mound (2)Verrucate (3)Bossy

10 Endocarp: ridging pattern – (0)Diffuse (1)Reticulate (2)Striate

11 Pit: shape – (0) Mainly circular (1)Occasionally elongate (2)Primarily elongate

12 Endocarp surface: vascularisation – (0)Resting on ridges (1)Resting between ridges mounds (2)On the channel of endocarp (3)Free

13 Areoles: free ending ridges – (0)Present (1)Rare or absent

14 Endocarp primary vascular strand: position – (0) Inside endocarp wall (1) Outside endocarp wall (2) In channel

15 Tubercles – (0)Present (1)Present but faintly protrude beyond wall (2)Absent

16 Micromorphology on locule surface – (0) Smooth (1) Papillae (2)Inflated

17 Locul: hairs –(0)Yes (1) No

18 Tubercle: morphology – (0)Conical (1)Peg shaped (2)Spiny (3)Cylindrical (4)Elongate-flattened (5)Shallow mound not protrude beyond wall (6) parallel sided protuberances

19 Tubercle apex: morphology – (0)Capitate Swollen head (1)Biphid (2)not elaborated more or less rounded or pointed

20 Ridges: shape – (0)Sharp (1)Rounded (2)Angular

21 Papillae: shape – (0)Rounded (1)Sessile rounded (2)Large

22 Endocarp wall: layers – (0)Divided into distinctive layers (1)Homogeneous

23 Endocarp wall cells: orientation – (0)Anticlinal (1)Periclinal (2)Isodiametric

24 Locule: number – (0)One (1)Two (2)Three (3)Five

25 Ridges: secondary– (0)Yes (1)No

26 Shallow mound invagination: shape – (0)Spiny (1)Areoles type

27 Pits: number by faces – (0)< 50 (1)50-100 (2)100-150 (3)>150

28 Endocarp thicker than wide– (0)No (1)Yes

29Fruit: fleshy appendage – (0)No (1)Yes

30 Fruit: Gynophore – (0)Yes (1)No

31 Endocarp wall: digitate cells– (0)No (1)Yes

Number of characters	1	2	3	4	5	6	7	8	9	10	11	13	14	15
Alsodeiopsis poggei	0	0	5	1	0	1	0	1	0	1	?	0	2	?
Casimirella	0	?	(01)	1	?	?	?	?	?	?	?	?	?	?
Cassinopsis madagascariensis	0	0	(01)	2	0	1	0	1	0	0	?	?	0	?
Desmostachys planchonianus	0	1	0	1	3	1	0	0	1	?	?	?	1	?
Hosiea japonica	0	0	0	1	0	1	0	1	0	1	?	0	1	?
Icacina mannii	0	0	0	1	2	1	0	0	1	?	?	?	0	?
Iodes cirrhosa	0	0	0	1	1	0	0	1	2	0	?	?	0	?
Iodes klaineana	0	0	0	1	0	1	0	1	0	1	?	0	0	?
Lavigeria macrocarpa	0	0	0	2	0	1	0	1	2	0	?	?	0	?
Leretia cordata	0	1	0	2	0	1	0	0	0	?	?	?	0	?
Mappia	0	1	(01)	1	0	1	0	0	1	?	?	?	1	?
Mappianthus iodoides	0	1	0	1	2	1	0	0	1	?	?	?	2	?
Merrilliodendron megacarpum	0	?	?	?	?	?	?	?	?	?	?	?	?	?
Miquelia caudata	0	0	0	1	0	1	1	1	0	(01)	0	1	1	0
Natsiatum herpeticum	0	0	(02)	1	0	1	0	1	0	1	?	0	1	?
Nothapodytes nimmoniana	0	0	5	2	3	1	0	0	1	?	?	?	1	?
Phytocrene borneensis	0	1	3	1	2	1	1	0	0	?	1	?	1	1
Pleurisanthes flava	0	1	0	(12)	0	1	0	0	1	?	?	?	1	?
Pyrenacantha malvifolia	0	0	0	1	0	1	1	1	0	0	1	?	1	0
Pyrenacantha rakotozafyi	0	0	0	1	0	1	1	1	0	0	2	?	1	0
Rhyticaryum macrocarpum	0	0	0	1	2	(01)	0	1	2	(01)	?	1	1	?
Sarcostigma paniculata	0	0	0	(12)	1	1	0	0	3	?	?	?	1	?
Stachyanthus zenkeri	0	0	0	1	0	1	1	1	0	0	0	?	1	0
Emmotum nitens Benth	0	0	1	2	0	1	0	0	0	?	?	?	1	?
Platea parvifolia	0	1	(02)	2	2	1	0	0	1	?	?	?	1	?
Apodytes dimidiata	0	?	1	1	0	0	0	1	0	2	?	?	1	?
Pittosporopsis kerrii	0	1	0	2	0	1	0	1	0	2	?	?	1	?
Oncotheca balansae	0	1	1	2	0	1	0	0	0	?	?	?	?	?
Iodes tubulifera F	0	0	0	1	1	1	0	1	0	1	?	1	0	?
Iodes rivecourtensis F	0	0	(01)	1	(12)	1	0	1	0	1	?	1	0	?
Iodes rigida F	0	0	(02)	1	0	1	0	1	0	1	?	1	0	?
Iodes acuere F	0	0	(02)	1	0	1	0	1	0	1	?	1	0	?
Iodes reidii F	0	0	0	1	1	1	0	1	0	1	?	1	0	?
Iodes parva F	0	0	(01)	1	1	1	0	1	0	1	?	1	0	?
Iodes sinuosa F	0	0	0	1	1	1	0	1	0	1	?	1	0	?
Iodes passiciensis F	0	0	0	1	1	1	0	1	0	1	?	1	0	?
Palaeophytocrene cf vancouverensis F	0	?	2	?	0	1	1	?	0	?	1	?	?	0

Number of characters	**16**	**17**	**18**	**19**	**20**	**21**	**22**	**23**	**24**	**25**	**26**	**27**	**28**	**29**	**30**	**31**
Alsodeiopsis poggei	0	1	?	?	2	?	0	(12)	0	1	?	?	0	0	1	1
Casimirella	?	0	?	?	?	?	?	?	0	?	?	?	0	0	1	?
Cassinopsis madagascariensis	0	0	?	?	1	?	1	2	0	1	?	?	0	0	1	1
Desmostachys planchonianus	0	1	?	?	?	?	0	(01)	0	?	?	?	0	0	1	1
Hosiea japonica	1	1	?	?	0	2	0	(01)	0	1	?	?	0	0	1	1
Icacina mannii	0	1	?	?	?	?	0	(12)	0	?	?	?	0	0	1	1
Iodes cirrhosa	1	1	?	?	(01)	0	0	(12)	0	1	?	?	0	0	1	1
Iodes klaineana	?	1	?	?	1	?	0	(12)	0	1	?	?	0	0	1	1
Lavigeria macrocarpa	0	0	?	?	1	?	0	(12)	0	1	?	?	0	0	1	1
Leretia cordata	0	0	?	?	?	?	1	1	0	?	?	?	0	0	1	1
Mappia	0	1	?	?	?	?	0	(01)	0	?	?	?	0	0	1	1
Mappianthus iodoides	1	1	?	?	?	0	0	(12)	0	?	?	?	0	0	1	1
Merrilliodendron megacarpum	?	?	?	?	?	?	?	?	0	?	?	?	0	0	1	1
Miquelia caudata	1	1	0	2	(01)	0	?	?	0	1	?	0	0	0	0	1
Natsiatum herpeticum	0	1	?	?	(12)	?	1	1	0	1	?	?	0	0	1	1
Nothapodytes nimmoniana	0	1	?	?	?	?	1	1	0	?	?	?	0	0	1	1
Phytocrene borneensis	2	1	5	2	?	?	0	(01)	0	?	0	2	0	0	1	1
Pleurisanthes flava	0	1	?	?	?	?	0	(01)	0	?	?	?	0	0	1	1
Pyrenacantha malvifolia	1	1	1	2	1	(02)	0	(12)	0	1	?	2	0	0	1	1
Pyrenacantha rakotozafyi	1	1	1	2	1	2	0	1	0	1	?	2	0	0	0	1
Rhyticaryum macrocarpum	1	1	?	?	1	2	0	(01)	0	1	?	?	0	0	1	1
Sarcostigma paniculata	1	1	?	?	?	0	0	(01)	0	?	?	?	0	0	1	1
Stachyanthus zenkeri	0	1	0	2	0	?	0	1	0	0	?	3	0	0	1	1
Emmotum nitens Benth	0	1	?	?	?	?	1	2	2	?	?	?	1	0	?	0
Platea parvifolia	0	1	?	?	?	?	1	1	0	?	?	?	0	0	?	0
Apodytes dimidiata	0	1	?	?	1	?	0	(01)	0	1	?	?	1	1	?	0
Pittosporopsis kerrii	0	1	?	?	1	?	1	1	0	1	?	?	0	0	?	0
Oncotheca balansae	0	1	?	?	?	?	0	(12)	3	?	?	?	1	0	?	0
Iodes tubulifera F	1	1	?	?	0	0	0	(12)	0	1	?	?	0	?	?	1
Iodes rivecourtensis F	1	1	?	?	1	0	0	(12)	0	1	?	?	0	?	?	1
Iodes rigida F	1	1	?	?	2	0	0	(12)	0	1	?	?	0	?	?	1
Iodes acuere F	1	1	?	?	0	0	0	(12)	0	1	?	?	0	?	?	1
Iodes reidii F	?	1	?	?	(12)	?	0	(12)	0	1	?	?	0	?	?	1
Iodes parva F	1	1	?	?	1	0	0	(12)	0	1	?	?	0	?	?	1
Iodes sinuosa F	1	1	?	?	0	0	0	(12)	0	1	?	?	0	?	?	1
Iodes passiciensis F	1	1	?	?	1	0	?	?	0	1	?	?	0	?	?	?
Palaeophytocrene cf vancouverensis F	?	?	(06)	?	?	?	?	?	0	?	?	1	?	?	?	?

Appendix 11

Modern endocarp species sampling.

(In italic specimens used for endocarp study, in regular specimens used for fruit study only)

Icacinaceae

***Alsodeiopsis poggei* Engl.** *P. Sita 1872, Congo, 1969, P04495916 (P)* ; A. Hladik 1859, s.p., 1971 P04495893 (P) ; M. Ekitiké 48, Cameroon, 1986, P04495907 (P) ; R. Letouzey 4485, Cameroon, 1962, P04495897 (P) ; C. Farron 4577, Congo, 1965, P04495914 (P). ***Cassinopsis madagascariensis* Baill.** *P. P. Lowry et al. 5162, Madagascar, 1999, P00724815 (P).* ***Desmostachys planchonianus* Miers** *B. Lewis & S. Razafimandimbison 735, Madagascar, 1993, P04561640 (P)* ; R. Rabevohitra et al. 4810, Madagascar, 2003, P04561628 (P); R. Rabevohitra et al. 4658, Madagascar, 2003, P04561629 (P) ; J. Rabenantoandro et al. 1155, Madagascar, 2002, P04561630 (P). ***Hosiea japonica* Makino** *Okudai 60474.* ***Icacina mannii* Oliv.** *J. Koechlin 2334, Brazzaville, 1953, P04495011 (P)* ; J. Koechlin 633, Brazzavile, 1950, P04495012 (P) ; R.P. Klaine 489, Gabon, 1897, P04495007 (P). ***Iodes cirrhosa* Turcz.** *B. Hayata 672, "Indo-chine", 1921, P06672331 (P)* ; E. Poilane 6622, "Indo-chine", s.d., P06672332 (P). ***Iodes klaineana* Pierre** *R.P. Klaine 3064, Gabon, 1902, P04472306 (P)* ; J.J.F.E. de Wilde 606, Gabon, 1983, P04472313 (P). ***Lavigeria macrocarpa* (Oliv.) Pierre** *Bos 4098 (MO); R. Letowsey 8970, Cameroon, 1968, (P); N. Hallé 3734, Gabon, 1966, P04494807 (P); J.J. Wieringa 5840, Cameroon, 2007, WAG. 1398985 (WAG).* ***Leretia cordata* Vell.** *J.C. Solomon 17073, Bolivia, 1987, U. 1343377 (U)* ; Centre Orstom 4687, Guyane, 1981, P05221896 (P). ***Mappia racemosa* Jacq.** *H. A. Van Hermann 250, West Indies, 1904, P04513543 (P)* ; C. Wright 1389, Cuba, s.d., P04513544 (P). ***Mappianthus iodoides* Hand.-Mazz.** *A. N. Steward & H.C. Cheo 1093, China, 1933, P04513538 5 (P)* ; Cavalerie 1518, China, s.d., P05274868 (P). ***Miquelia caudata* King** *Mohd, Shah & Sidek 1168, Malay, 1965, L2289517 (L)* ; *Othman S.56069 (MO).* ***Natsiatum herpeticum* Buch.-Ham. ex Arn.** *H. B. Cale s.n., China, 1903, P04513511 (P).* ***Nothapodytes nimmoniana* (J.Graham) Mabb.** *A. H. H. Jayasuriya 1922, Ceylon, 1975, L2289443 (L)* ; Thomson 359 ?, s.p., s.n., P04513576 (P) ; Thwaites 492, Ceylan, s.d., P04513579 (P). ***Phytocrene borneensis* Becc.** *No voucher, Borneo, 1979, L.2289394 (L).* ***Pleurisanthes flava* Sandwith** *J. J. Pipoly 10168, Guyana, 1987, P05279044 (P).* ***Pyrenacantha malvifolia* Engl.** *P. Polill 475, s.p., 1961, (P).* ***Pyrenacantha rakotozafyi* Labat, El-Achkar & R.Rabev.** *F. Barthelat 1764, Mayotte, 2007, P00631418 (P).* ***Rhyticaryum macrocarpum* Becc.** *W. Vink*

11381, New Guinea, 1961, L2293146 (L) ; Katik 46856 (MO). ***Sarcostigma paniculata*** **Pierre** *E. Poilane 6677, Vietnam, 1923, P05279454 (P)* ; DDS 14047, Vietnam, 2008, P06807857 (P). ***Stachyanthus zenkeri*** **Engl.** *Carvalho 3626, Guiana, 1988, P05030978 (P).*

Oncothecaceae

Oncotheca balansae **Baill.** *H.S. Mackee 37671, New-Caledonia, 1979, P00180992 (P).*

Mettenuisaceae

Emmotum nitens **(Benth.) Miers** *R. M. Harley & R. Souza 10028, Brazil, 1968, P05279304 (P)* ; M. Claussen 1838, Brazil, 1969, P04513313 (P) ; R. Quevedo 927, Bolivia, 1993, P04513320 (P) ; R. M. Harley et al. 15081, Brazil, 1974, P04513269 (P) ; A. Glaziou 22041, Brazil, 1894, P04513276 (P). ***Platea parvifolia*** **Merr.& Chun** *W. T. Tsang 27299, China, 1936, P04518074 (P).* ***Apodytes dimidiata*** **E.Mey. ex Arn.** *R. Ranaivojaona et al. 114, Madagascar, 1997, P05279728 (P)* ; S.T. Malcomber et al. 1212, Madagascar, 1992, P00379386 (P) ; H. Perrier De La Bathie 19254, Madagascar, 1933, P0044068 (P) ; M.Y. Ammann, M.C Madiomanana & A.J. Tahinarivo MYA495, Madagascar, 2009, P05279690 (P) ; G. Simon, L. Festo & G. Massawe 527, Kenya, 2000, P04499342 (P). ***Pittosporopsis kerii*** **Craib** *M.F. Newman et al. LAO 831, Laos, 2005, P05279702 (P).*

Appendix 12

Boostrap tree result with 10 000 replicates using Paup 4.0 and with a mixed matrix of molecular and morphology data (59 144 characters). In bold fossils from the Paris basin.

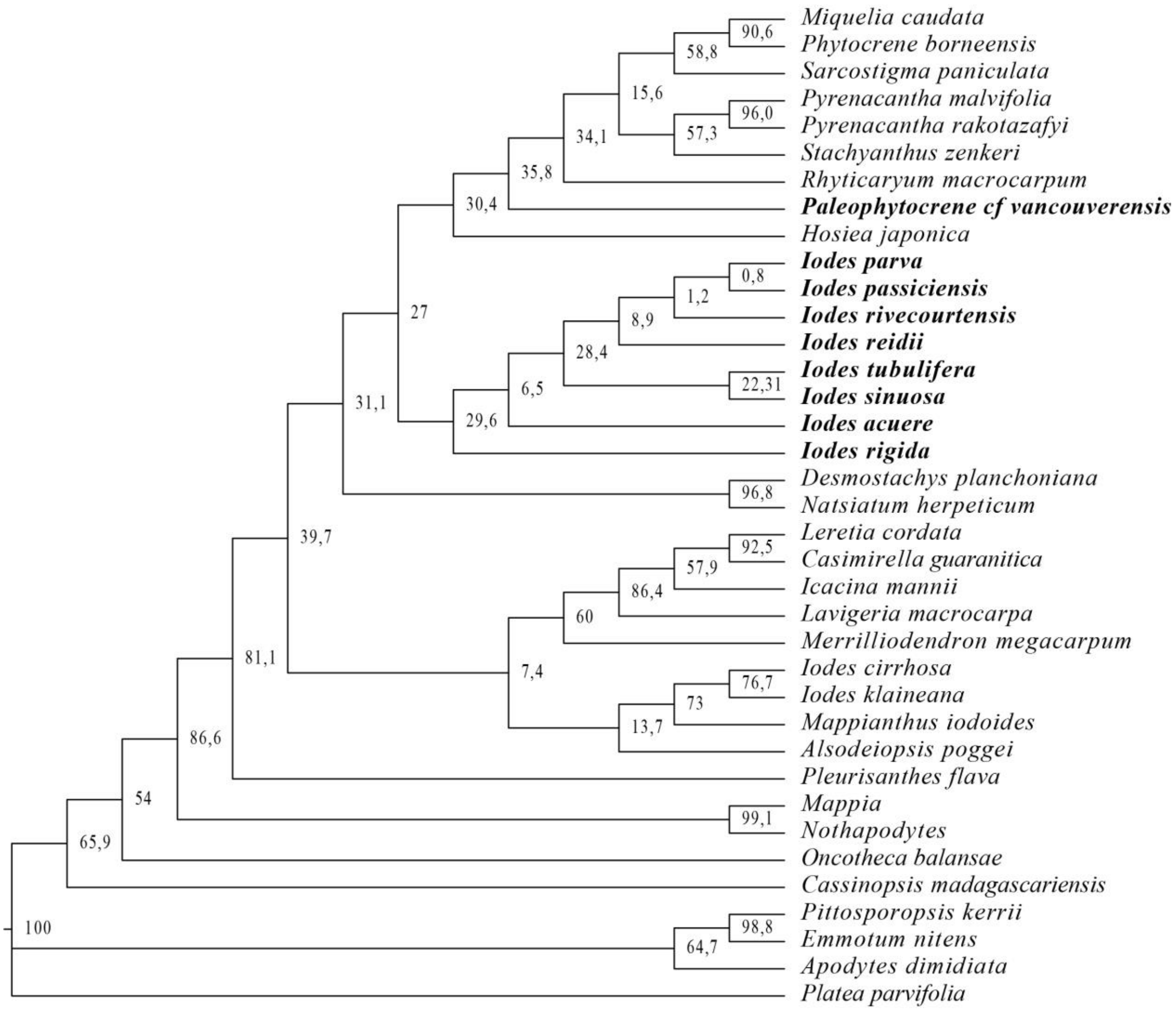

Appendix 13

Phylogenetic tree from a Bayesian inference implemented in Mrbayes 3.0 and with a mixed matrix of molecular and morphology data (59 144 characters). In bold, fossils from the Paris basin. The double slash in the branch of *Paleophytocrene* cf *vancouverensis* indicates that this branch have a greater length.

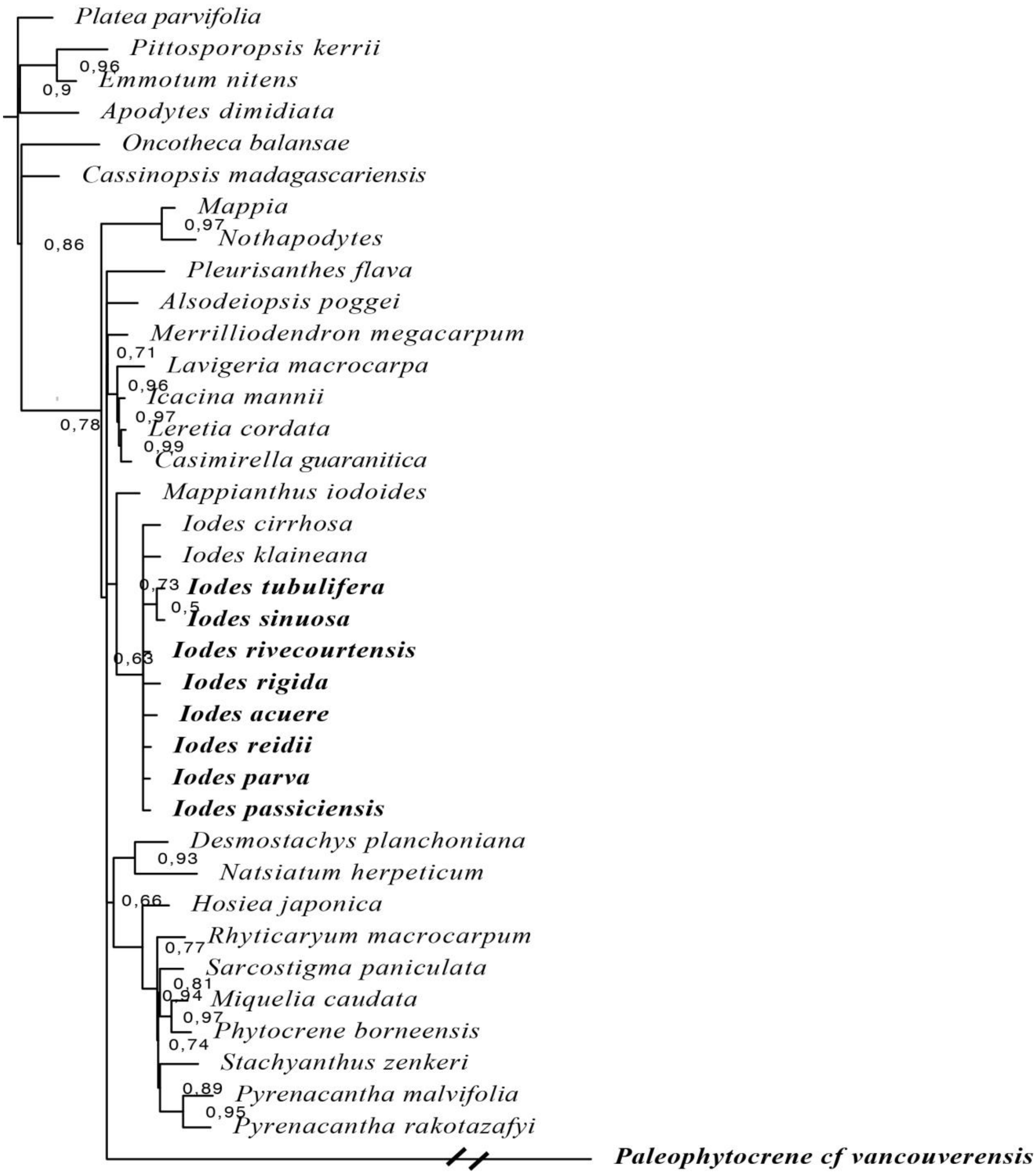

Résumé

La famille des Icacinaceae est une famille de plantes à fleurs possédant un registre fossile important durant le Paléogène, principalement en Amérique du Nord et en Europe. En particulier, des fossiles d'Icacinaceae ont été retrouvés au niveau de cinq sites du Bassin de Paris, principalement sous forme d'endocarpes datant du Thanétien et de l'Yprésien. Ces sites sont donc d'un grand intérêt pour étudier l'impact du maximum thermique de la limite Paléocene-Eocène sur les flores. En premier lieu, un travail sur les fruits actuels a permis de montrer la grande diversité des endocarpes et leurs valeurs en terme de reconnaissance spécifique chez les Icacinaceae. Par ailleurs, une clé d'identification Xper^3 accompagne cette étude. L'étude des fossiles du Bassin de Paris a permis de mettre en évidence huit nouvelles espèces appartenant au genre *Iodes*, une occurrence de *Paleophytocrene* et *Icacinicarya* ainsi que le nouveau genre *Icacinanthium* décrit à partir d'une fleur et de pollen pris dans de l'ambre. Sur les cinq espèces paléocènes, trois sont retrouvées au niveau des sites de l'Eocène, ce qui démontre au moins une continuité partielle des flores durant le réchauffement climatique. Cependant, une plus grande disparité morphologique est soulignée dans les sites éocènes. L'utilisation de l'ensemble du registre fossile a permis de reconstruire une histoire paléobiogéographique de la famille, en particulier de mettre en évidence une diversification de la famille durant l'Yprésien et plus généralement au cours de l'Eocène. Enfin, une étude de datation phylogénétique a permis de mettre en évidence la diversification d'un clade d'espèces grimpantes à la limite Paléocène-Eocène. Ainsi les différents niveaux d'études sont congruents et montrent que le réchauffement global du Paléocène-Eocène n'est pas un évènement catastrophique pour les Icacinaceae, mais plutôt une époque de diversification et d'apports nouveaux par migration, principalement en Hémisphère Nord.

Mots clés—endocarpe, *Iodes*, *Icacinanthium*, *Paleophytocrene*, Biogéographie, Paléobotanique

Abstract

The Icacinaceae family is a group of Angiosperm with a large fossil record, mainly from the North American and European Paleogene. Especially, fossils related to Icacinaceae were found in five sites from the Paris Basin, mainly as endocarp remains, in the Thanetian and Ypresian. Therefore, these sites constitute a good opportunity to study the impact of the global warming at the Paleocene-Eocene boundary in the floras. As a first step, we propose a survey of extant fruits; we show an important diversity of fruit shapes emphasizing the value of this organ in term of specific assignation. An Xper^3 database was built in addition to this study. The study of fossil's remains from the Paris Basin revealed the presence of eight new species belonging to the genus *Iodes*, an occurrence of genera *Paleophytocrene* and *Icacinicarya* and a new genus, *Icacinanthium*, described from a flower and pollen in amber. Among the five species described from the Paleocene, three were present in the Eocene sites, demonstrating at least a partial continuity of the Icacinaceae through the Paleocene-Eocene boundary. However, a greater morphological disparity was underlined in the Eocene sites. The use of all the fossil records allowed us to reconstruct the biogeographic history of the family and especially the diversification of the Icacinaceae during the Ypresian and more generally during the Eocene. Finally, a phylogenetic datating study highlighted a diversification of a climber clade at the Paleocene-Eocene boundary. Therefore, the different levels of studies are congruent and show that the Paleocene-Eocene Thermal Maximum was not a catastrophic event for the Icacinaceae family but rather a diversification event and new contributions by migration, mainly in the Northern Hemisphere.

Key Word—endocarp, *Iodes*, *Icacinanthium*, *Paleophytocrene*, Biogeography, Paleobotany